

# FINAL REPORT

## ENVIRONMENTAL SURVEY OF IDENTIFIED SAND RESOURCE AREAS OFFSHORE ALABAMA

### VOLUME I: MAIN TEXT

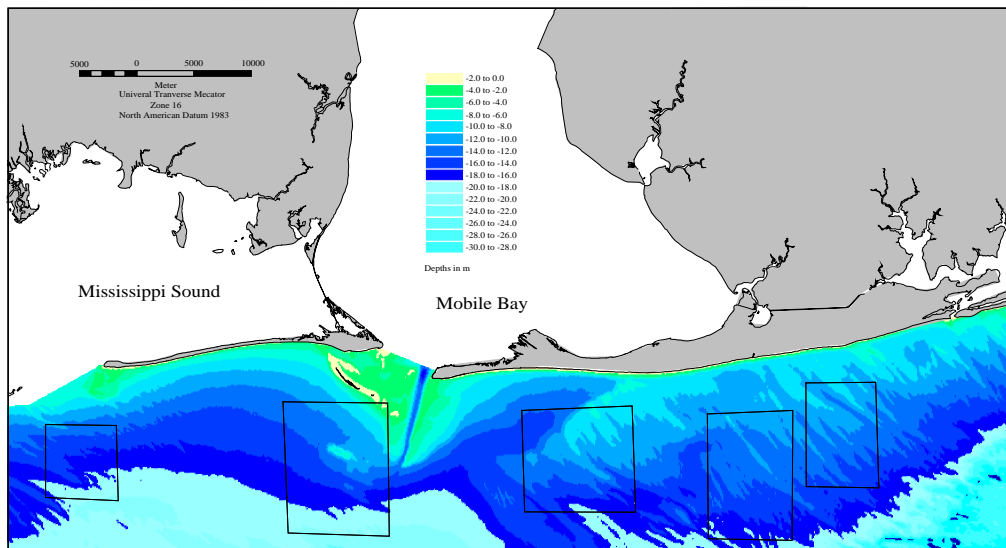
**Aubrey Consulting, Inc., Prime Contractor**

**Prepared by:**

**Applied Coastal Research and Engineering, Inc.  
766 Falmouth Road  
Building A, Unit 1-C  
Mashpee, MA 02649**

**In Cooperation With:**

**Continental Shelf Associates, Inc.  
Barry A. Vittor & Associates, Inc.  
Aubrey Consulting, Inc.**



**Prepared for:**

**U.S. Department of Interior  
Minerals Management Service  
International Activities and Marine  
Minerals Division (INTERMAR)**

**Funded Under Contract Number 14-35-01-97-CT-30840**

## **DISCLAIMER**

This report has been reviewed by the Minerals Management Service and approved for publication. Approval does not signify that the contents necessarily reflect the views and policies of the Service, nor does mention of trade names or commercial products constitute endorsement or recommendation for use.

## **SUGGESTED CITATION**

Byrnes, M.R., R.M. Hammer, B.A. Vittor, J.S. Ramsey, D.B. Snyder, K.F. Bosma, J.D. Wood, T.D. Thibaut, N.W. Phillips, 1999. Environmental Survey of Identified Sand Resource Areas Offshore Alabama: Volume I: Main Text, Volume II: Appendices. U.S. Department of Interior, Minerals Management Service, International Activities and Marine Minerals Division (INTERMAR), Herndon, VA. OCS Report MMS 99-0052, 326 pp. + 132 pp. appendices.

# **FINAL REPORT**

## **Environmental Survey Of Identified Sand Resource Areas Offshore Alabama**

**September 1999**

**Mark R. Byrnes**

Physical Processes Project Manager, Co-Editor  
(Applied Coastal Research and Engineering, Inc.)

**Richard M. Hammer**

Biological Component Project Manager, Co-Editor  
(Continental Shelf Associates, Inc.)

*With Contributions From:*

**Barry A. Vittor**

Barry A. Vittor & Associates, Inc.

**John S. Ramsey**

Applied Coastal Research and Engineering, Inc.

**David B. Snyder**

Continental Shelf Associates, Inc.

**Kirk F. Bosma**

Aubrey Consulting , Inc.

**Jon D. Wood**

Applied Coastal Research and Engineering, Inc.

**Tim D. Thibaut**

Barry A. Vittor & Associates, Inc.

**Neal W. Philips**

Continental Shelf Associates, Inc.

**Aubrey Consulting, Inc., Prime Contractor**

*Prepared by:*

**Applied Coastal Research and Engineering, Inc.  
766 Falmouth Road  
Building A, Unit 1C  
Mashpee, MA 02649**

*Prepared for:*

**U.S. Department of Interior  
Minerals Management Service  
International Activities and Marine  
Minerals Division (INTERMAR)  
381 Elden Street, MS 4030  
Herndon, VA 22070**

*In Cooperation With:*

**Continental Shelf Associates, Inc.  
Barry A. Vittor & Associates, Inc.  
Aubrey Consulting, Inc.**

**Contract Number 14-35-01-97-CT-30840**

## ACKNOWLEDGMENTS

Numerous people contributed to the project titled *Environmental Survey of Identified Sand Resource Areas Offshore Alabama*, which was funded by the U.S. Department of Interior, Minerals Management Service (MMS), International Activities and Marine Minerals Division (INTERMAR). Mr. Barry S. Drucker provided assistance and direction during the project as the MMS Contracting Officer's Technical Representative. Ms. Jane Carlson served as the MMS Contracting Officer. Mr. Barry Drucker, Mr. Khaled Bassim, and Mr. Keith Good of the MMS reviewed the draft document.

Dr. Mark R. Byrnes of Applied Coastal Research and Engineering, Inc. (Applied Coastal) served as Project Manager, Physical Processes Component Manager, co-authored Sections 1.0 (Introduction) and 3.0 (Regional Geomorphic Change), authored Section 2.1 (Offshore Sedimentary Environment), and was Co-Editor of the report. He was Program Manager from April 1997 to May 1998 while employed at Aubrey Consulting, Inc. (ACI). Dr. Richard M. Hammer of Continental Shelf Associates, Inc. (CSA) served as the Biological Component Manager, authored Sections 7.5.1 (Effects of Offshore Dredging on Benthic Fauna) and 7.5.2 (Recolonization Rate and Success), and was Co-Editor of the report. ACI was the prime contractor for the overall study, with Dr. David G. Aubrey serving as the Program Manager beginning May 1998.

Other Applied Coastal personnel who participated in the project included Mr. John S. Ramsey who led the nearshore sediment transport modeling component of the study. Mr. Ramsey authored Sections 2.2.6 (Nearshore Sediment Transport), 5.2.2 (Nearshore Sediment Transport Modeling), and 7.3.3 (Nearshore Sediment Transport Trends). Mr. Jon D. Wood designed and led the field data collection efforts to quantify short-term spatial and seasonal variability of shelf currents in the sand resource areas. Mr. Wood authored Sections 5.1.1 (Historical Data Set Analysis), 5.1.2 (Field Data Collection), 5.1.3 (Summary of Flow Regimes at Offshore Borrow Sites), 7.2 (Currents and Circulation), and co-authored Section 2.2 (Circulation and Physical Oceanography). Ms. Feng Li was responsible for shoreline and bathymetry change data compilation and surface modeling. Ms. Elizabeth A. Wadman provided report compilation and editorial assistance during production of the report.

Additional CSA personnel who contributed to the project included Mr. David B. Snyder who served as Chief Scientist during Biological Field Survey 1; authored Sections 2.3.2.1 and 7.6.1 (Zooplankton), 2.3.2.2 and 7.6.2 (Squids), and 2.3.2.3 and 7.6.3 (Fishes); and incorporated Sections 6.3.3 (Infauna), 6.3.4 (Epifauna and Demersal Ichthyofauna), and 6.4 (Discussion) into the remainder of Section 6.0 (Biological Field Surveys) which he authored. Dr. Alan D. Hart led the sampling design and statistical analyses for the biological data. Dr. Neal W. Phillips wrote Sections 2.3.2.4 and 7.6.4 (Sea Turtles), 2.3.2.5 and 7.6.5 (Marine Mammals), and reviewed the report. Mr. Paul S. Fitzgerald served as a Scientist during Biological Field Survey 1 and Chief Scientist for Survey 2. Messrs. Bruce D. Graham, Mark H. Schroeder, and Brock E. Stanaland served as Scientists during Survey 2. Mr. Frederick B. Ayer, III directed the field surveys and pre-plotted the station locations. Mr. Lynwood R. Powell, Jr. produced the field survey post-plot figures. Ms. Melody Powell provided editorial assistance and supervised CSA support staff during production of the biological sections of the report.

Personnel from Aubrey Consulting, Inc. who contributed to the project included Mr. Kirk F. Bosma who led the wave transformation numerical modeling effort and authored Sections 4.0 (Wave Transformation Numerical Modeling), 5.1.4 (Wave-Generated Currents), 5.2.1 (Sediment Transport at Borrow Sites), and 7.1 (Wave Transformation). Mr. Steven Jachec provided technical assistance on Sections 4.0 (Wave Transformation Numerical Modeling) and 5.2.1 (Sediment Transport at Borrow Sites). Ms. Imogene Bump provided technical assistance relative to analysis of currents and general circulation within the study area. Ms. Nadine Sweeney provided editorial assistance for the ACI portion of the report.

Personnel from Barry A. Vittor & Associates, Inc. (BVA) who contributed to the project included Dr. Barry A. Vittor, who served as Manager of BVA's responsibilities for the field surveys and report. Mr. Tim D. Thibaut authored Sections 2.3.1 (Benthic Environment), 6.3.3 (Infauna), 6.3.4 (Epifauna and Demersal Ichthyofauna), 6.4 (Discussion), and 7.5.3 (Predictions Relative to the Five Borrow Sites) of the report, with assistance from Dr. Vittor. Ms. Linda W. Sierke served as a Scientist during both field surveys. Ms. Sierke and Ms. Marianne P. Whitehurst supervised personnel associated with taxonomic identifications. Mr. Felix Fernandez served as Manager for BVA's benthic macroinfaunal data entry and analysis.

# TABLE OF CONTENTS

<b>1.0 INTRODUCTION</b>	<b>1</b>
1.1 STUDY AREA	2
1.2 STUDY PURPOSE	4
1.3 STUDY APPROACH	4
1.3.1 Baseline Ecological Conditions	5
1.3.2 Benthic Infaunal Evaluation	5
1.3.3 Project Scheduling	5
1.3.4 Wave Modifications	5
1.3.5 Sediment Transport Patterns	7
1.4 DOCUMENT ORGANIZATION	7
<b>2.0 ENVIRONMENTAL SETTING</b>	<b>8</b>
2.1 OFFSHORE SEDIMENTARY ENVIRONMENT	9
2.1.1 Seabed Morphology	12
2.1.2 Surface Sediments	13
2.1.3 Subsurface Deposits	16
2.1.4 Sand Resource Areas	16
2.2 CIRCULATION AND PHYSICAL OCEANOGRAPHY	32
2.2.1 Waves and Wave-Generated Currents	33
2.2.2 Wind-Generated Currents	34
2.2.3 Tidal Currents	35
2.2.4 Effects of Density	35
2.2.5 Gulf Loop Current	36
2.2.6 Nearshore Sediment Transport	36
2.3 BIOLOGY	37
2.3.1 Benthic Environment	37
2.3.1.1 Infauna	37
2.3.1.2 Epifauna and Demersal Ichthyofauna	40
2.3.2 Pelagic Environment	43
2.3.2.1 Zooplankton	43
2.3.2.2 Squids	52
2.3.2.3 Fishes	52
2.3.2.4 Sea Turtles	53
2.3.2.5 Marine Mammals	58
<b>3.0 REGIONAL GEOMORPHIC CHANGE</b>	<b>62</b>
3.1 SHORELINE POSITION CHANGE	62
3.1.1 Previous Studies	62
3.1.2 Shoreline Position Data Base	64
3.1.3 Historical Change Trends	66
3.1.3.1 1847/67 to 1917/18	66
3.1.3.2 1917/18 to 1934	68
3.1.3.3 1934 to 1957	68
3.1.3.4 1957 to 1978/82	71
3.1.3.5 Cumulative Shoreline Position Change (1847/67 to 1978/82)	71
3.2 NEARSHORE BATHYMETRY CHANGE	74
3.2.1 Bathymetry Data Base and Potential Errors	74
3.2.2 Digital Surface Models	75
3.2.2.1 1917/20 Bathymetric Surface	75
3.2.2.2 1982/91 Bathymetric Surface	78

3.2.3 Shelf Sediment Transport Dynamics.....	78
3.2.4 Magnitude and Direction of Change.....	83
3.2.5 Net Longshore Sand Transport Rates.....	85
3.3 SUMMARY.....	85
<b>4.0 WAVE TRANSFORMATION NUMERICAL MODELING .....</b>	<b>86</b>
4.1 ANALYSIS APPROACH .....	86
4.1.1 Wave Model Description.....	86
4.1.1.1 Refraction and Diffraction.....	90
4.1.1.2 Energy Dissipation.....	90
4.1.1.3 Wave Breaking.....	91
4.1.1.4 Radiation Stresses .....	92
4.1.1.5 Subgrids.....	92
4.1.2 Required Input Conditions .....	93
4.1.3 Wave Model Limitations and Modifications .....	93
4.2 WAVE CHARACTERISTICS AND INPUT SPECTRA.....	94
4.2.1 Wave Data Analysis and Sources .....	94
4.2.1.1 Wave Information Study and NOAA Buoy Data.....	94
4.2.1.2 Data Comparison.....	96
4.2.1.3 Seasonal Characteristics.....	96
4.2.1.4 High Energy Events.....	100
4.2.2 Seasonal Condition Parameters.....	102
4.2.2.1 Spectra Development.....	102
4.2.2.2 Selection of Wave Conditions .....	103
4.2.3 High Energy Event Parameters .....	104
4.3 GRID GENERATION .....	107
4.3.1 Existing Conditions .....	107
4.3.2 Post-Dredging Scenarios.....	109
4.3.2.1 Sand Borrow Site Selection.....	109
4.3.2.2 Numerical Excavation of Gridded Surfaces .....	111
4.4 PRE-DREDGING RESULTS .....	112
4.4.1 Seasonal Simulations .....	112
4.4.2 High Energy Wave Events Results .....	115
4.4.3 Model Results Relative to Historical Shoreline Change.....	116
4.5 COMPARISON OF PRE- AND POST-DREDGING RESULTS .....	118
4.5.1 Post-Dredging Results.....	118
4.5.2 Existing Conditions Versus Post-Dredging Seasonal Results .....	118
4.5.3 High Energy Wave Event Results .....	122
4.6 DISCUSSION.....	124
<b>5.0 CIRCULATION AND SEDIMENT TRANSPORT DYNAMICS .....</b>	<b>125</b>
5.1 CURRENTS AND CIRCULATION.....	125
5.1.1 Historical Data Analysis.....	125
5.1.1.1 Decomposition of Total Currents.....	127
5.1.1.2 Current Components .....	132
5.1.1.3 Total Observed Currents .....	132
5.1.1.4 Seasonal Variability .....	137
5.1.2 Field Data Collection.....	139
5.1.2.1 Survey Instrumentation and Techniques.....	139
5.1.2.2 Spring 1997 Survey Results.....	140
5.1.2.3 Fall 1997 Survey Results.....	151
5.1.3 Summary of Flow Regimes at Offshore Borrow Sites.....	159

5.1.4	Wave-Induced Bottom Currents .....	160
5.1.5	Wave-Induced Longshore Currents .....	162
5.1.5.1	Governing Equations .....	162
5.1.5.2	Lateral Mixing .....	164
5.1.5.3	Model Verification .....	166
5.1.5.4	Wave-Induced Currents Along the Alabama Coast.....	168
5.2	SEDIMENT TRANSPORT MODELING.....	170
5.2.1	Sediment Transport at Borrow Sites.....	170
5.2.1.1	Initiation of Sediment Motion Under Combined Wave and Current Action.....	170
5.2.1.2	Relative Magnitude and Direction of Transport.....	175
5.2.2	Nearshore Sediment Transport Modeling .....	183
5.2.2.1	Model Development.....	184
5.2.2.2	Sediment Transport Along the Alabama Coast.....	185
5.2.2.3	Nearshore Sediment Transport Versus Historical Shoreline Change .....	187
<b>6.0</b>	<b>BIOLOGICAL FIELD SURVEYS.....</b>	<b>192</b>
6.1	BACKGROUND .....	192
6.2	METHODS .....	192
6.2.1	Survey Design.....	192
6.2.2	Field Methods .....	200
6.2.2.1	Vessel .....	200
6.2.2.2	Navigation.....	200
6.2.2.3	Water Column.....	200
6.2.2.4	Sediment Grain Size.....	200
6.2.2.5	Infauna.....	201
6.2.2.6	Epifauna and Demersal Ichthyofauna .....	201
6.2.3	Laboratory Methods.....	201
6.2.3.1	Sediment Grain Size.....	201
6.2.3.2	Infauna.....	201
6.2.3.3	Epifauna and Demersal Ichthyofauna .....	201
6.2.4	Data Analysis .....	202
6.2.4.1	Water Column.....	202
6.2.4.2	Sediment Grain Size.....	202
6.2.4.3	Infauna.....	202
6.2.4.4	Epifauna and Demersal Ichthyofauna .....	203
6.3	RESULTS.....	203
6.3.1	Water Column.....	203
6.3.2	Sediment Grain Size .....	205
6.3.3	Infauna .....	205
6.3.4	Epifauna and Demersal Ichthyofauna .....	227
6.4	DISCUSSION.....	233
<b>7.0</b>	<b>POTENTIAL EFFECTS.....</b>	<b>239</b>
7.1	POTENTIAL SAND BORROW SITES .....	239
7.2	WAVE TRANSFORMATION .....	244
7.3	CURRENTS AND CIRCULATION.....	244
7.4	SEDIMENT TRANSPORT .....	247
7.4.1	Historical Sediment Transport Patterns.....	248
7.4.2	Sediment Transport Modeling at Potential Borrow Sites.....	248
7.4.3	Nearshore Sediment Transport Trends.....	249
7.4.3.1	Eastern Alabama Coast .....	249

7.4.3.2	Western Alabama Coast .....	254
7.4.3.3	Significance of Transport Trends .....	254
7.5	BENTHIC ENVIRONMENT .....	255
7.5.1	Effects of Offshore Dredging on Benthic Fauna .....	256
7.5.1.1	Sediment Removal .....	256
7.5.1.2	Sediment Suspension/Dispersion .....	257
7.5.1.3	Sediment Deposition .....	258
7.5.2	Recolonization Rate and Success.....	258
7.5.2.1	Adaptations for Recolonization and Succession.....	258
7.5.2.2	Successional Stages .....	259
7.5.2.3	Recolonization Rates.....	260
7.5.2.4	Recolonization Success and Recovery.....	261
7.5.3	Predictions Relative to the Borrow Sites .....	262
7.5.3.1	Potential Benthic Effects .....	263
7.5.3.2	Potential Recolonization Rate and Success .....	265
7.6	PELAGIC ENVIRONMENT.....	267
7.6.1	Zooplankton .....	267
7.6.1.1	Entrainment .....	267
7.6.1.2	Turbidity .....	267
7.6.1.3	Project Scheduling.....	268
7.6.2	Squids.....	269
7.6.2.1	Entrainment .....	269
7.6.2.2	Attraction.....	269
7.6.2.3	Project Scheduling.....	269
7.6.3	Fishes.....	269
7.6.3.1	Entrainment .....	269
7.6.3.2	Attraction.....	270
7.6.3.3	Turbidity .....	270
7.6.3.4	Project Scheduling.....	270
7.6.3.5	Essential Fish Habitat.....	270
7.6.4	Sea Turtles.....	272
7.6.4.1	Physical Injury.....	272
7.6.4.2	Turbidity and Anoxia.....	272
7.6.4.3	Noise.....	272
7.6.4.4	Project Scheduling.....	273
7.6.5	Marine Mammals .....	273
7.6.5.1	Physical Injury.....	273
7.6.5.2	Turbidity .....	274
7.6.5.3	Noise.....	274
7.6.5.4	Project Scheduling.....	274
7.7	POTENTIAL CUMULATIVE EFFECTS.....	274
<b>8.0</b>	<b>SUMMARY AND CONCLUSIONS .....</b>	<b>276</b>
8.1	WAVE TRANSFORMATION MODELING.....	276
8.2	CIRCULATION AND SEDIMENT TRANSPORT DYNAMICS .....	278
8.2.1	Historical Sediment Transport Patterns.....	278
8.2.2	Sediment Transport at Potential Borrow Sites .....	278
8.2.3	Nearshore Sediment Transport Modeling .....	279
8.3	BENTHIC ENVIRONMENT .....	280
8.4	PELAGIC ENVIRONMENT.....	281
8.5	SYNTHESIS.....	282
<b>9.0</b>	<b>LITERATURE CITED.....</b>	<b>283</b>

# APPENDICES

<b>APPENDIX A. HIGH-WATER SHORELINE POSITION CHANGE.....</b>	<b>A-1</b>
<b>APPENDIX B. WAVE TRANSFORMATION NUMERICAL MODELING INFORMATION .....</b>	<b>B-1</b>
B1. Directional and Frequency Verification .....	B-2
B2. Existing Conditions Wave Model .....	B-7
B3. Post-Dredging Wave Model Results.....	B-12
B4. Pre- and Post-Dredging Difference Plots.....	B-17
<b>APPENDIX C. SEDIMENT TRANSFORMATION NUMERICAL MODELING INFORMATION.....</b>	<b>C-1</b>
C1. Hydrodynamic and Sediment Transport Results at Sand Resource Areas 1, 2, and 3.....	C-2
C2. Longshore Sediment Transport Model Results .....	C-12
<b>APPENDIX D. FIELD SURVEY DATA .....</b>	<b>D-1</b>
D1. Sample Types, Sample Codes, Coordinates, and Water Depths.....	D-2
D2. Hydrolab Data .....	D-8
D3. Sediment Grain Size Data .....	D-10
D4. Infaunal Data.....	D-18
D5. Acoustic Doppler Current Profiler Data .....	D-49

## LIST OF FIGURES

Figure 1-1. Location diagram illustrating sand resource areas and State-Federal boundary relative to 1982/91 bathymetry. ....	3
Figure 1-2. Project Team. ....	6
Figure 2-1. Coastal Alabama and vicinity (from Hummell, 1996). ....	8
Figure 2-2. Sedimentary facies on the east Louisiana-Mississippi-Alabama shelf (after Ludwick, 1964; from Parker et al., 1997).....	10
Figure 2-3. Surface sediment texture map compiled from previous sediment texture data in the study area (from U.S. Army Corps of Engineers, 1984).....	11
Figure 2-4. Geomorphology of the ebb-tidal delta seaward of Mobile Bay entrance (from Hummell, 1996). ....	12
Figure 2-5. Vibracore, boring, and bottom grab locations in the Alabama EEZ study area (from Parker et al., 1997).....	14
Figure 2-6. Surface facies distribution in the Alabama EEZ study area (from Parker et al., 1997).....	15
Figure 2-7. Surficial sediment textures in the Alabama EEZ study area (from Parker et al., 1997).....	17
Figure 2-8. Surface sediment distribution in the west Alabama inner continental shelf (from Hummell, 1996). ....	18
Figure 2-9. Map of the mean grain size of Graded Shelly Sand Lithofacies vibracore sediment samples 0.1 m below the sediment-water interface (from Hummell and Smith, 1996).....	19
Figure 2-10. Generalized stratigraphic sequence of the Alabama EEZ study area (from Parker et al., 1997). ....	20
Figure 2-11. Map of the Sand Resource Area 1 (shaded area) showing location of cross section (A-A' and bathymetric profiles (1 and 2) (from Parker et al., 1997).....	22
Figure 2-12. Sand isopach (A) and surface sediment texture (B) maps for Sand Resource Area 1 (from Parker et al., 1997). ....	23
Figure 2-13. Map of Sand Resource Area 2 (shaded area) showing location of cross sections (A-A') and (B-B') and bathymetric profiles (1 and 2) (from Parker et al., 1997).....	24
Figure 2-14. Sand isopach (A) and surface sediment type (B) for Sand Resource Area 2 (from Parker et al., 1997).....	25
Figure 2-15. Map of Sand Resource Area 3 (shaded area) showing location of cross sections (A-A', B-B', and C-C') and bathymetric profiles (1 and 2) (from Parker et al., 1997).....	26
Figure 2-16. Sand isopach (A) and surface sediment texture (B) maps for Sand Resource Area 3 (from Parker et al., 1997). ....	27
Figure 2-17. Map of Sand Resource Area 4 showing location of vibracores and foundation borings (from Hummell and Smith, 1996).....	29
Figure 2-18. Surface facies distribution in Sand Resource Area 4 (from Hummell and Smith, 1996).....	30
Figure 2-19. Map of Sand Resource Area 5 (shaded area) showing location of cross sections (A-A' and B-B') and bathymetric profiles (1 and 2) (from Parker et al., 1997).....	31
Figure 2-20. Sand isopach (A) and surface sediment texture (B) maps for Sand Resource Area 5 (from Parker et al., 1997). ....	32

Figure 2-21. Infaunal assemblages associated with habitats on the inner continental shelf (<20 m depth) in the northeastern Gulf of Mexico study area (from Barry A. Vittor & Associates, Inc., 1985). .....	38
Figure 3-1. Map of southeastern Dauphin Island Gulf shoreline showing principal areas of erosion during the period 1955 to 1985 and estimated volumes of sand required for restoration of eroded areas (shaded) to the approximate position of the 1955 shoreline (from Parker et al., 1997).....	63
Figure 3-2. Gulf and Bon Secour Bay shoreline of Baldwin County, Alabama, showing locations of potential shoreline restoration and nourishment (from Parker et al., 1997).....	64
Figure 3-3. Shoreline position change along the Alabama coast, 1847/67 to 1917/20. ....	67
Figure 3-4. Shoreline position change along the Alabama coast, 1917/20 to 1934. ....	69
Figure 3-5. Shoreline position change along the Alabama coast, 1934 to 1957.....	70
Figure 3-6. Shoreline position change along the Alabama coast, 1957 to 1978/82. ....	72
Figure 3-7. Shoreline position change along the Alabama coast, 1847/67 to 1978/82. ....	73
Figure 3-8. Nearshore bathymetry (1917/20) for the southwestern Alabama coastal zone. ....	76
Figure 3-9. Nearshore bathymetry (1917/20) for the southeastern Alabama coastal zone. ....	77
Figure 3-10. Nearshore bathymetry (1985/91) for the southwestern Alabama coastal zone. ....	79
Figure 3-11. Nearshore bathymetry (1982/85) for the southeastern Alabama coastal zone. ....	80
Figure 3-12. Nearshore bathymetry change (1917/20 to 1985/91) for the southwestern Alabama coastal zone. ....	81
Figure 3-13. Nearshore bathymetry change (1917/20 to 1982/85) for the southeastern Alabama coastal zone. ....	82
Figure 3-14. Sand resource site location relative to dredged material deposition for Resource Area 4.....	84
Figure 3-15. Sand resource site location relative to sand ridge erosion and deposition in Resource Area 2.....	84
Figure 4-1. Comparison between a spectral (REF/DIF S) and monochromatic (REF/DIF 1) wave models. Wave height results are compared to measured data (*) collected by Vincent and Briggs (1989).....	87
Figure 4-2. Coordinate and angle convention used for the wave modeling in the present study.....	89
Figure 4-3. Diagram indicating the effects of refraction and diffraction as waves approach the coastline (from Svendsen and Jonsson, 1976).....	91
Figure 4-4. Example of subgrid development over a borrow pit feature (Kirby and Özkan, 1994).....	93
Figure 4-5. Comparison of WIS hindcast (dotted) and NOAA observed (solid) significant wave height for two time periods in 1988.....	97
Figure 4-6. Histogram plots of 20-yr averaged peak periods and associated wave directions for the month of May at WIS Station G1046. The vertical bars are normalized by the greatest occurrence bin. ....	98
Figure 4-7. Histogram plots of 20-yr averaged peak periods and associated wave directions for the month of November at WIS Station G1046. The vertical bars are normalized by the greatest occurrence bin. ....	98
Figure 4-8. Twenty-year averaged wave rose for May at WIS Station G1046.....	99
Figure 4-9. Twenty-year averaged wave rose for November at WIS Station G1046.....	99

Figure 4-10. Histogram plots of 20-yr averaged peak periods and associated wave directions for the spring season at WIS Station G1046. Vertical bars are normalized by the greatest occurrence bin.....	101
Figure 4-11. Twenty-year averaged wave rose for the spring season at WIS Station G1046.....	101
Figure 4-12. Energy and directional spectra verification and input set-up for the spring season at WIS Station G1047 (Grid A).....	105
Figure 4-13. Energy and directional spectra verification and input set-up for the summer season at WIS Station G1046 (Grid B).....	105
Figure 4-14. Illustration of reference grid notation (Kirby and Özkan, 1994).....	107
Figure 4-15. Bathymetry for Reference Grid A (Dauphin Island), with locations of WIS and NOAA stations, the defined sand resource areas, and the nearshore Dauphin Island subgrid.....	108
Figure 4-16. Bathymetry for Reference Grid B (Morgan Peninsula). With locations of WIS and NOAA stations, the defined sand resource areas, and the nearshore Morgan Peninsula subgrid.....	109
Figure 4-17. Potential borrow site locations (solid black lines) east of Main Pass.....	110
Figure 4-18. Potential borrow site location (solid black line) in Sand Resource Area 4.....	110
Figure 4-19. The four sand resource areas (outlined by the thick black line) and associated borrow sites (indicated by the thin black line).....	112
Figure 4-20. Spectral wave modeling results for existing conditions utilizing a typical spring season at reference Grid A.....	113
Figure 4-21. Spectral wave modeling results for existing conditions utilizing a typical spring season at reference Grid B.....	115
Figure 4-22. Spectral wave modeling results for existing conditions simulating a 50-yr storm event at reference Grid A.....	116
Figure 4-23. Wave height (thin line) taken from a baseline 100 m seaward of the Dauphin Island shoreline compared with historical shoreline change rates (thick line; 1847/67 to 1978/82). Points along the coastline that indicate increased wave height correspond to areas of historical erosion, while areas of historical accretion correspond to reduced wave heights.....	117
Figure 4-24. Wave height results (thin line) taken from a baseline 100 m seaward of the Morgan Peninsula shoreline compared to historical shoreline change rates (thick line; 1847/67 to 1978/82).....	119
Figure 4-25. Spectral wave modeling results for post-dredging scenario utilizing a typical spring season at reference Grid A.....	120
Figure 4-26. Wave height modifications resulting from potential offshore mining at Sand Resource Area 4 for a typical spring season. Hot colors (reds) identify areas of increased wave height, while cold colors (blues) identify areas of decreased wave height.....	121
Figure 4-27. Wave height modifications resulting from potential offshore mining at Sand Resource Areas 1, 2, and 3 for a typical spring season. Hot colors (reds) identify areas of increased wave height, while cold colors (blues) identify areas of decreased wave height.....	122
Figure 4-28. Wave height modifications resulting from potential offshore mining in Sand Resource Area 4 for a 50-yr storm event. Hot colors (reds) identify areas of increased wave height, while cold colors (blues) identify areas of decreased wave height.....	123
Figure 4-29. Wave height modifications resulting from potential offshore mining in Sand Resource Areas 1, 2, and 3 for the 50-yr storm event. Hot colors (reds) identify areas of increased wave height, while cold colors (blues) identify areas of decreased wave height.....	123

Figure 5-1. Map of sand resource areas east of Mobile Bay; Sand Resource Area 1 (far east) and Sand Resource Area 3 (far west). The five Gulf Shores mooring locations are shown as asterisks (*). Contours are labeled in m. ....	126
Figure 5-2. An example of the numerical separation of bottom current data collected within Shell Block 132, to the immediate southeast of the entrance to Mobile Bay (from Continental Shelf Associates, Inc. 1989). The data represent the east component of flow.....	129
Figure 5-3. Variance histogram for Shell Block 132 Mooring, representing the fraction of total energy attributed to individual forcing mechanisms. ....	130
Figure 5-4. Variance histogram for Gulf Shores Mooring 1M, representing the fraction of total energy attributed to individual forcing mechanisms. ....	130
Figure 5-5. Variance histogram for Gulf Shores Mooring 4S, representing the fraction of total energy attributed to the individual forcing mechanisms. ....	131
Figure 5-6. Variance histogram for Gulf Shores Mooring 4B, representing the fraction of total energy attributed to the individual forcing mechanisms. ....	131
Figure 5-7. Rose diagrams illustrating four historical data sets in the study area. The spokes of the diagram represent compass directions (90=east, 270=west, etc). The circumferential lines represent percent occurrence, with the inner annulus representing 10%, and the outside diameter representing 20% occurrence. A 'pie slice' extending to the outer circumference means that 20% of the time, currents are flowing in that direction. Current speeds are represented by the shading of the pie slice, with white (no shading) portions representing the fraction of time currents are between 0 and 5 cm/sec and black portions indicating the percent occurrence of currents over 50 cm/sec. ....	133
Figure 5-8. Rose diagrams for individual processes at Shell Block 132 (west of Mobile Bay, near-bottom) from September 30, 1987 to October 24, 1988. These data illustrate the relative strength of wind, and that water flow was directed primarily parallel to the isobaths, which are oriented northwest-southeast.....	134
Figure 5-9. Rose diagrams for individual processes at Mooring 4S (near-surface). These data illustrate that wind influence was primarily in the alongshore direction, the high- and low-frequency currents possessed the greatest directional variability, and that tides flowed predominantly to the east-northeast.....	135
Figure 5-10. Rose diagrams for individual processes at Mooring 4B (near-bottom). These data indicate that wind influence was rotated counter-clockwise relative to surface currents (Figure 5.9), that high- and low-frequency currents possessed the greatest directional variability, and that tides flowed predominantly to the northwest. ....	136
Figure 5-11. Rose diagrams for seasonal currents observed at Shell Block 132 (near-bottom currents). The individual plots represent the original time series divided into seasonal periods. ....	137
Figure 5-12. Comparison of seasonal winds versus seasonal wind-driven currents for Shell Block 132 (near-bottom) observations. Wind data were obtained from the NOAA station on Dauphin Island. Wind speed units are m/sec; current speed units are cm/sec. Radial circles of each plot represent the frequency of occurrence (in percent); the outer radius depicts 20%, the inner annulus depicts 10% occurrence. ....	138
Figure 5-13. Wind conditions prior to and during the field surveys on May 21-22, 1997. Dashed grid lines depict 0000 hours of the day labeled on the bottom axis. Winds are reported as direction from which the wind is blowing.....	142
Figure 5-14. Water elevation readings obtained from the NDBC station on Dauphin Island prior to and during field surveys on May 21-22, 1997. ....	143
Figure 5-15. Vector map of observed flow patterns for Sand Resource Area 4; May 21, 1997 from 0727 hours to 1150 hours. Current vectors represent average flow in the surface	

layer only (upper one-third of the water column). Bathymetry of Main Pass is noted in the upper right of the figure. The numbers in each corner of the transect grid ( 0727, 0948, 0848, and 1047) state the time (hour of day) that the transect line was started.....	144
Figure 5-16. Vector map of observed flow patterns for Sand Resource Area 4; May 21, 1997 from 0727 hours to 1150 hours. Current vectors represent average flow in the bottom layer only (lower one-third of the water column).....	145
Figure 5-17. Vector map of observed flow patterns for Sand Resource Area 4; May 21, 1997 from 1157 hours to 1620 hours. Current vectors represent average flow in the bottom layer only (lower one-third of the water column).....	146
Figure 5-18. Vector map of observed flow patterns for Sand Resource Area 4; May 21, 1997 from 1621 hours to 1930 hours. Current vectors represent average flow in the surface layer only (upper one-third of the water column). These currents were measured as wind squalls and thunderstorms passed the area, and demonstrate the rapid response of surface flow to sudden changes of wind speed and direction. ....	147
Figure 5-19. Example of a single vertical current profile measured in Sand Resource Area 2 on May 22, 1997. Strong vertical shear is apparent, as surface flow was directed to the east (90°) at approximately 35 cm/sec. Mid-layer and bottom flow were directed to the northwest (315°) at about 20 to 30 cm/sec. ....	148
Figure 5-20. Vector map of observed flow patterns for Sand Resource Area 2; May 22, 1997 from 0736 hours to 1130 hours. Current vectors represent average flow in the surface layer only (upper one-third of the water column).....	148
Figure 5-21. Vector map of observed flow patterns for Sand Resource Area 2; May 22, 1997 from 0736 hours to 1130 hours. Current vectors represent average flow in the bottom layer only (lower one-third of the water column).....	150
Figure 5-22. Vector map of observed flow patterns for Sand Resource Area 2; May 22, 1997 from 1534 hours to 1929 hours. Current vectors represent average flow in the bottom layer only (lower one-third of the water column). Note the 180° counterclockwise rotation of flow vectors since the beginning of the survey (see Figure 5-21). ....	151
Figure 5-23. Time series of wind speed and direction for 10 days preceding the fall 1997 field survey. Surveys were completed on September 30 and October 1, 1997. The horizontal dashed grid lines represent 0000 hours on the specified day.....	152
Figure 5-24. Water elevation readings obtained from the NDBC station on Dauphin Island prior to and during the fall field surveys. The data show the tides were near the equatorial (minimum) phase of the cycle on September 30 and October 1, 1997. ....	153
Figure 5-25. Vector map of observed flow patterns for Sand Resource Area 4; September 30, 1997 from 0829 hours to 1255 hours. Currents vectors represent average flow in the surface layer only (upper one-third of the water column).....	154
Figure 5-26. Vector map of observed flow patterns for Sand Resource Area 4; September 30, 1997 from 0829 hours to 1255 hours. Currents vectors represent average flow in the bottom layer only (lower one-third of the water column). ....	155
Figure 5-27. Vector map of observed flow patterns for Sand Resource Area 4; September 30, 1997 from 0829 hours to 1255 hours. Currents vectors represent average flow in the surface layer only (upper one-third of the water column).....	156
Figure 5-28. Vector map of observed flow patterns for Sand Resource Area 2; October 1, 1997 from 0827 hours to 1215 hours. Currents vectors represent average flow in the surface layer only (upper one-third of the water column).....	157
Figure 5-29. Vector map of observed flow patterns for Sand Resource Area 2; October 1, 1997 from 0827 hours to 1215 hours. Currents vectors represent average flow in the bottom layer only (lower one-third of the water column). ....	158
Figure 5-30. Shallow water and deep water wave orbits.....	160

Figure 5-31. Schematic of wave-induced bottom velocities. ....	161
Figure 5-32. Schematic longshore velocity profiles with and without cross-shore mixing (the abrupt reduction in velocity for the without mixing case occurs at the breaker line).....	165
Figure 5-33. Comparison of model and observed longshore current velocities from field measurements taken by Kraus and Sasaki (1979). ....	167
Figure 5-34. Comparison of modeled to observed longshore current velocities from field measurements taken by Thornton and Guza (1989). ....	168
Figure 5-35. $S_{xy}$ radiation stress and maximum longshore current velocities predicted by the wave-induced current model for the Morgan Peninsula during the spring season.....	169
Figure 5-36. Longshore current profiles along selected transects at Morgan Peninsula (colored transects in the top sub-plot correspond to like colored profiles in the bottom sub-plot). ....	170
Figure 5-37. Forces acting on grains resting on the seabed (Fredsoe and Deigaard, 1992). $F_L$ = lifting force, $F_D$ = drag force, and $W$ = grain weight. ....	171
Figure 5-38. Illustration indicating the angle between the apparent bottom current and wave-induced bottom current (Grant and Madsen, 1979). ....	172
Figure 5-39. Illustration of a particle on a (a) transverse slope, and on a (b) longitudinal slope. ....	174
Figure 5-40. Location of the offshore subgrid regions within Sand Resource Areas 1, 2, and 3. These subgrids were used to determine potential sediment transport at the borrow areas following numerical dredging. ....	176
Figure 5-41. Location of the offshore subgrid region within Sand Resource Area 4. This subgrid was used to determine potential sediment transport at the borrow area following numerical dredging. ....	176
Figure 5-42. Southeast winter hydrodynamic and sediment transport results at Sand Resource Area 4. The solid black lines represent depth contours, and sediment transport results are based on 200-m cell widths. ....	179
Figure 5-43. Northwest winter hydrodynamic and sediment transport results at Sand Resource Area 4. The solid black lines represent depth contours, and sediment transport results are based on 200-m cell widths. ....	179
Figure 5-44. Spring hydrodynamic and sediment transport results at Sand Resource Area 4. The solid black lines represent depth contours, and sediment transport results are based on 200-m cell widths. ....	180
Figure 5-45. Summer hydrodynamic and sediment transport results at Sand Resource Area 4. Solid black lines represent depth contours, and sediment transport results are based on 200-m cell widths. ....	180
Figure 5-46. Fall hydrodynamic and sediment transport results at Sand Resource Area 4. Solid black lines represent depth contours, and sediment transport results are based on 200-m cell widths. ....	181
Figure 5-47. Extreme hydrodynamic and sediment transport results at Sand Resource Area 4. Solid black lines represent depth contours, and sediment transport results are based on 200-m cell widths. ....	181
Figure 5-48. $S_{xy}$ radiation stress values and annualized sediment transport potential for the spring season at Morgan Peninsula. ....	186
Figure 5-49. $S_{xy}$ radiation stress and annualized sediment transport potential for existing conditions at Dauphin Island during the Summer season. ....	186
Figure 5-50. Cross-shore distribution of longshore current and sediment transport for three selected transects (spring season at Morgan Peninsula). ....	188
Figure 5-51. Annual longshore sediment transport potential, normalized change in longshore transport (modeled accretion/erosion potential), and observed shoreline change between 1847/67 and 1978/81 for the Morgan Peninsula. ....	189

Figure 5-52. Annual longshore sediment transport potential, normalized change in longshore transport (modeled accretion/erosion potential), and observed shoreline change between 1847/67 and 1978/81 for Dauphin Island. ....	190
Figure 6-1. Sampling locations for grain size and infauna relative to the five sand resource areas and the Alabama coast (adapted from Parker et al.,1997). ....	194
Figure 6-2. Sampling locations for Alabama Sand Resource Area 1. Inner box represents the limits of Area 1. Outer box provides reference coordinates. ....	195
Figure 6-3. Sampling locations for Alabama Sand Resource Area 2. Inner box represents the limits of Area 2. Outer box provides reference coordinates. ....	196
Figure 6-4. Sampling locations for Alabama Sand Resource Area 3. Inner box represents the limits of Area 3. Outer box provides reference coordinates. ....	197
Figure 6-5. Sampling locations for Alabama Sand Resource Area 4. Inner box represents the limits of Area 4. Outer box provides reference coordinates. ....	198
Figure 6-6. Sampling locations for Alabama Sand Resource Area 5. Inner box represents the limits of Area 5. Outer box provides reference coordinates. ....	199
Figure 6-7. Temperature (°C), salinity (ppt), and dissolved oxygen (mg/l) measured near-bottom by Hydrolab during May and December 1997 at the five sand resource areas offshore Alabama. Two sets of measurements were made in each sand resource area. ....	204
Figure 6-8. Station groupings (A to F) based on normal cluster analysis of infaunal samples collected during the May 1997 Survey 1 and December 1997 Survey 2 in the five sand resources areas (1 to 5) offshore Alabama. ....	209
Figure 6-9. Grain size composition of infaunal samples collected during the May 1997 Survey 1 and December 1997 Survey 2 in the five sand resource areas offshore Alabama. Sample order and Groups A-F are based on normal cluster analysis. ....	210
Figure 6-10. Normal cluster analysis of infaunal samples collected during the May 1997 Survey 1 (S1) and December 1997 Survey (S2) in Sand Resource Area 1 offshore Alabama. ....	213
Figure 6-11. Inverse cluster analysis of infaunal taxa from samples collected during the May 1997 Survey 1 and December 1997 Survey 2 in Sand Resource Area 1 offshore Alabama. ....	215
Figure 6-12. Normal cluster analysis of infaunal samples collected during the May 1997 Survey 1(S1) and December 1997 Survey 2 (S2) in Sand Resource Area 2 offshore Alabama. ....	217
Figure 6-13. Inverse cluster analysis of infaunal taxa from samples collected during the May 1997 Survey 1 and December 1997 Survey 2 in Sand Resource Area 2 offshore Alabama. ....	218
Figure 6-14. Normal cluster analysis of infaunal samples collected during the May 1997 Survey (S1) and December 1997 Survey 2 (S2) in Sand Resource Area 3 offshore Alabama. ....	220
Figure 6-15. Inverse cluster analysis of infaunal taxa from samples collected during the May 1997 Survey 1 and December 1997 Survey 2 in Sand Resource Area 3 offshore Alabama. ....	223
Figure 6-16. Normal cluster analysis of infaunal samples collected during the May 1997 Survey 1 (S1) and December 1997 Survey 2 (S2) in Sand Resource Area 4 offshore Alabama. ....	224
Figure 6-17. Inverse cluster analysis of infaunal taxa from samples collected during the May 1997 Survey 1 and December 1997 Survey 2 in Sand Resource Area 4 offshore Alabama. ....	226

Figure 6-18. Normal cluster analysis of infaunal samples collected during the May 1997 Survey 1 (S1) and December 1997 Survey 2 (S2) in Sand Resource Area 5 offshore Alabama.....	228
Figure 6-19. Inverse cluster analysis of infaunal samples collected during the May 1997 Survey 1 and December 1997 Survey 2 in Sand Resource Area 5 offshore Alabama.....	230
Figure 6-20. Normal cluster analysis of epifaunal trawl samples collected during the May 1997 Survey 1 (S1) and December 1997 Survey 2 (S2) in the five sand resource areas (A1 to A5) along the north (1) and south (2) transects offshore Alabama.....	234
Figure 7-1. Location of potential borrow sites for Resource Area 4.....	241
Figure 7-2. Location of potential borrow sites for Sand Resource Areas 1, 2 and 3.....	243
Figure 7-3. Present shoreline configuration (thick line) compared to differences in wave heights (thin line) caused by potential dredging scenarios offshore Dauphin Island. Wave heights (post-dredging minus pre-dredging) were taken from a baseline approximately 100 m seaward of the coastline.....	245
Figure 7-4. Present shoreline configuration (thick line) compared to differences in wave heights (thin line) caused by potential dredging scenarios offshore Morgan Peninsula. Wave heights (post-dredging minus pre-dredging) were taken from a baseline approximately 100 m seaward of the coastline.....	246
Figure 7-5. Difference in average annual transport rates associated with dredging sand resource sites along Morgan Peninsula.....	250
Figure 7-6. Difference in transport rates for 50-yr storm event associated with dredging sand resource sites along Morgan Peninsula.....	251
Figure 7-7. Difference in average annual transport rates associated with dredging sand resource area along Dauphin Island.....	252
Figure 7-8. Difference in transport rates for 50-yr storm event associated with dredging sand resource area along Dauphin Island.....	253

## LIST OF TABLES

Table 1-1. UTM Coordinates defining resource areas offshore Alabama (see Figure 1-1).....	2
Table 2-1. Sand resource area characteristics (Parker et al., 1997; Hummell, 1999).....	27
Table 2-2. Epifaunal assemblages of the northern Gulf of Mexico which pertain to the Alabama study area (from Defenbaugh, 1976).....	41
Table 2-3. Eight taxonomic groups resulting from a synthesis of community analyses of trawl samples collected in the northeastern Gulf of Mexico study area during the 1982 and 1983 SEAMAP groundfish surveys (from Barry A. Vittor & Associates, Inc., 1985).....	44
Table 2-4. Monthly occurrence of copepods collected in Mississippi Sound (adapted from McIlwain, 1968).....	47
Table 2-5. Spawning times of economically important fishes (F) and invertebrates (I) in the northern Gulf of Mexico (adapted from Barry A. Vittor & Associates, Inc., 1985).....	50
Table 2-6. Occurrence ( ) and peak seasonal occurrence ( ) of larval fishes in coastal waters of Mississippi (Adapted from: Stuck and Perry, 1981b). ....	51
Table 2-7. Food habits of coastal pelagic fishes collected from the northern Gulf of Mexico.....	54
Table 2-8. Monthly commercial landings (lbs) of coastal pelagic fishes for Alabama averaged over the years 1992 to 1996 (U.S. Department of Commerce, National Marine Fisheries Service, 1998).....	54
Table 2-9. Sea turtle species potentially occurring in coastal Alabama waters. ....	55
Table 3-1. Summary of shoreline source data characteristics for the coast between western Dauphin Island (at Petit Bois Pass) and Perdido Pass, Alabama.....	65
Table 3-2. Estimates of potential error associated with shoreline position surveys.....	65
Table 3-3. Maximum root-mean-square potential error for shoreline change data from western Dauphin Island (at Petit Bois Pass) to Perdido Pass, Alabama.....	66
Table 3-4. Summary of bathymetry source data characteristics for the offshore area between western Dauphin Island (at Petit Bois Pass) and Perdido Pass, Alabama.....	74
Table 4-1. Summary of relevant WIS stations in the modeling domain. ....	95
Table 4-2. Inventory of relevant NOAA stations in the modeling domain.....	96
Table 4-3. Summary of the seasonal breakdown of the 1976-1995 WIS data. ....	100
Table 4-4. Return periods based on the 1976 to 1995 WIS data.....	102
Table 4-5. Wave transformation numerical modeling input conditions and scenarios for Grid A (Dauphin Island).....	106
Table 4-6. Wave transformation numerical modeling input conditions and scenarios for Grid B (Morgan Peninsula).....	106
Table 4-7. Reference grid dimensions.....	108
Table 4-8. Subgrid dimensions. ....	109
Table 4-9. Dredged depth and resulting sand volume within respective sand resource area.....	111
Table 5-1. Current meter data sets collected in the study area.....	126
Table 5-2. Average salinity profiles at sand resource areas 1 – 5 May 1997 .....	143
Table 5-3. Sediment sizes at Sand Resource Areas 1 through 4. ....	177
Table 5-4. Summary of seasonally-averaged sediment transport results using potential cumulative dredged sand volumes.....	182
Table 5-5. Summary of seasonally-averaged sediment transport results relative to sand dredging volumes per beach replenishment event. ....	183
Table 6-1. Sample types and numbers for the May 1997 Survey 1 and December 1997 Survey 2 of the five sand resource areas offshore Alabama. Gravity coring was conducted only in Area 4 Station 14.....	193

Table 6-2. Five most abundant infaunal taxa from samples collected during the May 1997 Survey 1 and December 1997 Survey 2 in the five sand resource areas offshore Alabama.....	206
Table 6-3. Summary of infaunal statistics by survey and sand resource area offshore Alabama.....	207
Table 6-4. Infaunal species groups resolved from inverse cluster analysis of all samples collected during the May 1997 Survey 1 and December 1997 Survey 2 in the five sand resource areas offshore Alabama.....	211
Table 6-5. Two-way matrix from cluster analysis of infaunal samples collected during the May 1997 Survey 1 (S1) and December 1997 Survey 2 (S2) in Sand Resource Area 1 offshore Alabama.....	214
Table 6-6. Two-way matrix from cluster analysis of infaunal samples collected during the May 1997 Survey 1 (S1) and December 1997 Survey 2 (S2) in Sand Resource Area 2 offshore Alabama.....	219
Table 6-7. Two-way matrix from cluster analysis of infaunal samples collected during the May 1997 Survey 1 (S1) and December 1997 Survey 2 (S2) in Sand Resource Area 3 offshore Alabama.....	221
Table 6-8. Two-way matrix from cluster analysis of infaunal samples collected during the May 1997 Survey 1 (S1) and December 1997 Survey 2 (S2) in Sand Resource Area 4 offshore Alabama.....	225
Table 6-9. Two-way matrix from cluster analysis of infaunal samples collected during the May 1997 Survey 1 (S1) and December 1997 Survey 2 (S2) in Sand Resource Area 5 offshore Alabama.....	229
Table 6-10. Epifauna collected by mongoose trawl and ranked by numerical abundance from the May 1997 Survey (S1) in the five potential sand resource areas (A1 to A5) along north (1) and south (2) transects offshore Alabama.....	231
Table 6-11. Epifauna collected by mongoose trawl and ranked by numerical abundance from the December 1997 Survey (S2) in the five potential sand resource areas (A1 to A5) along north (1) and south (2) transects offshore Alabama.....	232
Table 7-1. UTM Coordinates defining borrow site polygons offshore Alabama.....	242
Table 7-2. Statistical parameters for annual average sediment transport conditions associated with Sand Resource Areas 1 through 4.....	254
Table 7-3. Statistical parameters for 50-year event sediment transport conditions associated with Sand Resource Areas 1 through 4.....	254
Table 7-4. Invertebrate and fish species managed by the Gulf of Mexico Fishery Management Council for which Essential Fish Habitat has been identified in the vicinity of the five sand resource areas offshore Alabama (adapted from Gulf of Mexico Fishery Management Council, 1998).....	271

## LIST OF ABBREVIATIONS

μ	micron
ACI	Aubrey Consulting, Inc.
ADCP	Acoustic Doppler Current Profiler
ASTM	American Society for Testing Materials
BVA	Barry Vittor & Associates, Inc.
CEQ	Council on Environmental Quality
CERC	Coastal Engineering Research Center
CHL	Coastal Hydraulics Laboratory
cm	centimeter
CSA	Continental Shelf Associates, Inc.
DGPS	Differential Global Positioning System
EA	Environmental Assessment
EEZ	Exclusive Economic Zone
EFH	Essential Fish Habitat
EIS	Environmental Impact Statement
ELMAS	East Louisiana-Mississippi-Alabama Shelf
ESA	Endangered Species Act
FMP	Fishery Management Plan
ft	feet
GMFMC	Gulf of Mexico Fishery Management Council
GSA	Geological Survey of Alabama
ha	hectare
INTERMAR	Office of International Activities and Marine Minerals
km	kilometers
kts	knots
LPIL	Lowest Practical Identification Level
m	meter
MAFLA	Mississippi-Alabama-Florida
MAME	Mississippi Alabama Marine Ecosystems
MCM	million cubic meters
mcy	million cubic yards
mi	statute mile
mm	millimeter
MWL	Mean Water Level
NAD	North American Datum
NDBC	National Data Buoy Center
NEGOM	northeastern Gulf of Mexico
NEPA	National Environmental Policy Act
NGVD	National Geodetic Vertical Datum
NMFS	National Marine Fisheries Service
NOAA	National Oceanic and Atmospheric Administration
OCS	Outer Continental Shelf
OCSLA	Outer Continental Shelf Lands Act
ppt	parts per thousand
SEAMAP	Southeastern Area Monitoring and Assessment Program
sec	second
USACE	U.S. Army Corps of Engineers
USDOI	U.S. Department of the Interior
USFWS	U.S. Fish and Wildlife Service
UTM	Universal Transverse Mercator
WIS	Wave Information Study
yd	yard
yr	year

## 1.0 INTRODUCTION

The coastal zone is a unique geological, physical, and biological area of vital economic and environmental value. Houston (1995) particularly discusses the value of beaches and their maintenance via beach nourishment to America's economy. Not only are beaches the dominant component of most coastal economies, but they also provide a measured level of protection against high winds and waves associated with storms. Miller (1993) stresses the importance of coastal and marine tourism as the world's largest industry and its continual rise over the past 50 years. As such, beaches are key elements of coastal tourism because they represent the leading tourist destination.

Coastal community master plans are being developed and revised to address concerns associated with population growth, storm protection, recreation, waste disposal and facilities management, and zoning (Williams, 1992). Often, problems stemming from these issues are in direct conflict with natural coastal processes. Some of the more direct problems are related to coastal erosion and storm protection. The practice of replenishing beaches with sand from upland and nearshore sources as protection for community infrastructure has increased in direct relation to population growth. As coastal and nearshore borrow areas become depleted, and our knowledge of environmental effects of coastal sand mining develop, alternate sources of aggregate and beach fill must be evaluated for offshore sites to meet specific societal needs. In many cases, sand resource extraction from the Outer Continental Shelf (OCS) may prove environmentally preferable to nearshore borrow areas due to potential changes in waves and currents as large quantities of sand are dredged from the seafloor.

Denmark, Japan, The Netherlands, and United Kingdom have been actively involved in marine mining of sand and gravel for the past few decades. The U.S. recognizes the potential benefits of sand and gravel mining on the Outer Continental Shelf (OCS), as well as the potential for environmental impacts. The U.S. Department of Interior (USDOI), Minerals Management Service (MMS) is responsible for managing the exploration and development of sand and gravel resources on the OCS seaward of State boundaries. In 1983, the MMS established the Office of Strategic and International Minerals for evaluating the prospects for and conditions under which sand and gravel mining would develop in the U.S. In 1991, the Office of International Activities and Marine Minerals (INTERMAR) was created to develop strategies for addressing specific concerns regarding offshore sand and gravel mining operations (Hammer et al., 1993).

The MMS has significant responsibilities with respect to the potential environmental impacts of sand and gravel mining. Existing regulations governing sand and gravel mining provide a framework for comprehensive environmental protection during operations. Specific requirements exist for evaluations and lease stipulations that include appropriate mitigation measures (Hammer et al., 1993). Guidelines for protecting the environment stem from a wide variety of laws, including the OCS Lands Act (OCSLA), National Environmental Policy Act (NEPA), Endangered Species Act, Marine Mammals Protection Act, and others. Regulations require activities to be conducted in a manner which prevents or minimizes the likelihood of any occurrences that may cause damage to the environment. The MMS takes a case-by-case approach in conducting environmental analyses, as required by NEPA and the Council on Environmental Quality (CEQ) regulations.

In recent years, there has been increasing interest in sand and gravel mining on the OCS. Currently, eight State-Federal task forces, several cooperative agreements, at least five negotiated agreements, and four environmental surveys exist to ensure substantive government and public involvement and attention to regional, State, and local concerns regarding leasing, engineering, economic, and environmental aspects of sand and gravel mining. Under the OCSLA, the MMS is required to conduct environmental studies to obtain information useful for decisions related to negotiated agreements and lease activities. As such, the MMS pursues its responsibilities for management of offshore sand and gravel mining vigorously by:

- protecting ocean and coastal environments by ensuring that all OCS sand and gravel mining activities are environmentally acceptable;
- ensuring the OCS sand and gravel activities are compatible with other uses of the ocean;
- involving coastal States in all aspects of sand and gravel mining activities; and
- evaluating the potential of the OCS as a domestic source for sand and gravel resources.

To this end, the MMS initiated four environmental studies along the Atlantic and Gulf coasts in FY97 to provide information for programmatic marine mining decisions at MMS Headquarters and OCS Regional Offices. This report presents the results of the first of four environmental studies administered through INTERMAR. Entitled "Environmental Study of Identified Sand Resource Areas Offshore Alabama", this program was initiated by Aubrey Consulting, Inc. (ACI) in April 1997 under MMS Contract No. 14-35-01-97-CT-30840. This report was prepared by Applied Coastal Research and Engineering, Inc. (Applied Coastal) in cooperation with Continental Shelf Associates, Inc. (CSA), ACI, and Barry A. Vittor & Associates, Inc. (BVA).

### 1.1 STUDY AREA

The inshore portion of the continental shelf, seaward of the State-Federal OCS boundary and within the Alabama Exclusive Economic Zone (EEZ), encompasses the project study area (Figure 1-1). The seaward limit of the study area is defined by the 30°05'N latitude line. The project area is located within the east Louisiana-Mississippi-Alabama Shelf (ELMAS). The continental shelf surface within the study area is relatively broad and featureless west of the Mobile Bay entrance; however, the Alabama shelf east of the entrance channel contains many northwest-southeast trending shoreface sand ridges, as well as other shoals (Figure 1-1).

Five potential sand resource areas were defined within the study area through a Federal-State cooperative agreement between MMS-INTERMAR and the Geological Survey of Alabama (GSA). Table 1-1 provides a list of coordinates defining the extent of each resource area. Parker et al. (1993, 1997) characterize the sand resource potential for each borrow area (defined by Parker [1990]) based on surface sediment samples and vibracore data. Hummell and Smith (1995, 1996) provide detailed geologic information on Sand Resource Area 4 to supplement existing information, identifying a specific low-relief shoal in the southeast quadrant of the sand resource area as the prime borrow area. Specific parts of Sand Resource Areas 1, 2, and 3 currently are being analyzed by the GSA using new vibracore and surface sediment samples to determine the quantity of sand available for future beach fills. The GSA report to MMS-INTERMAR is due in 1999. For the present study, four borrow sites within Sand Resource Areas 1 through 4 were defined to evaluate potential impacts of sand mining for beach replenishment (see Section 7.0). Sand Resource Area 5 was not included in the analysis because it is away from beach areas of greatest replenishment need, and the sediment was least compatible with native beach sand (see Parker et al., 1997).

Table 1-1. UTM Coordinates defining resource areas offshore Alabama (see Figure 1-1).				
Resource Area	UTM -x and -y coordinate pairs (easting, northing; Zone 16, NAD83)			
	Northwest	Northeast	Southeast	Southwest
1	433599.8, 3343440.7	439695.6, 3343497.7	439966.0, 3334262.3	433625.3, 3334390.6
2	424999.2, 3340725.8	432462.1, 3341046.5	432392.2, 3329688.6	425085.2, 3329834.3
3	408795.2, 3341033.2	418425.2, 3341418.9	418738.4, 3332150.8	409042.5, 3332165.5
4	387958.5, 3341778.8	397087.6, 3341691.0	397219.5, 3330053.1	388387.4, 3330323.6
5	367217.6, 3339795.0	373396.3, 3339722.0	373561.7, 3333162.2	367220.8, 3333422.7

See README.txt file to print this figure.

Figure 1-1. Location diagram illustrating sand resource areas and State-Federal boundary relative to 1982/91 bathymetry.

## 1.2 STUDY PURPOSE

The primary purpose of this study was to address environmental concerns raised by the potential for dredging sand from the OCS offshore the State of Alabama for beach replenishment and to document the findings in a technical report. The primary environmental concerns focused on biological and physical components of the environment. To this end, seven study objectives were identified:

- Compile and analyze existing oceanographic literature and data sets to develop an understanding of existing environmental conditions offshore Alabama and the ramifications of dredging operations at selected sand borrow sites;
- Design and conduct biological and physical field data collection efforts to supplement existing resources;
- Analyze the physical and biological field data sets to address basic environmental concerns regarding potential sand dredging operations;
- Use physical processes field data sets and wave climate simulations to predict wave transformation under natural conditions and in the presence of proposed dredging activities;
- Determine existing coastal and nearshore sediment transport patterns using historical data sets, and predict future changes resulting from proposed sand dredging operations;
- Evaluate the potential cumulative environmental effects of multiple dredging scenarios; and
- Develop a document summarizing the information generated to assist with decisions concerning preparation of an Environmental Assessment/Impact Statement to support a negotiated agreement.

In meeting these objectives, this document should provide invaluable information regarding environmental concerns examined relative to proposed future sand dredging in support of beach replenishment needs from offshore Alabama.

## 1.3 STUDY APPROACH

Biological and physical processes data were collected and analyzed to assess the potential impacts of offshore dredging activities within the study area to minimize or preclude long-term adverse environmental impacts at potential borrow sites and along the coastline landward of resource sites. In addition, wave transformation and sediment transport numerical modeling were employed to simulate the physical environmental effects of proposed sand dredging operations to ensure that offshore sand resources are developed in an environmentally sound manner.

Five primary study elements were outlined in Task 1 (Data Collection and Analysis) of the Request for Proposals for addressing environmental concerns associated with offshore sand dredging for beach replenishment. They included:

- Assessment of baseline benthic ecological conditions, using existing data sets and data collected from field work, in and around the five proposed sand borrow areas;
- Evaluation of the benthic infauna present in the five proposed borrow areas, and assessment of the potential effects of offshore sand dredging on these organisms, including an analysis of the potential rate and success of recolonization following dredging;
- Development of a schedule of best and worst times for offshore sand dredging in relation to transitory pelagic species;

- Evaluation as to the potential modification to waves that propagate within the study area due to offshore sand dredging within the proposed sand borrow areas; and
- Evaluation of the impact of offshore dredging and consequent beach replenishment in terms of potential alteration to sediment transport patterns, sedimentary environments, and impacts to local shoreline processes.

The first three study elements focused primarily on biology and associated ecological impacts relative to potential sand dredging operations. The final two elements concentrated on potential alterations to physical processes and sedimentary environments, as well as potential shoreline response to incident waves and currents resulting from dredging operations. The scientific approach used to address each of the study elements is presented below. The remaining study tasks (2-14) focused on document preparation and project management requirements. Figure 1-2 shows the organization of the project team and individual responsibilities.

### **1.3.1 Baseline Ecological Conditions**

The goal of this study element was to assess baseline ecological conditions (biology, water column parameters, physical processes, sedimentologic characteristics) in and around the five sand resource areas. This phase of the study primarily focused on field data collection efforts conducted in May, September, and December 1997 (presented in detail in Sections 5.0 and 6.0). However, existing literature and data were compiled and summarized to characterize the ecological environment and to form the foundation upon which field surveys were designed. Biological field surveys were conducted in May and December 1997 to characterize infauna, epifauna, demersal ichthyofauna, sediment grain size, and water column parameters (detailed in Section 6.0). Because Mobile Bay entrance flows potentially have significant impact on the physical processes (waves, currents, and sediment transport dynamics) affecting ecological conditions in the sand resource areas, total currents were measured at resource areas west and east of the entrance using an Acoustic Doppler Current Profiler (ADCP). Existing data sets were analyzed to document temporal variations in flow throughout the study area, whereas ADCP measurements were used to examine spatial variations throughout the water column (detailed in Section 5.0).

### **1.3.2 Benthic Infaunal Evaluation**

The goal of this study element was to assess the potential effects of offshore dredging on benthic infauna and analyze the potential rate and success of recolonization following cessation of dredging activities. Existing literature and data on dredging effects were searched and synthesized then combined with results from the biological field surveys to examine potential benthic effects and recolonization in the sand resource areas.

### **1.3.3 Project Scheduling**

The goal of this study element was to determine the best and worst times for offshore dredging relative to pelagic species. Environmental windows are temporal constraints placed on dredging activities to protect biological resources from potentially detrimental effects (Dickerson et al., 1998). Existing information was collected and summarized concerning the seasonal occurrence of pelagic species in the five sand resource areas and potential impacts from dredging. Project scheduling considerations for pelagic species then were analyzed based on this information.

### **1.3.4 Wave Modifications**

The goal of this study element was to perform wave transformation numerical modeling to predict the potential for adverse modification of waves resulting from sand dredging operations. Changes in bathymetry in sand resource areas can cause wave energy focusing resulting in

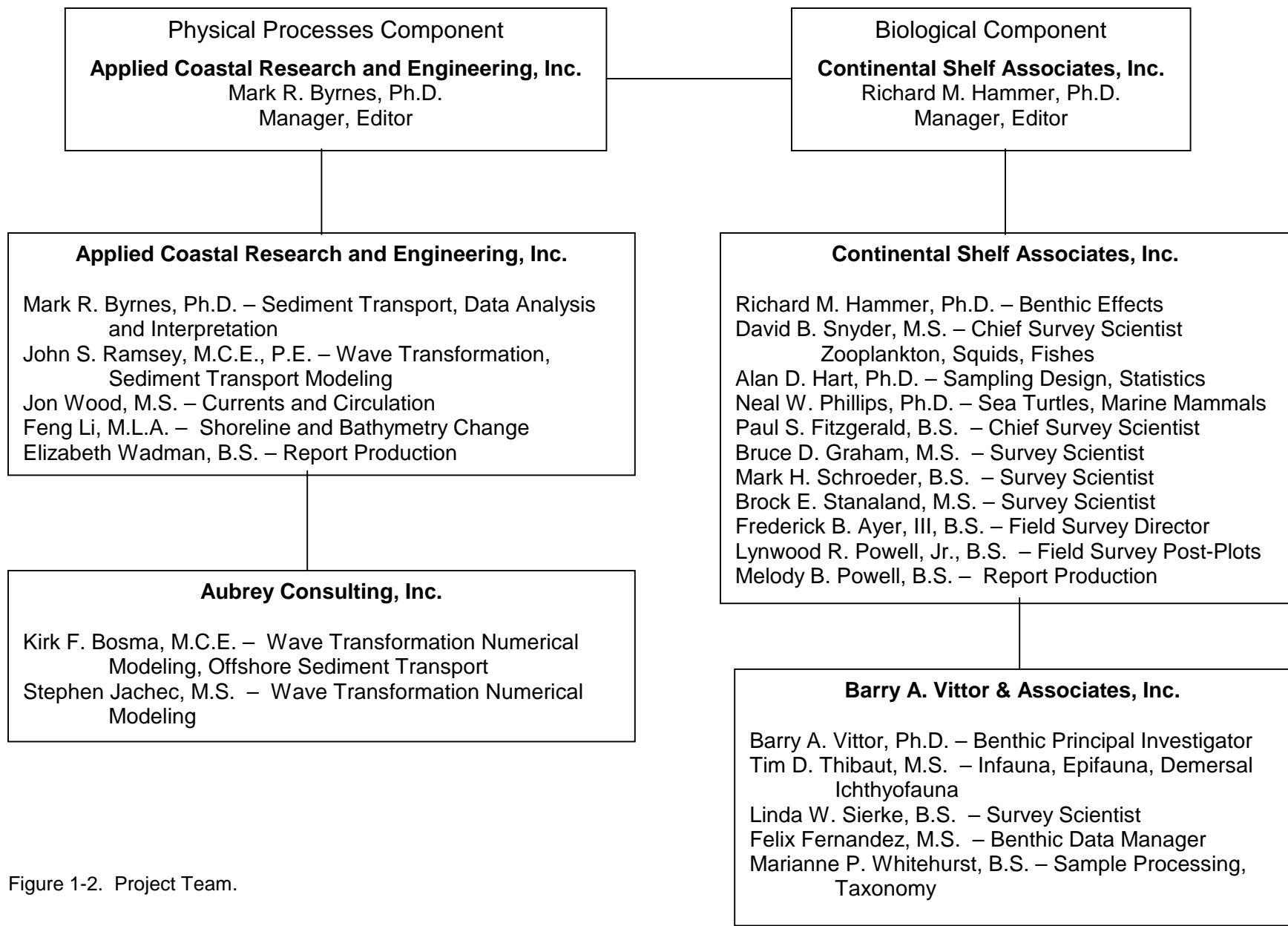


Figure 1-2. Project Team.

substantial alterations in sediment transport at the site of dredging operations, as well as along the shoreline landward of the borrow site. Because the purpose of dredging offshore sand from a specific site will be driven by the need for beach replenishment, it is critical to understand the impact of changing wave transformation patterns on shoreline response before potentially exacerbating a problem. Numerical comparisons of pre-and post-dredging impacts provided a means of documenting modifications to waves as they crossed the five sand resource areas.

### **1.3.5 Sediment Transport Patterns**

The goal of this study element was to predict changes in sediment transport patterns resulting from potential sand dredging operations using numerical information generated from wave transformation modeling, combined with offshore current data (ADCP). Sediment transport rates were quantified for sand resource sites using an analytical approach, whereas transport rates at the shoreline were determined numerically using output from wave transformation numerical modeling (detailed in Section 5.0).

Historical shoreline and bathymetry data were compiled to document regional sediment transport patterns over a 60-yr time period. Net changes in sediment erosion and deposition on the shelf surface offshore Alabama provided a direct method for identifying patterns of sediment transport and quantifying net rates of change throughout the potential sand resource areas (detailed in Section 3.0). These data also were used to calibrate numerical results for direction and magnitude of transport.

## **1.4 DOCUMENT ORGANIZATION**

Information presented in this document represents the culmination of a year and a half of work among experts in the fields of biology and benthic ecology (CSA and BVA) and coastal processes (Applied Coastal and ACI), under the direction of Mr. Barry Drucker (MMS INTERMAR). This document was organized into nine major sections as follows:

- Introduction
- Environmental Setting
- Regional Geomorphic Change
- Wave Transformation Numerical Modeling
- Circulation and Sediment Transport Dynamics
- Biological Field Surveys
- Potential Effects
- Conclusions
- Literature Cited

The sections are presented in a different order than the list of study elements in the RFP. Because benthic and pelagic biological characteristics are in part determined by spatially varying physical processes throughout the study area, physical processes analyses are summarized first.

In addition to the main document, appendices were prepared in support of many of the analyses presented in each section of the report. Furthermore, an Executive Summary, a Technical Summary, and a Non-Technical Summary were prepared as separate documents to provide a brief description of study methods and findings for audiences ranging from researchers to non-technical people.

## 2.0 ENVIRONMENTAL SETTING

Coastal Alabama, defined as the southern portions of Mobile and Baldwin Counties (Figure 2-1), is economically diverse and contains multiple coastal environments (Hummell, 1996). The outer coast extends approximately 90 km from about 87°30' longitude at Perdido Pass to about 88°25' longitude at Petit Bois Pass. There are about 75 km of shoreline along the open Gulf at about 30°15' latitude (Chermock et al., 1974). The offshore State-Federal jurisdictional boundary marks the direct landward limit of the study area; however, the ultimate use of sand extracted from the OCS is for beach replenishment along the Alabama outer coast. Consequently, a description of the environmental setting from the outer coast to the OCS is pertinent for addressing the overall study purpose.

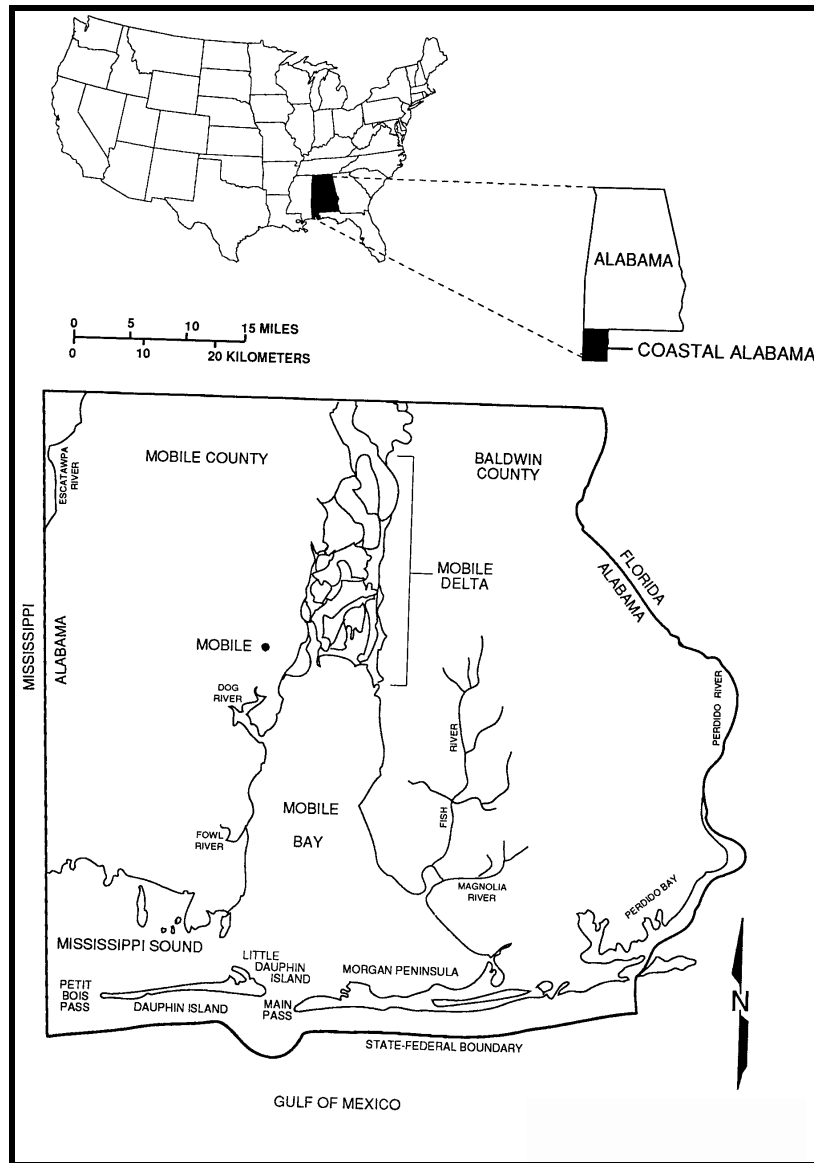


Figure 2-1. Coastal Alabama and vicinity (from Hummell, 1996).

Dauphin Island is the westernmost beach environment in coastal Alabama. The island is approximately 25 km long and extends from Main Pass at the Mobile Bay entrance to Petit Bois Pass, a 7-km-wide tidal inlet separating western Dauphin Island, Alabama and eastern Petit Bois Island, Mississippi (see Figure 2-1). The western two-thirds of Dauphin Island is a low-relief, washover barrier that is subject to overwash by Gulf of Mexico waters during tropical storms and hurricanes (Nummedal et al., 1980; Byrnes et al., 1991; Hummell, 1996). Maximum relief along this portion of the island is about 2 m relative to mean water level (MWL), except for dune features that may reach 3 m MWL in elevation. Island width varies between about 300 and 800 m. Currently, the main channel at Petit Bois Pass is located adjacent to Dauphin Island and extends to about 7 m below the MWL (McBride et al., 1991). The eastern end of Dauphin Island has an average elevation near the beach of about 3 m MWL; however, an extensive interior dune system that reaches an elevation of approximately 14 m MWL exists north of beach deposits on top of existing Pleistocene coastal deposits (Otvos, 1979).

Seaward of the beach along eastern Dauphin Island, an ephemeral, subaerial sand deposit called Pelican Island is associated with the ebb-tidal delta for Main Pass. This feature is prominent in its impact on shoreline response along eastern Dauphin Island (Parker et al., 1997). The island has continuously changed its shape, size, and location throughout the historical record in response to storm events and normal wave and current processes (Hummell, 1996).

Along the eastern Alabama coast in Baldwin County, the shoreline extends approximately 50 km from Morgan Point, at the eastern margin of Main Pass, along the Morgan Peninsula east to Perdido Pass (Figure 2-1). The Morgan Peninsula forms the southeastern terminus of Mobile Bay and consists of an extensive beach backed by parallel dunes and numerous sub-parallel beach ridges, formed as a result of net longshore sediment transport processes (Bearden and Hummell, 1990; Stone et al., 1992).

## **2.1 OFFSHORE SEDIMENTARY ENVIRONMENT**

Seafloor topography and Holocene sediment distribution on the Alabama EEZ reflect a combination of processes, including regression during the late-Pleistocene and reworking of the exposed shelf surface by ancient fluvial systems, and reworking of the exposed shelf surface by coastal processes during the subsequent Holocene rise in sea level (Ludwick, 1964; Parker et al., 1997). Redistribution of sediment by waves and currents during transgression partially or totally destroyed geomorphic features associated with Pleistocene fluvial environments. Concurrently, these same processes formed modern shelf deposits as subaerial coastal features became submerged and reworked during relative rising sea level. As such, much of the shelf offshore Alabama is sand (Figure 2-2) (Ludwick, 1964; Doyle and Sparks, 1980; Parker et al., 1997). On the inner shelf offshore Dauphin Island, an extensive deposit of sandy mud occurs as a result of sediment discharge from Mobile Bay through Main Pass (Figure 2-3; U.S. Army Corps of Engineers, 1984; Parker et al., 1997). Parker et al. (1992) indicate that sediment type can change from sand to mud over a distance of several meters within the large Mississippi-Alabama sand facies.

Parker et al. (1992) suggest that much of the variation is due to changes in bathymetry. Large ridges on the eastern part of the Alabama shelf extend for several hundred meters in length, a couple of hundred meters in width, and are composed of sand. Shell gravel is common on the landward flanks of the ridges with mud occasionally depositing in the troughs between ridges (Parker et al., 1992; McBride and Byrnes, 1995; Parker et al., 1997).

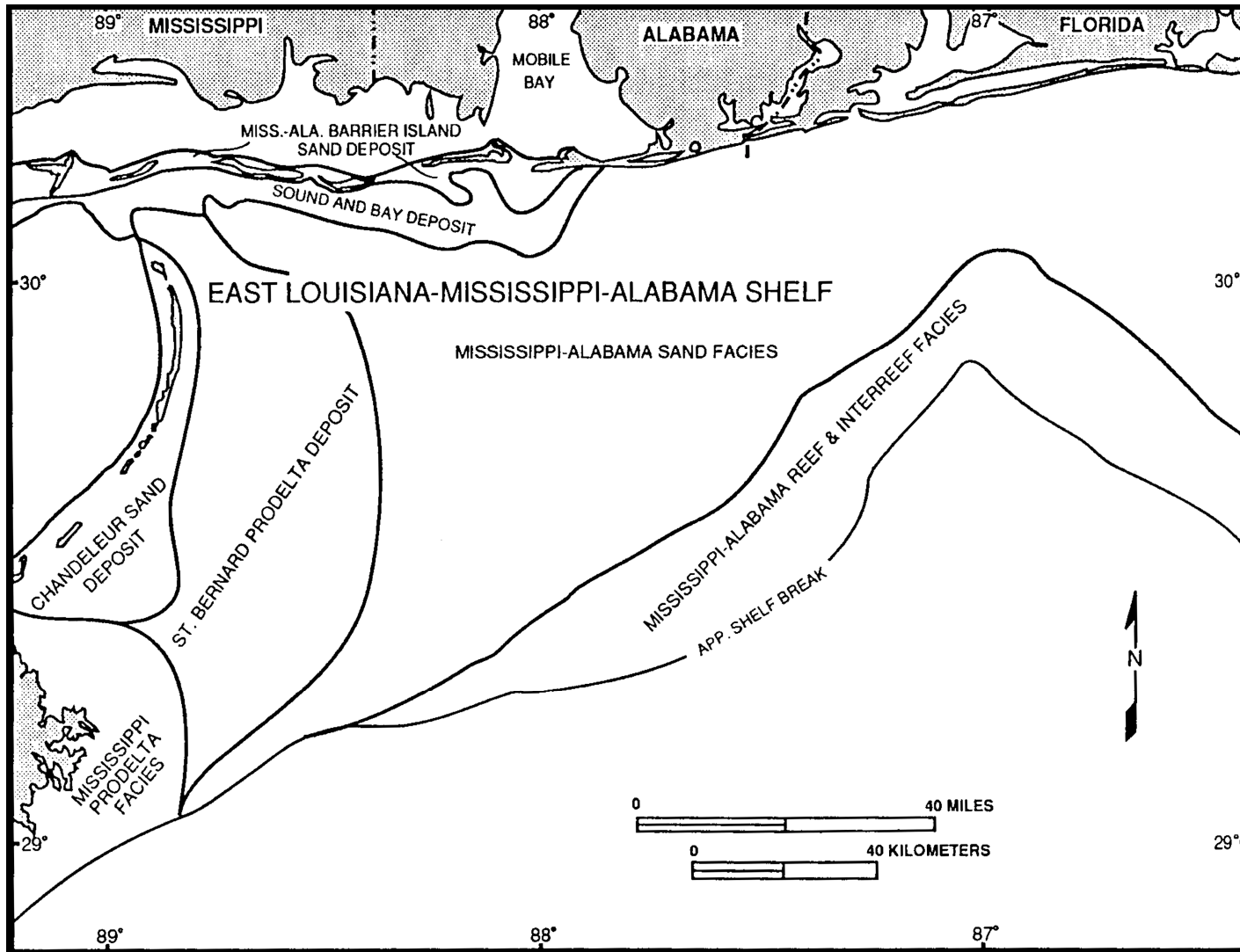


Figure 2-2. Sedimentary facies on the east Louisiana-Mississippi-Alabama shelf (after Ludwick, 1964; from Parker et al., 1997).

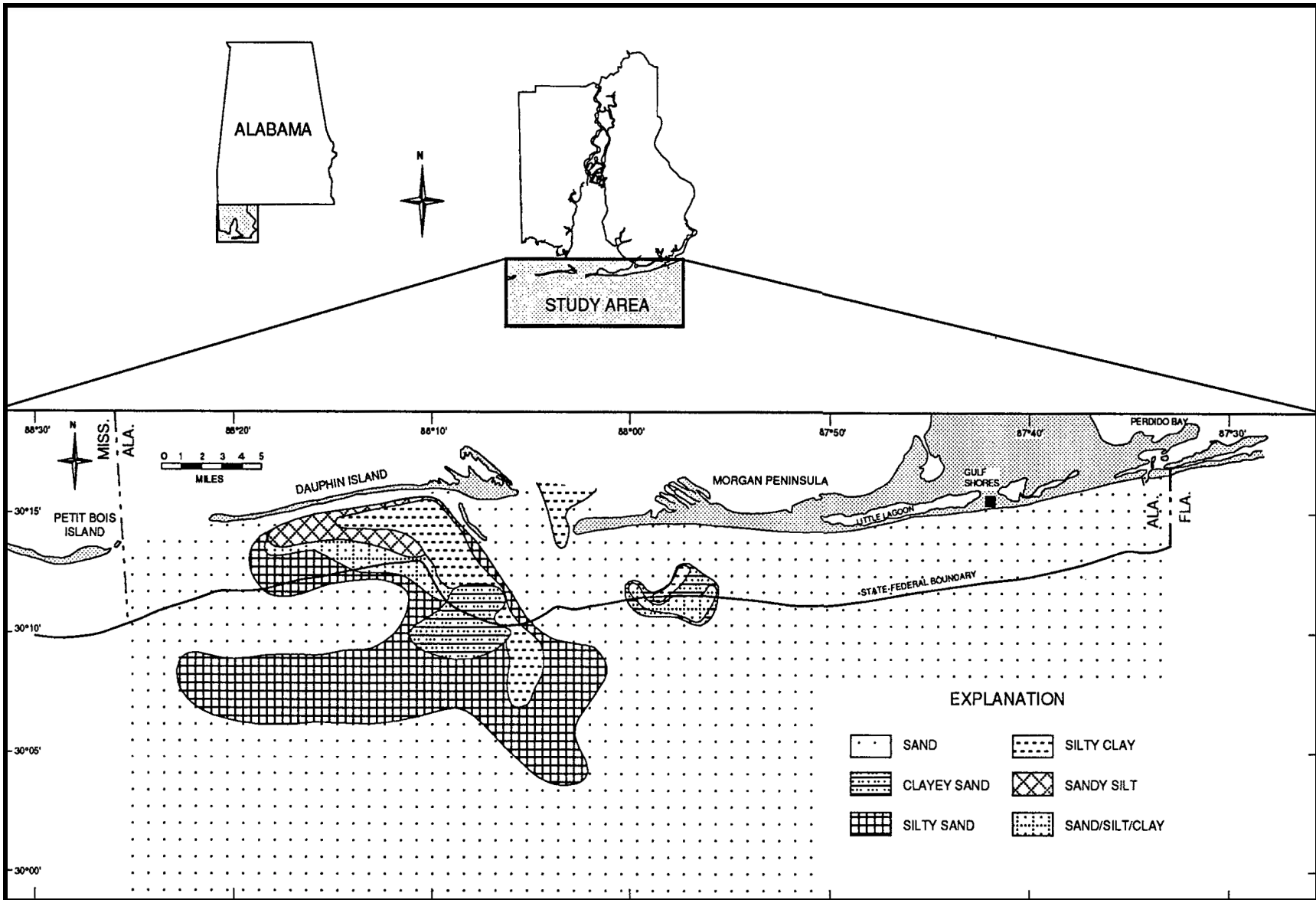


Figure 2-3. Surface sediment texture map compiled from previous sediment texture data in the study area (from U.S. Army Corps of Engineers, 1984).

### 2.1.1 Seabed Morphology

The Alabama continental shelf can be divided into two regions based on regional geomorphology and hydrology (Parker et al., 1997). The eastern shelf extends from the Alabama-Florida state boundary near Perdido Pass to Main Pass (see Figure 2-1). The western shelf extends from Main Pass to the Alabama-Mississippi state boundary at Petit Bois Pass. The large ebb-tidal delta at Main Pass is approximately 16 km wide, extends about 10 km offshore (Hummell, 1990), and separates the two regions (Figure 2-4). The subaerial portion of the ebb-tidal delta consists of Pelican Island, and occasionally Sand Island (an ephemeral shoal southeast of Pelican Island), both of which lie in the western shelf region.

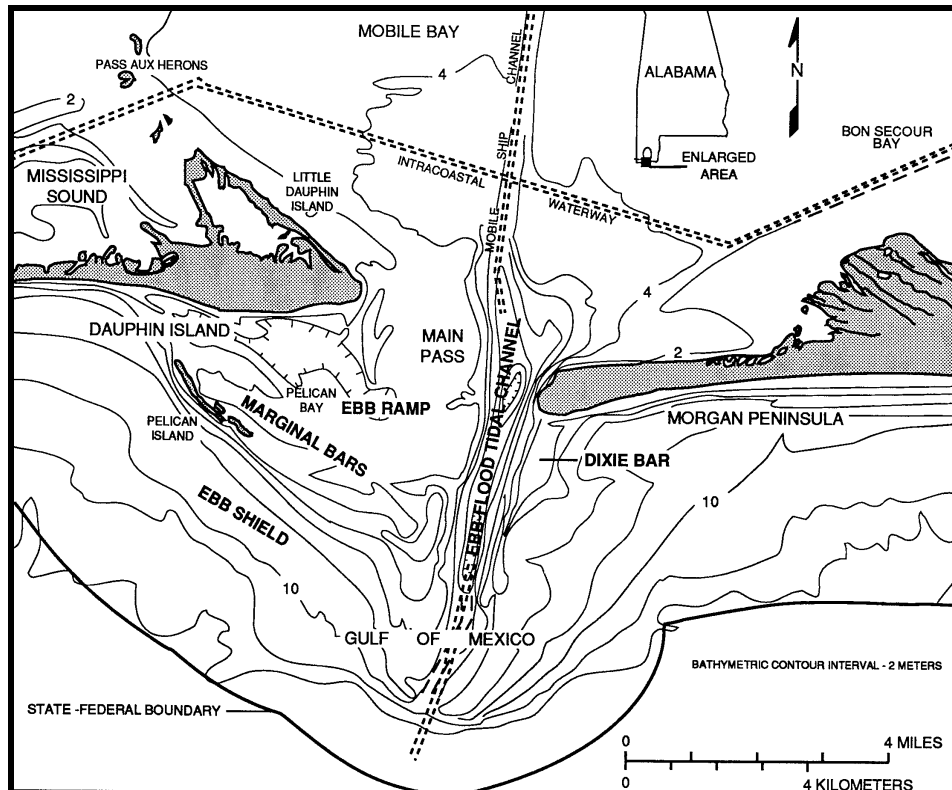


Figure 2-4. Geomorphology of the ebb-tidal delta seaward of Mobile Bay entrance (from Hummell, 1996).

The eastern portion of the study area is dominated by numerous shelf and shoreface sand ridges and swales that trend northwest to southeast (see Figure 1-1; McBride and Byrnes, 1995; Parker et al., 1997). The ridges are considered shoreface-attached and detached (Parker et al., 1992), and they form an oblique angle to the shoreline that opens to the east. Some of the ridges were identified by Parker et al. (1997) as pre-Holocene paleotopography draped with Holocene sand, rather than modern deposits resulting from marine hydrodynamic processes. The ridges average 6 km in length and range from 1 to 11 km long. Ridge widths range from 1 to 4 km with spacing between ridges varying between 1 and 7 km. Ridge side slopes average about  $1^\circ$ , and relief above the surrounding seafloor ranges from 1 to 5 m (McBride and Byrnes, 1995). The ridges recognized as shoreface-attached or shoreface-detached generally form opening angles with the east-west trending shoreline of  $30$  to  $60^\circ$ . Ridges formed as pre-Holocene paleohighs generally are oriented nearly perpendicular to the shoreline, reflecting their fluvial origin.

A large southwest-trending shoal, located approximately 16 km east of Mobile Point, is prominent in the eastern part of the study area (Figure 1-1). Although its origin is not known, evidence from Parker et al. (1997) suggests that it may be a drowned sand spit during the early Holocene as the western end of the Morgan Peninsula. Alternatively, it could be the remnants of a large ebb-tidal delta formed when an inlet was present through Morgan Peninsula. The sand shoal extends about 14 km offshore and has almost 6 m topographic relief, a potentially substantial sand resource target. The occurrence and character of ridges on the eastern shelf of the Alabama EEZ are described in detail by McBride and Byrnes (1995).

The upper shoreface of the eastern shelf region is much steeper than the western shelf region, and gradients range from 8 to 12 m/km (McBride and Byrnes, 1995; Parker et al., 1997). However, the eastern shelf surface from the shoreline to the shelf break averages approximately 1 m/km.

The western half of the study area, from Main Pass west to Petit Bois Pass, has relatively few geomorphic features compared with the eastern part of the study area. Shoals associated with deposition near the entrances to Main Pass and Petit Bois Pass are prominent; however, the shelf seaward of Dauphin Island is smooth and concave. The marginal shoals of the ebb-tidal delta are quite shallow to the west of Main Pass (see Figure 2-4; Pelican Island is subaerial and Sand Island is intermittently subaerial). Hummell (1990) discusses the importance of these features to sediment transport patterns along the shoreline of eastern Dauphin Island. Overall, the shelf surface in the western half of the study area slopes at about 1.5 m/km.

### **2.1.2 Surface Sediments**

Surface sediments throughout the study area are composed of two primary facies. The Mississippi-Alabama Sand Facies dominates the eastern portion of the study area (Figure 2-2; Ludwick, 1964). It consists predominantly of well-sorted clean quartz sand, with shelly sands occurring locally. McBride and Byrnes (1995) characterize samples taken from this area as >90% sand and <3% mud. Median grain size ranges from 0.14 to 0.46 mm or fine-to-medium sand. Ludwick (1964) characterized the sand in this area as 93% terrigenous and 7% carbonate, with a median grain diameter of 0.18 mm. Doyle and Sparks (1980) found the same general trend and named the facies the Mississippi-Alabama-Florida (MAFLA) sand sheet.

Along the coast between Little Lagoon and Dauphin Island is the Nearshore Fine-Grained Facies defined by Ludwick (1964) (Figure 2-2). This facies is similar to that found in Mobile Bay and Mississippi Sound (Chermock et al., 1974). Sand, muddy sand, sandy mud, and mud occur in water depths less than 20 m in a zone about 11 km wide. Near the Mobile Bay entrance, the zone extends seaward to encompass the ebb-tidal delta of Main Pass, before pinching out to the east near Little Lagoon.

Parker et al. (1997) collected 59 bottom sediment samples throughout the study area to characterize surface sediment distribution (Figure 2-5). Eight sediment facies were identified in the Alabama EEZ, two of which (graded shelly sand and echinoid sand facies) were found in 37 of 59 locations. The third most common surface sediment facies was orthoquartzite. Together, the three most common sand facies are represented in 81% of the samples (Figure 2-6), most of which are found in the eastern part of the study area, seaward of the Morgan Peninsula and Gulf Shores. Another large-scale pattern that is apparent is the presence of a muddier facies near the Main Pass of Mobile Bay. Sediment from Mobile Bay contributes fine-grained material to the shelf, particularly during times of heavy flow. Much of the fine-grained sediment is carried as a sediment plume offshore and to the west of Main Pass, due primarily to dominant wind, wave, and tidal current dynamics between the Bay and the Gulf (Wiseman et al., 1988; Stumpf and Gelfenbaum, 1990).

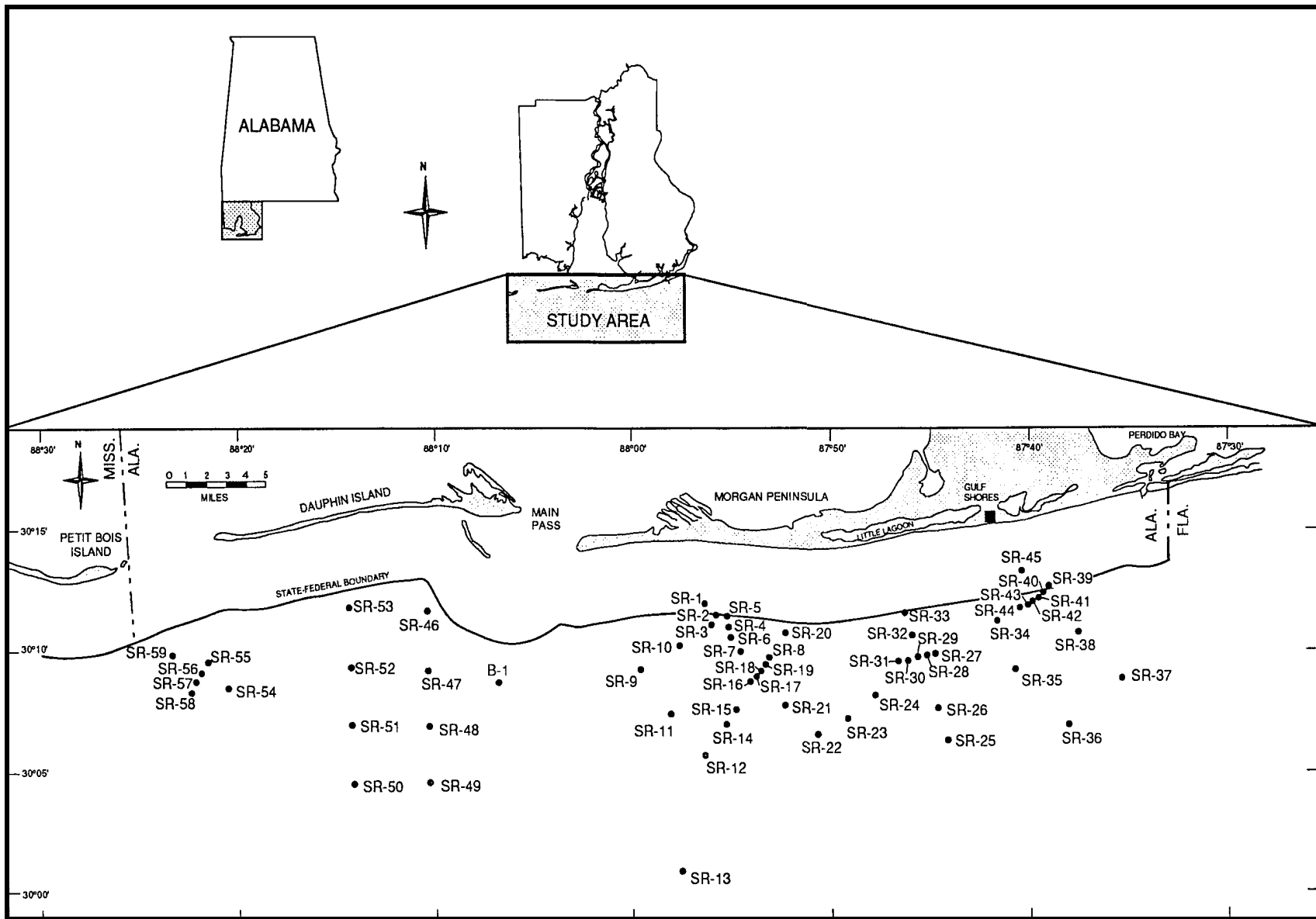


Figure 2-5. Vibracore, boring, and bottom grab locations in the Alabama EEZ study area (from Parker et al., 1997).

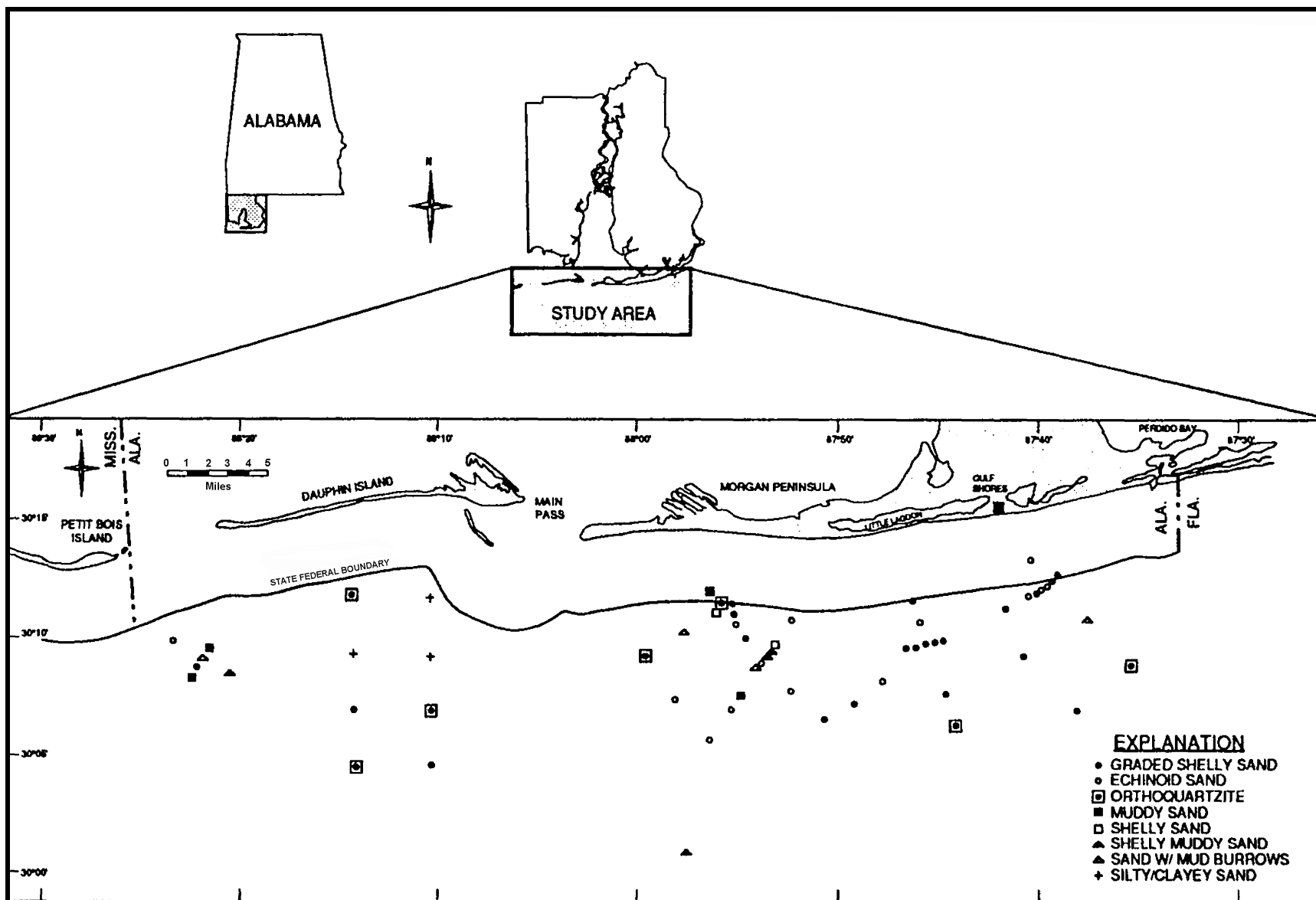


Figure 2-6. Surface facies distribution in the Alabama EEZ study area (from Parker et al., 1997).

Parker et al. (1993, 1997) illustrate the distribution of fine-grained sediment in the western portion of the study area based on limited samples (Figure 2-7), whereas Hummell and Smith (1995, 1996) use U.S. Army Corps of Engineers data to summarize the distribution of bottom sediment seaward of and adjacent to Main Pass and Dauphin Island (U.S. Army Corps of Engineers, 1984). Figure 2-8 illustrates the distribution of bottom sediment in the western portion of the study area where the influence of fine-grained sediment from Mobile Bay is recognized as areas of silty clay, silty sand, and sandy silt on an otherwise sandy shelf surface. Although the dominant surface sediment distribution in the vicinity of Area 4 is shown as sand/silt/clay to silty sand, Hummell and Smith (1996) collected additional surface sediment and vibracore samples to augment Parker et al. (1997) and U.S. Army Corps of Engineers (1984), and they identified a fine-to-medium sand deposit in the southeast quadrant of the area (Figure 2-9).

### **2.1.3 Subsurface Deposits**

The Holocene geologic framework of the Alabama EEZ has been documented by Parker et al. (1993, 1997), Hummell (1996), and Hummell and Smith (1996). Parker et al. (1997) obtained 59 vibracores from throughout the study area to document the history of sediment deposition on the continental shelf within the study area, with particular emphasis on identified potential sand resource areas. Based on core data analysis, five primary Holocene lithofacies were identified for the study area. They include a clean sand lithofacies, a graded shelly sand lithofacies, a dirty sand lithofacies, a biogenic sediment lithofacies, and a muddy sediment lithofacies. The sedimentologic characteristics of these facies are detailed in Parker et al. (1997; p. 33-71). As a summary, Figure 2-10 provides a generalized composite stratigraphic sequence of facies in the study area. Overall, much of the inner shelf of the Alabama EEZ is composed of a shelf sand sheet depositional environment formed during Holocene transgression. It is a deposit that grades into other sand depositional environments that have been reworked by high-energy storm events, as well as non-storm currents and bioturbation (Parker et al., 1997). On the eastern shelf region, numerous sand ridges have formed on top of the sand sheet in response to local and regional hydrodynamics (Swift and Niedoroda, 1985; McBride, 1997).

The western portion of the study area contains greater variability in depositional characteristics due to the influence of fine-grained sediment from Mobile Bay. The muddy sand lithofacies is common on the shelf west of Main Pass and seaward of Dauphin Island. Hummell and Smith (1996) used the classification criteria of Parker et al. (1993, 1997) to describe the lithology of deposits in Sand Resource Area 4. Hummell and Smith (1995, 1996) used 28 additional vibracores and seven Exxon foundation borings to determine the best location for a sand resource target in Area 4. Overall, sand deposits on the western shelf were finer-grained relative to shelf deposits to the east.

### **2.1.4 Sand Resource Areas**

The resource potential of offshore sand deposits within the study area was documented using geologic data from Parker et al. (1993, 1997) and Hummell and Smith (1995, 1996). In addition, sand volume estimates for Resource Areas 1, 2, and 3 have been updated by the GSA (Hummell, 1999) using newly acquired vibracores. A comparison of sediment characteristics (size and color) from each sand resource area with beach sediment size from eroding Gulf shorelines was completed by Parker et al. (1997) to document resource compatibility. Based on shoreline change trends, Parker et al. (1997) and Hummell and Smith (1996) documented three shoreline zones within the study area as eroding shoreline segments. They included eastern Dauphin Island, the Gulf shoreline south of Little Lagoon, and the beach downdrift of Perdido Pass.

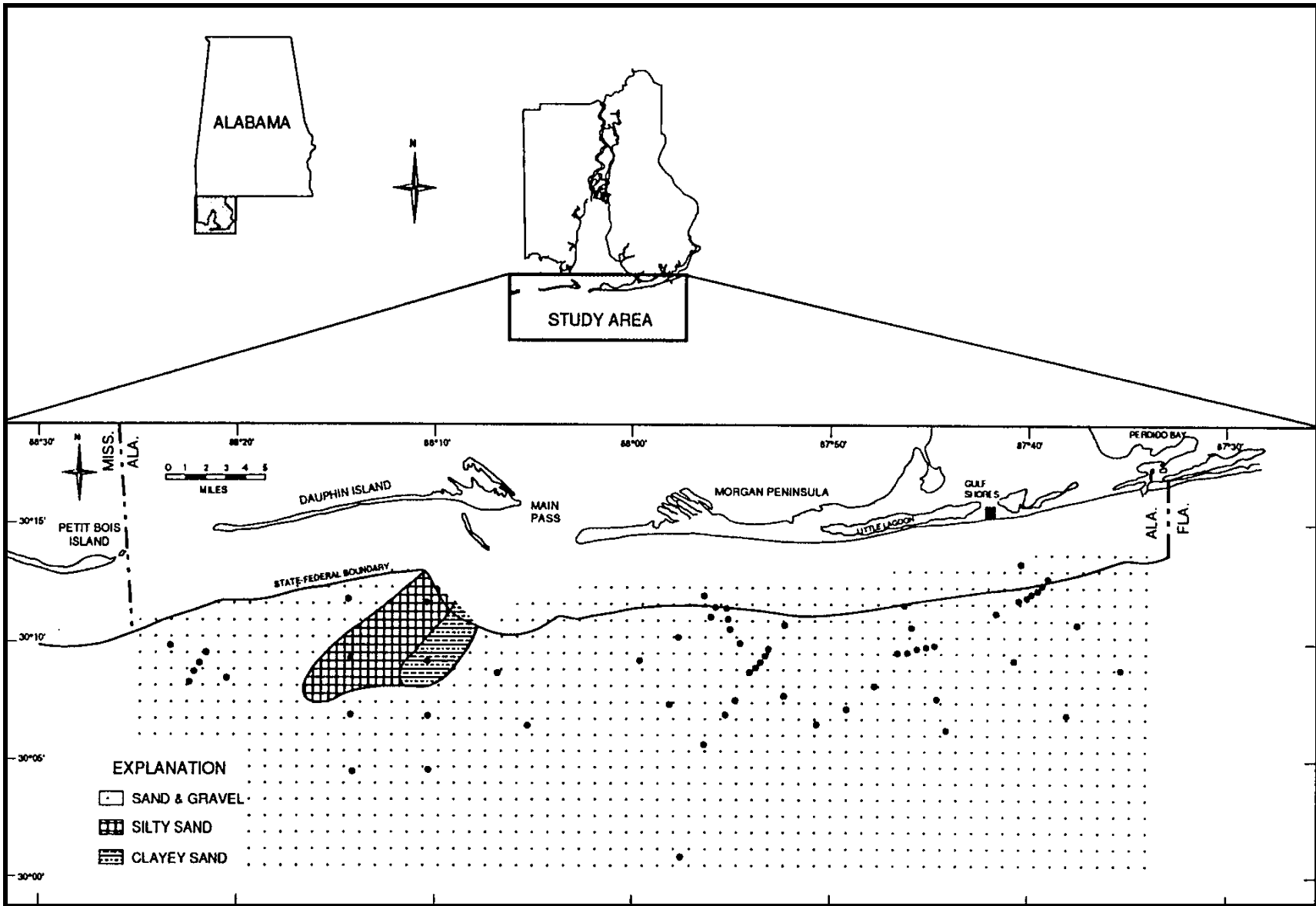


Figure 2-7. Surficial sediment textures in the Alabama EEZ study area (from Parker et al., 1997).

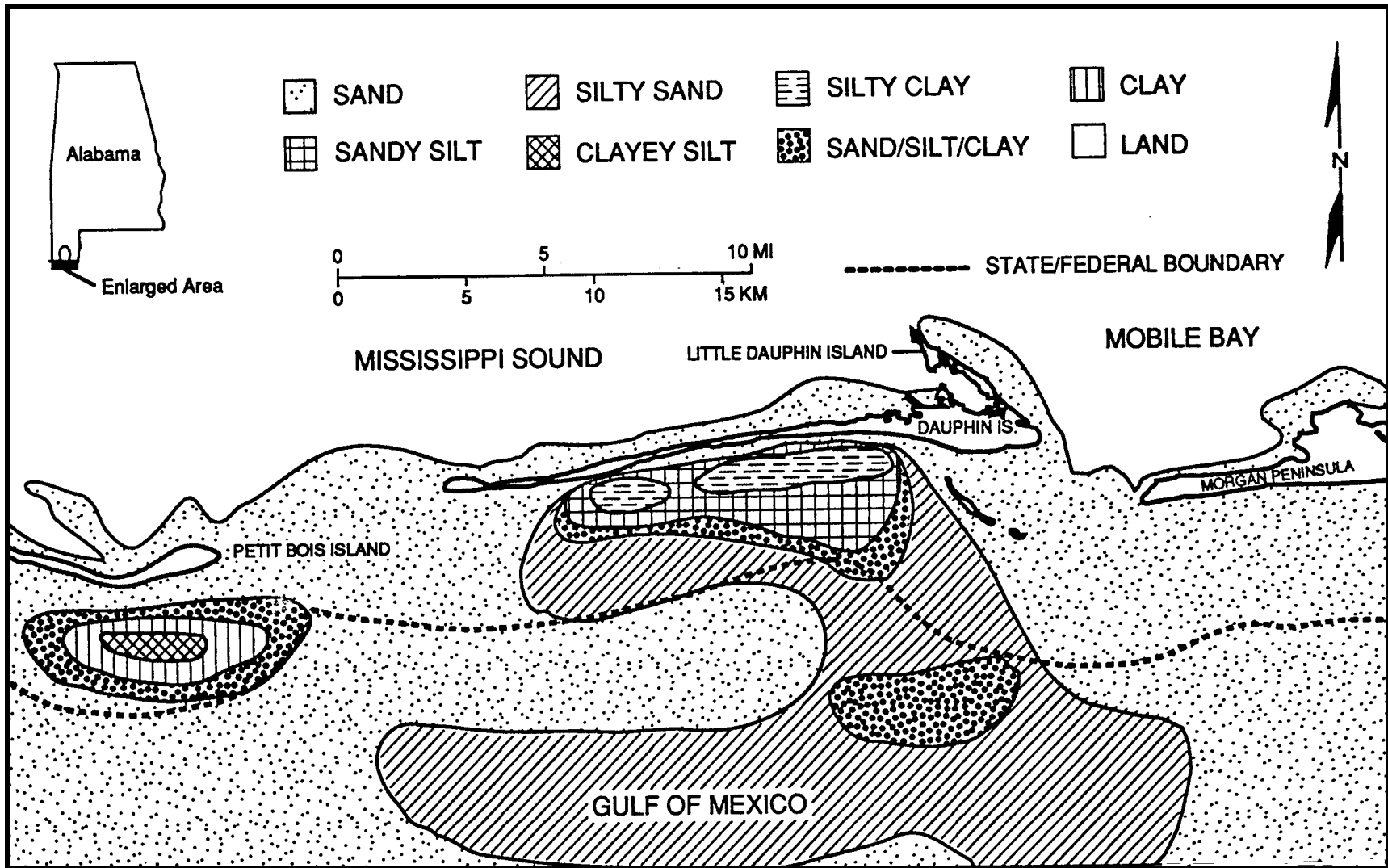


Figure 2-8. Surface sediment distribution in the west Alabama inner continental shelf (from Hummell, 1996).

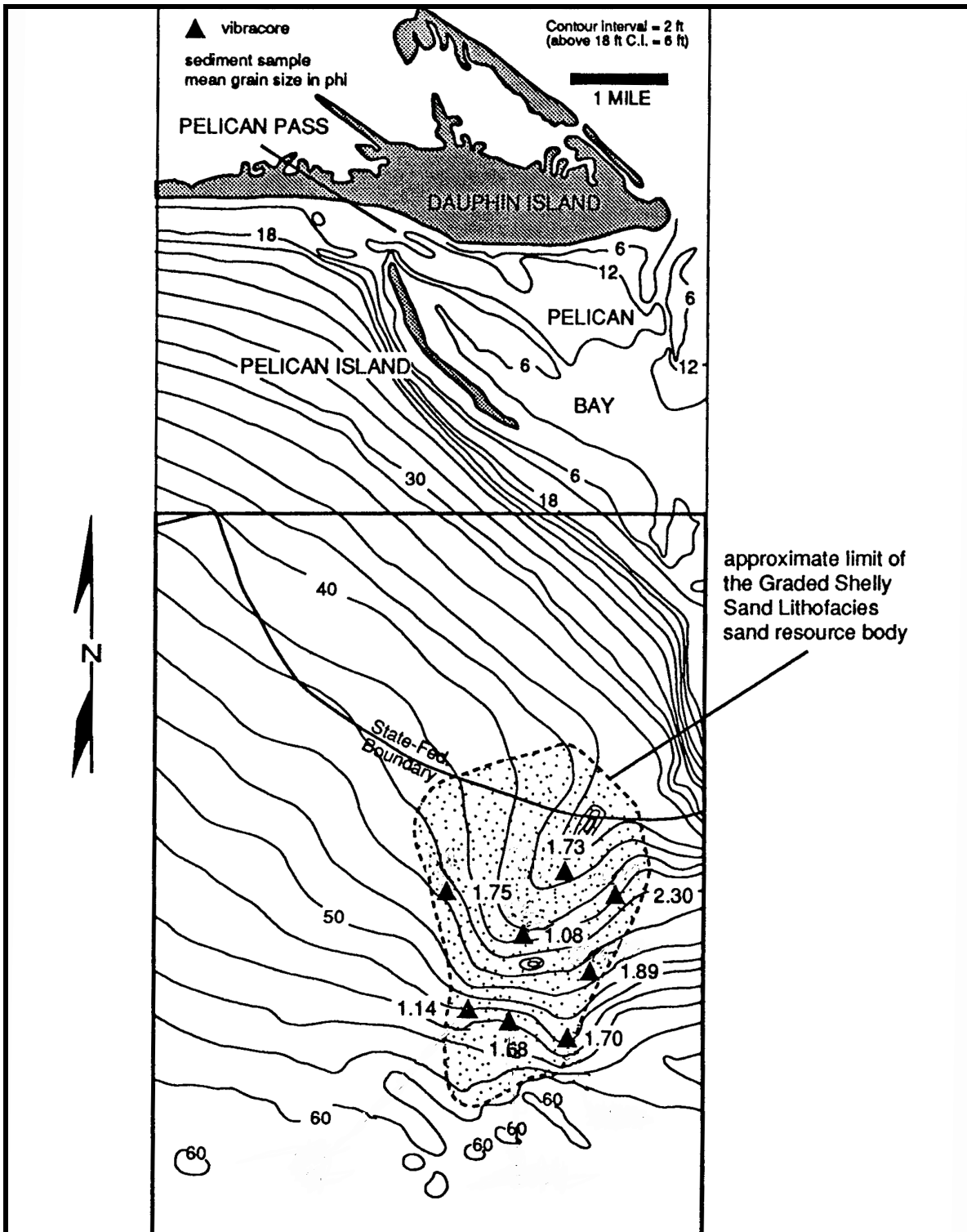


Figure 2-9. Map of the mean grain size of Graded Shelly Sand Lithofacies vibracore sediment samples 0.1 m below the sediment-water interface (from Hummell and Smith, 1996).

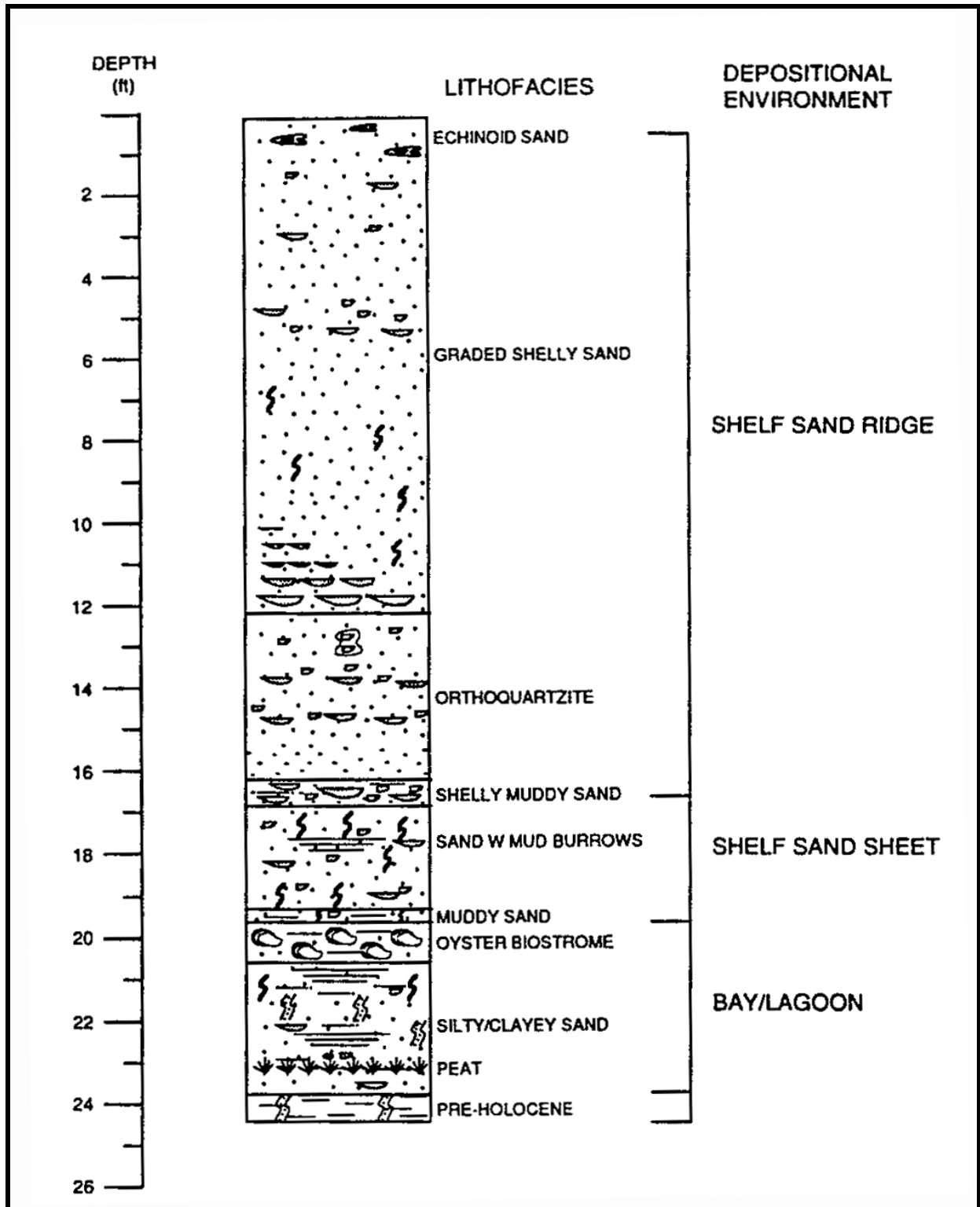


Figure 2-10. Generalized stratigraphic sequence of the Alabama EEZ study area (from Parker et al., 1997).

Sand Resource Area 1 is located on the eastern shelf south of Gulf Shores (Figures 1-1 and 2-11). The sand resource area in Federal waters encompasses approximately 4,200 ha (16 mi<sup>2</sup>) and extends 5.5 to 12 km offshore. Water depths range from about 8.5 m (28 ft) MWL on the shallowest sand ridge to 14.5 m (48 ft) MWL at the offshore boundary. Maximum relief associated with sand ridges in the resource area is about 3 m. Based on vibracores and sediment samples collected by Parker et al. (1997), the entire resource area consists of medium- to fine-grained sand, with an average grain size of 0.25 mm. Sediment samples from vibracores contain about 97% sand. Sand deposit thickness ranges from 1 to 4.25 m (3 to 14 ft), with thickest sequences occurring over the ridges (Figure 2-12). Hummell (1999) estimates that the volume of sand suitable for beach replenishment in Area 1 is approximately 130 MCM. Sediment overfill ratios were calculated for each of the shoreline retreat zones based on sand resource area sediment characteristics versus beach sediment characteristics. For Perdido Pass, Parker et al. (1997) estimate that about 210,000 m<sup>3</sup> of beach fill would be required from Area 1 to restore the beach back to its original condition in 1955 (1.75 overfill ratio). For the beach south of Little Lagoon, a sand volume of 160,000 m<sup>3</sup> would be required (4.0 overfill ratio) to restore the beach to 1955 conditions.

Sand Resource Area 2 is located south of Little Lagoon Pass, extending from about 5.5 to 15.5 km offshore. The sand resource area encompasses approximately 7,400 ha (28.5 mi<sup>2</sup>), and water depths range from about 10 to 18 m (33 to 60 ft; Figure 2-13) MWL. Parker et al. (1997) identify prominent sand ridges in the sand resource area that have relief ranging from 2 to 3.7 m (6 to 12 ft). Although sand quality is similar to that of Resource Area 1, sand deposits associated with shoals are noticeably thinner. Average mean grain size of the sand deposit is 0.27 mm, and sand content averages about 97%. Average sand thickness in the northern portion of the sand resource area is about 2 m (Figure 2-14), but sand thickness increases substantially in an offshore direction. Overall, Sand Resource Area 2 contains about 190 MCM of beach-quality sand (Hummell, 1999). The overfill ratios for beach replenishment sites at Perdido Pass and Little Lagoon are very similar to those identified for Area 1 (1.7 and 3.25, respectively). As such, the quantity of sand required to replenish these beaches would be about 155,000 m<sup>3</sup> and 100,000 m<sup>3</sup>, respectively.

Sand Resource Area 3 is located offshore the western Morgan Peninsula, approximately 13 km east of Main Pass (Figures 1-1 and 2-15). It extends from the State-Federal boundary (about 5 km from the shoreline) 7 km seaward to around the 18-m depth contour and includes about 6,800 ha (26 mi<sup>2</sup>) of seafloor (Parker et al., 1997). Water depths range from 8.5 to 18 m (28 to 60 ft) MWL, and a large northeast-southwest oriented shoal dominates seafloor morphology. This feature has almost 6 m of relief, and several individual sand ridges (1 to 2.5 m relief) are superimposed on the shoal and oriented in a direction perpendicular to its leading edge. Similar to Areas 1 and 2, sediment samples document an extensive medium- to fine-grained sand deposit. Sand content averages 96% and average mean grain size is 0.24 mm. According to Parker et al. (1997), average sand thickness in the area was difficult to determine because most cores did not penetrate the entire Holocene sequence. However, average sand thickness is greater than 3 m and may be as thick as 5 m in certain areas. Greatest sand thickness is associated with the main shoal and sand ridges, where sand is typically 3.5 to 4.5 m (12 to 15 ft) thick (Table 2-1; Figure 2-16). Based on core data from Parker et al. (1997) and Hummell (1999), Area 3 has the potential to provide approximately 245 MCM of beach-quality sand for beach replenishment. Calculated beach overfill ratios were similar but slightly greater than those identified for Area 2. As such, the volume of sand needed to restore the eroding shoreline downdrift of Perdido Pass to its 1995 position is about 175,000 m<sup>3</sup>. For the shoreline erosion area downdrift of Little Lagoon Pass, the sand volume requirements would be about 110,000 m<sup>3</sup>.

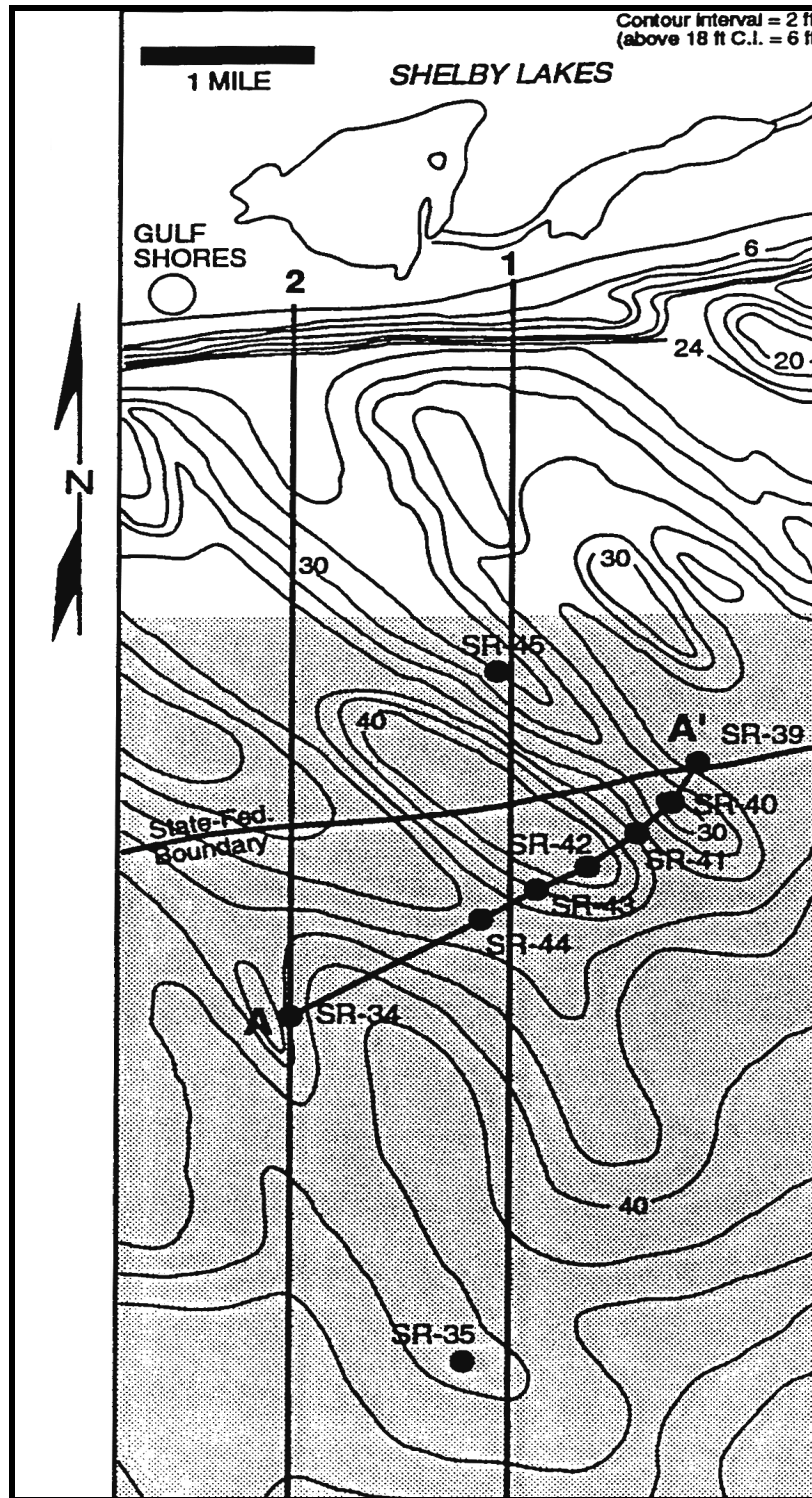


Figure 2-11. Map of the Sand Resource Area 1 (shaded area) showing location of cross section (A-A' and bathymetric profiles (1 and 2) (from Parker et al., 1997).

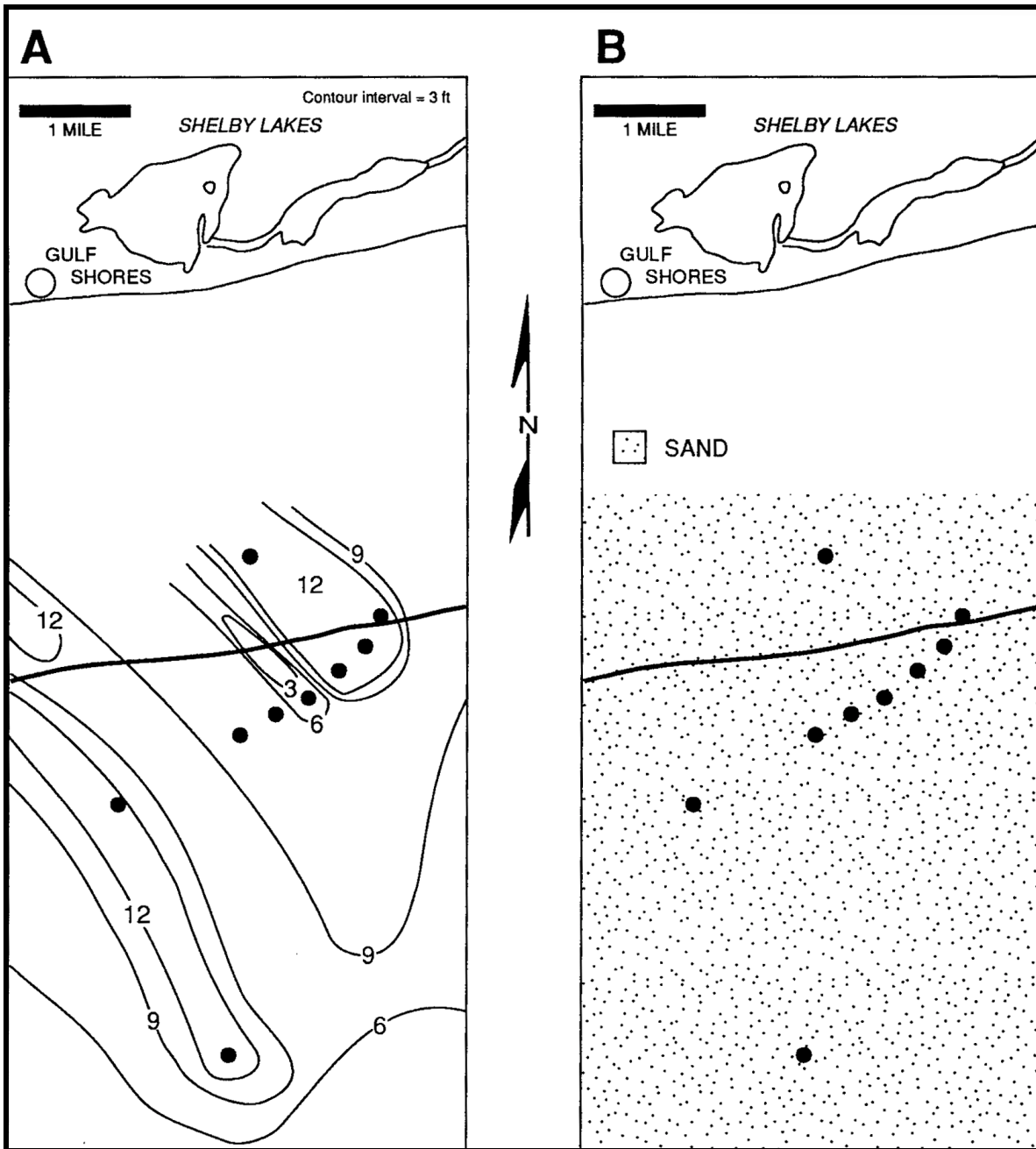


Figure 2-12. Sand isopach (A) and surface sediment texture (B) maps for Sand Resource Area 1 (from Parker et al., 1997).



Figure 2-13. Map of Sand Resource Area 2 (shaded area) showing location of cross sections (A-A') and (B-B') and bathymetric profiles (1 and 2) (from Parker et al., 1997).

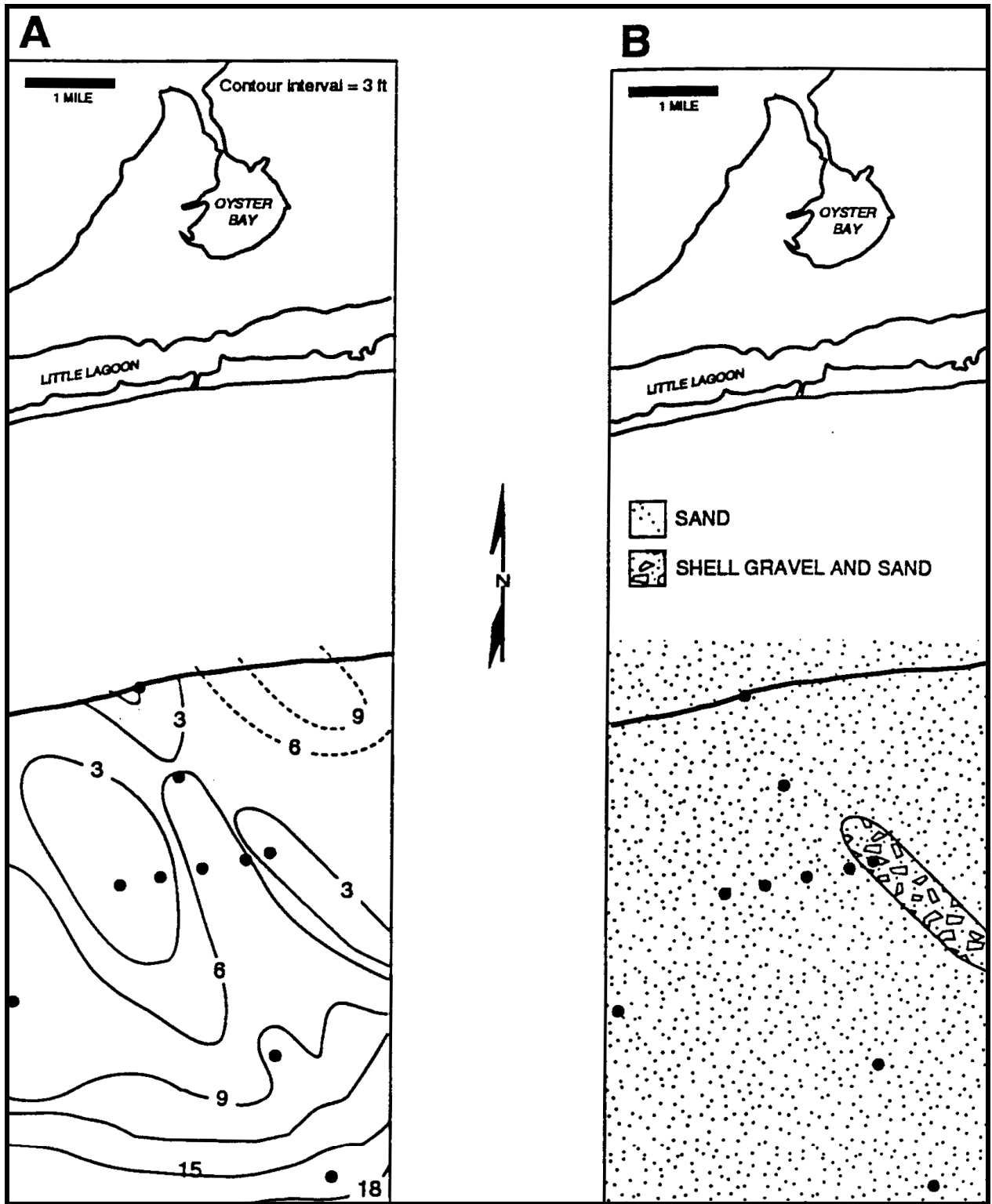


Figure 2-14. Sand isopach (A) and surface sediment type (B) for Sand Resource Area 2 (from Parker et al., 1997).

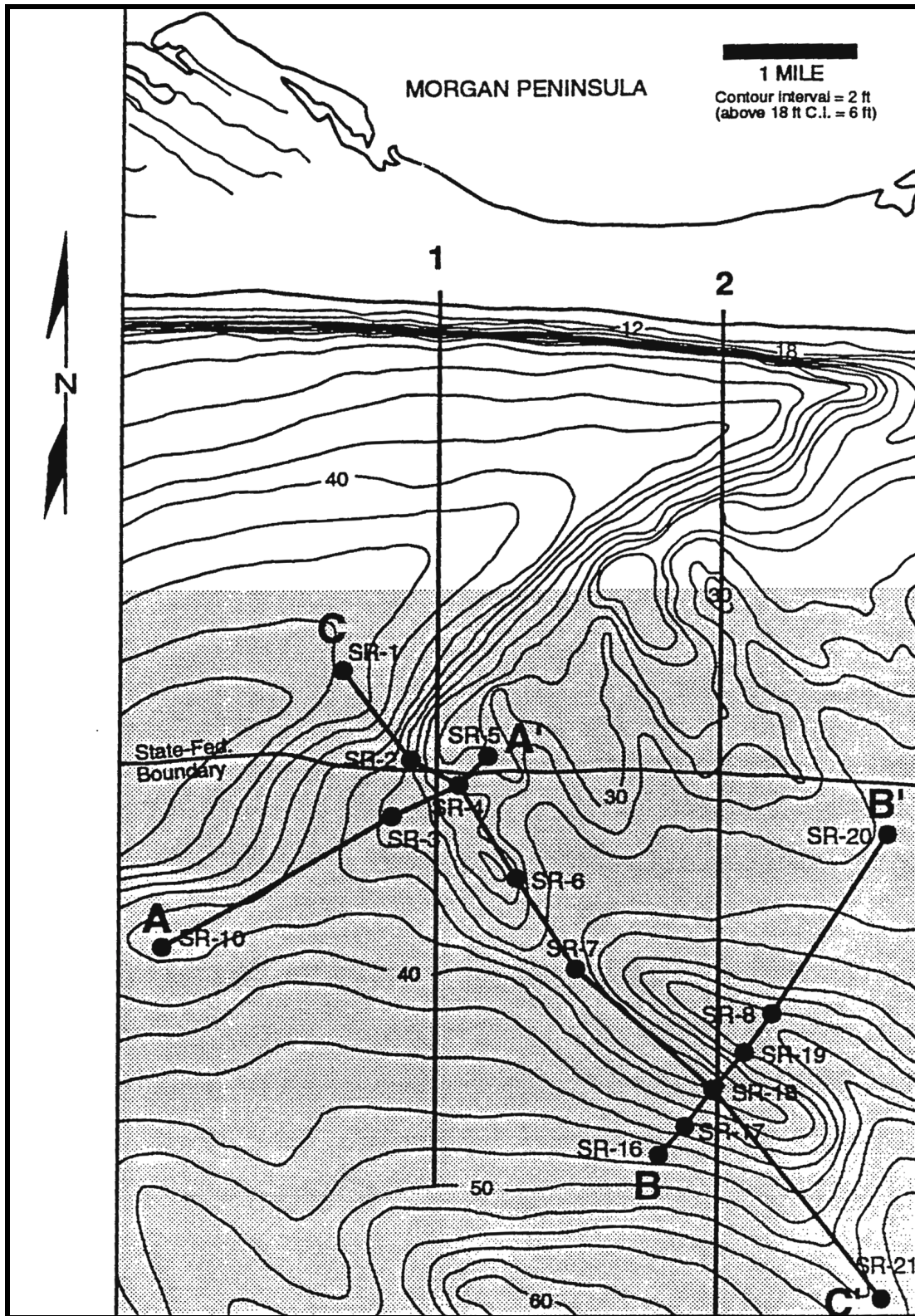


Figure 2-15. Map of Sand Resource Area 3 (shaded area) showing location of cross sections (A-A', B-B', and C-C') and bathymetric profiles (1 and 2) (from Parker et al., 1997).

Sand Resource Area	Distance from Shore (km)	Water Depth (m)	Seafloor Area (ha)	Mean Grain Size (mm)	Sand Content (%)	Average Sand Thickness (m)	Sand Volume (MCM)
1	5.5 to 12	8.5 to 14.5	4,200	0.25	97	1 to 4.25	130
2	5.5 to 15.5	10 to 18	7,400	0.27	97	2	190
3	5 to 7	8.5 to 18	6,800	0.24	96	3 to 5	245
4	8.5 to 16	18	400 *	0.35 *	96 *	3.0 *	12 *
5	6.5 to 12	12 to 18	3,300	0.25	90	2	60

\* - Characteristics for GSA shelly sand resource site within Resource Area 4 (see Figure 2-9).

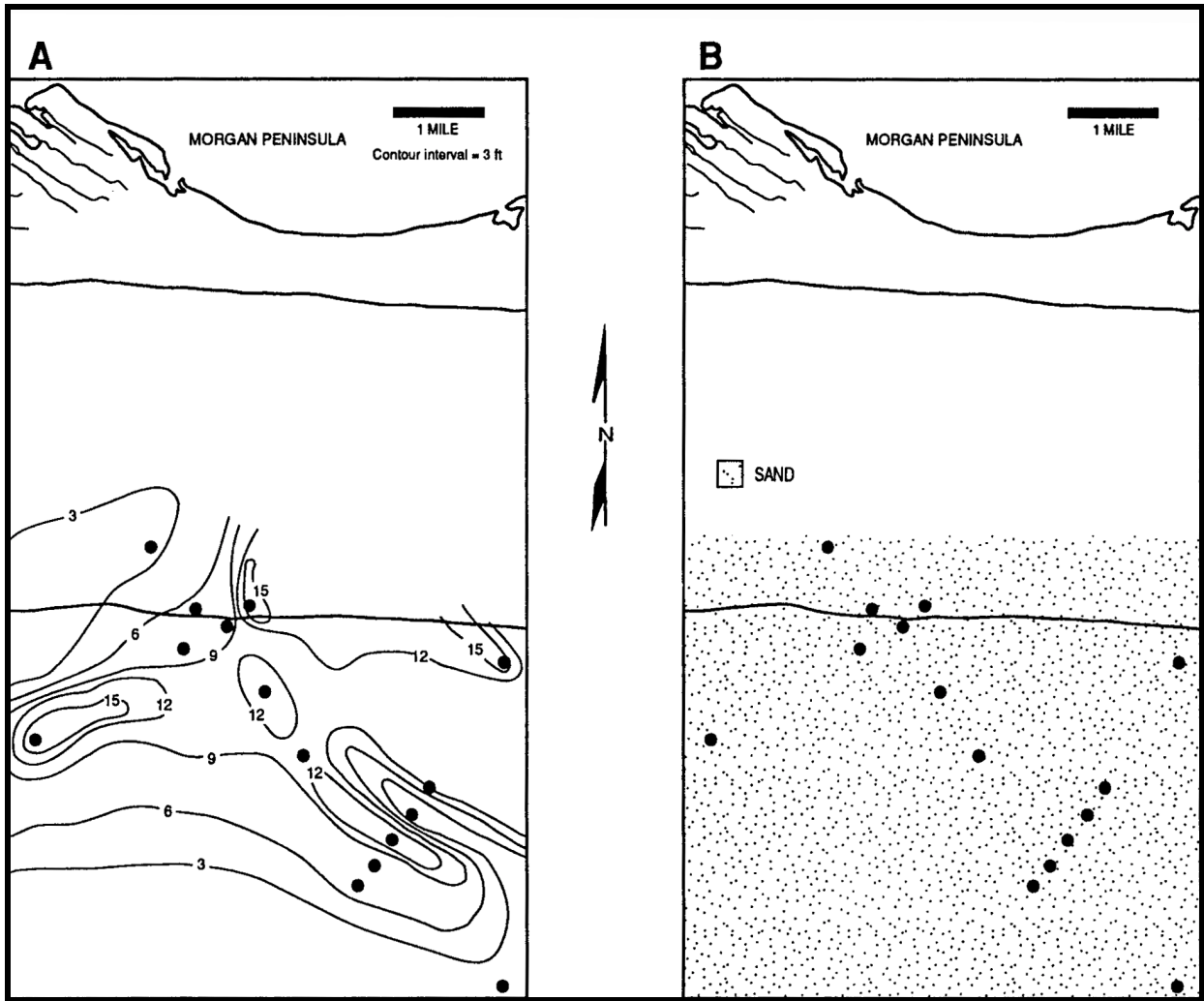


Figure 2-16. Sand isopach (A) and surface sediment texture (B) maps for Sand Resource Area 3 (from Parker et al., 1997).

West of Main Pass, Sand Resource Area 4 is located approximately 8.5 km south of eastern Dauphin Island adjacent to the western margin of the ebb-tidal delta for Main Pass (Figures 1-1 and 2-17). The seaward extent of Resource Area 4 is about 16 km offshore in 18-m (60-ft) MWL water depth, for a total seafloor area of about 7,700 ha (30 mi<sup>2</sup>). Little relief exists in this sand resource area except for a small rise in elevation in the southeastern quadrant. Although Parker et al. (1993, 1997) completed the original data collection and analysis for this area, Hummell and Smith (1995, 1996) augmented these data with additional vibracores and foundation borings. Unlike eastern shelf sand resource areas, sediments in Sand Resource Area 4 consist of mud and muddy sand ebb-tidal delta and shelf deposits, and shelf sand ridge sands (Hummell and Smith, 1996). Although all of Resource Area 4 is influenced by fine-grained deposition from Mobile Bay, Hummell and Smith (1995, 1996) were able to delineate a sand deposit in the northeast corner of the Federal sand resource area. Figure 2-18 illustrates surface sediment characteristics in Area 4; the Graded Shelly Sand lithofacies cluster of points denotes the location of the resource site. Average mean grain size for this area is about 0.35 mm, and sand thickness averages about 3.0 m. The sand deposit is in 12- to 16-m (39- to 53-ft) water depth, it increases in thickness to the south, and it grades into fine-grained facies on all sides (Hummell and Smith, 1996). Hummell and Smith estimated that this sand resource body contains approximately 12 MCM of compatible beach sand (about 97% sand), more than enough to suit the needs of eastern Dauphin Island (1.8 MCM; Table 2-1).

Area 5 is the westernmost sand resource site in the study area, occurring seaward of the western end of Dauphin Island in approximately 12- to 18-m (39- to 60-ft) MWL water depth (Figures 1-1 and 2-19). The sand resource site extends from the State-Federal boundary (about 6.5 km offshore) to approximately 12 km offshore Petit Bois Pass. The area of coverage is about 3,300 ha (12.5 mi<sup>2</sup>), the smallest of any of the five sand resource areas. Seafloor topography in Area 5 is characterized by one large ridge with a relief of about 3 m (Parker et al., 1997). Surface sediment samples and vibracores identified a medium-to-fine sand resource area with an average mean grain size of 0.25 mm. Average sand content was about 90% (Parker et al., 1997). Sand thickness averages approximately 2 m (7 ft), but the exact thickness of the sand deposit was difficult to determine because none of the cores penetrated pre-Holocene sediment (Figure 2-20; Table 2-1; Parker et al., 1997). The thickness of sand increases offshore but remains fairly constant over the ridge. Parker et al. (1997) estimate that 60 MCM of sand is available for beach replenishment. However, smaller mean grain size relative to beach sand on eastern Dauphin Island results in a larger volume of fill needed to mitigate erosion trends since 1955. Parker et al. (1997) estimate that 2.3 MCM are required to restore Dauphin Island.

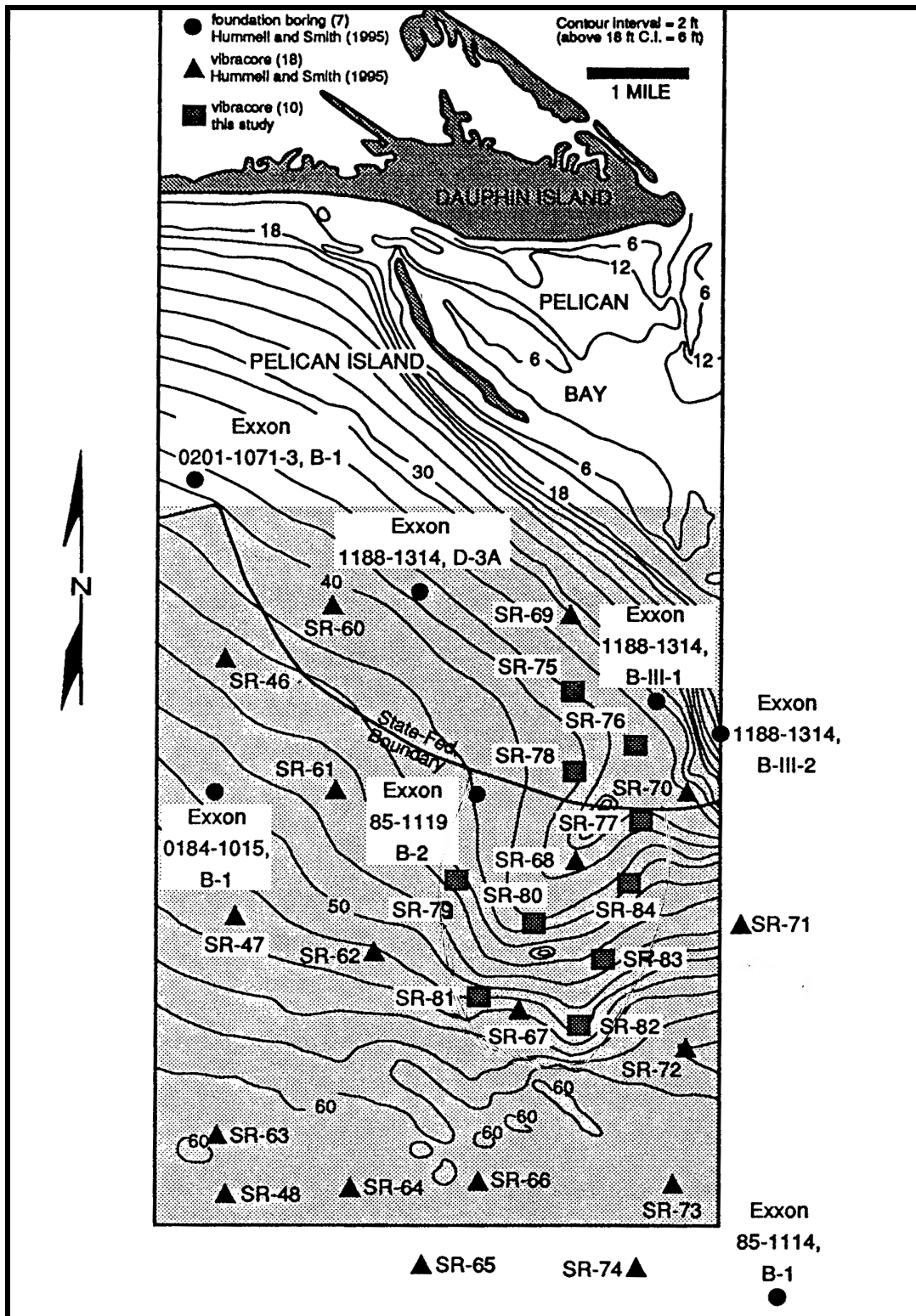


Figure 2-17. Map of Sand Resource Area 4 showing location of vibracores and foundation borings (from Hummell and Smith, 1996).

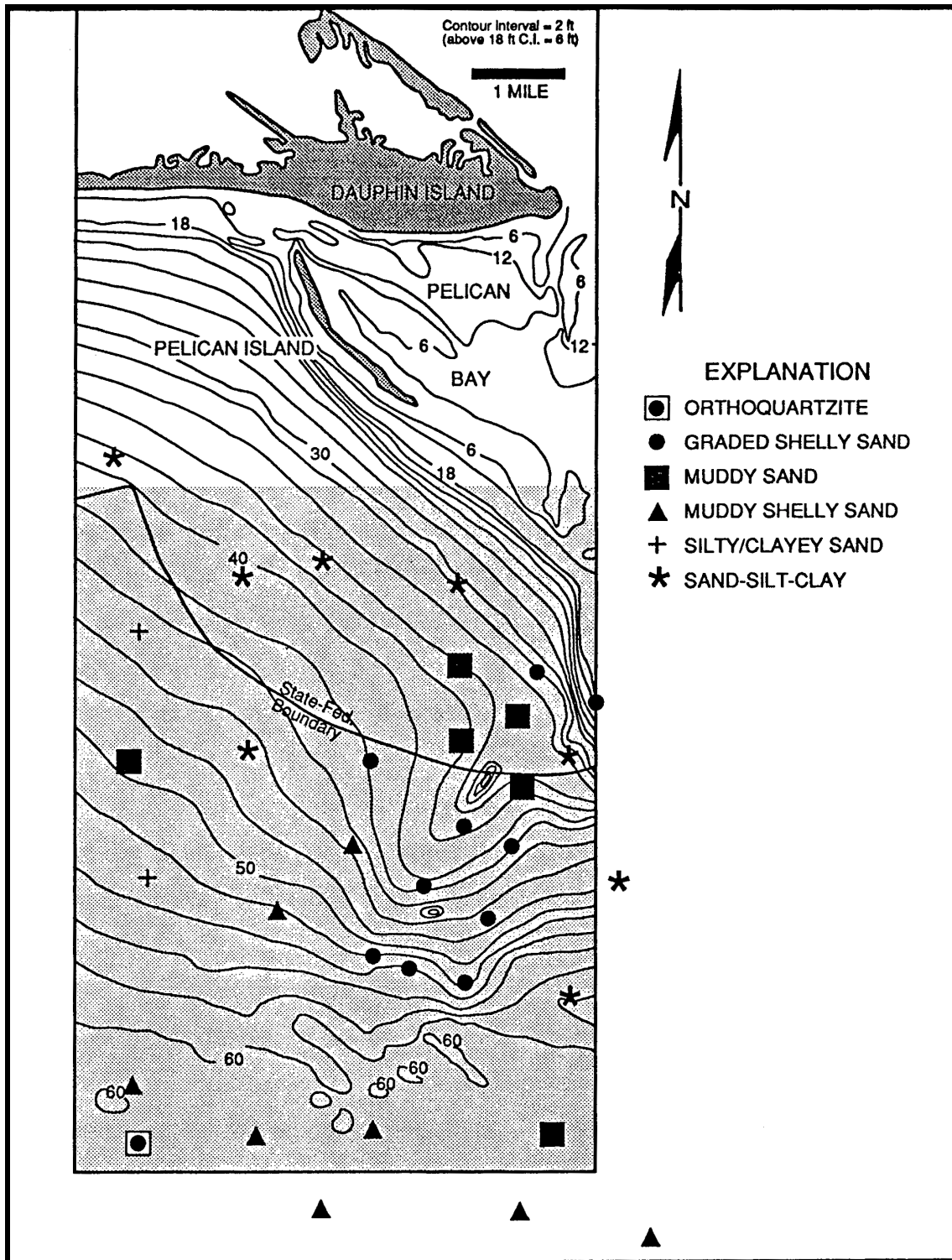


Figure 2-18. Surface facies distribution in Sand Resource Area 4 (from Hummell and Smith, 1996).

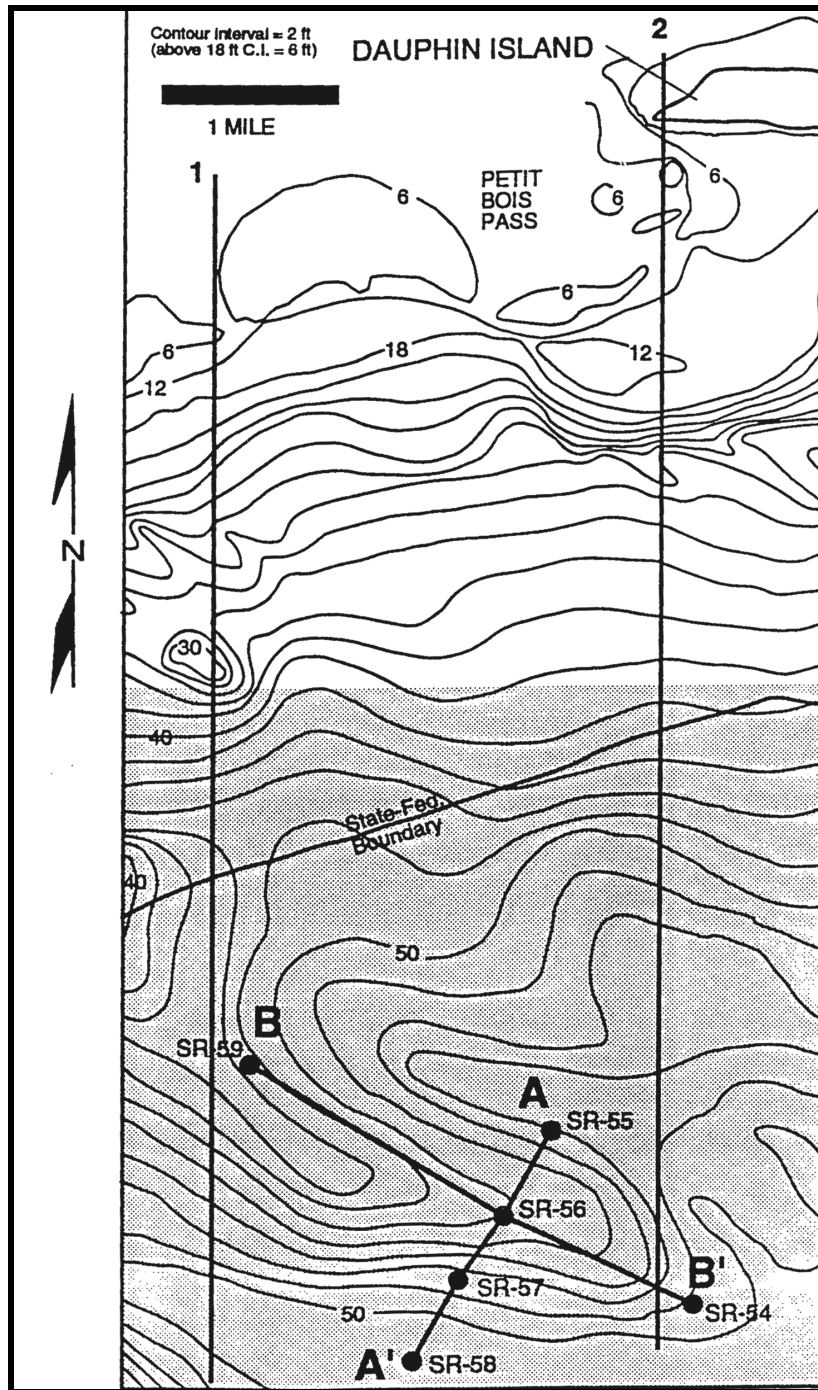


Figure 2-19. Map of Sand Resource Area 5 (shaded area) showing location of cross sections (A-A' and B-B') and bathymetric profiles (1 and 2) (from Parker et al., 1997).

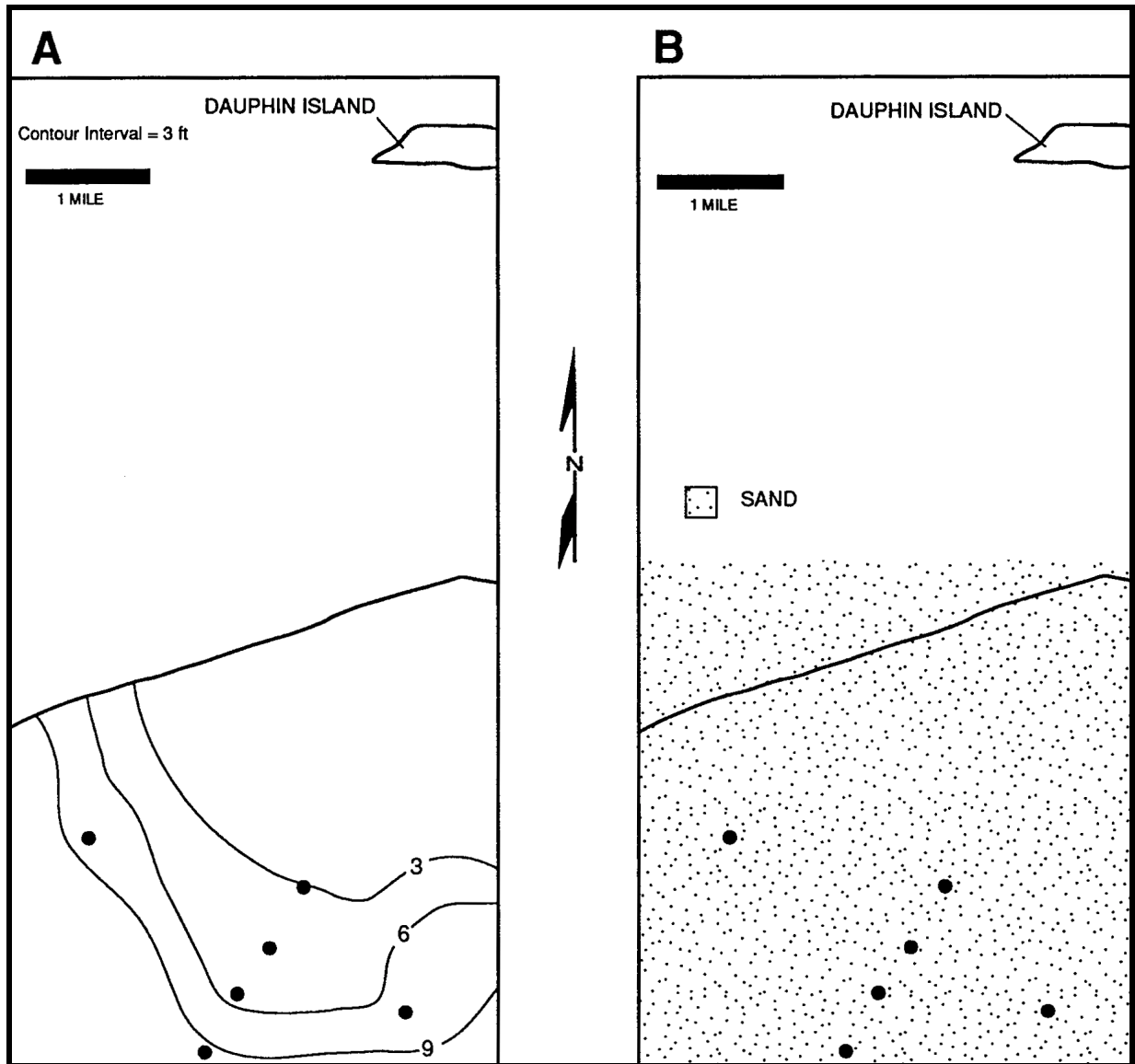


Figure 2-20. Sand isopach (A) and surface sediment texture (B) maps for Sand Resource Area 5 (from Parker et al., 1997).

## 2.2 CIRCULATION AND PHYSICAL OCEANOGRAPHY

Review of previously-published articles suggest circulation patterns in the offshore sand resource areas of Alabama result primarily from four dominant processes. These processes are wind-driven flow, tidal flow, buoyancy (or density)-driven flow, and influences of the Gulf Loop Current. Ocean currents at the sites display significant spatial and temporal variability, resulting from the relative strength of each of the forcing mechanisms. Total currents observed at any time (or location) typically are due to the sum responses of the water column to each of the individual forcing mechanisms mentioned above. There are interrelationships (or feedback responses) between different components that further complicate a description of these individual processes. The following review of literature will attempt to describe these processes, and how the circulation offshore of Alabama is affected by each component.

### 2.2.1 Waves and Wave-Generated Currents

The interaction of wind with the water surface generates waves. Once wind waves are generated, the forces of gravity, and to a lesser extent surface tension, allow waves to travel long distances across the sea surface. Waves are usually present at the shoreline because the sea surface is vast, winds are prevalent, and waves can travel long distances. Waves are primarily responsible for sediment transport in the nearshore zone and for subsequent shoreline change; therefore, waves are of fundamental interest to determine the potential effects of offshore sand mining on beach erosion.

As waves enter the nearshore zone, varying seafloor morphology causes the characteristics of waves (e.g., height and direction of travel) to change. As waves enter shallow water, their height increases (shoaling), and the direction of travel bends toward the coast so that wave crests become more parallel to the shoreline (refraction). As waves approach shore, shoaling and wavelength modifications overcome dissipation effects and cause wave height to increase and waves to steepen. Eventually wave steepness causes the wave to become unstable and break, which dissipates wave energy. Energy also is distributed along a wave crest by a process called wave diffraction. Together, wave shoaling, refraction, diffraction, and breaking can focus wave energy on particular areas, depending upon the characteristics of nearshore bathymetry.

General characteristics of waves that impact the Alabama Coast are as follows. Waves are generated by winds in the Gulf of Mexico. In general, there are seasonal variations in wave climate governed by seasonal characteristics of wind. Summer months (typically considered May through October) are characterized by relatively calm winds and low-energy waves, while winter months (typically considered December through April) are characterized by a more energetic wind and wave climate. Sporadic storms, such as hurricanes and cold fronts, generate the largest waves that impact the Alabama Coast.

More specific information about the waves impacting the Alabama Coast is provided in the published literature (although existing literature discussing waves and wave-generated currents is limited). For instance, Bedford and Lee (1994) collected short-term wave data in August and September 1989, approximately 760 m offshore of Dauphin Island and west of the Mobile ship channel. These authors deployed a pressure and current (PUV) sensor at a water depth of approximately 6 m. The pressure sensor was inoperative leaving only directional current measurements. Wave height was interpreted, therefore, from available data using linear wave theory. Spectral analysis showed that wave periods ranged from 3 to 10 sec, with the maximum wave energy associated with a peak wave period of 5.8 sec. Significant wave heights were approximately 80 cm. Although wave direction was not resolved well, given the failure of the pressure sensor, it was determined that waves were directed almost due north.

Another set of wave and current data in this region was collected by the USACE using wave gauges and near-bottom electromagnetic current meters as part of a monitoring program of nearshore dredged material disposal sites off the Alabama Coast. McGehee et al. (1994) provide details on the gauges and data collection procedures. Two wave gauges were installed by the National Data Buoy Center (NDBC) for that study between 1987 and 1990. The two wave gauges were deployed 1.3 and 2.6 km offshore.

Douglass et al. (1995) evaluated these long-term wave measurements, along with nearshore current measurements collected by the USACE in the vicinity of the disposal sites, to determine what mechanisms are responsible for long-term landward migration of large submerged sand bodies. These authors concluded that waves in this region provide the dominant mechanism responsible for moving Alabama berms persistently landward. Wave-driven sediment transport is due to faster landward current speeds under wave crests that are characteristic of shallow water, nonlinear waves. It was concluded that wave processes dominate other potential sediment transport processes, such as mean currents and short-term storms.

From more of a geological perspective, McBride and Byrnes (1995) performed a detailed study of nearshore sediment characteristics in this region. These authors concluded that ocean and wave-generated currents produce shelf and shoreface sand ridges in the region of southwestern Alabama/western Florida. This finding is consistent with that of Douglass et al. (1995), who concluded that waves provide a significant sediment transport mechanism offshore of Alabama.

### **2.2.2 Wind-Generated Currents**

The meteorological climate for the northeastern Gulf of Mexico (NEGOM) can be separated into two distinct seasonal periods: summer and winter (Clarke, 1994; Schroeder et al., 1994). Each of these periods is dominated by different types of air masses. The summer period is defined between May (late spring) through early fall (October), and it is characterized by stable high pressure air resulting from the more-northerly position of the Atlantic high pressure zone ('Bermuda High'). During this period, high pressure off the Atlantic coast brings relatively mild tropical air into the region, resulting in typically weak southerly winds. During the winter period, defined typically as December through April, the southern migration of the Atlantic high pressure zone allows polar air to intrude into the region, bringing with it Arctic frontal systems of cold, dry air. Northerly winds are more common during this period. These polar air intrusions occur at time scales of 3 to 10 days, and they result in more energetic air-sea disturbances. More vigorous vertical mixing of the water column is possible during the winter period.

The effect of these winds on nearshore barotropic currents can be exaggerated due to the presence of the shoreline, which creates an impermeable flow boundary, blocking typical Ekman response of the water column to wind forcing (Clarke, 1994). The result can be stronger response of the water column to wind forcing in nearshore zones than would be expected in deeper water. Lewis and Reid (1985) describe the along-shelf flow to be correlated to along-shelf winds. Reid (1994) stated that the longshore reversals in near-shore current directions (on subtidal time scales of order 3 to 10 days) observed during the Louisiana-Texas Shelf Physical Oceanography Program (LATEX; along the Louisiana-Texas coast west of the Mississippi River) result from similar reversals in the longshore wind component. For the Alabama locations, this suggests that wind-driven currents are likely strongest during the October to April period, when they are oriented approximately in the direction of the longshore wind component. Wind-driven currents in the summer months would be expected to be weaker.

Upwelling and downwelling processes may have an important effect on the spatial variability of nearshore barotropic currents. These processes produce a two-dimensional cross-shore circulation cell. In the upwelling case, surface waters are driven offshore by a longshore wind component that blows from the west with resulting bottom currents pulled shoreward to complete the circulation cell. Downwelling occurs when the longshore component drives surface flow onshore; bottom flow then retreats offshore. These processes can be modified significantly by density gradients in the cross-shore direction.

Storm events, typically hurricanes, passing the region can generate anomalous currents in the nearshore region. Measurements of currents during Hurricane Chantal (Douglass et al., 1995) show a modification to the mean bottom currents, increasing in magnitude to approximately 30 cm/sec from a pre-storm mean of approximately 10 cm/sec. Hurricane Chantal was considered a mild event (Category I hurricane) and passed about 800 km to the west of Alabama. Hence, these results probably do not adequately describe the expected local response to a more severe storm. Murray (1970) presented current observations obtained along the inner shelf (approximately 90 m offshore in 6.3-m water depth) offshore of Pensacola during the passage of Hurricane Camille. The eye of Camille passed approximately 160 km to the west of the mooring. The current meter collected readings exceeding 160 cm/sec (wave orbital velocities had been removed from the record) before malfunctioning. The winds had not yet reached peak speed at the time of

malfunction; extrapolating the current signal suggests the current speeds during the storm may have exceeded 200 cm/sec. These high speed flow responses to storm wind forcing were oriented in the direction of the wind stress vector; at that time, the wind was blowing out of the east. When the wind rotated to the southeast, blowing toward the shore, an offshore-directed flow was observed along the bottom. The bottom return flow in an offshore direction was produced in response to storm-surge setup along the shore and the need to balance the shore-normal pressure gradient.

### 2.2.3 Tidal Currents

Tidal currents in the NEGOM are strongly diurnal, dominated by the O1 (period of 25.82 hours) and K1 (period of 23.93 hours) tidal constituents (Clarke, 1994). Water elevation variations due to the tides average 45 to 60 cm, although the maximum range (tropic tides) can approach 80 cm while the minimum (equatorial tides) can be near-zero (Schroeder et al., 1994). Currents resulting from tidal elevation variations are assumed to vary along the same order.

Seim et al. (1987) found that tides on the Alabama-Mississippi inner shelf have a major axis oriented perpendicular to the shoreline with a shore-normal mean amplitude of approximately 6 to 8 cm/sec and a minor axis in the alongshore direction with a mean amplitude of 4 cm/sec. The tidal ellipses rotate in a clockwise sense on the shelf (Kinoshita and Noble, 1995).

Tidal currents on the inner shelf near the entrance to Mobile Bay are influenced by the ebb-tidal jet and, hence, dominated by the southward ebb flow from the Bay. However, current measurements made just west of the lighthouse at the entrance (near Sand Resource Area 4) show that the dominant tidal component is in the alongshore direction (Douglass et al., 1995), with a relatively weaker cross-shore component.

### 2.2.4 Effects of Density

Density-driven (baroclinic) currents on the continental shelf can be important in determining spatial variability of flow. Fresh water discharged from Mobile Bay is significant. This input of low density water creates a density gradient in the cross-shore direction. This gradient can result in an alongshore movement where the direction of flow will be to the right of the pressure gradient (Blanton, 1994). For Alabama, this suggests a baroclinic flow to the west when near-shore density gradients are present.

The structure of the near-shore density field can vary seasonally. In summer, a strong vertical stratification develops due to surface heating, as well as decreased vertical mixing (winds are milder). In winter, reduced heating and more vigorous vertical mixing tend to weaken the vertical stratification and produce a horizontal gradient (Clarke, 1994). Hence, the strength of the alongshore flow due to cross-shore density gradients is assumed to vary on a seasonal basis, with baroclinic flows likely strongest in winter.

Mobile Bay has the fourth-largest freshwater discharge in the United States (Morisawa, 1968), with an average annual mean of 1,850 m<sup>3</sup>/sec. Schroeder et al. (1994) states average mean discharge is more like 2,200 m<sup>3</sup>/sec. The peak discharge occurs in late winter/early spring and can be as high as 16,000 m<sup>3</sup>/sec; the minimum discharge is in autumn when the discharge can average 500 m<sup>3</sup>/sec (Stumpf et al., 1993). The result is a freshwater plume exiting Mobile Bay that persists for much of the year (Gelfenbaum and Stumpf, 1993). The plume is defined as a thin veneer (1 to 2 m thick) of fresh water overlying more saline ambient water (Gelfenbaum, 1994).

Schroeder et al. (1994) describes the plume as advecting to the east; however, no physical explanation of why this occurs was given. Other studies (Stumpf et al., 1993, Gelfenbaum and Stumpf, 1993) suggest the plume responds rapidly to local wind stress, hence the direction of the plume upon exit from the Bay likely depends on the direction of the alongshore wind stress component.

Gelfenbaum and Stumpf (1993) presented observations of current and waves collected on both sides of a well-developed buoyant plume front near the mouth of Mobile Bay. Measurements collected in ambient water were compared to those collected within the plume. Results indicated flow within the buoyant plume was largely decoupled from the ambient flow; the ambient flow moved around and beneath the plume. In addition, the plume created a buffer above the ambient water; this buffer retarded vertical mixing as well as attenuated surface waves. Surface wave heights within the plume were lower than those measured outside the plume. Also, wave periods within the plume were shorter than those detected outside the plume. This implies that the plume modifies the local wave field, and may modify sediment transport processes beneath it.

### **2.2.5 Gulf Loop Current**

The Gulf Loop Current has been studied extensively in past several decades, and it is a major influence on deep basin circulation. The Gulf Loop Current can impinge upon the shelf and significantly influence flow behavior on the NEGOM shelf. Kelly (1994) reported that intrusions of the Gulf Loop Current on the shelf occurs approximately 44% of the time. Intrusions were defined as observations of the warm-core ring itself, or filaments of the Gulf Loop Current. While these intrusions have significant influences on mid- and outer-shelf flow patterns, there was no mention of intrusions into the nearshore zone. There does not appear to be published evidence indicating the Gulf Loop Current has significant effect on the upper continental shelf.

### **2.2.6 Nearshore Sediment Transport**

Nearshore sediment transport is a complex process, which governs erosion and accretion of beaches. Sediment is moved alongshore and cross-shore (on and offshore) by physical coastal processes, such as wind, waves, tides, currents, and sea-level rise. The time scales of sediment transport and shoreline change vary from the initial formation of headlands and coasts on geologic time scales (thousands of years) to severe coastal erosion over a few days or hours during tropical storms and hurricanes.

In addition to physical coastal processes, sediment transport patterns are dependent upon the characteristics and supply of sediment. Grain size is the most important characteristic of the sediment. The quantity of sediment moved is inversely proportional to its grain size. Sediment transport rates decrease with increasing grain size, because heavier sediment requires more time and energy to be transported. Sediment density, durability, and shape also affect transport rates. In addition, the supply of sediment governs sediment transport rates, because transport rates are reduced where sediment is in short supply.

When waves break at an angle to the beach, alongshore-directed currents are generated, capable of lifting and moving sediment along the coast. For example, waves approaching the Gulf Shores shoreline from the east tend to move sand alongshore from east-to-west towards Main Pass. Because wave direction changes frequently, sand is moved back-and-forth along the beach. On an annual basis, however, there typically is a dominant wave direction that occurs most frequently on seasonal time scales.

Past work regarding longshore transport rates for Dauphin Island and the Morgan Peninsula is limited. According to Parker (1990), wave-generated longshore currents have the most apparent effect on sediment transport. Although it is generally accepted that the typical east-to-west currents dominate beach transport processes, the amount of sediment entrained in the littoral system along the Alabama barrier islands is not known with confidence. The only known quantitative estimates of littoral transport rates were calculated by the U.S. Army Corps of Engineers. Garcia (1977) determined that the total net longshore sediment transport rate at Dauphin Island was approximately 196,000 yd<sup>3</sup>/yr, and the U.S. Army Corps of Engineers (1955) estimated about 200,000 yd<sup>3</sup>/yr of net littoral transport at Perdido Pass.

## 2.3 BIOLOGY

### 2.3.1 Benthic Environment

The following subsections provide summaries of the existing literature concerning the benthic environment, including infauna (Section 2.3.1.1) and epifauna and demersal ichthyofauna (Section 2.3.1.2), in and around the five sand resource areas. This information, along with the assessment of ecological conditions from the biological field surveys (see Section 6.0), provides the framework for the evaluation of potential effects of dredging on these organisms (Section 7.5).

#### 2.3.1.1 Infauna

Previous infaunal studies in or near the sand resource areas include small-scale surveys (TechCon, Inc., 1980; Exxon Company, U.S.A., 1986; Barry A. Vittor & Associates, Inc., 1988; Continental Shelf Associates, Inc. and Barry A. Vittor & Associates, Inc., 1989) and regional surveys (Dames & Moore, 1979; Shaw et al., 1982; Harper, 1991). Organisms collected during these investigations consisted of members of the major invertebrate groups that commonly are found in sand bottom marine ecosystems, including crustaceans, echinoderms, mollusks, and polychaetous annelids. Generally, infaunal assemblages offshore Alabama tend to be numerically dominated by polychaetes (Shaw et al., 1982; Harper, 1991). Other conspicuous members of the infaunal community include amphipod crustaceans and bivalves. Seasonality is apparent in the overall abundance of infauna, with winter densities generally lower than during other seasons (Shaw et al., 1982; Barry A. Vittor & Associates, Inc., 1985; Harper, 1991).

Previous sampling efforts over broad areas of the northern Gulf of Mexico shelf have emphasized the importance of sediment type in determining infaunal community composition. Studies of the infauna of the Mississippi, Alabama, Florida Outer Continental Shelf (MAFLA OCS) by Dames & Moore (1979) revealed that inner shelf benthic habitats of the NEGOM can be described primarily on the basis of sediment texture and water depth. Shaw et al. (1982) surveyed infauna in the inner shelf area off Mississippi Sound, which included portions of Sand Resource Areas 4 and 5. This study is one of the most comprehensive historical surveys in the area, and describes distinct infaunal assemblages that are associated with mud, muddy sand, or sandy substrata within varied depth zones in shelf waters.

Based on a review of the studies cited above and other previous studies in the area, Barry A. Vittor & Associates, Inc. (1985) recognized four depth-related benthic habitats for infaunal communities in the region of the NEGOM: shallow beach habitat; inner shelf habitat; intermediate shelf habitat; and outer shelf habitat. Each of these habitats was further divided into sediment type (mud, sandy mud, muddy sand, or sand). Infaunal assemblage associations were recognized with each combination of water depth and substratum type. Cluster analysis revealed that infaunal taxa were closely tied to sediment type and texture (Figure 2-21).

The inner shelf habitat (4 to 20 m depth) of Barry A. Vittor & Associates, Inc. (1985) corresponds most closely with the location of the sand resource areas. Eight distinct infaunal assemblages were identified in this area. Three of these inner shelf assemblages exhibited narrow sediment texture preferences, while the other five assemblages showed transitional distributions (Figure 2-21). Muddy sand (50% to 90% sand) did not support a habitat-specific assemblage on the inner shelf, but instead was inhabited by transitional taxa that extended their range into areas characterized by other sediment types. Those assemblages that exhibited a narrow preference for a particular sediment texture were associated with mud, sandy mud, or sand. The mud (<20% sand) habitat assemblage was represented by the hemichordate *Balanoglossus* cf. *aurantiacus*, the polychaete *Paramphinome* sp. B, and the mollusks *Nassarius acutus* and *Utriculostra canaliculata*. The sandy mud (20% to 50% sand) habitat assemblage included the ophiuroids *Hemipholis elongata* and *Micropholis atra*, the bivalve *Nuculana concentrica*, and the crab *Pinnixa pearsei*.

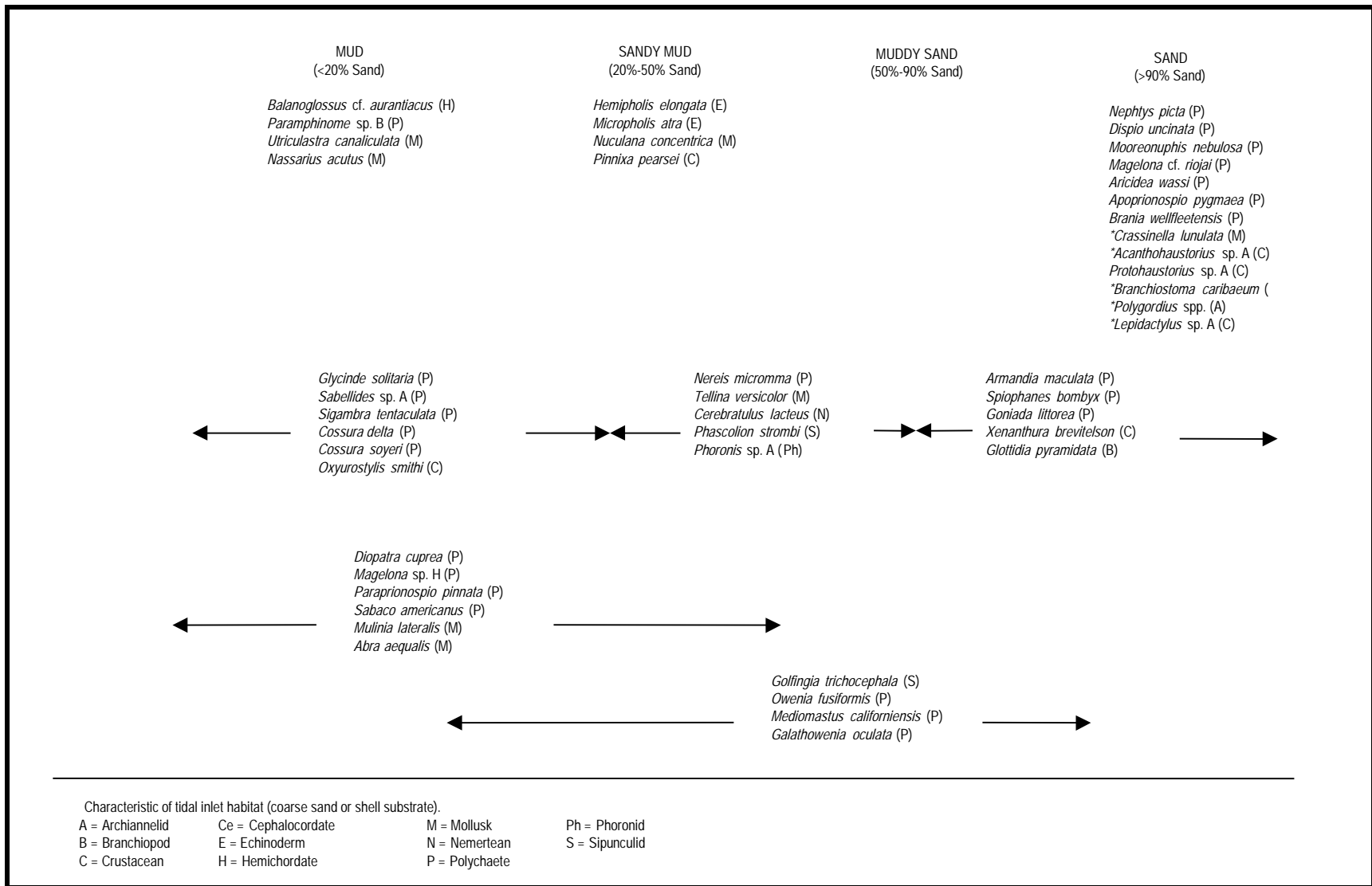


Figure 2-21. Infaunal assemblages associated with habitats on the inner continental shelf (<20 m depth) in the northeastern Gulf of Mexico study area (from Barry A. Vittor & Associates, Inc., 1985).

Inner shelf sand habitat (>90% sand) included amphipods of the genera *Acanthohaustorius*, *Protohaustorius*, and *Lepidactylus*, the archiannelid *Polygordius*, the lancelet *Branchiostoma caribaeum*, and a large number of polychaetes, including *Apoprionospio pygmaea*, *Aricidea wassi*, *Mooreonuphis nebulosa*, and *Nephtys picta* (Barry A. Vittor & Associates, Inc., 1985).

The Mississippi-Alabama Marine Ecosystems (MAME) study included sampling of infauna along three north-south transects in northern Gulf of Mexico shelf waters (Harper, 1991), and was the most recent large-scale shelf survey of sediment-inhabiting benthos. Infaunal densities were correlated with sediment particle size, with coarser sediments supporting higher densities. Inner stations of the De Soto Canyon and Mobile transects were located just within the southern edge of Sand Resource Areas 1 and 4, respectively. These two stations both were characterized by an infaunal assemblage associated with relatively coarse sediments, and included the amphipods *Ampelisca abdita* and *A. verrilli*, the bivalves *Parvilucina multilineata* and *Tellina versicolor*, the decapods *Euceramus praelongus* and *Spinocarcinus lobatus*, and various polychaetes, including *Aglaophamus verrilli*, *Mediomastus californiensis*, *Nereis micromma*, and *Spiophanes bombyx*.

The Geological Survey of Alabama reported benthic fauna sampled from various locations in Sand Resource Area 4 offshore Alabama (Hummell and Smith, 1995). In that study, about 82% of infaunal individuals sampled were unidentified polychaetous and oligochaetous annelids. Nearly 25% of the infauna collected consisted of a single taxon, the polychaete *Diopatra* sp. The second most abundant identified taxon was the rhynchocoel *Cerebratulus lacteus*, which contributed 6% of all organisms. Other identified taxa found in Area 4 included the echinoderm *Ophiolepis elegans* and the mollusks *Cerithium eburneum*, *N. concentrica*, and *Solen viridis*. The authors concluded that the assemblage was similar to that inhabiting the offshore mud habitat described by Shaw et al. (1982).

In addition to infaunal assemblages that exhibit narrow sediment texture preferences, regional surveys typically include other assemblages that show transitional distribution patterns (Barry A. Vittor & Associates, Inc., 1985). Several transitional species assemblages are commonly represented on the inner shelf habitat, each with affinities for broad ranges of sediment composition. These assemblages contain ubiquitous taxa, including the bivalve *Mulinia lateralis* and the polychaetes *Armandia maculata*, *Magelona* sp. H, *Mediomastus*, *Owenia fusiformis*, and *Paraprionospio pinnata* (Figure 2-21). These species are well adapted to burrowing and foraging in fine sediments.

Infaunal assemblages are comprised of species adapted to particular sedimentary habitats through differences in behavioral, morphological, physiological, and reproductive characteristics. Feeding is one of the behavioral aspects most closely related to sedimentary habitat (Rhoads, 1974). In general, habitats with coarse sediment and high water current velocities, where organic particles are maintained in suspension in the water column, favor the occurrence of suspension-feeding taxa that strain food particles from the water column. Coarse sediments also facilitate the feeding of carnivorous taxa that consume organisms occupying interstitial habitats (Fauchald and Jumars, 1979). At the other extreme, habitats with fine-textured sediments and little or no current are characterized by the deposition and accumulation of organic material, thereby favoring the occurrence of surface and subsurface deposit feeding taxa. In between these habitat extremes are a variety of habitat types that differ with respect to various combinations of sedimentary regime, depth, and hydrological factors, with each habitat type facilitating the existence of particular infaunal assemblages (Barry A. Vittor & Associates, Inc., 1985). An east-to-west transition of sedimentary regimes, from predominantly sands along the west Florida shelf to silts and clays along the Louisiana shelf, was evident during previous regional studies. Infaunal assemblages varied along this east-west gradient as well (Shaw et al., 1982; Barry A. Vittor & Associates, Inc., 1985).

The distribution and abundance of infaunal populations are influenced by factors other than sediment type. Results of previous studies also reflect the significance of local hydrology, with

euryhaline taxa occurring in lower densities east of Mobile Bay (Barry A. Vittor & Associates, Inc., 1985). The increase in salinity toward the west Florida shelf, due to a diminishing influence of riverine discharge from Mobile Bay, produces a diverse array of stenohaline taxa, especially crustaceans. Freshwater intrusion is one of the major environmental factors that affect the study area, especially in spring, bringing both lower salinities and increased sedimentation in waters near Mobile Bay. Infaunal assemblages of the Alabama inner shelf typically include taxa characteristic of muddy estuarine habitats, especially opportunistic species that inhabit areas that most taxa cannot. These euryhaline species predominate in inner shelf habitats during periods of elevated river discharge, and include the polychaetes *P. pinnata* and *Mediomastus* (Continental Shelf Associates, Inc. and Barry A. Vittor & Associates, Inc., 1989). These and other transitional taxa are able to numerically dominate habitats that experience various perturbations, including siltation, low salinity, and low levels of dissolved oxygen (hypoxia). Some transitional taxa are among the initial colonizers of disturbed areas offshore Alabama (Shaw et al., 1982).

Hypoxia is known to occur in the offshore Alabama region, and may be caused by water column organic enrichment, by stagnation due to water column stratification, or by other large-scale hydrological factors. Although a natural occurrence, some investigators believe that the frequency of hypoxic episodes may be increasing due to human influences (Turner and Rabalais, 1994). Hypoxia may negatively affect the distribution and abundance of some infaunal assemblages. Persistent hypoxia may result in defaunation of nearshore benthic habitats. In general, infauna are more negatively affected by hypoxia than are nektonic taxa because of their relative lack of mobility. The major invertebrate groups that comprise benthic assemblages exhibit varied levels of tolerance to hypoxia, with polychaetes being the most tolerant group, followed by bivalves. Crustaceans and echinoderms seem to be the least tolerant of hypoxic conditions (Stickle et al., 1989). Opportunistic infauna that commonly occur in offshore Alabama waters, such as the polychaetes *P. pinnata*, *Heteromastus filiformis*, and *Streblospio benedicti*, commonly inhabit hypoxic areas.

The relatively shallow-water benthic habitats of the inner shelf offshore Alabama are strongly influenced by abiotic factors such as temperature, wind and waves, river discharge (salinity and turbidity), currents and circulation, and tropical storms. The inherent variability of local benthic habitats causes the inner shelf infaunal community to be dynamic and unstable and to remain in an immature level of development, compared to a mature and stable community comprised of large, deep-dwelling, head-down deposit feeders. The Alabama inner shelf community probably remains in various stages of succession due to sporadic environmental disturbances, including seasonal and annual fluctuations in environmental parameters (Continental Shelf Associates, Inc. and Barry A. Vittor & Associates, Inc., 1989).

#### **2.3.1.2 Epifauna and Demersal Ichthyofauna**

Defenbaugh (1976) based the most detailed account of benthic macroinvertebrates of the northern Gulf region on extensive collections. The pro-delta sound assemblage includes the inshore and nearshore OCS from the Chandeleur Islands to the eastward boundary of the study area. Depths range from 4 to 20 m, and sediments are composed primarily of soft mud mixed with sand or shell hash; however, sediments are sandy east of Mobile Bay. Equivalent to Parker's (1960) open sound habitat, this assemblage is composed of such taxa as sea pansy *Renilla mulleri*; baby's ear gastropod *Sinum perspectivum*; bivalves *Chione clenchi* and *Noetia ponderosa*; brown shrimp *Penaeus aztecus*; shame-face crabs *Calappa sulcata* and *Hepatus epheliticus*; purse crabs *Persephona* spp.; and echinoderms *Hemipholis elongata* and *Mellita quinquiesperforata* (Table 2-2).

The intermediate shelf assemblage is a relatively broad area seaward of the pro-delta sound assemblage (Defenbaugh, 1976). Sediments are composed of muddy sand or sand in depths ranging from 20 to 60 m. This habitat contains the following taxa representative of the faunal assemblage: gastropods *Busycon*, *Fasciolaria*, *Murex*, and *Strombus*; bivalves *Argopecten*, *Pitar*,

Table 2-2. Epifaunal assemblages of the northern Gulf of Mexico which pertain to the Alabama study area (from Defenbaugh, 1976).

<u>PRO-DELTA SOUND ASSEMBLAGE (4-20 m depth)</u>	
<p>Cnidaria</p> <p><i>Leptogorgia virgulata</i></p> <p><i>Renilla mulleri</i></p> <p>Gastropoda</p> <p><i>Cantharus cancellarius</i></p> <p><i>Sinum perspectivum</i></p> <p>Bivalvia</p> <p><i>Chione clenchi</i></p> <p><i>Noetia ponderosa</i></p> <p>Natantia</p> <p><i>Penaeus aztecus</i></p> <p><i>Sicyonia dorsalis</i></p> <p><i>Trachypeneus similis</i></p>	<p>Reptantia</p> <p><i>Calappa sulcata</i></p> <p><i>Callinectes similis</i></p> <p><i>Hepatus epheliticus</i></p> <p><i>Pagurus pollicaris</i></p> <p><i>Persephona aquilonaris</i></p> <p><i>Persephona crinata</i></p> <p><i>Portunus gibbesi</i></p> <p>Stomatopoda</p> <p><i>Squilla empusa</i></p> <p>Echinodermata</p> <p><i>Hemipholis elongata</i></p> <p><i>Luidia clathrata</i></p> <p><i>Mellita quinquesperforata</i></p> <p><i>Ophiolepis elegans</i></p>
<u>INTERMEDIATE SHELF ASSEMBLAGE (20-60 m depth)</u>	
<p>Annelida</p> <p><i>Diopatra cuprea</i></p> <p>Gastropoda</p> <p><i>Busycon contrarium</i></p> <p><i>Conus austini</i></p> <p><i>Distorsio clathrata</i></p> <p><i>Faciolaria l. hunteri</i></p> <p><i>Murex fulvescens</i></p> <p><i>Pleurobranchaea hedgpethi</i></p> <p><i>Polystira albida</i></p> <p><i>Strombus alatus</i></p> <p><i>Tonna galea</i></p> <p>Bivalvia</p> <p><i>Amusium papyraceus</i></p> <p><i>Argopecten gibbus</i></p> <p><i>Chione clenchi</i></p> <p><i>Gouldia cerina</i></p> <p><i>Pitar cordata</i></p> <p><i>Tellina nitens</i></p> <p><i>Tellina squamifera</i></p> <p>Natantia</p> <p><i>Penaeus aztecus</i></p> <p><i>Penaeus setiferus</i></p> <p><i>Sicyonia brevirostris</i></p> <p><i>Sicyonia dorsalis</i></p> <p><i>Trachypeneus similis</i></p>	<p>Reptantia</p> <p><i>Anasimus latus</i></p> <p><i>Calappa sulcata</i></p> <p><i>Callinectes similis</i></p> <p><i>Hepatus epheliticus</i></p> <p><i>Libinia emarginata</i></p> <p><i>Parthenope serrata</i></p> <p><i>Persephona crinata</i></p> <p><i>Petrochirus diogenes</i></p> <p><i>Portunus gibbesi</i></p> <p><i>Portunus spinicarpus</i></p> <p><i>Portunus spinimanus</i></p> <p>Stomatopoda</p> <p><i>Squilla chydaea</i></p> <p><i>Squilla empusa</i></p> <p>Echinodermata</p> <p><i>Astropecten duplicatus</i></p> <p><i>Clypeaster ravenelli</i></p> <p><i>Echinaster sp.</i></p> <p><i>Encope michelini</i></p> <p><i>Luidia alternata</i></p> <p><i>Luidia clathrata</i></p> <p><i>Ophiolepis elegans</i></p> <p><i>Stylocidaris affinis</i></p>

and *Tellina*; shrimps *Peneaus* and *Sicyonia*; crabs *Anasimus*, *Calappa*, *Libinia*, *Parthenope*, and *Portunus*; echinoids *Encope* and *Stylocidaris*; and sea stars *Astropecten* and *Luidia* (Table 2-2).

The MAME study (Harper, 1991) was the most recent major investigation of epifauna in the region of the sand resource areas. During this study, 310 species were collected by trawl, with decapods accounting for 48% of the species and 78% of the individuals collected. The numerical dominance of decapods was due to the large number of shrimps collected. Other than decapods, mollusks and echinoderms were the major contributors, comprising 30% and 18% of collected species, and 8% and 10% of individuals, respectively. Patterns of epifaunal similarity among stations in the MAME study were examined using cluster analysis. The inner stations of the De Soto Canyon and Mobile transects were located just within the southern edge of Sand Resource Areas 1 and 4, respectively, and were characterized by a common epifaunal assemblage that generally included shallow water and estuarine-related taxa. Numerical dominants common to both stations included the decapods *Sicyonia brevirostris* and *Trachypenaeus constrictus* and the squid *Loligo pealei*. Other numerical dominants were *Sicyonia dorsalis*, *Portunus gibbseii*, and the asteroid *Luidia clathrata*. Sediment at both MAME stations was characterized as sand (Harper, 1991).

Continental Shelf Associates, Inc. (1989) conducted a diver tow and photographic survey in OCS Pensacola Area Block 881 to characterize bottom habitats. The site of the survey was situated at the southern end of Sand Resource Area 2. Sandy sediments characterized the area, often consisting of shell hash and coarse sand. Frequently observed epifauna included burrowing anemones (cerianthids), portunid decapods, and echinoderms (*Astropecten duplicatus*, *Encope michelini*, and *L. clathrata*).

Darnell and Kleypas (1987) provided a comprehensive survey of demersal ichthyofauna of the eastern Gulf of Mexico shelf, from the Mississippi Delta to southwest Florida. Regional shelf waters supported about 347 species plus another 85 unresolved taxa from 80 families. The most speciose families included Bothidae (23 species), Serranidae (21 species), Sciaenidae (18 species), Triglidae (14 species), Ophidiidae (13 species), Carangidae (12 species), Sparidae (11 species), Gobiidae (11 species), Balistidae (10 species), Syngnathidae (10 species), and Scorpaenidae (9 species). Pinfish (*Lagodon rhomboides*) and longspine porgy (*Stenotomus caprinus*) were the most abundant species, together comprising about 19% of the catch. Total abundance was dominated by relatively few species; the top 13 species contributed over 50% of the entire catch.

In their survey, Darnell and Kleypas (1987) described several distinctive fish assemblages based on the co-occurrence of species in trawl samples. Within the study region, they identified the Mississippi Bight assemblage extending from the Mississippi Delta eastward to about Perdido Bay, Florida and out to the shelf break. Of six assemblages discussed by Darnell and Kleypas (1987), the Mississippi Bight fauna was by far the most diverse assemblage in the eastern Gulf of Mexico. Abundant species included striped anchovy (*Anchoa hepsetus*), rock seabass (*Centropristis philadelphica*), silver seatrout (*Cynoscion arenarius*), pinfish (*Lagodon rhomboides*), spot (*Leiostomus xanthurus*), Atlantic croaker (*Micropogonias undulatus*), and longspine porgy (*Stenotomus caprinus*).

The Geological Survey of Alabama (Hummell and Smith, 1995) summarized unpublished Southeastern Area Monitoring and Assessment Program (SEAMAP) trawl data collected during June 1985 and 1991 and October 1988 and 1993 from Sand Resource Area 4. Epifaunal taxa collected most consistently during these SEAMAP surveys included crab (*Callinectes similis*), shrimps (*Penaeus aztecus* and *P. setiferus*), squid (*Lolligunculus brevis*), and stomatopod (*Squilla empusa*). Demersal ichthyofauna collected most consistently during the SEAMAP surveys in Area 4 included bay anchovy (*Anchoa mitchilli*), silver seatrout, pinfish, Atlantic croaker, searobin (*Prionotus longispinus*), and lizardfish (*Synodus foetens*).

The Mississippi Bight area encompasses a zone of faunal transition for demersal fishes. This is presumably due to a sediment textural change from the mud of the Mississippi Delta to the more

sandy, biogenic carbonate sediments of the West Florida Shelf. The affinity of certain demersal species for particular sediment types is often related to the types of prey items supported by those sediments (Rogers, 1977). Another factor thought to influence the distribution and abundance of fishes in this area is the reduced freshwater discharge (and sediment load) to shelf waters east of Mobile Bay (Barry A. Vittor & Associates, Inc., 1985).

Seasonally, the Mississippi Bight assemblage (Darnell and Kleypas, 1987) showed peak abundance (due to movement by a few species) in winter months on the middle and outer shelf. In general, this assemblage exhibited much less seasonality when compared with the northwestern Gulf fish assemblages. Mild winter temperatures and reduced riverine discharge east of the Mississippi River may contribute to the reduced seasonal movements by demersal species. Pattern analyses were performed by Comiskey et al. (1985) on various data sets from trawl surveys in the area of the present study, including 1974 to 1975 National Marine Fisheries Service (NMFS) fishery independent surveys and 1982 to 1983 SEAMAP surveys. These analyses indicated that the nearshore environment off Alabama was characterized by low numbers of taxa and individuals relative to areas nearer the Mississippi Delta. Inner shelf waters off Alabama apparently support a demersal community of spatially widespread taxa that migrate inshore seasonally, rather than distinct resident assemblages (Comiskey et al., 1985).

Barry A. Vittor & Associates, Inc. (1985) analyzed 1982 to 1983 SEAMAP trawl data using cluster analysis. This provided a fine-scale analysis of proximate environmental factors, such as hydrography and substratum type, that influence the distribution of demersal taxa (including motile epifauna) within the Darnell and Kleypas (1987) Mississippi Bight assemblage. Cluster analysis produced eight taxonomic groups explained primarily by sediment type and water depth (Table 2-3). Species diversity of the groupings was positively correlated with depth and salinity and negatively correlated with temperature, indicating that the deeper, more hydrographically stable habitats support a more diverse demersal community.

## **2.3.2 Pelagic Environment**

Existing information on the pelagic environment is provided in this section to support discussions in Section 7.6 concerning potential impacts and schedules of best and worst times for offshore dredging with regards to transitory pelagic species. Ecological characteristics and seasonal distribution of zooplankton (including ichthyoplankton) and nekton (i.e., squids, fishes, sea turtles, and mammals) which occur in nearshore shelf waters of Alabama are described. Available literature for the Alabama coastal region was supplemented with data and information from surrounding waters when necessary to fill gaps and provide descriptions of organisms in the sand resource areas given their water depth and distance from shore.

### **2.3.2.1 Zooplankton**

Zooplankton form essential links in the marine food web between primary producers (phytoplankton and bacteria) and larger marine species such as fishes, birds, and marine mammals. They are relatively weak swimmers that drift with water currents. Zooplankton transport organic matter through the water column by their vertical migration and production of organically rich fecal pellets which sink to the seafloor.

There have been numerous studies of zooplankton species composition and distribution in the eastern Gulf of Mexico and its estuaries, but few were directly applicable to the sand resource areas. Most studies in the region have been conducted in Mississippi coastal waters, Mississippi Sound, and Mobile Bay. Results of these studies provided general information on abundance and seasonality of various species groups.

Table 2-3. Eight taxonomic groups resulting from a synthesis of community analyses of trawl samples collected in the northeastern Gulf of Mexico study area during the 1982 and 1983 SEAMAP groundfish surveys (from Barry A. Vittor & Associates, Inc., 1985).

<b>Group 1. Shallow Water, Low Salinity Habitat</b>	
<b><u>Scientific Name</u></b>	<b><u>Common Name</u></b>
<i>Anchoa mitchilli</i>	Bay anchovy
<i>Anchoa nasuta</i>	Longnose anchovy
<i>Arius felis</i>	Hardhead catfish
<i>Chloroscombrus chrysurus</i>	Atlantic bumper
<i>Larimus fasciatus</i>	Banded drum
<i>Menticirrhus americanus</i>	Southern kingfish
<i>Polydactylus octonemus</i>	Atlantic threadfin
<i>Stellifer lanceolatus</i>	Star drum
<i>Trinectes maculatus</i>	Hogchoker
<b>Group 2. Widespread in Low Salinity Waters and in High Salinity Waters Overlying Muddy Sediments</b>	
<b><u>Scientific Name</u></b>	<b><u>Common Name</u></b>
<i>Anchoa hepsetus</i>	Striped anchovy
<i>Callinectes sapidus</i>	Blue crab
<i>Callinectes similis</i>	Crab
<i>Citharichthys spilopterus</i>	Bay wiff
<i>Cynoscion arenarius</i>	Sand seatrout
<i>Leiostomus xanthurus</i>	Spot
<i>Lolliguncula brevis</i>	Squid
<i>Penaeus aztecus</i>	Brown shrimp
<i>Penaeus setiferus</i>	White shrimp
<i>Peprilus burti</i>	Gulf butterflyfish
<i>Symphurus plagiusa</i>	Blackcheek tonguefish
<i>Trichiurus lepturus</i>	Atlantic cutlassfish
<b>Group 3. Widespread in High Salinity Waters Overlying Muddy Sediments</b>	
<b><u>Scientific Name</u></b>	<b><u>Common Name</u></b>
<i>Brotula barbata</i>	Bearded brotula
<i>Calappa sulcata</i>	Crab
<i>Cynoscion nothus</i>	Silver seatrout
<i>Etropus crossotus</i>	Fringed flounder
<i>Lepophidium graellsii</i>	Blackedge cusk-eel
<i>Ophidion welschi</i>	Crested cusk-eel
<i>Porichthys plectrodon</i>	Atlantic midshipman
<i>Prionotus rubio</i>	Blackfin searobin
<i>Sicyonia dorsalis</i>	Rock shrimp
<i>Squilla</i> LPIL	Mantis shrimp
<i>Trachypenaeus</i> LPIL	Hardback shrimp
<b>Group 4. High Salinity Waters Overlying Muddy Sediments East of the Mississippi River</b>	
<b><u>Scientific Name</u></b>	<b><u>Common Name</u></b>
<i>Portunus gibbesii</i>	Portunid crab
<i>Prionotus tribulus</i>	Bighead searobin
<i>Saurida brasiliensis</i>	Largescale lizardfish
<i>Serranus atrobranchus</i>	Blackear bass
<i>Sphoeroides parvus</i>	Least puffer
<i>Urophycis cirratus</i>	Gulf hake
<i>Urophycis floridanus</i>	Southern hake

Table 2-3. Continued.

<b>Group 5. High Salinity Waters Overlying Muddy Sediments West of the Mississippi River Outfall</b>	
<b><u>Scientific Name</u></b>	<b><u>Common Name</u></b>
<i>Antennarius radiosus</i>	Singlespot frogfish
<i>Bollmania communis</i>	Ragged goby
<i>Gunterichthys longipennis</i>	Gold brotula
<i>Hoplunnis macrurus</i>	Silver conger
<i>Nezumia bairdi</i>	Grenadier
<i>Parapenaeus</i>	Shrimp
<i>Steindachneria argentea</i>	Luminous hake
<b>Group 6. High Salinity Waters Overlying Muddy and Sandy Sediments</b>	
<b><u>Scientific Name</u></b>	<b><u>Common Name</u></b>
<i>Centropristis philadelphicus</i>	Rock sea bass
<i>Diplectrum bivattatum</i>	Dwarf sand perch
<i>Etrumeus teres</i>	Round herring
<i>Halieutichthys aculeatus</i>	Pancake batfish
<i>Lepophidium jeannae</i>	Mottled cusk-eel
<i>Lutjanus campechanus</i>	Red snapper
<i>Ophidion grayi</i>	Blotched cusk-eel
<i>Ovalipes guadulpensis</i>	Portunid crab
<i>Penaeus duorarum</i>	Pink shrimp
<i>Portunus spinicarpus</i>	Portunid crab
<i>Prionotus roseus</i>	Bluespotted searobin
<i>Solenocera atlantidis</i>	Shrimp
<i>Stenotomus caprinus</i>	Longspine porgy
<i>Syacium gunteri</i>	Shoal flounder
<i>Synodus foetens</i>	Inshore lizardfish
<b>Group 7. Nearshore High Salinity Waters Overlying Sandy Sediments</b>	
<b><u>Scientific Name</u></b>	<b><u>Common Name</u></b>
<i>Centropristis ocyurus</i>	Bank sea bass
<i>Doryteuthis plei</i>	Squid
<i>Haemulon aurolineatum</i>	Tomtate
<i>Loligo pealei</i>	Squid
<i>Orthopristis chrysoptera</i>	Pigfish
<i>Prionotus carolinus</i>	Northern searobin
<i>Prionotus martis</i>	Barred searobin
<i>Prionotus scitulus</i>	Leopard searobin
<i>Raja eglanteria</i>	Cleannose skate
<i>Sicyonia brevirostris</i>	Rock shrimp
<i>Sphoeroides spengleri</i>	Bandtail puffer
<b>Group 8. Offshore High Salinity Waters Overlying Sandy Sediments</b>	
<b><u>Scientific Name</u></b>	<b><u>Common Name</u></b>
<i>Bellator militaris</i>	Horned searobin
<i>Lagodon rhomboides</i>	Pinfish
<i>Monacanthus hispidus</i>	Planehead filefish
<i>Neomerinthe hemingwayi</i>	Spinycheek scorpionfish
<i>Ophidion holbrooki</i>	Bank cusk-eel
<i>Prionotus salmonicolor</i>	Blackwing searobin
<i>Scorpaena calcarata</i>	Smoothhead scorpionfish
<i>Syacium papillosum</i>	Dusky flounder
<i>Synodus intermedius</i>	Sand diver
<i>Synodus poeyi</i>	Offshore lizardfish
<i>Trachinocephalus myops</i>	Snakefish
<i>Urophycis regius</i>	Spotted hake

Zooplankton can be functionally divided into holoplankton and meroplankton. Holoplankton spend their entire lives in the water column, whereas meroplankton occur as plankton only during certain stages (generally larval stages) of their life cycle. Many important commercial and sport fish species have planktonic eggs and larvae. Almost without exception, the commercially important shellfish have planktonic larvae. Fish eggs and larvae are discussed separately in the ichthyoplankton section, which occurs after the sections on holoplankton and meroplankton.

## Holoplankton

Major constituents of the holoplankton include protozoa, gelatinous zooplankton, copepods, mysids, and chaetognaths. Other groups include amphipods, euphausiids, heteropods, ostracods, polychaetes, and pteropods.

Among protozoans, ciliates have received the most attention. Approximately 116 ciliate genera and about 215 ciliate species are known in the Gulf of Mexico (Borror, 1962). Tintinnids are a group of common, marine, ciliated protozoans which live within a tube-like covering. Balech (1967) reported 55 tintinnid species from the NEGOM.

Gelatinous zooplankton constitute an important group in the northern Gulf of Mexico. Phillips et al. (1969) studied macroplanktonic jellyfishes in the northern Gulf of Mexico and found them to be essential links via food webs and symbiotic relationships to the benthos, nekton, and other zooplankters. Phillips et al. (1969) and Burke (1975, 1976) listed 1 chondrophore, 2 ctenophores, 12 hydromedusae, 7 scyphomedusae, and 5 siphonophores from nearshore waters off Mississippi. Hydromedusae (i.e., *Liriope tetraphylla*, *Bougainvillia carolinensis*, *Nemopsis bachei*) were most abundant. Scyphomedusae were numerically dominated by the sea nettle *Chrysaora quinquecirrha* and the cabbagehead jellyfish *Stomolophus meleagris*. The cabbagehead jellyfish, along with the ctenophore *Mnemiopsis mccradyi*, can be so plentiful (up to 10/m<sup>2</sup> or more) that they interfere with commercial shrimp and fish trawling operations. In the Mississippi Sound region, Christmas (1973) found that *M. mccradyi* was always the dominant zooplankton species in terms of biomass. The ctenophore *M. mccradyi* is a major predator of microzooplankton, including copepods and bivalve larvae (Reeve and Walter, 1978).

Another small, but important, group of filter-feeding gelatinous zooplankton includes the larvaceans. They are one of the few zooplankton groups that can feed on bacteria-sized particles. The only larvacean that is common in northern Gulf of Mexico inshore waters is *Oikopleura dioica*. Off Florida, Hopkins (1966) reported that *O. dioica* formed about 8% of the total zooplankton densities in St. Andrew Bay. Edmiston (1979) found that this species constituted about 3% of the zooplankton densities off Apalachicola Bay.

Copepods are the numerically dominant group of net-collected zooplankton. These small crustaceans are mainly herbivorous and opportunistic, forming an important link in the food web between phytoplankton and micronekton. Copepods feed on whatever species of phytoplankton is most abundant within a size range of about 5 to 75  $\mu\text{m}$  (Turner, 1984a,b,c,d, 1986). McIlwain (1968) reported 15 copepod taxa from Mississippi Sound. Numerically dominant species in his samples were *Acartia tonsa*, *Labidocera aestiva*, *Oithona brevicornis*, and *Paracalanus parvus*. Table 2-4 shows the monthly occurrence of all copepod taxa collected by McIlwain (1968). Zooplankton collections from nearshore waters offshore Mississippi and Alabama (<25 m water depths) included the copepod genera *Acartia*, *Centropages*, *Eucalanus*, *Oithona*, and *Paracalanus* (Alexander et al., 1977).

Mysids are shrimp-like crustaceans which are categorized (depending on their size and behavior) as either zooplankton, micronekton, or epibenthos. They are important food for fishes. Seventeen species of mysids are known from nearshore shelf waters in the northern Gulf of Mexico (Stuck et al., 1979). In the vicinity of Dauphin Island, Alabama, five mysid species are common, with

three species (*Mysidopsis almyra*, *Bowmaniella brasiliensis*, and *B. floridana*,) accounting for about 85% of the mysids collected (Modlin, 1982).

Chaetognaths are a small, but significant, group of zooplankton. They form an important trophic link between copepods and larger predators, including commercially important fishes (McLelland, 1989). Twenty-four species are known from the Gulf of Mexico, but only a few are common inshore (McLelland, 1989). In nearshore waters of the NEGOM, four species of *Sagitta* predominate: *S. friderici*, *S. helenae*, *S. hispida*, and *S. tenuis*, (McLelland, 1984). The onshore/offshore distribution of these species is affected by tolerance to salinity changes (McLelland, 1984).

Species	Month											
	J	F	M	A	M	J	J	A	S	O	N	D
<i>Acartia tonsa</i>	•	•		•	•	•	•	•	•	•	•	
<i>Centropages furcatus</i>						•	•	•	•	•	•	•
<i>Centropages hamatus</i>											•	•
<i>Corycaeus</i> sp.						•	•	•	•			
<i>Eucalanus pileatus</i>		•				•	•	•	•		•	
<i>Euterpina acutifrons</i>		•				•	•	•	•		•	•
<i>Labidocera aestiva</i>				•	•	•	•	•	•	•	•	
<i>Labidocera</i> sp.	•	•					•		•	•	•	
<i>Oithona brevicornis</i>				•	•	•	•	•	•	•	•	•
<i>Oithona</i> sp.		•					•					
<i>Oncaea venusta</i>						•	•	•				
<i>Paracalanus parvus</i>				•	•	•	•		•	•	•	
<i>Sapphirina nigromaculata</i>		•						•				
<i>Temora longicornis</i>						•	•	•	•	•	•	
<i>Temora stylifera</i>								•				

## Meroplankton

Meroplankton includes organisms occurring as plankton only during certain stages (generally larval stages) of their life cycle. Major meroplanktonic groups are planktonic larvae of benthic invertebrates (e.g., polychaetes, gastropods, bivalves, decapods, echinoderms, and cephalochordates) and fishes. Fish eggs and larvae are discussed separately in the following ichthyoplankton section.

Planktonic larvae of benthic invertebrates are a significant component of the coastal zooplankton. The occurrence of crab larvae in the northern Gulf of Mexico was studied by Truesdale and Andryszak (1983). They found larvae of portunid (swimming) crabs at every station, with *Callinectes* spp. (mostly *C. sapidus* [blue crab] and *C. similis*) and *Portunus* spp. larvae being most abundant. Early zoeal stages of *Callinectes* spp. were confined mostly to inshore waters, whereas later stages occurred mostly offshore. Other numerically important crab larvae were *Uca* spp. (fiddler crabs) and *Pagurus pollicaris* and *Clibanarius vittatus* (hermit crabs). Stuck and Perry (1981a) described the seasonal distribution of blue crab megalops larvae in Mississippi coastal

waters. They collected megalopae in all months of the year, but peak settlement occurred in fall. More recently, Perry et al. (1995) and Rabalais et al. (1995) investigated the seasonal recruitment patterns of blue crab megalopae near major passes in the north-central Gulf of Mexico including Mobile Bay and Mississippi Sound. Settlement of blue crab megalops larvae was estimated using collecting traps that provided continuous sampling over time. Over a 2-yr monitoring period, the settlement of megalopae occurred primarily from August to November (with intra-month peaks). Despite their relative proximity, there was a 5-day lag in settlement between Mississippi Sound and Mobile Bay (Rabalais et al., 1995).

Although not strictly planktonic, the occurrence of post-larval (recently settled) penaeid shrimps provides a clue to the seasonality of the late-stage planktonic larvae. Christmas et al. (1966) described the seasonal distribution of post-larval penaeid shrimps in Mississippi Sound using towed nets. Brown shrimp post-larvae appeared as early as February and continued through August. White shrimp post-larvae occurred in April and persisted through September. Pink shrimp post-larvae first appear in June and were collected until October.

Many meroplankters that use estuarine habitats as juveniles originate offshore in adult spawning areas where eggs and larvae are released in the water. Although exact mechanisms are not well understood, the transport of meroplankters to their juvenile habitat depends upon local and regional circulation processes including coastal currents, wind regime, and tidal influence as well as the behavior of the organism (Shaw et al., 1988). Parcels of coastal water can be displaced for hundreds of kilometers, thus larvae do not necessarily enter estuaries nearest to the offshore spawning sites (Shaw et al., 1988).

The ingress (inshore migration) of penaeid shrimp larvae was modeled by Rogers et al. (1993) for Louisiana coastal waters. This process was thought to involve behavioral responses to environmental cues that allow the post-larval shrimp to take advantage of prevailing physical forces. These researchers suggested that the ingress of larval brown shrimp from offshore waters to inshore marsh habitats was facilitated by environmental cues provided by the passage of cold fronts. The post-cold front southerly winds generated northward flowing currents which transported the brown shrimp post-larvae shoreward (Rogers et al., 1993).

## **Ichthyoplankton**

Most fishes inhabiting the Gulf of Mexico, whether pelagic or benthic as adults, have pelagic larval stages. For various lengths of time (10 to 100 days, depending on the species), these pelagic fish eggs and larvae become part of the planktonic community known as ichthyoplankton (Leis, 1991). Variability in survival and transport of pelagic larval stages is thought to be an important determinant of future year class strength in adult populations of fishes and invertebrates (Underwood and Fairweather, 1989). For this reason, larval fishes and the physical and biological factors that influence their abundance and distribution have received increasing attention from marine ecologists. In general, the distribution of fish larvae depends upon 1) spawning behavior of adults; 2) hydrographic structure at a variety of scales; 3) duration of the pelagic period; 4) behavior of larvae; and 5) larval mortality and growth (Leis, 1991).

In this section, major ichthyoplankton studies relevant to the project area are reviewed and discussed. There was no information on ichthyoplankton available for the immediate vicinity of the five sand resource areas. Therefore, available information was used from studies conducted in nearby areas such as lower Mobile Bay, Mississippi Sound, and coastal Mississippi.

Ichthyoplankton assemblages in nearshore shelf waters of the region are composed of species that also are common as adults (Ditty, 1986; Ditty et al., 1988). The temporal occurrence of these taxa in ichthyoplankton samples reflects the spawning times of adults. In the northern Gulf of Mexico, spawning activity can be broadly classified as cold water and warm water periods which parallel the seasons (Barry A. Vittor & Associates, Inc. 1985). Because generally expected

seasonal patterns of fish egg and larval occurrence can be inferred from knowledge of the known adult spawning times, this information is presented to augment information on the temporal patterns of ichthyoplankton occurrence. Table 2-5 gives the spawning times for economically important species from the region.

Ditty et al. (1988) summarized information from over 80 ichthyoplankton studies from the northern Gulf of Mexico (north of 26°N) and reported 200 coastal and oceanic fishes from 61 families. Many taxa were only collected over waters within certain depth ranges. Species found exclusively in water depths shallower than 25 m were mostly inshore demersal species such as Atlantic bumper (*Chloroscombrus chrysurus*), spotted seatrout (*Cynoscion nebulosus*), pigfish (*Orthopristis chrysoptera*), and black drum (*Pogonias cromis*). At depths <100 m, several clupeids (*Brevoortia patronus*, *Opisthonema oglinum*, and *Sardinella aurita*), several serranids (*Centropristis striata*, *Diplectrum formosum*, and *Serraniculus pumilio*), Atlantic croaker (*Micropogonias undulatus*), and spot (*Leiostomus xanthurus*) were most common in collections.

Local ichthyoplankton surveys from near Mobile Bay (Marley, 1983; Shipp, 1982, 1984, 1987) and offshore of Mississippi (Stuck and Perry, 1981b) revealed less diverse assemblages. Stuck and Perry (1981b) collected 95 taxa in 43 families during a year-long survey. Monthly occurrences of the most important taxa collected in their survey are given in Table 2-6. Three families numerically dominated the catches: jacks (Carangidae), anchovies (Engraulidae) and drums (Sciaenidae). Atlantic bumper was the most abundant taxon collected, representing 38.8% of the catches. Most larval fishes were collected during a 7-month period from April to October; catches decreased considerably during colder months (November to March).

Species such as Atlantic croaker, spot, and Gulf menhaden (*Brevoortia patronus*) migrate to the outer shelf during winter months to spawn. Consequently, larvae of these species often are numerically dominant during winter months (Shipp, 1987). Larvae of speciose families such as engraulids (*Anchoa* spp.), searobins (*Prionotus* spp.), tonguefishes (*Symphurus* spp.), and pufferfishes (*Sphoeroides* spp.) were collected during all months (Shipp, 1984, 1987).

Larval fishes are highly dependent on small zooplankton until they can feed on larger prey. In the northern Gulf of Mexico, the diets of Atlantic croaker, Gulf menhaden, and spot consist mainly of copepods and copepod nauplii, larval bivalves, pteropods, and the dinoflagellate *Prorocentrum* sp. (Govoni et al., 1989).

Although Mobile Bay has not been studied specifically, its discharge plume could serve as an important aggregation site for larval fishes. A series of investigations has shown that ichthyoplankton aggregate at the frontal zone of the Mississippi River discharge plume (Govoni et al., 1989; Grimes and Finucane, 1991; Govoni and Grimes, 1992). Grimes and Finucane (1991) sampled larval fishes, chlorophyll *a*, and zooplankton along transects traversing the discharge plume. Total ichthyoplankton catch per tow, individual surface chlorophyll *a* values, and zooplankton volumes were all significantly greater in frontal waters than adjacent shelf or plume waters. Hydrodynamic convergence and the continually reforming turbidity fronts associated with the discharge plume probably accounted for the concentration of larval fishes at the front. These investigators hypothesized that frontal waters provide feeding and growth opportunities for larvae. Bothids (lefteye flounders), carangids, cynoglossids (tonguefishes) engraulids, exocoetids (flying fishes and halfbeaks), gobiids (gobies), sciaenids, scombrids (mackerels and tunas), synodontids (lizardfishes), and tetraodontids (pufferfishes) were the 10 most frequently caught taxa in the plume/shelf samples off the Mississippi River Delta (Grimes and Finucane, 1991).

Table 2-5. Spawning times of economically important fishes (F) and invertebrates (I) in the northern Gulf of Mexico (adapted from Barry A. Vittor & Associates, Inc., 1985).												
Species	Month											
	J	F	M	A	M	J	J	A	S	O	N	D
<b>Cold Water Spawners</b>												
<i>Archosargus probatocephalus</i> (F)												
<i>Brevoortia patronus</i> (F)												
<i>Leiostomus xanthurus</i> (F)												
<i>Micropogonias undulatus</i> (F)												
<i>Mugil cephalus</i> (F)												
<i>Paralichthys albigutta</i> (F)												
<i>P. lethostigma</i> (F)												
<i>Peprilus burti</i> (F)												
<i>Pogonias cromis</i> (F)												
<i>Pomatomus saltatrix</i> (F)												
<i>Penaeus aztecus</i> (I)												
<b>Warm Water Spawners</b>												
<i>Arius felis</i> (F)												
<i>Caranx hippos</i> (F)												
<i>Cynoscion arenarius</i> (F)												
<i>C. nothus</i> (F)												
<i>Lutjanus campechanus</i> (F)												
<i>L. synagris</i> (F)												
<i>Peprilus alepidotus</i> (F)												
<i>Rachycentron canadum</i> (F)												
<i>Sciaenops ocellatus</i> (F)												
<i>Scomberomorus maculatus</i> (F)												
<i>Tarpon atlanticus</i> (F)												
<i>Penaeus duorarum</i> (I)												
<i>P. setiferus</i> (I)												
<b>Year Round Spawners</b>												
<i>Anchoa mitchilli</i> (F)												
<i>Caranx crysos</i> (F)												

Table 2-6. Occurrence ( ) and peak seasonal occurrence ( • ) of larval fishes in coastal waters of Mississippi (Adapted from: Stuck and Perry, 1981b).

Family	Genus/Species	Month											
		J	F	M	A	M	J	J	A	S	O	N	D
Clupeidae	<i>Brevoortia</i> spp.												
	<i>B. patronus</i>			•	•					•	•	•	
Engraulidae	<i>Anchoa</i> spp.	•	•								•	•	•
	<i>A. hepsetus</i>	•	•	•	•	•	•	•	•	•	•	•	•
Ophidiidae	<i>Brotula barbata</i>	•										•	•
Syngnathidae	<i>Hippocampus erectus</i>				•	•			•		•		
	<i>Syngnathus floridae</i>				•	•	•		•	•			
	<i>S. louisianae</i>				•	•	•	•	•	•	•	•	•
Serranidae	<i>Centropristis</i> spp.	•	•	•	•	•		•		•	•	•	•
	<i>C. striata</i>	•	•	•		•				•	•	•	
	<i>Diplectrum</i> spp.	•	•	•	•					•	•	•	•
	<i>D. formosum</i>	•	•	•			•	•			•	•	
Carangidae	<i>Caranx</i> sp.	•	•	•	•	•	•	•	•	•	•	•	•
	<i>C. crysos</i>			•	•	•				•	•	•	
	<i>Chloroscombrus chrysurus</i>				•	•					•		
	<i>Decapterus punctatus</i>			•							•	•	
	<i>Oligoplites saurus</i>				•	•				•	•	•	
	<i>Selar crumenophthalmus</i>				•	•	•	•	•	•	•		
	<i>Selene</i> spp.					•	•				•	•	
	<i>Trachinotus</i> spp.				•	•	•	•	•	•			
Sparidae	<i>Archosargus probatocephalus</i>				•	•							
	<i>Lagodon rhomboides</i>	•	•	•	•							•	•
Sciaenidae	<i>Bairdiella chrysoura</i>			•						•	•		
	<i>Cynoscion arenarius</i>		•			•	•			•	•		
	<i>C. nebulosus</i>		•	•						•	•		
	<i>C. nothus</i>					•	•	•	•			•	
	<i>Larimus fasciatus</i>				•	•	•	•	•		•	•	
	<i>Leiostomus xanthurus</i>		•	•	•						•	•	
	<i>Menticirrhus</i> spp.		•	•	•	•	•	•	•	•	•	•	•
	<i>Micropogonias undulatus</i>		•	•	•					•			
	<i>Sciaenops ocellatus</i>								•			•	
	<i>Stellifer lanceolatus</i>				•	•	•	•	•	•	•		
Mugilidae	<i>Mugil cephalus</i>	•	•	•	•	•	•	•	•	•	•	•	•
Scombridae	<i>Scomberomorus maculatus</i>				•	•	•	•	•	•			

Stromateidae	<i>Peprilus alepidotus</i>				•	•	•	•	•	•	•	•	
	<i>P. burti</i>	•	•	•	•	•	•				•	•	•
Triglidae	<i>Prionotus</i> spp.				•	•	•	•		•	•	•	
Bothidae	<i>Citharichthys/Etropus</i> spp.				•	•	•	•	•	•	•	•	•
	<i>Citharichthys spilopterus</i>	•	•	•		•	•				•	•	
	<i>Paralichthys</i> spp.			•	•				•				
Cynoglossidae	<i>Symphurus</i> spp.				•	•				•	•	•	•
Balistidae	<i>Monacanthus hispidus</i>					•	•	•	•	•	•		•
Tetraodontidae	<i>Sphoeroides</i> spp.				•	•	•	•	•				
	<i>S. parvus</i>					•	•	•		•		•	

### 2.3.2.2 Squids

Squids (cephalopods) display patchy distributions and periodic vertical and horizontal migrations. Water quality, currents, and temperature principally control the occurrence of squids, while food and population density affect movements within suitable water masses.

Squids most likely to occur in or near the project area include *Doryteuthis plei*, *Loligo pealei*, and *Loliguncula brevis*. *Loliguncula brevis* is common nearshore, frequenting salinities as low as 17 ppt. *Doryteuthis plei* and *L. pealei* usually live in the more saline shelf waters (Lipka, 1975). The most recent commercial catch statistics from the NMFS (U.S. Department of Commerce, NMFS, 1998) indicate that some squids are caught and sold in the eastern Gulf, particularly the northernmost locations. *Loligo* and *Loliguncula* make up the bulk of this catch, although neither the fishermen nor the markets separate the catch by species. This catch is both temporally and geographically variable, but is consistently of minimal commercial importance, contributing much less than 1% of the total commercial catch of all species from any reporting grid. The bulk of the squid catch appears to be bycatch from the commercial shrimping fleet.

### 2.3.2.3 Fishes

Pelagic fishes occur throughout the water column from the beach to the open ocean. Water column structure (temperature, salinity, turbidity) partitions this vast habitat. On a broad scale, pelagic fishes recognize different water masses based upon physical and biological characteristics. The basic subdivision of pelagic fishes is oceanic pelagic and coastal pelagic. Primarily coastal pelagic species are found in the vicinity of the sand resource areas.

Major coastal pelagic families occurring in the region are Carcharhinidae (requiem sharks), Elopidae (ladyfish), Engraulidae (anchovies), Clupeidae (herrings), Scombridae (mackerels and tunas), Carangidae (jacks and scads), Mugilidae (mulletts), Pomatomidae (bluefish), and Rachycentridae (cobia). Coastal pelagic species traverse shelf waters of the region throughout the year. Some species form large schools (e.g., Spanish mackerel, *Scomberomorus maculatus*), while others travel singly or in small groups (e.g., cobia, *Rachycentron canadum*). The distribution of most species depends upon water column structure, which varies spatially and seasonally. Some coastal pelagic species show an affinity for vertical structure and are often observed around natural or artificial structures (e.g., dredges or oil and gas platforms), where they are best classified as transients rather than true residents. This is particularly true for Spanish sardine (*Sardinella aurita*),

round scad (*Decapterus punctatus*), blue runner (*Caranx crysos*), king mackerel (*Scomberomorus cavalla*), and cobia (Klima and Wickham, 1971; Chandler et al., 1985).

Coastal pelagic fishes can be divided into two ecological groups. The first group includes large predatory species such as king and Spanish mackerels, bluefish (*Pomatomus saxatilis*), cobia, jacks (*Caranx* spp.), and little tunny (*Euthynnus alletteratus*). These species typically form schools, undergo migrations, grow rapidly, mature early, and exhibit high fecundity. Each of these species is important to some extent to regional fisheries. The second group exhibits similar life history characteristics, but the species are smaller in body size and planktivorous. This group is composed of anchovies (*Anchoa* spp.), Gulf menhaden (*Brevoortia patronus*), round scad, Spanish sardine, striped mullet (*Mugil cephalus*), and thread herring (*Opisthonema oglinum*). Species in the second group are preyed upon by the larger species in the first group; thus, the two are ecologically important in energy transfer in the nearshore environment (Saloman and Naughton, 1983a,b, 1984a,b). The food habits of five predatory species (bluefish, cobia, crevalle jack [*Caranx hippos*], and king and Spanish mackerels) in the northern Gulf of Mexico are given in Table 2-7.

With the exception of king mackerel, migratory routes and schedules of the large-bodied, predatory coastal pelagic species are not well known or documented. King mackerel occurring in the shelf waters of the region actually may come from two distinct populations (Johnson et al., 1994). The eastern population migrates from near the Mississippi Delta eastward, then southward around the Florida peninsula, wintering off southeastern Florida (Sutter et al., 1991). The western population travels to waters off the Yucatan Peninsula during winter. In summer, both populations migrate to the northern Gulf of Mexico, where they intermix to an unknown extent (Johnson et al., 1994). Spanish mackerel, cobia, bluefish, crevalle jack, and coastal sharks (*Carcharhinus* spp.) are migratory, but their routes have not been studied. Spanish mackerel, bluefish, and crevalle jack generally migrate westward along the shelf in warm months and back eastward towards Florida during cold months (Barry A. Vittor & Associates, 1985).

Coastal pelagic fishes are important to both commercial and recreational fisheries of the region. Fisheries landings provide the best available source of temporal patterns in occurrence of coastal pelagic species in the region (Table 2-8). Commercial purse seine fisheries landed 392 metric tons of coastal pelagic species offshore Alabama in 1997 (U.S. Department of Commerce, NMFS, 1998). Some species are targeted by the purse seine fishery while others are captured incidentally (Da Silva and Condrey, 1998). The Gulf menhaden fishery perennially produces the highest fishery landings in the continental U.S. (U.S. Department of Commerce, 1991). Menhaden form large, surface feeding schools in waters near the Mississippi Delta and eastward to Florida from April through September. Fishermen take advantage of this schooling behavior, capturing millions of pounds each year with large purse nets. Other coastal pelagic species contributing high commercial landings in the region include striped mullet and Spanish mackerel (Table 2-8).

#### **2.3.2.4 Sea Turtles**

Five species of sea turtles may occur offshore Alabama (Table 2-9). All are protected under the Endangered Species Act of 1973. The loggerhead sea turtle (*Caretta caretta*) is a threatened species. The hawksbill (*Eretmochelys imbricata*), Kemp's ridley (*Lepidochelys kempii*), and leatherback (*Dermochelys coriacea*) sea turtles are endangered species. The Atlantic green sea turtle (*Chelonia mydas*) is threatened, except for the Florida breeding population, which is endangered.

Loggerheads are expected to be the most common turtle in the project area, as they are the most abundant turtle on the northern Gulf shelf (Lohofener et al., 1990; Mullin and Hoggard, 1998). Lohofener et al. (1990) estimated that 92% of the turtles they observed during aerial surveys of the northern Gulf were loggerheads. Leatherbacks are abundant in the northern Gulf, but primarily in deep waters of the continental slope and beyond (Hansen et al., 1996; Mullin and Hoggard, 1998);

COMMON NAME	Scientific Name	Primary Stomach Contents (based on percent occurrence)	Area and Source
Bluefish	<i>Pomatomus saltatrix</i>	Fishes (herrings, jacks, drums, and seatrout)	Northwest Florida (Saloman and Naughton, 1984b)
Cobia	<i>Rachycentron canadum</i>	Crustaceans (swimming crabs and mantis shrimps)	Louisiana, Mississippi, Alabama, and Florida (Meyer and Franks, 1996)
Crevalle jack	<i>Caranx hippos</i>	Fishes (herrings and jacks)	Northwest Florida (Saloman and Naughton, 1984a)
King mackerel	<i>Scomberomorus cavalla</i>	Fishes (herrings, jacks, and unidentified)	Northwest Florida (Saloman and Naughton, 1983a)
Spanish mackerel	<i>Scomberomorus maculatus</i>	Fishes (herrings, jacks, and unidentified)	Northwest Florida (Saloman and Naughton, 1983b)

Species	Month												Total
	Jan	Feb	Mar	Apr	May	Jun	Jul	Aug	Sep	Oct	Nov	Dec	
Menhaden	144,828	74,133	160,974	656,885	1,015,611	640,227	1,086,096	663,861	881,567	247,331	50,219	126,992	5,748,724
Striped mullet	186,366	143,129	202,929	129,637	122,614	134,230	167,661	211,244	248,348	346,568	890,641	207,599	2,990,966
Other mullets	0	0	0	0	0	0	0	0	0	113,875	557,210	37,315	708,400
Spanish mackerel	0	0	0	523,550	21,232	1,016	7,560	34,089	12,324	5,989	0	0	605,760
Sharks (Unclassified)	0	15,146	4,857	15,008	0	0	0	0	0	67,946	0	0	102,957
Blue runner	0	0	0	18,777	0	0	0	0	0	0	0	0	18,777
Bluefish	0	0	0	2,079	0	2,507	1,160	1,484	6,578	226	0	0	14,034
Cobia	0	0	0	613	1,486	1,241	831	0	313	0	0	0	4,484

Table 2-9. Sea turtle species potentially occurring in coastal Alabama waters.				
Common Name	Scientific Name	Habitat Associations	Diet (adults)	Nesting Season <sup>a</sup> (Fla. Panhandle area)
Loggerhead sea turtle	<i>Caretta caretta</i>	Coastal, shelf, and slope waters	Benthic fauna (generalist)	May 1 - Nov 30
Green sea turtle	<i>Chelonia mydas</i>	Shallow coastal waters, seagrass beds	Seagrasses, algae, associated organisms	May 1 - Oct 31 <sup>b</sup>
Leatherback sea turtle	<i>Dermochelys coriacea</i>	Coastal, shelf, and slope waters (most abundant on slope)	Cnidarians (e.g., jellyfishes)	May 1 - Sept 30 <sup>b</sup>
Kemp's ridley sea turtle	<i>Lepidochelys kempii</i>	Shallow coastal waters, seagrass beds	Crabs, shrimps, etc.	(no nesting in area)
Hawksbill sea turtle	<i>Eretmochelys imbricata</i>	Coral reefs, hard bottom areas	Sponges	(no nesting in area)

<sup>a</sup> Sea turtle nesting seasons for the Florida Panhandle area as stated by the Minerals Management Service (1997).

<sup>b</sup> Green sea turtles are listed as nesting on Alabama beaches, but leatherbacks are not (Alabama Game and Fish Division, 1997). However, occasional nests and false crawls for both species have been observed nearby in the Florida Panhandle area (summarized by Minerals Management Service, 1997).

however, they also occur on the shelf in smaller numbers. Green, hawksbill, and Kemp's ridley turtles are typically inshore species that may occur in the project area, but little is known of their abundance.

There is a significant nesting subpopulation of loggerhead turtles along the Florida Panhandle, and some loggerhead nesting on Alabama beaches. Therefore, increased loggerhead densities may be expected during nesting season, which in the Panhandle region extends from 1 May through 30 November (Minerals Management Service, 1997). Although green turtles may nest on Alabama beaches (Alabama Game and Fish Division, 1997), the Minerals Management Service (1997) indicates that green turtle nesting in the northern Gulf is "isolated and infrequent" during the season lasting from 1 May through 31 October. Leatherbacks occasionally nest on Florida Panhandle beaches from 1 May through 30 September (Minerals Management Service, 1997) but are not listed as nesting in Alabama by the Alabama Game and Fish Division (1997). Hawksbill and Kemp's ridley turtles do not nest anywhere near the project area.

In addition to the occurrence of sea turtle adults, juveniles, and hatchlings in the water column, some adults may partially bury themselves in bottom sediments to avoid cold spells during winter. This phenomenon is known as "brumation" (essentially another term for hibernation) (Carr et al., 1981; Byles and Dodd, 1989). Little is known of the frequency of this behavior or the likelihood of turtles brumating in bottom sediments of the project area during winter. Lohofener et al. (1990) reported that some loggerheads observed in the northern Gulf during February and March had mud lines on their carapaces, possibly indicating that the turtles had buried themselves in bottom sediments. In south Florida, Byles and Dodd (1989) noted that a female loggerhead brumated for periods up to 5 days when water temperatures fell below 18°C. Green sea turtles also may brumate during cold weather (Ehrhart, 1977).

### **Loggerhead Sea Turtle**

The loggerhead sea turtle is found in estuarine, coastal, and shelf waters from South America to Newfoundland. Adults of this predominantly subtropical species occur widely in coastal and shelf waters of the northern Gulf of Mexico, where they are the most abundant turtles seen during aerial surveys (Lohofener et al., 1990; Mullin and Hoggard, 1998). Juveniles are pelagic, inhabiting wrack lines and *Sargassum* rafts and drifting in current gyres for several years. It is believed that subadults move into nearshore and estuarine areas.

Loggerhead nesting in U.S. waters occurs from New Jersey to Texas (Frazier, 1995), and at least four nesting subpopulations have been identified (Byles et al., 1996). The major U.S. nesting area is in southeastern Florida, which is second only to Oman in worldwide importance (Dodd, 1988; National Research Council, 1990; NMFS, 1990). Much smaller but important regular nesting aggregations occur in South Carolina, Georgia, and North Carolina. In the NEGOM, there is a Florida Panhandle nesting subpopulation located in the vicinity of Eglin Air Force Base and the Panama City area (Byles et al., 1996). Nesting has been reported on Gulf Shores and Dauphin Island, Alabama (Fuller et al., 1987). The Florida Panhandle nesting season extends from 1 May through 30 November (Minerals Management Service, 1997). Incubation lasts about 60 to 95 days. Hatchlings swim offshore and begin a pelagic existence within *Sargassum* rafts.

Loggerhead adults are generalist carnivores feeding primarily on nearshore benthic mollusks and crustaceans (Dodd, 1988). Pelagic stages feed on coelenterates and cephalopods.

### **Atlantic Green Sea Turtle**

The Atlantic green sea turtle has a circumglobal distribution in tropical and subtropical waters. In the U.S., it occurs in Caribbean waters around the U.S. Virgin Islands and Puerto Rico, and along

the mainland coast from Texas to Massachusetts. Green turtles are typically found in shallow coastal waters, particularly in association with seagrass beds.

The primary nesting sites in U.S. Atlantic waters are high-energy beaches along the east coast of Florida, with additional sites in the U.S. Virgin Islands and Puerto Rico (NMFS and U.S. Fish and Wildlife Service [USFWS], 1991). The Minerals Management Service (1997) indicates that reports of green turtle nesting in the northern Gulf are “isolated and infrequent,” including beaches of the Florida Panhandle and unconfirmed reports of nesting in Alabama. The Alabama Game and Fish Division (1997) lists green turtles as nesting on Alabama beaches. Hatchlings swim out to sea and enter a pelagic stage in *Sargassum* mats associated with convergence zones.

Adult green turtles commonly feed on seagrasses, algae, and associated organisms, using reefs and rocky outcrops near seagrass beds for resting areas. Important feeding grounds in Florida, including Indian River Lagoon, the Florida Keys, Florida Bay, Homosassa, Crystal River, and Cedar Key, are all well to the south of the project area.

### **Leatherback Sea Turtle**

The leatherback sea turtle is a circumglobal species, currently divided into two subspecies (Thompson and Huang, 1993). The subspecies of interest here is *Dermochelys coriacea coriacea* which inhabits waters of the western Atlantic Ocean from Newfoundland to northern Argentina. The leatherback is the largest living turtle (Eckert, 1995), and with its unique deep-diving abilities (Eckert et al., 1986) and wide-ranging migrations, is considered the most pelagic of the sea turtles (Marquez, 1990). It is the most abundant turtle on the continental slope of the northern Gulf (Hansen et al., 1996; Mullin and Hoggard, 1998). However, leatherbacks also can be present in shelf waters (Lohofener et al., 1990; Mullin and Hoggard, 1998).

Leatherbacks nest on coarse-grained, high-energy beaches (i.e., beaches exposed to strong wave action) in tropical latitudes (Eckert, 1995). Florida is the only location in the continental U.S. where significant leatherback nesting occurs. Nesting on the Atlantic coast of Florida may sometimes approach that reported in the Caribbean, but nest density is considerably lower. Some nesting along the Florida Panhandle has been reported between 1 May and 30 September (Minerals Management Service, 1997), but leatherbacks are not listed as nesting on Alabama beaches (Alabama Game and Fish Division, 1997). Incubation lasts about 60 to 75 days. Very little is known of the pelagic distribution of hatchling and/or juvenile leatherback turtles.

Adult leatherbacks feed primarily on cnidarians (medusae, siphonophores) and tunicates (salps, pyrosomas) (Eckert, 1995). The turtles are sometimes observed in association with jellyfishes, but actual feeding behavior only occasionally has been documented. Foraging has been observed at the surface, but also is likely to occur at depth (Eckert, 1995).

### **Kemp's Ridley Sea Turtle**

The Kemp's ridley sea turtle is the smallest and most endangered of the sea turtles. Its distribution extends from the Gulf of Mexico to New England, and occasionally as far north as Nova Scotia. Adult turtles are usually found in the Gulf of Mexico, primarily in shallow coastal waters less than 50 m deep (Byles, 1988). Juveniles may move northward along the U.S. Atlantic coast in spring with the Gulf Stream to feed in productive, coastal waters between Georgia and New England (NMFS and USFWS, 1992); these migrants then move southward with the onset of cooler temperatures in late fall and winter. In the Gulf of Mexico, juvenile Kemp's ridleys occupy nearshore waters (Rudloe et al., 1991; Shaver, 1991; Renaud, 1993), but they may move to deeper waters as temperatures cool during winter (Henwood and Ogren, 1987).

Nesting of Kemp's ridleys occurs almost entirely at Rancho Nuevo beach, Tamaulipas, Mexico, where 95% of the nests are laid along 60 km of beach (NMFS and USFWS, 1992; Weber,

1995). More than half of the adult females nest every year between April and mid-August, while the remainder may or may not skip certain years (National Research Council, 1990). In the U.S., nesting occurs infrequently on Padre and Mustang Islands in south Texas from May to August. No Kemp's ridley nesting occurs near the project area.

After emerging, Kemp's ridley hatchlings swim offshore to inhabit *Sargassum* mats and drift lines associated with convergences, eddies, and rings, where they feed at the surface. Adult Kemp's ridleys are carnivorous benthic feeders, preferring crabs, but also occasionally eating mollusks, shrimp, dead fishes, and vegetation (Mortimer, 1982; Lutcavage and Musick, 1985; Shaver, 1991; Burke et al., 1993; Werner and Landry, 1994). When adult ridleys are not migrating to or from their nesting beach, they inhabit crab-rich waters, such as those close to the Mississippi River Delta (Pritchard, 1989; National Research Council, 1990). The distribution of Kemp's ridleys also is associated with seagrass beds, which support a rich crustacean fauna (Lutcavage and Musick, 1985).

### **Hawksbill Sea Turtle**

Hawksbill sea turtles occur in tropical and subtropical seas of the Atlantic, Pacific, and Indian Oceans. In the western Atlantic, hawksbill turtles are generally found in clear tropical waters near coral reefs, including the Caribbean, Bahamas, Florida Keys, and southwestern Gulf of Mexico. Hawksbills are the least frequently reported turtle in the Gulf of Mexico (Hildebrand, 1982) and are not expected to be common off the Alabama coast.

Nesting areas for hawksbills in the Atlantic are found in the U.S. Virgin Islands, Puerto Rico, and south Florida. Within the continental U.S., nesting beaches are restricted to the southeast coast of Florida (i.e., Volusia through Dade Counties) and the Florida Keys (Monroe County), as noted by Meylan (1992) and the NMFS and USFWS (1993). No hawksbill nesting occurs near the project area.

Adult hawksbills typically are associated with coral reefs and similar hard bottom areas, where they forage on sponges. Hatchlings are pelagic, drifting with *Sargassum* rafts. Juveniles shift to a benthic foraging existence in shallow waters, progressively moving to deep waters as they grow and become capable of deeper dives for sponges.

### **2.3.2.5 Marine Mammals**

Up to 28 cetacean species occur in the northern Gulf of Mexico, including 7 species of mysticetes (baleen whales) and 21 species of odontocetes (toothed whales) (Jefferson and Schiro, 1997). However, only two cetacean species commonly occur in Gulf coastal waters: the Atlantic spotted dolphin (*Stenella frontalis*) and the bottlenose dolphin (*Tursiops truncatus*) (Davis et al., 1996, 1998). These two are the most likely marine mammals to be found in and near the project area. Two other marine mammals potentially occurring in the region are a sirenian (the Florida manatee, *Trichechus manatus latirostris*) and an exotic pinniped (the California sea lion, *Zalophus californianus*). Of these four marine mammals, only the Florida manatee is a listed species (endangered) under the Endangered Species Act of 1973. All marine mammals are protected under the Marine Mammal Protection Act of 1972.

### **Atlantic Spotted Dolphin**

Atlantic spotted dolphins are widely distributed in warm temperate and tropical waters of the Atlantic Ocean, including the Gulf of Mexico (Perrin et al., 1987, 1994). In the northern Gulf, these animals occur mainly on the continental shelf (Jefferson and Schiro, 1997). During recent aerial and shipboard surveys in the northern Gulf of Mexico for the MMS-sponsored GulfCet II program,

Atlantic spotted dolphins were seen at water depths ranging from 22 to 222 m (Mullin and Hoggard, 1998).

Atlantic spotted dolphins can be expected to occur near the project area during all seasons. However, they may be more common during spring. According to Blaylock et al. (1995), it has been suggested that there may be a seasonal movement of this species onto the continental shelf in spring, but data supporting this hypothesis are limited (Fritts et al., 1983). Jefferson and Schiro (1997) indicate that there is a peak in sightings and sightings per unit effort during spring. The GulfCet II data confirm that Atlantic spotted dolphins are present on the shelf during all seasons with the highest number of sightings during spring (Mullin and Hoggard, 1998).

Favored prey of Atlantic spotted dolphins include herrings, anchovies, and carangid fishes (Schmidly, 1981). Mating has been observed in July, with calves born offshore. Atlantic spotted dolphins often occur in groups of up to 50 individuals.

### **Bottlenose Dolphin**

Bottlenose dolphins in the western Atlantic range from Nova Scotia to Venezuela, as well as the waters of the Gulf of Mexico (Hansen and Blaylock, 1994). This species is distributed worldwide in temperate and tropical inshore waters.

Bottlenose dolphins along the U.S. coastline are believed to be organized into local populations, each occupying a small region of coast with some migration to and from inshore and offshore waters (Schmidly, 1981). The NMFS recognizes a northern Gulf of Mexico coastal stock of bottlenose dolphins (Blaylock et al., 1995). It has been defined for management purposes as those bottlenose dolphins occupying the nearshore coastal waters in the Gulf of Mexico from the Mississippi River mouth to about 84°W longitude and extending from shore, barrier islands, or presumed bay boundaries to 9.3 km seaward of the 18.3-m isobath. Bottlenose dolphins in the project area are presumed to belong to this stock.

During GulfCet II aerial and shipboard surveys, bottlenose dolphins were sighted on the continental shelf off Mobile Bay during all seasons (Mullin and Hoggard, 1998). Water depths of sightings ranged from 30 to 702 m. Bottlenose dolphins were the most abundant cetacean sighted on the continental shelf.

Bottlenose dolphins feed on a variety of fishes, mollusks, and arthropods. Mating and calving occur from February to May. Gestation lasts about 12 months, and the calving interval is 2 to 3 years (Schmidly, 1981). They are found in groups of up to several hundred individuals with group sizes decreasing with distance from shore.

### **Florida Manatee (Endangered Species)**

The West Indian manatee is one of the most endangered marine mammals in U.S. coastal waters. In the southeastern U.S., manatees are limited primarily to Florida and Georgia. This group constitutes a separate subspecies called the Florida manatee that appears to be divided into at least two virtually separate populations -- one centered along the Atlantic coast and the other on the Gulf coast of Florida (USFWS, 1996). Despite concerted research, it has not been possible to develop a reliable estimate of manatee abundance in Florida. The highest single-day count of manatees from an aerial survey is 1,856 animals in January 1992 (Ackerman, 1995).

During winter months, the manatee population confines itself to the coastal waters of the southern half of peninsular Florida and to springs and warm water outfalls as far north as southeast Georgia (USFWS, 1996). As water temperatures rise in spring, manatees disperse from winter aggregation areas. During summer months, they may migrate as far north as coastal Virginia on the east coast and the Louisiana coast in the Gulf of Mexico (USFWS, 1996). On the Florida west coast, sightings drop off sharply north of the Suwannee River (Marine Mammal Commission, 1986),

although about 12 to 15 manatees are seen each summer in the Wakulla River at the base of the Florida panhandle. Louisiana is considered the western limit of the Florida manatee's range (Powell and Rathbun, 1984; Lefebvre et al., 1989).

Manatees inhabit both salt and fresh water of sufficient depth (1.5 m to usually less than 6 m) throughout their range. They may be encountered in canals, rivers, estuarine habitats, saltwater bays, and on occasion have been observed as much as 6 km off the Florida Gulf coast (USFWS, 1996)

Based on their known distribution patterns, a few Florida manatees occasionally could be present in Alabama waters during summer months. However, because these animals tend to stay in shallow water, they are considered unlikely to be present in the project area. The Alabama Game and Fish Division (1997) lists them as a Federally endangered species, but with the notation "not believed to occur in Alabama."

Critical habitat for this endangered species has been designated by the USFWS. All of the critical habitat areas are in peninsular Florida, predominantly along the southwest and southeast coasts (USFWS, 1996).

### **California Sea Lion**

One exotic pinniped species, the California sea lion, is present in the northern Gulf. This species normally occurs only on the Pacific coast. However, a few feral animals are present in the northern Gulf, probably individuals that escaped or were released from marine parks (Schmidly, 1981; Minerals Management Service, 1997).

In the northern Gulf, California sea lions often are seen on or near sea buoys, where they may remain for several months (Schmidly, 1981). There have been sightings off Mobile Bay and near the mouth of the Mississippi River. According to Schmidly (1981), Lowery (1974) reported that a California sea lion visited an oil company barge 51.5 km south of Cameron, Louisiana daily for about a month in August and September 1971, sunning itself on the deck. It seems possible, though unlikely, that a California sea lion could occur in the project area during any season.

California sea lions feed on squids and small fishes. They are polygamous and have a single pup after a gestation period of 11 to 12 months (Schmidly, 1981).

### **Other Listed Species**

In addition to the Florida manatee, endangered marine mammals potentially occurring in the northern Gulf of Mexico include six species of mysticetes (blue whale, *Balaenoptera musculus*; fin whale, *B. physalus*; humpback whale, *Megaptera novaeangliae*; northern right whale, *Eubalaena glacialis*; and sei whale, *B. borealis*) and one odontocete (the sperm whale, *Physeter macrocephalus*). However, the Gulf of Mexico is outside the normal range of most mysticetes, and Bryde's whale (*B. edeni*, a non-listed species) is the only mysticete commonly occurring there (Davis and Fargion, 1996; Jefferson and Schiro, 1997; Mullin and Hoggard, 1998). The endangered mysticetes are likely to be represented in the Gulf only by occasional strays (Jefferson and Schiro, 1997) and because these large whales prefer deep waters well offshore of the continental shelf (Davis et al., 1998), they would be very unlikely to occur in the project area. Sperm whales are common in the northern Gulf and particularly favor an area just south of the Mississippi River mouth (Hansen et al., 1996; Mullin and Hoggard, 1998). However, these large whales also prefer deepwater habitats and would be very unlikely to occur in the project area. No critical habitat for these endangered large whales is located near the project area.

Another endangered species formerly known from the Gulf of Mexico (the Caribbean monk seal, *Monachus tropicalis*) is now extinct (Schmidly, 1981). The Caribbean monk seal was listed as endangered throughout its range on 10 April 1979. The last reliable sighting of a Caribbean

monk seal occurred in 1952. No confirmed sightings have been reported since then. Many scientists believe that the species has been extinct since the early 1950's. No recovery effort is currently being made for this species (NMFS, 1998).

Boyd and Stanfield (1998) reported circumstantial evidence for the presence of monk seals in the West Indies, suggesting that they may not be extinct. The conclusion was based on interviews with fishermen, some of whom chose monk seals when asked to select pictures of marine species known to them. Some fishermen also gave information about size and color that was consistent with many of these seals being monk seals. However, Early (1998) suggested that extralimital arctic seals may account for at least some of the sightings. Even if monk seals are found to be not extinct, they can be assumed not to occur in the project area based on the absence of sightings in the Gulf of Mexico in recent decades.

## **3.0 REGIONAL GEOMORPHIC CHANGE**

Nearshore sediment transport processes influence the evolution of shelf sedimentary environments to varying degrees depending on temporal and spatial response scales. Although micro-scale processes, such as turbulence and individual wave orbital velocities, determine the magnitude and direction of individual grain motion, variations in micro-scale processes are considered noise at regional-scale and only contribute to coastal response in an average sense. By definition, regional-scale geomorphic change refers to the evolution of depositional environments for large coastal stretches (10 km or greater) over extended time periods (decades or greater) (Larson and Kraus 1995). An underlying premise for modeling long-term morphologic change is that a state of dynamic equilibrium is reached as a final stage of coastal evolution. However, the interaction between the scale of response and forces causing change may result in a net sediment deficit or surplus within a system, creating disequilibrium. This process defines the evolution of coastal depositional systems.

Topographic and hydrographic surveys of coastal and nearshore morphology provide a direct source of data for quantifying regional geomorphology and change. Historically, hydrographic data have been collected in conjunction with regional shoreline position surveys by the U.S. Coast and Geodetic Survey (USC&GS); currently Coast and Geodetic Survey of the National Ocean Service [NOS], National Oceanographic and Atmospheric Administration). Comparison of digital bathymetric data for the same region but different time periods provides a method for calculating net sediment movements into (accretion) and out of (erosion) an area of study. Coastal scientists, engineers, and planners often use this information for estimating the magnitude and direction of sediment transport, monitoring engineering modifications to a beach, examining geomorphic variations in the coastal zone, establishing coastal erosion setback lines, and verifying shoreline change numerical models. The purpose of this portion of the study is to document patterns of geomorphic change throughout the sand resource areas and quantify the magnitude and direction of net sediment transport over the past 60 to 100 years. These data, in combination with wave and current measurements and model output, provide a temporally integrated technique for evaluating the potential physical impacts of offshore sand mining on sediment transport dynamics.

### **3.1 SHORELINE POSITION CHANGE**

Creation of an accurate map is always a complex surveying and cartography task, but the influence of coastal processes, relative sea level, sediment source, climate, and human activities make shoreline mapping especially difficult. In this study, shoreline surveys are used to define landward boundaries for bathymetric surfaces and to document net shoreline movements between specified time periods. Consequently, net change results can be compared with wave model output and nearshore sediment transport simulations to evaluate cause and effect. Results integration provides a direct method of documenting potential environmental impacts related to sand dredging on the OCS.

#### **3.1.1 Previous Studies**

The Gulf shoreline of Alabama is dissected by the entrance to Mobile Bay, creating a barrier island shoreline to the west (Dauphin Island) and a peninsular barrier beach to the east (Morgan Peninsula). Hardin et al. (1976) used USC&GS topographic sheets and U.S. Geological Survey (USGS) 7.5-minute quadrangle maps for the dates 1917/18, 1942, 1958, and 1974 to document shoreline advance and retreat. The 1917 shoreline illustrated a hurricane breach along central Dauphin Island (about 8.5 km wide) that filled with sediment by 1942. Concurrently, the western end of the island extended about 1.3 km into Petit Bois Pass (Hardin et al., 1976). Between 1942 and 1974, Hardin et al. (1976) documented shoreline retreat along most of western two-thirds of Dauphin Island (about 3 m/yr) and westward migration of the island of about 2 km. Byrnes et al. (1991)

quantified the lateral migration rate of western Dauphin Island for the period 1848 to 1986. They documented a rate of 55.3 m/yr (slightly higher than that reported by Hardin et al. [1976]), or about 7.6 km for the period of record. Parker et al. (1993, 1997) updated the analysis of Hardin et al. (1976) by including a 1985 shoreline interpreted from aerial photography. Because most inhabitants live on the eastern third of Dauphin Island, specific attention was given to shoreline change trends in that area between 1955 and 1985. Figure 3-1 documents specific areas of erosion with estimates of sand volume necessary to restore the beach back to its 1955 condition (Parker et al. 1993, 1997). Hummell and Smith (1996) updated the findings of Parker et al. (1993, 1997) to 1995, concluding that increased erosion in this area between 1985 and 1995 resulted in a sand volume requirement of about 1.85 MCM to restore beaches to the 1955 condition.

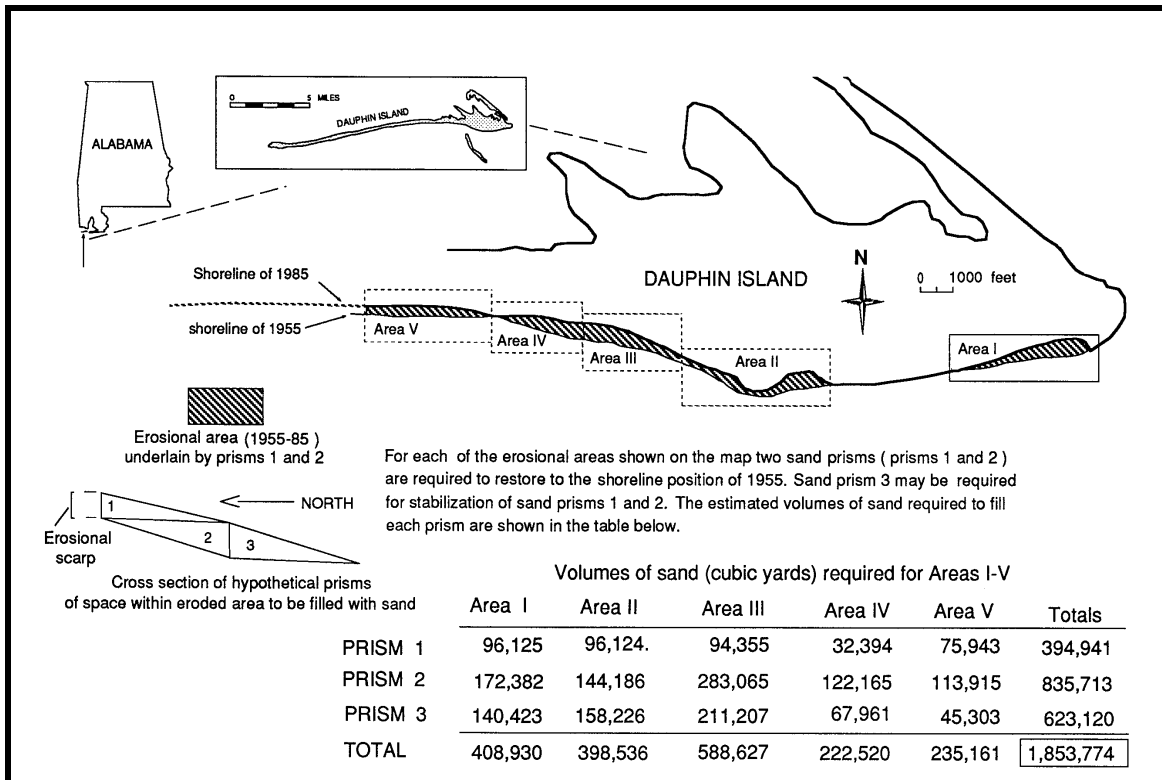


Figure 3-1. Map of southeastern Dauphin Island Gulf shoreline showing principal areas of erosion during the period 1955 to 1985 and estimated volumes of sand required for restoration of eroded areas (shaded) to the approximate position of the 1955 shoreline (from Parker et al., 1997).

For the Gulf shore of the Morgan Peninsula, from Mobile Point to Perdido Pass (about 50 km long), Hardin et al. (1976) monitored shoreline position change at five specific locations. For the period 1917 to 1974, they documented about 6 m/yr shoreline advance near Mobile Point, -0.5 m/yr at Gulf Highlands, no significant change at Gulf Shores, and -0.8 m/yr at Romar Beach. A detailed analysis of shoreline change at Perdido Pass also was included in Hardin et al. (1976), illustrating the dynamic nature of the inlet system between 1867 and 1974. Parker et al. (1997) updated this data set to 1985, documenting coastal structure placement associated with erosion hot spots (Figure 3-2) and sand volume requirements to restore beaches to 1955 conditions (about 120,000 cubic meters). Significant hurricane impacts near Gulf Shores and Orange Beach over the past few years has resulted in a reassessment of sand volume needs along the Morgan Peninsula (Hummell, 1999). It is now estimated that approximately 750,000 cubic meters of sand may be needed for beach restoration in this area in the near future.

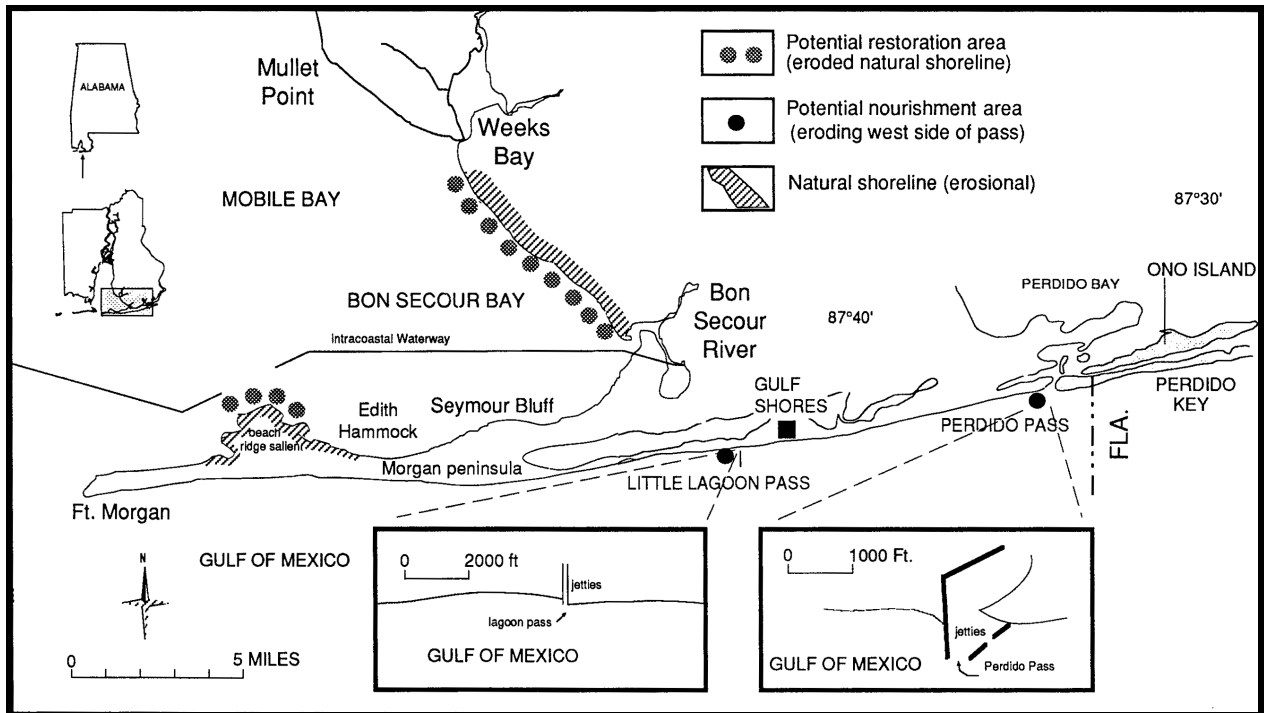


Figure 3-2. Gulf and Bon Secour Bay shoreline of Baldwin County, Alabama, showing locations of potential shoreline restoration and nourishment (from Parker et al., 1997).

### 3.1.2 Shoreline Position Data Base

For the present study, five primary outer coast shoreline surveys, conducted by the U.S. Coast and Geodetic Survey (USC&GS; predecessor to NOS) in 1847/67, 1917/18, 1934, 1957, and 1978/82 between Petit Bois Pass (west) and Perdido Pass (Table 3-1), were used to quantify historical shoreline change. The 1847/67 and 1917/18 surveys were completed as field surveys using standard planetable techniques, whereas the final three shoreline surveys were interpreted from aerial photography. Methods used for compiling and analyzing historical data sets are described in Byrnes and Hiland (1994a, b).

When determining shoreline position change, all data contain inherent errors associated with field and laboratory compilation procedures. These errors should be quantified to gauge the significance of measurements used for research/engineering applications and management decisions. Table 3-2 summarizes estimates of potential error for the shoreline data sets used in this study. Because these individual errors are considered to represent standard deviations, root-mean-square error estimates are calculated as a realistic assessment of combined potential error.

Positional errors for each shoreline can be calculated using the information in Table 3-2; however, change analysis requires comparing two shorelines from the same geographic area but different time periods. Table 3-3 is a summary of potential errors associated with change analyses computed for specific time periods. As expected, maximum positional errors are associated with the oldest shorelines (1847/67 and 1917/18) at smallest scale (1:40,000), but most change estimates for the study area document shoreline advance or retreat greater than these values.

Date	Data Source	Comments and Map Numbers
1847/67	USC&GS Topographic Maps 1:10,000 (T-1035, T-1042) 1:20,000 (T-240, T-245, T-277)	First regional shoreline survey throughout study area using standard planetable surveying techniques; 1847 - western end of Dauphin Island to entrance to Mobile Bay (T-245, T-240); 1849 - outer coastline south of Bon Secour Bay (T-277); 1867 - shoreline south of Shelby Lakes east to Perdido Pass (T-1035, T-1042).
1917/18	USC&GS Topographic Maps 1:40,000 (T-3711, T-3714)	Second regional shoreline survey along the seaward coast of the study area using standard planetable surveying techniques (regional-scale reconnaissance survey); 1917 - Dauphin Island (T-3711); 1918 - Mobile Point east to Perdido Pass (T-3714).
June/July 1934	USC&GS Topographic Maps 1:10,000	First regional shoreline survey completed using aerial photography; central Dauphin Island (T-5537); shoreline adjacent to Mobile Bay Entrance (T-5536); outer shoreline south of Bon Secour Bay (T-5535); shoreline south of Little Lagoon (T-5534); Gulf Shores (T-5497); shoreline south of Shelby Lakes (T-5498); Perdido Pass (T-5495).
November 1957	USC&GS Topographic Maps 1:10,000	All maps produced from interpreted aerial photography; Dauphin Island (T-sheets 10761, 10762, 10770, 10771, 10772); Morgan Peninsula east to shoreline south of Shelby Lakes (T-sheets 10773, 10774, 10775, 10776, 10993, 10994, 10996).
1978/82	USC&GS Topographic Maps 1:20,000	All maps produced from interpreted aerial photography; 1978 - shoreline south of Little Lagoon east to Perdido Pass (TP-sheets 00542, 00543); 1981/82 - Mobile Bay east to shoreline south of Bon Secour Bay (TP-sheets 00931, 00932); Dauphin Island (TP-sheets 00929, 00930).

Traditional Engineering Field Surveys (1847/67, and 1917/18)			
Location of rodded points	±1 m		
Location of plane table	±2 to 3 m		
Interpretation of high-water shoreline position at rodded points	±3 to 4 m		
Error due to sketching between rodded points	up to ±5 m		
Cartographic Errors (all maps for this study)	Map Scale		
	1:10,000	1:20,000	1:40,000
Inaccurate location of control points on map relative to true field location	up to ±3 m	up to ±6 m	up to ±12 m
Placement of shoreline on map	±5 m	±10 m	±20 m
Line width for representing shoreline	±3 m	±6 m	±12 m
Digitizer error	±1 m	±2 m	±4 m
Operator error	±1 m	±2 m	±4 m
Aerial Surveys (1934, 1957, 1978/82)	Map Scale		
	1:10,000	1:20,000	1:40,000
Delineating high-water shoreline position	±5 m	±10 m	±20 m
Sources: Shalowitz, 1964; Ellis 1978; Anders and Byrnes, 1991; Crowell et al., 1991.			

Table 3-3. Maximum root-mean-square potential error for shoreline change data from western Dauphin Island (at Petit Bois Pass) to Perdido Pass, Alabama.				
	1917/18	1934	1957	1978/81
1847/67	$\pm 31.7^1$	$\pm 17.3$	$\pm 17.3$	$\pm 22.6$
	$(\pm 0.5)^2$	$(\pm 0.2)$	$(\pm 0.2)$	$(\pm 0.2)$
1917/18		$\pm 20.9$	$\pm 20.9$	$\pm 32.4$
		$(\pm 1.7)$	$(\pm 0.7)$	$(\pm 0.5)$
1934			$\pm 11.8$	$\pm 18.7$
			$(\pm 0.5)$	$(\pm 0.4)$
1957				$\pm 18.7$
				$(\pm 0.8)$

<sup>1</sup> Magnitude of potential error associated with high-water shoreline position change (m); <sup>2</sup> Rate of potential error associated with high-water shoreline position change (m/yr).

### 3.1.3 Historical Change Trends

Regional change analysis completed for this study provides a without-project assessment of shoreline response for comparison with predicted changes in wave-energy focusing at the shoreline resulting from potential offshore sand dredging activities. It differs from previous studies in that continuous measurements of shoreline change are provided at 100 m alongshore intervals for the period 1847/67 to 1978/82 (see Appendix A). This way, model results (wave and sediment transport) at discreet intervals along the coast can be compared with historical data to develop process/response relationships for evaluating potential impacts. The following discussion focuses on incremental changes in shoreline response (1847/67 to 1917/18, 1917/18 to 1934, 1934 to 1957, 1957 to 1978/82) relative to net, long-term trends (1847/67 to 1978/82).

#### 3.1.3.1 1847/67 to 1917/18

Shoreline response along Dauphin Island was dramatic for the earliest time interval, illustrating a large gap in the central portion of the island in response to storm wave impacts (Figure 3-3). Although the exact timing of hurricane impact relative to this feature is not know, the U.S Army Corps of Engineers (1967) reported significant storm surge associated with the 1915 hurricane, where erosion along the Mississippi Sound barrier islands was particularly severe. The hurricanes of 1916 and 1917 likely sustained the large barrier breach, but they inflicted less damage to coastal areas than the 1915 event. The absence of a high-water shoreline in 1917 for the central portion of Dauphin Island signifies the importance of overwash processes on island evolution; however, longshore sediment transport have had a profound influence on lateral migration of western Dauphin Island into Petit Bois Pass. The rate of lateral island migration for this time period is about 54 m/yr to the west.

Along the eastern third of Dauphin Island, zones of shoreline retreat and advance alternate from the entrance of Mobile Bay to the central island breach (Figure 3-3). Shoreline retreat adjacent to the breach is consistent with the formation of ephemeral inlet features, and zones of shoreline advance away from this area mimic long-term change trends. Shoreline advance along the eastern 4.6 km of Dauphin Island averages about 1 m/yr; however, a short zone of retreat is present in the middle of this shoreline reach (Figure 3-3) where natural wave energy focusing by nearshore ebb-tidal shoal deposits is persistent.

### SHORELINE POSITION CHANGE FOR COASTAL ALABAMA 1847/67 TO 1917/20

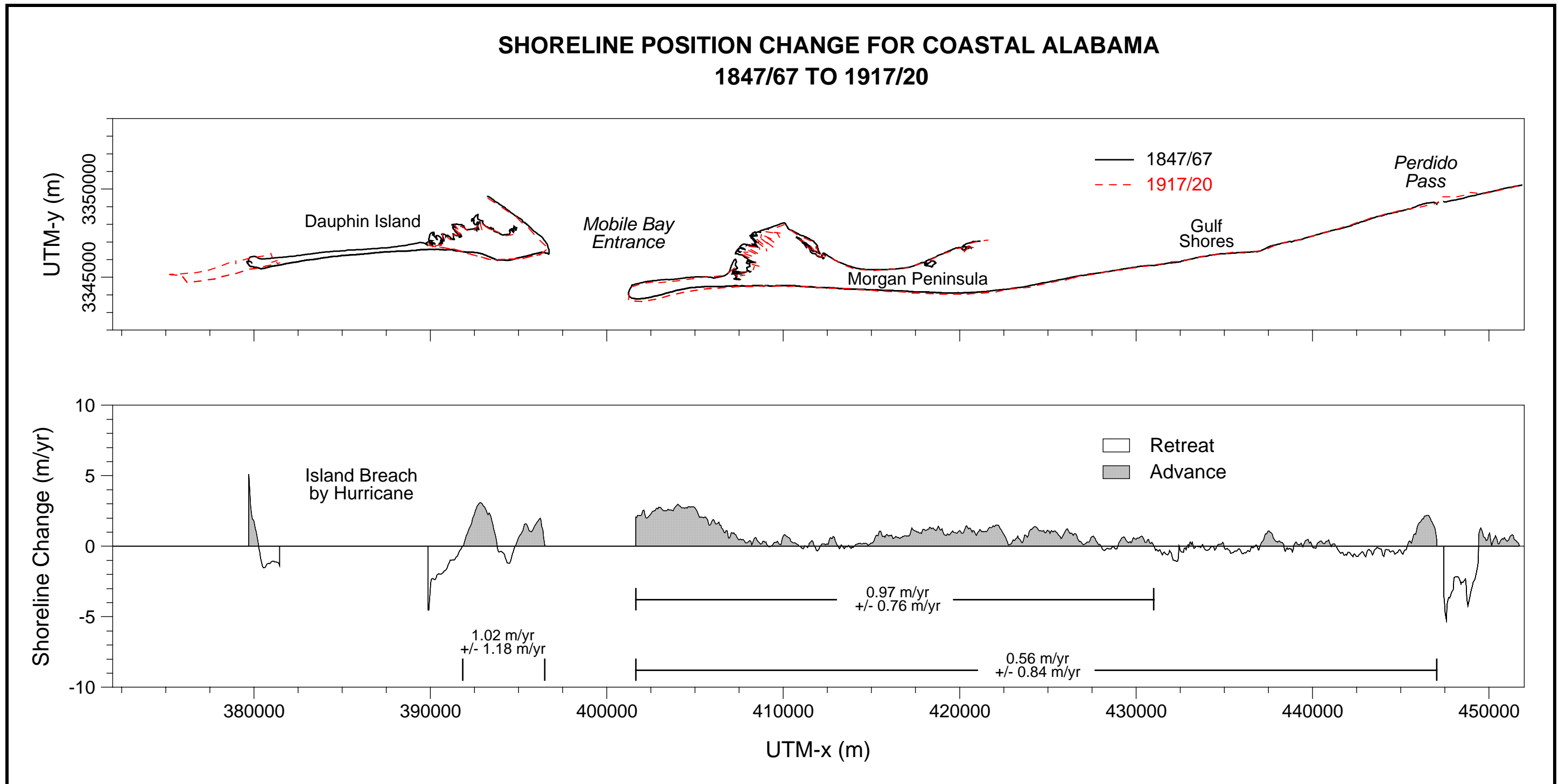


Figure 3-3. Shoreline position change along the Alabama coast, 1847/67 to 1917/20.

To the east, along the Morgan Peninsula, average shoreline advance of about 1 m/yr is recorded for the western 29 km of beach. In fact, the entire 45 km of outer coast from Perdido Pass to Mobile Point (Figure 3-3) averages about 0.6 m/yr shoreline advance. Net shoreline retreat does occur within the 16 km of beach downdrift of Perdido Pass; however, on average, the shoreline is stable. The most significant change in this area is associated with Perdido Pass, particularly the shoreline east of the inlet where maximum retreat rates are greater than 5 m/yr and average change is -2.9 m/yr. Overall, spatial change trends along the Morgan Peninsula indicate a net surplus of sediment to the beaches between 1867 and 1918.

### **3.1.3.2 1917/18 to 1934**

Between 1917/18 and 1934, major changes in shoreline position occurred throughout the study area. Whether the magnitude of change reflects reality or inaccuracies in mapping procedures is debatable. The 1917/18 shoreline was mapped as a reconnaissance shoreline at a scale of 1:40,000, whereas the 1934 shoreline represents the first interpreted shoreline from aerial photography. Inherent mapping errors at a scale of 1:40,000 would be approximately double those associated with field mapping at a scale of 1:20,000. Potential error associated with interpretation of high-water shoreline position from the 1934 photography could be substantially greater. In addition, the period of time between surveys is quite short (17 years); the longer the time period, the smaller the rate of change due to natural averaging of short-term event impacts. Regardless, it is expected that the trend of change is reasonable for the analysis period (Figure 3-4).

Although fluctuations in shoreline advance and retreat characterize eastern Dauphin Island, the dominant direction of shoreline movement is advance at an average rate of 0.2 m/yr. Relative to potential error estimates (Table 3-3), this value does not seem significant, but if zones of shoreline retreat and advance are evaluated separately, average change rates are -1.6 m/yr and 1.8 m/yr, respectively. Similar to changes documented for 1847/67 to 1917/18, a noticeable zone of erosion exists just downdrift of eastern Dauphin Island where wave energy focusing occurs in relation to the position of shallow offshore shoals associated with the ebb-tidal delta of Main Pass.

The western 30 km of the Morgan Peninsula exhibits average shoreline retreat of about 4.1 m/yr. Compared with the previous time interval, the magnitude of change is much greater and the trend of change is opposite (see Figures 3-3 and 3-4). Farther to the east towards Perdido Pass, shoreline change trends continue to indicate average shoreline retreat, but areas of accretion are present near Gulf Shores and a few other locations. The area of shoreline retreat east of Perdido Pass for the previous time period has been replaced by shoreline advance. For this 17-yr period of record, a net sediment deficit is indicated throughout the study area.

### **3.1.3.3 1934 to 1957**

Shoreline position change along the eastern 60% of Dauphin Island for this 23-yr period is dominated by shoreline retreat. Small areas of accretion exist along the eastern end of the island, consistent with trends for the previous two time periods (Figure 3-5). Average shoreline retreat for the central and eastern erosion zone (14 km long) is about 1.5 m/yr. Although shoreline position in 1934 was not available for the western third of the island, it is expected that shoreline retreat would persist west of the erosion area shown on Figure 3-5, and lateral migration into Petit Bois Pass would continue at historical rates.

### SHORELINE POSITION CHANGE FOR COASTAL ALABAMA 1917/20 TO 1934

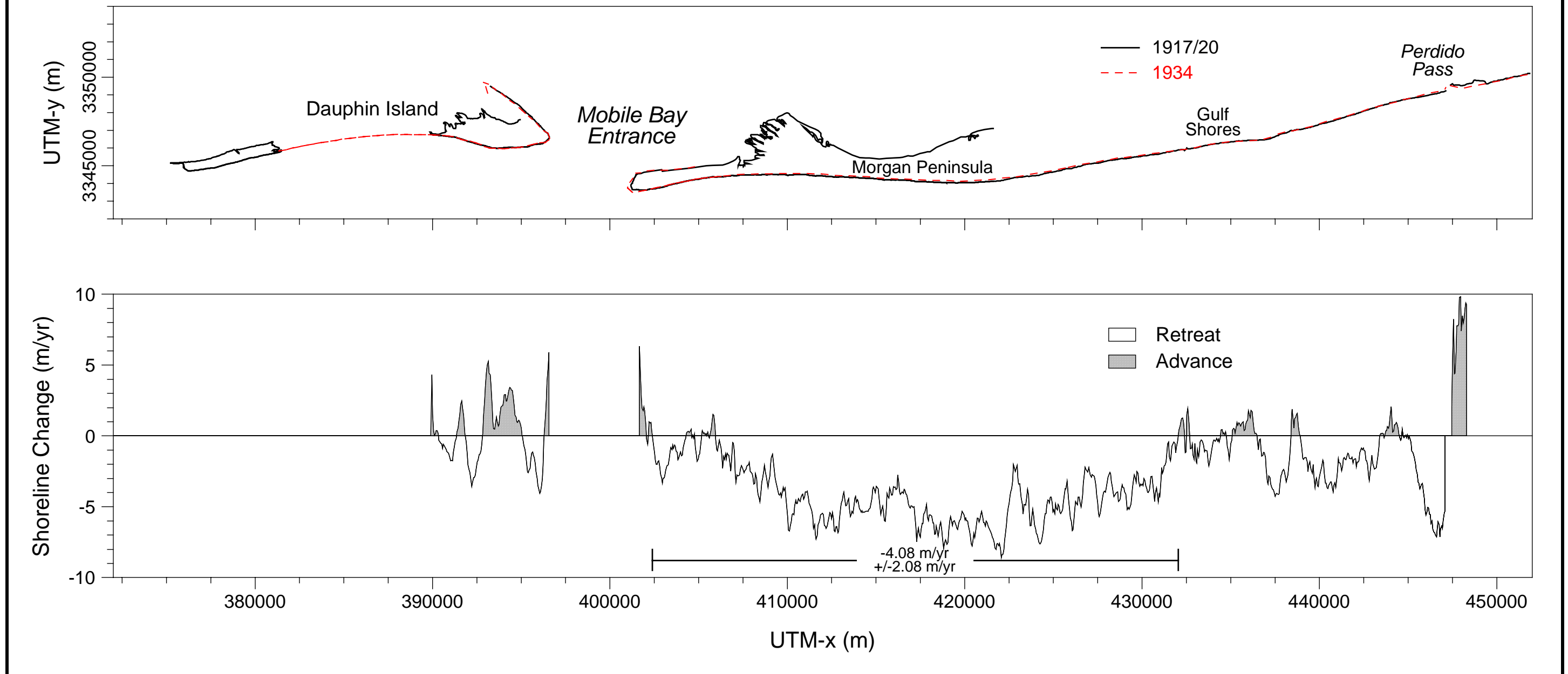


Figure 3-4. Shoreline position change along the Alabama coast, 1917/20 to 1934.

### SHORELINE POSITION CHANGE FOR COASTAL ALABAMA 1934 TO 1957

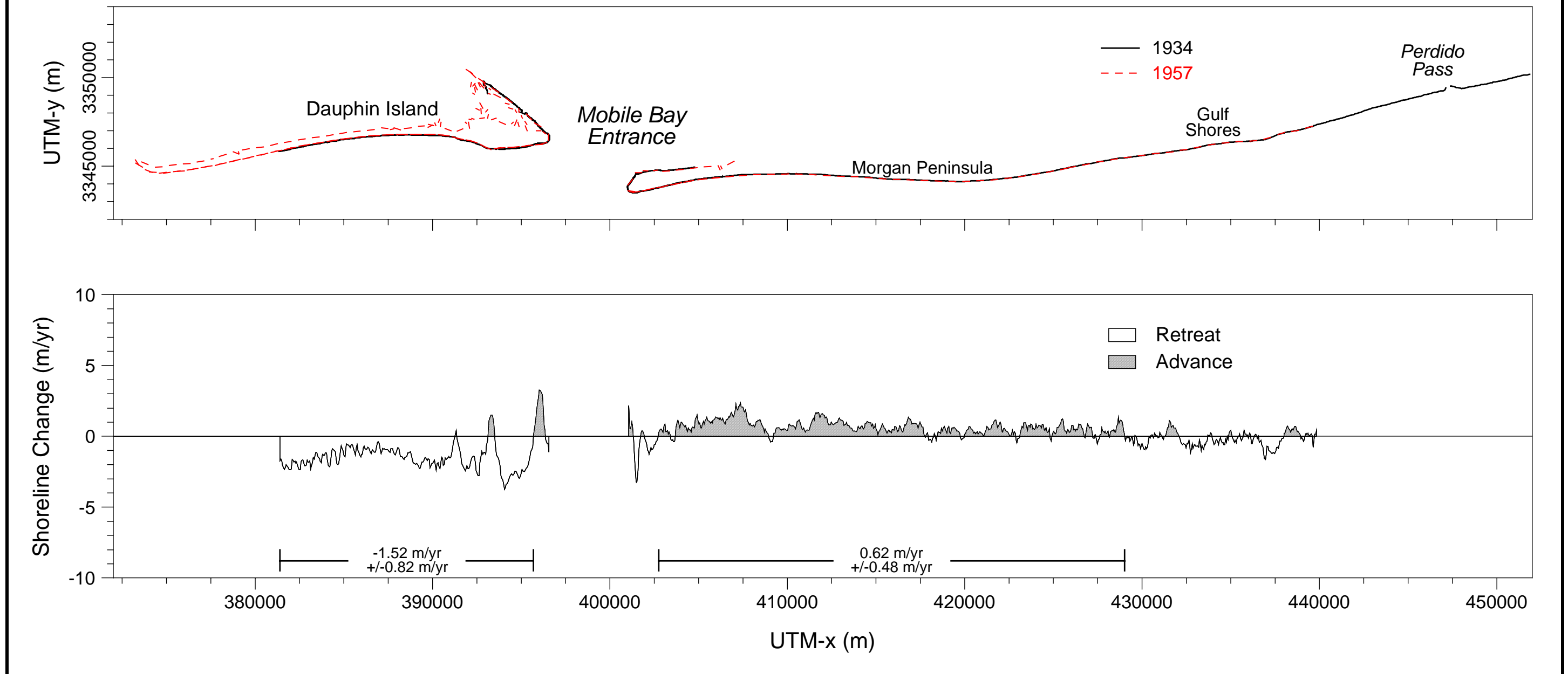


Figure 3-5. Shoreline position change along the Alabama coast, 1934 to 1957.

Except for a short length of beach along the western end of the Morgan Peninsula, shoreline change for a 26 km stretch of beach west of Gulf Shores is dominated by accretion at an average rate of about 0.6 m/yr. West of this area to the limit of data coverage, shoreline retreat is common, but the average rate of change is relatively small (-0.3 m/yr; Figure 3-5). Overall, shoreline advance along the Alabama Gulf shoreline west of Mobile Bay averaged 0.3 m/yr between 1934 and 1957. Although this trend is contrary to the previous time interval, it is consistent with change results identified for the period 1847/67 to 1917/18.

#### **3.1.3.4 1957 to 1978/82**

Shoreline change calculations relative to shoreline position in 1955 were used by Parker et al. (1993, 1997) to estimate sand volume requirements for maintaining beaches along the Alabama coast. Hummell and Smith (1995, 1996) updated these calculations to 1995. Shoreline retreat and advance for the period 1957 to 1978/82 illustrates regional trends relative to specific areas of concern identified by Parker et al. (1997). Comparison of change trends with earlier time intervals provides a means of gauging the reliability of results relative to the entire historical record.

The spike of sand accretion along western Dauphin Island is the result of lateral island migration. East of this point, shoreline retreat is dominant for about 20 km at an average rate of about 3 m/yr (Figure 3-6). Patterns of shoreline advance and retreat along eastern Dauphin Island are similar to those for all other time intervals. Parker et al. (1997) identified these same trends in their analysis of shoreline change along eastern Dauphin Island (Figure 3-1). Rates of change for independent analyses (present analysis versus Parker et al., 1997) were similar for the erosion zones identified in Figure 3-1 (about -2.5 m/yr on average).

Along the Morgan Peninsula, rates of shoreline position change exhibit relatively small variations (1.1 to -1.7 m/yr); however, average change for the easternmost 32 km of coast (Figure 3-6) is about -0.35 m/yr. Other than the 1917/18 to 1934 period, this 23-yr time interval is the only one recording a net sediment deficit for eastern Alabama beaches. Impacts from hurricanes over the past few years have at least maintained this trend and have likely increased the long-term rate of shoreline retreat for areas directly effected by extreme storm conditions.

#### **3.1.3.5 Cumulative Shoreline Position Change (1847/67 to 1978/82)**

Shoreline position change between 1847/67 and 1978/82 documents dramatic lateral migration of western Dauphin Island (about 7.3 km or 55 m/yr) into Petit Bois Pass and constant shoreline retreat along the western 60% of the island (about -2.2 m/yr; Figure 3-7). Following the trend of incremental change data, the eastern end of Dauphin Island exhibits net shoreline advance of 0.4 m/yr, even though a small erosion zone persists throughout the period of record. Although shoreline retreat dominates the record of change along the island, concurrent lateral growth of the beach to the west appears to balance losses recorded elsewhere.

Historical rates of change to the east along the Morgan Peninsula document net deposition within 6 km of the Mobile Bay entrance (about 1 m/yr; Figure 3-7). West of this area for the next 28 km, net shoreline retreat is persistent at an average rate of about 0.3 m/yr (average net retreat of 40 m). Averaging shoreline change rates along the eastern Alabama coast yields a net change of about 0, indicating a net sediment balance in this area. In addition, sediment accretion along the western margin of the Morgan Peninsula illustrates the dominant east to west direction of transport.

### SHORELINE POSITION CHANGE FOR COASTAL ALABAMA 1957 TO 1978/82

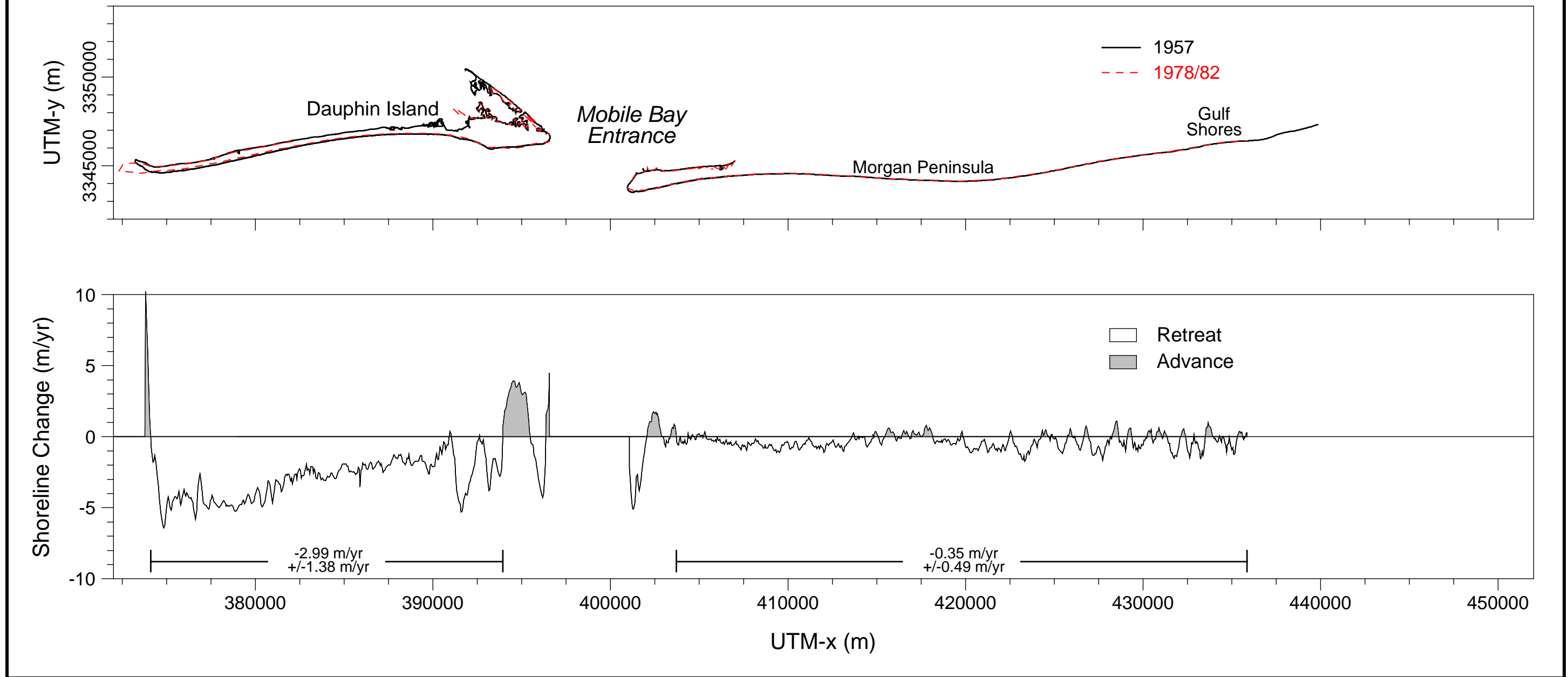


Figure 3-6. Shoreline position change along the Alabama coast, 1957 to 1978/82.

### SHORELINE POSITION CHANGE FOR COASTAL ALABAMA 1847/67 TO 1978/82

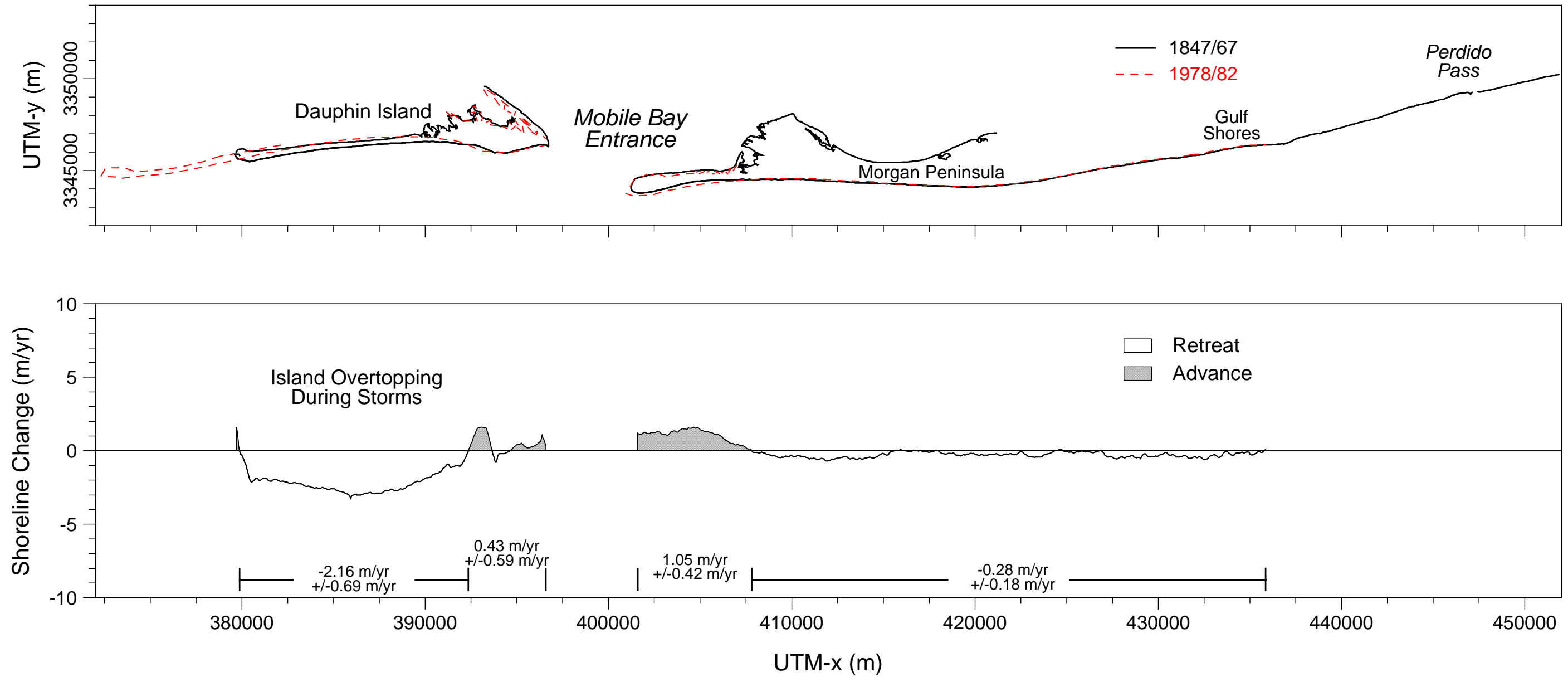


Figure 3-7. Shoreline position change along the Alabama coast, 1847/67 to 1978/82.

## 3.2 NEARSHORE BATHYMETRY CHANGE

### 3.2.1 Bathymetry Data Base and Potential Errors

Seafloor elevation measurements collected during historical hydrographic surveys are used to identify changes in nearshore bathymetry for quantifying sediment transport trends relative to natural processes and engineering activities. Two USC&GS bathymetry data sets were used to document seafloor changes between 1917/20 and 1982/91. Temporal comparisons were made for an 85-km coastal segment from 34 km west of Main Pass at the entrance to Mobile Bay to 51 km east of Main Pass at the Alabama/Florida border (Perdido Pass). Data extend offshore to about the 30-m depth contour (about 20 km offshore). The survey sets consist of digital data compiled by the National Geophysical Data Center (NGDC) and analog information (maps) that had to be compiled in-house using standardized digitizing procedures (see Byrnes and Hiland, 1994b).

The first regional USC&GS bathymetric survey was conducted in 1917/20 (Table 3-4); data were registered in units of feet. The scale of the surveys (1:40,000 and 1:80,000) suggests that they were primarily reconnaissance surveys used to provide a regional overview of bathymetry for that time period. The density of points was good for characterizing coastal and shelf topography; however, the most recent survey (1982/91) recorded many more points for describing surface characteristics in the same area. The 1917/20 offshore survey recorded an adequate number of depths along a survey line, and longshore spacing of lines was about 1 km. As such, depth values appear reasonable for describing bathymetric features and compared well with the 1982/91 survey set. The 1982/91 bathymetry data were available as digital data from the National Geophysical Data Center (NGDC).

Date	Data Source	Comments and Map Numbers
1917/20	USC&GS Hydrographic Sheets 1:40,000 (H-4020, H-4023, H-4023a) 1:80,000 (H-4139, H-4171)	First regional bathymetric survey that includes all potential resource sites in the study area; 31°05'00", 88°25'00" to 30°15'00", 87°30'00" (western Dauphin Island east to Perdido Pass); 1917/18 – Dauphin Island to Gulf Shores (H-4020, H-4-23, H-4023a); 1919/20 - Offshore and east of Gulf Shores to Perdido Pass (H-4139); 1920 - Offshore Mobile Bay Entrance and Dauphin Island (H-4171)
1982/91	USC&GS Hydrographic Sheets 1:20,000 (from NGDC data set) 1:10,000 (from NGDC data set)	Most recent offshore regional bathymetric survey; 1982 - Perdido Pass and Offshore (H-10041); 1983 - Gulf Shores to Perdido Pass and offshore (H-10114); 1984 - seaward of Little Lagoon (H-10151a); 1985 - Morgan Peninsula and offshore (H-10179); offshore Petit Bois Pass (H-10208); 1986 - offshore Main Pass and eastern Dauphin Island (H-10226); 1987 - offshore Dauphin Island and Petit Bois Pass (H-10247, H-10261); 1991 - offshore Mobile Bay entrance, including USACE placement of Mobile Outer Mound (H-10393 and H-10394)

As with shoreline data, measurements of seafloor elevation contain inherent errors associated with data acquisition and compilation. Potential error sources for horizontal location of points are identical to those for shoreline surveys (see Table 3-2). These shifts in horizontal position translate to vertical adjustments of about  $\pm 0.3$  to 0.5 m based on information presented in USC&GS and USACE hydrographic manuals (e.g., Adams, 1942). Corrections to soundings for tides and sea level change introduce additional errors in vertical position of  $\pm 0.1$  to 0.3 m. Finally, the accuracy of the depth measurement adds error that is variable depending on the measurement method. Using this information, it is estimated that the combined root-mean-square error for bathymetry

surface comparisons between 1917/20 and 1982/91 is about  $\pm 0.6$  m. This estimate was used to denote areas of no significant change on surface comparison maps.

Because seafloor elevations are temporally and spatially inconsistent for the entire data set, adjustments to depth measurements were made to bring all data to a common point of reference. These corrections include changes in relative sea level through time and differences in reference vertical datums. Vertical adjustments were made to each data set based on the time of data collection. All depths were adjusted to NGVD and projected average sea level for 1991. The unit of measure for all surfaces is meters, and final values were rounded to one decimal place before cut and fill computations were made.

### **3.2.2 Digital Surface Models**

Historical bathymetry data within the study area provide geomorphic information on characteristic surface features that form in response to dominant coastal processes (waves and currents) and relative sea level change. Comparing two or more surfaces documents net sediment transport patterns relative to incident processes and sediment supply. The purpose for conducting this analysis throughout the study area is to document net sediment transport trends on the shelf surface and to quantify the magnitude of change to calibrate the significance of short-term wave and sediment transport numerical modeling results. Net sediment transport rates on the shelf are determined using these historical data sets to address potential infilling rates for sand borrow sites.

#### **3.2.2.1 1917/20 Bathymetric Surface**

Bathymetry data for the period 1917/20 were combined with the 1917/18 shoreline data to create a continuous surface from the shoreline seaward to about the 30-m depth contour (NGVD). The most prominent geomorphic feature throughout the study area is the ebb-tidal delta associated with Main Pass at the Mobile Bay entrance (Figure 3-8). A series of well-defined ebb shoals (primarily on the western side of the entrance) and a prominent entrance channel dominate the entrance area to a distance approximately 10 km offshore. The channel exits the coast in a northeast-southwest direction, and the shape of the shoal is skewed to the west. This observation is consistent with all other geomorphic evidence documenting the dominant direction of net sediment transport along the shelf and shoreline to the west.

The linear sand shoal east of the Main Pass and parallel to the channel represents a zone of net deposition supplied by longshore sand transport from the east. Channel currents create a dynamic diversion to east-west transport (Todd, 1968), resulting in a shoal that parallels the channel to the seaward margin of the ebb-delta (Figure 3-8). Extensive subaerial and subaqueous islands and shoals have formed and dissipated during the historical evolution of the ebb-delta (Hummell, 1990). All of these deposits exist west of Main Pass, indicating the dominant direction of net transport is from east to west. Petit Bois Pass, at the western margin of Dauphin Island, illustrates the same pattern of deposition, where the ebb shoals and main channel are skewed to the west (Figure 3-8). Between these two passes, offshore depth contours appear relatively straight and parallel to shoreline orientation.

East of Mobile Pass (Figure 3-9), shelf bathymetry is dominated by a large shore-oblique sand shoal (northeast-southwest orientation) just west of Little Lagoon, a relatively steep shoreface west of this deposit, and numerous northwest-southeast trending sand ridges to the east (McBride and Byrnes, 1995). The prominent sand shoal extending southwest from Little Lagoon reaches approximately 11 km offshore and has topographic relief of about 6 m. The steep shoreface and deep trough west of this sand ridge may be the remnant of a Pleistocene paleochannel for Mobile Bay (Hummell and Parker, 1995). However, Parker et al. (1997) show with vibracore data that the extensive sand shoal east of this bathymetric low contains Holocene sediment, indicating a depositional process of formation during Holocene sea level rise.

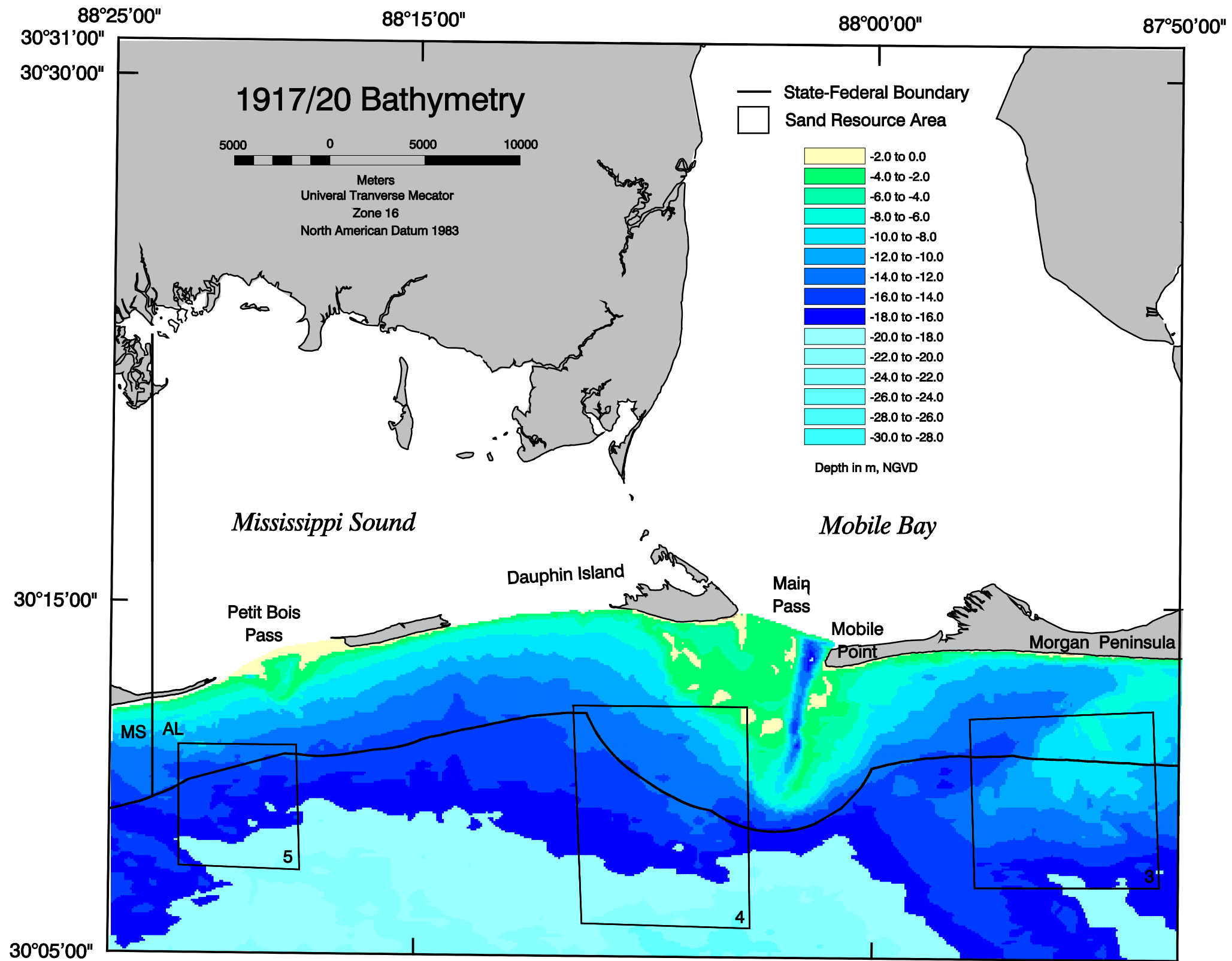


Figure 3-8. Nearshore bathymetry (1917/20) for the southwestern Alabama coastal zone.

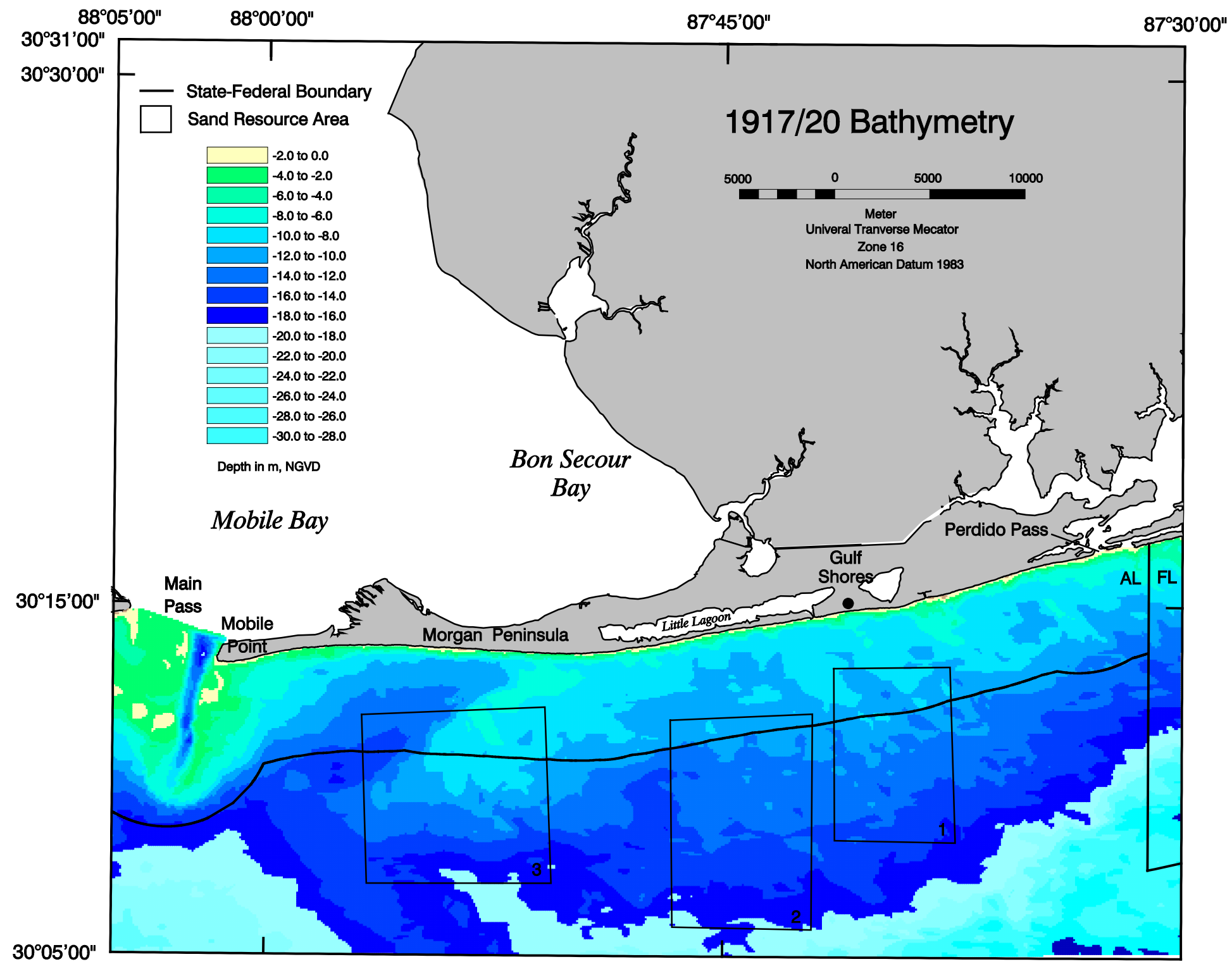


Figure 3-9. Nearshore bathymetry (1917/20) for the southeastern Alabama coastal zone.

### **3.2.2.2 1982/91 Bathymetric Surface**

The general character of the bathymetric surface for the period 1982/91 is very similar to the 1917/20 surface with a few exceptions (Figure 3-10). First, geomorphic features are better defined because the number of data points is larger for the most recent time period. The general shape and position of shoals is consistent for both surfaces. Second, subaqueous deposition seaward of the western end of Dauphin Island changed in shape and position due to rapid migration of the beach to the west during the intervening years (see Byrnes et al., 1991). Third, an elongated sediment shoal was deposited to the southwest of the ebb-tidal delta by the U.S. Army Corps of Engineers between 1988 and 1990. Approximately 13 MCM of sediment was deposited about 10 km southwest of the Mobile Bay entrance in 14-m water depth as an experimental berm for dissipating wave energy (Hands, 1994). Known as the Mobile Outer Mound, sediment accumulation thickness was about 6 m. The sand resource target identified in Area 4 for the present study is due south of this deposit in 14- to 16-m water depth.

Shoal geometry for the ebb-tidal delta at Main Pass was better defined than in 1917/20. Main Pass channel is now on a routine maintenance schedule, and the channel extends farther seaward in 1982/91. The shoal east of the channel remains prominent in 1982/91, and sand deposits on the dominant western portion of the ebb-delta have become more extensive. Pelican Island is very well-defined and appears to be bypassing sand to the beach along eastern Dauphin Island. Shoal deposition along western Dauphin Island illustrates that sediment transport trends are dominant from east to west (Figure 3-10).

For the eastern portion of the study area, shelf morphology is characterized by three prominent features: 1) a large northeast-southwest shoal trending seaward from the Little Lagoon area; 2) a substantial nearshore bathymetric low and shoreface steepening west of the shoal; and 3) a well-defined sand ridge field (northwest-southeast trending) on and east of the large sand shoal, extending seaward to 20-m water depth (Figure 3-11). The entire shelf surface in this area is composed of clean, medium-to-fine sand. As such, almost any site within the potential sand resource areas provides quality sand for beach replenishment.

### **3.2.3 Shelf Sediment Transport Dynamics**

Although bathymetric surfaces appear similar for 1917/20 and 1982/91, a comparison of bathymetry data yields a difference plot that isolates areas of erosion and accretion between the two surfaces for documenting sediment transport patterns and quantifying trends (Figures 3-12 and 3-13). The most significant changes occurring during the 68-yr interval were associated with deposition (and erosion) at and seaward of the Mobile Bay entrance, erosion along Dauphin Island, deposition along the Morgan Peninsula shoreline, and alternating patterns of erosion and deposition on the shelf surface in the northwest-southeast-trending sand ridge field east of Mobile Bay.

Fluid flow and sediment transport at and seaward of the entrance to Mobile Bay is most dynamic for the study area. Spring runoff and storm water outflow from Mobile Bay export substantial quantities of sediment to the shelf surface seaward and west of the entrance through suspended sediment transport (Stumpf and Gelfenbaum, 1990). Polygons of green in this area represent zones of natural deposition and human-induced deposition through dredged material disposal (large dark green areas west of the channel near the State-Federal boundary; Figure 3-12). North of this site, deposition landward of an erosion zone near Pelican Island suggests a net flux of sediment towards the beaches from offshore shoals, feeding the longshore sediment transport system. However, significant sand transport to the beach has not occurred by 1986 because beach erosion is present landward of this accretion zone. In the western portion of the study area, south of Petit Bois Pass, alternating bands of erosion and accretion illustrate the dynamic nature of shelf sand ridge deposits.

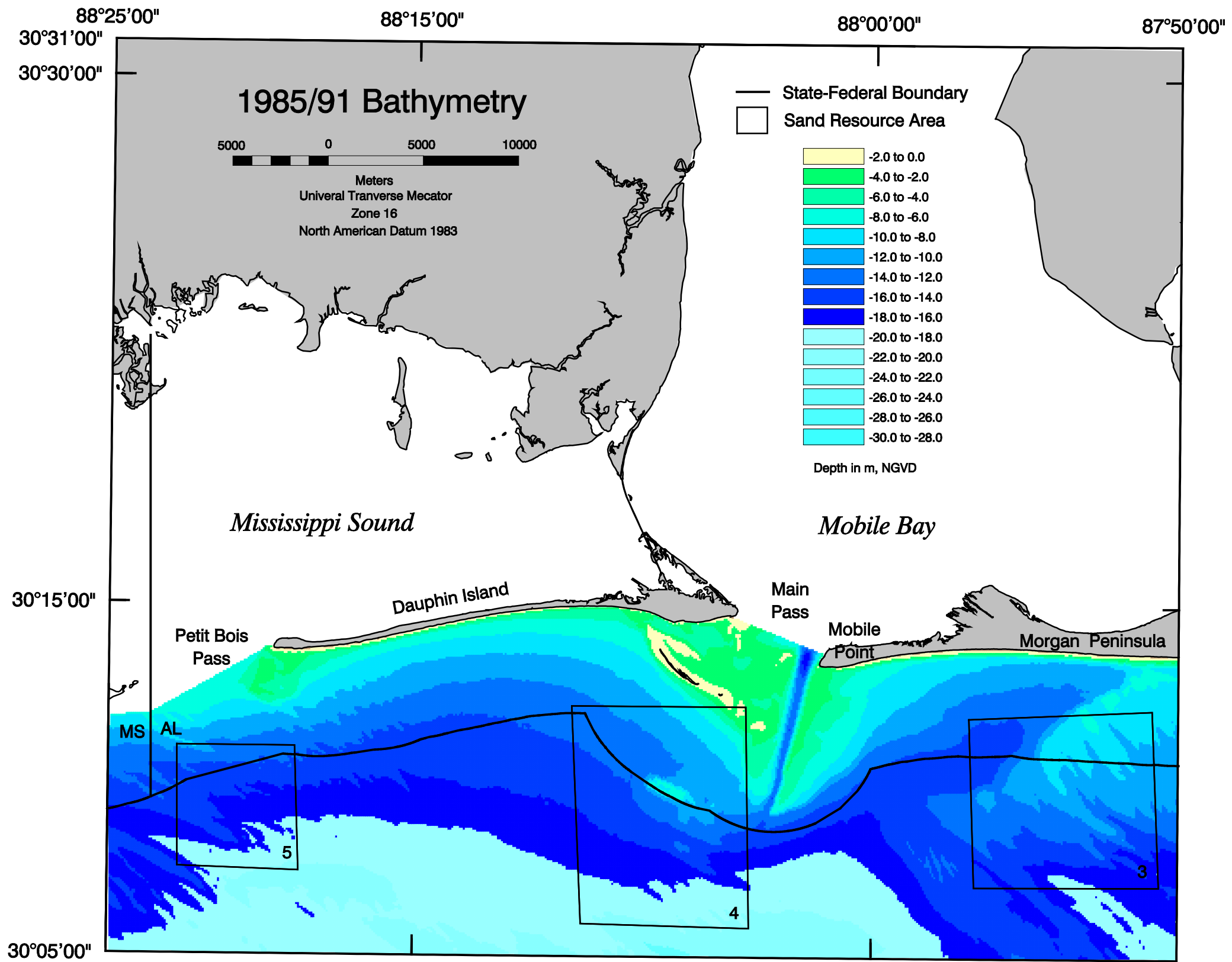


Figure 3-10. Nearshore bathymetry (1985/91) for the southwestern Alabama coastal zone.

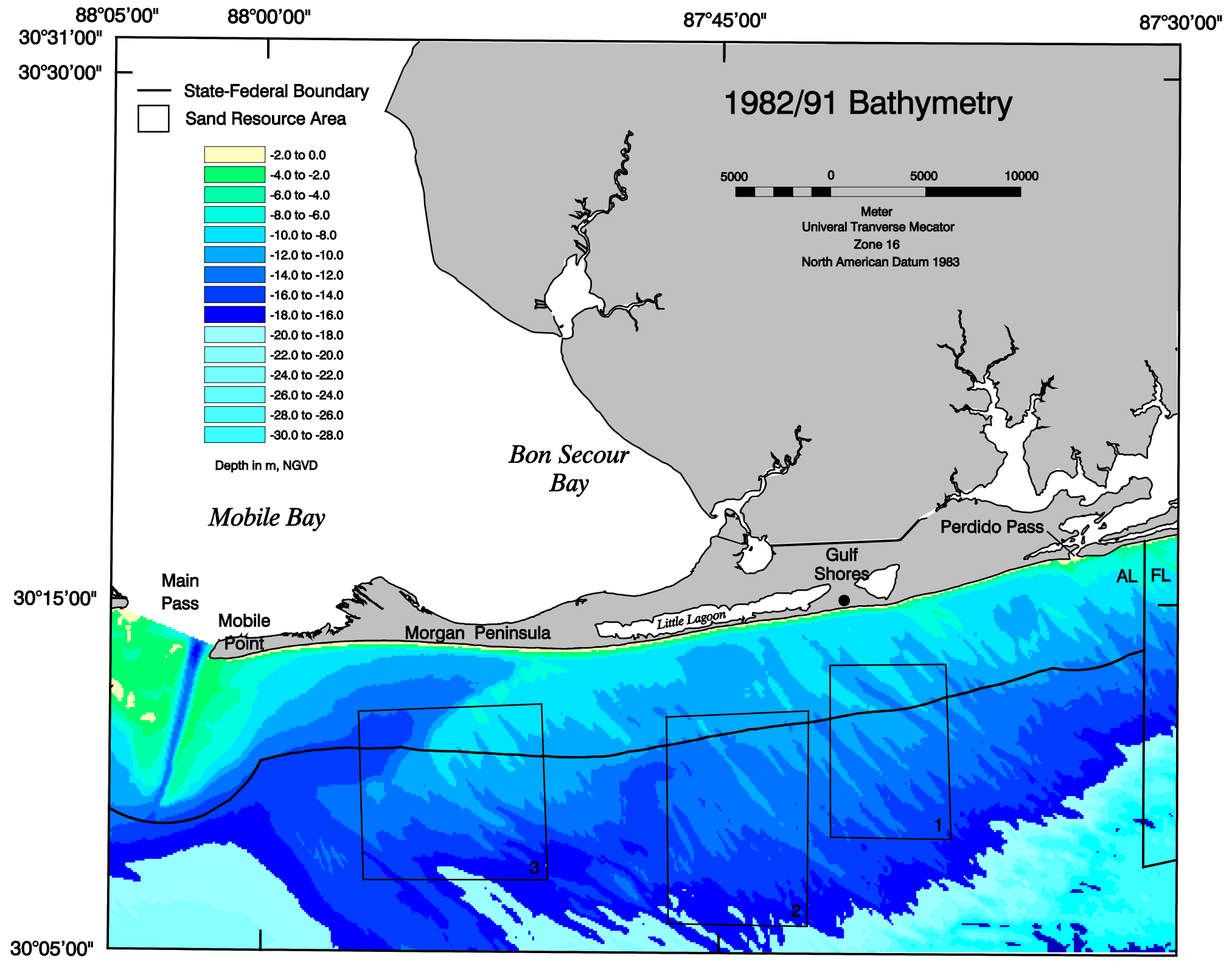


Figure 3-11. Nearshore bathymetry (1982/85) for the southeastern Alabama coastal zone.

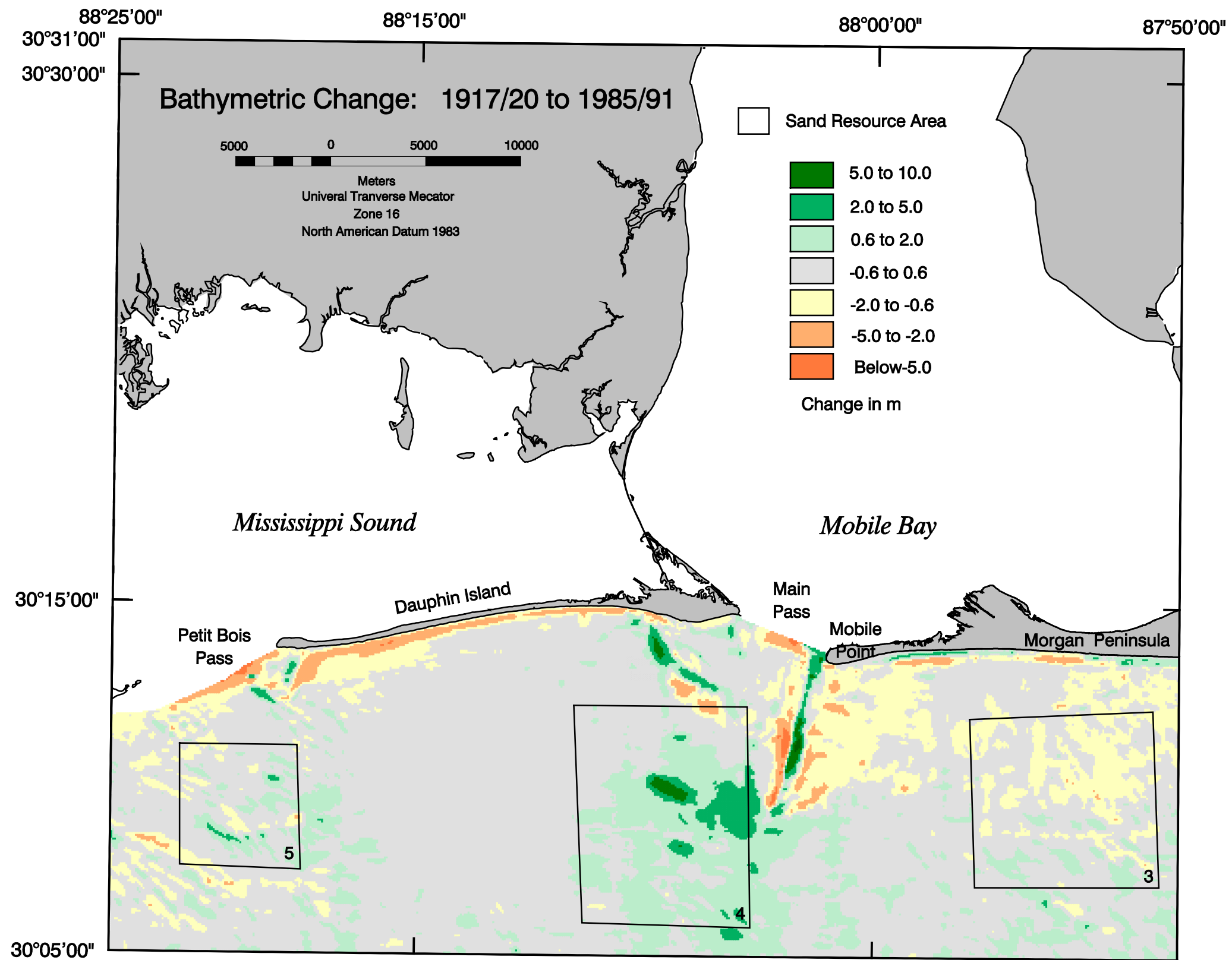


Figure 3-12. Nearshore bathymetry change (1917/20 to 1985/91) for the southwestern Alabama coastal zone.

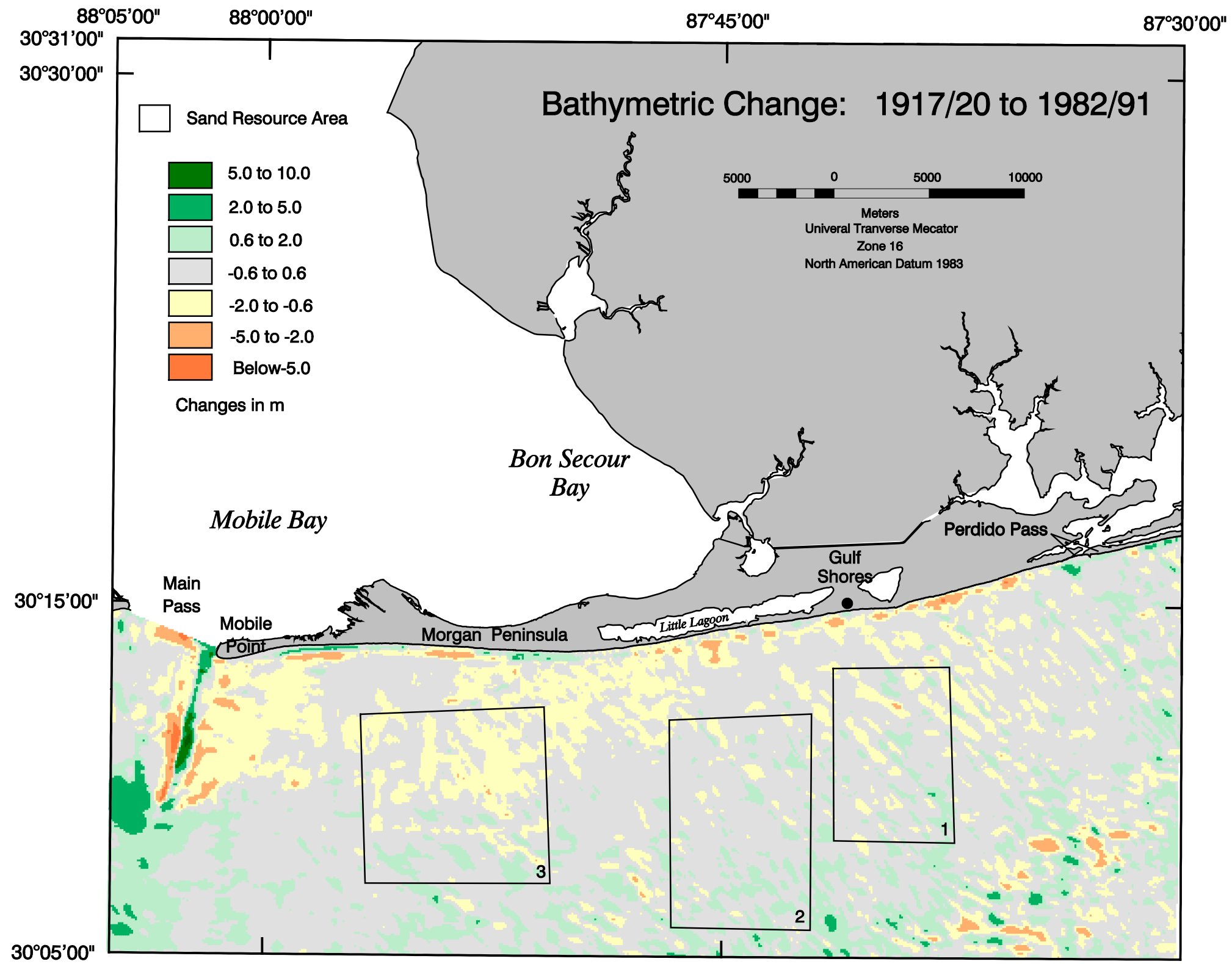


Figure 3-13. Nearshore bathymetry change (1917/20 to 1982/85) for the southeastern Alabama coastal zone.

Figure 3-13 illustrates historical sediment transport patterns east of Mobile Bay. Deposition and erosion in a thin band paralleling the coast indicates the zone of littoral sand transport. Seaward of this zone, shelf sediment transport is reflected by the migration of shoreface sand ridge deposits and alternating bands of erosion and accretion. Sand volume change calculations for these zones are used to estimate net sand transport rates along the shore and on the shelf surface (see Sections 3.2.4 and 3.2.5). Historical transport rates are used to calibrate simulations of borrow site infilling and nearshore sand transport (Section 5.2).

### 3.2.4 Magnitude and Direction of Change

Patterns of seafloor erosion and accretion on the continental shelf seaward of the Alabama coast documented the net direction of sediment transport throughout the study area (Figure 3-12 and 3-13). For the period 1917/20 to 1982/91, net sediment movement is to the west. This direction of transport is consistent with historical shoreline change trends and dredging practice at Main Pass channel (disposal is always west of the channel). Although overall trends are helpful for assessing potential impacts of sand extraction from the OCS, the specific purpose of the historical bathymetry change assessment is to quantify sediment erosion and accretion and to derive transport rates specifically related to potential sand extraction sites. Of the five potential borrow sites, four were chosen for evaluating sand extraction scenarios based on discussions of beach replenishment needs with Geological Survey of Alabama personnel (Hummell, 1999). Area 5 at the western end of the study area was not evaluated as a sand borrow source because it is substantially removed from beach areas of greatest replenishment needs and the sediment was least compatible with native beach sand (see Parker et al., 1997).

For Sand Resource Area 4, sediment deposition resulting from water and sediment outflow from Main Pass and dredged material disposal by the USACE was prominent on the change surface. Three specific sub-sites documented sediment deposition at 1) the potential sand resource area, 2) the Mobile Outer Mound (constructed by the USACE), and 3) the dredged material disposal site used by the USACE (and approved by EPA) during channel dredging operations (Figure 3-14). For the resource site, total sediment deposition was about 4.8 MCM between 1917/20 and 1991, or about 66,000 m<sup>3</sup>/yr accretion. At the dredged sediment disposal site, approximately 23.5 MCM was deposited since 1917/20. At the Mobile Outer Mound, where about 13 MCM of sediment was placed by the USACE between 1988 and 1990, net deposition since 1917/20 was about 13 MCM (equal to the amount placed by the USACE as reported by Hands [1994]).

For Sand Resource Area 3, primarily erosion is indicated at the sand resource site. The total amount of sand volume change at the site between 1917/20 and 1982/85 was about 585,000 m<sup>3</sup> or about 8,800 m<sup>3</sup>/yr. At Sand Resource Area 2, a well-defined zone of erosion exists adjacent to a zone of deposition as a shoreface sand ridge migrates to the west under the influence of incident shelf processes (Figure 3-15). The zone of deposition indicates an accretion rate of about 6,200 m<sup>3</sup>/yr, whereas the erosion rate is calculated as about 9,100 m<sup>3</sup>/yr (rates of change are normalized using the potential resource site surface area). As such, the average, long-term transport rate for the resource site is 7,300 m<sup>3</sup>/yr.

At Sand Resource Area 1, the rates of erosion and accretion associated with sand ridge migration were quite variable over short distances. Shoal migration near the sand resource site illustrated net transport from east to west, but associated transport rates vary from 34,000 to 9,000 m<sup>3</sup>/yr, respectively. Net sand volume change at the proposed resource site indicated no significant movement for the period of record; however, absolute sand volume change averaged about 8,500 m<sup>3</sup>/yr. Although the potential for transport (and borrow site infilling) is high in this area, the average sand transport rate is consistent with other sand resource areas south of the Morgan Peninsula.

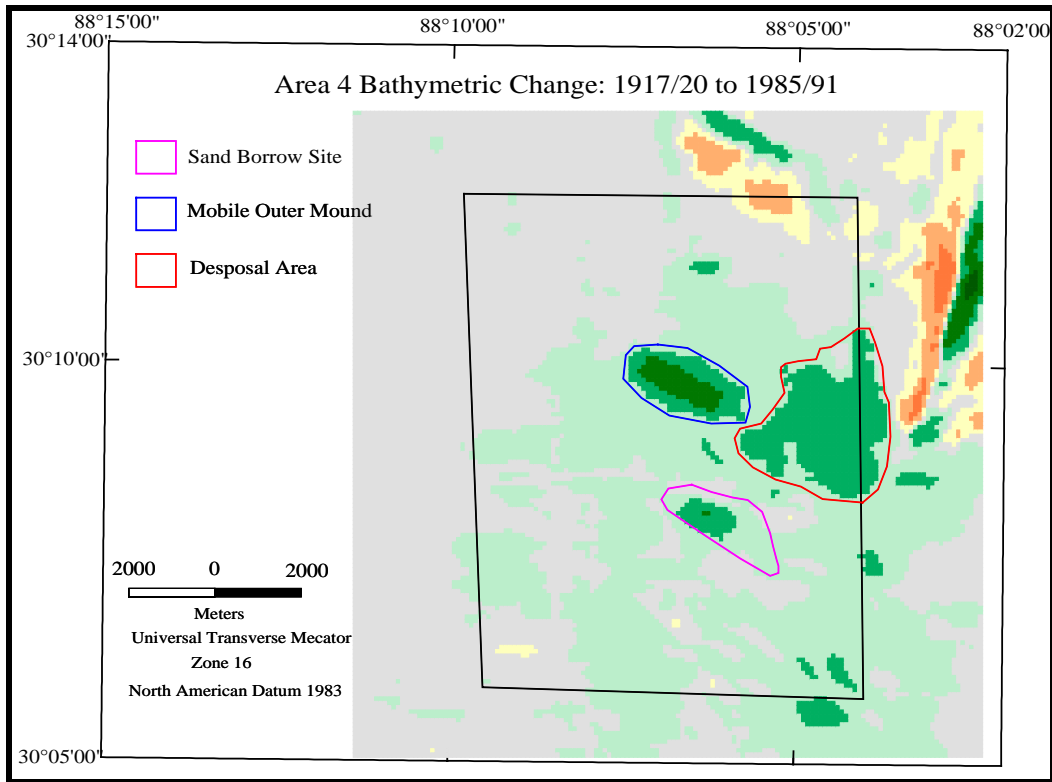


Figure 3-14. Sand resource site location relative to dredged material deposition for Resource Area 4.

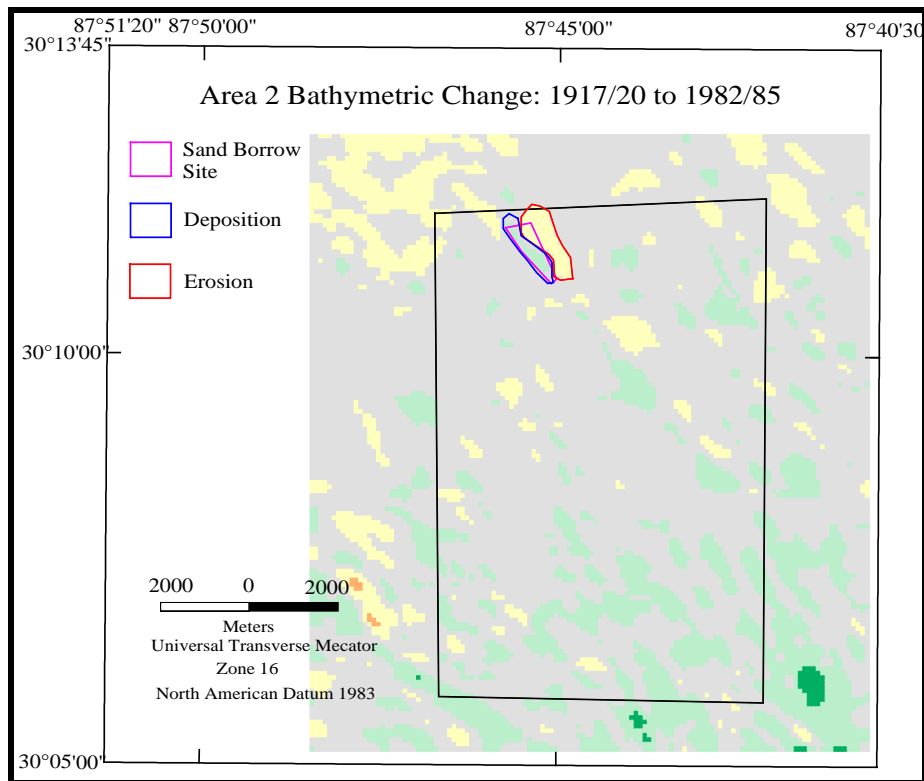


Figure 3-15. Sand resource site location relative to sand ridge erosion and deposition in Resource Area 2.

### 3.2.5 Net Longshore Sand Transport Rates

Well-defined zones of erosion and accretion are documented in Figure 3-13 as the region of littoral sand transport along the Morgan Peninsula. This zone extends seaward to about the 6-m (NGVD) depth contour (see Figure 3-11), which represents the approximate depth of closure (based on calculations of  $d_c$  from Hallermeier [1981] using USACE Wave Information Study [WIS] data statistics). Between Perdido Pass and Main Pass, alternating zones of erosion and accretion were evaluated with respect to the net sediment budget to determine a net longshore sand transport rate for the area. With the western boundary defined by the present location of Main Pass channel, the net long-term sand transport rate was determined as approximately 106,000 m<sup>3</sup>/yr. Unfortunately, an estimate of sand transport for the littoral zone of Dauphin Island could not be determined from the existing data set, due in part to the absence of a 1917/20 shoreline boundary along much of the island (see Figure 3-4). However, because incident wave processes do not vary significantly throughout the study area (see Section 4), it is expected that the longshore sand transport rate determined for the area east of Main Pass is representative for Dauphin Island as well.

### 3.3 SUMMARY

Shoreline position and nearshore bathymetry change document four important trends relative to study objectives. First, the predominant direction of sediment transport throughout the study area is east to west. Western Dauphin Island has migrated at a rate of 56 m/yr to the west since 1917. The ebb-tidal shoals at Main Pass and Petit Bois Pass are skewed to the west, and the natural channel at Petit Bois Pass is aligned in a northeast-southwest direction. Deposition associated with outflow from Mobile Bay is illustrated primarily west of the channel, and a pattern of downdrift deposition (west) and updrift erosion (east) is documented for shoreface sand ridge deposits seaward of Morgan Peninsula.

Second, the most dynamic portion of the study area, in terms of sediment transport, is the ebb-tidal delta at Mobile Bay entrance. Areas of significant erosion and accretion are documented for the period 1917/20 to 1982/91, reflecting USACE channel dredging and sediment disposal practice, wave and current dynamics at the entrance and influence on sediment deposition seaward and west of the ebb-delta, and the contribution of littoral transport from the east to channel infilling adjacent to Mobile Point.

Third, alternating bands of erosion and accretion on the continental shelf east of Main Pass illustrate relatively slow but steady reworking of the upper shelf surface as sand ridges migrate to the west. The process by which this is occurring suggests that a borrow site in this area would fill with sand transported from an adjacent site at a rate of about 10,000 m<sup>3</sup>/yr. Sand Resource Area 1 illustrates the largest variability in potential transport rates, whereas Areas 2 and 3 are fairly consistent for the period of record. Although long-term sand transport rates are relatively low, sediment filling the borrow area(s) would be primarily sand because the shelf surface in the area contains about 95% sand (Parker et al., 1993, 1997; Hummell and Smith, 1995, 1996; McBride and Byrnes, 1995). For Sand Resource Area 4, the potential borrow site area appears to be accreting at a fairly rapid rate (approximately 66,000 m<sup>3</sup>/yr), but much of the sediment encountered near the surface is silt and clay.

Finally, the net longshore transport rate determined from seafloor changes in the littoral zone between Perdido Pass and Main Pass indicate a gradient in transport to the west at a rate of about 106,000 m<sup>3</sup>/yr. Variations in transport rate are evident in the patterns of change recorded on Figure 3-13. It appears that areas of largest net transport exist just east of Gulf Shores where coastal erosion is greatest in the littoral zone.

## **4.0 WAVE TRANSFORMATION NUMERICAL MODELING**

### **4.1 ANALYSIS APPROACH**

A quantitative understanding of wave characteristics, storm surge, sediment transport, and other natural processes is key to implementing an effective borrow site management plan. Computer models provide predictive tools for evaluating various forces governing wave climate, sediment transport processes, and the performance of beach fill extraction from offshore borrow sites. Quantitative information produced from numerical models can be used to maximize the design life of beach replenishment projects and examine the effects of dredging at offshore borrow sites. As a result, management strategies can be developed to explain the physical processes that dominate a region and to furnish appropriate recommendations/solutions for each stretch of coast.

An assessment of potential impacts caused by dredging offshore borrow sites can be determined using wave modeling to estimate refraction, diffraction, shoaling, and wave breaking. Refraction and diffraction may have a significant effect on the impacts waves have on a shoreline. Wave refraction and diffraction generally result in an uneven distribution of wave energy along the coast that affects sediment transport in the region. Wave modeling results provide information on wave propagation across the continental shelf and to the shoreline, revealing areas of increased erosion (“hot spots”) or areas of increased wave energy. These data then provide the basis for nearshore circulation and sediment transport models. In addition, one of the primary advantages of wave modeling is its ability to simulate multiple scenarios. The model domain can be modified (e.g., comparison of existing and post-dredging scenarios, different structural configurations, evaluation of varying beach nourishment templates, etc.) to determine the effect various changes have on the wave climate. Wave input also can be modified to simulate a wide range of wave conditions (e.g., storm events, seasonal variations) to determine changing impacts on shoreline response.

This section focuses on the application and results of wave transformation numerical modeling for offshore Alabama. A combined refraction and diffraction spectral wave model was used to propagate random waves from offshore to the nearshore region and investigate potential changes in the wave field caused by dredging of offshore borrow areas. The purpose of this section is to describe the framework and capabilities of the wave model, explain its application to the Alabama coastline, and provide analysis of the modeling results used as input to the numerical circulation and sediment transport models.

#### **4.1.1 Wave Model Description**

The spectral wave refraction/diffraction model REF/DIF S (Kirby and Özkan, 1994) was employed to evaluate changes in wave propagation across the Alabama continental shelf relative to potential sand mining scenarios. REF/DIF S is a combined refraction and diffraction spectral wave model, which can simulate the behavior of a random sea state and incorporates the effects of shoaling, wave breaking, refraction, diffraction, and energy dissipation. Using wave data collected in the Alabama coastal region, appropriate input can be developed and used to specify offshore wave boundary conditions. Then, using local bathymetry to create an accurate grid, the model is able to propagate waves to an area of interest (e.g., Dauphin Island, Gulf Shores). The following discussion provides a comprehensive description of the REF/DIF S, including a brief summary of the theoretical background.

Understanding water wave propagation over an irregular bathymetry can be improved greatly through the implementation of a spectral wave model rather than a monochromatic wave model. The use of a spectral wave model provides the capability to propagate all components of ocean waves simultaneously through the model domain. The spectral approach makes it possible to calculate

nearshore statistical wave parameters and represent the actual sea surface more accurately. Typically, ocean wave energy is composed of a large variety of waves moving in different directions and with different frequencies, phases, and heights. By simulating all wave components that propagate towards the Alabama shoreline, a spectral wave model is superior to a monochromatic wave model.

To illustrate the increased accuracy gained when using a spectral wave model, a comparison was made between spectral model results (REF/DIF S), monochromatic results (REF/DIF 1), and experimental data collected by Vincent and Briggs (1989) for waves propagating over a submerged shoal. The upper left-hand panel of Figure 4-1 illustrates bathymetry used in the experiments conducted by Vincent and Briggs (1989). The bottom panels present normalized wave height results for two (monochromatic and spectral) model simulations. The dashed black lines on the bottom two plots show contours of the submerged shoal, while the solid white lines are contours of normalized wave height (also presented as a color map). Both monochromatic (REF/DIF 1, lower left-hand panel) and spectral (REF/DIF S, lower right-hand panel) results illustrate wave focusing that occurs behind the submerged shoal; however, the monochromatic wave model tends to focus wave energy to a much greater degree than the spectral wave model. In addition, monochromatic wave model results show more “jagged” wave height patterns induced by the presence of the shoal.

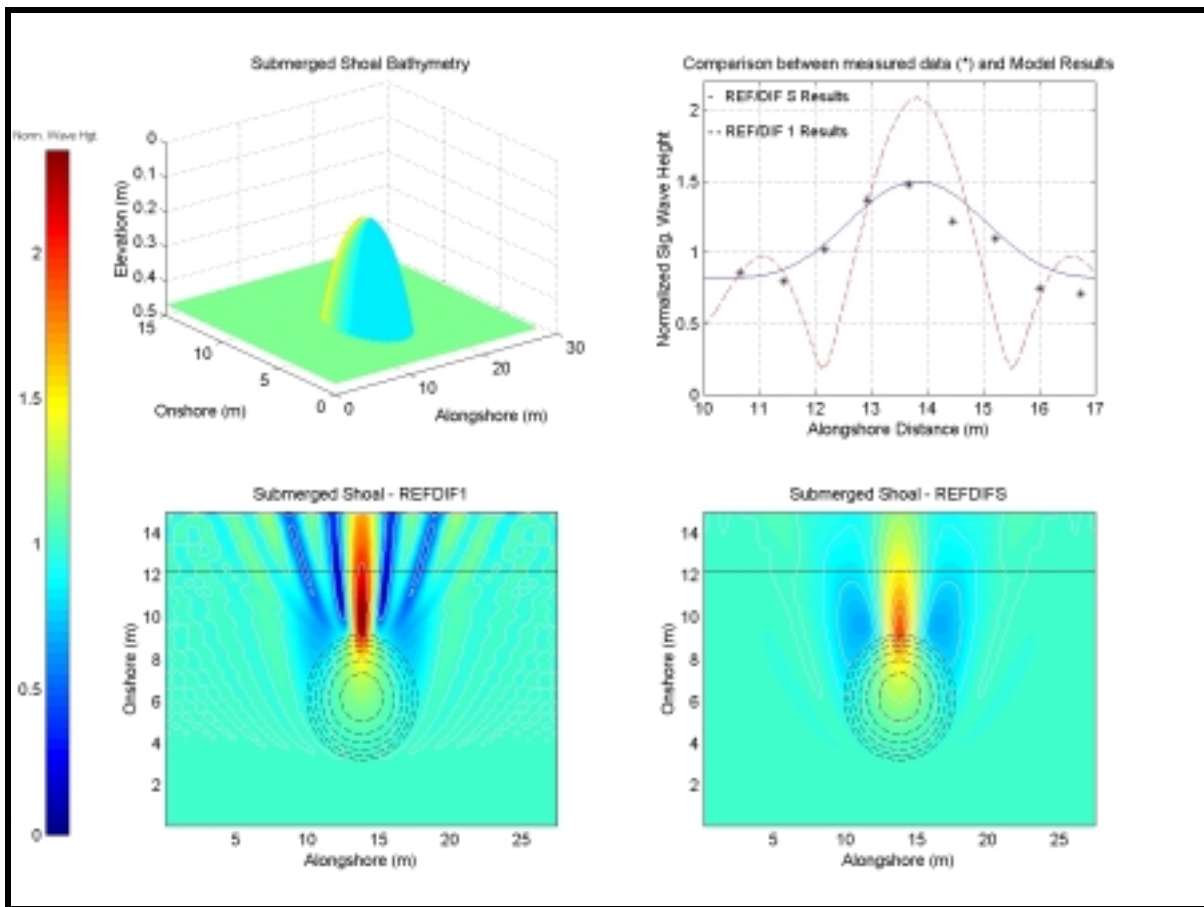


Figure 4-1. Comparison between a spectral (REF/DIF S) and monochromatic (REF/DIF 1) wave models. Wave height results are compared to measured data (\*) collected by Vincent and Briggs (1989).

The upper-right hand plot shows a comparison between spectral model results (-), monochromatic model results (- -), and measured data (\*) for a transect taken 12.2 m from the offshore boundary (indicated by the solid black line in the lower panel plots). Spectral wave model results compare well with the general shape of the curve depicted by the measured data, while monochromatic wave model results over-predict wave focusing and under-predict wave height on either side of the focusing.

REF/DIF S simulates the behavior of a random sea surface by describing wave energy density as a function of direction (directional spectrum) and frequency (frequency spectrum). The two-dimensional wave spectrum is discretized into separate wave components, which make up an essential part of the input for REF/DIF S. Therefore, at any point  $(x,y)$  in the model domain, water surface elevation is represented as

$$\eta(x, y, t) = \sum_f \sum_\theta \left\{ \frac{A(x, y, f, \theta)}{2} e^{i\psi} \right\} \quad (4.1)$$

where  $A(x,y,f,\theta)$  is the complex amplitude,  $f$  is the component's frequency,  $\theta$  is the direction of any individual wave component, and

$$\psi = \int k \cdot dx - \omega t \quad (4.2)$$

is the phase of the wave component,  $k$  is the wave number, and  $\omega$  is the radian frequency. The wave number vector,  $k$ , can be defined in terms of its components in the  $x$  and  $y$  directions and related to the direction of any individual wave component,  $\theta_n$ , by:

$$k_x = k_n \cos \theta_n \quad (4.3)$$

$$k_y = k_n \sin \theta_n \quad (4.4)$$

Figure 4-2 shows the coordinate convention used in the present wave modeling study and the angle made by each wave component relative to the  $x$ -axis.

Input wave spectra are comprised of discrete, bin-centered values of frequency and direction specified at the offshore boundary. A description of the development of specific input conditions for the Alabama wave modeling grids is presented in Section 4.1.3. Computations in the model domain are performed simultaneously for all wave components,  $n$ . After each shoreward step in the model grid, the complex amplitudes,  $A(x,y)_n$ , are known for all wave components contained within the selected spectra. REF/DIF S calculates the significant wave height ( $H_{1/3}$ ), based on all the components, as:

$$H_{1/3}(x, y) = \sqrt{8 \sum_{n=1}^N |A(x, y)_n|^2} \quad (4.5)$$

where  $N$  is the total number of wave components and  $A(x,y)_n$  is the complex amplitude of the wave component  $n$ . Historically, significant wave height, which is the average of the one-third highest waves, has been referenced for characterizing the sea state, and it is used throughout REF/DIF S in additional computations (e.g, wave breaking).

As waves propagate over irregular bathymetry, complex interactions between individual waves and other natural physical phenomena create modifications to the wave field that result in a complicated three-dimensional problem. REF/DIF S is a parabolic model that solves this complex problem based on the mild slope equation developed by Berkhoff (1972).

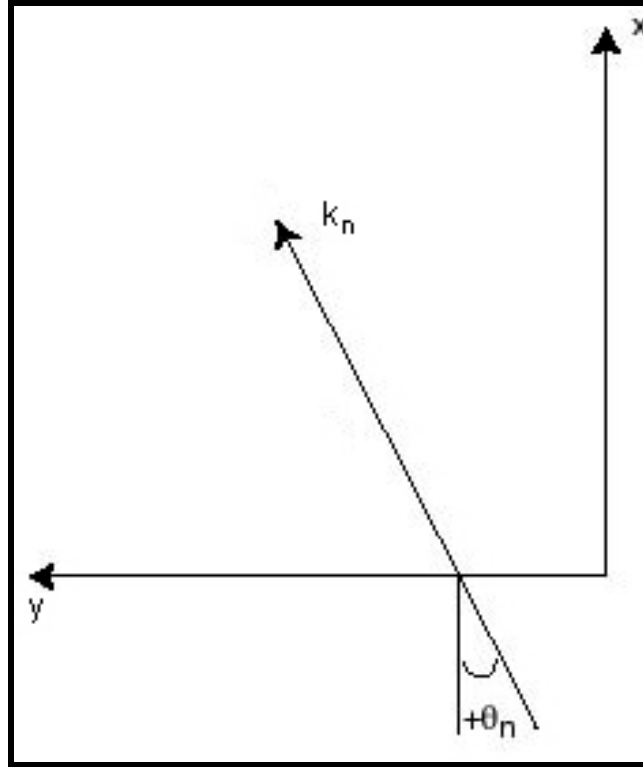


Figure 4-2. Coordinate and angle convention used for the wave modeling in the present study.

The vertically integrated mild slope equation can be written in terms of the horizontal gradient operator as:

$$\nabla_h \cdot (CC_g \nabla_h \eta) + k^2 CC_g \eta = 0 \quad (4.6)$$

where,

$$C = \sqrt{(g/k) \tanh kh} \quad (\text{Wave Celerity}) \quad (4.7)$$

$$C_g = C(1 + 2kh / \sinh 2kh) / 2 \quad (\text{Group Velocity}) \quad (4.8)$$

and  $g$  = acceleration of gravity and  $h$  = local water depth.

Although the mild slope equation is an approximation, it is accurate in both deep and shallow water and is sufficient even for large local bottom slopes (Booij, 1983). REF/DIF S uses the linear form of the mild slope equation and includes the effects of shoaling, non-linear refraction and diffraction (Kirby, 1983; Kirby and Dalrymple, 1983a), wave breaking, energy dissipation, and wave-current interaction (Kirby, 1984; Kirby and Dalrymple, 1983b). Equation 4.9 presents the complete form of the revised mild slope equation.

$$\frac{\partial A_n}{\partial x} = \frac{i}{2k_n} \frac{\partial^2 A_n}{\partial y^2} - \frac{\omega_n}{2C_{gn}} A_n - \alpha A_n \quad (4.9)$$

where  $\omega_n$  is the dissipation factor.

Through a combination of the various wave directions and frequencies, REF/DIF S is able to simulate the behavior of a random sea. In addition, detailed analysis and selection of input spectrum allows the model to assess the impact of different seasonal conditions and storms.

#### 4.1.1.1 Refraction and Diffraction

Wave refraction and diffraction have a significant impact on wave transformation along the coast. Wave refraction (Figure 4-3) tends to align wave crests parallel to offshore depth contours and eventually the shoreline. Wave energy may be distributed unevenly along the coast; therefore, wave refraction results indicate potential variations in sediment transport pathways. Wave diffraction (Figure 4-3) tends to spread wave energy as a wave passes a structure or a shoal. This effect is most evident behind shore parallel breakwaters. As waves propagate past a breakwater, they bend towards the shadow zone behind the structure. Wave energy is then transferred along wave crests towards regions of smaller wave height. As with wave refraction, diffraction also will result in an uneven distribution of wave energy along the coast.

In some cases, refraction and diffraction occur simultaneously, and it is important to be able to simulate both phenomena. REF/DIF S simulates refraction and diffraction using a parabolic approximation developed by Radder (1979) and Lozano and Liu (1980) to solve the mild-slope equation. This parabolic model was further extended by Kirby and Dalrymple (1983a) to be weakly non-linear. Comparisons with laboratory data (Kirby and Dalrymple, 1984) show the importance of non-linear dispersion terms in the governing equations as the weakly non-linear model indicated better agreement with the observed laboratory data.

#### 4.1.1.2 Energy Dissipation

In nature, sea floor characteristics vary from muddy substrates to sandy, rippled beds to rough, rocky bottoms. Therefore, assuming a rigid, impermeable horizontal seafloor is inadequate for quantifying wave transformation. To varying degrees, water waves are influenced by these bottom characteristics through wave damping. Energy dissipation is accounted for in REF/DIF S with three potential energy dissipation options assigned to the dissipation factor,  $\omega_n$ , presented in Equation 4.9.

1. *Laminar Surface and Bottom Boundary Layers* - accounts for the damping associated with boundary layers caused by viscosity at the surface and bottom as

$$\omega_n = \frac{\sigma_n k_n \sqrt{(\nu/2\sigma_n)(1-i)}}{\tanh k_n h} \quad (\text{Surface}) \quad (4.10)$$

$$\omega_n = \frac{2\sigma_n k_n \sqrt{(\nu/2\sigma_n)(1-i)}}{\sinh 2k_n h} \quad (\text{Bottom}) \quad (4.11)$$

where  $\sigma_n$  is the frequency and  $\nu$  is the kinematic viscosity.

2. *Turbulent Bottom Boundary Layer Damping* - accounts for wave conditions that result in a turbulent bottom boundary layer, as would occur in nature. The dissipation term is

$$\omega_n = \frac{2\sigma_n k_n f |A_n|}{3\pi \sinh 2k_n h \sinh k_n h} \quad (4.12)$$

where  $f$  represents the Darcy-Weisbach friction factor.

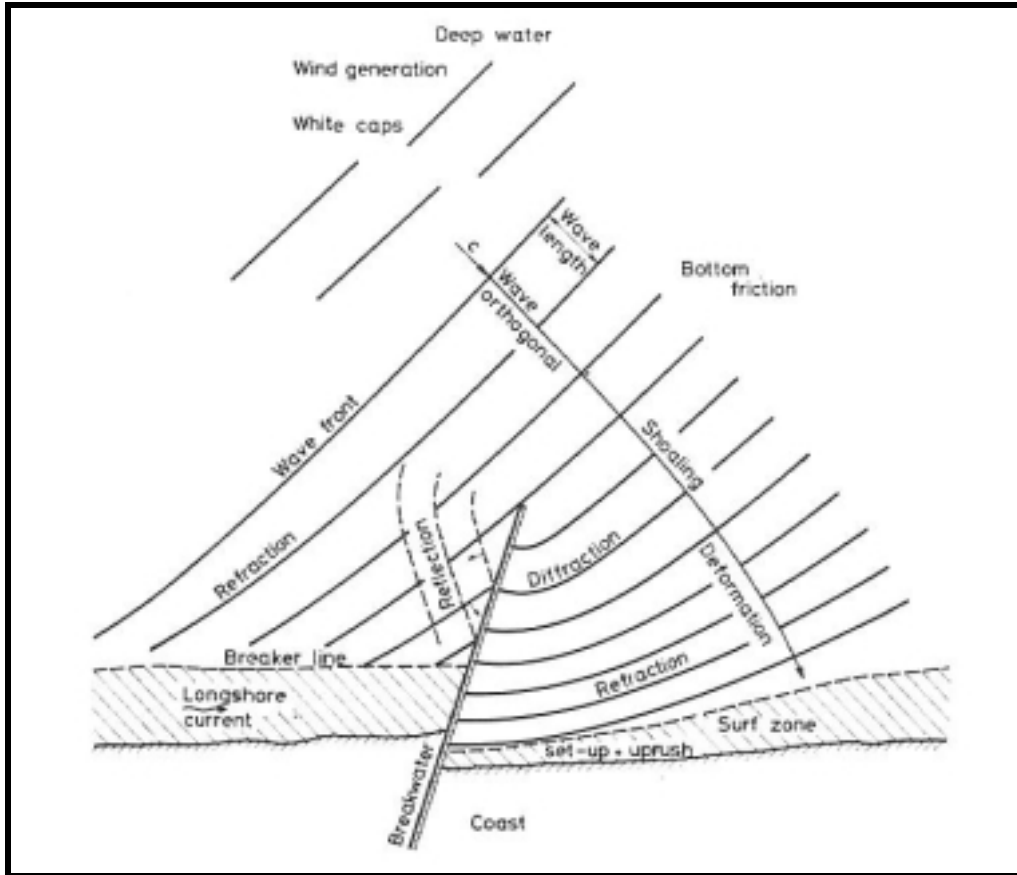


Figure 4-3. Diagram indicating the effects of refraction and diffraction as waves approach the coastline (from Svendsen and Jonsson, 1976).

3. *Porous Sand Damping* - accounts for wave damping due to the Darcy flow into sand bed where the dissipation term is

$$\omega_n = \frac{gk_n C_p}{\cosh^2 k_n h} \quad (4.13)$$

and  $C_p$  is the coefficient of permeability.

For this study, wave damping was simulated using a turbulent bottom boundary layer to most accurately represent natural conditions in the northeastern Gulf of Mexico. The assumed Darcy-Weisbach friction factor,  $f$ , in REF/DIF S is set equal to 0.01 by the model.

#### 4.1.1.3 Wave Breaking

As a wave proceeds into shallow water, it continues to shoal and increase in wave height. However, at some depth, a wave will become unstable and break. Seafloor and wave characteristics determine how a wave will break. In REF/DIF S, the breaking model developed by Thornton and Guza (1983) is employed to dissipate energy in the form of turbulence. Energy dissipation is expressed as:

$$-\varepsilon_b = \frac{\partial EC_{gn}}{\partial x} \quad (4.14)$$

where energy,  $E$ , is expressed as

$$E = \frac{1}{8} \rho g H_{rms}^2 \quad (4.15)$$

and bore dissipation,  $\varepsilon_b$ , is

$$\varepsilon_b = \frac{3\sqrt{\pi}}{16} \frac{\rho g f_p B^3}{\gamma^4 h^5} H_{rms}^7 \quad (4.16)$$

In Equation 4.16,  $f_p$  is the peak spectral frequency,  $H_s = 1.41H_{rms}$ , and  $B$  and  $\gamma$  are constants equal to 1 and 0.6, respectively. The breaking coefficient,  $\alpha$ , as presented in Equation 4.9, is a function of the bore dissipation and is very small when breaking does not occur. However, once breaking starts,  $\alpha$  begins to take on significant values and energy is dissipated from the wave field.

$$\alpha = \frac{4\varepsilon_b}{\rho g H_{rms}^2} \quad (4.17)$$

#### 4.1.1.4 Radiation Stresses

After each forward computational step, REF/DIF S calculates radiation stresses for waves propagating at angle  $\theta$  and outputs the values at every grid point in the model domain. For spectral modeling, radiation stresses are computed as a summation over all of the spectral wave components. Radiation stress in the y-direction due to the excess momentum flux in the x-direction is given by

$$S_{xy}(x, y) = \frac{1}{4} \rho g \sum_{n=1}^N \left( \frac{C_{gn}}{C_n} \right) (x, y) |A(x, y)_n|^2 \sin 2\theta(x, y)_n \quad (4.18)$$

Likewise, radiation stress in the x-direction due to the momentum flux in the x-direction and radiation stress in the y-direction due to the momentum flux in the y-direction are given by:

$$S_{xx}(x, y) = \frac{1}{2} \rho g \sum_{n=1}^N |A(x, y)_n|^2 \left\{ \left( \frac{C_{gn}}{C_n} \right) (x, y) (1 + \cos^2 \theta(x, y)_n) - \frac{1}{2} \right\} \quad (4.19)$$

$$S_{yy}(x, y) = \frac{1}{2} \rho g \sum_{n=1}^N |A(x, y)_n|^2 \left\{ \left( \frac{C_{gn}}{C_n} \right) (x, y) (1 + \sin^2 \theta(x, y)_n) - \frac{1}{2} \right\} \quad (4.20)$$

respectively. Radiation stress results are used as input to the nearshore circulation model and sediment transport simulations.

#### 4.1.1.5 Subgrids

Another feature of REF/DIF S is its capability to use a coarse-scale (typically hundreds of meters) reference grid and a fine-scale subgrid, which can have many times the resolution of the reference grid. The subgridding option can be implemented to resolve important topographic features (e.g., artificial islands, shoals, borrow pits, etc.) or increase resolution for coupling with

additional models (e.g., nearshore circulation). Figure 4-4 illustrates a case where a subgrid becomes important to increase resolution at a sand borrow site. The selection and development of reference grids and subgrids for the present study can be found in Section 4.3.

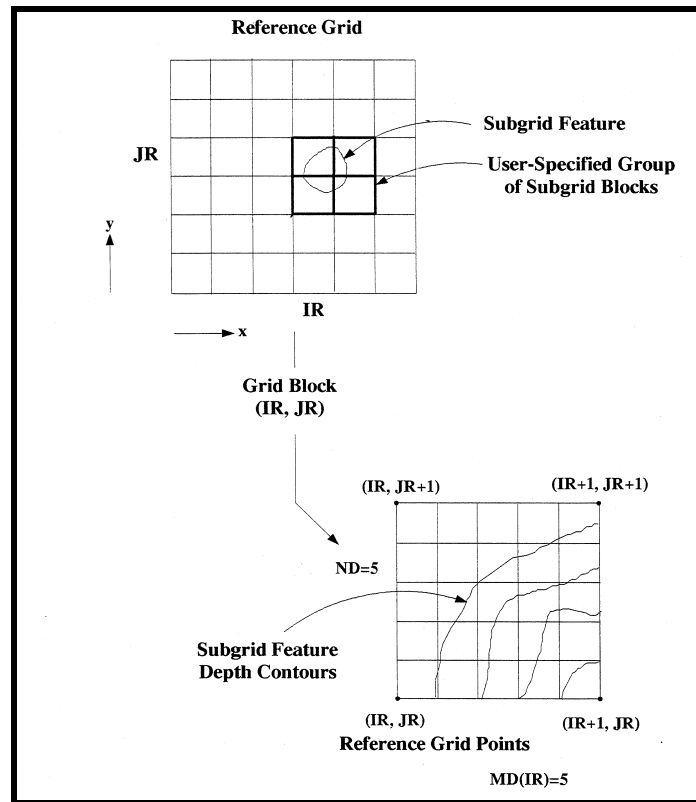


Figure 4-4. Example of subgrid development over a borrow pit feature (Kirby and Özkan, 1994).

#### 4.1.2 Required Input Conditions

Wave modeling requires an offshore wave specification and a bathymetric grid. By analyzing collected offshore wave data (National Oceanic and Atmospheric Administration [NOAA] wave buoys as well as other sources) or USACE WIS hindcast wave data, the appropriate wave input (spectra) can be developed and used to specify the offshore forcing boundary condition. By using local bathymetry to create an accurate grid, determine lateral boundary conditions, and select appropriate dissipation parameters, the model is capable of propagating waves to the area of interest. A comprehensive description of wave characteristics and spectral input determination can be found in Section 4.2, while development of site-specific reference grids (both existing and post-dredging) for the Alabama wave transformation numerical modeling can be found in Section 4.3.

#### 4.1.3 Wave Model Limitations and Modifications

The version of REF/DIF S used in this study was modified from REF/DIF S version 1.2 and obtained from Dr. James Kaihatu of the Naval Research Laboratory, Oceanographic Division at the Stennis Space Center, Mississippi. Dr. Kaihatu discovered limitations in the calculation method of the wave group velocity in REF/DIF S, which constrained the selection of y-subdivisions to the value of one. He also updated the finite difference scheme used for calculating peak wave approach angle, as well as disabled the internal, numerical filtering mechanism to reduce energy loss from the wave field. The removal of numerical filtering eliminated alongshore smoothing.

Additional modifications were made to REF/DIF S for the present study. The limitation discovered in the calculation of wave group velocity was corrected, allowing an uninhibited selection of y-subdivisions. The number of y-subdivisions can become critical depending on reference model grid spacing and bathymetric changes in the model domain. The ability to increase the number of alongshore subdivisions improves model resolution in the alongshore direction and allows more accurate calculation of wave field characteristics. REF/DIF S also was upgraded to run in either monochromatic or spectral modes, to allow for larger reference grids and subgrids, and to provide user-controlled output of major parameters (i.e., wave height, radiation stresses, etc.) within subgrid regions.

Although more advanced wave models are currently under development (i.e., Boussinesq modeling), the wave modeling presented here is similar to other currently accepted spectral wave modeling techniques and is adequate for gauging potential changes in the wave field caused by offshore sand mining. However, wave prediction capabilities are still limited even when using the spectral approach. Required computation time limits the spectral representation to discrete bins in the directional and frequency domains. Simulation of a continuous spectra, rather than discrete bins, would yield a more comprehensive and accurate representation of the wave field. In addition, REF/DIF S does not define the peak angle approach well in directional, multi-component seas or when waves become short crested. Wave modeling also requires detailed input (wave fields and bathymetric information) to produce high quality results, specifically those required to drive nearshore circulation and sediment transport models.

Existing modeling techniques also may be limited for simulating long-period, high-energy wave events (or storms), and the accuracy of results for these simulations is questionable. The reduced number of spectral components used for simulating long-period, high-wave events, as well as the lack of internal alongshore energy dispersion, produce wave modeling results with substantial gradients in alongshore wave height. These gradients (or streaks) associated with long wave period events indicate the limitation of REF/DIF S for areas with highly-variable offshore bathymetric contours, such as the eastern Alabama shelf. For these cases, REF/DIF S tends to over-predict wave focusing.

Despite some of the limitations of spectral wave modeling, it is the best overall technique currently available to simulate wave propagation. REF/DIF S is capable of accurately simulating most wave fields, and it is efficient for identifying potential modifications to the wave field caused by offshore sand mining.

## **4.2 WAVE CHARACTERISTICS AND INPUT SPECTRA**

A key component of accurate wave modeling is the analysis and selection of input wave data. The results derived from numerical wave transformation modeling are controlled by the quality of selected input data and parameters. This section describes the analysis and selection of input wave parameters for the modeling effort and focuses specifically on the development of seasonal and extremal spectra.

### **4.2.1 Wave Data Analysis and Sources**

#### **4.2.1.1 Wave Information Study and NOAA Buoy Data**

The U.S. Army Corps of Engineers Wave Information Study (WIS) has met a critical need for wave information in coastal engineering studies since the 1980s. WIS contains time series information of spectrally-based, significant wave height, peak period, peak direction, and wind speed and direction produced from a computer hindcast model. The hindcast wave model, WISWAVE (Resio and Tracy, 1983), is run using wind data (speed and direction) at selected coastal locations around the United States. The model provides wave climate based on local/regional wind

conditions. Because the data are numerically generated, consistent and long-term wave data are available at most coastal locations. WIS data used in this study include the effects of storms; however, the effects of extreme events, such as hurricanes, are not included. Simulation of an extreme, high energy event for the study area is incorporated using extremal analysis. WIS information originally was calculated by hindcasting deepwater waves from historical surface pressure and wind data (Brooks and Corson, 1984). The Phase I-type model used large-scale atmospheric conditions, a large grid size (hundreds of kilometers), and only one type of wave process, air-sea interaction. Phase I results do not include such effects as shoaling, bottom friction, or long waves. Although simplifications are present in Phase I-type modeling, it still provides adequate approximations of time-series results.

Wave measurements made by the NOAA during the 1980's made verification of WIS results possible by comparing the statistics and the distributions of wave heights and periods from different time periods (Hubertz et al., 1993). Improvements have been made through subsequent modeling efforts to increase the accuracy of WIS relative to NOAA measurements. Phase II-type WIS data, which include the effects of shoaling, refraction, diffraction, and bottom friction, were used in the present study. The Phase II WIS data provide wave parameter results every three hours.

The availability and long-term records make WIS information attractive when considering average or seasonal wave conditions. Since the data are widespread and continuous, adoption of the WIS data for development of spectral wave conditions is applicable. WIS stations used are located at or near the offshore boundary of the wave transformation model grid. Table 4-1 provides a summary of the WIS stations used in the present spectral wave modeling effort along the Alabama coast.

WIS Station	G1046	G1047
Reference Grid	B (Resource Areas 1, 2, & 3)	A (Resource Areas 4 & 5)
UTM Northing (m)	3,318,842	3,319,262
UTM Easting (m)	427,661	403,547
Depth (m)	28	28
Time Period (yrs)	1976 to 1995	1976 to 1995

Each of these stations is located seaward of the five sand resource areas in 28-m water depth. Input data (energy and directional spectra) for the reference grids are developed from simulated wave data for these two stations. Wave parameters do not differ significantly between the two stations. However, due to the significant distance between the two modeling grids, input spectra are generated for each grid separately.

Another source of wave data readily available in the Gulf of Mexico is NOAA observed wave data. The benefit of using NOAA data is that it is measured rather than hindcasted (predicted). Therefore, it includes high energy events, such as hurricanes. However, because NOAA buoys are collecting actual observations, the buoys are subject to severe weather and mechanical problems, and therefore, a consistent long-term wave record is more difficult to attain. Table 4-2 presents the locations and availability of NOAA data for offshore Alabama. The observed data consist of numerous gaps, limited deployment times, and changes in deployment location. These variables resulted in an incomplete and unfavorable wave data set. For example, directional wave data were collected only during time periods when the NOAA buoys were deployed landward of the sand resource areas (Table 4-2). Only during a brief deployment (Buoy 42015, December 1987 to December 1988) were wave data collected seaward of the sand resource areas. Spatial and

temporal data limitations made it difficult to use NOAA observations for anything more than ancillary data.

Station ID	Location	Deployment Time	Wave Data	Wind Data	Wave Direction
42015	30.1 N / 88.2 W	4/87-8/87	O	X	O
		9/87-10/87	O	X	O
		11/87	O	X	O
		12/87-12/88	X	X	X
42015	30.2 N / 88.2 W	12/88-9/90	X	X	X
42016	30.2 N / 88.1 W	4/88-9/88	X	X	X
		9/88-12/88	X	X	X
		4/89-11/89	X	X	X
		2/90-5/90	X	X	X
		7/90	X	X	O
		8/90-9/90	X	X	X
42016	29.9 N / 88.0 W	12/93-1/94	O	X	O
		2/94-3/95	O	X	O
42016	30.2 N / 88.2 W	5/95	O	X	O
		6/95	O	X	O

X = data collected; O = no data collected

#### 4.2.1.2 Data Comparison

In order to verify the accuracy of WIS hindcast data used in this study, a comparison was made between hindcast data and a time period (December 1987- December 1988) when wave data (NOAA Station 42015) were collected at approximately the same location. Figure 4-5 presents the results of the comparison from two distinct time periods in 1988 (January through April and May through September). Although differences exist between the data sets, WIS information simulates the structure and peaks of observed wave data fairly well. For the time period when WIS and NOAA data were available at similar locations (approximately one year), observed wave heights were within  $\pm 0.25$  meters approximately 70% of the time, and within  $\pm 0.5$  meters 93% of the time. The observed wave periods were within  $\pm 1$  second of the hindcast data 72% of the time, and within  $\pm 2$  seconds 96% of the time. A comparison of wave directions was not performed since the measured NOAA data did not include directional information during this deployment interval. Based on the results of the comparison, it was determined that the WIS data set was adequate for developing seasonal wave input conditions.

#### 4.2.1.3 Seasonal Characteristics

A detailed understanding of local wave climate is required to produce representative wave modeling simulations. The 20-yr (1976-1995) WIS data offer a synopsis of the wave climate offshore Alabama. An examination of local WIS stations (G1047 and G1046) provides a detailed description of the wave climate and development of appropriate input spectra.

Rather than selecting the most common wave heights and directions, a detailed analysis was conducted to summarize existing WIS data into average seasonal wave conditions and spectra. Each season may contain distinct differences in energy and/or directional spectra, and consequently produce varying impacts at borrow locations. Simulation of seasonal characteristics (averaged over 20 years) provides a method to identify these changes. For example, if there is a difference in mean

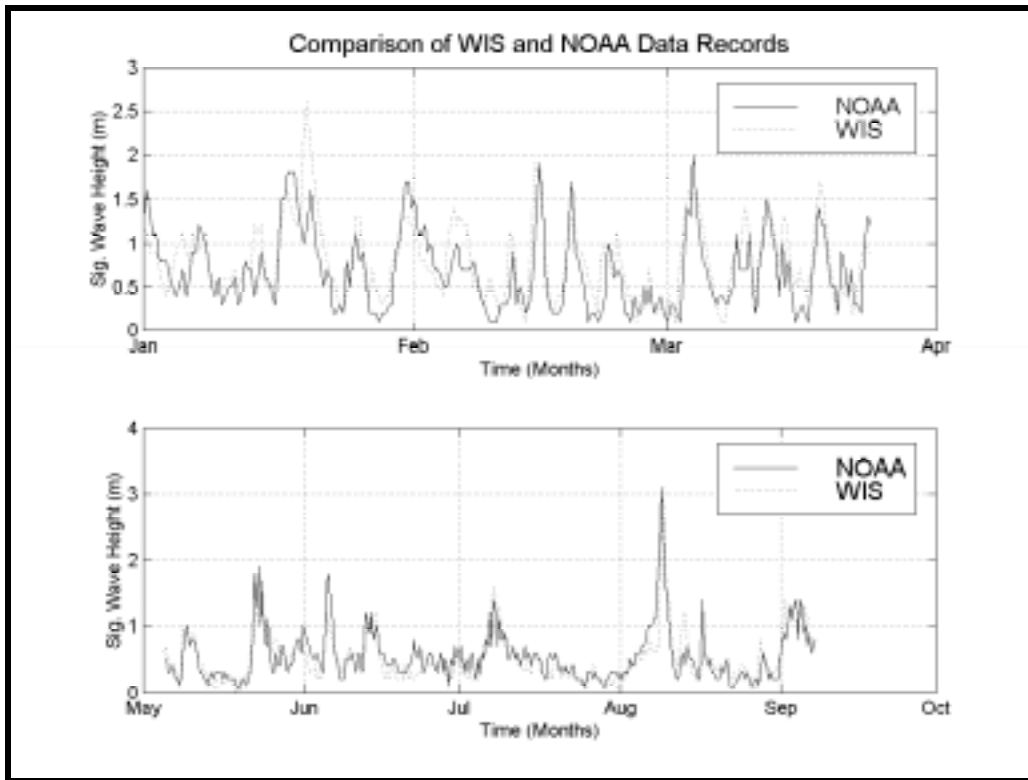


Figure 4-5. Comparison of WIS hindcast (dotted) and NOAA observed (solid) significant wave height for two time periods in 1988.

direction of wave approach during the summer and winter seasons, simulations for these two seasons may result in varying impacts caused by removal of sediment from potential borrow sites. Also, averaging 20 years of wave data creates typical seasonal wave conditions offshore Alabama. Spectra developed for the Alabama shoreline indicate that all seasonal waves propagate from east-to-west. Therefore, seasonal spectra do not incorporate the effects of occasional reversals in wave direction.

To summarize the historical data into appropriate seasons by energy and directional spectra, monthly wave conditions were examined for each WIS station. Figures 4-6 through 4-9 present examples of the monthly breakdown conducted using historical data. Figure 4-6 shows histograms of peak wave period and associated direction for the month of May, averaged over 20 years (1976 to 1995) for Station G1046 (Grid B). Figure 4-7 presents similar plots for the month of November. The analysis uses a high frequency cut off of 0.2 Hertz (5 sec) to eliminate periods of low wave energy from the analysis. Although wave components with periods less than 5 sec do contribute to the wave field, they do not contribute significantly to the sediment transport analysis. Wave periods of less than 5 seconds would require a higher resolution model grid, which would substantially increase model simulation time. Due to the extensive region evaluated, as well as the negligible impact to sediment transport calculations, wave periods less than 5 seconds were excluded from the analysis. During the month of May, the direction of wave approach is concentrated around a primary direction (narrow spreading), while during the month of November, an increase in spreading is evident. Also, greater low frequency (high period) waves appear during November than May. These differences illustrate the importance of evaluating specific seasonal phenomena rather than focusing only on overall average conditions.

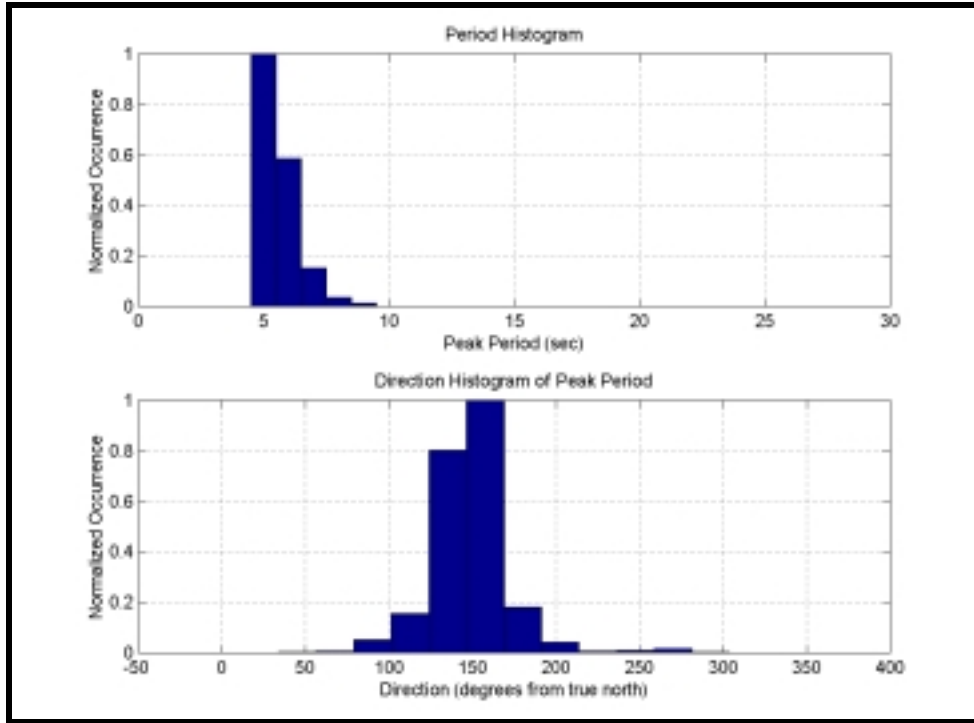


Figure 4-6. Histogram plots of 20-yr averaged peak periods and associated wave directions for the month of May at WIS Station G1046. The vertical bars are normalized by the greatest occurrence bin.

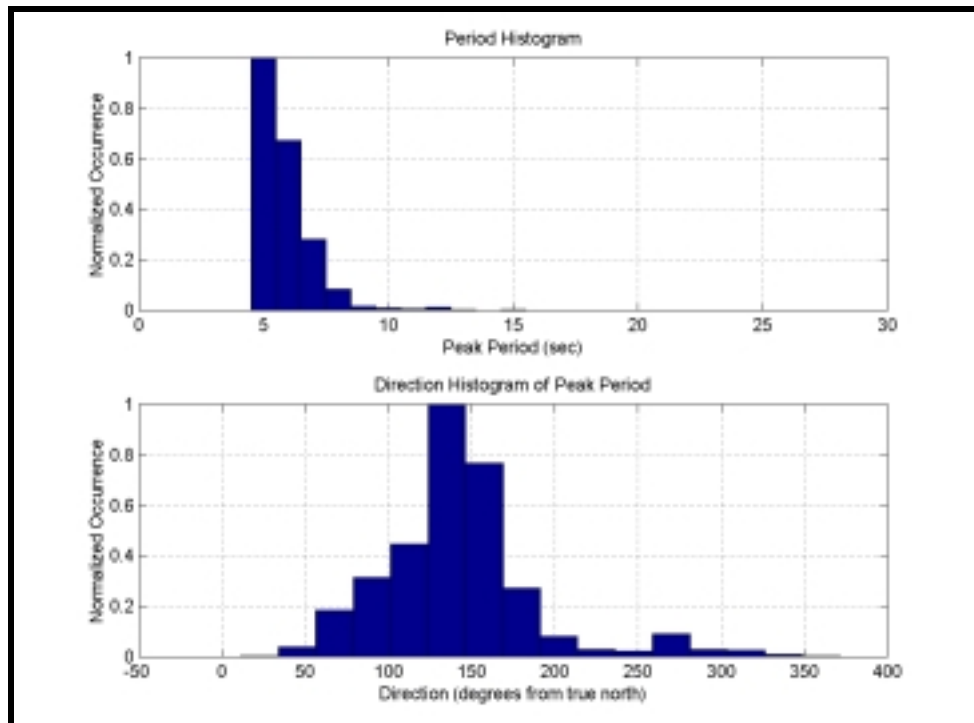


Figure 4-7. Histogram plots of 20-yr averaged peak periods and associated wave directions for the month of November at WIS Station G1046. The vertical bars are normalized by the greatest occurrence bin.

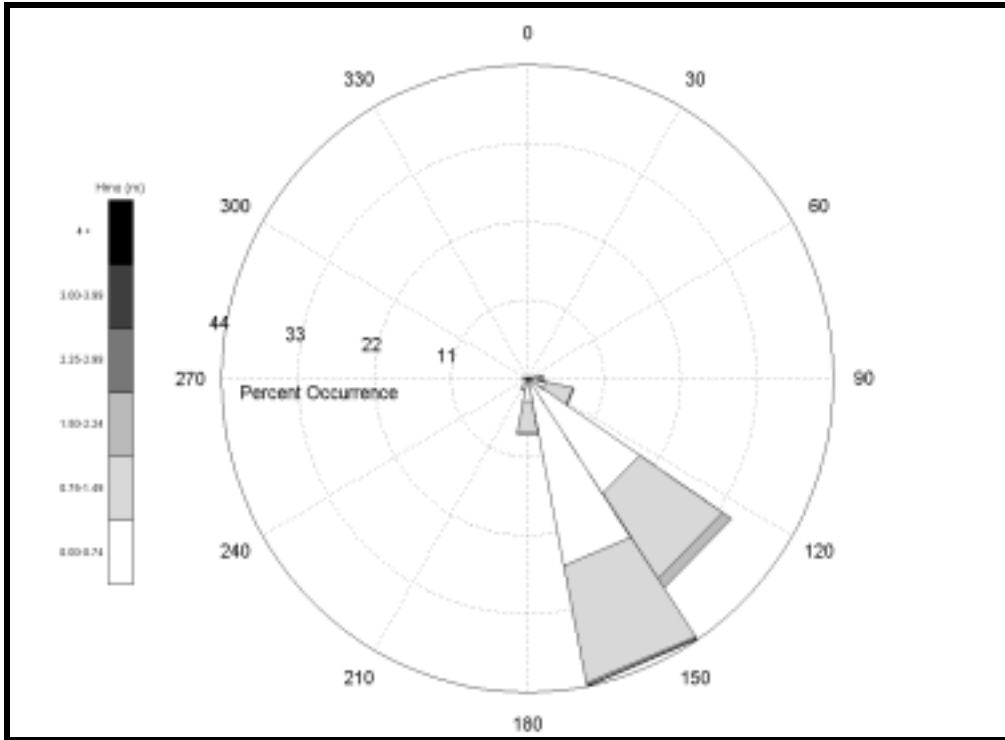


Figure 4-8. Twenty-year averaged wave rose for May at WIS Station G1046.

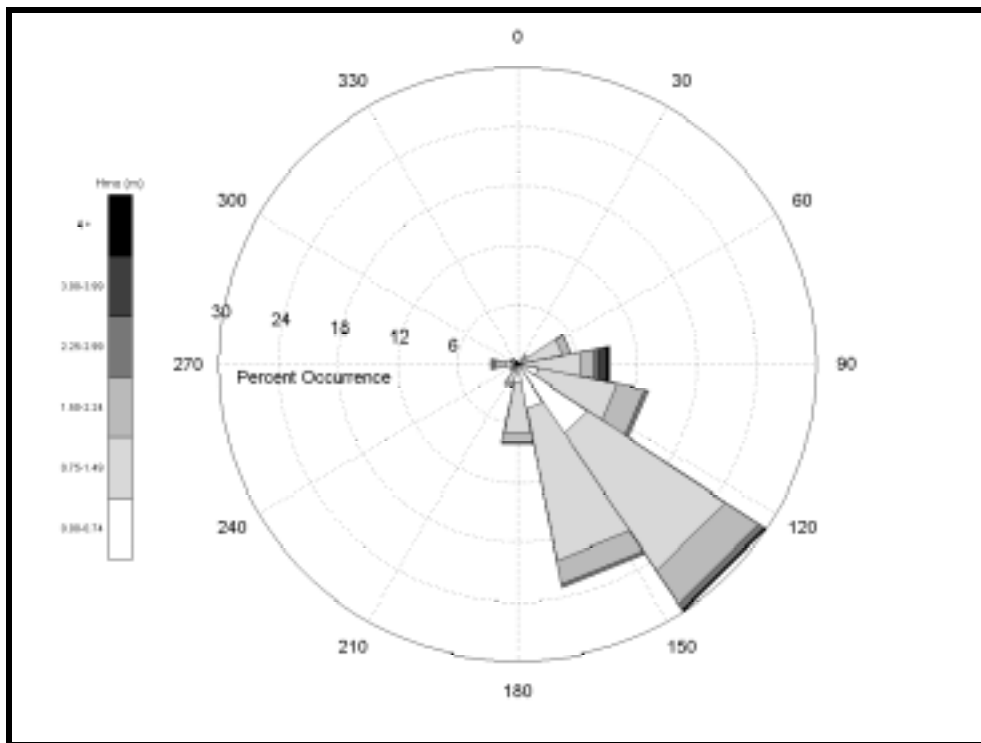


Figure 4-9. Twenty-year averaged wave rose for November at WIS Station G1046.

The distribution of significant wave height data (illustrated using a wave rose plot) for the months of May and November is presented in Figures 4-8 and 4-9, respectively. The color scale indicates the magnitude of wave height, the circular axis represents the direction of wave approach (coming from) relative to North (0 degrees), and the extending radial lines indicate percent occurrence within that magnitude and directional band. The month of November consists of higher energy waves and, as indicated with the directional spread of energetic wave periods (Figure 4-9), greater directional spreading. In contrast, the month of May has smaller wave heights and less directional spreading. Similar average breakdowns were completed for both WIS stations and all months.

Evaluation of wave characteristics for individual months provided a breakdown of the data set into specific seasonal averages. Using statistical summaries of monthly wave data (i.e., mean significant wave height, standard deviation of the significant wave height, mean direction, mean peak period, etc.), as well as the visual summary of data presented above, average seasons were determined. Monthly data were grouped by similar wave conditions (i.e., wave height, directional spread, frequency distribution, etc.) to form representative wave seasons and provide a convenient way to delineate the changes in wave climate. For example, summer seasons may be characterized by smaller wave heights and shorter wave periods, while winter seasons may consist of larger waves with longer periods. Table 4-3 presents the seasonal breakdown for each of the WIS stations. Due to the reduced wave climate in the Gulf of Mexico, seasonal variability is not quite as evident as it is along many open ocean coastlines.

WIS Station	G1046	G1047
Winter	December to February	December to February
Spring	March to May	March to May
Summer	June to August	June to August
Fall	September to November	September to November

Following the seasonal delineation, frequency and directional histograms, as well as wave rose plots, were developed for the four seasons. For example, Figure 4-10 presents the peak period and associated directional histograms for the spring season extracted from Station G1046. Figure 4-11 presents the wave height distribution in a wave rose for the same spring season. As before, the color scale indicates the magnitude of wave height, the circular axis represents the direction of wave approach (coming from) relative to North (0 degrees), and the extending radial lines indicate percent occurrence within that magnitude and directional band.

The recasting of WIS data into seasonal wave conditions was used in the development of energy and directional input spectra for REF/DIF S. A more detailed discussion on the development of individual seasonal spectra can be found in Section 4.2.2.1.

#### 4.2.1.4 High Energy Events

As discussed in Section 4.2.1.1, WIS data used in this study do not include hurricanes. Since these high energy events have a significant impact on many physical processes (and in most cases, dominate sediment transport), it is crucial to include storm simulations in wave modeling to assess their impact of potential borrow sites. Therefore, high energy events are simulated using wave transformation modeling, in addition to evaluating average seasonal conditions.

High energy events were evaluated by reviewing existing literature on hurricanes in the Gulf of Mexico, investigating the storm tracks, and using an extremal-value approach to analyze historical data sets. Results of the analysis, coupled with historical storm tracks and wave directions, were used to determine wave heights, directions, and frequencies for simulating a high-energy wave

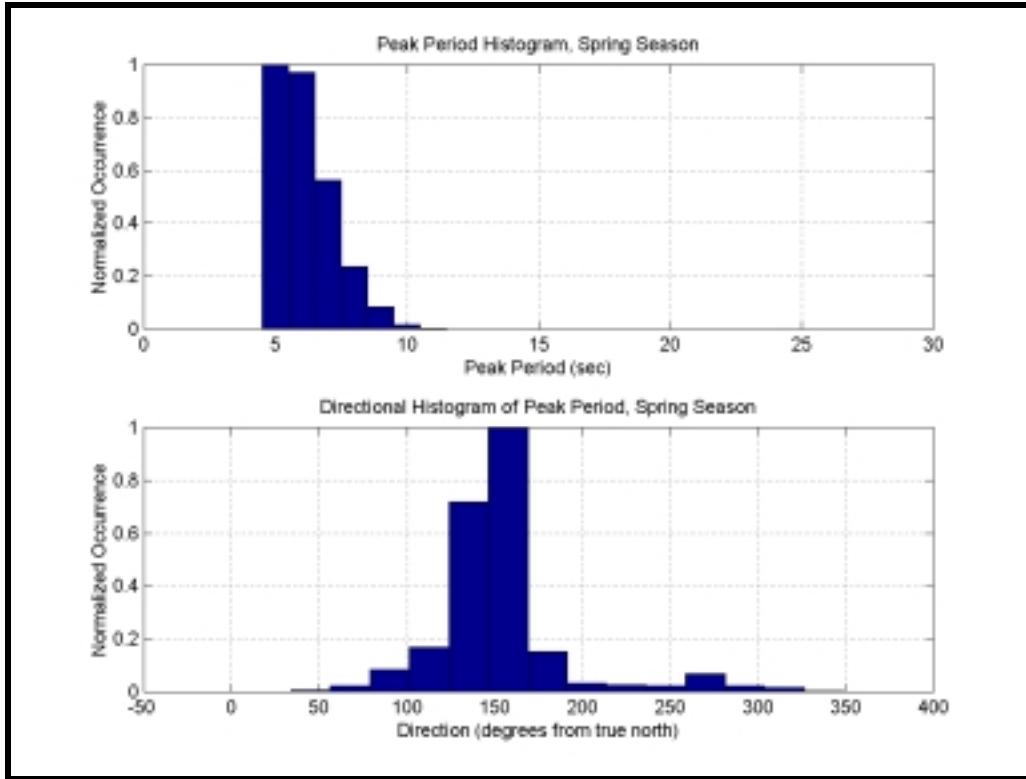


Figure 4-10. Histogram plots of 20-yr averaged peak periods and associated wave directions for the spring season at WIS Station G1046. Vertical bars are normalized by the greatest occurrence bin.

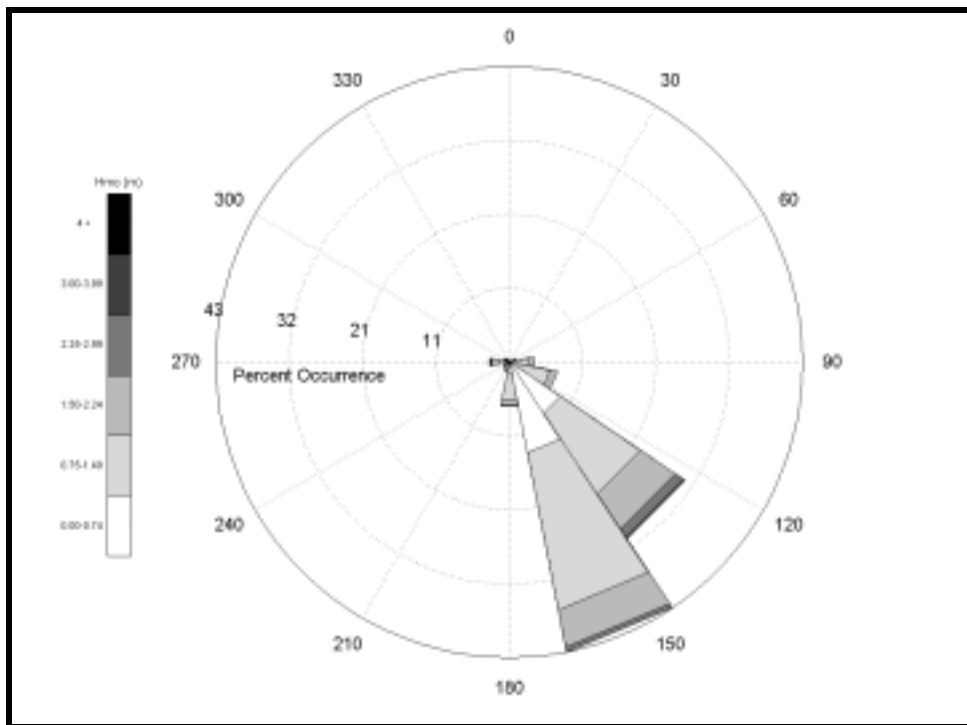


Figure 4-11. Twenty-year averaged wave rose for the spring season at WIS Station G1046.

event. Murray (1970) measured bottom currents near the coast during Hurricane Camille and also presented the track of the hurricane as it approached Gulf Shores. More recently, directional wave spectra observed during the passage of a frontal storm in the Gulf of Mexico were evaluated by Van de Voorde and Dinnel (1998).

Table 4-4 presents return periods calculated by the Coastal Hydraulics Laboratory (CHL), formerly the Coastal Engineering Research Center (CERC), based on WIS data (1976-1995). The return period can be thought of as the average period of waiting between events exceeding some specified value. Generally, return values are presented for 10 years, 25 years, 50 years, and 100 years, although any arbitrary return period can be calculated. The return periods calculated here are 2, 5, 10, 20, 25, and 50 years. For instance a 20-yr return value for a wave height of 6.4 m means that for any given year, there is a 1/20 chance that waves of 6.4 m will be reached. However, the return period is not the same as the probability that an event of a specific size will occur within a interval of time. Nor is the return period the frequency of occurrence of events of a given intensity. The specific selection of parameters representing the high energy (or extreme) wave event can be found in Section 4.2.3.

Return Period (yr)	Significant Wave Height (m)	
	Station G1046	Station G1047
2	4.14	4.17
5	5.10	5.19
10	5.76	5.90
20	6.40	6.58
25	6.60	6.79
50	7.22	7.46

## 4.2.2 Seasonal Condition Parameters

### 4.2.2.1 Spectra Development

REF/DIF S requires input of a directional wave spectrum, which represents the distribution of wave energy in the frequency and direction domains. The two-dimensional spectrum is given as the product of the energy and directional spectra as:

$$S(f, \theta) = E(f)D(\theta) \quad (4.21)$$

where  $S(f, \theta)$  is the directional wave spectral density function,  $D(\theta)$  is the directional spreading function, and  $E(f)$  is the frequency spectra. The directional spreading function provides the relative magnitude of directional spreading of wave energy, while the frequency spectra provides the absolute value of wave energy density.

Numerous empirical approximations have been developed to represent frequency and directional distributions. The frequency distribution for fully developed wind waves was approximated by Bretschneider (1968), or for deep water swell the JONSWAP formulation may be applied (Hasselmann et al., 1973). More recently, the TMA spectrum (Hughes, 1984) was developed for finite depths and is utilized in the present study. The TMA spectrum is given by the energy density,  $E(f)$ , for frequency  $f$  as:

$$E(f) = \frac{\alpha g^2}{(2\pi)^4 f^5} \exp \left\{ -1.25 \left( \frac{f_m}{f} \right)^4 + (\ln \gamma) \exp \left[ \frac{-(f - f_m)^2}{2\sigma^2 f_m^2} \right] \right\} \phi(f, h) \quad (4.22a)$$

where  $\alpha$  = Phillips' constant  
 $f_m$  = peak frequency  
 $\gamma$  = peak enhancement factor

The shape parameter,  $\sigma$ , is defined as

$$\sigma = \begin{cases} \sigma_a = 0.07 & \text{if } f < f_m \\ \sigma_b = 0.09 & \text{if } f \geq f_m \end{cases} \quad (4.22b)$$

The factor  $\phi(f,h)$  incorporates the effect of depth on the frequency distribution by

$$\phi = \begin{cases} 0.5[\omega_h^2] & \text{if } \omega_h < 1 \\ 1 - 0.5(2 - \omega_h)^2 & \text{if } 1 \leq \omega_h \leq 2; \quad \omega_h = 2\pi f \sqrt{\frac{h}{g}} \\ 1 & \text{if } \omega_h > 2 \end{cases} \quad (4.22c)$$

where  $h$  = water depth.

The peak enhancement factor,  $\gamma$ , can be manipulated to represent the narrowness (or broadness) of the input frequency spectra. A narrow frequency spectrum means the waves in the wave group have a relatively compressed frequency range, while broad spectra contain waves ranging over a greater frequency distribution.

In a similar manner, the directional spreading distribution can be represented through various formulations. Borgman (1985) developed the following relationship, which is applied in the current study:

$$D(\theta) = \frac{1}{2\pi} + \frac{1}{\pi} \sum_{j=1}^J \exp\left[-\frac{(j\sigma_m)^2}{2}\right] \cos j(\theta - \theta_m) \quad (4.23)$$

where

$\theta_m$  = the mean wave direction  
 $J$  = the number of terms in the series  
 $\sigma_m$  = the directional spreading parameter

The directional spreading parameter,  $\sigma_m$ , can be selected to produce narrow or wide directional range. A broad directional spectrum identifies waves approaching the coast from many different directions, whereas a narrow directional spectrum centers the wave group around the primary wave direction.

#### 4.2.2.2 Selection of Wave Conditions

Using the frequency distribution and directional spreading from WIS data, energy and directional spectra are generated to represent each seasonal scenario. WIS data distributions are matched with TMA frequency and directional spreading functions to obtain a best-fit of the data. The matching procedure involves adjustment and optimization of the peak enhancement factor and directional spreading parameter, as well as appropriate bin selection and energy conservation. After approximating the data with continuous and appropriate spectra, representative discrete components (in frequency and directional domains) are selected by discretizing the continuous spectra into energy conserving bins. Each component is representative of an energy conserving bin (equal area under the continuous curve).

Figure 4-12 illustrates the matching of spectra to spring season data at Station G1047 (Grid A). The upper two panels present the directional spreading verification (left-hand side) and the discretization of the continuous directional spreading function (right-hand side). The normalized amplitude histogram shows the directional distribution of WIS data (over 20 years) at Station G1047 during the spring season (Section 4.2.1.3). The triangles on both plots identify the discrete directional components representing continuous directional spectra. More spectral influence is placed at locations along the distribution where occurrences are more frequent. In this case, nine directional bins are used and the spreading is skewed slightly towards the negative direction of wave approach (southeast). Due to the directional limitation imposed in forward propagating wave models, a minimal portion of the directional energy may be lost for wide directional spreading. The lower two panels in Figure 4-12 present the frequency spectra verification (left-hand side) and the discretization of the continuous TMA spectrum function (right-hand side). As in the upper panels, the normalized amplitude histogram shows the frequency distribution of the WIS data (over 20 years) at Station G1047 during the spring season. The triangles on both plots identify the discrete directional components representing the continuous energy spectra. The cutoff frequency is evident in the derived spectra at 0.2 Hertz (5 sec). Again, discrete components are placed based on the makeup of each individual season while maintaining energy conservation. Nine components are used to divide the frequency spectra for the spring season.

As a second example, Figure 4-13 presents the matching of the spectra to the summer season data at WIS Station G1046 (Grid B). In this case, the energy and directional spectra are very narrow. Similar figures for all seasons and stations can be found in Appendix B1.

Following generation of the energy and directional spectra, values are coupled to produce discrete wave components forming a comprehensive seasonal wave group. For example, ten frequency bins and ten directional bins produces a wave field consisting of 100 individual waves. Tables 4-5 and 4-6 present a season-by-season summary of the spectral parameters used to develop input conditions corresponding to Grid A and Grid B, respectively. The parameters are used to develop the seasonal input wave conditions at the offshore boundaries.

### 4.2.3 High Energy Event Parameters

As an extreme simulation, a 50-yr storm event is modeled using the analysis presented in Section 4.2.1.4. Extremal wave heights were determined from return period calculations performed by the Army Corps of Engineers Coastal Hydraulics Laboratory (CHL). These calculations were based on WIS data from 1976 to 1995 at Stations G1046 and G1047. The corresponding storm event wave period was determined using the following equation:

$$T = 12.1 \sqrt{\frac{H_o}{g}} \quad (4.24)$$

as presented in the Shore Protection Manual (US Army Corps of Engineers, 1984).

Directional and energy spectra are estimated for the 50-yr event through comparisons of previous storm spectra (Van de Voorde and Dinnel, 1998) and application of Borgman's (1985) spreading function and a TMA spectra, respectively. The observed spectra (Van de Voorde and Dinnel, 1998) are used for comparison purposes only because the 50-yr storm does not represent a specific hurricane or storm event. Tables 4-5 and 4-6 present the spectral parameters used to develop the 50-yr storm input conditions corresponding to Grids A and B.

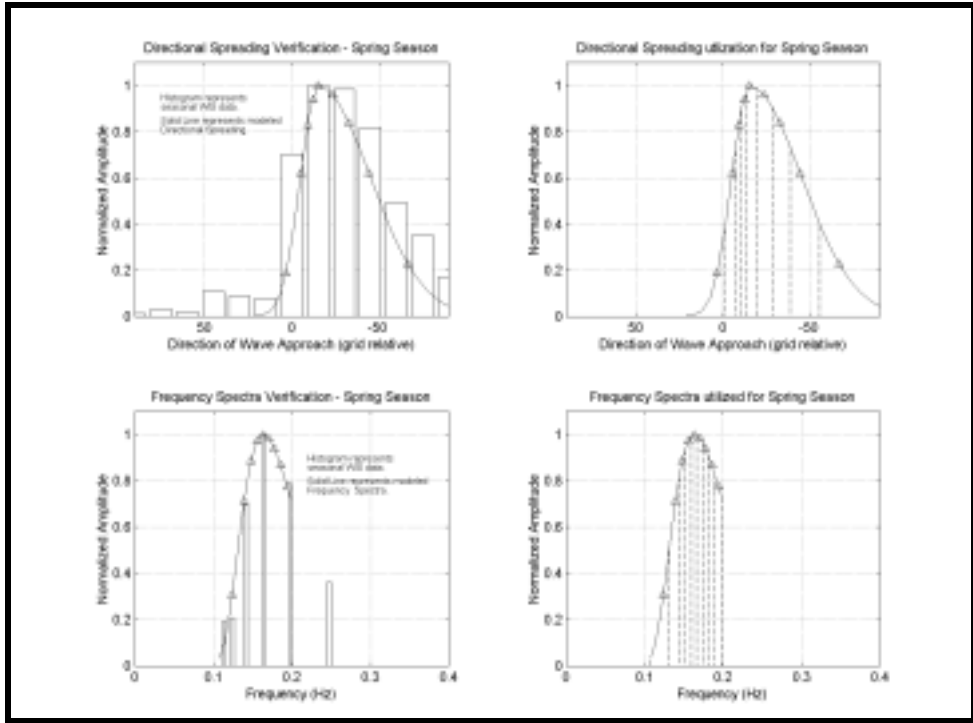


Figure 4-12. Energy and directional spectra verification and input set-up for the spring season at WIS Station G1047 (Grid A).

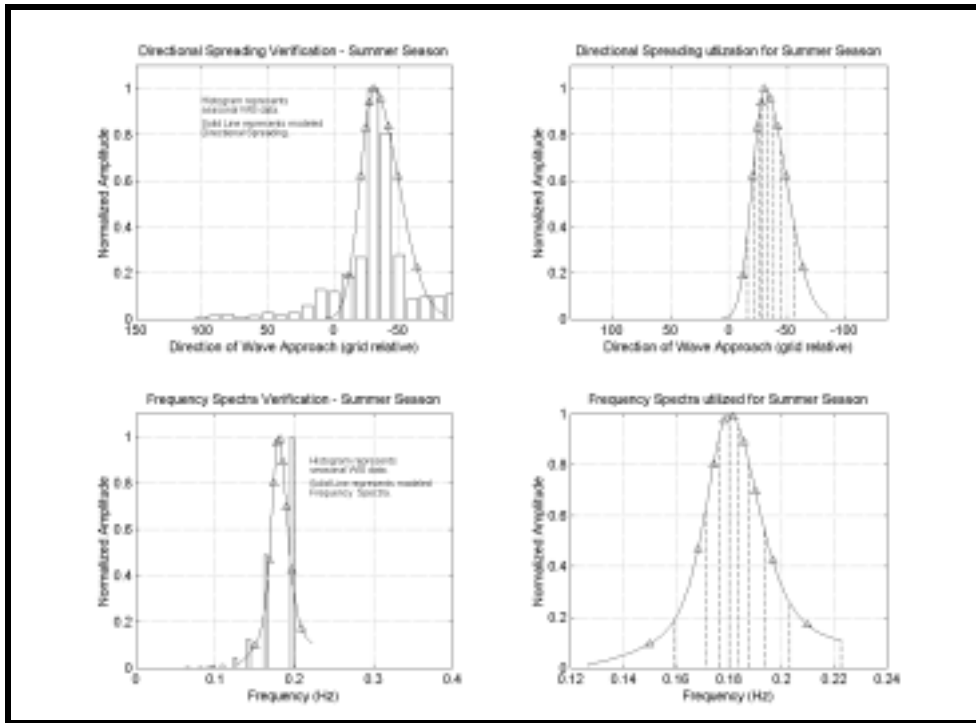


Figure 4-13. Energy and directional spectra verification and input set-up for the summer season at WIS Station G1046 (Grid B).

Scenario	Y-Sub	Spectra Type	# of E Bins	# of $\theta$ Bins	$T_{1/3}$	$f_p$	$f_{max}$	$\sigma_m$ (+)	$\sigma_m$ (-)	$\gamma$	$H_s$ (m)	$\theta_m$ (grid relative)
Spring (Significant)	10	TMA	9	9	6.76	0.160	0.20	10	30	1.0	1.56	15°
Summer (Significant)	10	TMA	7	9	6.14	0.167	0.23	35	25	2.0	1.36	45°
Fall (Significant)	10	TMA	9	9	6.68	0.21	0.3	25	40	1.0	1.82	45°
Winter (Significant)	10	TMA	10	11	6.60	0.185	0.3	12	30	1.0	1.70	10°
50-yr Storm	10	TMA	7	5	10.6	0.095	0.125	5	5	1.0	7.46	5°
$\gamma$ = Directional Peak Enhancement Factor (adjusted to fit seasonal spectra)								$\sigma_m$ = Directional Spreading Parameter				

Scenario	Y-Sub	Spectra Type	# of E Bins	# of $\theta$ Bins	$T_{1/3}$	$f_p$	$f_{max}$	$\sigma_m$ (+)	$\sigma_m$ (-)	$\gamma$	$H_s$ (m)	$\theta_m$ (grid relative)
Spring (Significant)	10	TMA	10	9	6.89	0.165	0.20	15	17	1.0	1.66	30°
Summer (Significant)	10	TMA	9	9	6.01	0.180	0.225	10	19	7.0	1.25	30°
Fall (Significant)	10	TMA	9	9	6.51	0.180	0.225	25	25	7.0	1.83	38°
Winter (Significant)	10	TMA	9	9	6.52	0.170	0.225	20	27	3.0	1.69	30°
50-yr Storm	10	TMA	7	5	10.3	0.096	0.125	5	5	1.0	7.22	5°
$\gamma$ = Directional Peak Enhancement Factor (adjusted to fit seasonal spectra)								$\sigma_m$ = Directional Spreading Parameter				

A storm surge value was also included in the wave modeling simulation to represent the increased water level experienced during the passage of a large storm event. Surge values for 25 storms from 1772 to 1969 (Chermock, et al., 1974) were used in an extremal analysis to estimate the value of a 50-year storm surge. A storm surge height of 3.0 m was determined from the extremal analysis and used as input for model simulations.

### 4.3 GRID GENERATION

#### 4.3.1 Existing Conditions

In REF/DIF S, the reference grid consists of a mesh of points with dimensions IR and JR, as shown in Figure 4-14. At each point within the domain, water depth, as well as ambient current data, can be specified. Reference points are separated by spacing DXR (x-direction) and DYR (y-direction). Because REF/DIF S uses at least 5 points per wavelength of the shortest modeled wave, reference grid selection is not always trivial. In addition, boundaries of the model domain should be outside of the study area of interest, so that interference from the boundaries does not affect modeling results.

The model domain for the present study is divided into two reference grids due to the large region that is required for wave transformation numerical modeling. The western grid (Grid A) is used to focus on the Dauphin Island coastline, whereas the eastern grid (Grid B) is used to evaluate changes along the coastline of Morgan Peninsula. The two reference grids overlap near the entrance to Mobile Bay to include potential effects from tidal flow in both grids.

Grids A and B were created from the most recent bathymetric information available (see Section 3). The offshore grid boundary was selected to correspond closely to the location of WIS stations used to develop spectral input. Table 4-7 presents the UTM coordinates for the corners of each of the reference grids.

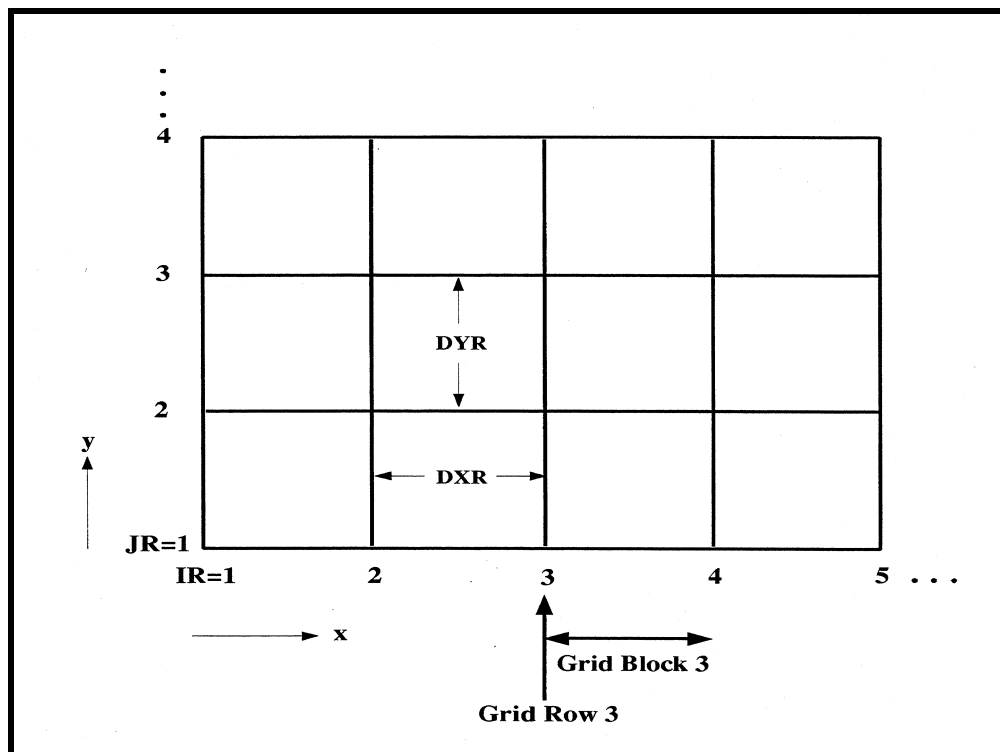


Figure 4-14. Illustration of reference grid notation (Kirby and Özkan, 1994).

Reference Grid	UTM Easting extents (m)	UTM Northing extends (m)
A	363,797 to 409,597	3,317,290 to 3,350,690
B	392,900 to 442,700	3,317,290 to 3,350,690

The reference grids cell size is 200 by 200 m with interpolated depths obtained from the bathymetric data at each grid intersection point. The interpolated depths were smoothed using a 5-point matrix smoothing routine. Figure 4-15 (Grid A) and 4-16 (Grid B) show the associated bathymetric grids, sand resource areas, and subgrids for each study region, as well as the location of WIS and NOAA stations in the region.

Although the reference grid spacing was fixed at 200 m, subgrids and other input parameters allow REF/DIF S to calculate information at intermediate points within the reference grid. Depths at intermediate points are computed by REF/DIF S by fitting a twisted surface to the reference grid through linear interpolation. In the alongshore direction, the grid was subdivided by ten to yield a spacing of 20 m. This subdivision spacing was chosen to optimize computational time versus spatial resolution in the longshore direction, as well as to provide adequate information for nearshore sediment transport modeling. In the onshore direction, REF/DIF S automatically subdivides each reference grid step by the smallest calculated wavelength in the spectrum. Therefore, the onshore spacing varies throughout the domain as a function of the propagating wave field, unless the model is in a subgrid region. In areas where a subgrid is specified, the onshore subdivision must be fixed to correspond to the defined subgrid spacing (i.e., locations where depths and currents are specified).

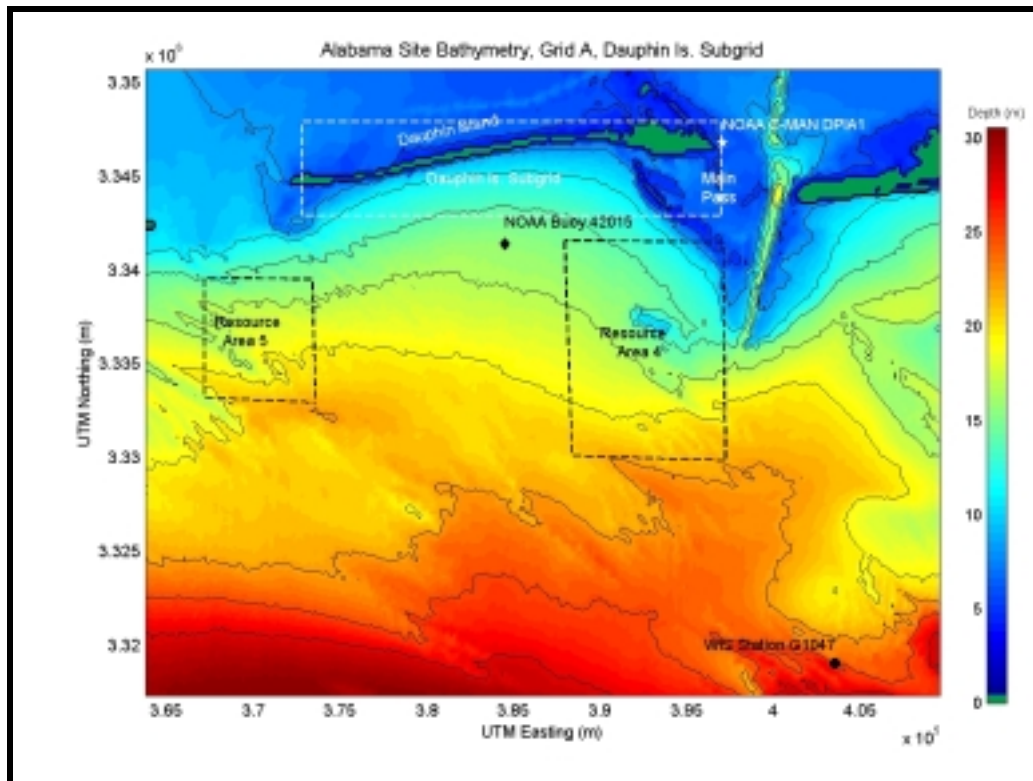


Figure 4-15. Bathymetry for Reference Grid A (Dauphin Island), with locations of WIS and NOAA stations, the defined sand resource areas, and the nearshore Dauphin Island subgrid.

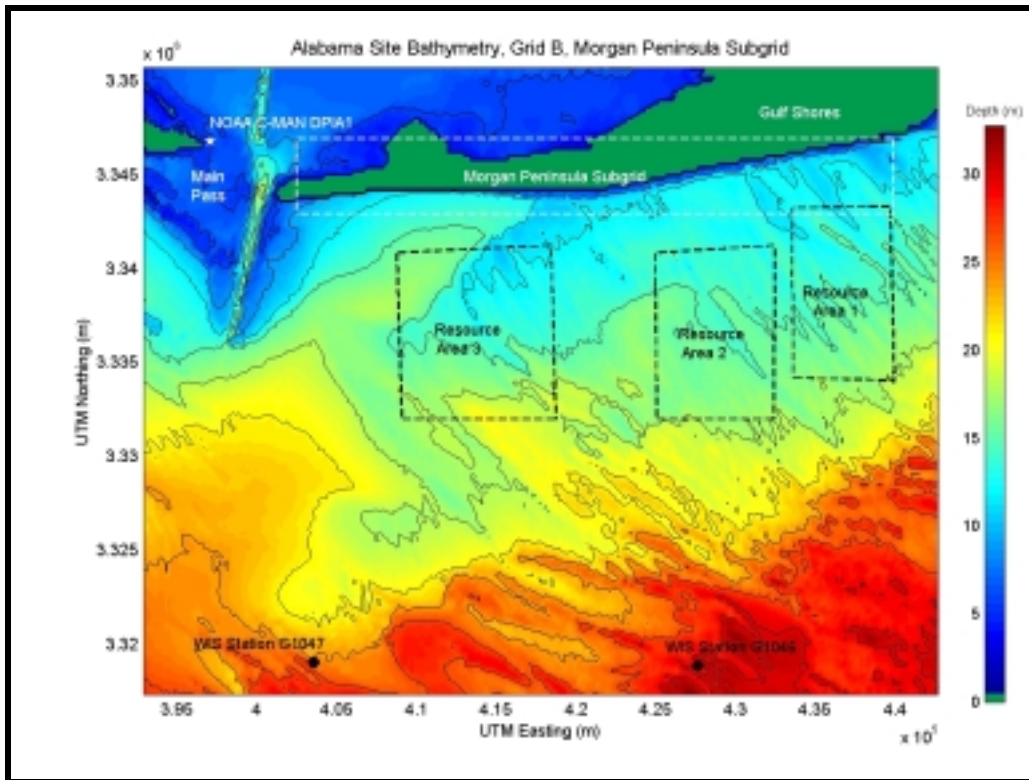


Figure 4-16. Bathymetry for Reference Grid B (Morgan Peninsula). With locations of WIS and NOAA stations, the defined sand resource areas, and the nearshore Morgan Peninsula subgrid.

Nearshore subgrids were created in the reference domains for Dauphin Island and Morgan Peninsula shorelines. Subgrids were used to generate detailed results in the nearshore zone as input to nearshore circulation and sediment transport models. Table 4-8 presents the dimensions and extents of each of the subgrids, as shown in Figures 4-15 and 4-16. Wave heights, water depth, and radiation stress results were output from each grid node in the subgrid domain.

Reference Grid	Subgrid	Onshore Spacing (m)	Alongshore Spacing (m)	UTM Easting extents (m)	UTM Northing extents (m)
A	Dauphin Is.	5	20	372,797 to 396,997	3,342,890 to 3,347,890
B	Morgan Peninsula	5	20	402,500 to 439,900	3,342,890 to 3,346,690

## 4.3.2 Post-Dredging Scenarios

### 4.3.2.1 Sand Borrow Site Selection

Four offshore borrow sites were identified as potential sources of beach quality sediment (see Section 7.0 for details); these data were used to numerically excavate wave modeling grids to simulate the impacts dredging may have on physical processes in the region (e.g., wave transformation and sediment transport). Three borrow sites are located east of Main Pass, one each within Sand Resource Areas 1, 2, and 3 (Figure 4-17). The final potential borrow site is located within Sand Resource Area 4 (Figure 4-18).

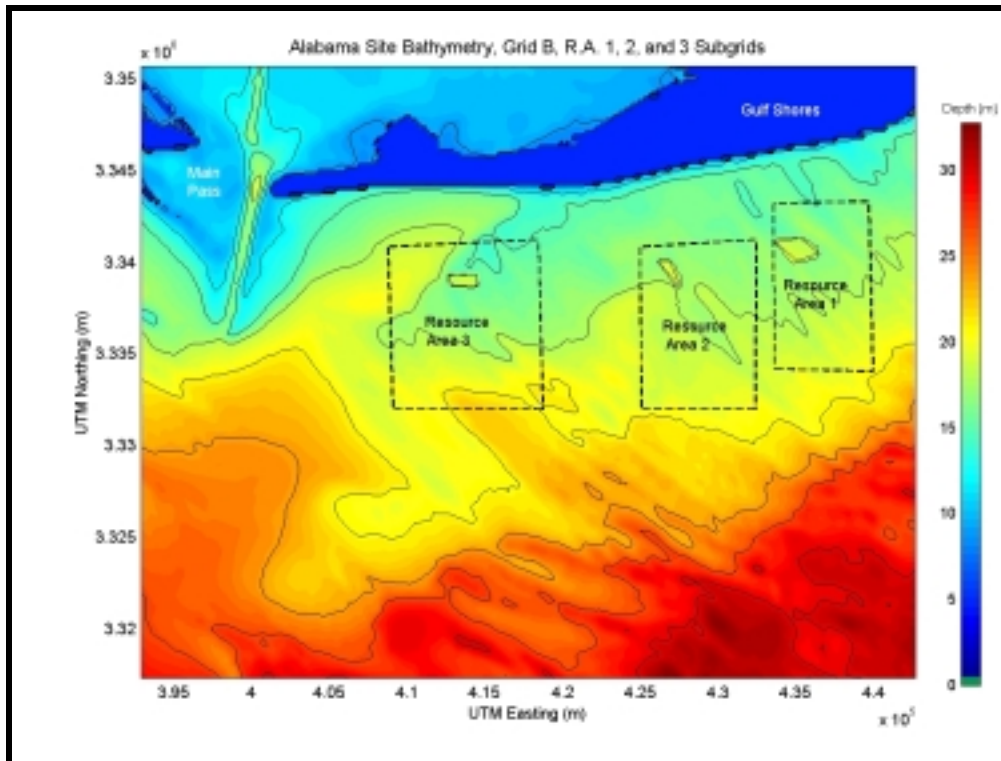


Figure 4-17. Potential borrow site locations (solid black lines) east of Main Pass.

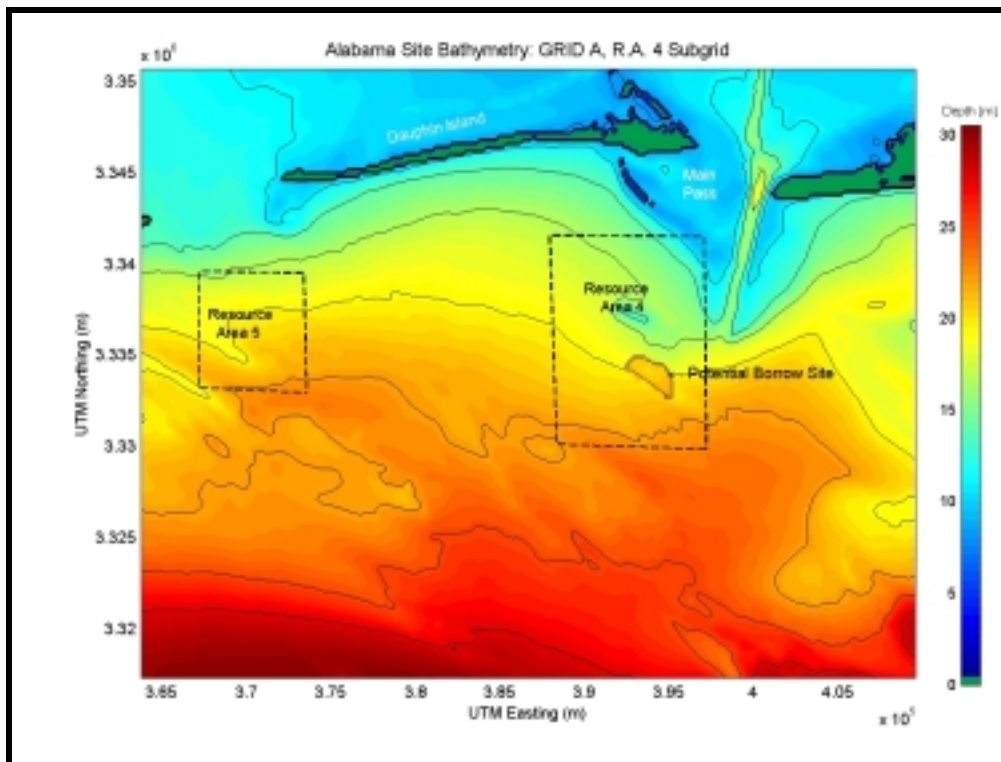


Figure 4-18. Potential borrow site location (solid black line) in Sand Resource Area 4.

The areas and volumes of the potential sand borrow sites were selected using the following guidelines.

- Sand Resource Areas - borrow site selection was limited to regions within the sand resource areas defined by the Mineral Management Service (MMS) and the Geological Survey of Alabama (GSA).
- Shoaling Regions - based on geomorphology within each sand resource area, regions characterized by shoaling features were selected. In this manner, the proposed dredging creates a flat bottom rather than a hole in the bathymetry surface. In addition, shoaling indicates regions that should replenish more quickly than others.
- Thickness of Sediment Layer - depth of dredging was based on the thickness of available sediment at each borrow location. The thickness of the sediment layer was determined from GSA core data sets.
- Extreme Dredge Scenarios - dredge volumes were selected to represent large sediment extraction scenarios or cumulative impact scenarios (e.g., dredging the same region before it replenishes with sediment). Although it is unlikely that the total sand volume extracted in the scenarios would ever be reached, extreme dredge scenarios are useful for evaluating at potential long-range and extreme impacts caused by sand dredging. The large borrow sites will have a greater impact on the physical processes, and therefore, indicate worst case situations.
- Beach Quality Sediment and Proximity to Nourishment Locations - the selection of borrow sites also considered the quality of beach compatible sediment and the relative proximity to nourishment locations.

Each of the four borrow sites were numerically dredged to simulate post-extraction scenarios. In the eastern reference modeling grid (Grid B), borrow sites within Sand Resource Areas 1, 2, and 3 are dredged simultaneously to simulate the combined impact from all three borrow sites and limit the number of model simulations.

#### 4.3.2.2 Numerical Excavation of Gridded Surfaces

Following the selection of potential dredging locations, four sand resource areas were numerically excavated to evaluate the impact of bathymetry changes on wave transformation, nearshore circulation, and the beach and borrow location sediment transport. The depths of the sand borrow areas were increased to reflect the effects of potential dredging scenarios. Table 4-9 lists the sand resource areas where each numerical excavation was performed, as well as the excavation depth and resulting dredged sand volume. For example, if the pre-dredging depth at a grid point within Sand Resource Area 1 is 16 m, the post-dredging depth is increased to 19 m. As the wave field propagates into the grid, it is affected by a number of factors, including the increased water depth at the dredged location.

Sand Resource Area	Depth to be Dredged (m)	Resulting Sand Volume(x 10 <sup>6</sup> m <sup>3</sup> )
1	3	5.8
2	3	1.7
3	4	4.7
4	3	8.4

Figure 4-19 illustrates the size, shape, and location of each borrow site within the sand resource areas. Because each grid consists of hundreds of cells, every grid point in the model domain has a water depth associated with it. Therefore, each grid point within the dredged borrow site can be artificially deepened to simulate effects of various dredging scenarios.

#### 4.4 PRE-DREDGING RESULTS

##### 4.4.1 Seasonal Simulations

Model simulations were performed for existing conditions (pre-dredging) with seasonal spectra and a 50-yr storm spectrum. This section discusses results for simulations of existing conditions. Figure 4-20 illustrates REF/DIF S results for the Dauphin Island grid (Grid A) for a typical spring season. The color map corresponds to the distribution of significant wave height (m) throughout the modeling domain. Solid black lines represent bathymetric contours. Land masses are shown in brown and are represented as thin film layers in REF/DIF S. Therefore, some wave energy is able to advance beyond the narrower sections of coastline into Mobile Bay and Mississippi Sound (e.g., the western end of Dauphin Island). Similar plots for a typical spring season can be found in Appendix B2.

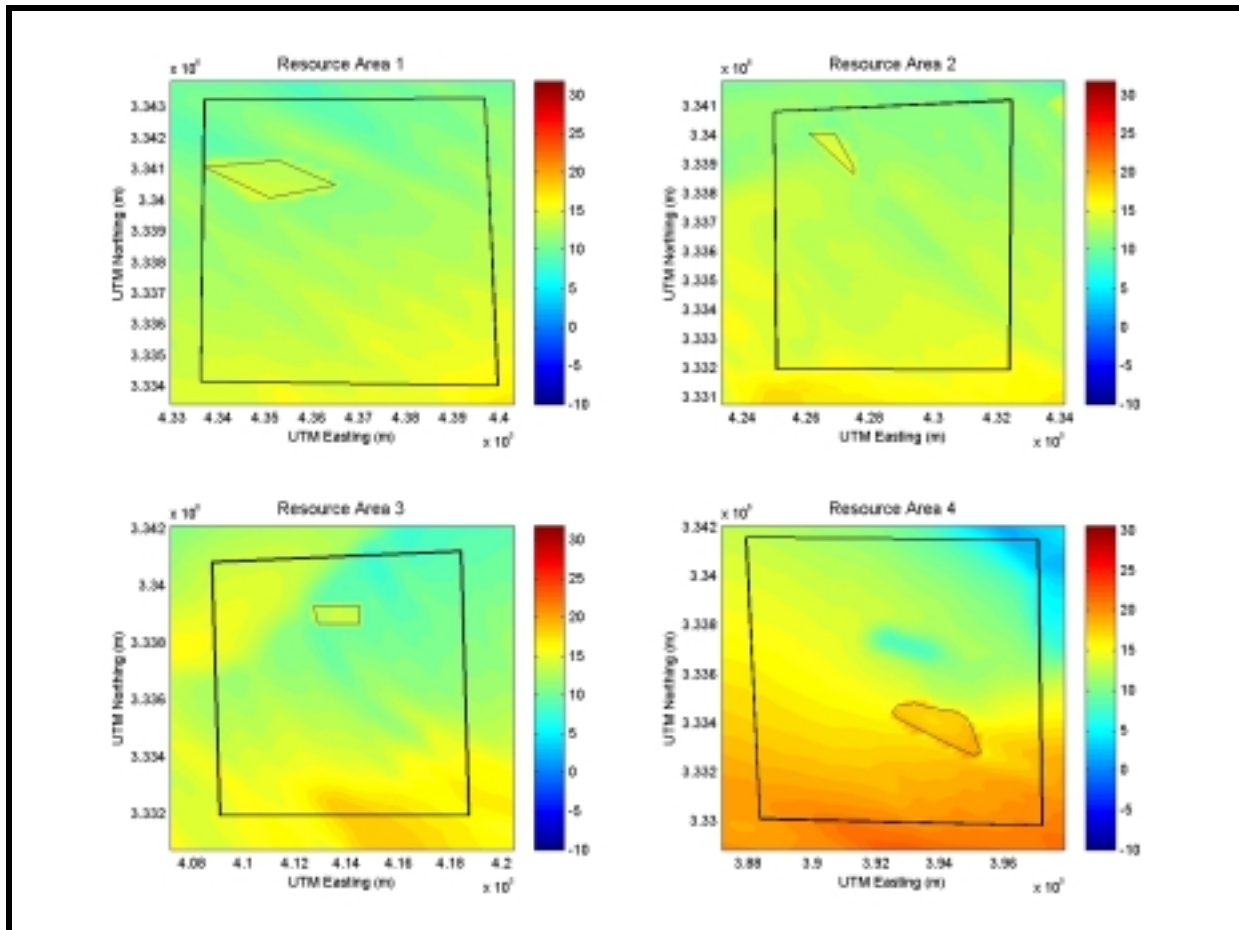


Figure 4-19. The four sand resource areas (outlined by the thick black line) and associated borrow sites (indicated by the thin black line).

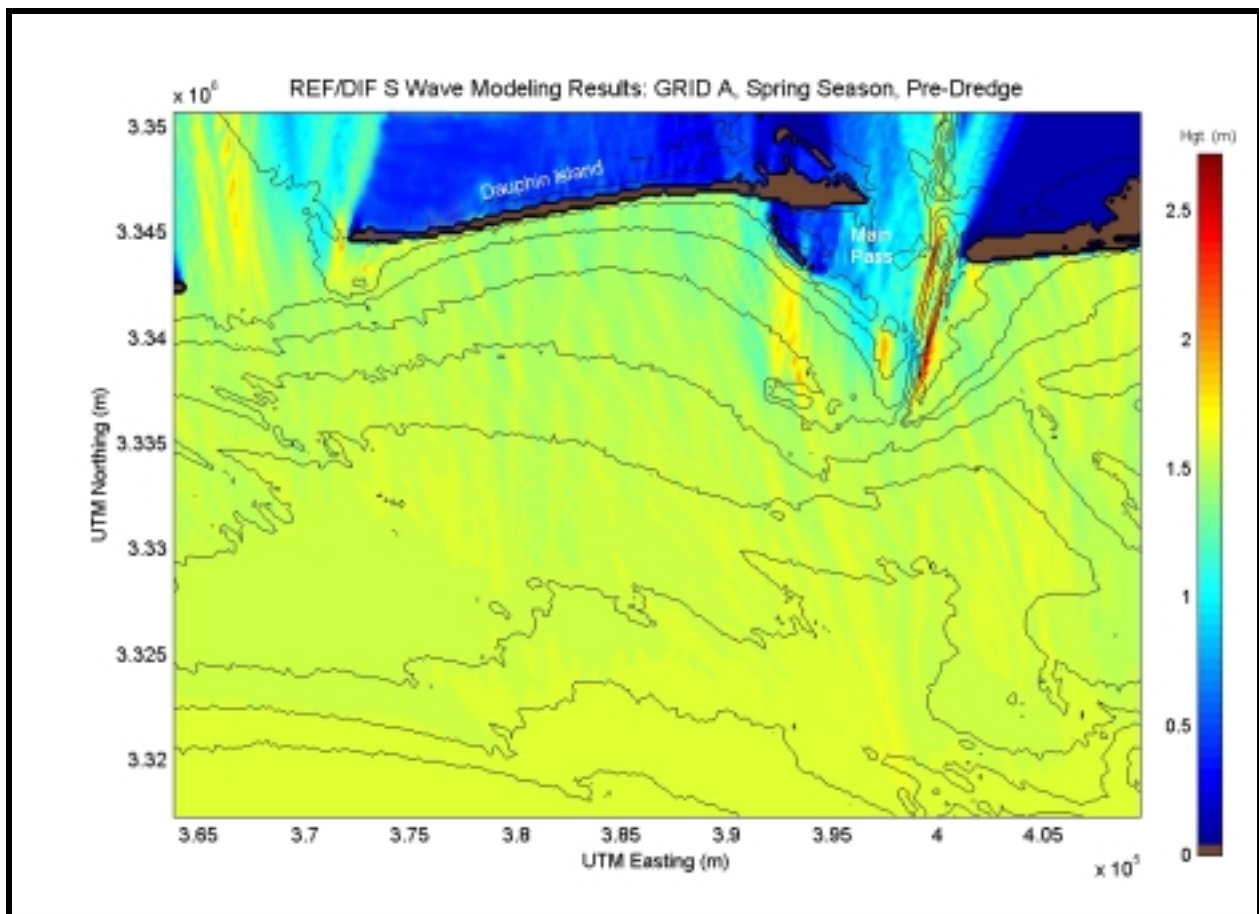


Figure 4-20. Spectral wave modeling results for existing conditions utilizing a typical spring season at reference Grid A.

There is minimal variation in wave heights in the offshore region for the spring simulation results (Figure 4-20). Because most of the spectral wave components do not interact with the seafloor at this depth, the wave field is not significantly affected by changes in bathymetry. The influence of bathymetry becomes significant at approximately the 15-m depth contour, where wave height and direction begins to change.

Wave focusing, divergence, and shadowing occur at several locations around Dauphin Island. Significant wave focusing is evident behind the Mobile Outer Mound disposal area. Wave refraction around this feature creates increased wave heights of approximately 0.25 to 0.5 m in the lee of the disposal area, and decreased wave heights adjacent to the mound. Wave focusing caused by Mobile Outer Mound produces an increase of energy that advances towards Pelican Island. Pelican Island offers a natural protective buffer against wave action for the eastern end of Dauphin Island, as indicated by the shadow zone behind the Pelican Island region. Wave focusing caused by Mobile Outer Mound most likely results in increased erosion at Pelican Island, which may significantly consume this protective wave buffer during a storm event.

An increase in wave height is also apparent west of the dredged navigational channel into Mobile Bay (397,500 Easting; 3,340,000 Northing). Bathymetric contours in this area focus wave energy into a region just before the eastern edge of the ebb shoal. The shape of contours in this

region causes waves to refract and converge. The resultant increase in wave height (approximately 0.5 m) dissipates quickly as the wave field propagates over the ebb shoal.

A similar increase in wave energy also is evident near the western end of Dauphin Island as the bathymetric contours refract the waves towards the western tip of Dauphin Island. Because the western end of Dauphin Island is the terminal end to net longshore sediment transport (east to west), an increase in wave energy in this region will not create significant erosion, though sediment transported into the region may be moved north and into Mississippi Sound as it encounters Petit Bois Pass. A significant amount of wave energy propagates through the pass between Dauphin Island and Petit Bois Island into Mississippi Sound as the bathymetry in this region remains relatively deep.

Another area of increased wave energy is located in regions adjacent to the dredged navigational channel (Main Pass) of Mobile Bay. Waves entering the region shoal in shallower areas (less than 5 m) adjacent to the dredged channel. Waves approaching from the southeast, as in the typical spring scenario, reform in deeper water of the navigation channel and shoal against the western edge of the channel.

Wave heights are relatively constant along the Dauphin Island shoreline. The eastern end of Dauphin Island is protected from significant wave energy by a shadow zone produced from Pelican Island and subaerial portions of the ebb shoals. A small amount of wave energy advances through the relatively narrow gap between the aerial and subaerial portions of the ebb shoal (approximately 394,000 Easting; 3,344,000 Northing).

The existing conditions simulation for the winter season, as presented in Appendix B2, produces results that are very similar to the results discussed for a typical spring season. Minor differences appear due to the increased significant wave height and subtle changes in the frequency and directional spread of the incident spectrum. Slightly larger wave energy increases are located in areas where wave shoaling was identified for the spring season, although the maximum increase is greater for the spring season near the dredged navigational channel into Mobile Bay.

During a typical summer season (figure presented in Appendix B2), average wave heights are significantly reduced (approximately 0.3 to 0.5 m) in regions where wave shoaling is apparent. Wave focusing caused by Mobile Outer Mound and regions near the dredged navigational channel is less concentrated and less severe. This is the result of a combination of reduced wave energy during the summer season, the change in peak spectral wave direction, and a broader directional spectrum. A slight increase in wave energy is allowed to proceed through the area between Pelican Island and the subaerial portion of the ebb shoal due to the angle of wave approach.

Fall season results (illustrated in Appendix B2) are similar to results for a typical summer season. Patterns of wave convergence and divergence during the two seasons are similar, with wave heights during the fall season 0.5 to 0.6 m higher than in summer.

Figure 4-21 illustrates results for a typical spring season along the Morgan Peninsula (Grid B). The color map corresponds to the distribution of significant wave height (m) throughout the model domain, while the solid black lines represent bathymetric contours. Similar plots for the entire season can be found in Appendix B2. As with Grid A, there is little variation in wave heights in the offshore region.

Areas of wave convergence and divergence seaward of the Morgan Peninsula shoreline are caused by the irregular bathymetry and the southwest-oriented seaward extending shoal located at approximately 414,000 Easting; 3,337,500 Northing. Wave energy converges in regions where bathymetric contours are aligned shore perpendicular as waves refract to match the bathymetry. In areas where bathymetric contours experience sudden changes in the along shore direction, wave convergence and divergence are apparent. Grid A simulations document an increase in wave height near the edges of the dredged navigational channel.

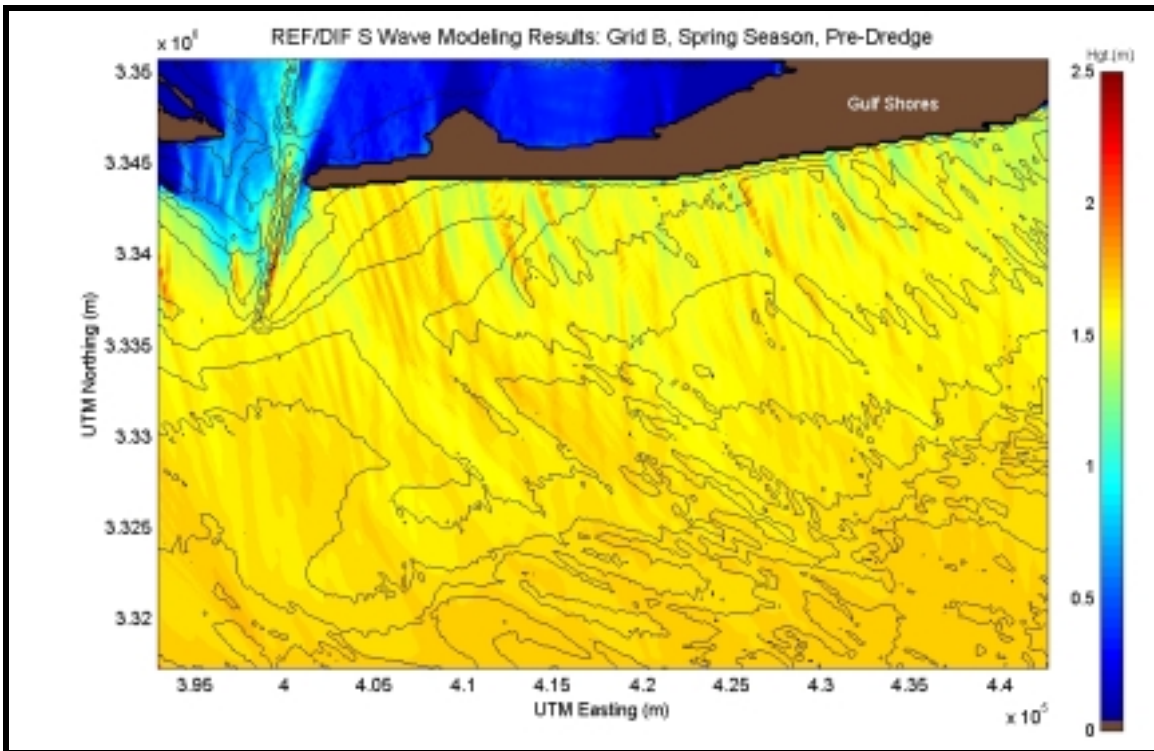


Figure 4-21. Spectral wave modeling results for existing conditions utilizing a typical spring season at reference Grid B.

Because of the irregular nature of the nearshore shoals, wave approach angles experience significant changes on the continental shelf. Summer, fall, and winter season results for Morgan Peninsula (presented in Appendix B2) indicate similar patterns of wave convergence and divergence. There are no visible differences in wave height patterns for different seasons. The winter season is slightly more energetic (wave heights approximately 0.2 to 0.3 m greater). Spring and fall results are almost identical, with only a slight variation in directional spreading.

#### 4.4.2 High Energy Wave Events Results

Figure 4-22 illustrates wave transformation results for the 50-yr storm at Dauphin Island (Grid A). Fifty-year storm results for Morgan Peninsula are presented in Appendix B2. Storm wave propagation patterns are similar to those documented for seasonal trends. For example, Mobile Outer Mound now concentrates a 4.0- to 4.5-m wave field on southeastern Pelican Island and a significant reduction in wave height is evident adjacent to this area. Wave shoaling in other areas (e.g., the dredged navigation channel) appears to be less important when considering larger storm waves, though the increased color scale (Figure 4-22) reduces visible identification of previously significant wave height modifications (shown in Figure 4-20). Wave approach directions are modified further offshore since the large storm waves interact with the seafloor in deeper water than average seasonal waves.

Due to the reduced number of spectral components used with storm simulations (closer to a monochromatic simulation) and the increased wave height, increased patterns of convergence and divergence are more evident in model results. These streaks are typically caused by large variations in bathymetry in the modeling grid. Comparison of pre- and post-dredging results in the next section will not include existing areas of convergence and divergence, but will concentrate only on changes caused by the dredging scenarios.

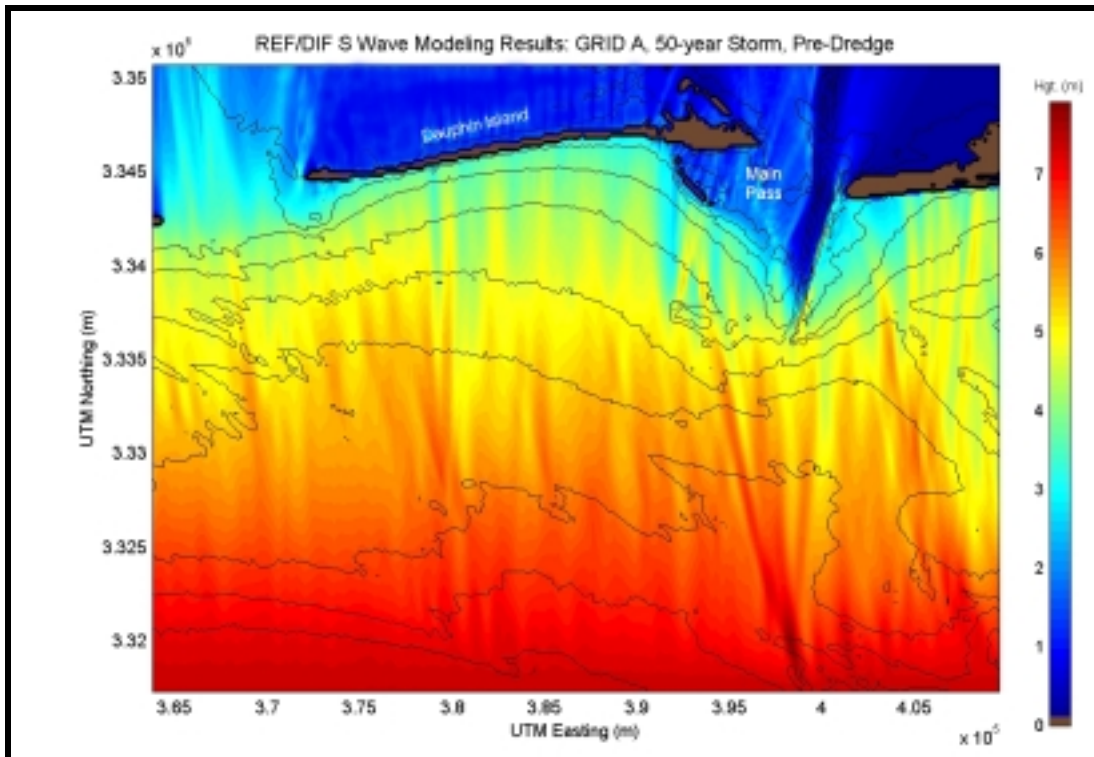


Figure 4-22. Spectral wave modeling results for existing conditions simulating a 50-yr storm event at reference Grid A.

#### 4.4.3 Model Results Relative to Historical Shoreline Change

When comparing average seasonal wave modeling results to historical shoreline change, the overall influence of each season on coastal and nearshore change can be investigated. Figure 4-23 shows significant wave heights extracted along a baseline 100 m seaward of the Dauphin Island coastline. The seasonal results, an average result for all four seasons, and the 50-yr storm result are illustrated on the panels within the figure. Historical shoreline change for Dauphin Island is represented by a thick line and is scaled by the left-hand axis. Significant wave height is represented by a thin line and is scaled by the right-hand axis.

Historically, the western portion of Dauphin Island has been dominated by lateral island growth and shoreline retreat. The eastern end illustrates accretion in the shadow zone behind Pelican Island and relative stability near Mobile Bay entrance since 1847. A small erosional area is located landward of the gap between Pelican Island and subaerial portions of the ebb shoal, where wave energy propagates landward, as indicated in the wave model results presented above. Wave height distribution correlates with shoreline change rates relatively well. Wave heights are generally higher in areas that have experienced historical shoreline retreat, while wave height reduction is indicated in areas of historical accretion (e.g., the shadow zone behind Pelican Island). Wave heights during the summer season are smaller than in other seasons. Therefore, it is expected that less erosion or accretion occurs during that portion of the year. The 50-yr storm exhibits higher wave heights along the entire coastline, yet still maintains a form similar to the seasonal results. The correlation between wave height results and historical shoreline change rates suggests that the wave model is performing reasonably.

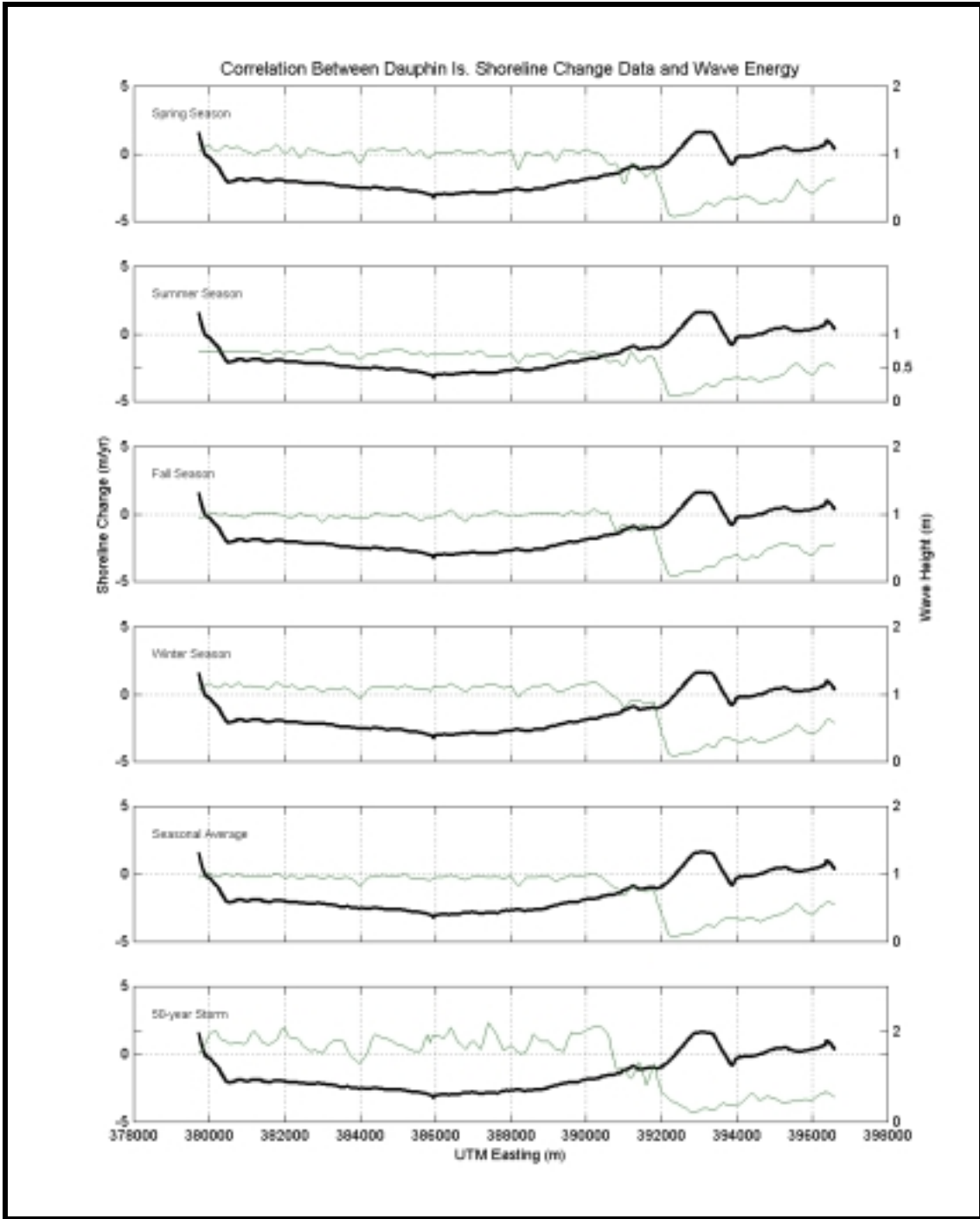


Figure 4-23. Wave height (thin line) taken from a baseline 100 m seaward of the Dauphin Island shoreline compared with historical shoreline change rates (thick line; 1847/67 to 1978/82). Points along the coastline that indicate increased wave height correspond to areas of historical erosion, while areas of historical accretion correspond to reduced wave heights.

Figure 4-24 shows similar results for the Morgan Peninsula. Historical shoreline change rates indicate a relatively stable coastline with accretion occurring at the western end of the peninsula (again due to the dominant sediment transport to the west). Significant wave heights presented in Figure 4-24 were smoothed using a weighted 11-point filter to identify general trends in wave height. Correlation between wave heights and historical shoreline change rates can again be made at certain points along the coast. For example, a region of historical erosion evident at approximately 432,500 m (Easting), is also indicated as an area of increased wave energy. In addition, wave heights increase from west to east along Morgan Peninsula. Smaller wave heights exhibited at the western end of the peninsula may also contribute to the accretion trend seen in shoreline change rates.

In a regional context, shoreline change and wave height distribution correlate well along Morgan Peninsula. However, slight changes in the orientation and location of offshore shoals result in a shift in the location of areas of energy convergence and divergence. Historically, these shore-oblique shoals have experienced some movement, thereby changing the location of increased wave energy along the coast.

## **4.5 COMPARISON OF PRE- AND POST-DREDGING RESULTS**

### **4.5.1 Post-Dredging Results**

Following wave modeling runs for existing conditions, simulations were performed for post-dredging scenarios. Results were produced for each of the seasonal spectra and the 50-yr storm event to evaluate potential physical impacts of offshore sand mining. Figure 4-25 presents the results for Dauphin Island (Grid A) simulating a typical spring season for the post-dredging scenario in Sand Resource Area 4. As in Figure 4-20, the color map corresponds to the distribution of significant wave height (m) throughout the model domain. The solid black lines represent bathymetric contours. Other than the differences in bathymetry, the same boundary conditions were used in the simulation to produced results shown in Figure 4-20.

The same wave patterns described in Section 4.4 are evident in the post-dredged model results (e.g., the wave focusing behind Mobile Outer Mound; the increase in wave height along the edges of the dredged navigational channel). It is difficult to visually identify any significant differences between the pre- and post-dredging results. This is true for all seasonal and 50-yr storm simulations. Because the modifications to the wave field are not very evident after initial inspection of results, the impact of the potential sand mining operations on the wave field can be considered small compared with natural changes occurring throughout the model domain. Figures similar to Figure 4-25 for all the simulated post-dredging model results can be found in Appendix B3.

### **4.5.2 Existing Conditions Versus Post-Dredging Seasonal Results**

Differences in wave heights (between pre- and post-dredging results) were computed at each grid point within the model domain to document potential impacts caused by specific sand mining scenarios. Pre-dredging wave simulations were subtracted from the post-dredging wave results so that positive (negative) differences indicate an increase (decrease) in wave height related to sand mining at potential borrow sites. Figure 4-26 shows the difference plot for the spring season presented above. As expected, sand mining creates a zone of decreased wave energy behind the sand borrow site and increased energy adjacent to the borrow site. A maximum increase of approximately 0.17 m (11% increase relative to offshore significant wave height) and a maximum decrease of 0.2 m result from the sediment extraction scenario for Resource Area 4 (Table 4-9) during the typical spring season. Increased wave energy is focused near the southwest end of Pelican Island and on the eastern end of Dauphin Island. Increased wave heights dissipate relatively quickly once breaking begins. A decrease in wave energy is evident in the lee of the borrow site, and therefore reduces the magnitude of wave height focused by the Mobile Outer

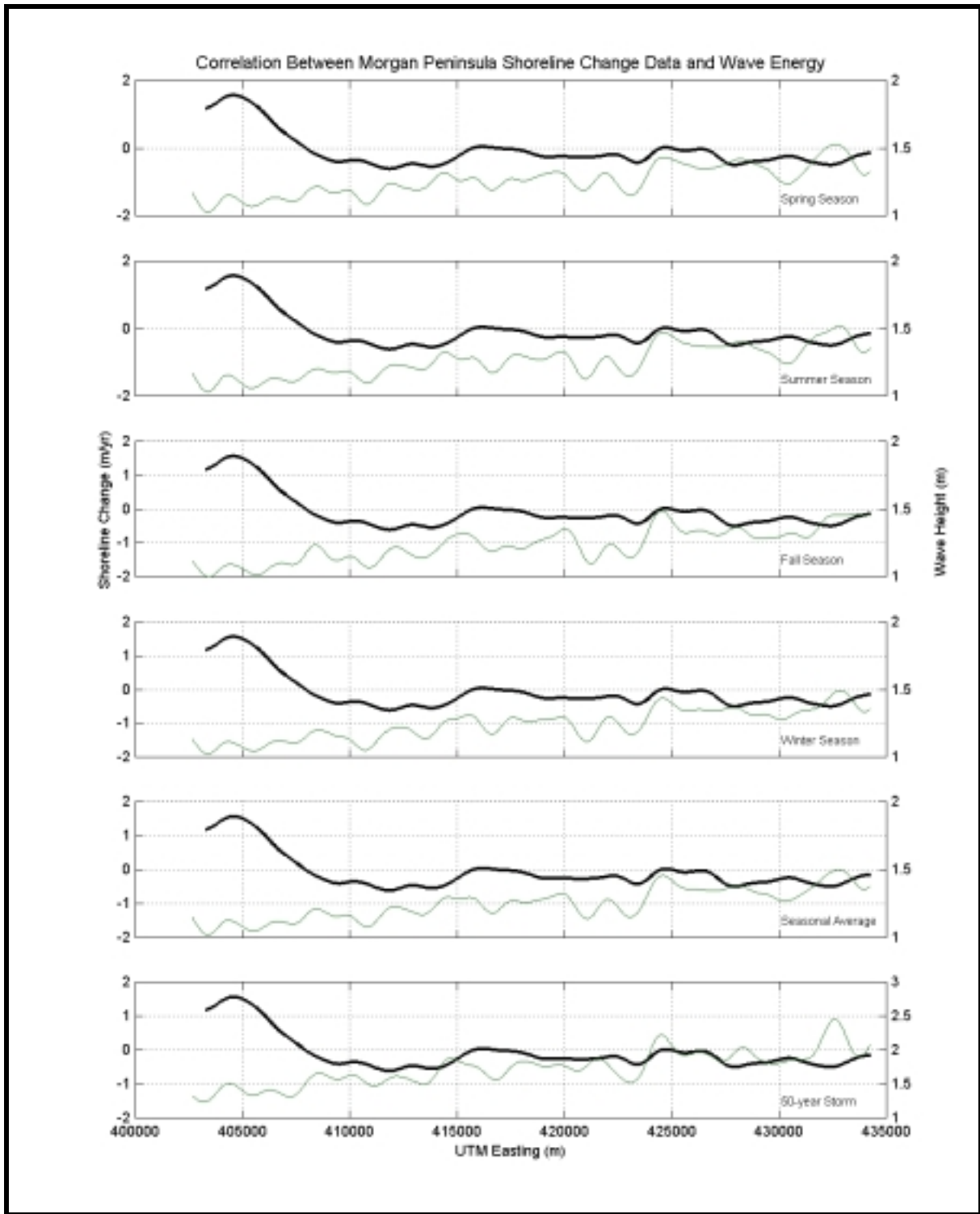


Figure 4-24. Wave height results (thin line) taken from a baseline 100 m seaward of the Morgan Peninsula shoreline compared to historical shoreline change rates (thick line; 1847/67 to 1978/82).

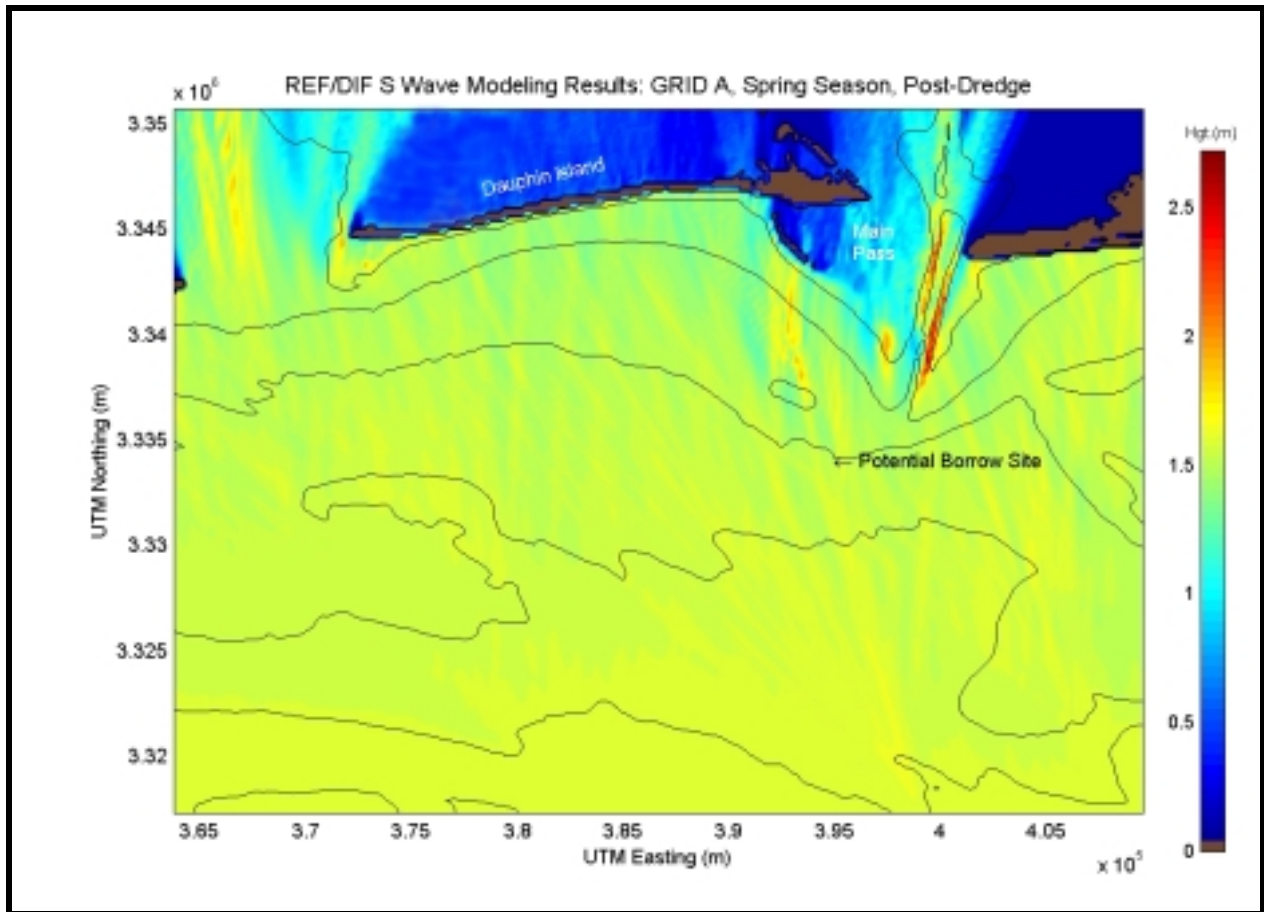


Figure 4-25. Spectral wave modeling results for post-dredging scenario utilizing a typical spring season at reference Grid A.

Mound. Because wave energy focused on Pelican Island is reduced during a typical spring season, potential sand mining operations may be beneficial for protecting Pelican Island.

Difference plots for the remaining simulations at Grid A are presented in Appendix B4. Winter season differences indicate a slight shift in the impact zone to the east due to variations in peak spectral wave approach. The magnitude of wave height differences is slightly smaller than the spring simulations and the western edge of Pelican Island experiences an insignificant increase in wave height (0.02 to 0.04 m).

For fall and summer seasons, wave transformation trends were similar, and the impact of potential sand excavation scenarios was insignificant (changes less than 0.06 m). During the summer season, waves were smaller, consisted of shorter periods, and the directional spread was quite wide. Modifications to the wave field were not well-defined, and changes were negligible. The fall season model runs produced slightly larger changes in wave height differences on a portion of Pelican Island; however, changes were determined to be insignificant (5- to 6-cm increase) relative to source wave data (WIS). Overall, modifications to the wave field are insignificant during the fall and summer.

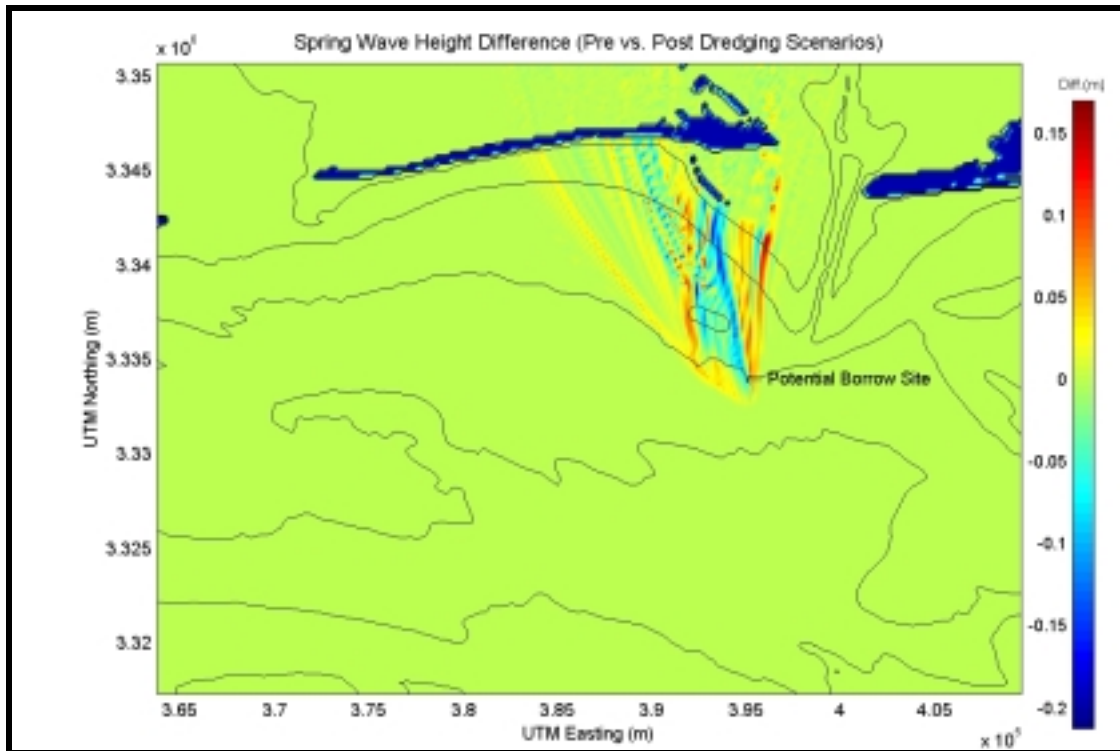


Figure 4-26. Wave height modifications resulting from potential offshore mining at Sand Resource Area 4 for a typical spring season. Hot colors (reds) identify areas of increased wave height, while cold colors (blues) identify areas of decreased wave height.

Figure 4-27 illustrates wave height differences for the spring season at Grid B (Morgan Peninsula). Wave heights were modified by the dredged regions as waves are refracted away from each borrow site by local changes in water depth, creating a shadow zone directly behind the borrow site and an increase in wave height in adjacent waters. This phenomena is evident at all three of the proposed sand borrow sites within Grid B. A maximum wave height increase of 0.4 m (24% increase) at the western edge of Sand Resource Areas 2 and 3 is caused by the large sediment extraction scenarios (Table 4-9) for the typical spring season. A maximum decrease of 0.4 m is evident in the lee of the dredged locations. The shadow zone behind the Sand Resource Area 2 borrow site is more concentrated due to the orientation of the dredged area. Wave height modifications are larger for borrow sites within Grid B, with maximum changes in significant wave height approaching 0.3 to 0.4 m. The increase in wave height is due to borrow-site location relative to the shoreline and borrow site size and orientation. However, waves dissipate energy as they advance toward the shoreline and negligible increases in wave height (0.1 m or less) are observed at potential impact areas along the coastline.

Difference plots for the remaining simulations at Grid B are presented in Appendix B4. During the summer, winter, and spring, patterns of wave modifications are comparable. Maximum increases/decreases in wave height are slightly smaller ( $\pm 0.2$  to 0.3 m) than observed during the spring season. In the fall, modifications to the wave field are less consolidated due to the less direct wave approach direction. During the summer and winter, a small area of increased wave height observed at the western edge of the borrow site within Sand Resource Area 3 appears to propagate to the shoreline (at approximately 412,500 Easting; 3,344,000 Northing). However, changes at the shoreline are negligible.

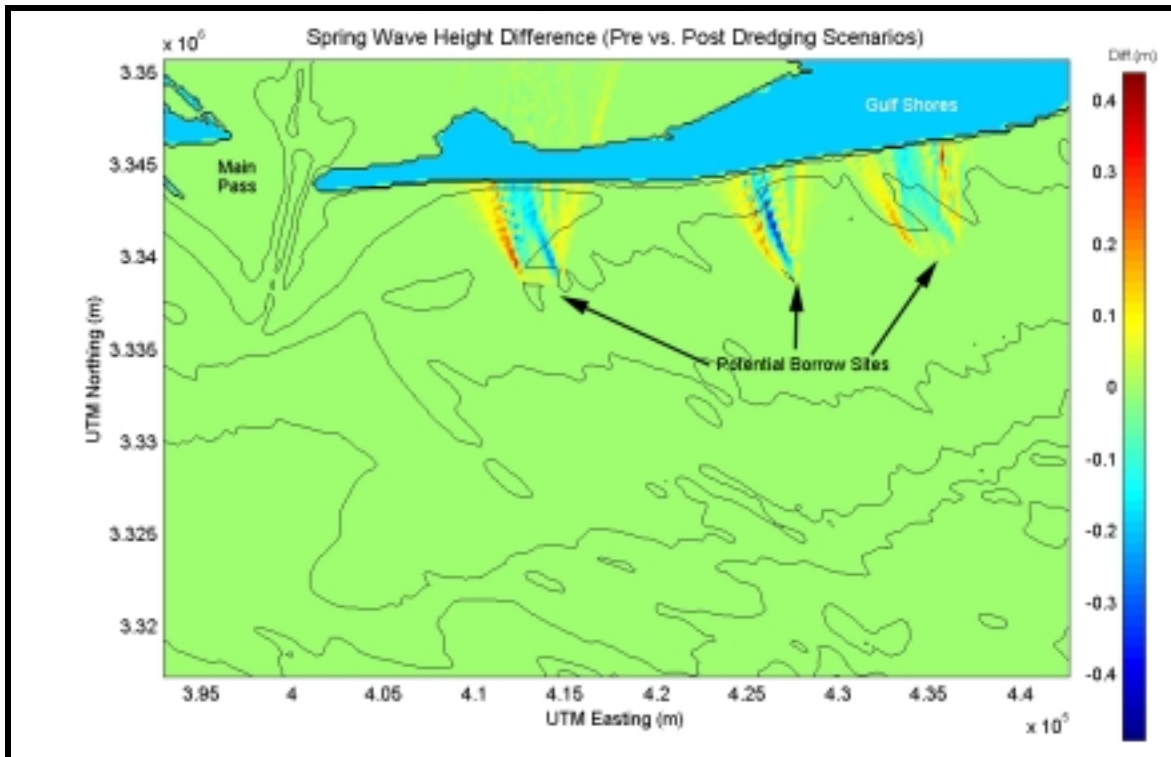


Figure 4-27. Wave height modifications resulting from potential offshore mining at Sand Resource Areas 1, 2, and 3 for a typical spring season. Hot colors (reds) identify areas of increased wave height, while cold colors (blues) identify areas of decreased wave height.

Overall, the impact caused by potential offshore dredging at sand borrow sites during normal conditions is relatively small. At most, only minor changes are expected in the wave field and the nearshore sediment transport potential.

#### 4.5.3 High Energy Wave Event Results

Differences in wave heights were also computed for 50-yr storm simulations to identify potential impacts of offshore sand mining. Figures 4-28 and 4-29 show results for Dauphin Island and Morgan Peninsula, respectively. A similar distribution of wave energy change as that indicated in the seasonal results is illustrated (i.e., wave energy reduction directly behind the dredged area and an adjacent increase in energy). Both change plots indicate a maximum increase in wave height of approximately 1.5 m (20% increase over offshore wave heights). A wave reduction of 1.5 to 2.0 m is observed in the shadow zones of borrow sites.

In Grid A (Dauphin Island), a significant amount of wave energy is dissipated before the waves reach the shoreline as modifications to wave heights are less than 0.5 m along a majority of Pelican Island. As with seasonal results, a beneficial reduction in wave height is obtained due to borrow site characteristics and Mobile Outer Mound for a portion of Pelican Island. However, a smaller amount of the wave energy dissipates before reaching the shoreline landward of borrow sites in Sand Resource Areas 1, 2, and 3. Therefore, during storm events, changes may be large enough to result in significant impacts at certain locations along the eastern Alabama shoreline.

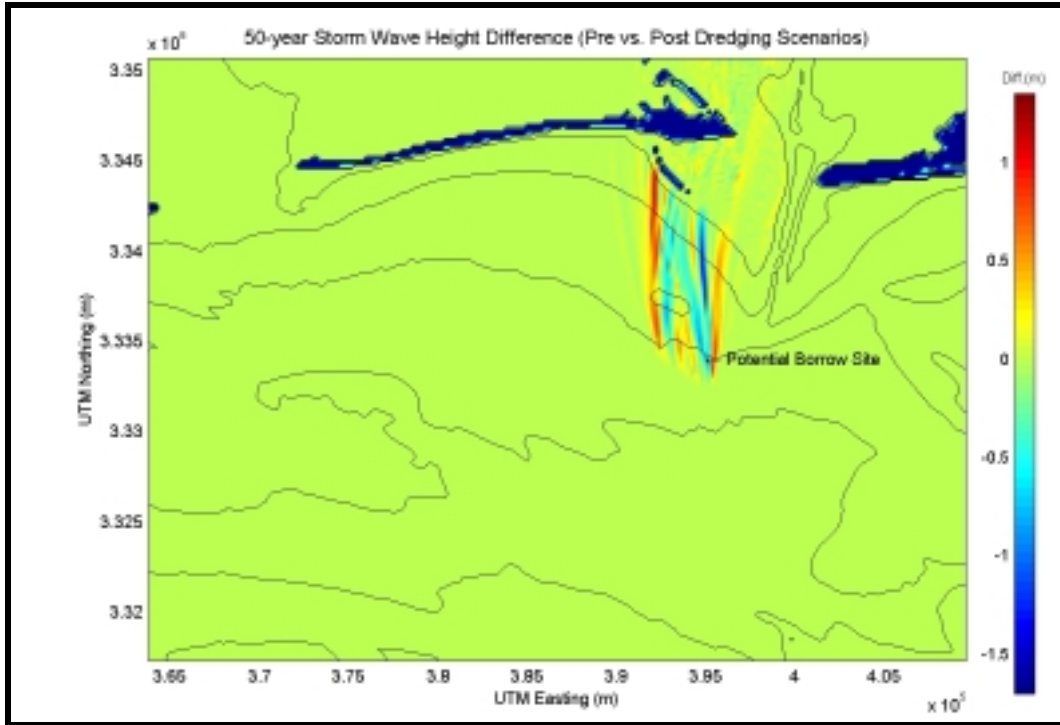


Figure 4-28. Wave height modifications resulting from potential offshore mining in Sand Resource Area 4 for a 50-yr storm event. Hot colors (reds) identify areas of increased wave height, while cold colors (blues) identify areas of decreased wave height.

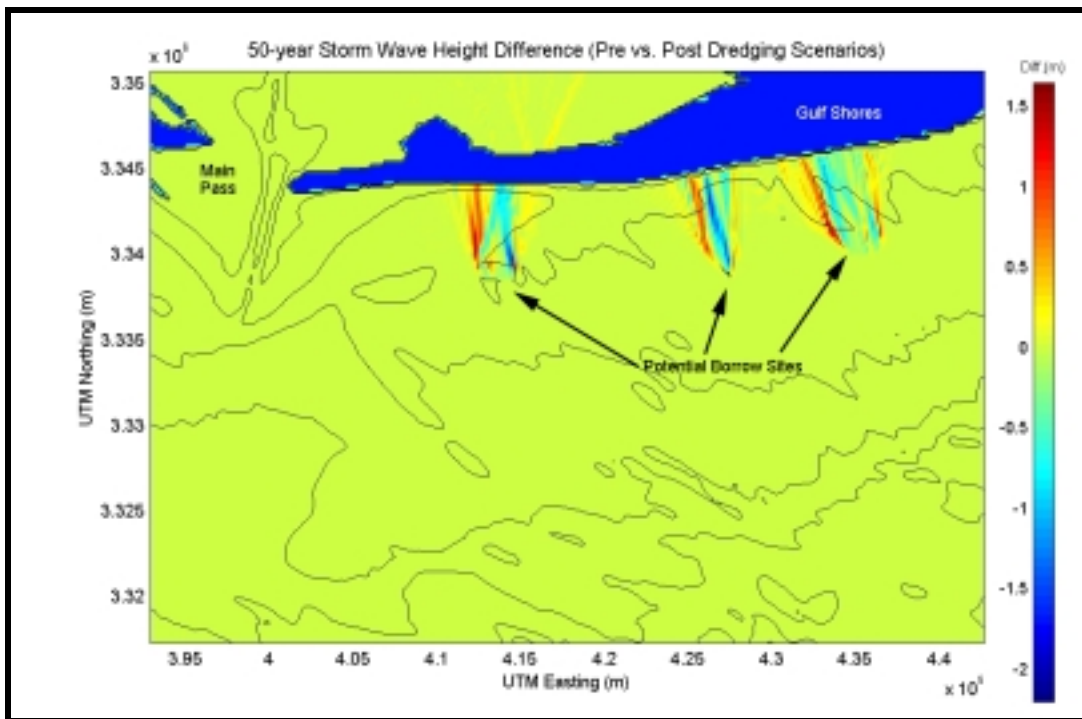


Figure 4-29. Wave height modifications resulting from potential offshore mining in Sand Resource Areas 1, 2, and 3 for the 50-yr storm event. Hot colors (reds) identify areas of increased wave height, while cold colors (blues) identify areas of decreased wave height.

## 4.6 DISCUSSION

This section presented an analysis of potential impacts to the nearshore wave climate caused by sand mining offshore Alabama. The analysis approach relied upon the spectral wave model REF/DIF S to simulate the behavior of a random sea state, incorporating the effects of shoaling, wave breaking, refraction, diffraction, and energy dissipation. Accuracy of the wave transformation model is affected by quality of the selected input data and parameters. Data analysis revealed a relatively consistent wave climate throughout the year (wave height, direction, periods, etc.). The Gulf of Mexico experiences minimal variation in wave climate, and with the exception of storm events, typical conditions are directionally narrow and energetically mild.

Wave transformation modeling simulations were performed for existing conditions with seasonal and 50-yr storm spectra. The model results identify key areas of wave convergence, divergence, and shadow zones offshore Alabama. In the seasonal simulations, significant wave heights experience little variation up to the 15-m depth contour where the wave field begins to feel the influence of bathymetry. For Dauphin Island, wave heights are relatively consistent along the shoreline while the eastern end of the island is protected from significant wave energy by Pelican Island and subaqueous portions of the ebb shoal. Several areas of wave convergence were identified in the Dauphin Island grid, including Mobile Outer Mound, which focuses wave energy on Pelican Island during most seasons. Wave focusing caused by Mobile Outer Mound results in an increase in erosion at Pelican Island, and during a storm event may significantly erode the island. Areas of wave convergence and divergence along the Morgan Peninsula are primarily caused by the southeast-oriented linear shoals on the continental shelf.

For the 50-yr storm, the wave patterns are similar to the normal seasonal results. An increase in wave height is significant in many areas where wave convergence occurs. For example, the Mobile Outer Mound disposal site concentrates 4.0- to 4.5-m wave heights on Pelican Island during an event of this kind. The 50-yr storm event simulated in the present study represents a major storm that will have significant impact on the approaching wave field and sediment transport patterns.

Differences in wave height between pre- and post-dredging scenarios offshore Dauphin Island indicate maximum wave height changes (increases and decreases) for seasonal simulations ranged from  $\pm 0.02$  to 0.2 m. These maximum changes dissipate relatively quickly as waves break and advance towards the coast. For the Morgan Peninsula, maximum wave height differences were larger ( $\pm 0.2$  to 0.4 m) due to borrow site sizes and orientations as well as proximity to the shoreline. However, the waves dissipate energy as they propagate towards the shoreline and increases in wave height of 0.1 m or less are observed at potential impact areas along the coast. Overall, the impact caused by the potential offshore dredging during normal seasonal conditions is negligible.

During extreme wave conditions (e.g., a 50-yr storm event), wave heights are modified up to  $\pm 1.5$  to 2.0 m, indicating a rather significant change. For the sand borrow site located in Sand Resource Area 4, a significant amount of wave energy is dissipated before the waves reach the coast. As such, wave height increases are less than 0.5 m along a majority of Pelican Island. During a storm event, waves are large (4 to 8 m), even without modifications caused by dredging. Therefore, a maximum change of 0.5 m (7% of the offshore wave height) may not significantly increase nearshore erosion above existing conditions near Dauphin Island.

Borrow sites within Sand Resource Areas 1, 2, and 3, which are located closer to the coast, have a greater impact on the wave field. A small amount of wave energy is dissipated before reaching the shoreline. Changes to the wave heights are large enough to result in significant impacts at certain locations along Morgan Peninsula. A moderate to large storm event will produce changes in the wave field and in the sediment transport patterns along the coastline.

## **5.0 CIRCULATION AND SEDIMENT TRANSPORT DYNAMICS**

This section analyzes the physical regime of the Alabama continental shelf and discusses circulation, wave, and sediment transport processes to evaluate the potential environmental impact of offshore sand mining. Current and wave processes provide physical mechanisms for moving sediment throughout the Alabama coastal zone. The following discussion documents the physical mechanisms potentially impacted by sand mining within specific offshore locations.

### **5.1 CURRENTS AND CIRCULATION**

Circulation patterns observed at specific areas within the study region were evaluated within the context of potential offshore sand mining operations. The following discussion uses long-term current measurements obtained during previous studies in the region, as well as current meter data collected during field surveys for this program, to describe circulation at the study site. Long-term observations were analyzed to provide an understanding of temporal variations of inner shelf circulation (time scales of hours to months), while field survey data sets provided detail regarding to spatial variability within specific borrow sites. Combined, the analyses presented in this section describe circulation characteristics within the study region, including major forcing influences, time scales of variability, and the magnitude of resulting currents. The results from this section were used to provide estimates of sediment transport potential at potential offshore borrow sites.

#### **5.1.1 Historical Data Analysis**

Long-term observations of currents, previously collected by various investigators on the Alabama/Florida inner-continental shelf, were obtained and analyzed for this study. These data were used to estimate the major forcing influences throughout the region and to determine the seasonal variability of the flow regime. The goal of the analyses was to develop an understanding of current patterns throughout the study region, and to use this information to determine how sediment transport at potential sand resource sites may be affected by the flow regime on the inner shelf.

Two current meter data sources were used for evaluating seasonal and annual variations in flow throughout the study area. These data represent current observations at specific mooring locations along the Alabama inner shelf (Table 5-1). Supporting data, such as observations of atmospheric winds, were included in the analysis as well. Unfortunately, observations of density stratification on the shelf or freshwater discharge from Mobile Bay, two important parameters identified from previous investigations which influence circulation in the region, were unavailable for this analysis.

Continental Shelf Associates (CSA), Inc., of Jupiter, FL, provided current meter observations at Sand Resource Area 4, specifically near Shell Oil Platform #132, during the time period September 28, 1987 to October 24, 1988 (Hart et al., 1989). The mooring was deployed west of the main ship channel and due east of the dredged material disposal mound. Observations represent a year-long record of near-bottom currents (approximately 1.6 m above the seafloor in approximately 12-m water depth). These data were used to develop an understanding of the most-frequent flow characteristics near Sand Resource Area 4.

The second data set resulted from an Environmental Protection Agency (EPA) study offshore of Gulf Shores, AL (Dinnell, 1997). A series of five moorings were deployed in areas within Sand Resource Areas 1 and 2 (Figure 5-1). Data were collected between late March 1986 and late March 1987. Data coverage at any single mooring site was sporadic during this time. A nearshore site, named Gulf Shores Current Meter Mooring 1 (GSCM1), had observations collected in approximately 5-m water depth with a single meter located approximately at mid-depth (GSCM1M) within Sand Resource Area 1. These data were almost complete for the period April 1986 to March 1987. A

second location (GSCM4) is within Sand Resource Area 2 in approximately 10-m water depth and yielded observations at near-bottom (GSCM4B) and near-surface depths (GSCM4S). Data were collected at both depths during the period early May 1986 to mid-November 1986. These three data sets formed the basis for developing an understanding of flow field characteristics for Sand Resource Areas 1, 2, and 3.

Data Set Name	Location	Water depth (sensor depth)	Dates
Shell Block 132	Resource Area 4 30° 09.6N 88° 4.8W	12.0 m (10.6 m)	28-Sep-87 to 24-Oct-88
GSCM1M	Resource Area 1 30° 13.8N 87° 41.1W	5.0 m (2.5 m)	29-Mar-86 to 04-Mar-87
GSCM4B	Resource Area 2 30° 11.3N 87° 44.4W	10.0 m (2.0 m)	11-May-86 to 25-Nov-86
GSCM4S	Resource Area 2 30° 11.3N 87° 44.4W	10.0 m (8.0 m)	24-Apr-86 to 23-Nov-86

Sources: Continental Shelf Associates (Hart et al., 1989); Dinnell, 1997

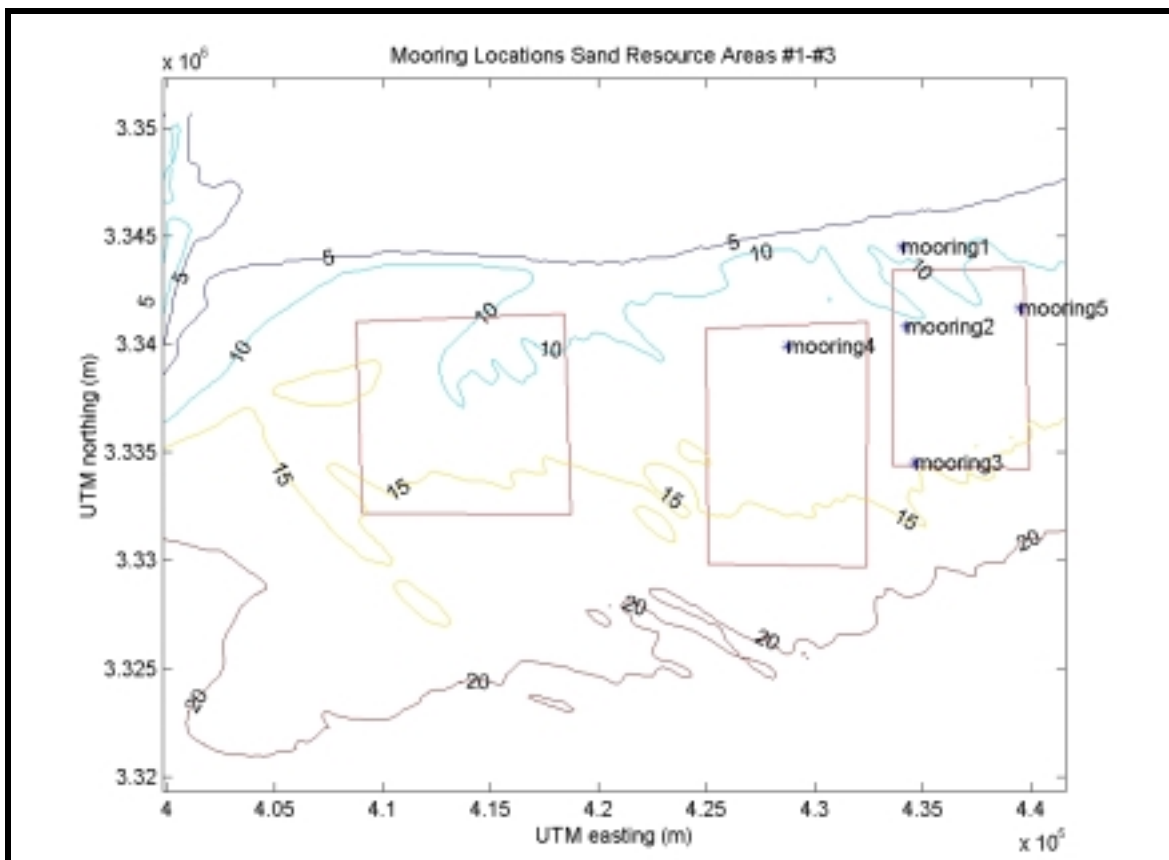


Figure 5-1. Map of sand resource areas east of Mobile Bay; Sand Resource Area 1 (far east) and Sand Resource Area 3 (far west). The five Gulf Shores mooring locations are shown as asterisks (\*). Contours are labeled in m.

### 5.1.1.1 Decomposition of Total Currents

Currents observed at each mooring site during the deployments represent the cumulative effects of many physical processes active in this region; processes which have a variety of time scales and amplitudes. These processes occur simultaneously; hence, the current observed at any one time can be considered a superposition of all individual processes. This section describes the numerical procedures used to separate the observed currents into individual subsets, each with specific time scales of variability. This procedure allows analysis of each process to determine their relative importance to total circulation in the region.

Separation of the total signal into specific process components was performed using various numerical analysis techniques, such as tidal harmonic decomposition, as well as the application of a series of low-, band-, and high-pass filters. The results of the analyses represent subsets of individual time series. Each time subset represents a specific physical process, such as:

- high-frequency currents (less than approximately 33-hour periodicity)
- tidal currents (diurnal, semi-diurnal, fortnightly)
- wind-driven currents (1 to 15 day frequency band)
- low frequency or seasonal currents (greater than 15 day periodicity).

The first step in the separation analysis is to remove tidal currents from the raw data using harmonic analysis. Harmonic analysis calculates the amplitude and phase of 23 individual tidal constituents using a least-squares fit of the constituent sinusoid to the raw data signal. The tidal constituents removed included **K1, M2, M4, M6, S2, N2, O1, S4, S6, M8, MK3, MN4, MS4, 2N2, OO1, M1, J1, Q1, 2Q1, L2, 2SM2, Mf, and MSF**. A majority of these constituents represent high frequency tides, or tides having periods less than approximately 28 hours (diurnal tides). The exception is the MSf and Mf tides, which vary on an approximate 14.7-day and 13.6-day period, respectively.

The result of this analysis is a separation of the total observed currents into two time series; one is predicted tides, based on a reconstruction of individual tidal components, and the second is non-tidal or residual currents. The residual current was generated by subtracting (point by point) the reconstructed tidal series from the original signal.

The residual signal became the basis for subsequent analyses. The first step in processing was to remove the remaining high frequency energy. This was accomplished by applying a PL33 low-pass filter over the residual signal. The PL33 is a standard oceanographic filter which uses 1/(33 hours) as the cutoff frequency, and is used primarily to remove tidal energy (or all signal energy with periodicity less than 33 hours) from oceanographic time series. Some energy leakage can occur near the cutoff frequency using this filtering method; however, this effect is minimal since the significant diurnal (and higher frequency) tides had been removed prior to this step. The low-passed time series was termed the subtidal signal.

The subtidal signal was subtracted from the previous residual signal, resulting in a high frequency time series containing all non-tidal currents having periods less than approximately 33 hours. This high-frequency signal (typically referred to as noise) contained significant energy, which can be due to several sources, including actual flow field turbulence, wave-induced flow, as well as possible data contamination due to mooring motions. The high frequency signal was saved as a separate time series for later analysis and comparison.

The subtidal signal was then reduced further into distinct frequency bands. The first frequency band was defined as processes with time scales of 1-15 days. It was assumed to include wind-driven flows, as well as other processes of similar time scales. Buoyancy-driven flow may be included in this frequency band. This wind-driven band was expected to yield significant energy.

The signal was derived by high-pass filtering the subtidal signal with a 15-day cutoff, and was termed the wind-driven signal.

The second time band defined processes with periodicity greater than 15 days. It was termed the seasonal band, although processes with higher frequencies than seasonal (e.g., 15 to 30 days) are inherently included in this band. This series was derived by subtracting the wind-driven signal from the subtidal signal.

Each time series was extracted in sequential manner from the raw signal to a set of individual process-specific signals, each representing the dominant current occurring at specific time scales. This separation procedure was repeated for every data set.

An example of this analysis with the resulting time series signals is shown in Figure 5-2. Figure 5-2 depicts the time series decomposition of the east component of near-bottom velocity measured at Shell Block 132 (eastern side of Mobile Bay entrance channel) from 1987 to 1988. The top plot is the original signal sampled every 15 minutes. Small data gaps associated with instrument turnarounds had been filled prior to numerical separation using cubic spline interpolation. The subsequent time series represent tidal, high-frequency, wind-driven, and low-frequency (or seasonal) components, respectively. Visually, the high-frequency and wind-driven signals appear to have the most signal variability.

Separating these processes from the whole illustrated the relative contribution of each to the total observed circulation at a selected sand resource site. The signal variance of each resulting time series represents its energy level. Comparing the variance of each process to the total signal variance yields a representation of how much energy the process contributed to the whole. Results are depicted as histograms in Figures 5-3 through 5-6. The original (raw) signal variance was included to show what percentage each individual process contributed to the total signal energy.

Figure 5-3 shows the signal variance for the Shell Block 132 data, collected in an area located to the west of Main Pass at Mobile Bay. The bars to the left of the figure show the total energy of east (light blue) and north (dark purple) velocity components. Total current energy in the east-west direction appears to be equivalent to the north-south current energy. This distribution of energy is consistent with the orientation of local bathymetric contours at the site, and they are aligned along an approximate SE-NW axis. Consistent with results shown in Figure 5-2, the variance of the high-frequency and wind-driven signals contain a majority of the total signal energy. Wind-driven processes dominate the east-west currents with over half (52%) of the total signal energy. North-south flow appears equally distributed between high-frequency and wind-driven processes. Tides and low-frequency processes have little contribution to the overall signal at this location. The tidal signal shows a more dominant north-south component than east-west component of flow. The entrance to Mobile Bay is to the north of the mooring location; hence, a north-south bias of these near-bottom tidal currents would be expected.

Comparing the variance histograms at different locations also illustrates how individual processes vary spatially throughout the region. Figures 5-4 through 5-6 represent the variance histograms for locations to the east of Mobile Bay, near Sand Resource Areas 1 and 2. In these areas, the east-west current is approximately parallel to the shoreline and bathymetric contours, with the north-south component parallel to the cross-shore direction. Mooring 1M is relatively close to shore in shallow water (see Figure 5-1), whereas Mooring 4S and 4B are located in slightly deeper water on the northern fringe of Sand Resource Area 2. Data from 4S represent near-surface observations, whereas data from 4B represent near-bottom flow.

Histogram plots show that the total alongshore component of currents have significantly higher energy than the total cross-shore component, and that energy dissipates close to the seafloor and shoreline boundaries. Alongshore current energy is approximately 40% greater at Mooring 4S location, in deeper-water, than at Mooring 1M, which was located closer to shore.

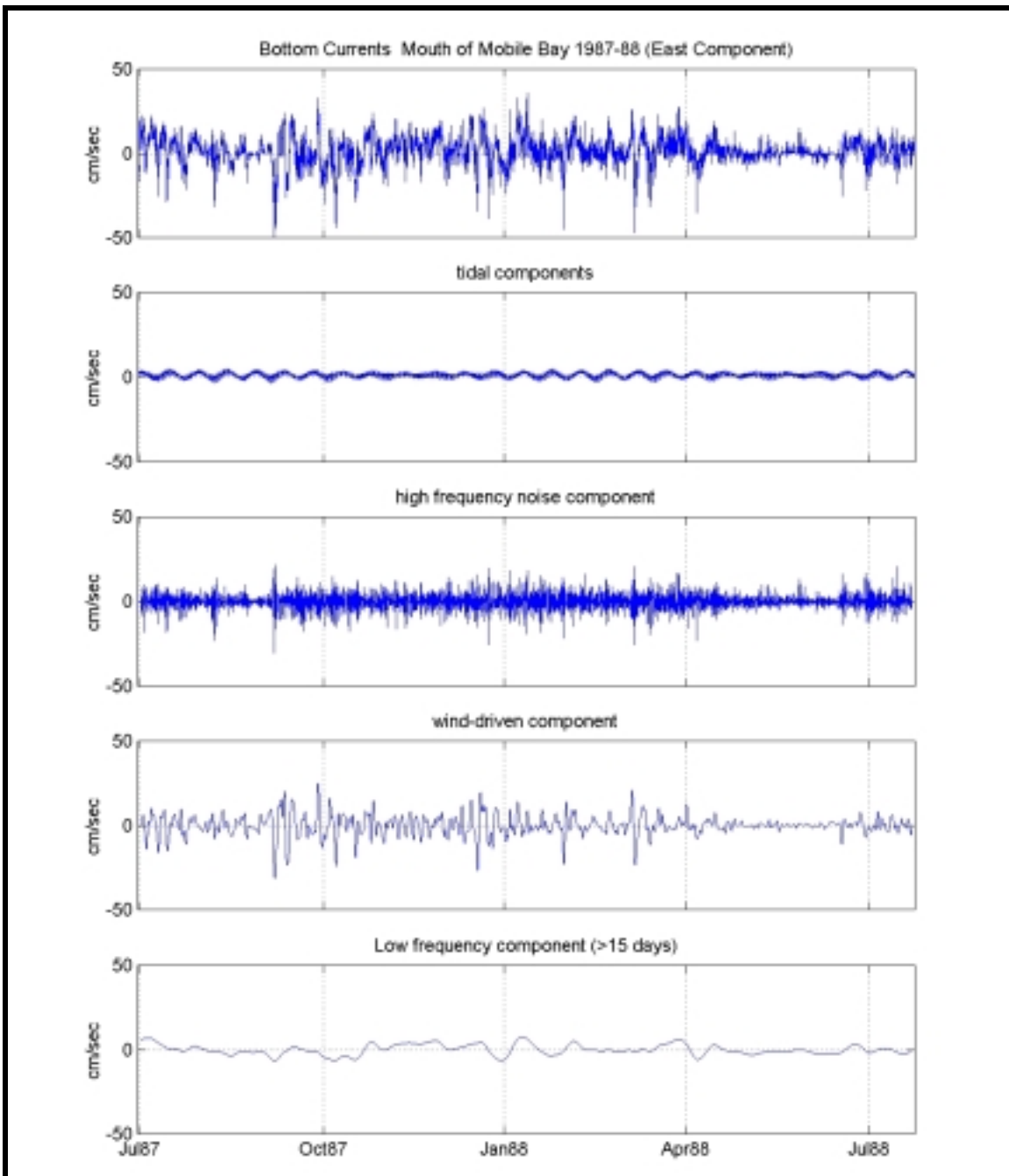


Figure 5-2. An example of the numerical separation of bottom current data collected within Shell Block 132, to the immediate southeast of the entrance to Mobile Bay (from Continental Shelf Associates, Inc. 1989). The data represent the east component of flow.

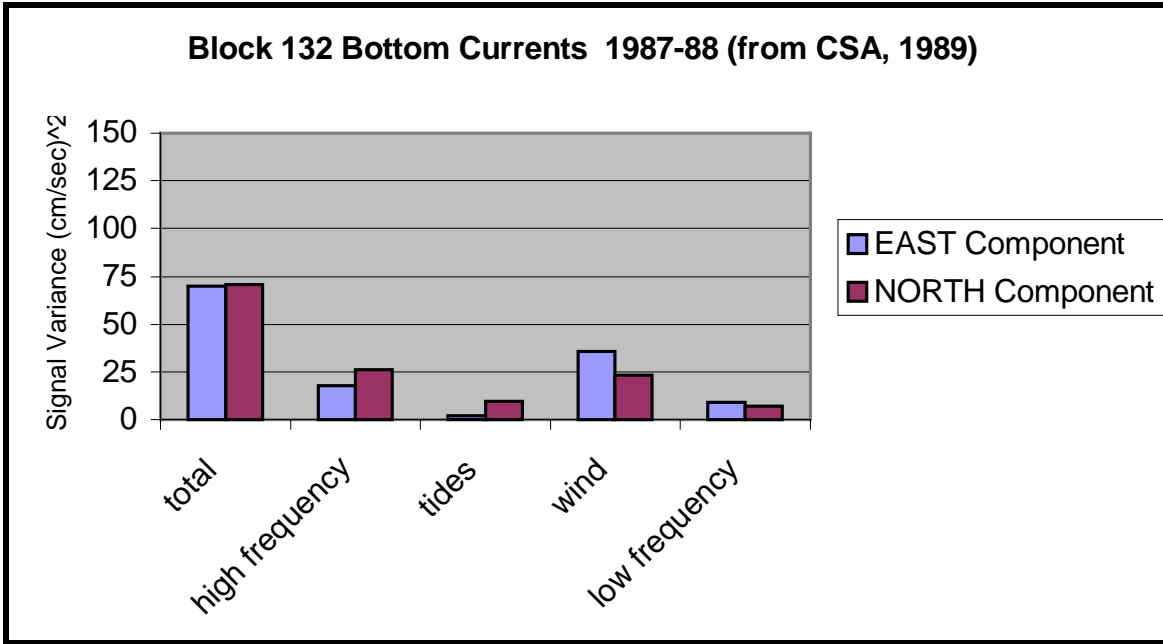


Figure 5-3. Variance histogram for Shell Block 132 Mooring, representing the fraction of total energy attributed to individual forcing mechanisms.

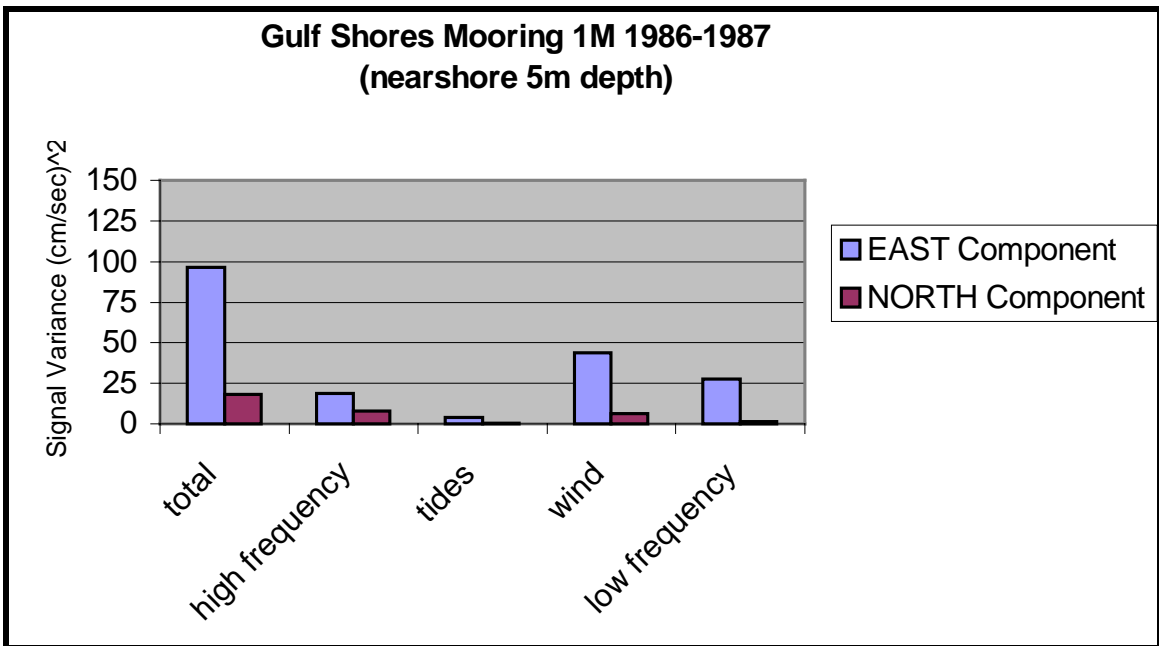


Figure 5-4. Variance histogram for Gulf Shores Mooring 1M, representing the fraction of total energy attributed to individual forcing mechanisms.

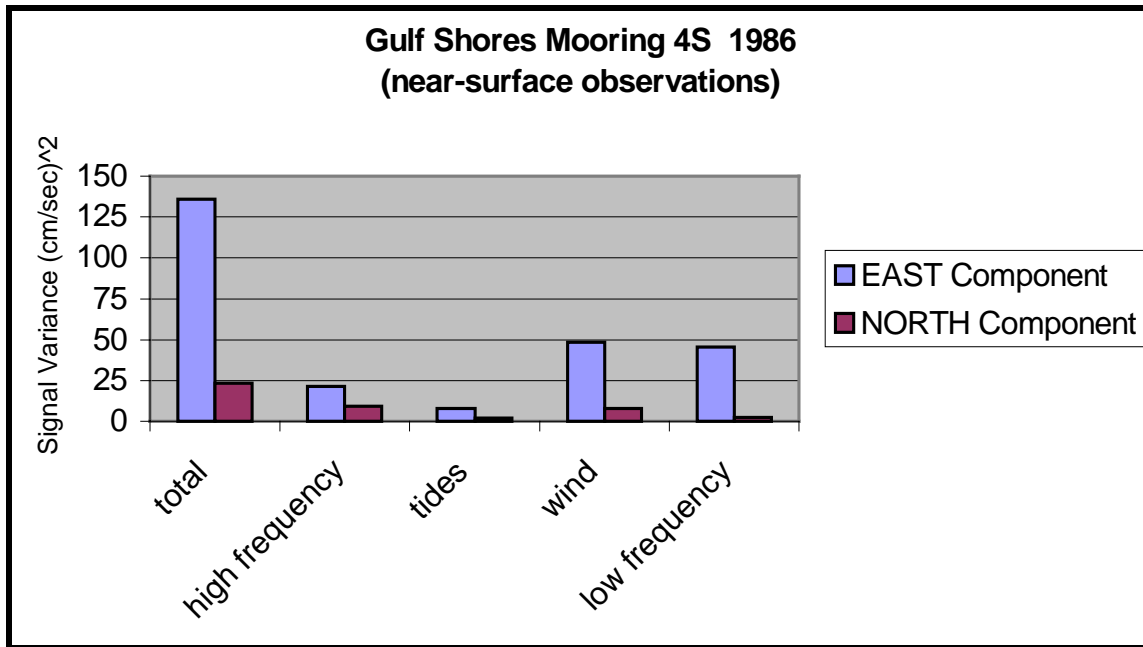


Figure 5-5. Variance histogram for Gulf Shores Mooring 4S, representing the fraction of total energy attributed to the individual forcing mechanisms.

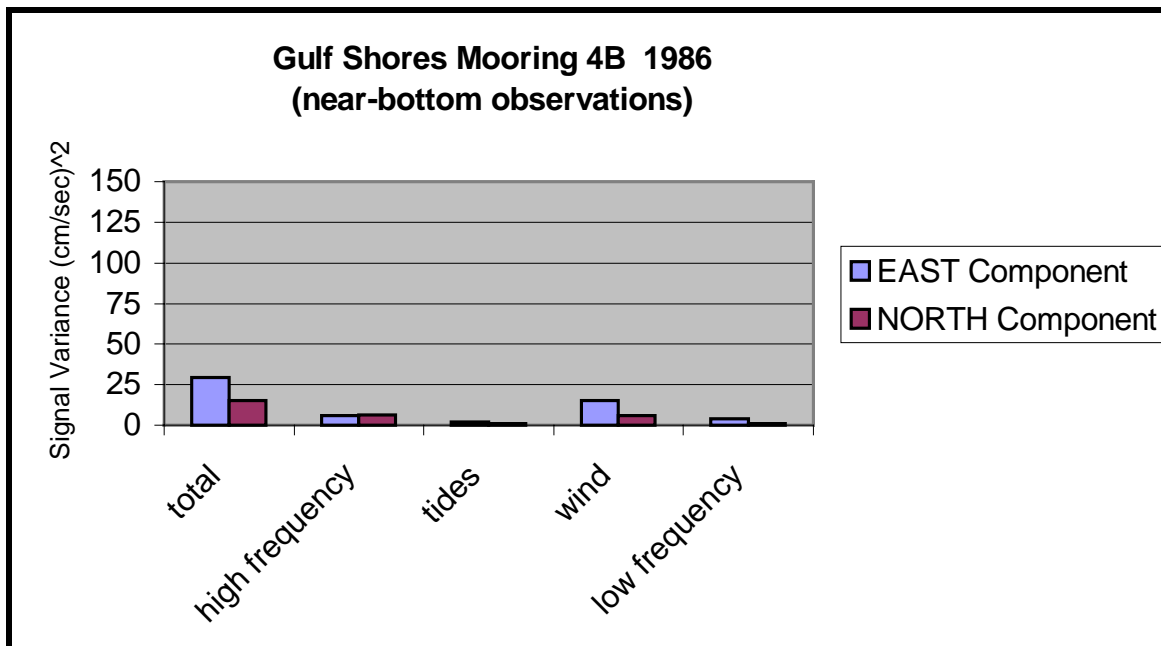


Figure 5-6. Variance histogram for Gulf Shores Mooring 4B, representing the fraction of total energy attributed to the individual forcing mechanisms.

The energy associated with alongshore flow at near-surface 4S was approximately 5 times the energy of the alongshore flow near the seafloor. The attenuation of alongshore current energy near the shoreline and seafloor likely was due to boundary frictional effects. The energy associated with cross-shore currents was similar between the 1M and 4S moorings, with a 50% reduction in cross-shore energy observed at site 4B. Damping of the cross-shore signal should occur in the vertical axis alone, as there is no shoreline boundary to affect flow between site 1M and 4S. The decrease of cross-shore flow at 4B relative to 4S is consistent with frictional damping of the seafloor; a factor of two decrease (versus a factor of five decrease in the alongshore direction) also is consistent with the relatively slower speeds of cross-shore flow versus alongshore flow. Frictional losses are proportional to the square of velocity; at low speeds frictional losses are proportionally smaller than at higher speeds.

#### **5.1.1.2 Current Components**

Tidal signals in the eastern part of the study area have a small contribution to the overall current energy, accounting for approximately 3 to 7% of the total observed currents. Of this contribution, alongshore-directed tidal currents were stronger than cross-shore flows. Tidal flow along the sea floor was quite small, with a stronger effect at the surface and near-shore environments.

High-frequency currents, defined as non-tidal variability of frequency less than approximately 33 hours, contribute approximately 16-20% of the total alongshore signal, and approximately 40-45% of the total cross-shore signal. High-frequency currents may stem from several sources: wave-induced flow, high-frequency wind-driven flow where the water column responded rapidly to sudden changes in wind stress, or simply from measurement noise inherent to the current meter. Figure 5-2 shows a high-frequency time series that is well-correlated with the wind-driven time series. As such, the assumption that the high-frequency signal is attributed to wave-induced flow or high-frequency responses to changes in wind stress appears accurate.

Wind-driven flow had the greatest influence on total observed currents at all sites. Approximately 36 to 51% of the total alongshore current was due to winds; in the cross-shore direction, wind-generated flow accounts for approximately 34 to 38% of the signal. Alongshore wind-driven flow was approximately 6 to 7 times stronger than cross-shore wind-driven flow, specifically at sites 4S and 1M. At site 4B, alongshore flow was approximately three times the energy of the cross-shore component. The energy associated with cross-shore wind-driven flow was quite similar between all sites, with little spatial variability.

Low-frequency currents varied considerably with location. These currents may be attributed to many sources, including variations in discharge from Mobile Bay, variations in seasonal wind patterns, and basin-wide fluctuations that may impinge upon the coastline. Low-frequency currents were relatively strong in the alongshore direction relative to the cross-shore direction, and they had greater influence on the site 4S signal (approximately 33% of the total) than at the 4B site (13%) or 1M site (approximately 28%). There appears to be some correlation between these low-frequency signals and the wind-driven signals, suggesting that low-frequency currents may be due to seasonal shifts in prevailing wind patterns.

#### **5.1.1.3 Total Observed Currents**

Total observed currents as frequency-of-occurrence rose diagrams illustrate the directional character of flow at each site (Figure 5-7). These rose plots show percent occurrence as a function of earth direction and current speed. Radial (circular) lines define the percent occurrence magnitude, with currents divided into discrete directional bins. The length of the pie slices indicates

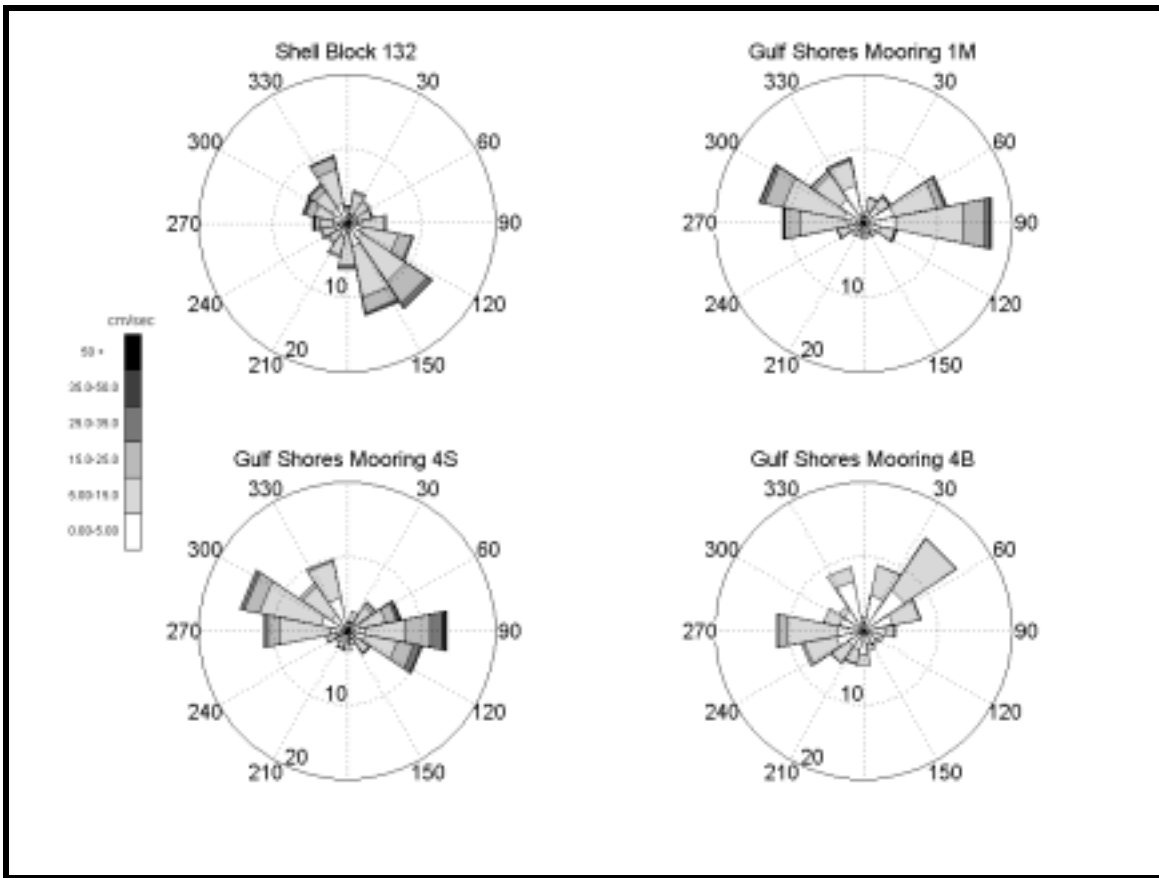


Figure 5-7. Rose diagrams illustrating four historical data sets in the study area. The spokes of the diagram represent compass directions (90=east, 270=west, etc). The circumferential lines represent percent occurrence, with the inner annulus representing 10%, and the outside diameter representing 20% occurrence. A 'pie slice' extending to the outer circumference means that 20% of the time, currents are flowing in that direction. Current speeds are represented by the shading of the pie slice, with white (no shading) portions representing the fraction of time currents are between 0 and 5 cm/sec and black portions indicating the percent occurrence of currents over 50 cm/sec.

percent occurrence; longer slices indicate that currents flow in the specified direction more often than if the pie slice were short. The shading of each pie slice indicates the magnitude of current speed; no shading means the speeds were quite small (between 0 to 5 cm/sec), with increasing intensity as current speeds increase. Portions of the pie slice shaded black infer that speeds were greater than 50 cm/sec. Figure 5-7 shows that currents at all the mooring sites flow predominantly in the alongshore direction with typical speeds of order 5 to 15 cm/sec.

Near-bottom currents west of Mobile Bay entrance, represented by the Shell Bock 132 rose diagram in the upper left corner of Figure 5-7, typically were oriented along a northwest-southeast axis which is parallel to the bathymetry contours at the site. The strongest flow at this site was to the southeast with speeds of order 15 to 25 cm/sec occurring approximately 8 to 10% of the time. Occasional currents with speeds exceeding 25 cm/sec were observed, although these higher speed currents occurred less than 2% of the time.

Currents to the east of Mobile Bay, represented by rose diagrams for Gulf Shores Moorings 1M, 4S, and 4B, were strongest at the surface (Mooring 4S) and weakest at the bottom (Mooring 4B). Flow was stronger offshore (Mooring 4S) than nearer to shore (Mooring 1M), consistent with the variance plots detailed earlier. Currents from these sites also were oriented primarily in the

alongshore direction. The strongest flow was observed at the surface (Mooring 4S), and while surface flow was oriented to the west and northwest most commonly (approximately 33% of the time), this westward flow was typically weaker than flow to the east. Westward flow at Mooring 4S greater than 15 cm/sec occurred approximately 5% of the time, while eastward flow exceeding 15 cm/sec occurred approximately 17% of the time. Approximately 1% of the time, eastward flow exceeded 35 cm/sec, whereas the westward flow never exceeded 35 cm/sec.

The separated signals (tides, high-frequency, wind-driven, and low-frequency currents) were also depicted as rose diagrams to understand the directional distribution for each individual process. Figure 5-8 depicts the frequency of occurrence rose diagrams for each individual process for the Shell Block 132 data set. High- and low-frequency processes illustrate much greater directional variability than either tidal or wind-driven currents. Tidal currents along the bottom at this location appear to flow principally offshore (to the south-southeast) for a majority of the time; the offshore-directed tidal flows were stronger (5 to 15 cm/sec) than the on-shore directed tidal flows (0 to 5 cm/sec). The rose plot of wind-driven flow shows that wind processes dominated total observed currents at the site (compare to Figure 5-7). The dominant wind-driven flows were oriented southeast and northwest, also parallel to the isobaths in the area, which is consistent with the alongshore dominance of currents in the inner shelf region. Near-bottom wind-driven currents were approximately 5 to 15 cm/sec, with occasional currents exceeding 15 cm/sec. Less than 1% of the time, wind-driven currents were oriented to the northwest at speeds exceeding 25 cm/sec.

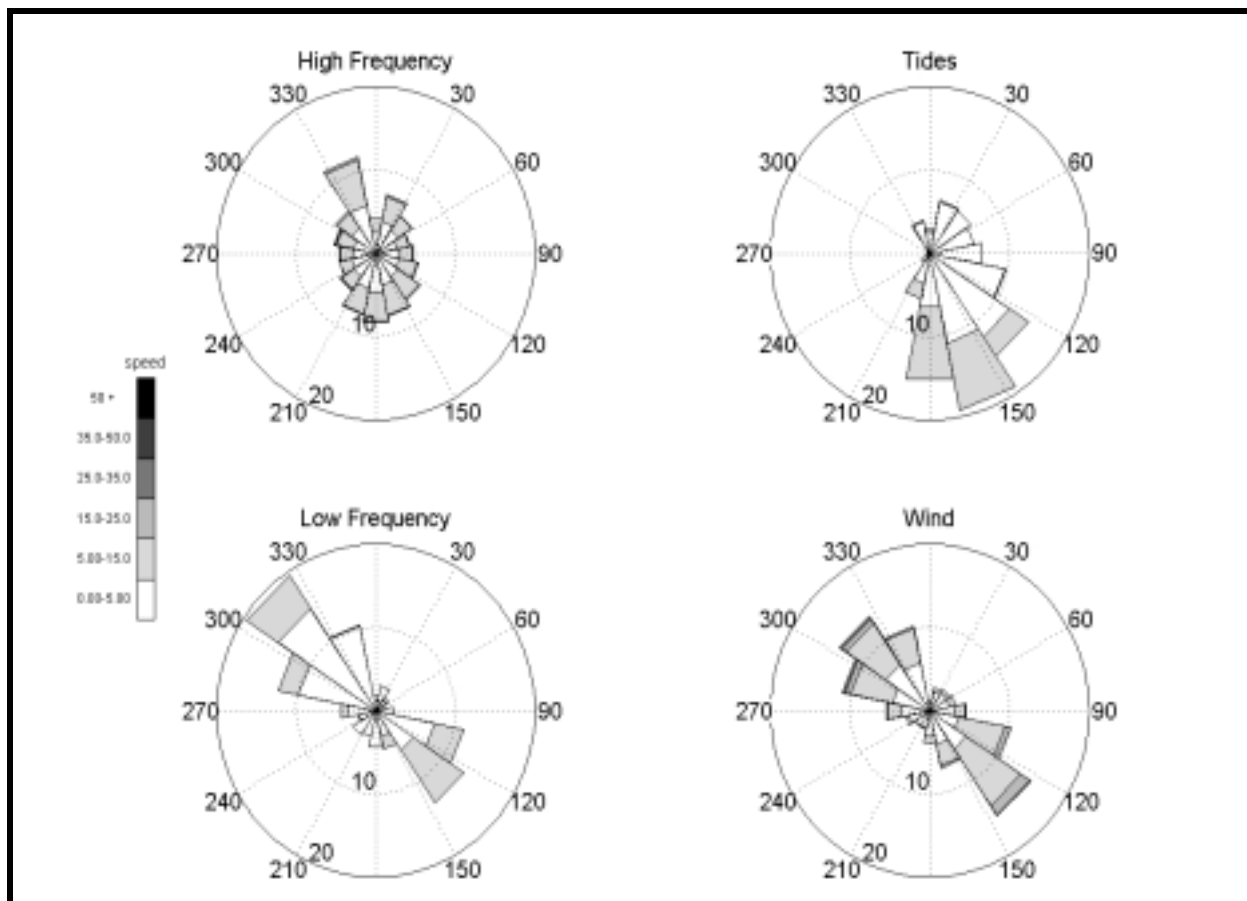


Figure 5-8. Rose diagrams for individual processes at Shell Block 132 (west of Mobile Bay, near-bottom) from September 30, 1987 to October 24, 1988. These data illustrate the relative strength of wind, and that water flow was directed primarily parallel to the isobaths, which are oriented northwest-southeast.

Figure 5-9 shows the rose diagrams for separated signals for Mooring 4S. Figure 5-10 shows the rose diagrams for near-bottom currents collected at Mooring 4B. The high-frequency and low-frequency rose diagrams for both sites indicate these processes are distributed in all directions and do not seem as polarized as wind-driven or tidal currents. Wind-driven currents dominate these sites as well.

The wind-driven signal at Moorings 4S and 4B had an obvious alongshore orientation. Comparison of rose plots for Mooring 4S and 4B show the predominant directional axes are rotated slightly with depth. The predominant direction of flow at 4S was along an approximate east-west axis, whereas the direction of flow at the bottom was an approximate northeast-west turn. The flow appeared to be rotated slightly (perhaps 45 degrees) counterclockwise with increasing depth. This observation at the Mooring 4 location is not consistent with classical Ekman response of the water column to wind forcing, which expects flow to rotate to the right of the wind, or clockwise with depth.

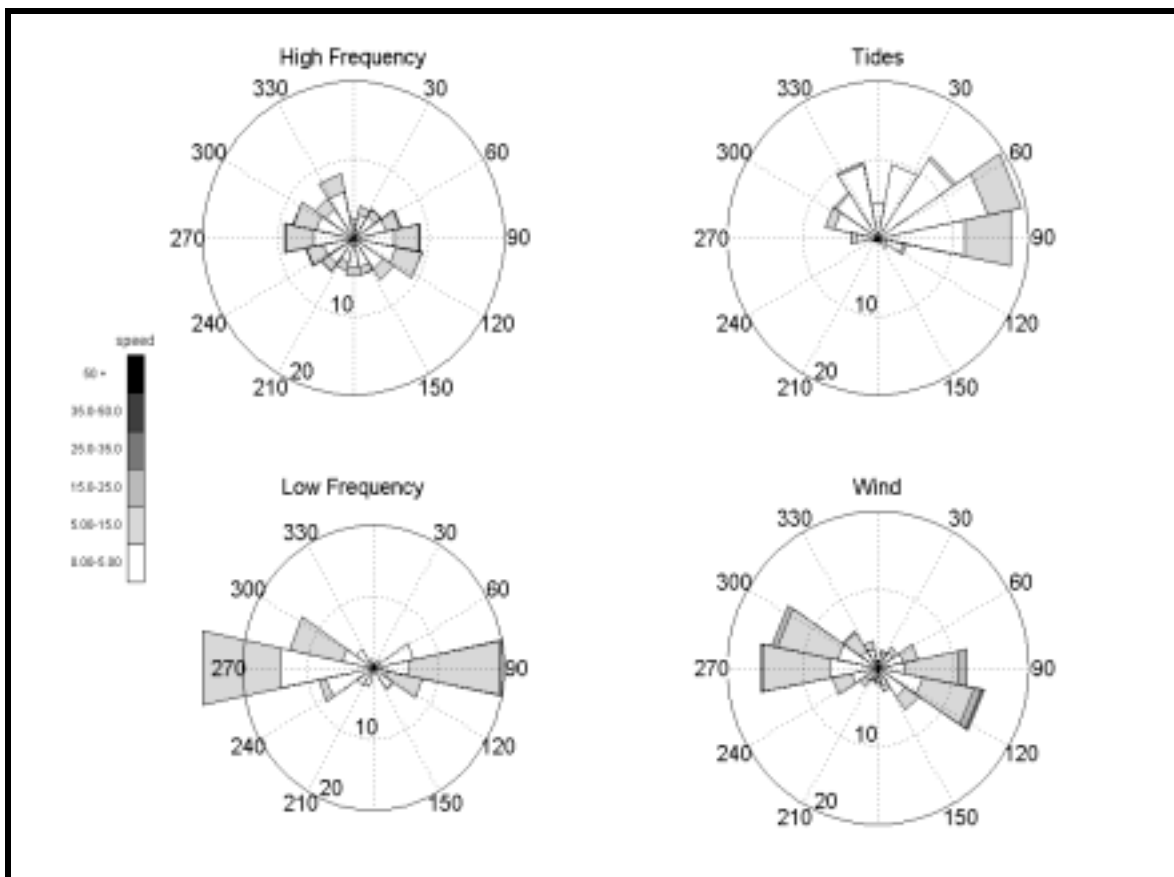


Figure 5-9. Rose diagrams for individual processes at Mooring 4S (near-surface). These data illustrate that wind influence was primarily in the alongshore direction, the high- and low-frequency currents possessed the greatest directional variability, and that tides flowed predominantly to the east-northeast.

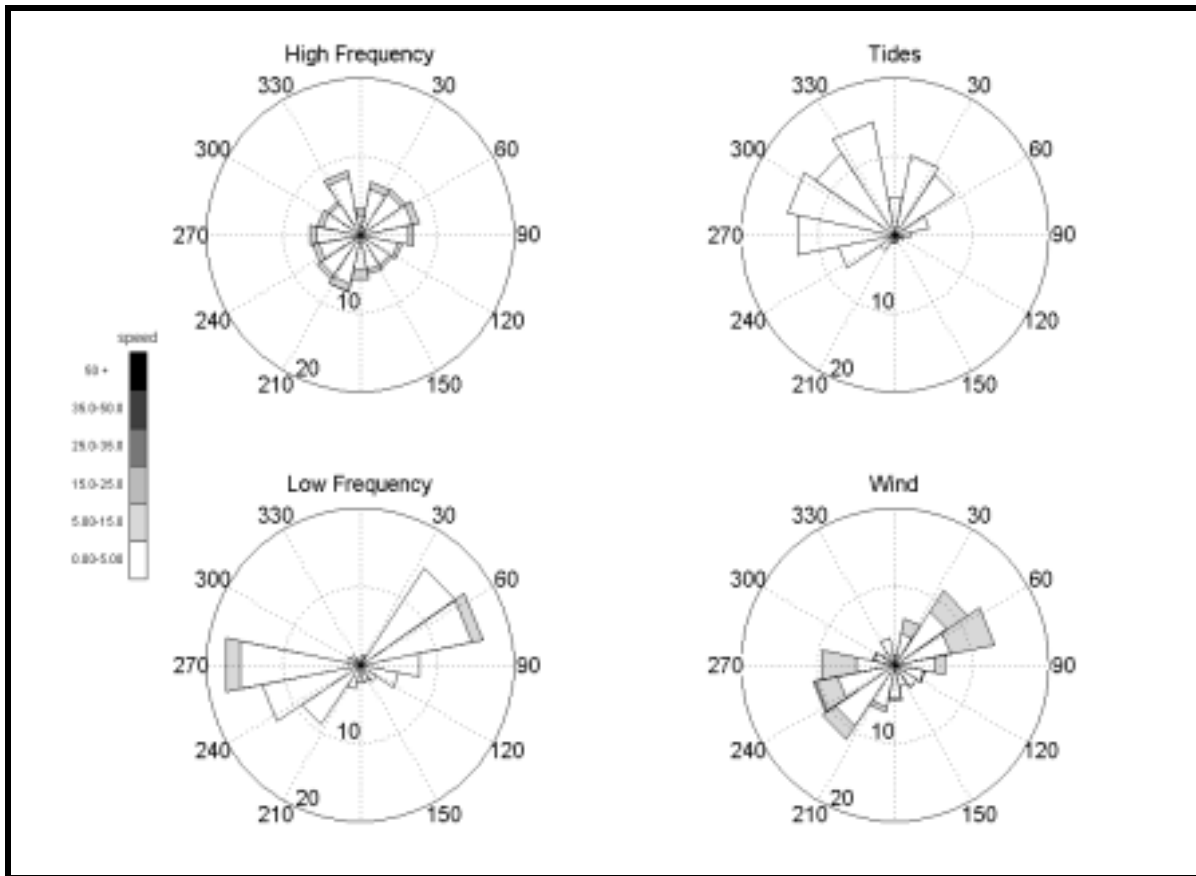


Figure 5-10. Rose diagrams for individual processes at Mooring 4B (near-bottom). These data indicate that wind influence was rotated counter-clockwise relative to surface currents (Figure 5.9), that high- and low-frequency currents possessed the greatest directional variability, and that tides flowed predominantly to the northwest.

An explanation for this vertical counterclockwise rotation may be found by exploring the cross-shore response to wind stress. West winds (winds from the west) force flow to the east and create an upwelling-favorable situation, where the surface flow will tend to drift slightly offshore (or to the right in the northern hemisphere). This drift to the right of a west wind creates a small cross-shore component directed offshore. This offshore component at the surface requires an onshore return flow along the bottom to balance. This balance maintains a cross-shore circulation cell, where bottom water will be driven on-shore, or up-welled, in response to offshore drift of surface flow. East winds will create a downwelling-favorable situation, where surface flow to the west will tend onshore, with bottom waters balancing this cross-shore cell with a slightly offshore bias. Thus, for east winds, the surface flow will tend slightly to the right of the alongshore direction, with bottom waters tending slightly to the left (or onshore) of the alongshore direction. For west winds, the surface flow will again be slightly to the right of the alongshore direction, with bottom waters deflected slightly to the offshore side of the alongshore direction. This cross-shore balance, combined with direct wind forcing, creates the effect of a counter-clockwise rotation of flow with increasing depth. The same counterclockwise rotation of flow in the vertical was observed by Murray (1970) analyzing inner-shelf flow response to high winds during Hurricane Camille.

The rose diagrams for tidal currents at site 4B (Figure 5-9 and Figure 5-10) illustrate different behavior for near-surface tidal currents versus near-bottom tidal currents. Tidal currents at the surface appear to flow to the east-northeast most of the time, with little or no current to the southern

quadrants of the compass. Tidal current speeds were below 15 cm/sec most of the time. At the bottom, tidal behavior was quite different than at the surface. Tides flowed to the northwest quadrant most of the time. Near-bottom tidal currents were less than 5 cm/sec most of the time.

#### 5.1.1.4 Seasonal Variability

The previous section provided evidence that currents along the inner shelf were controlled primarily by surface winds. Currents with 1 to 15 day periodicity (termed wind-driven currents) were shown to be the largest contributor to overall observed currents. Analysis of historical data sets also revealed that wind-driven currents were steered by local bathymetric features. Thus, predominant current directions were controlled not only by the direction of alongshore wind but also by the shape of the shoreline and bottom boundaries. Winds with a western component (from the south-southwest to the north-northwest) appeared to drive flow generally in the alongshore direction to the east. The pattern reverses for winds from the east, which tend to push flow alongshore to the west. This understanding implies that seasonal variability of currents within the sand resource areas is likely to be governed by seasonal wind characteristics.

Figure 5-11 shows the frequency-of-occurrence distribution of currents for the winter (December to February), spring (March to May), summer (June to August), and fall (September to November) seasons for Shell Block 132 observations. This figure represents the directional distribution of flow during specific time periods, and is a further synthesis of data presented in

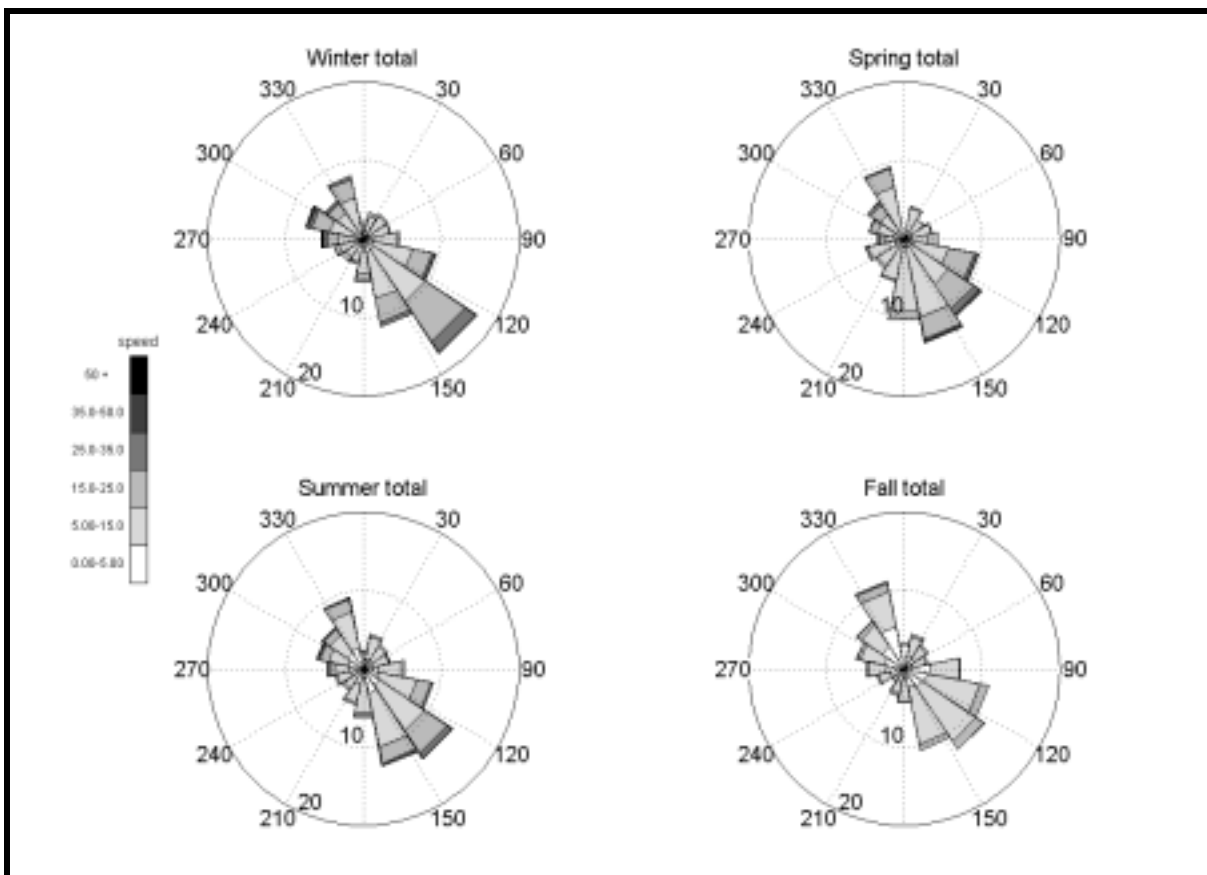


Figure 5-11. Rose diagrams for seasonal currents observed at Shell Block 132 (near-bottom currents). The individual plots represent the original time series divided into seasonal periods.

Figure 5-7 (upper left plot). The data show that the direction of flow changed little with season and maintained a predominant orientation parallel to isobaths. There was also the indication of strengthened flow in the winter, when flows exceeding 15 cm/sec occurred more frequently than at other times of year. The diagrams for the spring and summer seasons show that currents exceeding 15 cm/sec occur less frequently in the spring than in winter; the frequency of these stronger currents diminished further into the summer. For this data set, it appears that currents observed between September and November were the weakest.

Existing literature suggests the wind climatology of this region is influenced in winter by periodic intrusions of cold Arctic air fronts and in summer by milder tropical air due to the northerly position of the Atlantic Bermuda High pressure zone. In winter, stronger northerly winds were more common, while in summer milder southern winds were predominate. Figure 5-12 illustrates observed wind data from the 1987 to 1988 time period separated into winter (December-April) and summer (May-October). Wind-driven currents during this time period are also shown. Wind patterns

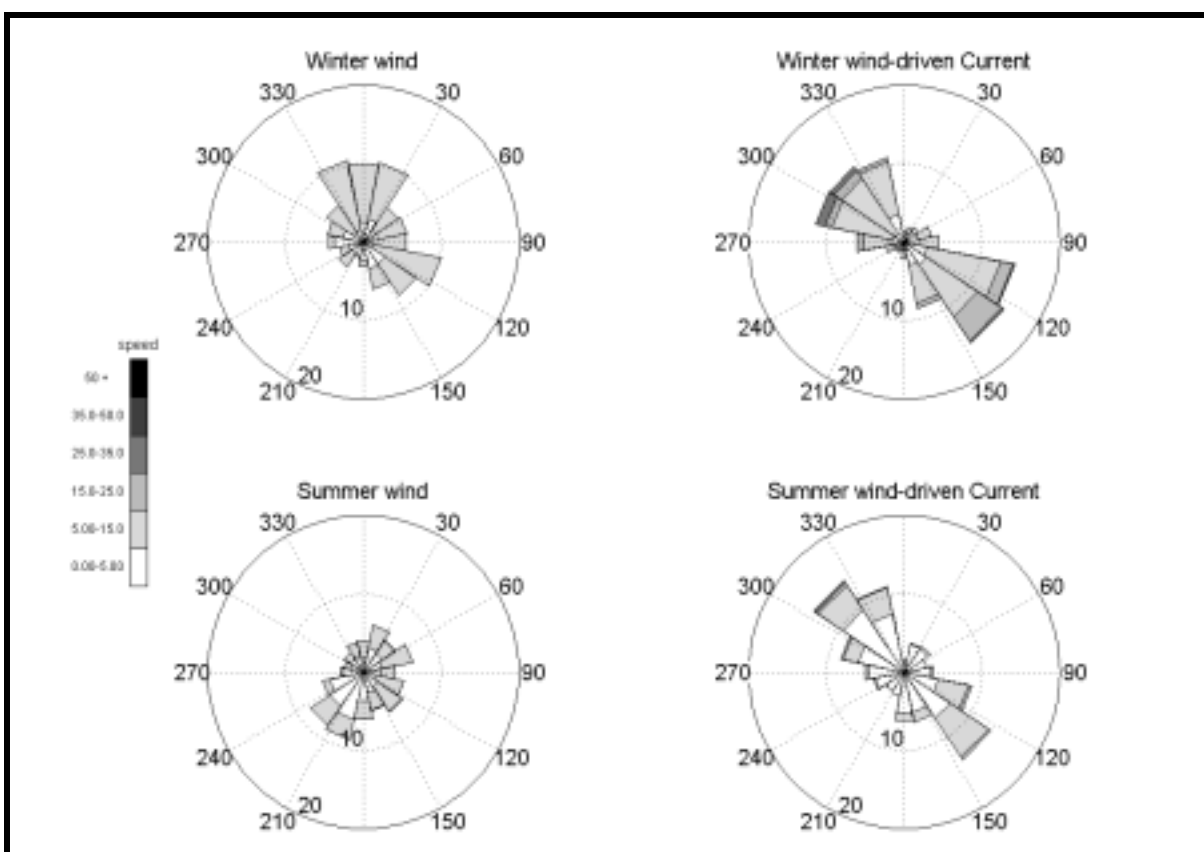


Figure 5-12. Comparison of seasonal winds versus seasonal wind-driven currents for Shell Block 132 (near-bottom) observations. Wind data were obtained from the NOAA station on Dauphin Island. Wind speed units are m/sec; current speed units are cm/sec. Radial circles of each plot represent the frequency of occurrence (in percent); the outer radius depicts 20%, the inner annulus depicts 10% occurrence.

during this period were consistent with historical observations, showing winter winds relatively strong and from the north, with a significant but less frequent southeastern direction. The summer winds were generally weaker and more frequently from the southwest. Wind-driven currents maintained an alongshore direction (northwest to southeast) and were generally consistent with variations in seasonal wind strength. In summer, wind-driven currents exceeded 5 cm/sec approximately 23%

of the time and exceeded 15 cm/sec only about 3% of the time. In winter, wind-driven currents exceeded 5 cm/sec approximately 60% of the time, 15 cm/sec 13% of the time, and greater than 25 cm/sec 3% of the time. In summer, wind-driven flow did not exceed 25 cm/sec.

The analysis suggests that while local bathymetric features govern the predominant directional axis of flow, driving the current in the direction of the alongshore wind stress, it is the strength of the wind that gives an indication of the strength of the current. Throughout the year, flow observed at Shell Block 132 ran either to the southeast (if winds were generally out of the west) or to the northwest (if winds were generally out of the east). In winter, when wind speeds were relatively strong, wind-driven currents also were strong. In summer, when mild wind conditions were most common, flow was relatively weak.

### **5.1.2 Field Data Collection**

Field measurements of currents within the Sand Resource Areas 2 and 4 were conducted in Spring and Fall of 1997. The purpose of these measurements was to observe spatial flow-variations in eastern and western portions of the study area. A total of four surveys were completed; one survey in each of Areas 2 and 4 in the Spring and Fall of 1997. The results of the surveys yielded observations on flow variations throughout the region, and were used in concert with long-term historical current data to augment our understanding of flow characteristics on the inner-continental shelf offshore Alabama. The observations support the results of historical data analyses, suggesting the flow offshore Alabama is dependent upon local bathymetry and changes in wind conditions; tides appear to have little effect on the observed flow.

This section briefly describes field data collection procedures, including instrumentation, survey techniques, and data processing. Furthermore, flow conditions observed at each site during the surveys are discussed. The setup conditions determining flow characteristics (i.e. winds, tides, freshwater discharge) were different during each survey. The following discussion describes how flow in Areas 2 and 4 responded to different forcing conditions. Survey data results are presented in more detail in Appendix D5.

#### **5.1.2.1 Survey Instrumentation and Techniques**

Each survey was designed to measure currents throughout the east and west portions of the study area during an approximate 12-hour period. A survey transect grid was created with transect lines traversed repeatedly throughout the survey. Currents were measured using an acoustic doppler current profiler (ADCP) mounted rigidly to a small vessel. The ADCP is capable of high-resolution measurements of the vertical structure of current flow beneath the instrument transducer. When mounted to a moving platform, such as a small vessel, and used to traverse regional areas, a detailed synoptic view of the current field can result. Repeating these transects at regular time intervals throughout a complete tidal cycle provides a method for evaluating the spatial and temporal variation in current structure in the study area.

The survey transect lines were designed to approximate a butterfly pattern, with two parallel lines running cross-shore (longitudinally north-to-south) separated by approximately 5.6 km (3 nautical miles). Two return lines were run diagonally from the (offshore) end of one cross-shore line to the start of the second cross-shore line in the near-shore zone. The intersection of the two diagonal return lines was located in the approximate center of each sand resource area. The two north-south longitudinal transects were traversed in the offshore-onshore direction, while the two diagonal return lines were run in the onshore-offshore direction.

Each line was completed in approximately one hour, with an entire four-line cycle traversed every four hours. The transect schedule allowed for three complete cycles for Area 2, and two and a half complete cycles for Area 4. The intersection point (center of the sand resource area) was

passed at twice the cycle frequency, resulting in six measurements in the center of the site (once every two hours) per survey. This survey technique provided adequate spatial coverage of the sites with reasonable synopticity, and it was designed with the cross-shore bias to more adequately observe the more dominant alongshore flow processes.

For this study, the ADCP was configured to balance maximum accuracy with reasonable vertical resolution, resulting in a standard deviation (or accuracy of current measurement) of approximately 1.3 cm/sec. The vertical resolution was 1 m, or one velocity observation every 1-m water depth. Each vertical profile took approximately 4 seconds to collect. Averaging parameters resulted in a horizontal resolution of approximately 10 to 12 m along the transect line.

Position information was collected using Hypack, an integrated navigation software package running on a PC computer, linked to a NorthStar 941DX differential GPS. Position data were read from the device in WGS-84 coordinate system and transformed on-the-fly to NAD 1983 State Plane Alabama West zone. Position updates were available every 2 sec, although brief interruptions of position data were experienced when thunderstorms were in the area. These brief losses of position data (less than 10 sec) did not compromise results. Raw position data was also sent to the ADCP Toshiba laptop to assist in verifying clock synchronization between the GPS and ADCP.

The survey resulted in two types of data: current velocity profiles (or ensembles) and vessel position. The ADCP data for a single transect consisted of velocity components at every depth bin for every profile. For these surveys, the two earth-referenced velocity components ( $V_{east}$  and  $V_{north}$ ) were reported, as well as current speed, current direction, and error velocity. The conversion process outputs each ensemble profile as a function of depth (i.e.,  $V_{east}$  vs. depth,  $V_{north}$  vs. depth, etc.). The entire data file represents each ensemble profile along the transect. Approximately 1000 individual profiles were obtained per transect. Twelve (12) transects were completed each survey day, resulting approximately 12,000 independent current profiles through the study area per day.

Position data were recorded as time-northing-easting within Hypack. The ensemble profiles were merged with the position data to assign a unique x-y pair to every ensemble. This merging operation was done using time and GPS position as the common link between the Hypack and ADCP data files. By searching for the unique position at a specific time for each of the data sets, an accurate x-y location was assigned to each ensemble.

Current measurements were presented as vector maps throughout the survey areas. The vector maps represented spatially-averaged current velocities at specific locations within the survey domain. Velocity profiles were separated into near-surface, mid-depth, and near-bottom layers, and grouped within discrete segments along the transect paths. Each survey transect was divided into 16 segments, with an average velocity value calculated for each transect segment at the three depth layers. Each segment was approximately 450 m (1500 ft) long. The resulting vector was located within the center of each segment. The vectors corresponding to a single survey cycle (4 transects) were then displayed on an area map. These vector maps were produced for each of the three depth layers and for each of the three survey cycles. Each survey cycle took approximately four hours to complete. A series of plots shows temporal and spatial variation in horizontal and vertical currents during the survey. A complete set of vector maps for each survey is presented in Appendix D5. Examples of the data will be presented in the next section.

#### **5.1.2.2 Spring 1997 Survey Results**

Sand Resource Area 4 was surveyed May 21, 1997. This site is located immediately south of eastern Dauphin Island (Figure 1-1). The area has complex bathymetric features associated with the Main Pass ebb-tidal delta that influence local circulation patterns. Flow exchange between the Bay and the inner shelf occur primarily through Main Pass. The northeast corner of the area is highlighted by sloping bathymetric contours (along a southeast-northwest axis) which define Pelican Island, a portion of the ebb-tidal delta due south of the eastern tip of Dauphin Island and to the north

of the sand resource area. The ebb-tidal delta is dissected by the dredged channel at Main Pass. An experimental sediment mound lies in the center of the Area 4; elevations on the mound are 2 to 6 m higher than the surrounding region (Hands, 1994). Sand Resource Area 2 was surveyed May 22, 1997. This site is east of the entrance to Mobile Bay in a region of complex bathymetry associated with shore-oblique linear shoals across the entire continental shelf. However, abrupt bathymetric changes related to ebb shoals at Main Pass likely have greater influence on shelf flow patterns throughout the study area.

In the days preceding the surveys, winds were generally blowing onshore (from the south or southeast) at 10 to 15 kts (Figure 5-13). Winds shifted south-southwest three days before the survey. These southwest winds abated to less than 10 kts. On May 21, the day of the Area 4 survey, winds were approximately 10 kts from the west. During the survey, field notes document intense rain squalls and thunderstorms passed the area. On the night of May 21, the winds shifted offshore (from the north) with speeds less than 10 kts. The winds strengthened to 12 to 15 kts in the morning of May 22 and originated from the northeast. These winds calmed during the afternoon of the Site 2 survey to approximately 5 kts.

Tidal elevations during the survey were collected from the NDBC site on Dauphin Island (Figure 5-14). Diurnal tides dominate the region, specifically the K1 and O1 tidal constituents, resulting in one high and one low each day. On May 21, 1997, low water occurred after midnight and high water was observed in early afternoon (1500 hours). The tide range on this day was of order 0.4 m, which appeared to be close to the maximum tidal range in the tropic/equatorial cycle. On May 22, 1997, low water occurred at approximately 4 AM (EDT) and high water was observed at approximately 1600 hours (EDT). The tide range on this day was also 0.4m.

Salinity profiles obtained by CSA during the survey showed the surface layer at all sites to be less saline than underlying layers (see Table 5-2), particularly those close to the mouth of Mobile Bay. Sand Resource Area 1 showed the least vertical variation in salinity, suggesting the freshwater plume had not been carried fully to that location. The strong vertical density stratification between surface and underlying layers affects the flow regime (Stumpf et al., 1993), and it may help to explain both the spatial and temporal current variations observed during the surveys.

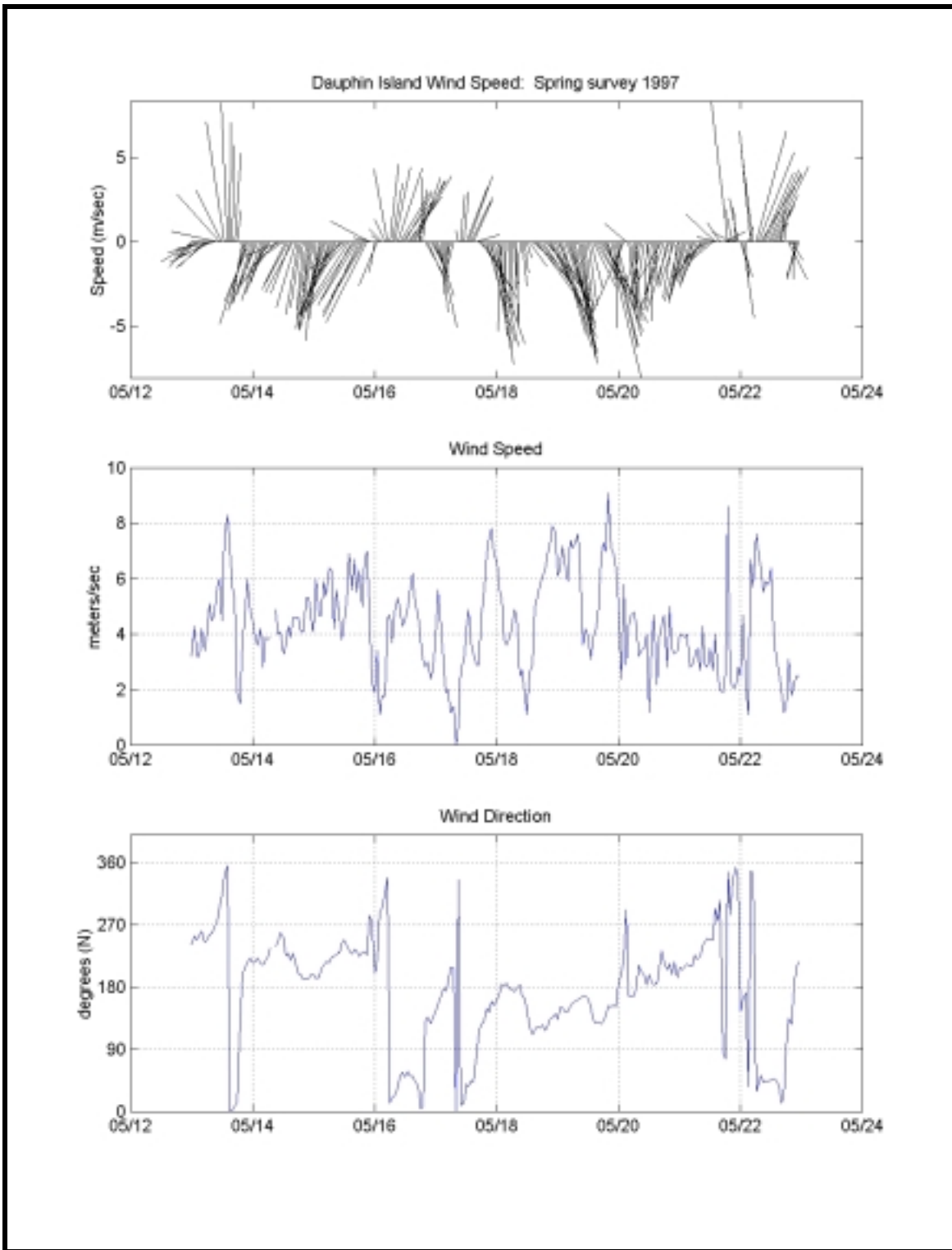


Figure 5-13. Wind conditions prior to and during the field surveys on May 21-22, 1997. Dashed grid lines depict 0000 hours of the day labeled on the bottom axis. Winds are reported as direction from which the wind is blowing.

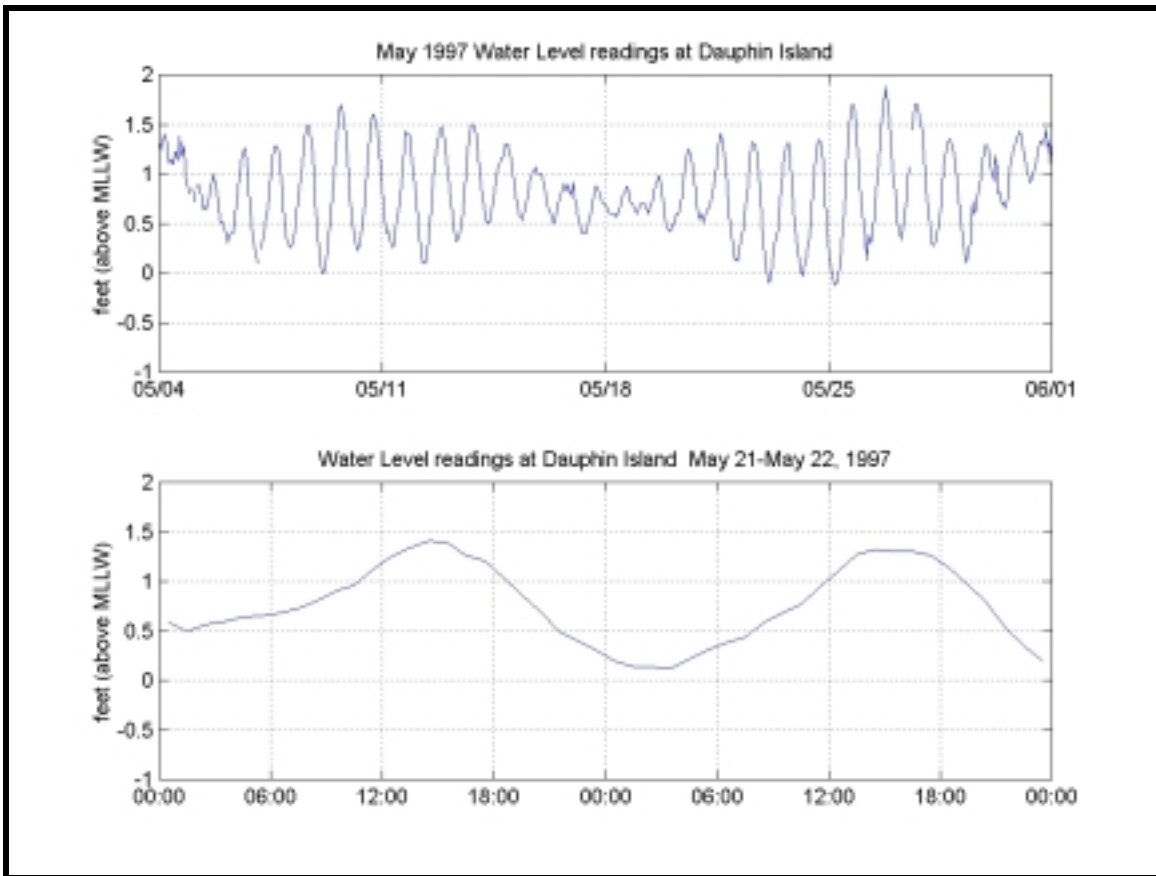


Figure 5-14. Water elevation readings obtained from the NDBC station on Dauphin Island prior to and during field surveys on May 21-22, 1997.

Practical Salinity Units					
Depth Layer	Area 5	Area 4	Area 3	Area 2	Area 1
Surface	18.8	20.2	17.8	19.6	26.6
Mid-layer	30.0	30.5	27.5	26.6	30.2
Bottom	33.6	33.5	28.3	28.4	31.9

Obtained by Continental Shelf Associates, Inc. (see Section 6.0).

#### Spatial Variability at Sand Resource Area 4

The vertical and horizontal variability observed at Area 4 appeared to be due to flow exchange with Mobile Bay, as well as modifications of the flow regime by bathymetric features. The surface and mid-layer currents observed during the survey showed small horizontal variation at any given time (Figure 5-15). Flow in these upper layers was directed primarily west to east, responding to the westerly longshore component of the winds that had been blowing for the previous few days. Flow in the southern (deeper) portion of the area was to the east, consistent with the direction of the depth contours, with amplitudes of approximately 25 to 35 cm/sec. Flow in the northern (shallow) regions was southeast, steered by the local bathymetry around Pelican Island, with similar magnitude as flow in deeper areas. Surface flow was greater (25 to 35 cm/sec) than flow in the mid-depth layers (20 to 25 cm/sec). Flow in the upper vertical layers of Area 4 appeared to be dependent upon the shape and direction of the bottom depth contours.

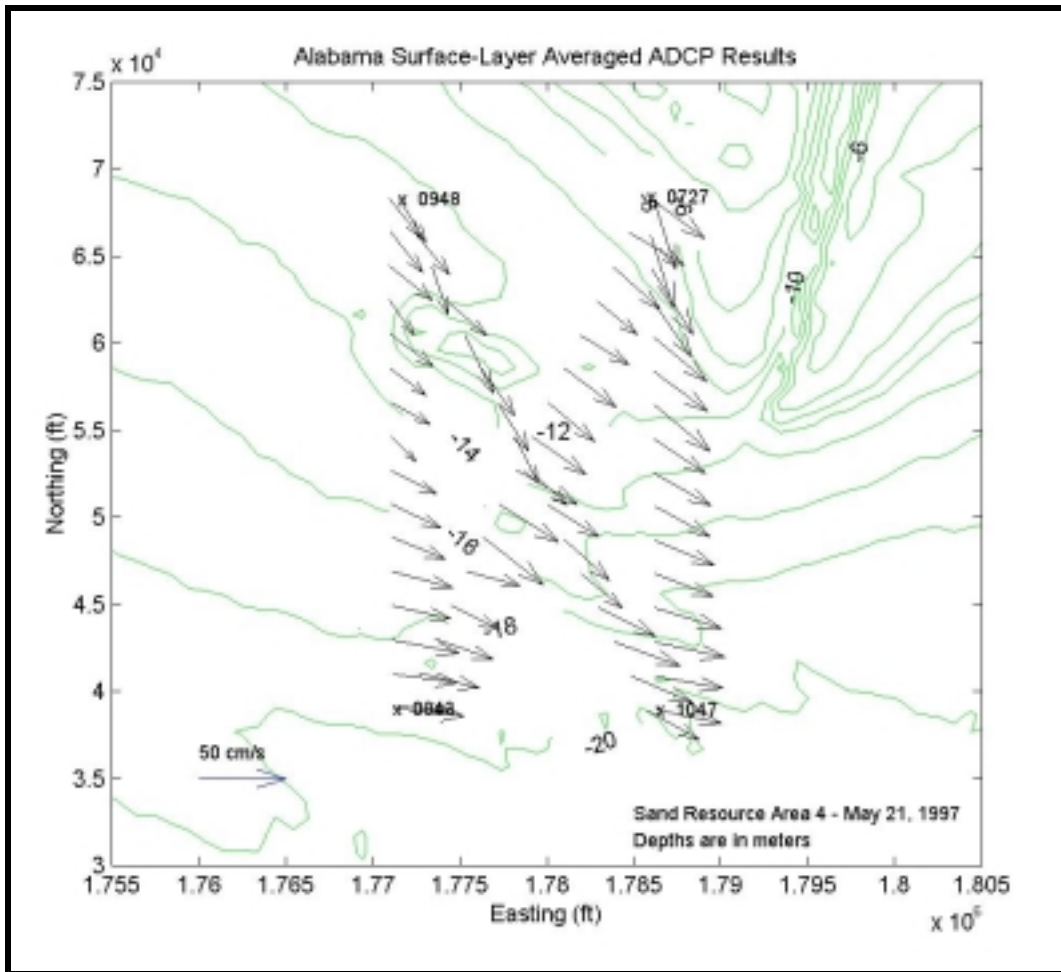


Figure 5-15. Vector map of observed flow patterns for Sand Resource Area 4; May 21, 1997 from 0727 hours to 1150 hours. Current vectors represent average flow in the surface layer only (upper one-third of the water column). Bathymetry of Main Pass is noted in the upper right of the figure. The numbers in each corner of the transect grid ( 0727, 0948, 0848, and 1047) state the time (hour of day) that the transect line was started.

Bottom flow was not similar to surface flow. During a rising tide (early in the survey only), current vectors along the seafloor were oriented toward the mouth of the Bay, which was perpendicular (not parallel) to the bottom depth contours, with speeds approximately 15 to 25 cm/sec (Figure 5-16). The vectors varied slightly in the bottom layer, but each appeared directed toward the narrow Main Pass opening between Pelican Island and Mobile Point. As tide slackens later in the survey, bottom vectors changed to a west-east orientation, consistent with overlying layers.

The dredged material mound located within the northeast quadrant of the sand resource area appeared to modify the bottom flow field weakly, as current vectors shown near the sediment mound (Mobile Outer Mound; Hands, 1994) bend slightly around the obstruction. No significant acceleration of currents was noted due to this diversion.

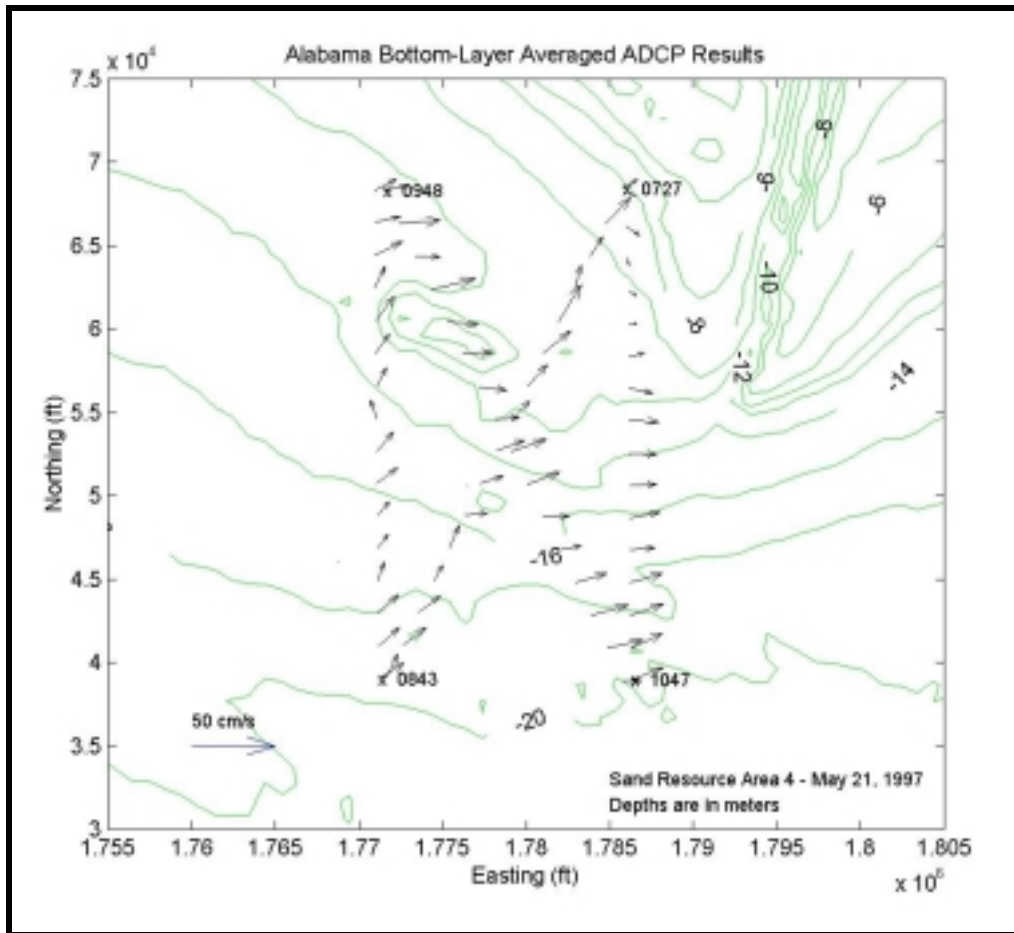


Figure 5-16. Vector map of observed flow patterns for Sand Resource Area 4; May 21, 1997 from 0727 hours to 1150 hours. Current vectors represent average flow in the bottom layer only (lower one-third of the water column).

During the survey, the current regime appeared to respond to temporal changes in tide as well as wind. Early in the survey, water elevations at Dauphin Island approached a peak (high tide was approximately at 1500 hours). The flood of water into the Bay early in the survey was observed along the bottom in areas closest to the Main Channel. Mid-way through the survey, flood flow at the bottom weakened to near-zero conditions (Figure 5-17). When the tide was ebbing from Mobile Bay, bottom currents exhibited alongshore flow consistent with the upper layers. These observations illustrate the manner in which water flows into Mobile Bay in the presence of a persistent freshwater outflow. The near-constant freshwater plume discharged from Mobile Bay at this time may create a vertical layering to the water column, with less-dense fresh water atop a dense layer of ambient shelf water. Surface water discharged from the Bay to the inner shelf is driven either east or west depending on the direction of local winds. Tidal exchange between the inner shelf and the bay may occur in bottom and, to a lesser extent, mid-depth layers as dense shelf water floods into Mobile Bay along the bottom and less-dense fresh water from Mobile Bay is discharged at the surface.

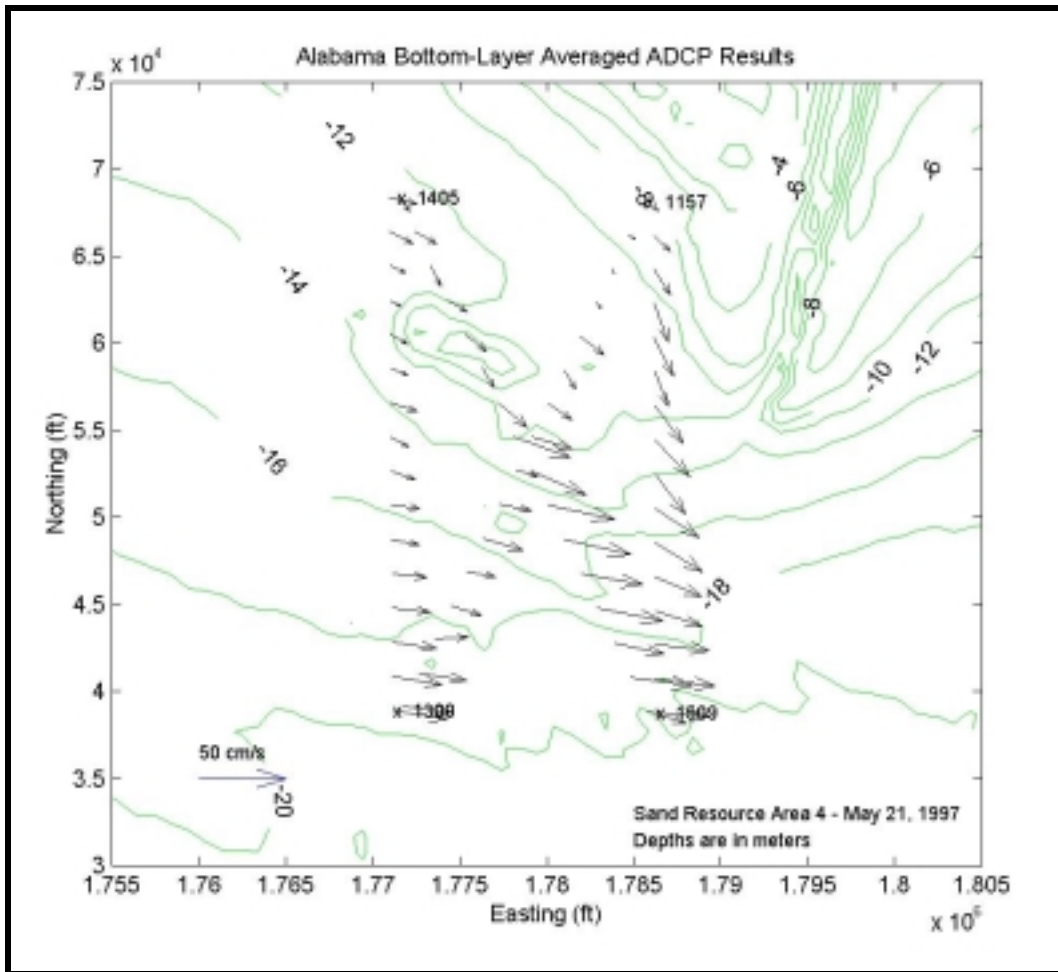


Figure 5-17. Vector map of observed flow patterns for Sand Resource Area 4; May 21, 1997 from 1157 hours to 1620 hours. Current vectors represent average flow in the bottom layer only (lower one-third of the water column).

The surface flow field also demonstrated the tidal influence of Mobile Bay. During flood tide, surface flow was observed west-to-east, consistent with long shore wind forcing in the absence of an inlet. At the northern portion of the area, near the shoals of Pelican Island, surface flow was directed southeast, modified more strongly by the bathymetry than flow in the deeper southern portions of the area. As the tide reached peak approximately mid-day, near-bottom flood currents weakened. However, the surface flow vectors appeared to bend to the southeast around Main Pass, perhaps deflected southerly by a surface discharge from the Bay.

Winds were from the west early in the survey, later in the afternoon wind squalls and thunderstorms passed the area, creating localized flow responses to this variable wind field (Figure 5-18). When wind squalls were observed later in the afternoon the surface flow was quite variable, with directions changing by more than 90° in less than three hours. This directional variability was detected most noticeably in shallow regions to the north, demonstrating the rapid response of the surface flow field to changes in wind stress. Amplitudes of flow during the wind squalls were less than 15 cm/sec, suggesting the wind stress directed to the west may be counteracting the predominant eastward flow.

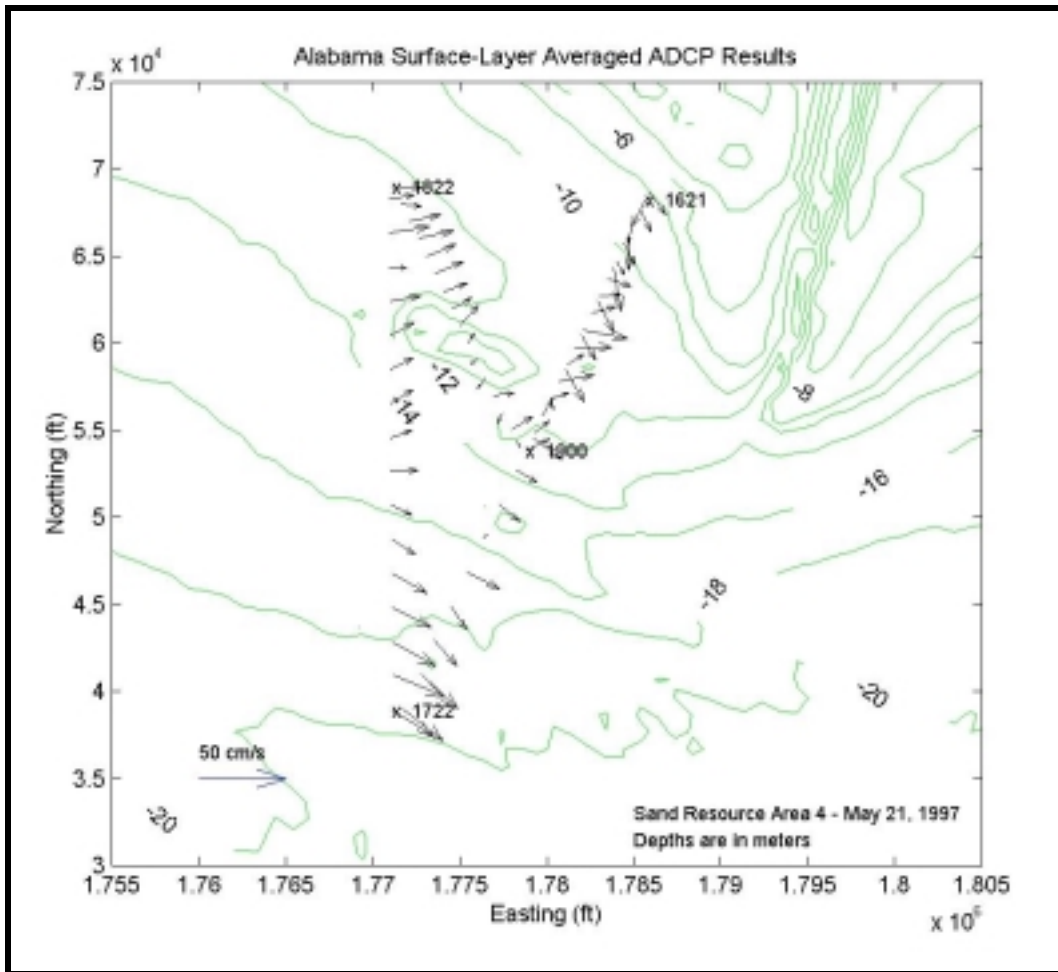


Figure 5-18. Vector map of observed flow patterns for Sand Resource Area 4; May 21, 1997 from 1621 hours to 1930 hours. Current vectors represent average flow in the surface layer only (upper one-third of the water column). These currents were measured as wind squalls and thunderstorms passed the area, and demonstrate the rapid response of surface flow to sudden changes of wind speed and direction.

### Spatial Variability at Sand Resource Area 2

Sand Resource Area 2 has equally-complex bathymetric relief as Sand Resource Area 4; however, the influence of flow processes at Mobile Bay entrance complicates shelf flow patterns in Area 4. Currents in Area 2 were separated initially into three depth layers: the near-surface layer (1 to 4 m from the surface), the mid-depth layer (4 to 8 m below the surface), and the near-bottom layer (8 to 12 m below the surface). Each of the three layers appeared to possess distinct flow characteristics, with the mid-depth and bottom layers exhibiting a strongly coupled relationship. Near-surface flows appeared to be somewhat decoupled from underlying flows.

Distinctions in flow characteristics between the surface layer and underlying layers can be traced to a strong vertical stratification of the water column, likely resulting from the eastward advection of fresh water discharged from Mobile Bay due to southwest and west winds earlier in the week. An example of a single vertical profile is shown as Figure 5-19, showing the abrupt variation of flow within the upper layer.

Currents in the surface layer were relatively uniform in a directional sense, with flows oriented north-northeast at speeds of approximately 15 to 30 cm/sec early in the day (Figure 5-20). Later

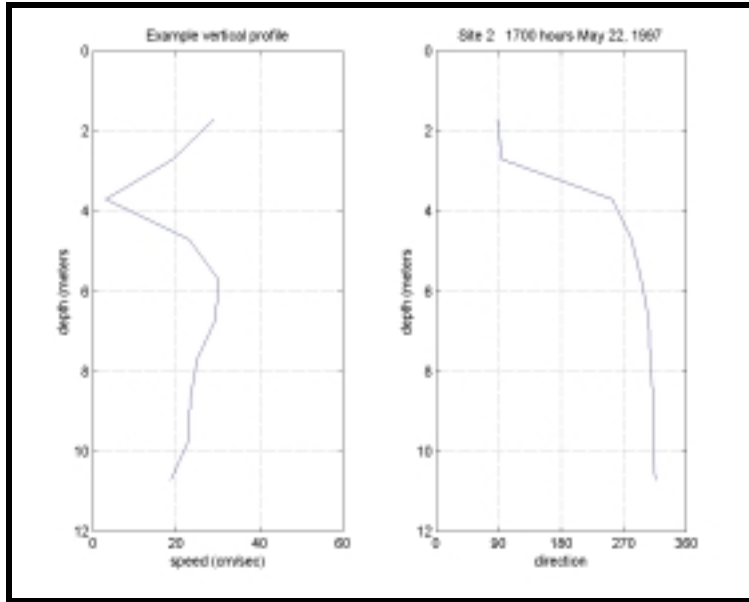


Figure 5-19. Example of a single vertical current profile measured in Sand Resource Area 2 on May 22, 1997. Strong vertical shear is apparent, as surface flow was directed to the east (90°) at approximately 35 cm/sec. Mid-layer and bottom flow were directed to the northwest (315°) at about 20 to 30 cm/sec.

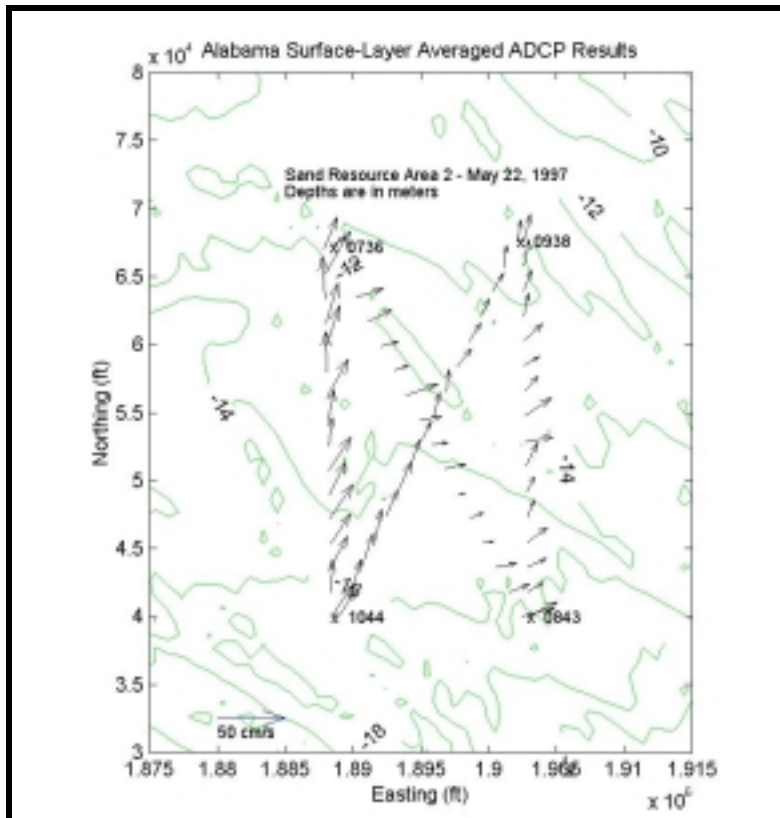


Figure 5-20. Vector map of observed flow patterns for Sand Resource Area 2; May 22, 1997 from 0736 hours to 1130 hours. Current vectors represent average flow in the surface layer only (upper one-third of the water column).

in the day, surface currents shifted east-northeast and maintained a range of speeds approximately 15 to 40 cm/sec. The slight shift in current direction may correspond weakly to a shift in wind direction from the north to the northeast. The entire surface flow field appeared oriented in a uniform direction at any one time with little horizontal directional variability. There did not appear to be specific locations within the survey area where some currents were consistently weaker or stronger than others. The range of surface current speeds throughout the survey was approximately 15 cm/sec in isolated locations to more commonly observed speeds of 30 to 40 cm/sec throughout the region. Speeds of around 45 cm/sec were observed briefly.

The surface layer appeared to be influenced by freshwater discharge from Mobile Bay, as winds had been blowing from the southwest and west for the previous 36 hours. Using an average speed of 30 cm/sec over a duration of 36 hours yields a translation distance of approximately 39 km, a value greater than the distance between Area 2 from the mouth of Mobile Bay. Note that salinity at Area 1, farthest to the east, did not show as strong a vertical gradient in salinity as Areas 3 and 2, suggesting the freshwater plume had not fully reached that far to the east (Table 5-2). The relatively low salinity values measured in underlying (middle and bottom) layers at Areas 3 and 2 suggest that some vertical mixing had occurred between the surface plume and underlying layers.

Mid-depth and near-bottom flows also indicated little horizontal variability for any time period. Flow vectors were oriented in a relatively consistent direction. Near-bottom vectors appeared slightly more variable than mid-depth layer currents, owing to the modification of near-bed flows by bathymetric features. The region is a gently sloping area with few relief features; hence, the observation of low directional variability near the bottom is reasonable. Current speeds decreased with depth and were observed to be approximately 10 to 35 cm/sec in the mid-depth layer and approximately 5 to 25 cm/sec in the near-bottom layer (Figure 5-21). As with observations of surface flow, there did not appear to be localized pockets of weak or strong flow. Speed variability was due more likely to the weak turbulent conditions characteristic of shallow water inner-shelf flow and less dependent upon site-specific behavior resulting from flow modification from seabed bathymetric features.

Two distinct vertical layers (surface and middle/bottom layers) exhibited different temporal changes through the duration of the survey. The surface layer tended to move eastward early in the day, correlated well with the wind direction (from the southwest). Observations that the freshwater plume discharged from Mobile Bay is highly correlated to local wind stress has been reported by Gelfenbaum and Stumpf (1993). As wind shifted to the northeast on the day of the survey, surface currents appeared to rotate slightly to the east-northeast, perhaps as an initial response to the shift in wind direction. The survey did not extend later in the day to observe a continuation of the surface flow field response to this shift in wind direction.

The mid-depth and near-bottom layers appeared to rotate clockwise throughout the survey duration. Mid-depth layers were observed in the morning to flow east-southeast, rotating with time to the southeast (at mid day) and subsequently to the northwest at the end of the survey. The near-bottom layer showed this same rotation, with flow directions oriented east and southeast early in the day, shifting south and then west and northwest late in the day (Figure 5-22). The near-bottom flow was rotated slightly clockwise with respect to the overlying flow. The clockwise rotation of the regional current vectors appeared to make an approximate 180° turn (half a complete cycle) during the approximate 12-hour duration of the survey. This extrapolates to a complete cycle over a 24-hour time period, falling approximately upon both major tidal periods for this region.

The decoupling of surface layer currents with underlying flows was observed during the survey, specifically with surface currents appearing to respond rapidly to variations in wind stress, and the underlying flows forced by processes of longer time scales. Gelfenbaum and Stumpf (1993) report a similar finding in this region, with the upper layer of a stratified water column having little

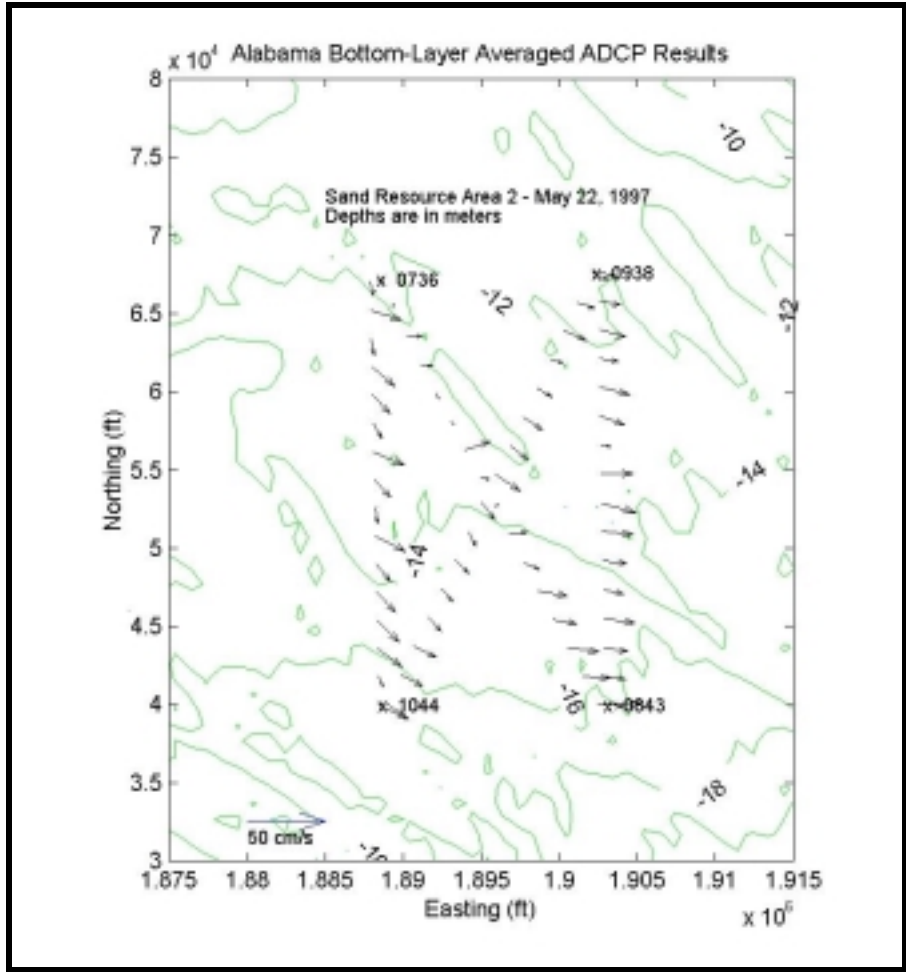


Figure 5-21. Vector map of observed flow patterns for Sand Resource Area 2; May 22, 1997 from 0736 hours to 1130 hours. Current vectors represent average flow in the bottom layer only (lower one-third of the water column).

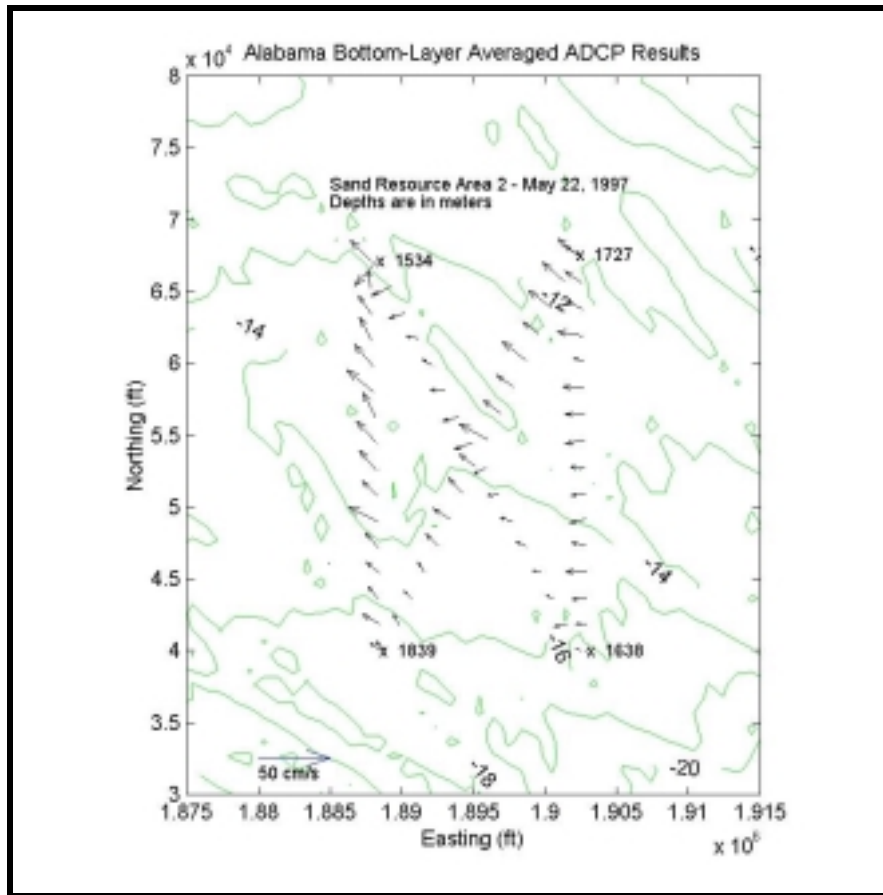


Figure 5-22. Vector map of observed flow patterns for Sand Resource Area 2; May 22, 1997 from 1534 hours to 1929 hours. Current vectors represent average flow in the bottom layer only (lower one-third of the water column). Note the 180° counterclockwise rotation of flow vectors since the beginning of the survey (see Figure 5-21).

effect on the movement of underlying water. These authors suggest two layers do not mix very efficiently in the vertical, however the observation of lower salinity waters in the region (Areas 3 and 2) suggest some vertical mixing between layers can occur.

### 5.1.2.3 Fall 1997 Survey Results

Area 4 was surveyed again after the summer to determine flow characteristics during a different season. On September 30, the same survey transects were occupied as the Spring survey. Area 2 was surveyed the following day, October 1, 1997. The wind field was relatively constant, and tidal variation was small. While no discharge data were collected from Mobile Bay, historical data suggest that discharge during the survey was less than discharge during the previous survey in May.

On September 30, winds were steady from the west at about 10 kts (Figure 5-23), weakening slightly in the afternoon. On October 1, winds maintained a speed of 10 kts from the west, shifting north to less than 10 kts during the afternoon. A strong wind event four to five days before the surveys produced winds from the northwest in excess of 20 kts. This event persisted for approximately 24 hours. After this event, winds blew offshore (from the north) at approximately 10 to 15 kts for the next two days. Winds rotated southwest and west at approximately 10 kts during the two-to-three days before the surveys.

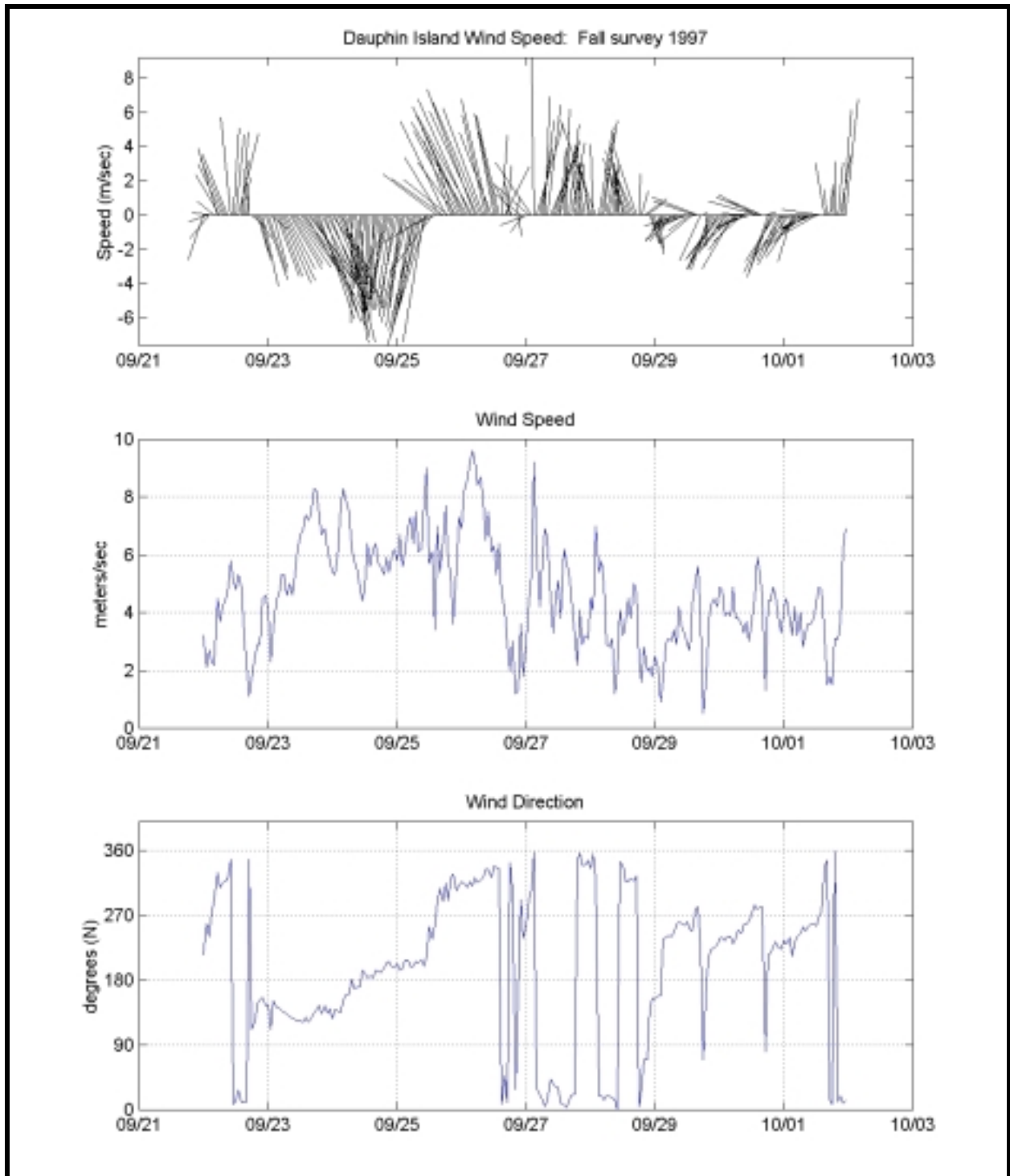


Figure 5-23. Time series of wind speed and direction for 10 days preceding the fall 1997 field survey. Surveys were completed on September 30 and October 1, 1997. The horizontal dashed grid lines represent 0000 hours on the specified day.

Tides during the survey were in the equatorial (minimum) phase, producing small elevation changes at the Dauphin Island station (Figure 5-24). This is in contrast to the spring survey, which occurred during the tropic (or maximum) phase of tide. On September 30, the change in water level was 12 cm. The usual tidal variations observed earlier in the week appeared to be contaminated by non-tidal influences, as the tidal record for October 1 appears almost as a flat line, with a water elevation variation of less than 8 cm. It is unclear what caused this perturbation in the water elevation record.

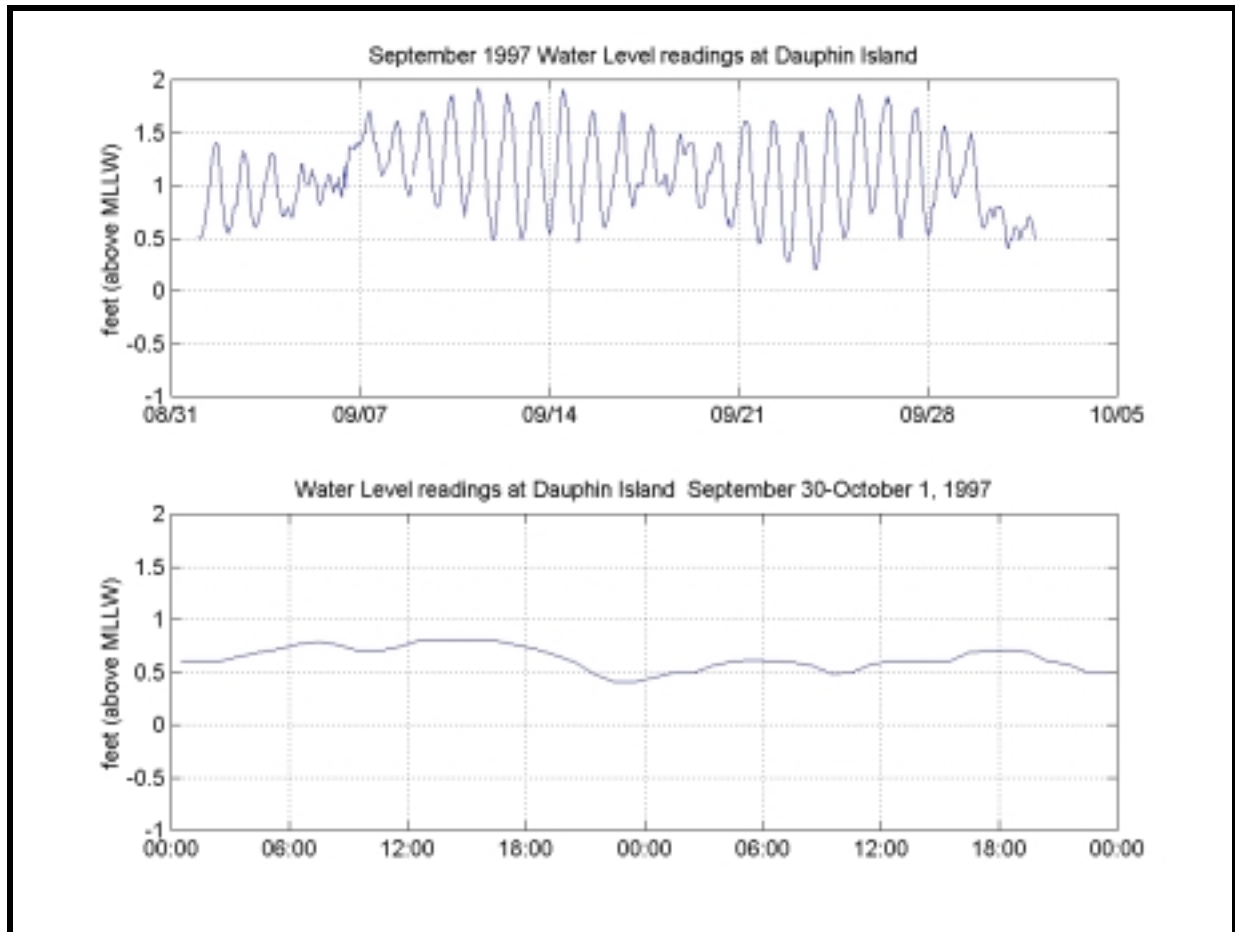


Figure 5-24. Water elevation readings obtained from the NDBC station on Dauphin Island prior to and during the fall field surveys. The data show the tides were near the equatorial (minimum) phase of the cycle on September 30 and October 1, 1997.

The strong vertical stratification observed during the previous survey in May, and resulting decoupling of surface layer versus underlying currents, was absent during the fall. The lack of a highly stratified water column results in more efficient vertical mixing, and therefore, a more homogeneous behavior to the flow field. While no profiles of temperature and salinity were obtained during the October survey, there were profiles obtained during a subsequent cruise in early December, 1997. These observations show the water column to be extremely well-mixed, with little vertical gradient to these parameters. This mixing may be related to two sources; the reduced fresh water input discharged from Mobile Bay in this season, and the more frequent and energetic storms that pass the region during the autumn, providing sufficient vertical mixing forces to the water column. The absence of vertical variability of currents during the October survey suggests the water column was less stratified than during the May survey.

### Spatial Variability at Sand Resource Area 4

Current flow through the region appears to result from wind forcing and shows a dependence upon bottom bathymetry, with the flow generally oriented parallel to depth contours. There was vertical variation between surface and bottom layers, suggesting a well-mixed water column.

Surface flow throughout the sand resource area generally followed the depth contours, with flow in the deeper south regions oriented to the southeast (Figure 5-25). Currents were likely wind-driven, but there could have existed a surface plume discharged from the Bay that may have deflected the flow slightly to the south as well. Currents in shallower regions of the northeast quadrant were also directed to the southeast, including currents measured adjacent to the Main Channel. Currents near the Main Channel appeared to be deflected weakly to the south, perhaps influenced by some surface discharge from the Bay. However, this deflection was observed late in the afternoon when there was a small decrease in tidal elevation at Dauphin Island. The range of speeds for currents measured in the surface layer was 40 to 50 cm/sec.

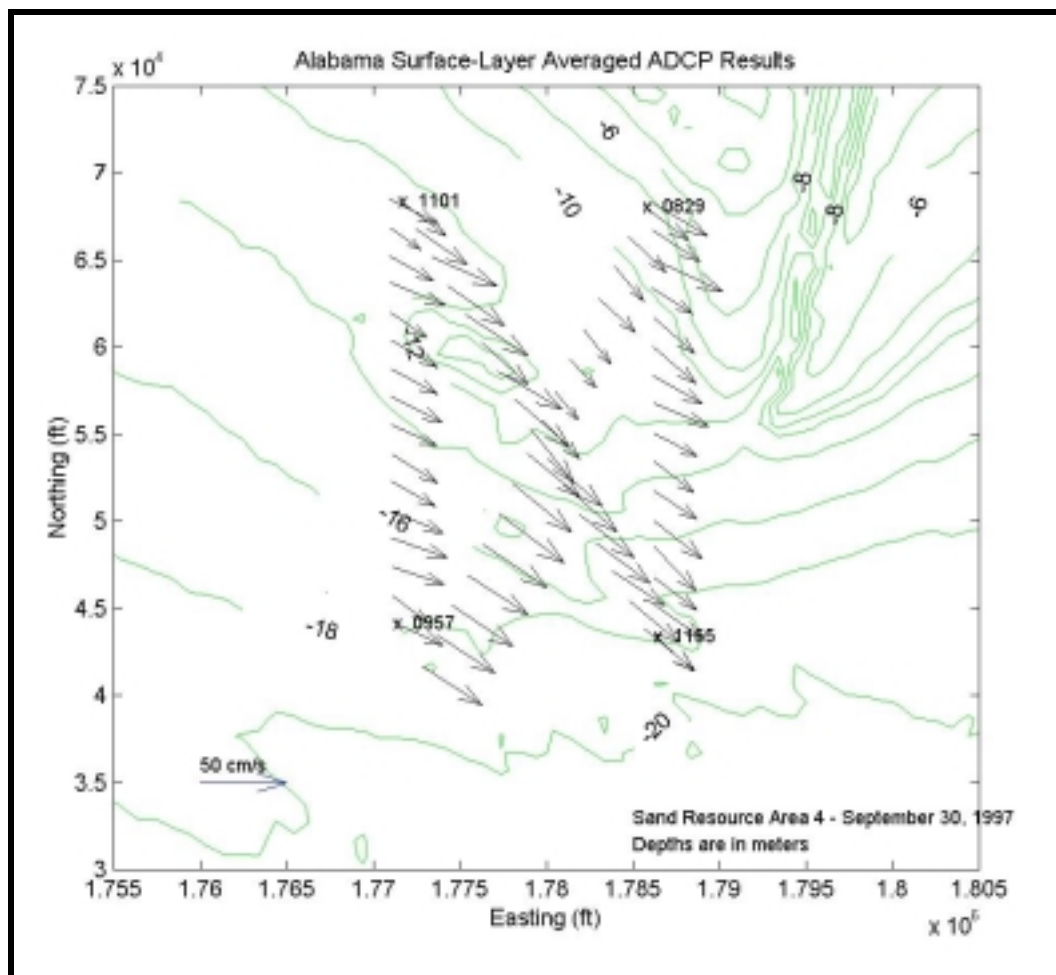


Figure 5-25. Vector map of observed flow patterns for Sand Resource Area 4; September 30, 1997 from 0829 hours to 1255 hours. Currents vectors represent average flow in the surface layer only (upper one-third of the water column).

Mid-layer flow had a similar southeast directional orientation, with speeds slightly reduced to approximately 25 to 35 cm/sec throughout the region. Bottom flow was weaker than overlying layers, with areas of low speed flow (approximately 15 cm/sec) and other areas where the speed was approximately 25 cm/sec (Figure 5-26). The weakest bottom currents appeared to be located on the down-current side of the dredged material mound; the strongest bottom currents were located in deeper water and those near the Main Channel. Bottom layer flow generally was oriented to the east, versus overlying flow to the southeast. This may be due to the presence of a surface plume discharged from the Bay, affecting more strongly the surface layers and hence deflecting surface currents weakly to the southeast. Meanwhile, bottom flow was relatively unaffected and free to follow the bottom contours.

Temporal changes in the flow field during the survey consisted of a slight weakening in surface current speed in the afternoon due likely to decreasing west winds (to approximately 6 kts versus 10 kts early in the day). The observed surface currents decreased from speeds of 40 to 50 cm/sec in the morning to speeds ranging from 20 to 30 cm/sec in the late afternoon. No directional changes were evident.

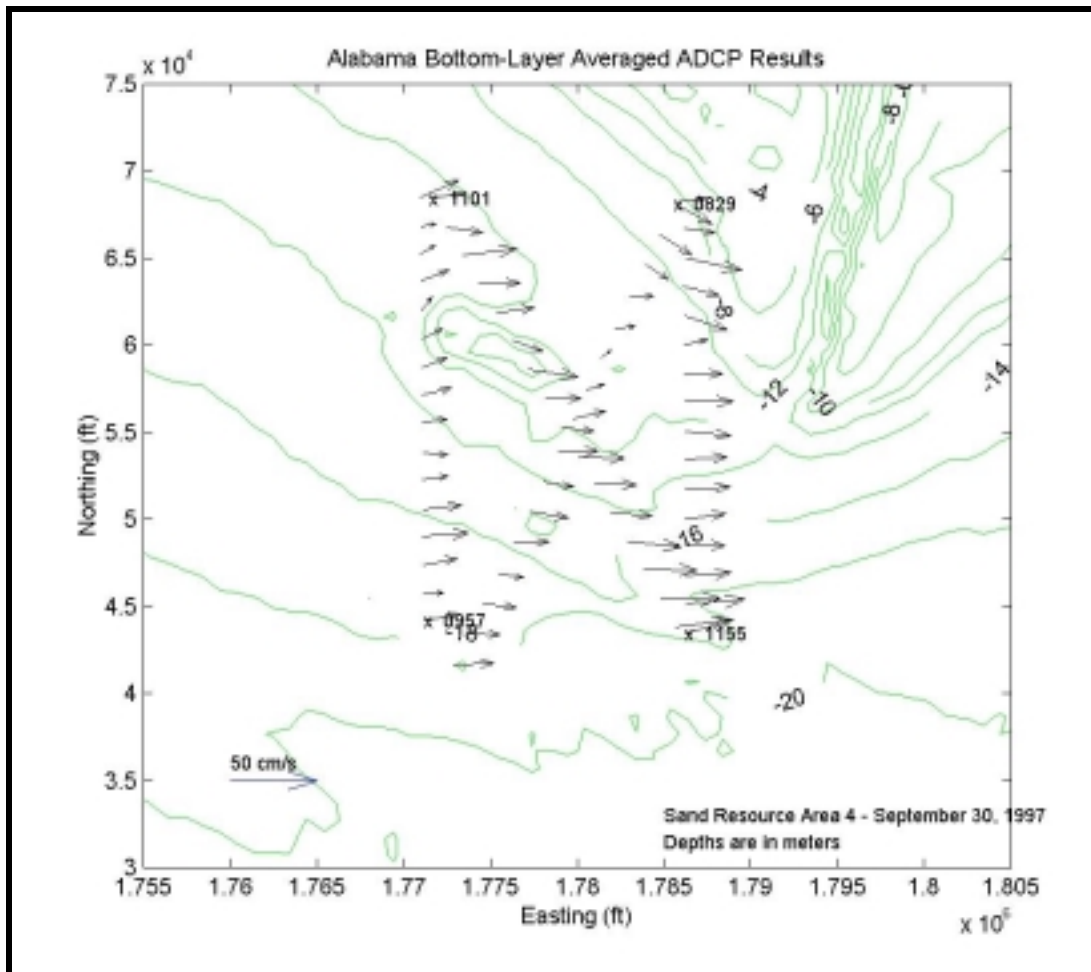


Figure 5-26. Vector map of observed flow patterns for Sand Resource Area 4; September 30, 1997 from 0829 hours to 1255 hours. Currents vectors represent average flow in the bottom layer only (lower one-third of the water column).

A slight modification of flow was observed later in the survey, likely due to weak ebb flow from Mobile Bay. The tide curve shows a decrease in water elevations in the afternoon, although this decrease was quite small (8 cm). Flow near Main Pass was observed to deflect slightly to the south, consistent with flow interaction between ambient west-to-east coastal currents and a southward discharge from the Bay entrance (Figure 5-27). This flow collision modified both surface currents as well as bottom currents. Flow along the bottom shifted southeast, versus an eastward flow earlier. Upper and middle layer flow was deflected to the south, versus an earlier southeast orientation.

### Spatial Variability at Sand Resource Area 2

Currents throughout Area 2 were again quite uniform, meaning there was little directional variability observed at any one time. A slight clockwise rotation was observed during the survey, however the rotation appeared to be approximately 45° over the 12-hour period, and likely due to changes in the wind stress field.

No significant horizontal variation was observed in the surface layer, as the flow field was uniformly directed to the east or east-southeast (Figure 5-28). Speeds were relatively consistent and ranged from approximately 25 to 50 cm/sec. The mean speed at the surface was approximately 40 to 45 cm/sec. The relatively large range of observed current speeds at the surface indicates

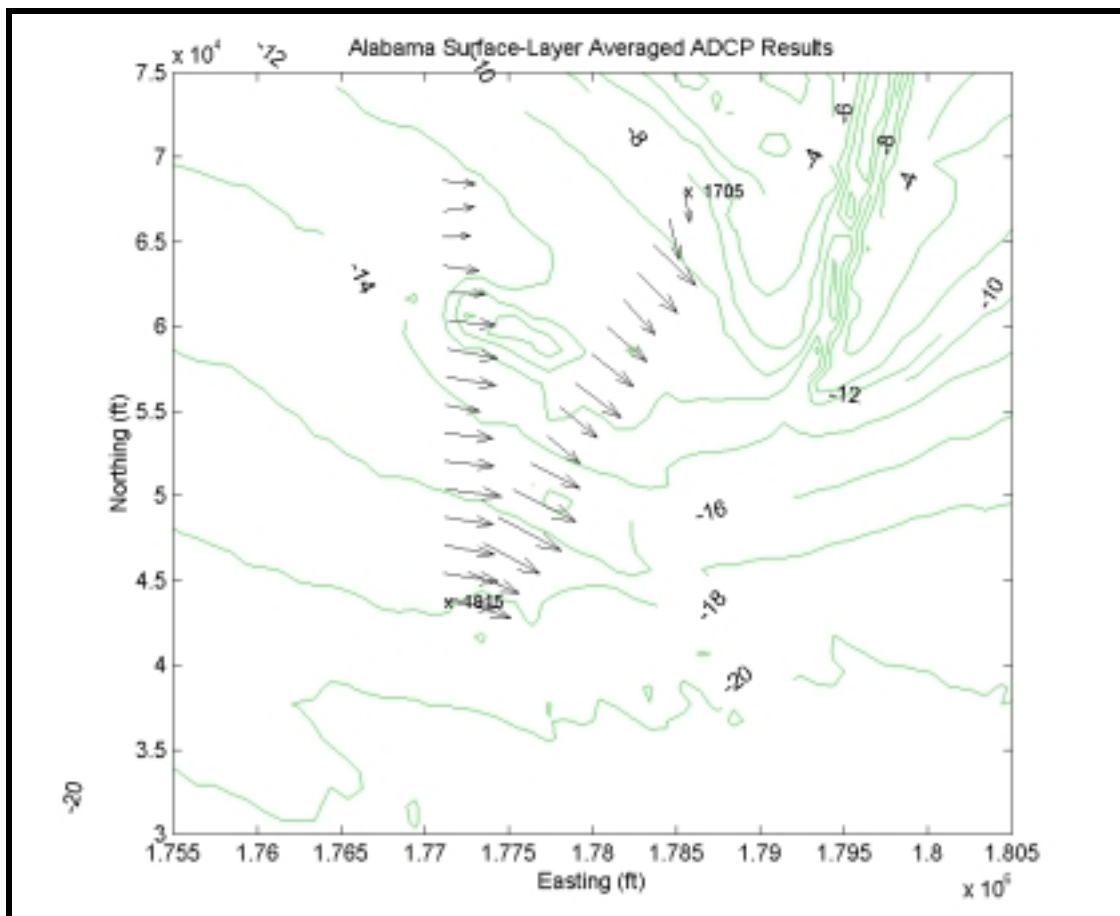


Figure 5-27. Vector map of observed flow patterns for Sand Resource Area 4; September 30, 1997 from 0829 hours to 1255 hours. Currents vectors represent average flow in the surface layer only (upper one-third of the water column).

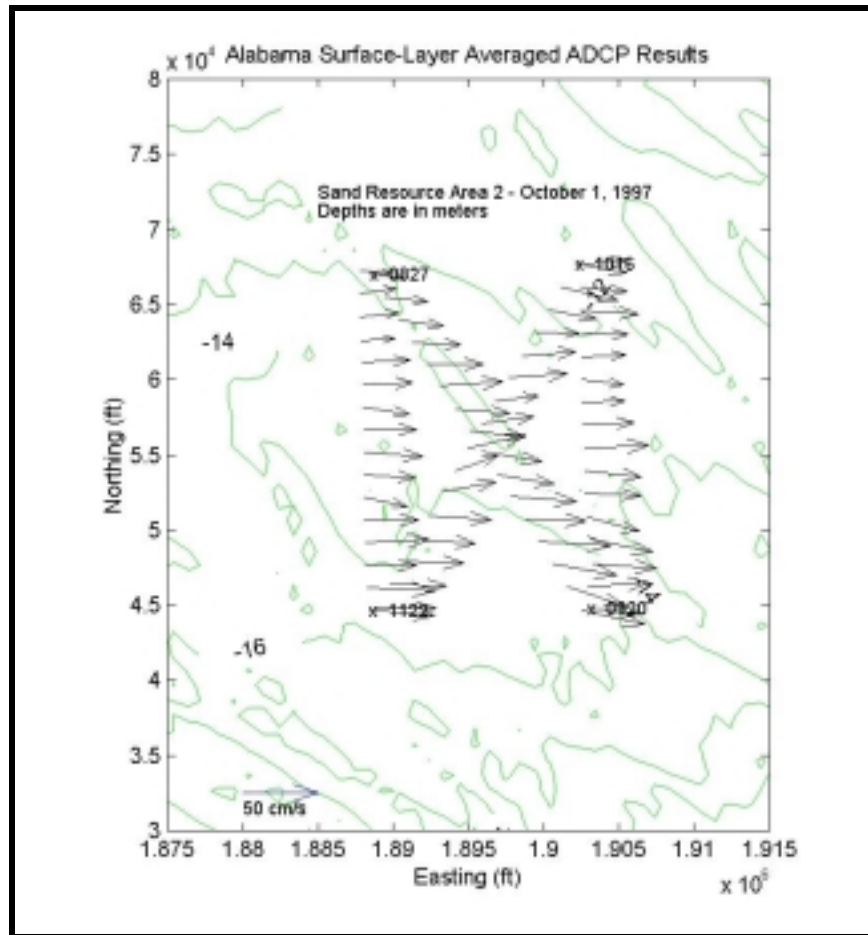


Figure 5-28. Vector map of observed flow patterns for Sand Resource Area 2; October 1, 1997 from 0827 hours to 1215 hours. Currents vectors represent average flow in the surface layer only (upper one-third of the water column).

a weakly turbulent flow regime. The mid-depth and near-bottom layers also exhibited this same uniformity, with all mid-depth currents flowing to the east-northeast. Speeds in this middle layer were approximately 15 to 40 cm/sec, with an average speed of approximately 30 cm/sec. Near-bottom currents showed slightly more directional variance, again due to the moderate influence of bathymetric relief; however, the currents generally pointed northeast. Mean speeds were approximately 20 cm/sec in the near-bottom layer, with a range from 10 to approximately 25 cm/sec (Figure 5-29).

The vertical variation in currents was much weaker than observed during the previous survey. In autumn, as river discharge abates, it is expected that the nearshore water column would lose vertical stratification and become more homogeneous with more efficient mixing between the surface and underlying layers. During the Fall survey, there was little difference between flows at the surface and near-bottom. A slight rotation was observed with depth; however, the rotation was counterclockwise to surface flows directed east and near-bottom flows directed to the northeast. This counterclockwise rotation may be the result of coastal upwelling. For a west wind producing a wind-driven flow to the east, there will be a slight cross-shore component produced to the right of the flow vector, or in this case, offshore. Bottom flow compensates for this offshore-directed transport to create a weak on-shore return component. The net result of this is an apparent counterclockwise rotation of flow with increasing depth.

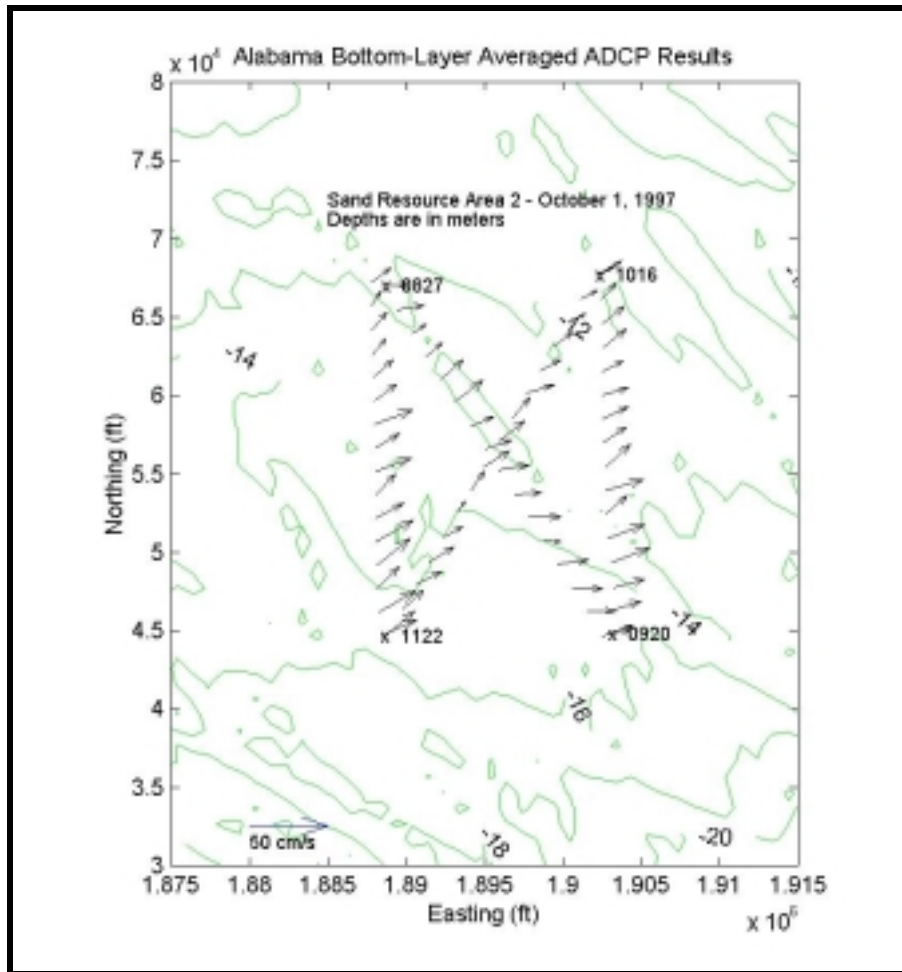


Figure 5-29. Vector map of observed flow patterns for Sand Resource Area 2; October 1, 1997 from 0827 hours to 1215 hours. Currents vectors represent average flow in the bottom layer only (lower one-third of the water column).

The flow field varied little throughout the survey, maintaining an approximate eastward direction with speeds ranging from 40 cm/sec at the surface to approximately 20 cm/sec in the near-bottom layer. During the 12-hour duration of the survey, a slight modification of near-surface current vectors was observed in response to a shift in the wind direction. This response to changes in wind stress was noticed initially in the surface layer; underlying layers appeared unaffected by this change, likely because the survey ended prior to the effects passing through the surface to underlying layers.

The response of the near-surface flow field to changes in wind stress is identified by a gradual shift in current direction from east-southeast and east, the predominant orientation of the flow during the early morning and afternoon, to the southeast later in the day. The shift in wind direction occurred at approximately 1500 hours. The first evidence of surface layer response was noted approximately two hours later at 1700 hours, when currents began deflecting southeasterly. This deflection of flow to the south appeared more consistently in shallower near-shore regions of the survey grid than in the deeper (offshore) regions of the area. There was also some evidence that surface flow vectors were decelerated by this deflection, with speeds measured in the range of 5 to 30 cm/sec (versus a range of 25 to 50 cm/sec early in the day, and a range of 15 to 45 cm/sec at mid-day).

### 5.1.3 Summary of Flow Regimes at Offshore Borrow Sites

The information presented above indicates the flow regimes within the study area are dependent upon wind forcing, density stratification, seafloor topography, and coastal boundaries. Tides had little influence on observed currents.

Historical data, in the form of long-term current observations at specific locations, were separated by time scales of individual physical processes: winds, tides, high-frequency currents, and low-frequency currents. For this analysis, it was clear that the observed currents at each location flowed predominantly in an alongshore direction. Wind-driven flow, defined as flow occurring at time scales between 1 and 15 days, had the greatest fraction of total signal energy. Wind distributes energy to the water column at a variety of time scales, from high-frequency bands (periods less than 24 hours) to low-frequency bands (periods greater than 15 days), so it must be assumed that some wind influence was included inherently in other separated signals as well. The separated low- and high-frequency signals also possessed significant energy, though not as great as the energy attributed to the defined wind-driven processes. These low- and high-frequency signals also appeared to be correlated to the strength of the wind.

Seasonal variation in currents also was correlated to seasonal changes in wind. Comparison of wind data in winter versus summer indicated the winter season was characterized by relatively strong northern winds, while the summer period was characterized by weak winds from the south. Generally, winter current speeds were shown to be greater than those observed in summer. Although wind directions varied considerably between seasons, the direction of the currents at these locations did not vary. The predominant alongshore orientation of currents at all sites did not change throughout the year.

The separation analysis also noted that tides have small influence on the overall observed currents. Tide accounts for less than 10% of the total signal energy. Tidal currents were greatest in the alongshore direction, as well as stronger at the surface than at the bottom. Tidal current speeds reached approximately 5 cm/sec (at the bottom) during tropic (maximum) phases and less than 1 cm/sec during equatorial phases; at the surface, maximum tidal speeds were approximately 8 cm/sec.

Results of the field surveys showed the spatial influence of bathymetric features, tidal exchange between Mobile Bay and the inner shelf, and the wind forcing on the nearshore circulation patterns. Wind conditions prior to and during both surveys had significant westerly longshore components. As a result, the prevailing currents flowed generally eastward, consistent with previous analyses. This wind-driven longshore flow was influenced locally by bathymetric features, specifically the ebb-tidal delta of Main Pass, which tended to steer longshore flow to the south, while flow in areas farther offshore, removed from this coastal boundary, did not have such strong deflections. At Area 2, east of Mobile Bay and in an area of gently sloping bathymetry with no abrupt features, the spatial variation of flow was small.

Survey data also illustrate the rapid response of surface flow to sudden changes in wind stress. During wind squalls on May 21, the surface flow field became quite variable just a few hours after wind gusts blew through the area. Also, on October 1, the surface flow regime was observed to respond rapidly to shifts in wind direction. This response occurred approximately two hours following a shift in the wind. This high-frequency response to changes in the wind field offers evidence that high-frequency signals, separated numerically from the original signal during the historical analysis, must be influenced by wind forcing as well. The directional distribution (rose diagrams) for this high-frequency component lacks the directional polarity of the wind-driven (1 to 15 day) signal, suggesting that sudden changes in wind direction result in flow in the same direction.

However, comparison of the spring and fall surveys revealed some distinctions, the most obvious difference was the vertical structure of the water column and the resulting effect of this

vertical stratification on the current field. In May, especially at Area 2, the water column appeared strongly stratified, due mostly to eastward advection of the freshwater plume discharged from Mobile Bay. Circulation was modified by vertical stratification with the surface appearing to respond strongly to localized wind stress. The underlying layers had little direct response to these sudden changes. In October, when freshwater discharge from the Mobile Bay estuary is generally smaller than discharges during the spring, there was little evidence of a stratified water column. Flow at the surface had similar characteristics as flow along the bottom. There seemed to be some dependence of the near-bottom flows on overlying near-surface flow. The lack of a stratified water column in October suggests that the freshwater plume had smaller influence on circulation dynamics during this season.

Tidal conditions were also quite different during the two surveys. In May, tides were in the tropic phase, at or near the largest range of elevations (approximately 0.45 m). In October, tides were in the equatorial phase, or the minimum range of the tide, and the water elevation changes during the survey were less than 15 cm. Tides were identified in the historical analysis to be a small contributor to the overall circulation dynamic in this region; however, during the May survey in Area 2, a significant clockwise rotation was observed which dominated current direction variations. This rotation may have been tidal in origin, although the magnitude of the currents suggest other processes (possibly baroclinic). In October, when small water elevation changes were observed (as well as weak vertical stratification), no such rotational phenomena was observed. During the spring survey at Area 4, tidal currents were observed briefly along the bottom during flood tide, as denser shelf water entered the Bay during the rising tide. This suggests that tides, while generally of lesser importance than wind effects, may have localized and transient importance, such as during tropic tide phases when freshwater discharge is significant. At these times (tropic flood tides in springtime when discharge is high), tidal currents flooding into Mobile Bay may be relatively strong, with magnitudes of order 15 to 25 cm/sec, versus more prevalent tidal currents of approximately 5 cm/sec.

#### 5.1.4 Wave-Induced Bottom Currents

A propagating wave not only causes a displacement in the water surface, but also displaces water particles beneath the passing wave. This displacement induces local currents, which over the period of the passing wave take on an orbital shape (orbital velocities). In shallow water, the orbits of water particles tend to take on an elliptical shape, while in deeper water the orbits are more circular (Figure 5-30). Associated with these water particle trajectories are the particle horizontal ( $u_{orbit}$ ) and vertical ( $w_{orbit}$ ) orbital velocity components. These velocity components contribute to the initiation and transport of sediment at the seabed. Therefore, knowledge of orbital velocities at the seabed is a key parameter for determining sediment transport characteristics at potential offshore borrow areas. This section describes the method used to calculate wave-induced orbital velocities at the seabed.

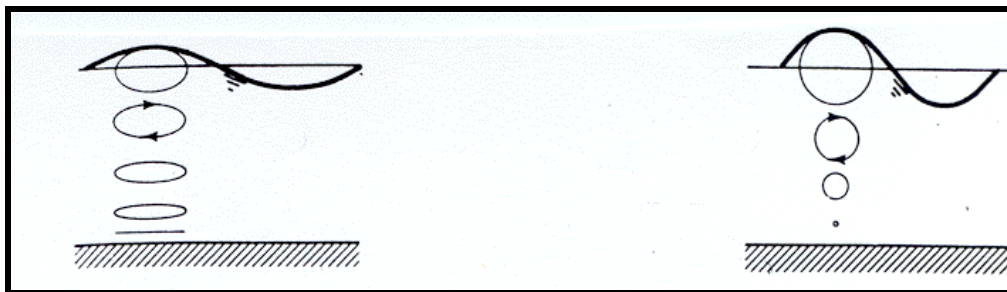


Figure 5-30. Shallow water and deep water wave orbits.

The relationship between a progressive wave and the particle motion it generates beneath the surface is well described by linear wave theory. Linear wave theory is used to derive the expression of the velocity potential ( $\phi$ ) as:

$$\phi = -\frac{Hg}{2\sigma} \frac{\cosh k(h+z)}{\cosh(kh)} \cos(kx) \sin(\sigma t) \quad (5.1)$$

where H is the wave height;  $\sigma$  is the wave frequency; k is the wave number; h is the still water depth; z is the point of interest in the water column (positive upwards from still water); x is the horizontal point of interest along the wave, g is the gravitational constant, and t is the temporal point of interest. The resulting horizontal and vertical velocities under the wave are given by:

$$u_{orbit} = \frac{-\partial\phi}{\partial x} = \frac{H}{2} \sigma \frac{\cosh k(h+z)}{\sinh(kh)} \cos(kx - \sigma t) \quad (5.2)$$

$$w_{orbit} = \frac{-\partial\phi}{\partial z} = \frac{H}{2} \sigma \frac{\sinh k(h+z)}{\sinh(kh)} \sin(kx - \sigma t) \quad (5.3)$$

Equations (5.2) and (5.3) reveal that the velocity at the bottom ( $z = -h$ ) consists only of the  $u_{orbit}$  component, while  $w_{orbit}$  is zero. Thus, at the seabed, the motion of the water particles is purely horizontal (assuming the water cannot penetrate the seabed). This allows the reduction of the velocity at the bottom to:

$$U_B = \frac{H}{2} \frac{\sigma}{\sinh(kh)} \quad (5.4)$$

The horizontal motion, as the seabed oscillates positively (under a crest) and negatively (under a trough), depends on the spatial and temporal position of the wave (Figure 5-31). Therefore, the absolute maximum bottom currents induced by the wave occur at the crest and/or the trough of the passing wave.

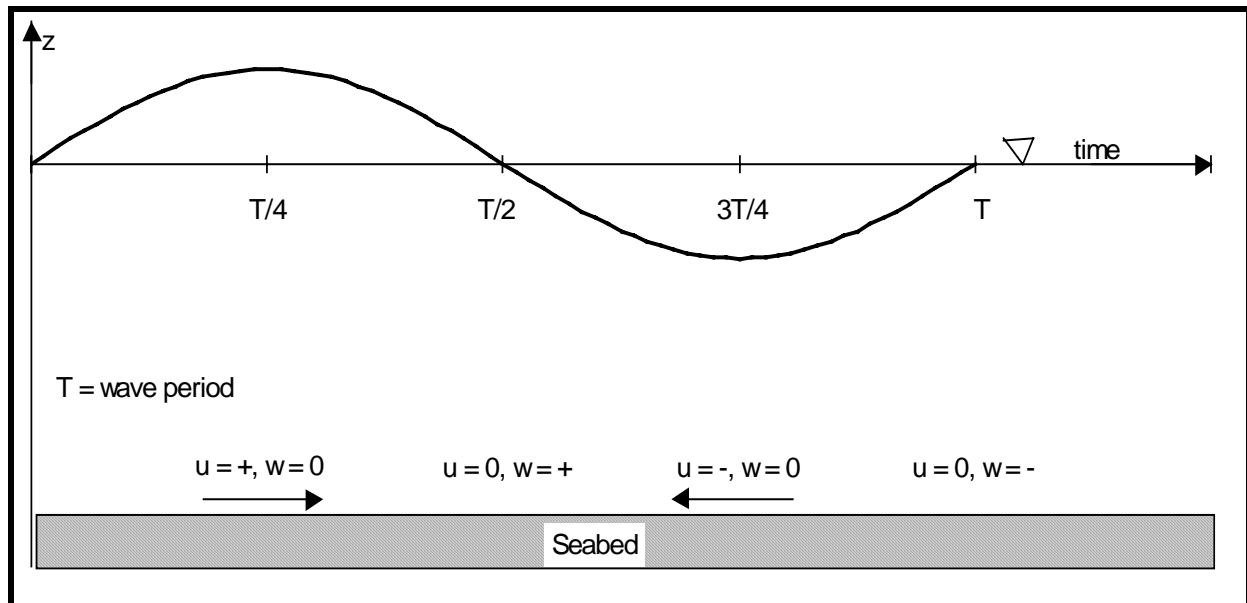


Figure 5-31. Schematic of wave-induced bottom velocities.

Applying linear wave theory, coupled with the wave model results at the dredged borrow areas, wave-generated bottom currents can be determined. Wave height, wave period, wave

direction, and water depth are extracted from the wave model at each of the designated borrow areas (and for each season/event scenario) and used to calculate the maximum bottom horizontal orbital velocity at the seafloor for each grid point within the selected domain. Wave-induced bottom velocities can then be combined with ambient currents and utilized to determine sediment initiation and potential transport at the offshore borrow sites.

The wave-induced bottom velocity is a key factor contributing to the initiation and transport of sediment. Although for purely sinusoidal motion, no net sediment transport is caused by the orbital motions, shearing velocities created at the seabed by the waves are a primary contributor to the initialization of sediment into the water column (Fredsoe and Deigaard, 1992).

### 5.1.5 Wave-Induced Longshore Currents

In addition to orbital velocities generated beneath a propagating wave, longshore currents are generated in the nearshore zone (generally landward of the breaker line) by waves approaching obliquely to the coast. This longshore current is the primary advective force generating littoral drift along the beach. Several models have been developed that take simplified information from monochromatic wave models to develop empirical or semi-empirical relationships between calculated wave information and longshore sediment transport rate. However, the use of REF/DIF S allowed development of a sediment transport model based on spectral wave parameters. As part of the output, REF/DIF S calculates radiation stress values ( $S_{xx}$ ,  $S_{xy}$ , and  $S_{yy}$ ) at each model grid cell for the entire spectra. Therefore, a single set for radiation stress values at each grid cell provides the basis of sediment transport analyses. The methodology requires a two-part procedure: wave-induced currents were developed following the work of Ebersole and Dalrymple (1980), and the cross-shore distribution of currents was utilized to generate local longshore sediment transport rates based on the work of Bodge (1986).

The governing equations of the wave-induced current model are the depth-averaged continuity equation and the depth-averaged x and y direction momentum equations. All of these equations are developed by integrating the standard form of the equations over the depth of the water column and then time averaging the results. Previous work incorporating this methodology includes Birkemeier and Dalrymple (1976), Ebersole and Dalrymple (1979), Yan (1987), Winer (1988), and Ramsey (1991).

Due to the inherent complexities of wave-induced current formation in the surf zone, certain assumptions are required in the derivation of governing equations for the wave-induced current model. A primary simplification is that the flow field may be represented in two dimensions by depth and time averaging the equations. Therefore, the vertical variation in the velocity profile is lost. The advantage of depth averaging the equations is to reduce the complicated three-dimensional problem to a more tractable two-dimensional one. However, some details of the flow field may be missed by only considering horizontal flow.

#### 5.1.5.1 Governing Equations

The form of the continuity equation used in this model assumes that the water density is constant and can be represented by:

$$\frac{\partial \bar{\eta}}{\partial t} + \frac{\partial}{\partial x}(UD) + \frac{\partial}{\partial y}(VD) = 0 \quad (5.5)$$

where

- $U$  = the x component of the mean current
- $V$  = the y component of the mean current

$\bar{\eta}$  = the mean water surface elevation

$D$  = the total water depth ( $h + \bar{\eta}$ )

$h$  = the local still water depth

The continuity equation represents the conservation of mass per unit surface area under the assumption that the water density does not change with depth or time. Although seasonal temperature variations may affect water density, the influence of density variability on wave-induced current velocities within the surf zone can be considered negligible.

The horizontal depth-averaged momentum equations were originally derived by Phillips (1969) and for the purpose of the wave-induced current model take the form:

$$\begin{aligned} \frac{\partial}{\partial t}(UD) + \frac{\partial}{\partial x}(U^2D) + \frac{\partial}{\partial y}(UVD) = -gD \frac{\partial \bar{\eta}}{\partial x} - \frac{D}{\rho} \frac{\partial \bar{\pi}}{\partial y} \\ - \frac{1}{\rho} \frac{\partial S_{xy}}{\partial y} - \frac{1}{\rho} \frac{\partial S_{xx}}{\partial x} + \frac{1}{\rho} \tau_{sx} - \frac{1}{\rho} \tau_{bx} \end{aligned} \quad (5.6)$$

and

$$\begin{aligned} \frac{\partial}{\partial t}(VD) + \frac{\partial}{\partial x}(UVD) + \frac{\partial}{\partial y}(V^2D) = -gD \frac{\partial \bar{\eta}}{\partial x} - \frac{D}{\rho} \frac{\partial \bar{\pi}}{\partial x} \\ - \frac{1}{\rho} \frac{\partial S_{xy}}{\partial x} - \frac{1}{\rho} \frac{\partial S_{yy}}{\partial y} + \frac{1}{\rho} \tau_{sy} - \frac{1}{\rho} \tau_{by} \end{aligned} \quad (5.7)$$

for the  $x$  and  $y$  direction, respectively, where

$U$  =  $x$  component of mean current

$V$  =  $y$  component of mean current

$\bar{\eta}$  = mean water surface elevation

$D$  = total water depth

$\rho$  = water density

$\bar{\pi}$  = lateral stress due to turbulent mixing

$\tau_{bx}$  =  $x$  component of bottom shear stress

$\tau_{by}$  =  $y$  component of bottom shear stress

$\tau_{sx}$  =  $x$  component of surface shear stress

$\tau_{sy}$  =  $y$  component of surface shear stress.

Many of the terms in the depth-averaged momentum equations require certain empirical guidelines to compute their values. The theory governing bottom friction and lateral mixing are not completely understood and, therefore, need empirical formulations or scaling arguments to estimate their values.

First, the bottom shear stress typically is based on some type of drag coefficient and can be expressed as:

$$\tau_{bi} = \rho f u_{ti} |u_t| \quad (5.8)$$

where  $u_t$  is composed of the mean current and the wave orbital velocity,  $u_{ti}$  is its component form (either in the  $x$  or  $y$  direction), and the overbar indicates time averaging over one wave period. The

empirical friction factor is represented by  $f$ . The magnitude of the total velocity, expressed as  $|u_t|$ , is equal to  $\sqrt{u^2 + v^2}$  where the  $u$  and  $v$  velocity components are

$$u = U + u_{xw} = U + u_w \cos \theta \quad (5.9)$$

$$v = V + u_{yw} = V + u_w \sin \theta \quad (5.10)$$

$U$  and  $V$  are the mean current speeds defined previously. The wave orbital velocities in the  $x$  and  $y$  direction are  $u_{xw}$  and  $u_{yw}$ , respectively, where  $u_w = \sqrt{u_{xw}^2 + u_{yw}^2}$ . The total velocity can then be expressed as

$$|u_t| = \sqrt{U^2 + V^2 + u_w^2} = 2Uu_w \cos \theta = 2Vu_w \sin \theta \quad (5.11)$$

The wave orbital velocity exhibits oscillatory behavior which may be expressed as

$$u_w = u_{\max} \cos \sigma t \quad (5.12)$$

where  $u_{\max}$  is the maximum orbital velocity at the bottom which can be written as

$$u_{\max} = \frac{\sigma |a|}{\sinh kh} \quad (5.13)$$

For numerical efficiency, a simplified model that includes wave orbital velocities and a strong current assumption may be formulated as

$$\tau_{bi} = pf |u'_t| U_i \quad (5.14)$$

where

$$|u'_t| = \sqrt{U^2 + V^2} + u_{\max} \quad (5.15)$$

This equation implies that there is no interaction between the wave orbital velocity and the mean current velocity. The equations for  $x$  and  $y$  components may be expressed as

$$\tau_{bx} = pf |u'_t| U \quad (5.16)$$

and

$$\tau_{by} = pf |u'_t| V \quad (5.17)$$

This simplification allows calculation of bottom shear stresses without the computational demands of full integral equations. Increasing the friction factor may offset any differences between this approach and the more complete integral equations. The selection of a proper value for the friction factor is very important in modeling currents and will be discussed in Section 5.1.5.3.

### 5.1.5.2 Lateral Mixing

Longshore currents vary with distance offshore, where strongest currents typically are found near the wave break point. If the wave-induced current model did not include cross-shore mixing, the predicted longshore velocity profile would change abruptly to zero at the breaker line as shown in Figure 5-32. To simulate the effect of turbulent mixing in the surf zone, some type of cross-shore mixing within the velocity profile is required. In addition, longshore mixing may be required if morphologic controls (e.g. shore perpendicular channels or shoals in the surf zone) or groins create rip currents. Since this application of the wave-induced current model for the Alabama coast

involves a sandy coast with no major shore protection structures, the focus of lateral mixing only involves the cross-shore direction.

Harris et al. (1963) were the first to conduct field and laboratory studies to measure the intensity of mixing within the surf-zone. Their work involved releasing known amounts of tracer in the nearshore region and calculating the strength of mixing based on measured concentration of the tracer at a later time. Qualitative results indicated that the tracer dispersed rapidly in the on/offshore direction and that, in the absence of rip currents, cross-shore mixing was confined mainly to the surf zone. In addition, they noted that mixing in the longshore direction was largely due to advection of the dye by the longshore current.

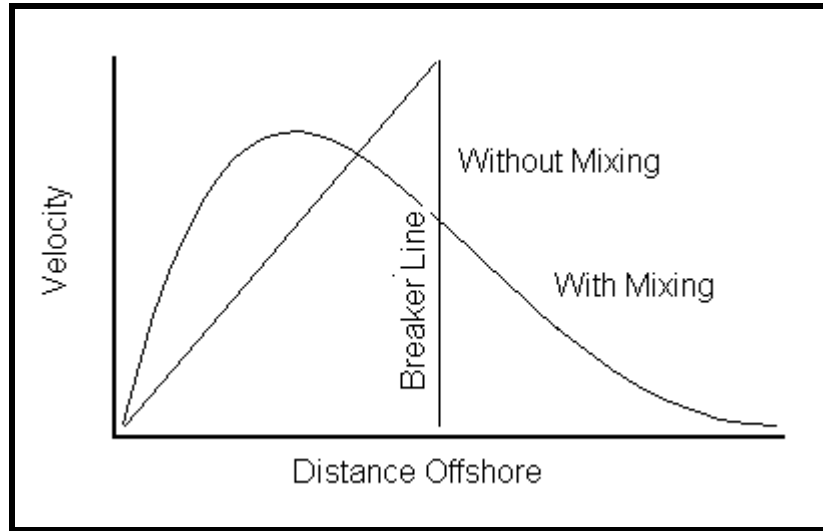


Figure 5-32. Schematic longshore velocity profiles with and without cross-shore mixing (the abrupt reduction in velocity for the without mixing case occurs at the breaker line).

Longuet-Higgins (1970) used the two depth integrated equations of motion which assumed that the turbulent fluctuation term,  $-\overline{\rho u'v'}$ , is independent of depth to derive a different equation for cross-shore mixing. Another major assumption required in the derivation was that the momentum transfer due to turbulent fluctuations may be represented as a product of the mixing length coefficients ( $\epsilon_x, \epsilon_y$ ) and derivatives of the mean current. In equation form, this can be expressed as

$$\tau_t = -\rho \left( \epsilon_y \frac{\partial U}{\partial y} + \epsilon_x \frac{\partial V}{\partial x} \right) \quad (5.18)$$

Longuet-Higgins made additional assumptions regarding horizontal mixing in the surf-zone based on the horizontal eddy viscosity coefficient,  $\epsilon_x$ . Since the turbulent eddies responsible for lateral mixing must be smaller than the distance from an arbitrary point to the shoreline, it follows that  $\epsilon_x$  must tend to zero as the shoreline is approached. However, the decrease in  $\epsilon_x$  between the breakerline and the shoreline is not necessarily linear. The approach adopted by Longuet-Higgins was to assume that  $\epsilon_x$  is proportional to the offshore distance,  $x$ , multiplied by a typical shallow water wave celerity,  $\sqrt{gh}$ . When the bottom slope is uniform, a simple equation governs the longshore current profile. Although beach profiles in nature are not uniform, the simplified approach provides a reasonable method for determining an appropriate mixing coefficient. Expressing the cross-shore mixing coefficient as

$$\varepsilon_x = Nx\sqrt{gh} \quad (5.19)$$

and using a number of scaling arguments for the variables, the probable limits for the constant  $N$  were found to be  $0 < N < 0.016$ .

This equation or some slight modification has become the standard formula for calculating mixing in longshore current models. Seaward of the plunge line,  $\varepsilon_x$  is kept at the maximum value. Since there is little turbulence seaward of the plunge line, the high value of the mixing coefficient ensures that there is a reasonable amount of lateral mixing in the cross-shore direction. For the spectral wave model, much of the cross-shore mixing is represented by gradual breaking of waves, where longer wave components break further from shore. This representation of a wave breaking envelope tends to distribute longshore currents in a manner similar to the with mixing case shown in Figure 5-32. Therefore, significant redistribution of longshore currents using the above methodology was not necessary, and values for the cross-shore mixing coefficient were minimized.

### 5.1.5.3 Model Verification

Because the primary purpose for calculating the cross-shore distribution of the longshore current was to calculate the littoral drift rate, model validation to field experiments was required to gauge computational accuracy. The model was verified using the field data sets of Kraus and Sasaki (1979) and Thornton and Guza (1989). These data represented a broad range of field conditions, with wave periods ranging from 4.1 to 12.8 sec. Kraus and Larson (1991) used both data sets to verify the one-dimensional longshore current model, NMLONG. Unfortunately, these field test cases provide only cross-shore variation in the longshore current. No two-dimensional field data sets were found for model verification. Several laboratory experiments have been performed to evaluate two-dimensional wave-induced current fields, including currents near groins (Winer, 1988) and shore parallel breakwaters (Ramsey, 1991).

For the field cases modeled, radiation stresses were calculated based on the results of a monochromatic wave refraction model designed to estimate wave heights and directions within the nearshore region. Since this wave model over-simplified nearshore wave conditions, limited wave-induced current model verification was anticipated. However, results of the current model compared favorably with both data sets. In addition, the modeled longshore current distribution was similar to those predicted by the NMLONG model.

Kraus and Sasaki (1979) measured the longshore current profile along seven transects on a sandy beach facing the Sea of Japan. Current measurements were made simultaneously along each transect by divers positioned at 5 m intervals. The current was measured by timing the migration of neutrally buoyant floats located at about mid-depth. An average current velocity was computed based on three successive measurements along each transect. Field observations during the field experiment indicated the waves arrived as clean swell, with a significant wave height of 1.0 m, a period of 4.1 sec, and a angle at breaking of 9 degrees relative to the shoreline.

A comparison of field experiment results and wave-induced current model output used in this study is shown in Figure 5-33. Due to the relatively steep waves, two significant peaks of longshore current velocity were computed by the model: one peak just landward of the observed breaker line (about 40 m offshore) and one peak adjacent to the shoreline. This increase in current strength near the swash zone is typical of steep wave conditions (Bodge, 1986). The results from two different model runs are shown, with the friction factor ranging between 0.0025 and 0.0030. Both the magnitude and offshore position of the maximum longshore current compare well with field data. In addition, the modeled prediction of current strengths seaward of the breaker line closely matched the data. However, the modeled current magnitude was under-predicted relative to field measurements.

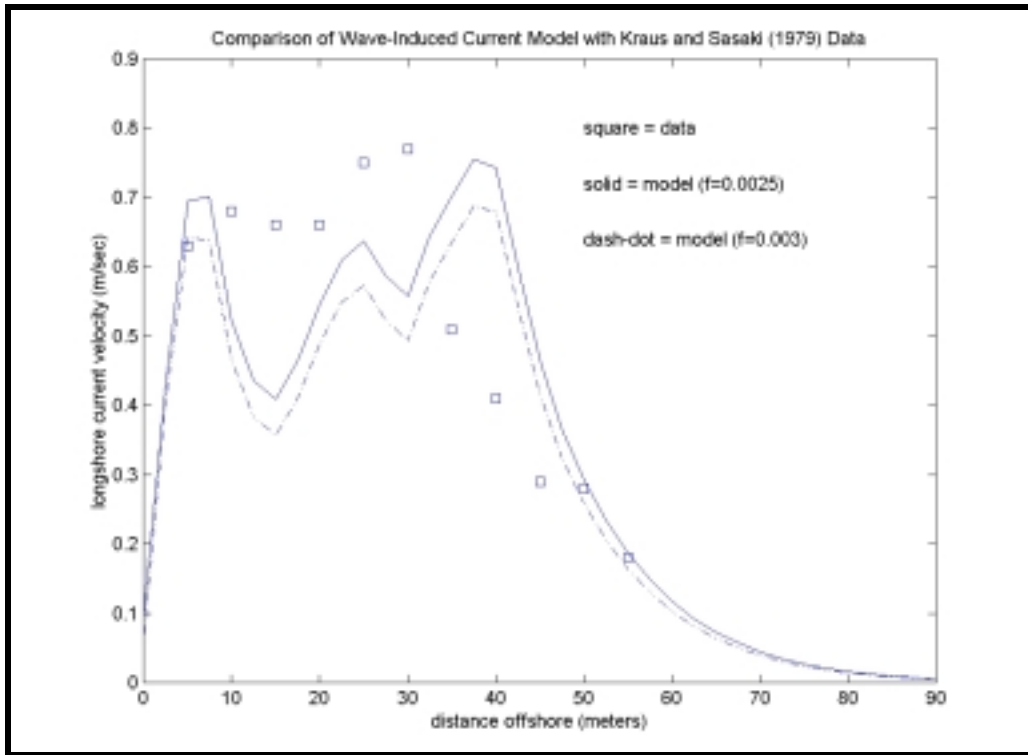


Figure 5-33. Comparison of model and observed longshore current velocities from field measurements taken by Kraus and Sasaki (1979).

To further verify the applicability of the wave-induced current model, wave and longshore current data from Thornton and Guza (1989) were utilized. The data were collected at Leadbetter Beach, California at a location where nearshore contours were relatively straight and parallel. Although four cases were presented in the initial work, only the February 5<sup>th</sup> Case was used for comparison with the wave model. Wave conditions for this case were a root-mean-square wave height of 0.45 m, a wave period of 12.8 sec, and an angle at breaking of 8.4 degrees relative to the shoreline.

A comparison of field data and wave-induced current model output is shown in Figure 5-34. The results from three different model runs are shown, with the friction factor ranging between values of 0.002 and 0.004. This range of friction values is similar to those employed by Kraus and Larson (1991). The magnitude of the maximum longshore current compares well with field data; however, the model predicted the location of the peak current much closer to the shoreline than the data indicated. In this case, use of a monochromatic wave model to generate radiation stresses for the wave-induced current model effectively eliminated cross-shore mixing associated with various spectral components.

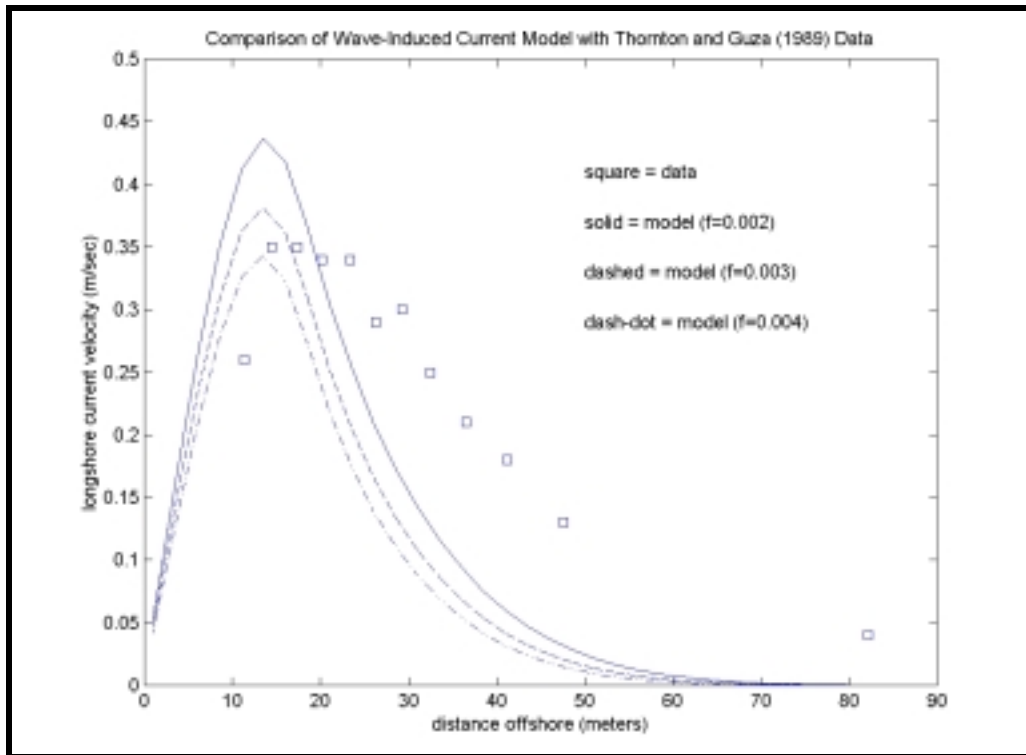


Figure 5-34. Comparison of modeled to observed longshore current velocities from field measurements taken by Thornton and Guza (1989).

#### 5.1.5.4 Wave-Induced Currents Along the Alabama Coast

Model verification provided confidence that the wave-induced current model could be used to effectively evaluate longshore currents as the basis for littoral drift prediction. A sensitivity analysis was performed to determine appropriate values for the friction coefficient. Based on the verification runs, as well as previous work by Ramsey (1991), the appropriate value of  $f$  was determined to be 0.003. This value was utilized for all model runs associated with the Alabama study.

Because the results of the wave-induced current model are merely an intermediary step in the calculation of longshore sediment transport, only sample results from the current model are presented in this report. The wave-induced current model was run for the Dauphin Island and Morgan Peninsula wave modeling grids, for each spectral wave condition (total of five), and for both existing conditions and post-dredging scenarios. This required a total of 20 model runs. The results of one run (the existing conditions at Morgan Peninsula for the spring wave conditions) are described in more detail below. This example provides an overview of typical wave-induced current predictions associated with the modeling effort.

First, radiation stress in the longshore direction across a shore perpendicular transect is denoted as  $S_{xy}$ . Although the combined effects of the other two radiation stress components ( $S_{xy}$ ,  $S_{yy}$ ) are important to the two-dimensional current regime,  $S_{xy}$  provides the primary driving force for longshore currents. As waves reach the break point, it is the variation in  $S_{xy}$  across the surf zone that induces longshore current motion. Therefore, Figure 5-35 illustrates the longshore and cross-shore distribution of  $S_{xy}$ , indicating regions of longshore energy focus. As expected, areas of higher  $S_{xy}$  values have higher maximum current velocities.

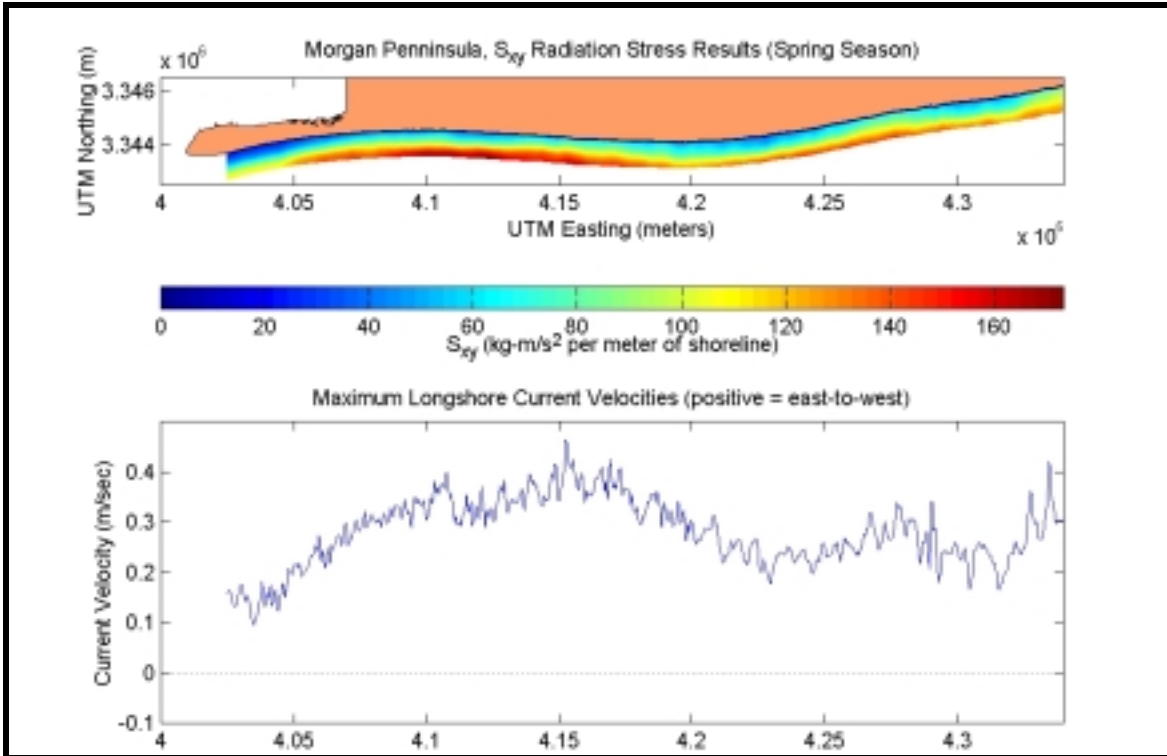


Figure 5-35.  $S_{xy}$  radiation stress and maximum longshore current velocities predicted by the wave-induced current model for the Morgan Peninsula during the spring season.

Cross-shore variability of the longshore current also can impact the volume of longshore sediment transport. Areas with relatively wide surf zones may exhibit low maximum longshore current velocities; however, currents exist over a larger area on these beaches and if the currents are strong enough to mobilize sediment, longshore transport rates can be higher than beaches with higher maximum currents. Along much of the Morgan Peninsula, beach slope is consistent and steep; therefore, the maximum current strengths shown on Figure 5-35 directly reflect the transport trends along this stretch of beach. Figure 5-36 provides several longshore current profiles indicating the variability of currents along the Morgan Peninsula shoreline. Although there is some variability in profile shape along the Morgan Peninsula shoreline, longshore current velocities become negligible within 60 m of the shoreline at all locations. The surf zone width appears to be slightly wider near the eastern end of the project area, likely due to larger wave heights in this region. For the Spring season, maximum longshore current speeds vary by more than 50%, ranging from approximately 0.1 to 0.4 meters per second. Although not a direct link, the longshore variation in maximum current is an indication of longshore sediment transport trends. Typically, areas with greater wave-induced current velocities will have a higher longshore sediment transport potential. A detailed analysis of longshore sediment transport potential is provided in Section 5.2.2.

Because the wave-induced current analysis was an intermediary step between wave transformation modeling and longshore sediment transport modeling, detailed results for each seasonal or extremal cases have not been provided. As described above, variations in longshore currents were similar to trends depicted in nearshore sediment transport modeling described in Section 5.2.2.

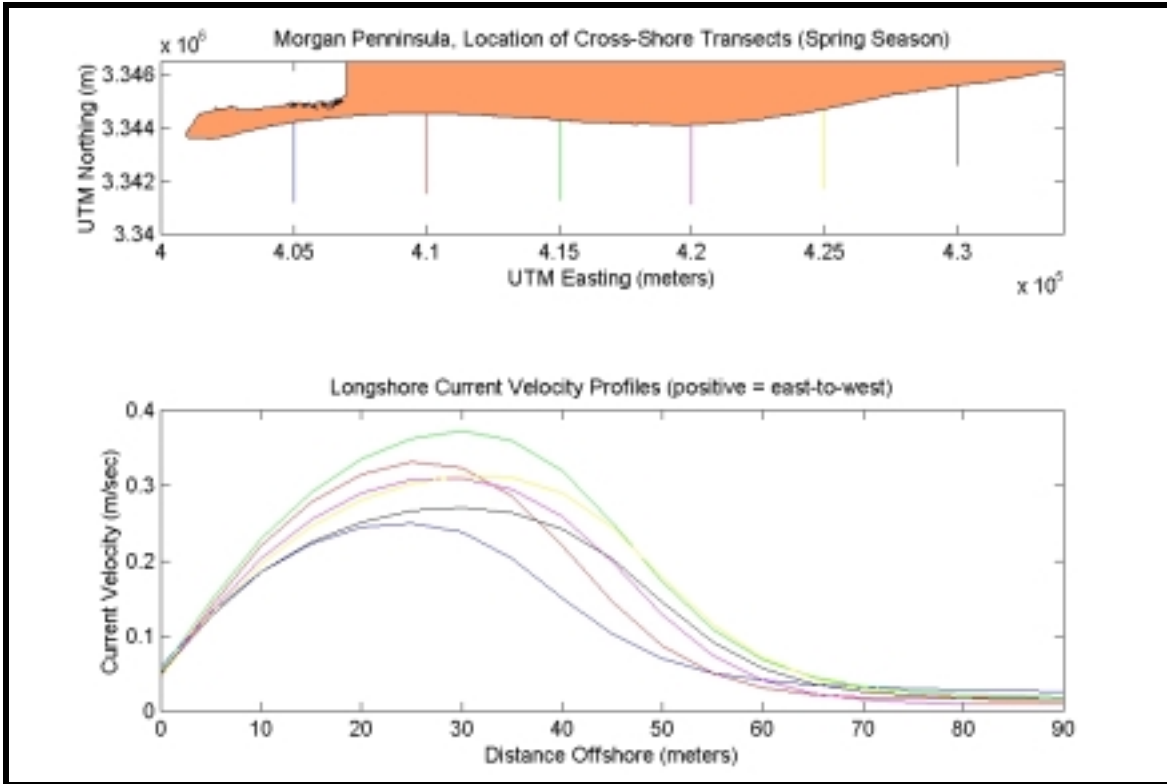


Figure 5-36. Longshore current profiles along selected transects at Morgan Peninsula (colored transects in the top sub-plot correspond to like colored profiles in the bottom sub-plot).

## 5.2 SEDIMENT TRANSPORT MODELING

### 5.2.1 Sediment Transport at Borrow Sites

Potential sand mining activities at offshore borrow areas may lead to changes in sediment transport mechanics occurring at or near proposed offshore dredging locations. The purpose of this section is to identify the approximate quantity and direction of sediment transport at potential borrow sites and estimate the duration for infilling of borrow areas. Spectral wave model results, along with historical and measured current observations, were employed for the analysis of sand transport at borrow sites. This section examines the interaction of wave-induced bottom orbital velocities and ambient currents, the initiation of sediment motion at potential borrow areas, and the relative magnitude and direction of sediment transport.

#### 5.2.1.1 Initiation of Sediment Motion Under Combined Wave and Current Action

Assuming purely oscillatory wave motion (linear theory) without currents results in no net sediment transport at offshore borrow areas. Even if sediment is lifted from a non-sloping seafloor into the water column, the amount of sediment transported forward (in the direction of wave propagation) during half of the cycle will equal the amount being transported backwards during the other half of the cycle under linear waves. In order to cause a net difference in sediment transport, additional physical phenomena are required. These include:

- bottom slopes on the seafloor
- tidal and/or wind-driven currents
- wave asymmetry (non-linearity)
- wave-induced mass transport

In areas outside the surfzone, it is critical to account for wave and current interactions inside the bottom boundary layer when evaluating potential sediment transport. Introducing coastal currents to wave motions adds difficulty in estimating shear, dissipation, and sediment transport dynamics. A number of approaches have been developed by Lundgren (1972), Bakker (1974), Smith (1977), and Bakker and van Doorn (1978) to attempt to solve this problem.

Only Madsen and Grant (1976, 1977), Grant and Madsen (1978, 1979) and Tanaka and Shuto (1981), considered current and wave interaction situations, where the current and wave have an arbitrary angle with each other. Tanaka and Shuto used a one-layer eddy viscosity approach, which most likely over simplified the problem. Madsen and Grant (1976, 1977), and Grant and Madsen (1978, 1979) derived sediment transport relationships for predicting net sediment transport rates in the presence of second order effects such as bottom slope, wave asymmetry, coastal currents, and mass transport currents. They concluded that only cases involving small amplitude wave theory and a steady current are understood to a level that it is reasonable to evaluate resulting sediment transport rates with any degree of confidence. Fortunately, this is the situation for offshore Alabama, including the potential offshore borrow areas.

Before sediment can be transported, it must be moved from the seabed by combined wave and current motion. When sufficient stress is applied to the bed, sediment may begin to move. Typically, a mild steady flow over a bed of cohesionless grains will not result in sediment transport (Fredsoe and Deigaard, 1992). However, when subjected to a large enough flow, the driving forces impacting sediment grains exceed the stabilizing forces, and sediment will begin to move.

Through dimensional analysis, Shields (1936) derived an expression that identifies the point where bed stress equals bed resistance. The threshold of particle motion is based on a ratio between the driving forces (drag and lifting forces) and stabilizing forces (frictional forces) as seen in Figure 5-37. The Shields parameter ( $\Psi$ ) results from equating the driving and stabilizing forces. For a flat bed:

$$\psi = \frac{\tau_b}{(s-1)\rho g d_{50}} \quad (5.20)$$

where

- $\tau_b$  = maximum bottom shear stress
- $\rho$  = density of the sea water
- $s$  = relative density (equals 2.65 for natural sediment)
- $g$  = acceleration due to gravity
- $d_{50}$  = grain diameter which corresponds to 50% by weight finer

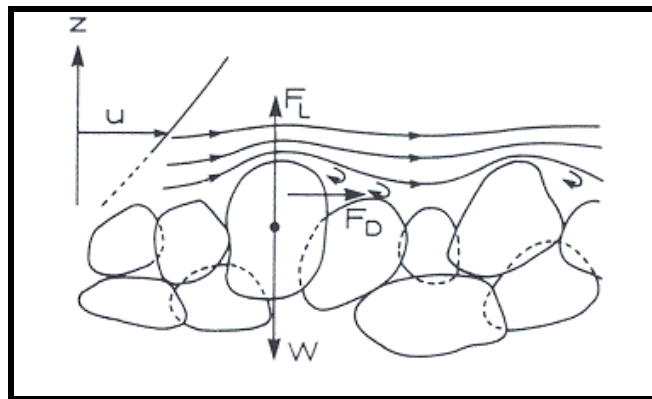


Figure 5-37. Forces acting on grains resting on the seabed (Fredsoe and Deigaard, 1992).  $F_L$  = lifting force,  $F_D$  = drag force, and  $W$  = grain weight.

The shear stress at the bed,  $\tau_b$ , is given by Madsen and Grant (1976) and Raudkivi (1990) as:

$$\tau_b = \frac{1}{2} \rho f_{cw} |u_{cw}| u_{cw} \quad (5.21)$$

where  $f_{cw}$  is the combined wave/current friction factor and  $u_{cw}$  is the combined wave/current reference velocity.

In this study,  $u_{cw}$  includes the effects of waves and a steady current. A combination of the two creates a more realistic representation of maximum bottom velocity and bed shear stress. Proper combination of wave-induced and ambient currents requires an accurate representation of flow dynamics located directly at the seabed. In most cases, it is difficult to measure ambient current magnitude and direction directly at the seafloor. In the present study, historical current observations were measured a certain distance from the bottom. For example, current data used to derive the current field at Sand Resource Area 4 were sampled at a distance of 1.2 m above the sea floor.

The combined wave/current reference velocity,  $u_{cw}$ , is a function of the wave-induced bottom orbital velocity (Equation 5.4) and the apparent current velocity at the bottom,  $U_a$ , as given by:

$$u_{cw} = (U_b \cos \omega t + U_a \cos \phi_a, U_a \sin \phi_a) \quad (5.22)$$

where,  $U_b$  = wave-induced bottom velocity  
 $U_a$  = apparent ambient current bottom velocity  
 $\phi_a$  = the angle between the apparent current and wave-induced current (Figure 5-38)

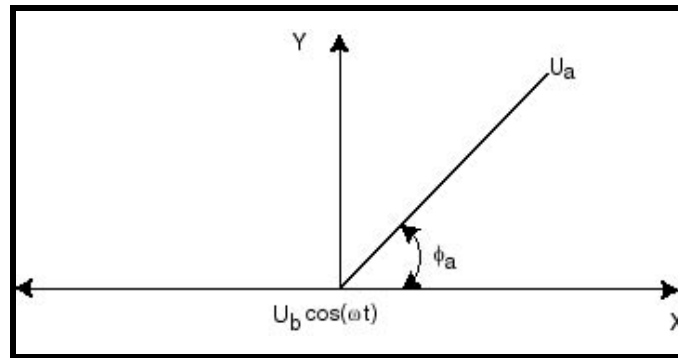


Figure 5-38. Illustration indicating the angle between the apparent bottom current and wave-induced bottom current (Grant and Madsen, 1979).

Because current observations were not measured at the bottom, they must be translated to the seafloor based on the application of a current profile through the bottom boundary layer. In order to determine the appropriate vertical current profile, the thickness of the bottom wave/current boundary layer ( $\delta_w$ ) must be determined and compared to the observed current location within the water column. A significant amount of work has been completed relative to the wave/current bottom boundary layer (Kajiura, 1964; Kajiura, 1968; Kamphuis, 1975; Knight, 1978; Bakker and van Doorn, 1978; Grant and Madsen, 1979; Trowbridge and Madsen, 1984). In addition, Trowbridge and Agrawal (1995) collected field data within the bottom boundary layer. Jonsson (1980) presents an equation for the thickness of the wave boundary layer in oscillatory rough turbulent flow, which is most common in nature, as:

$$\delta_w = \frac{2\kappa U_{*m}}{\omega} \quad (5.23)$$

$\kappa$  = Von Karman's constant (0.4)

$U_{*m}$  = the maximum current velocity at the seabed  
 $\omega = 2\pi/T$

If observed currents were measured outside of the bottom boundary layer ( $z > \delta_w$ ), which is usually the case in field measurements, a logarithmic current profile is assumed, as:

$$U_c = \frac{U_{*c}}{\kappa} \ln\left(\frac{30z}{k_{bc}}\right) \quad (5.24)$$

where  $U_{*c}$  = the critical bottom velocity  
 $z$  = height above the bed  
 $U_c$  = the magnitude of the measured current  
 $k_{bc}$  = the apparent bed roughness

The apparent bed roughness presented in Equation 5.24 is defined as:

$$k_{bc} = k_b \left(60\kappa \frac{U_{*m}}{k_b \omega}\right)^\beta \quad (5.25)$$

where  $k_b$  is the roughness coefficient, which is assumed to be equivalent to  $d_{50}$  of the local sediment, and  $\beta = 1 - (U_{*c}/U_{*m})$ .

In the present study, the observed current was measured outside of the wave boundary layer at all of the measurement stations; therefore, Equation 5.24 was applied to translate the observed current data to the seabed for each of the borrow site regions (Areas 1, 2, 3, and 4).

Having defined the ambient current velocity at the bottom, the bottom shear stress resulting from combined wave/current interaction can be determined. Maximum bottom shear stress,  $\tau_{b,max}$ , due to the combined current and wave action can be determined from

$$\tau_{b,max} = \rho U_{*m}^2 = \frac{1}{2} \rho f_{cw} U_b^2 (1 + 2\varepsilon \cos \phi_a) \quad (5.26)$$

where  $\varepsilon = (U_a/U_b)$ .

The combined wave/current friction factor,  $f_{cw}$ , is provided by Madsen and Grant (1976) as:

$$f_{cw} = \frac{U_c f_c + U_b f_w}{U_c + U_b} \quad (5.27)$$

where  $f_c$  and  $f_w$  are friction factors corresponding to ambient current flow and wave-induced flow, respectively. The wave friction factor was presented by Jonsson (1966a) and is a function of the wave Reynolds number and  $(U_b/k_b\omega)$ .

$$f_w = f_w \left( \frac{U_b^2}{\nu \omega}, \frac{U_b}{k_b \omega} \right) \quad (5.28)$$

The wave friction factor can be determined using Jonsson's wave friction factor diagram (Jonsson, 1966a). In a similar manner, the current friction factor can be determined from the standard Darcy-Weisbach approach:

$$f_c = \frac{1}{4} f \left( \frac{U_m 4h}{\nu}, \frac{d_{50}}{4h} \right) \quad (5.29)$$

The maximum bottom shear stress under the combined wave/current interaction is then used to calculate the Shields parameter ( $\Psi_{\max}$ ) from Equation 5.20, recast as:

$$\Psi_{\max} = \frac{U_{*m}^2}{g(s-1)d_{50}} \quad (5.30)$$

Once the Shields parameter ( $\Psi_{\max}$ ) has been calculated at points of interest, the resulting values can be compared to a critical Shields parameter ( $\Psi_{\text{crit}}$ ) to determine if sediment initiation occurs at each point of interest. The critical Shields parameter may be determined using a modified Shields diagram developed for sediment transport in the coastal environment (Madsen and Grant, 1976, 1977).

In addition, modifications have been made to the critical Shields parameter to account for sloped bed forms, such as the sideslopes of the dredged area. If sand grains are placed on a bed with a transverse slope or longitudinal slope, it is either easier or more difficult to initiate movement based on the direction of current flow (Figure 5-39). In the transverse case, the flow direction is perpendicular to the slope, while in the longitudinal case, the flow travels parallel to the slope. Therefore, sediment is initiated more easily on a downward slope than an upward slope and the critical Shields parameter decreases or increases according to bathymetry. Equations (5.31) and (5.32) take into account the transversely and longitudinally sloped bed forms, respectively, and provide an adjusted  $\Psi_{\text{crit}}$ :

$$\Psi_{\text{crit}} = \Psi_{\text{critical for a flat bed}} \cos \beta \sqrt{1 - \frac{\tan^2 \beta}{\tan^2 \phi_s}} \quad (5.31)$$

$$\Psi_{\text{crit}} = \Psi_{\text{critical for a flat bed}} \cos \gamma \left[ 1 - \frac{\tan \gamma}{\tan \phi_s} \right] \quad (5.32)$$

where  $\beta$  = transverse bed slope,  $\gamma$  = longitudinal bed slope, and  $\phi_s$  = angle of repose.

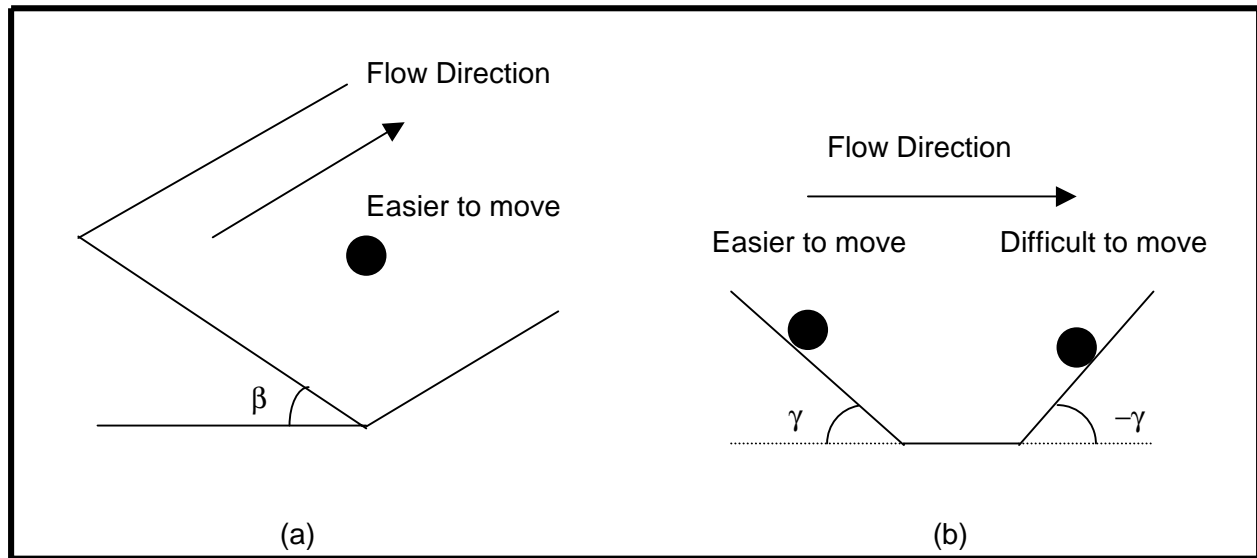


Figure 5-39. Illustration of a particle on a (a) transverse slope, and on a (b) longitudinal slope.

Finally, by comparing maximum and critical Shields parameters, sediment initiation can be determined at locations within and surrounding the offshore borrow areas. If  $\Psi_{\max}$  exceeds  $\Psi_{\text{crit}}$ , then sediment will move. At each of the potential borrow locations, a subgrid encompassing the dredged region and surrounding area, was extracted from the reference modeling domain (Figures 5-40 and 5-41). At each point within the selected subgrid, the Shields parameter was determined and compared to the critical Shields parameter at that same grid point using wave modeling results for post-dredging scenario runs. In this manner, sediment initiation was determined at each point within the domain. The results of the sediment initiation analysis for each of the potential borrow sites (within Sand Resource Areas 1, 2, 3, and 4) are documented below.

#### **5.2.1.2 Relative Magnitude and Direction of Transport**

Sediment initiation provides valuable insight into sediment movement, but does not provide information as to how much sediment moves and in what direction is it traveling. Therefore, sediment transport rates and transport directions need to be calculated in and around the offshore borrow areas to assess overall sediment transport potential as well as provide insight into:

- approximate rates of sediment transport,
- estimates on borrow site infilling rates,
- seasonal fluctuations in sediment transport patterns, and
- impact of storm events on borrow site infilling.

This section presents the results of offshore sediment transport analyses at the potential borrow site locations following a large dredging episode. Sediment initiation and potential sediment transport rates were estimated in and around the dredged area.

Offshore sediment transport rates are based on analytical expressions developed by Madsen and Grant (1976). They involve:

1. determining the time-varying values of sediment transport in the northing (y) and easting (x) directions,
2. period-averaging these sediment transport component results, and
3. calculating the net sediment transport magnitude and direction.

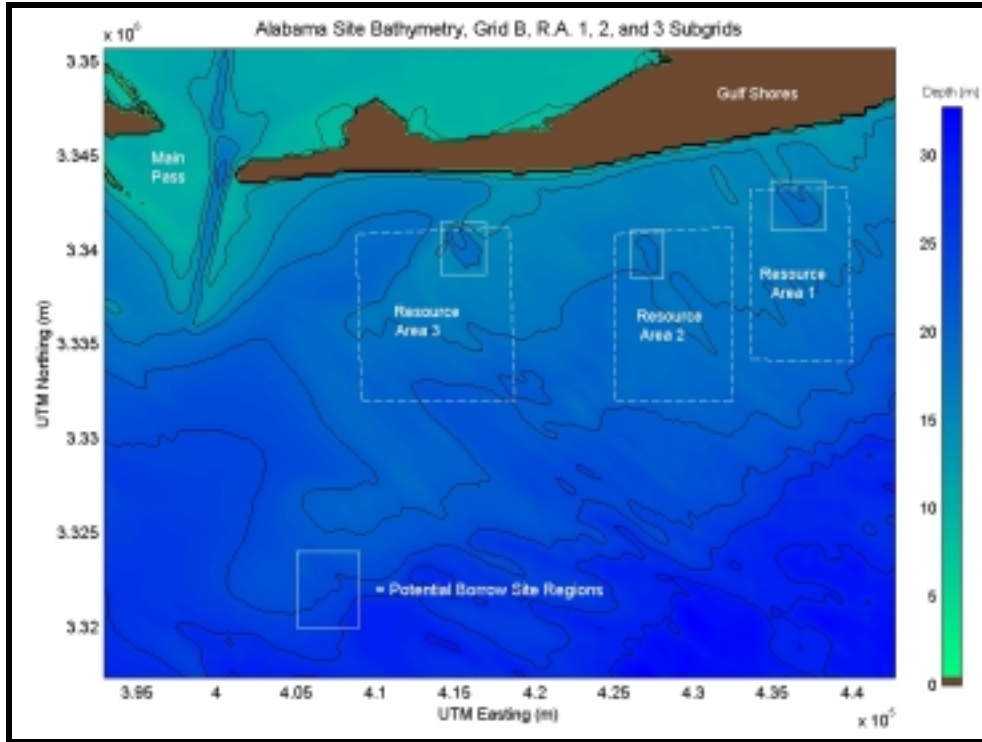


Figure 5-40. Location of the offshore subgrid regions within Sand Resource Areas 1, 2, and 3. These subgrids were used to determine potential sediment transport at the borrow areas following numerical dredging.

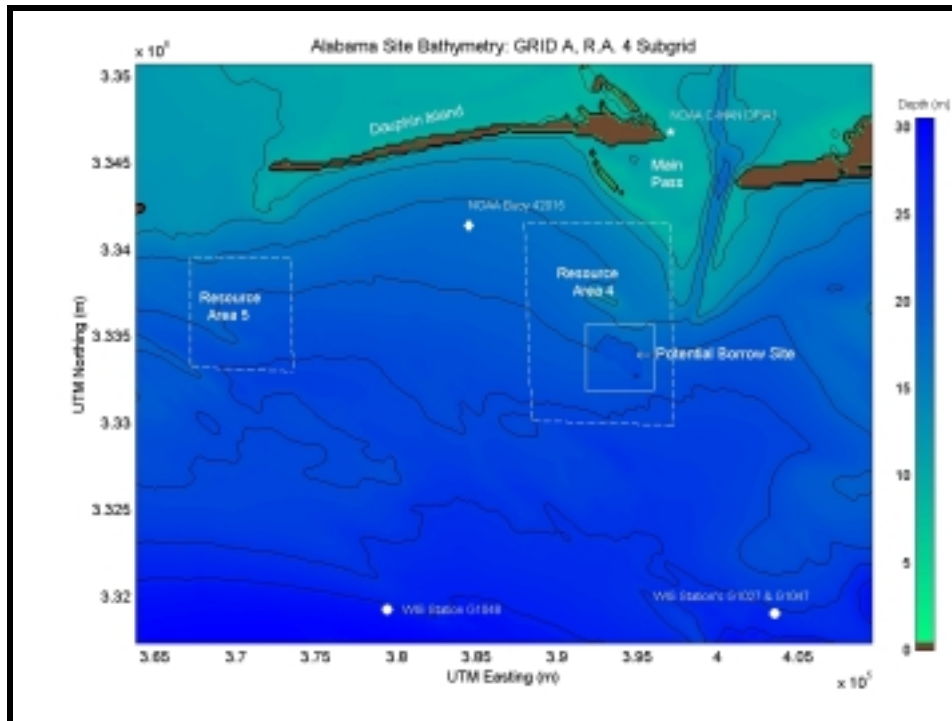


Figure 5-41. Location of the offshore subgrid region within Sand Resource Area 4. This subgrid was used to determine potential sediment transport at the borrow area following numerical dredging.

Determination of the instantaneous sediment transport rate is given by the following equations:

$$q(t)_{\text{sediment}, y} = 40 \omega_{\text{fall}} d_{50} \left[ \frac{1/2 f_{\text{cw}} (u(t)^2 + v(t)^2)}{(s-1) g d_{50}} \right]^3 * \frac{v(t)}{\sqrt{u(t)^2 + v(t)^2}} \quad (5.33)$$

$$q(t)_{\text{sediment}, x} = 40 \omega_{\text{fall}} d_{50} \left[ \frac{1/2 f_{\text{cw}} (u(t)^2 + v(t)^2)}{(s-1) g d_{50}} \right]^3 * \frac{u(t)}{\sqrt{u(t)^2 + v(t)^2}} \quad (5.34)$$

where  $q(t)_{\text{sediment}, y}$  = sediment transport rate in northing direction  
 $q(t)_{\text{sediment}, x}$  = sediment transport rate in easting direction  
 $v(t)$  = time-dependent wave orbital bottom velocity and steady near bottom current in the northing direction  
 $u(t)$  = time-dependent wave orbital bottom velocity and steady near bottom current in the easting direction  
 $\omega_{\text{fall}}$  = sediment fall velocity

The above equations require information about sediment sizes at each of the four sand resource areas. Table 5-3 summarizes various sediment sizes that were needed to calculate sediment transport rates, as well as initiation. The values were obtained from grain size analyses performed on samples taken at each of the four sand resource areas.

Table 5-3. Sediment sizes at Sand Resource Areas 1 through 4.			
Resource Area	$d_{10}$ (mm)	$d_{50}$ (mm)	$d_{90}$ (mm)
1	0.18	0.25	0.93
2	0.14	0.22	0.44
3	0.14	0.27	0.44
4	0.20	0.34	0.50

To determine the net sediment transport rate per wave cycle, sediment transport rates were period-averaged. The net period-averaged sediment transport rates in the northing ( $\bar{q}(x, y)$ ) and easting ( $\bar{q}(x, y)$ ) directions, respectively, are:

$$\bar{q}(x, y)_y = \frac{1}{T} \int_0^T q(t)_y dt \quad (5.35)$$

$$\bar{q}(x, y)_x = \frac{1}{T} \int_0^T q(t)_x dt \quad (5.36)$$

The northing and easting components can be combined by determining the sediment transport magnitude ( $\bar{q}(x, y)$ ) defined as:

$$\bar{q}(x, y) = \sqrt{[\bar{q}(x, y)_y]^2 + [\bar{q}(x, y)_x]^2} \quad (5.37)$$

In addition to magnitude, the net direction can be calculated based on the sediment transport components. Results of the analyses were used to visualize the rate of sediment movement and the direction of transport.

Four potential sand borrow sites were investigated to determine: 1) sediment transport rate estimates into and around the dredged areas, 2) indications of sediment supply areas, and 3) approximate infilling rates. Seasonal and extreme (50-yr storm) results are presented and discussed. In addition, a yearly average is interpolated from seasonal results, including the effects of a storm.

The results for Sand Resource Area 4 are discussed and presented within this section. The results for Sand Resource Areas 1, 2, and 3 are summarized in subsequent tables and Appendix C1. Figures 5-42 through 5-47 illustrate seasonal (winter, spring, summer, and fall) and extreme (50-yr storm) hydrodynamic and sediment transport results at the sand borrow site in Area 4. The figures include maximum wave-induced bottom velocities (upper left panel), steady near bottom currents (upper right panel), sediment initiation potential (lower left panel), and period-averaged sediment transport (lower right panel). For the upper left panel, solid lines indicate the depth contour of the numerically-dredged bathymetry, and the overlaid color map illustrates the magnitude of wave-induced bottom velocity (m/s). Red areas indicate regions of higher bottom velocity, while blue areas indicate lower velocities. Vectors indicate the direction and magnitude (length) of wave-induced bottom velocity at each grid point. The x-axis (easting) and the y-axis (northing) indicate the exact location on the subgrid within the sand resource area.

The upper right panel presents near bottom steady current results (m/s). Again, the bathymetry, including the dredged area, is illustrated with solid black lines while the color map shows the magnitude associated with the current. The vectors give the direction of the current in and around the borrow site.

Potential sediment initiation is presented in the lower left-hand panel. Bathymetry is shown as solid lines, while the color map illustrates the potential for sediment initiation. Red areas indicate regions of certain initiation while blue areas illustrate areas of minimal or no initiation.

Net sediment transport ( $\text{m}^3/\text{day}/\text{cell width}$ ) and direction are shown in the lower right panel. This figure shows the direction of period-averaged transport (represented by vectors), and the color map provides a visual scale to determine the rate of transport per cell width (cell width = 200 m). Red areas indicate relatively high zones of transport, while blue areas indicate zones of no or minimal transport.

The winter season (Figures 5-42 and 5-43) is represented by two scenarios: a near bottom ambient current heading to the southeast, and a near bottom current heading to the northwest. During the winter season, historical current observations indicate that a near bottom current flows to the southeast 38% of the time and to the northwest 34% of the time (near Sand Resource Area 4). When coupled with the wave-induced bottom currents, it yields two different sediment transport patterns during the winter season. Ambient currents from the southeast initiate sediment north and northeast of Sand Resource Area 4 (Figure 5-42) in the shallower depths near the Mobile Outer Mound disposal site. The combined ambient and wave-induced current magnitude is high enough to move sediment in these areas, and the resulting sediment transport is in a southeasterly direction traversing across the dredged area. The pattern differs when compared to the northwest winter.

Initiation occurs in similar areas, but transport is in the northwest direction and occurs throughout the northern section of the subgrid. Also, the sediment transport rates for the northwest winter scenario are slightly less than the southeast winter case.

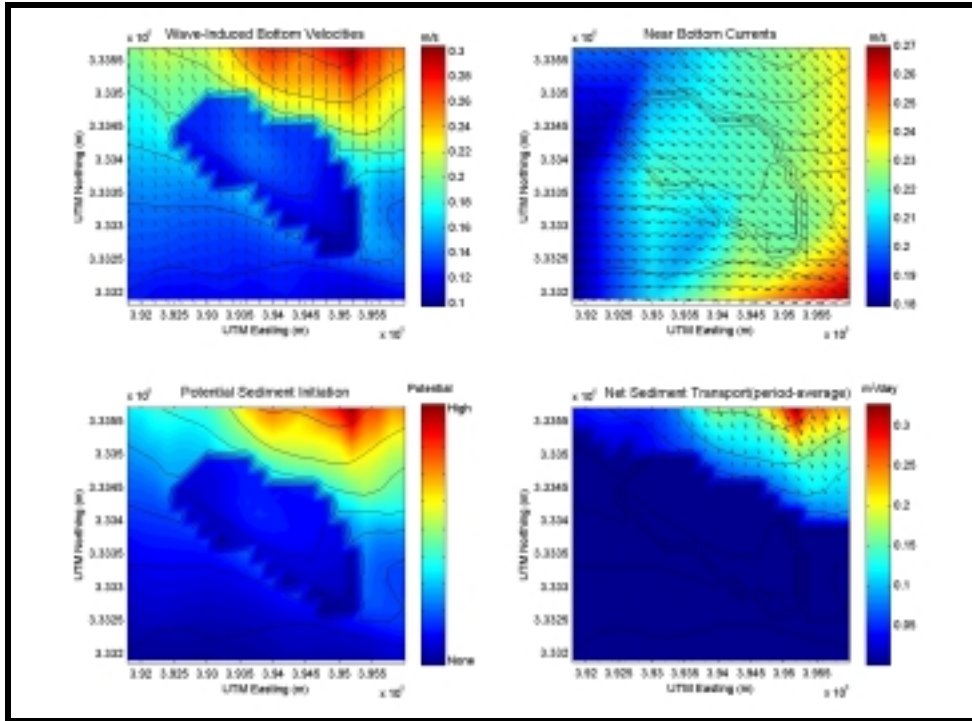


Figure 5-42. Southeast winter hydrodynamic and sediment transport results at Sand Resource Area 4. The solid black lines represent depth contours, and sediment transport results are based on 200-m cell widths.

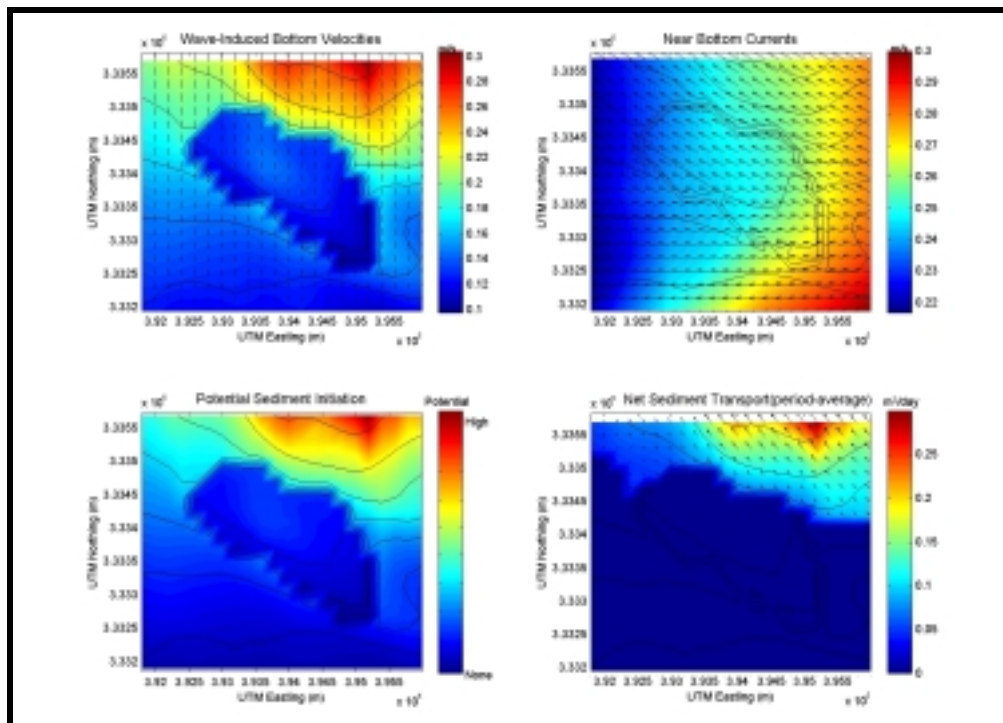


Figure 5-43. Northwest winter hydrodynamic and sediment transport results at Sand Resource Area 4. The solid black lines represent depth contours, and sediment transport results are based on 200-m cell widths.

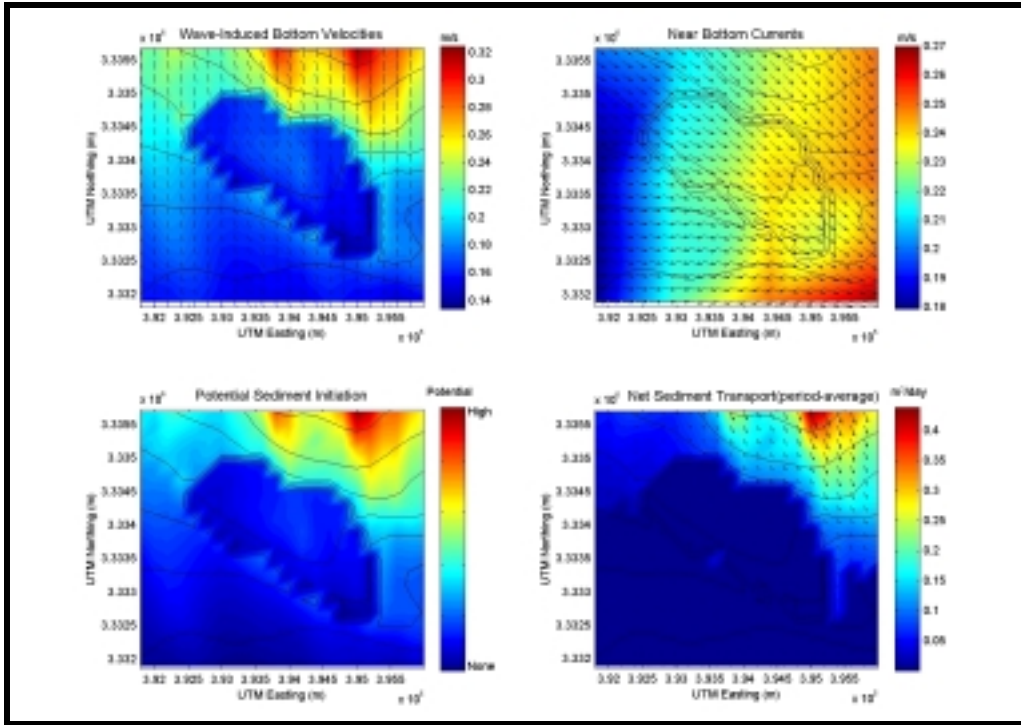


Figure 5-44. Spring hydrodynamic and sediment transport results at Sand Resource Area 4. The solid black lines represent depth contours, and sediment transport results are based on 200-m cell widths.

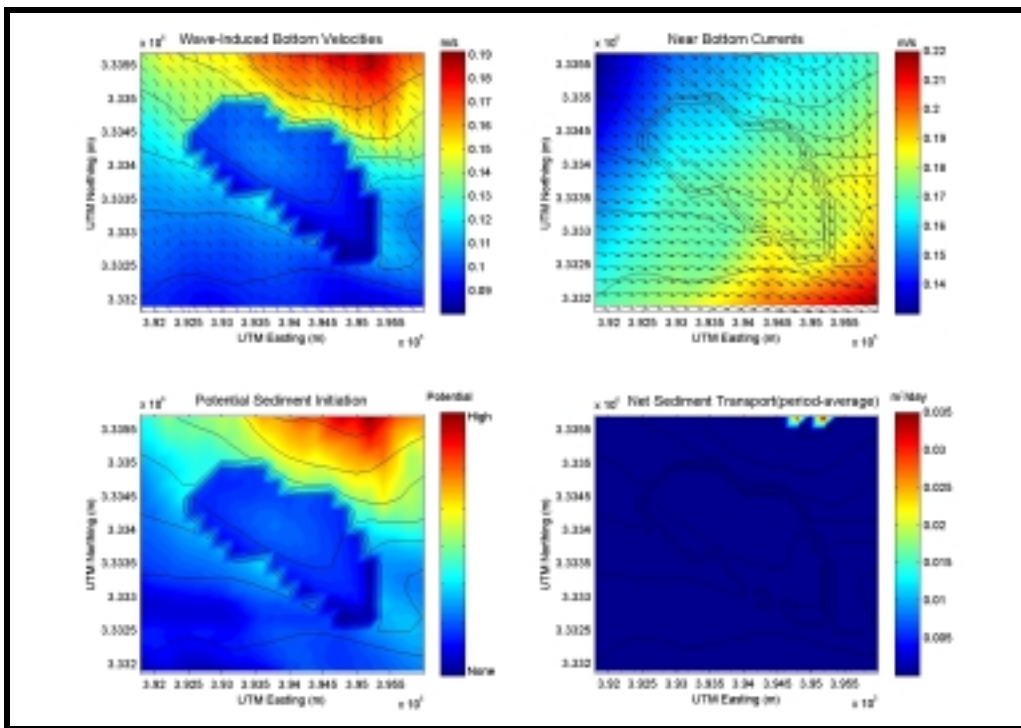


Figure 5-45. Summer hydrodynamic and sediment transport results at Sand Resource Area 4. Solid black lines represent depth contours, and sediment transport results are based on 200-m cell widths.

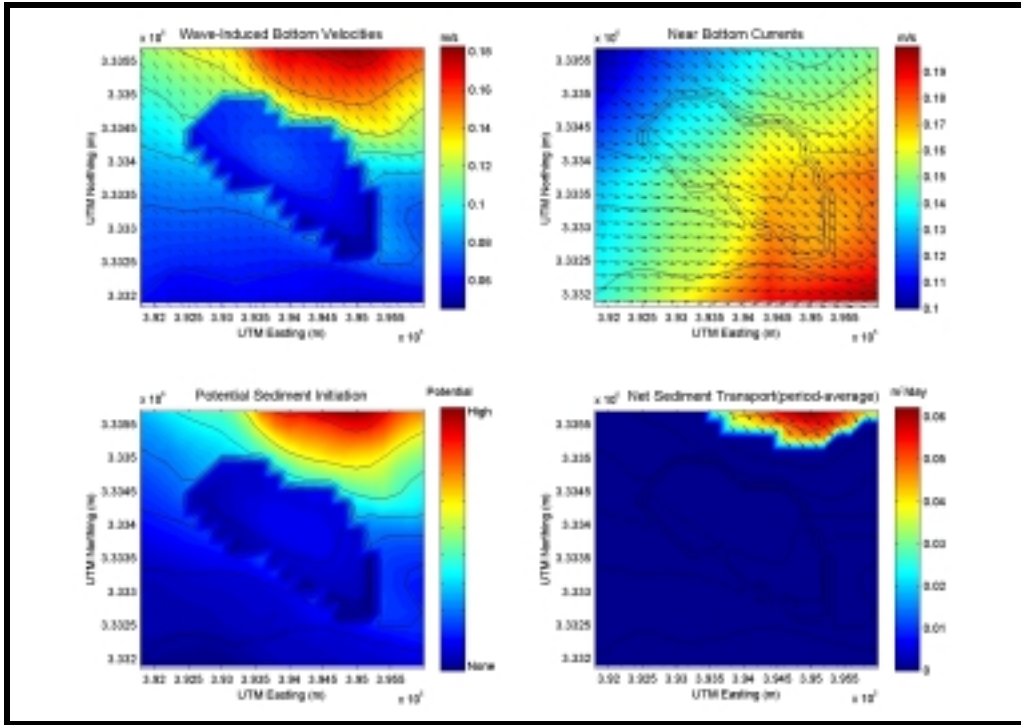


Figure 5-46. Fall hydrodynamic and sediment transport results at Sand Resource Area 4. Solid black lines represent depth contours, and sediment transport results are based on 200-m cell widths.

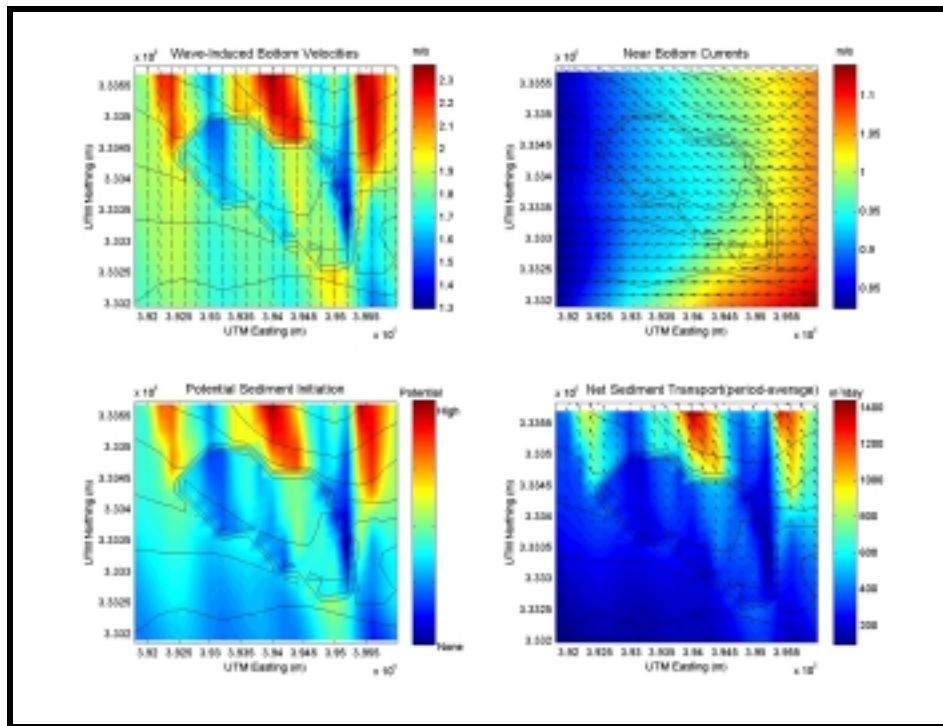


Figure 5-47. Extreme hydrodynamic and sediment transport results at Sand Resource Area 4. Solid black lines represent depth contours, and sediment transport results are based on 200-m cell widths.

During the spring (Figure 5-44), net sediment transport is similar to the southeast winter case. The spring season is comprised of relatively high wave-induced bottom currents and comparable near bottom currents. When combined, results initiate sediment over a larger area and increase the net transport rate slightly. Sediment is transported toward the east/southeast portion of the sand resource area.

Minimal transport occurs during the summer season. Summer wave heights are relatively small; therefore, the resulting wave-induced bottom velocities are small, allowing most of the sediment in and around the sand resource area to remain in place on the seafloor. Although a few cells indicate minimal transport (~ 0.035 m<sup>3</sup>/day/cell width), it is practical to conclude that sediment transport does not occur at the potential borrow site in Resource Area 4 during typical summer conditions.

During the fall, sediment transport increases in limited areas adjacent to the borrow site; however, it is still of the same order as the summer season. Net sediment transport occurs in the northeast corner of the subgrid (in shallow depths near Mobile Outer Mound), and it is moved in a southeasterly direction.

Extreme (50-yr storm) conditions transport more sediment than any season. Concentrations of high initiation and transport (200 to 1400 m<sup>3</sup>/day) are documented throughout the domain in the lower panels. Because maximum wave-induced orbital velocities and bottom currents are directed to the northwest, it follows that sediment transport occurs in the northwest direction.

All potential dredging scenarios for each of the selected borrow sites are summarized in the Table 5-4. The table includes information on the magnitude and direction of sediment transport into the sand resource areas, sand volume from the dredged area, and the approximate time to fill in the dredged site.

Table 5-4. Summary of seasonally-averaged sediment transport results using potential cumulative dredged sand volumes.				
Resource Area	Magnitude of Sediment Transport (m <sup>3</sup> /day)	Direction of Sediment Transport (to)	Dredged Sediment Volume (x 10 <sup>6</sup> m <sup>3</sup> )	Time to Fill Dredged Area (yr)
1	117	NW	5.8	136
2	40	N	1.7	116
3	50	NE	4.7	257
4	37	SE	8.4	622

The analysis for infilling time assumes a constant rate of transport through each season and does not include the effects of modified bathymetry. For example, as the dredged region begins to fill, sediment transport dynamics and morphodynamics change. Therefore, sediment transport rates will fluctuate as the borrow site begins to fill. This dynamic, time-dependent process is not accounted for in the present analysis. In addition, our analysis does not include suspended sediment entering the local region. For example, a significant amount of fine material will enter the borrow site in Sand Resource Area 4 from Mobile Bay, significantly reducing the infilling time for that borrow area. Also, the two winter seasons are combined and weighted with other seasons to yield an average year. In spite of these assumptions, the analysis presented here does give an order of magnitude estimate of infilling times.

The magnitude of sediment transport can be interpreted as the rate during an average day. In addition, the third column presents the associated seasonally-averaged direction. The magnitudes and directions may fluctuate from day to day, but the magnitude and direction presented here are for an average year. Transport rates range from a minimum of 37 m<sup>3</sup>/day to a high of

117 m<sup>3</sup>/day. The fill time is determined by assuming a constant average infilling rate. The infilling times presented in Table 5-4 requires more than a century for all seasonal cases, likely due to the absence of storms in the analysis.

It is likely that dredged volumes will be smaller than the cumulative extraction scenarios utilized to investigate potential impacts. As such, Table 5-5 uses dredged sand volumes per beach replenishment event to compute the infilling time (see Section 7.1 for dredging volume details). These volumes were estimated based on quantities required to restore Alabama beaches after a major storm event. As expected, infilling times are drastically reduced. For Sand Resource Area 4, the time required to fill the sand borrow site is reduced by approximately a factor of 5.6.

Table 5-5. Summary of seasonally-averaged sediment transport results relative to sand dredging volumes per beach replenishment event.				
Resource Area	Magnitude of Sediment Transport (m <sup>3</sup> /day)	Direction of Sediment Transport (to)	Dredged Sediment Volume (x 10 <sup>6</sup> m <sup>3</sup> )	Time to Fill Dredge Area (yr)
1	117	NW	.75	18
2	40	N	.75	51
3	50	NE	.75	41
4	37	SE	.50	111

### 5.2.2 Nearshore Sediment Transport Modeling

Nearshore sediment transport is a complex process that depends on waves, wind, and tidal action to affect coastal change. Although infrequent storm events represent the most significant erosion process, it is long-term variations in wave climate (combination of storm and normal conditions) that govern beach planform. Wave action constantly moves sand in the longshore direction due to wave-induced currents created by breaking waves. Waves incident from the east will tend to cause littoral drift to be directed to the west. Although wind and tides also govern sediment transport, the quantity of sand moved by these forcing mechanisms is minor when compared with wave-induced movement.

To adequately evaluate sediment transport along the Alabama coastline, a methodology incorporating wave orbital velocities needed to suspend sediment and mean wave-induced currents to advect sediment alongshore was employed. Grant (1943) first investigated the combined effect of orbital velocities and longshore currents on sediment transport processes. Over the past three decades, numerous researchers have developed methodologies for evaluating longshore transport rates based on calculations of the longshore current (e.g. Komar and Inman [1970], Thornton [1968], Grant and Madsen [1978], Sawaragi and Deguchi [1978], and Bodge [1986]). Due to the inherent complexities of surf zone dynamics caused by turbulent flow and energy dissipation, none of the methods provide perfect agreement with field data. However, utilizing reasonable assumptions, as well as a longshore sediment transport analysis technique based on sound scientific principles, a quantitative estimate of wave-induced transport can be determined.

To date, expressions for evaluating the distribution of longshore sediment transport across the surf zone have assumed that sediment is mobilized by (a) energy dissipation from breaking waves, (b) bottom shear stress induced by the peak horizontal orbital velocities alone, or (c) combined peak orbital velocities and the mean longshore current (Bodge, 1989). Mobilized sediment is then advected by the mean longshore current. Therefore, the distribution of longshore currents across the surf zone provides the driving force needed to predict local longshore transport

rates. Based on the review provided by Bodge (1989), most investigators have relied on the expression for longshore current on a planar beach developed by Longuet-Higgins (1970).

The existing models indicate that longshore sediment transport is largest between the breaker line and approximately midway across the surf zone, and that the transport rate tends to zero at the shoreline and outside the breaker line. Most models do not account for the often-significant longshore transport that occurs in the swash zone. Field data have indicated that significant sediment transport may occur in the swash zone; about 10% to 30% of the total transport occurs seaward of the breaker line, and greater transport is often associated with shallower depths such as bars. Overall, there is large variability in the shape of the transport distribution profile (Bodge, 1989). Although existing models have limitations, many of these models have been used successfully to evaluate the general characteristics of the longshore transport distribution.

### 5.2.2.1 Model Development

Stresses exerted by waves vary in the cross-shore direction, typically decreasing from the breaker line to the shoreline. However, this decrease may not occur in a uniform manner due to the presence of bars and troughs. The longshore current also has a characteristic profile, and because sand transport is the result of combined waves and currents, its distribution will be related to the distribution of waves and currents. Using data from field and laboratory experiments, Bodge and Dean (1987) tested five existing cross-shore distribution relationships. They provided a rating system for each relationship, ranging from fair to poor based on comparisons with measurements. Bodge and Dean (1987) also proposed a relationship for the cross-shore distribution of longshore sediment transport which assumed that sediment is mobilized in proportion to the local rate of wave energy dissipation per unit volume and transported alongshore by the mean current. In equation form, this expression is

$$q_x(y) = k_q \frac{1}{d} \frac{\partial}{\partial x} (EC_g) V \quad (5.38)$$

where  $q_x(y)$  is the local longshore transport per unit width offshore,  $y$  represents the cross-shore coordinate,  $k_q$  is a dimensional normalizing constant,  $d$  is the local water depth in the surf zone (including wave-induced setup),  $E$  represents the local wave energy density,  $C_g$  is the local wave group celerity, and  $V$  is the local mean longshore current speed. The above expression can be expanded by assuming shallow water wave conditions, small angles of wave incidence, and a nonlinear value for the wave group celerity ( $C_g = (g(H+d))^{1/2}$ ) as:

$$q_x(y) = k_q \frac{1}{8} \rho g \frac{H}{\sqrt{H+d}} \left[ 2 \frac{dH}{dy} + \frac{H}{2(H+d)} \frac{d}{dy} (H+d) \right] V \quad (5.39)$$

in which  $H$  is the local wave height in the surf zone. This shallow water equation represents conditions landward of the breakpoint. Seaward of the breakpoint, transport is assumed to be negligible since no energy dissipation occurs. This simplification could underestimate the transport rate by between 10% and 30%, since field measurements have indicated that this amount of transport occurs seaward of the breaker line. However, the REF/DIF S wave model employed in this study used a spectral wave breaking model. By employing this type of wave breaking model, no definitive breakpoint exists and a small amount of transport will occur in the region where some of the high period spectral components break. Therefore, sediment transport occurs seaward of the standard definition of the breakpoint. Energy dissipation, as well as the associated transport, within this offshore region was assumed to characterize transport seaward of the breakpoint. The distribution of  $q_x(y)$  was integrated across the nearshore zone to compute longshore transport rates for each cross-shore profile.

### 5.2.2.2 Sediment Transport Along the Alabama Coast

The REF/DIF S wave and wave-induced current models provided needed information for the littoral drift evaluation. Longshore currents were derived from the wave-induced current model, and wave parameters (wave height and water depth) were derived from wave modeling results. Because the purpose of the sediment transport modeling task was to determine impacts of offshore sand mining on the nearshore region, a sensitivity analysis of the empirical constants utilized in the transport equation was not required. Instead, the  $k_q$  value was determined from the bathymetric change analysis. Based on maximum annual transport rates of between 100,000 and 200,000 m<sup>3</sup>/yr, the  $k_q$  value was set and remained constant for all model runs. By comparing existing sediment transport potential rates to variations in the rates resulting from the various dredging scenarios, the relative impact of dredging on nearshore transport processes were quantitatively evaluated.

Similar to the wave-induced current model, the longshore sediment transport model was run for the Dauphin Island and Morgan Peninsula wave modeling grids, for each spectral wave condition (total of five) under existing conditions and post-dredging scenarios. This required a total of 20 model runs. Results from all model runs are included in Appendix C2. As an example, the results of one run (the existing conditions at Morgan Peninsula for spring wave conditions) are described in more detail below. This example provides an overview of typical wave-induced sediment transport predictions associated with the modeling effort.

The  $S_{xy}$  radiation stress component provided the primary driving force for wave-induced currents and longshore sediment transport. Radiation stress values were generated from REF/DIF S modeling; therefore, results of the wave-induced current and longshore sediment transport models was dependent on the numerical evaluation of the nearshore wave climate. Figure 5-48 illustrates the longshore and cross-shore distribution of  $S_{xy}$ , indicating regions of wave energy focus. As expected, areas of higher  $S_{xy}$  values have higher longshore sediment transport rates. Because all sediment transport is directed east-to-west, the general decrease in sediment transport rate from UTM Easting coordinate 415,000 m to approximately 403,000 m would indicate a tendency toward accretion. The opposite is also true, where the increase in sediment transport rate from UTM Easting coordinate 423,000 m to approximately 415,000 m would be indicative of a shoreline segment experiencing erosion.

Morgan Peninsula and Dauphin Island sediment transport modeling results indicated a large variation in transport magnitude; however, the overall tendency along both shorelines was an east-to-west littoral drift. Over the entire study area, the only exception to this transport trend was the region at the eastern terminus of Dauphin Island. In this region, wave protection afforded by Pelican Island and the numerous offshore shoals caused a reversal in net transport direction. However, the magnitude of this west-to-east transport is low due to wave energy dissipation on the shoal system.

For the Morgan Peninsula, sediment transport rates generally increased from west-to-east for seasonal model runs. Due to specific regions of wave focusing associated with seasonal wave characteristics, some areas of increased sediment transport potential existed along the shoreline. For example, sediment transport calculations for the spring and winter season indicated relatively high transport rates at UTM Easting coordinate 415,000 m (Figure 5-48). Along the Dauphin Island shoreline, greater seasonal variability in transport rates was evident (Appendix C2). Again, results from the spring and winter model runs indicated similar results, due to similar wave spectra characteristics. For both seasons, the transport rate generally increased from east-to-west. The mild wave climate in the summer season indicated sediment transport potential at a lower magnitude than other seasons. In addition, a reversal in transport direction was predicted at UTM Easting coordinate 382,000 m (Figure 5-49). The broad spectral spreading characteristics of the fall season indicated highest transport rates near the middle portion of Dauphin Island (between

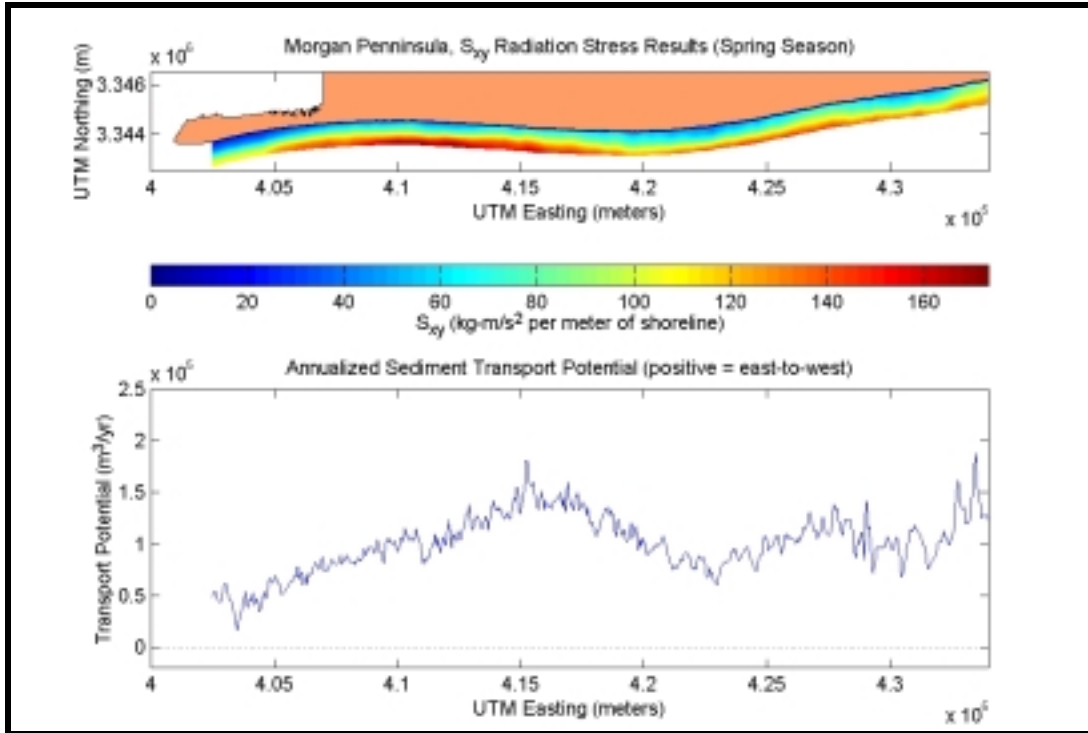


Figure 5-48.  $S_{xy}$  radiation stress values and annualized sediment transport potential for the spring season at Morgan Peninsula.

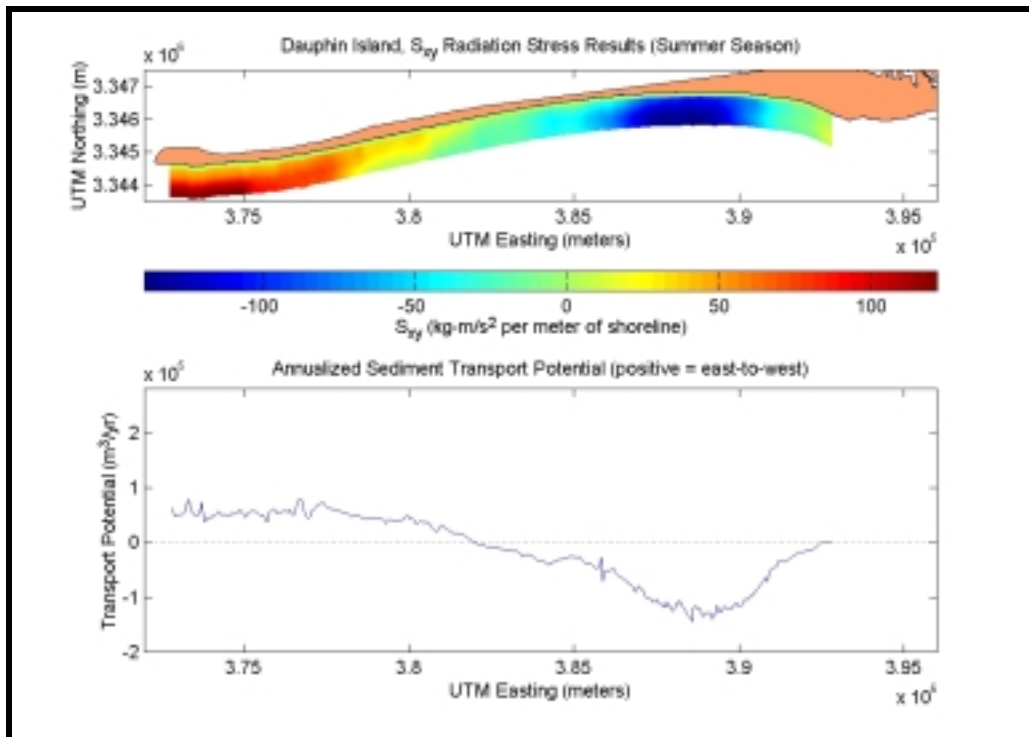


Figure 5-49.  $S_{xy}$  radiation stress and annualized sediment transport potential for existing conditions at Dauphin Island during the Summer season.

UTM Easting coordinates 380,000 and 385,000 m. Because transport rates predicted for the spring and winter seasons were significantly greater than the other two seasons, these seasons tended to dominate the long-term sediment transport trends along Dauphin Island.

Similar to the wave modeling results, the sediment transport rates calculated for the 50-year event illustrated significant longshore variability. Along Dauphin Island, the relative magnitude of transport was similar to the seasonal trend, where the transport rate was lowest adjacent to the Mobile Bay entrance and generally increased in magnitude from east-to-west. Along Morgan Peninsula, the transport rate was highest near the eastern end of the modeled region.

In addition to providing net sediment transport rates, the transport model provided the cross-shore distribution of longshore sediment transport across the surf zone. Figure 5-50 illustrates this cross-shore distribution in relation to the cross-shore distribution of the mean longshore current at three selected transects. Based on the results of the sediment transport model, peak current velocities occur landward of the peak sediment transport. Since most wave models predict rapid energy dissipation at the breaker line, and the sediment transport equation used strongly depends on the wave energy dissipation rate, the highest sediment transport rate can be expected relatively close to the break point. Field and laboratory data collected by Bodge and Dean (1987) indicate that peak transport rates often occur near the breakpoint. The current distribution predicted by the longshore current model also corresponds to other model approaches, where the maximum currents occur in the seaward half of the surf zone.

### **5.2.2.3 Nearshore Sediment Transport Versus Historical Shoreline Change**

As a simplistic measure of the longshore sediment transport model's applicability to the Alabama shoreline, an attempt was made to compare accretion/erosion potential predicted by the model to shoreline change results. The accretion/erosion potential was determined through calculation of sediment transport change normalized to the maximum computed change. In this manner, the relative magnitude of erosion and accretion could be evaluated for the entire shoreline segment. Because the calculation of accretion/erosion potential was dependent on the slope of the net sediment transport curve, smoothing of this curve was performed to determine general transport trends. Shoreline change for the entire time period (1847/67 to 1978/81) was plotted for comparison purposes. The results of this analysis are shown in Figures 5-51 and 5-52 for Morgan Peninsula and Dauphin Island, respectively.

Figure 5-51 illustrates large variability in accretion/erosion trends predicted by the sediment transport model, as well as the variability of observed shoreline change. Due to this high variability, it is difficult to determine obvious trends for either the normalized transport change or the observed shoreline change. Erosion indicated by shoreline change results between UTM Easting coordinates 418,000 and 423,000 m, as well as between 427,000 and 431,000 m, was predicted by the sediment transport model. However, some other regions of observed shoreline change did not correspond to model predictions. For example, the model predicted a general tendency toward shoreline accretion between UTM Easting coordinates 404,000 and 415,000 m (immediately east of the Mobile Bay entrance). However, shoreline change indicated that the long-term trend of accretion only extended to approximately UTM Easting coordinate 408,000 m. The relatively stable region between 415,000 and 427,000 m (low annual shoreline change rates) was adequately predicted by the modeled sediment transport trends in this region.

Although many of the trends indicated by the observed shoreline change and the computed accretion/erosion potential were predicted well, several shoreline reaches indicated opposite trends, where the observed and computed accretion/erosion contradicted each other. Direct comparisons of measured shoreline change and computed sediment transport have several sources of potential error and variability. First, the modeled change in longshore transport represents sediment moving

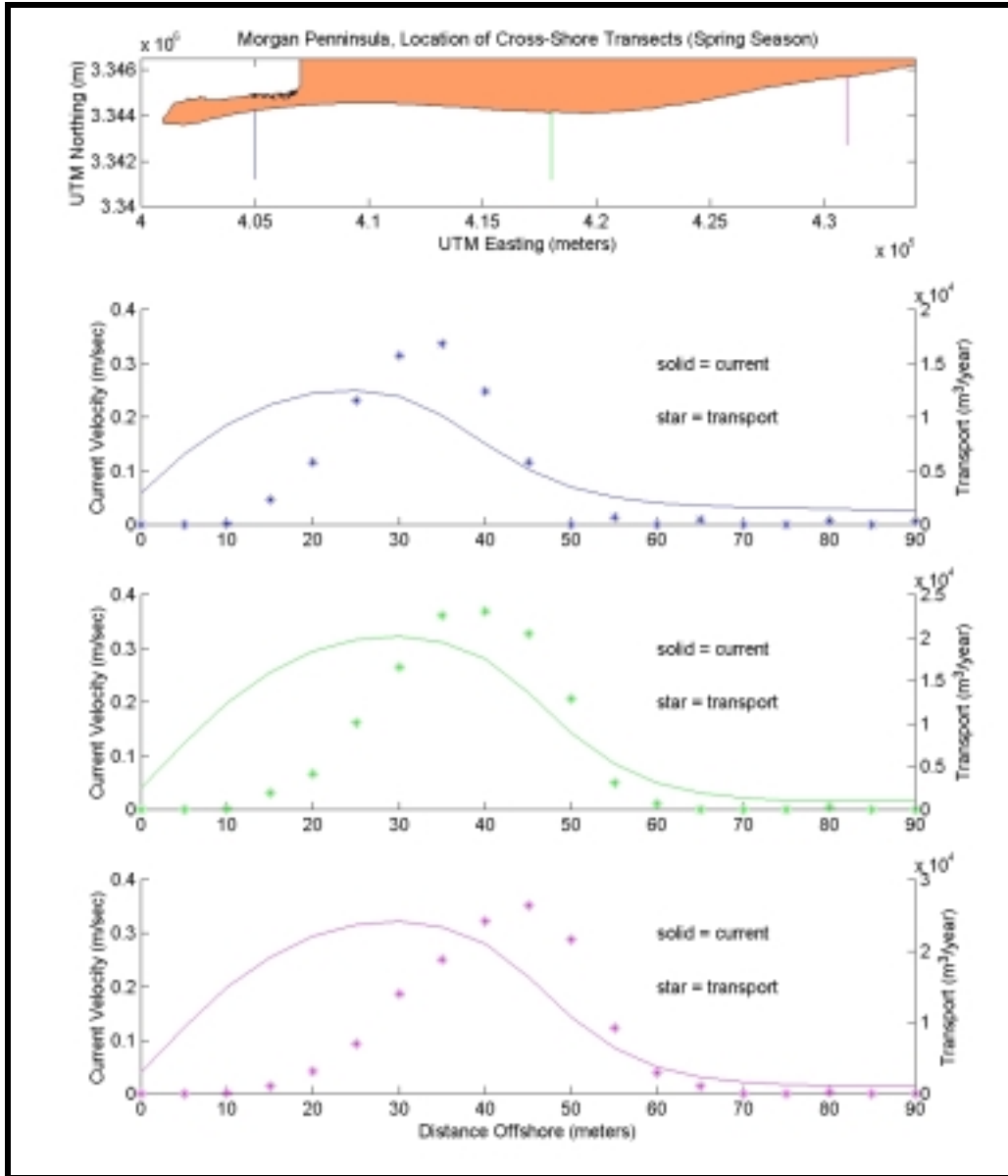


Figure 5-50. Cross-shore distribution of longshore current and sediment transport for three selected transects (spring season at Morgan Peninsula).

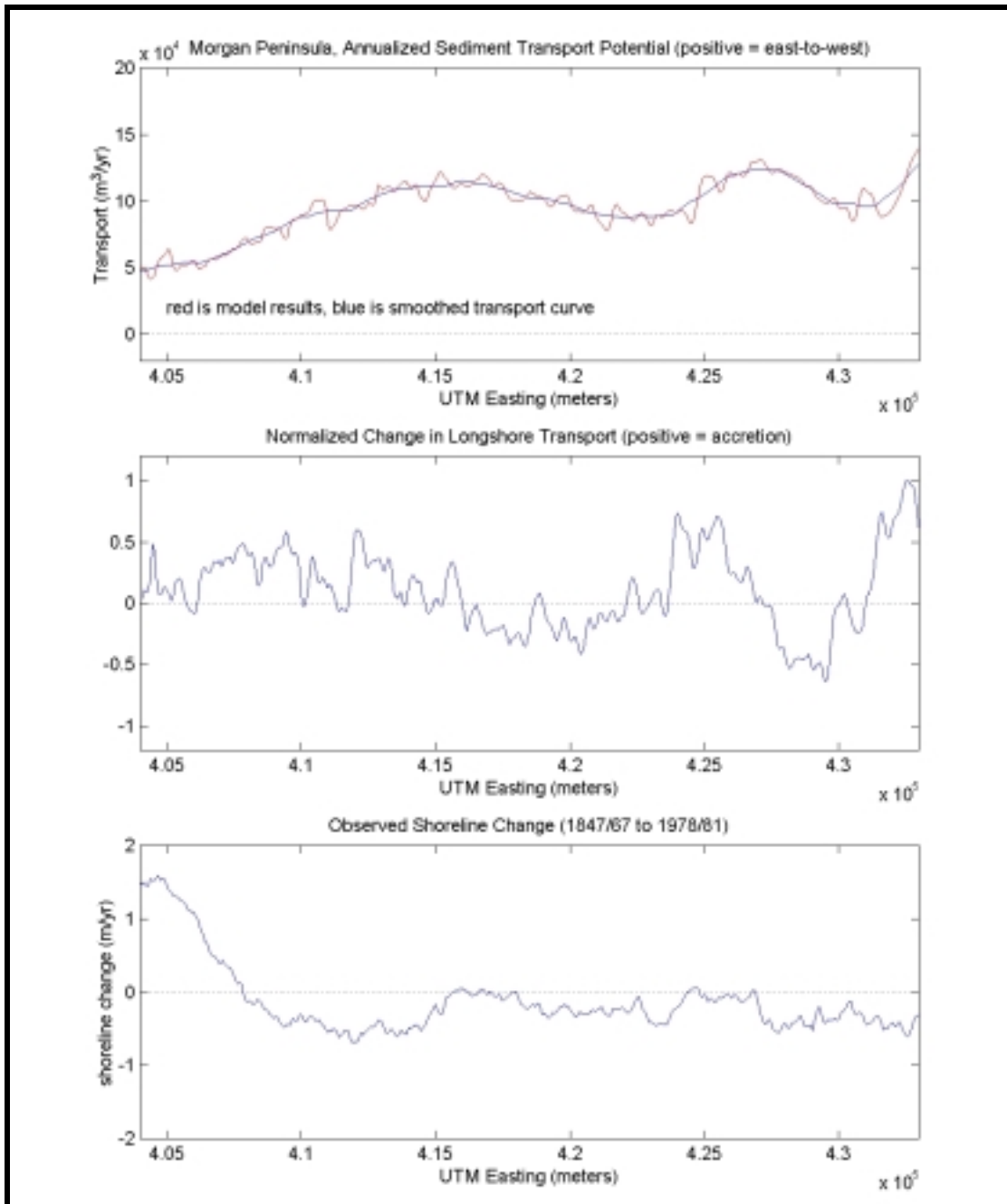


Figure 5-51. Annual longshore sediment transport potential, normalized change in longshore transport (modeled accretion/erosion potential), and observed shoreline change between 1847/67 and 1978/81 for the Morgan Peninsula.

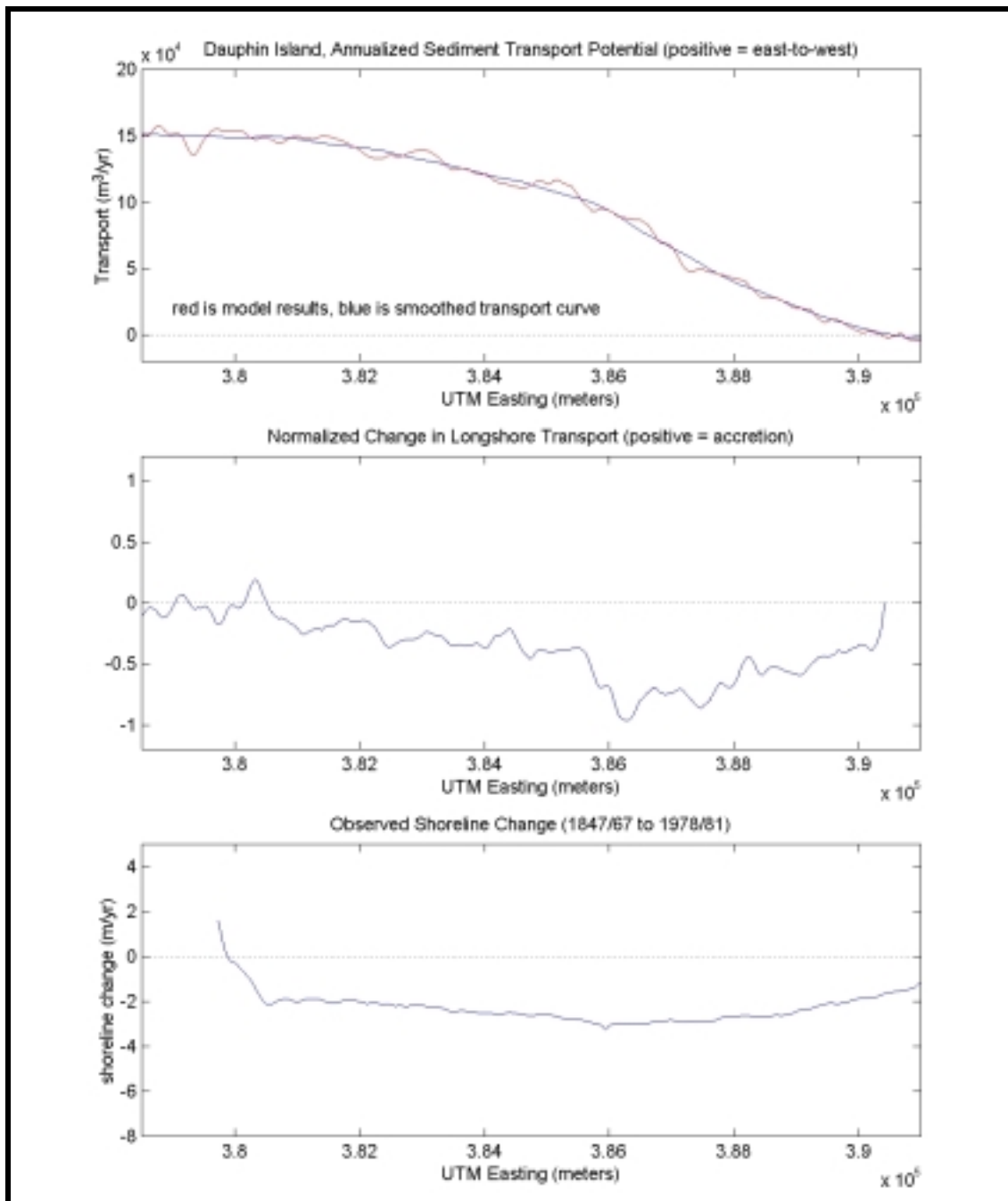


Figure 5-52. Annual longshore sediment transport potential, normalized change in longshore transport (modeled accretion/erosion potential), and observed shoreline change between 1847/67 and 1978/81 for Dauphin Island.

throughout the surf zone and shoreline change merely indicates migration of a single line. For example, the bathymetric change analysis indicated accretion in the nearshore area (surf zone) at the western end of the Morgan Peninsula. Therefore, observations of bathymetric change are in direct conflict with shoreline change results, indicating that shoreline change alone may not be a valid indicator of coastal change.

Sediment transport modeling also assumes an infinite sediment source. If erosion potential is high along a certain stretch of shoreline, the model assumes that this volume is available for transport. However, natural beaches typically are in a state of constant adjustment toward equilibrium based on current environmental conditions (waves, tides, winds, etc.). Therefore, the shoreline may not be able to provide the sand volume required by wave conditions, a sediment deficit is created downdrift, and the beach does not behave exactly as the model predicts. Typically, sediment transport models are appropriate for use on sandy coasts like Dauphin Island and the Morgan Peninsula because they can accurately predict long-term trends in these areas.

Figure 5-52 illustrates accretion/erosion potential and observed shoreline change at Dauphin Island. Due to wave sheltering provided by Pelican Island and the numerous offshore shoals, there is a marked decrease in transport rates between the central portion of the Island and its eastern terminus. Because net direction of transport is from east-to-west, the increase in modeled transport rates from the east end of Dauphin Island to the center of the Island creates an erosional trend. This result compares well with observed shoreline change between 1847/67 and 1978/81, where the peak observed erosion, as well as the peak computed erosion, occur at approximately the same location (UTM Easting coordinate 386,000 m). Along the western portion of the Island, the modeled longshore transport rate decreases, indicating a tendency toward lower erosion rates and/or a stable shoreline. This result also agrees with the observed shoreline change, where the high annual shoreline erosion rate (approximately 2 m per year) becomes negligible at UTM Easting coordinate 380,000 m.

Although similar potential errors exist for comparing observed shoreline change with computed accretion/erosion tendency, the results for Dauphin Island compare favorably for the entire shoreline. The larger magnitude of observed shoreline change for Dauphin Island made general trends more obvious than trends observed along the Morgan Peninsula. In addition, bathymetric contours offshore of Dauphin Island were predominantly shore parallel, unlike the shore-oblique sand ridges offshore of Morgan Peninsula. This more simplistic bathymetry facilitated more accurate modeling of the nearshore wave field; therefore, prediction of erosion/accretion trends also was more accurate.

## **6.0 BIOLOGICAL FIELD SURVEYS**

### **6.1 BACKGROUND**

Two biological field surveys were conducted to collect data in and around the five sand resource areas. The primary objective of the field surveys was to obtain descriptive data on benthic biological conditions (i.e., infauna, epifauna, demersal ichthyofauna, and sediment grain size) and water column characteristics (i.e., temperature, salinity, dissolved oxygen, and depth) in the five proposed sand resource areas. A secondary objective was to obtain descriptive data on the infauna and sediment grain size adjacent to the five proposed sand resource areas.

The locations and dimensions of the five sand resource areas were based on reports by Parker et al. (1993, 1997) and Hummell and Smith (1995, 1996). Although the sand resource areas as described by these authors overlap state/federal boundaries, only the portion of each sand resource area in federal waters was considered for the biological program.

Sample types and numbers for the May 1997 Survey 1 and December 1997 Survey 2 are summarized in Table 6-1. Sampling locations are illustrated in Figures 6-1 through 6-6 and tabulated in Appendix D1.

### **6.2 METHODS**

#### **6.2.1 Survey Design**

A total of 20 grab samples for infauna and sediment grain size were collected inside and outside (adjacent to) each sand resource area (16 samples inside and 4 samples outside). The goal in the placement of these sampling stations was to provide uniform coverage within a sand resource area and, at the same time, ensure that the samples would be independent of one another to satisfy statistical assumptions. This systematic sampling with an unaligned grid approach provides more uniform coverage of the target populations that, in many cases, yields more accurate estimates of the mean than simple random sampling (Gilbert, 1987). To achieve uniform sampling coverage, 4 x 4 grids (=16 cells) were placed over figures of each sand resource area. For Sand Resource Areas 1, 2, 3, and 5, the 16-cell grid was placed over a map of the entire sand source area in federal waters. Because the sand resource site within Area 4 was very localized based on surficial sediment samples and subsurface core data of Parker et al. (1993, 1997) and Hummell and Smith (1995, 1996), the 16-cell grid was placed over this specific target site within Area 4. To achieve independence, one sampling station then was randomly placed within each grid cell of each sand resource area. Randomizing within grid cells eliminated biases that could be introduced by unknown spatial periodicities in the sampling area. All station locations then were pre-plotted on geodetically corrected maps from Parker et al. (1993, 1997) and Hummell and Smith (1996).

To sample epifauna and demersal ichthyofauna, two trawl transects were located within each of the sand resource areas. One east-west transect was placed near the northern boundary and one east-west transect was placed near the southern boundary of each sand resource area. This approach allowed characterization of the existing assemblages with respect to water depth. Water column measurements were made near the beginning point of each trawl transect prior to actual trawling.

To satisfy the secondary objective, four stations were placed outside Areas 1, 2, 3, and 5. Four stations were placed outside the specific target site within Area 4. The location of these stations was based upon sedimentary information in Parker et al. (1993, 1997) and Hummell and Smith (1995, 1996).

Table 6-1. Sample types and numbers for the May 1997 Survey 1 and December 1997 Survey 2 of the five sand resource areas offshore Alabama. Gravity coring was conducted only in Area 4 Station 14.

Sand Resource Area	Number of Stations							
	Smith-McIntyre Grab				Epifaunal and Demersal Ichthofaunal Trawls		Water Column	
	Grain Size		Infauna		Survey 1	Survey 2	Survey 1	Survey 2
	Survey 1	Survey 2	Survey 1	Survey 2				
1	20 (16 inside; 4 outside)	20 (16 inside; 4 outside)	20 (16 inside; 4 outside)	20 (16 inside; 4 outside)	2 (1 north; 1 south)	2 (1 north; 1 south)	2 (1 north; 1 south)	2 (1 north; 1 south)
2	20 (16 inside; 4 outside)	20 (16 inside; 4 outside)	20 (16 inside; 4 outside)	20 (16 inside; 4 outside)	2 (1 north; 1 south)	2 (1 north; 1 south)	2 (1 north; 1 south)	2 (1 north; 1 south)
3	20 (16 inside; 4 outside)	20 (16 inside; 4 outside)	20 (16 inside; 4 outside)	20 (16 inside; 4 outside)	2 (1 north; 1 south)	2 (1 north; 1 south)	2 (1 north; 1 south)	2 (1 north; 1 south)
4	20 (16 inside; 4 outside)	20 (16 inside; 4 outside)	20 (16 inside; 4 outside)	20 (16 inside; 4 outside)	2 (1 north; 1 south)	2 (1 north; 1 south)	2 (1 north; 1 south)	2 (1 north; 1 south)
5	20 (16 inside; 4 outside)	20 (16 inside; 4 outside)	20 (16 inside; 4 outside)	20 (16 inside; 4 outside)	2 (1 north; 1 south)	2 (1 north; 1 south)	2 (1 north; 1 south)	2 (1 north; 1 south)
TOTAL	100	100	100	100	10	10	10	10

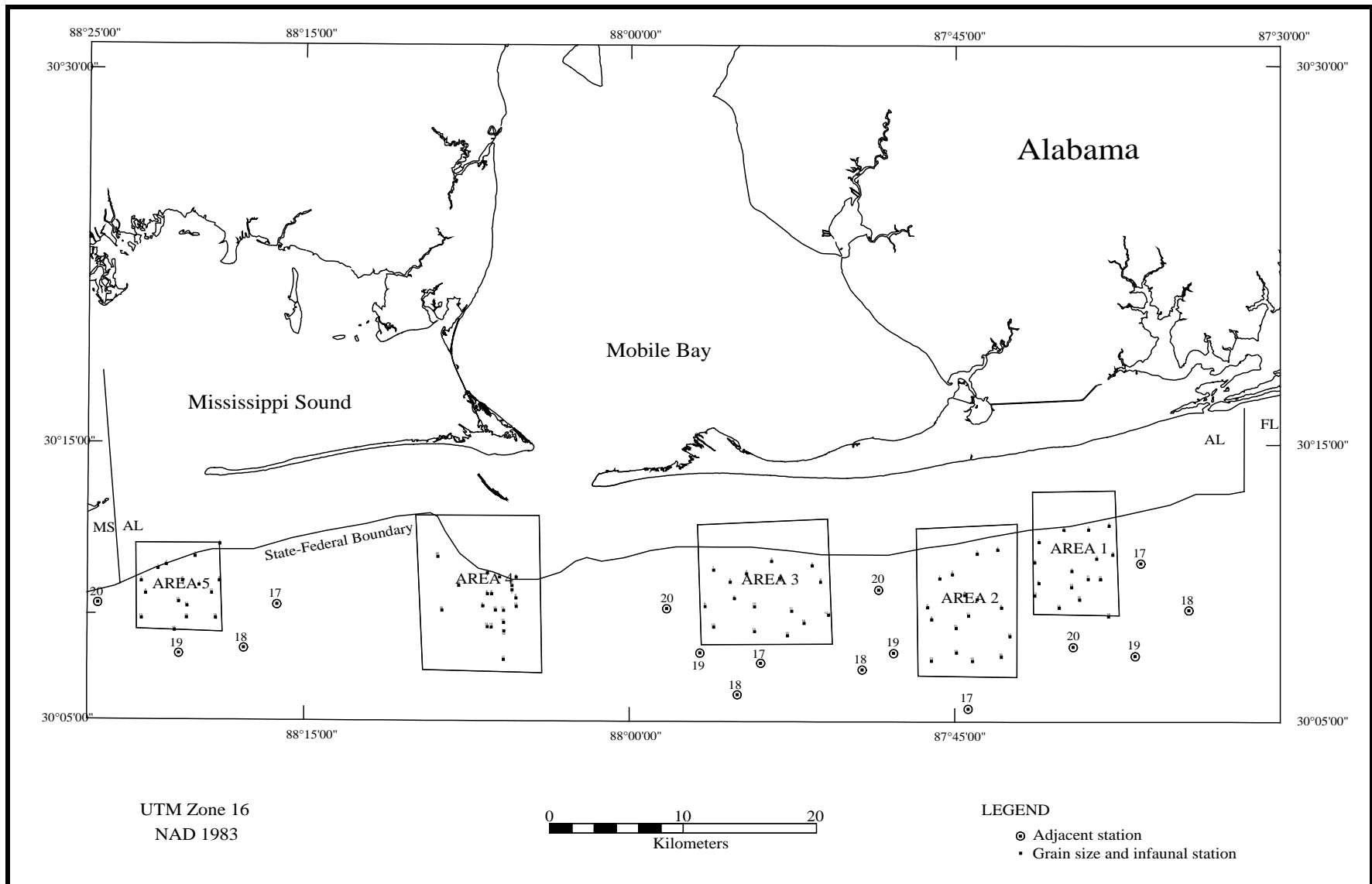


Figure 6-1. Sampling locations for grain size and infauna relative to the five sand resource areas and the Alabama coast (adapted from Parker et al., 1997).

# AREA 1

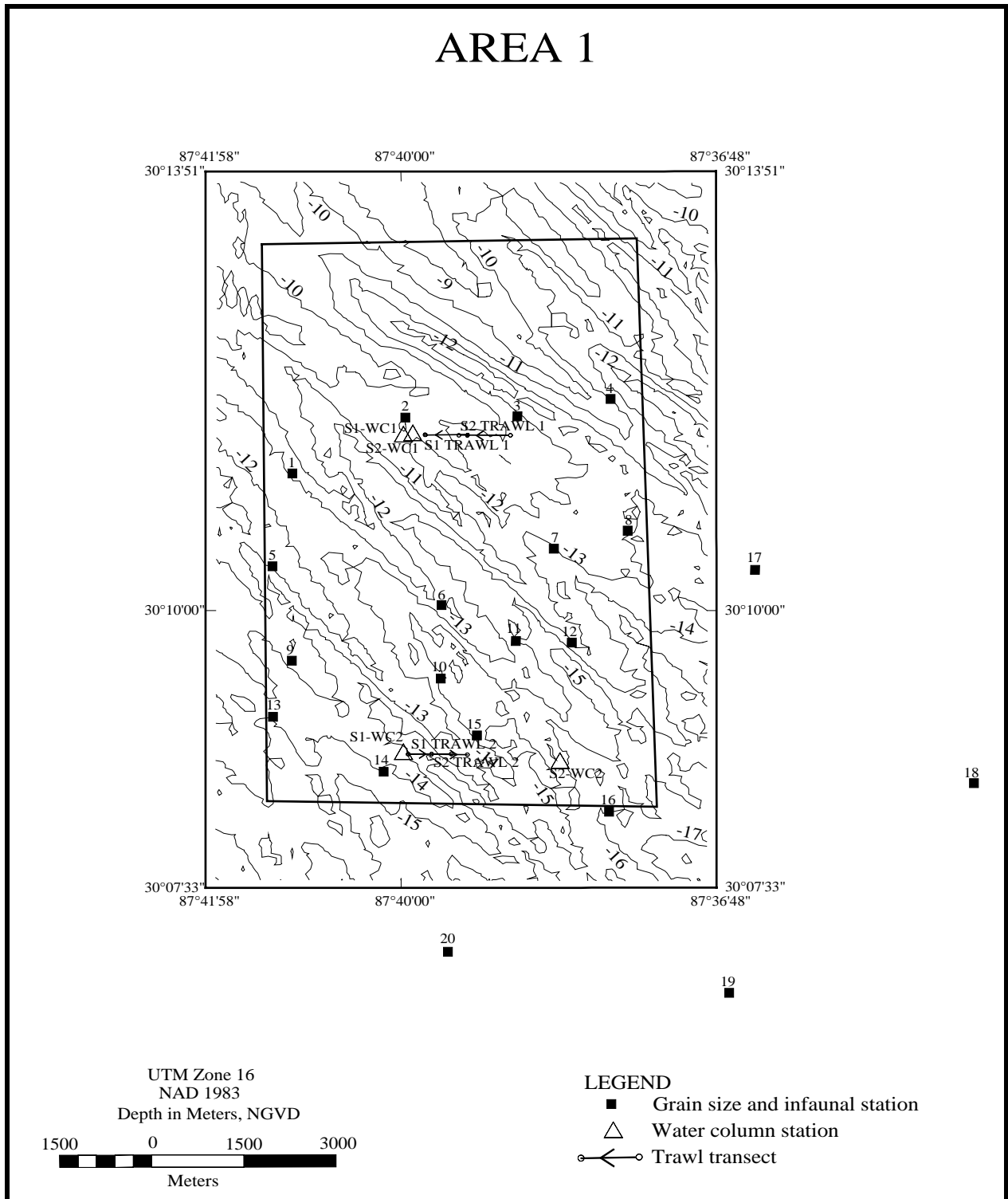


Figure 6-2. Sampling locations for Alabama Sand Resource Area 1. Inner box represents the limits of Area 1. Outer box provides reference coordinates.

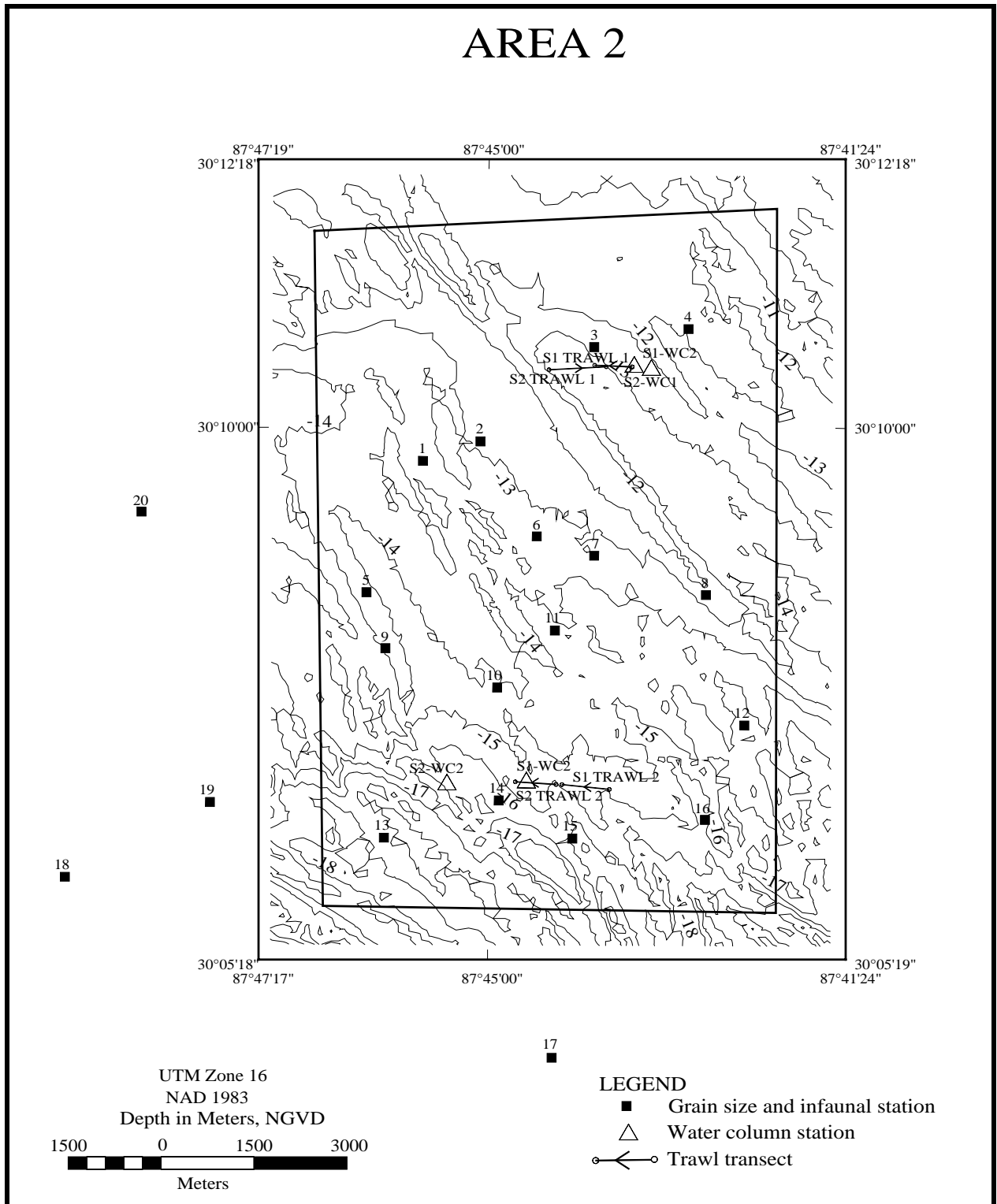


Figure 6-3. Sampling locations for Alabama Sand Resource Area 2. Inner box represents the limits of Area 2. Outer box provides reference coordinates.

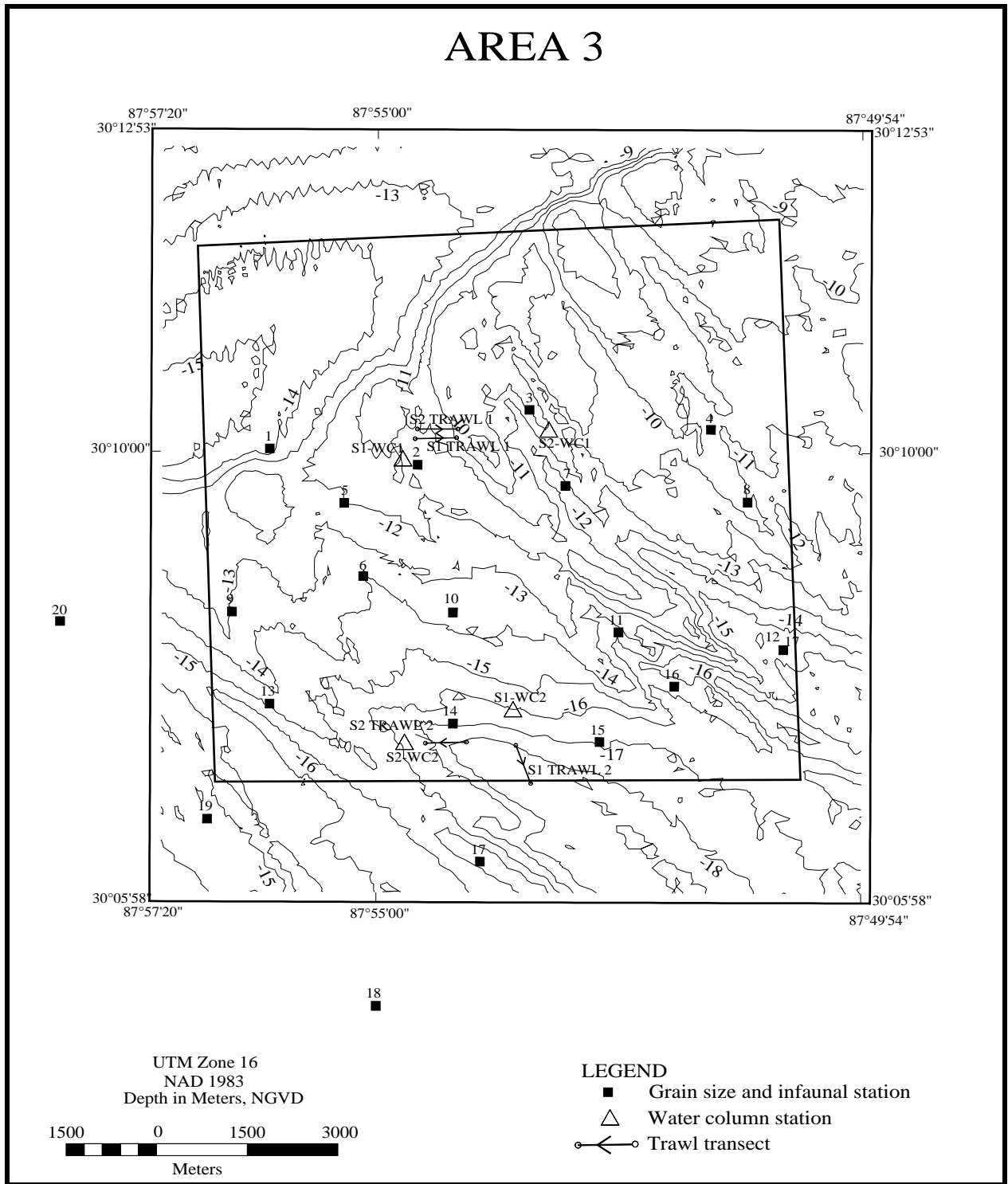


Figure 6-4. Sampling locations for Alabama Sand Resource Area 3. Inner box represents the limits of Area 3. Outer box provides reference coordinates.

# AREA 4

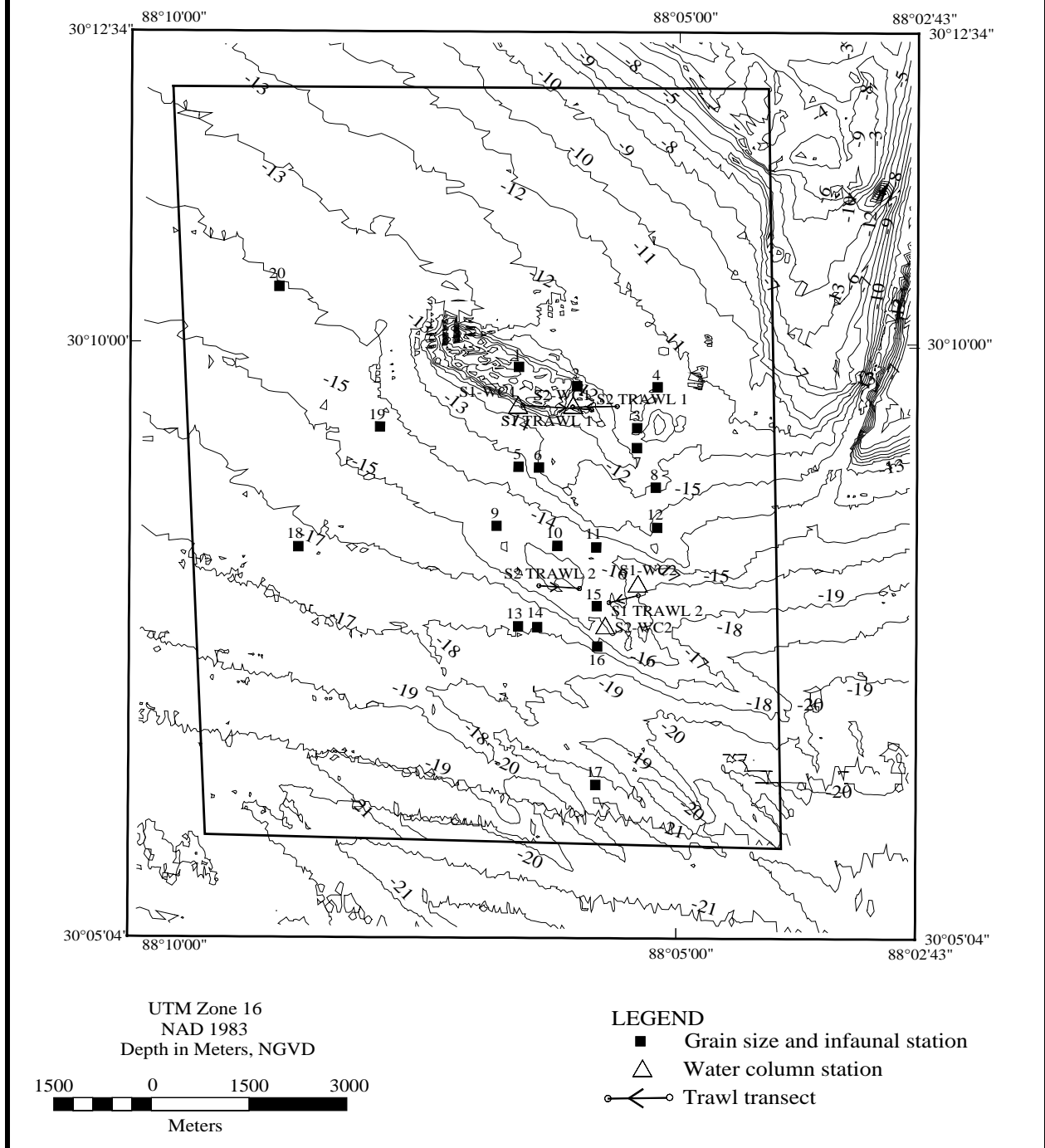


Figure 6-5. Sampling locations for Alabama Sand Resource Area 4. Inner box represents the limits of Area 4. Outer box provides reference coordinates.

# AREA 5

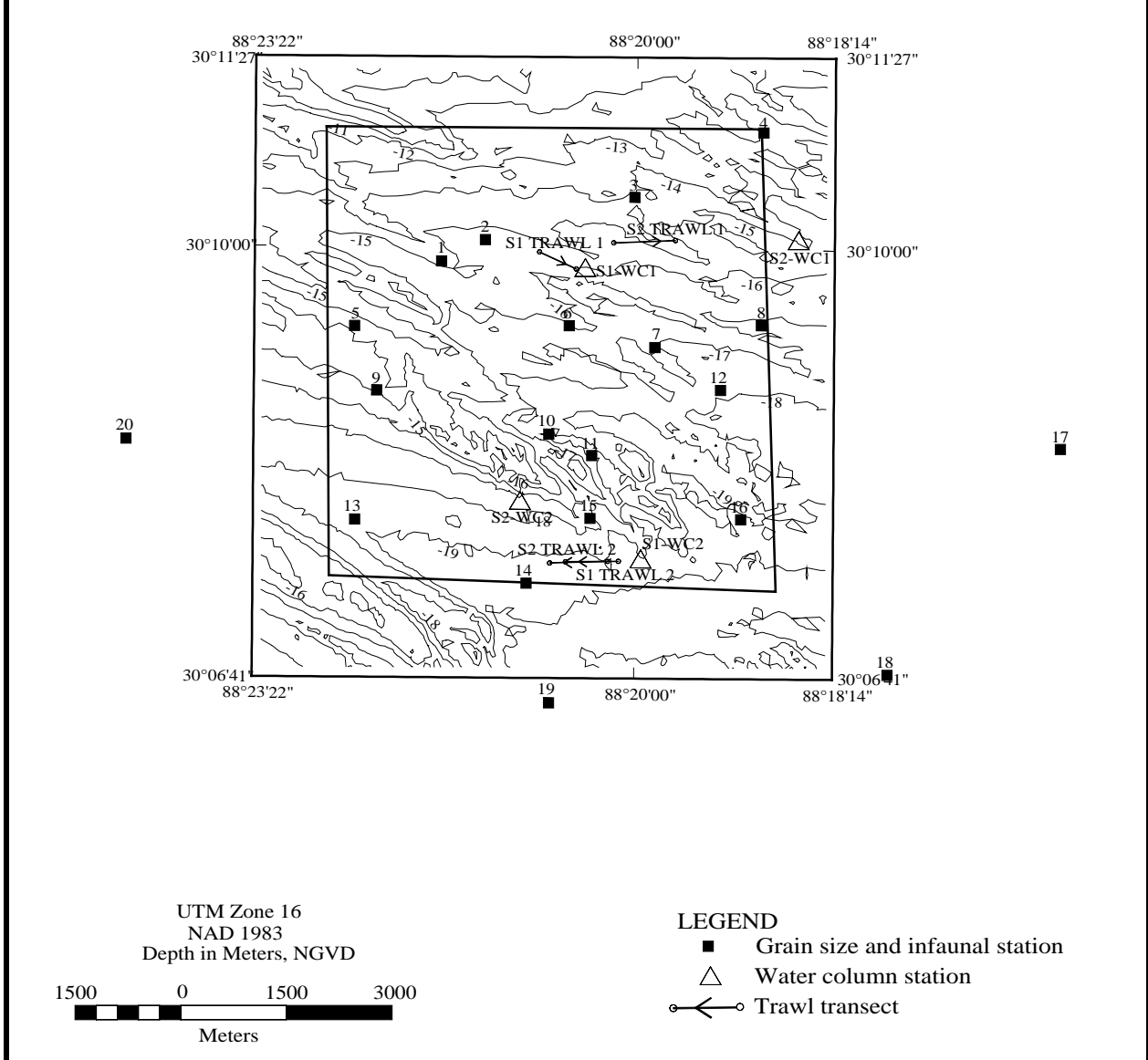


Figure 6-6. Sampling locations for Alabama Sand Resource Area 5. Inner box represents the limits of Area 5. Outer box provides reference coordinates.

Visual observations and laboratory analyses of some Survey 1 grab samples indicated that the surficial sediment in Sand Resource Area 4 contained more silt and clay than expected, rather than sand as identified in the reports by Hummell and Smith (1995, 1996). A small-scale data collection effort was proposed for Survey 2 to further investigate the discrepancy. In a limited reconnaissance effort gravity coring was used to investigate whether there was sand below the mud layer in Area 4.

## **6.2.2 Field Methods**

### **6.2.2.1 Vessel**

The two field surveys were conducted from different vessels. The May survey was completed aboard the M/V CAPTAIN JOHN based at Dauphin Island, Alabama. This cruise took place from 18 May to 24 May 1997 (field sampling occurred from 19 to 23 May). For the December survey, the R/V BEACON based in Bayou La Batre, Alabama was used. This cruise was conducted from 10 December to 16 December 1997 (field samples were collected from 11 to 15 December).

### **6.2.2.2 Navigation**

A differential global positioning system (DGPS) was used to navigate the survey vessels to all sampling stations. The DGPS was connected to an on-board computer equipped with Hypack Navigation Software Version 6.4 (Coastal Oceanographics, 1996). With this system, the ship's position was displayed in real-time on a monitor affixed to a counter top in the wheel house. All sampling stations were pre-plotted and stored in the Hypack program. While in the field, actual positions of all samples collected were recorded and stored by the program.

### **6.2.2.3 Water Column**

Temperature, conductivity, dissolved oxygen, and depth were measured with a portable Hydrolab unit. The Hydrolab was calibrated as needed each working day. Hydrolab measurements of temperature (°C), conductivity (mS), and dissolved oxygen (mg/L) were taken at three depths: surface, middle, and near-bottom. The Hydrolab was fastened to a weighted line, then lowered to depth by hand. All measurements were recorded on standard data sheets. Two water column profiles from each sand resource area produced 10 profiles for each survey.

### **6.2.2.4 Sediment Grain Size**

One grab sample was taken with a Smith-McIntyre grab at each pre-plotted sediment sampling station. Once a sample was deemed acceptable (i.e., adequate penetration and undisturbed surface layer), a subsample of sediment (about 250 g) was removed with a 5-cm diameter acrylic core tube and placed in a labeled plastic bag for grain size analyses. This sample was stored on ice. A total of 20 grain size samples was taken from each sand resource area during each field survey for a total of 100 grain size samples per survey.

As part of the limited reconnaissance coring effort, 12 attempts to collect gravity cores were made at Station 14 in Area 4 using a 1.2-m core tube. Although penetration occurred, the gravity core tube did not hold sediment very well upon retrieval due to a combination of factors, including consistency of the sediment, the shallow water depth for the gravity core drop, vessel movement from strong water currents and high wind conditions, and depth of penetration relative to the core tube length. Eight additional attempts were made using a shorter 0.6-m core tube at Station 14, and a core was retrieved. A Van Veen sampler also was used at Station 14 in Area 4, resulting in only 15 to 18 cm of penetration.

#### **6.2.2.5 Infauna**

One grab sample was taken with a Smith-McIntyre grab at each pre-plotted sediment sampling station. Once a sample was deemed acceptable (i.e., adequate penetration and undisturbed surface layer), a subsample of sediment was removed for grain size analysis, and the remainder of the grab sample was sieved through a 0.5-mm sieve for infaunal analyses. The infaunal sample was placed in a container and preserved in 10% formalin with rose bengal stain. At each sand resource area, 20 grab samples were taken, which produced a total of 100 infaunal samples per field survey.

#### **6.2.2.6 Epifauna and Demersal Ichthyofauna**

A 25-ft mongoose trawl was towed for 10 min (bottom time) along the pre-plotted transects. The tow path of each trawl tow was logged into the Hypack navigation system. Once the trawl was on deck, the contents of the catch bag were identified, then sorted to the lowest practical taxon. Organisms that could be identified in the field were counted and returned to the sea. Any specimens not identified were saved and preserved with 10% formalin. All specimens identified and counted in the field were recorded on standard trawl data sheets. Each sand resource area yielded two trawl samples for a total of 10 samples per survey.

### **6.2.3 Laboratory Methods**

#### **6.2.3.1 Sediment Grain Size**

Sediment grain size analyses were conducted using combined sieve and hydrometer analyses according to recommended American Society for Testing Materials (ASTM) procedures. Grain size samples were washed in demineralized water, dried, and weighed. Coarse and fine fractions (sand/silt) were separated by sieving through a U.S. Standard Sieve Mesh No. 230 (62.5  $\mu\text{m}$ ). Sediment texture of the coarse fraction was determined at half-phi intervals by passing the sediment through nested sieves. The weight of the materials collected in each particle size class was recorded. Boycouse hydrometer analyses were used to analyze the fine fraction (<62.5  $\mu\text{m}$ ).

#### **6.2.3.2 Infauna**

Formalin-preserved infaunal samples were rinsed on a U.S. Standard No. 30 (0.59 mm) sieve and transferred to 70% isopropanol. Before sorting, samples were passed through a series of sieves (0.3, 0.5, 0.6, 1, and 2 mm) to separate the organisms into size classes. Samples were sorted by hand under dissecting microscopes. All sediment in each sample was examined by a technician who removed all infauna observed. Organisms were identified to lowest practical taxon and counted. A minimum of 10% of all samples were resorted by different technicians as a quality control measure. Voucher specimens of each taxon were archived at the Barry A. Vittor & Associates, Inc. laboratory.

#### **6.2.3.3 Epifauna and Demersal Ichthyofauna**

Most fishes and invertebrates were identified, sorted, and counted on board the survey vessels. Specimens returned to the laboratory were rinsed in fresh water then transferred to 70% isopropanol. Specimens were sorted and counted then placed in 70% isopropanol for storage. All fish specimens were deposited in the Florida Museum of Natural History ichthyological collection.

## 6.2.4 Data Analysis

### 6.2.4.1 Water Column

Temperature, conductivity, dissolved oxygen, and depth values were entered into an electronic spreadsheet and tabulated. Salinity was calculated from conductivity and temperature using standard formulae.

### 6.2.4.2 Sediment Grain Size

A computer algorithm was used to determine size distribution and provide interpolated size information for the fine fraction at 0.25-phi intervals. Median grain size, percentages of gravel, sand, silt, clay, and Folk descriptions were provided for each sample (see Appendix D3).

### 6.2.4.3 Infauna

Summary statistics including number of taxa, number of individuals, density, diversity ( $H'$ ), evenness ( $J'$ ), and species richness ( $D$ ) were calculated for each sampling station. Diversity ( $H'$ ), also known as Shannon's Index (Pielou, 1966), was calculated as follows:

$$H' = -\sum_{i=1}^S p_i \ln(p_i)$$

where  $S$  is the number of taxa in the sample,  $i$  is the  $i$ th taxa in the sample, and  $p_i$  is the number of individuals of the  $i$ th taxa divided by ( $N$ ) the total number of individuals in the sample.

Evenness ( $J'$ ) was calculated using Pielou's (1966) index of evenness:

$$J' = \frac{H'}{\ln(S)}$$

where  $H'$  is Shannon's index as calculated above and  $S$  is the total number of taxa in a sample.

Species richness ( $D$ ) was calculated by using Margalef's index:

$$D = \frac{(S-1)}{\ln(N)}$$

where  $S$  is the total number of taxa in the sample, and  $N$  is the number of individuals in the sample.

Spatial and temporal patterns in the infaunal assemblage as a whole were examined by cluster analysis of the entire data set. Additional cluster analyses also were performed on data from each sand resource area. Cluster analyses were performed on similarity matrices constructed from raw data matrices consisting of taxa and samples (station-survey). Species included in the cluster analysis for each of the individual sand resource areas comprised at least 0.4% of total infaunal abundance within the sand resource area being analyzed. Raw counts of each individual infaunal taxon in a sample ( $n$ ) were transformed to logarithms [ $\log_{10}(n+1)$ ] prior to similarity analysis. Both normal (stations) and inverse (taxa) similarity matrices were generated using the Bray-Curtis index which was calculated using the following formula:

$$B_{jk} = \frac{2 \sum_i \min(x_{ij}, x_{ik})}{\sum_i (x_{ij} + x_{ik})}$$

where  $B_{jk}$  (for normal analysis) is the similarity between samples  $j$  and  $k$ ;  $x_{ij}$  and  $x_{ik}$  are the abundances of species  $i$  in samples  $j$  and  $k$ .  $B$  ranges from 0.0 when two samples have no species in common to 1.0 when the distribution of individuals among species is identical between samples. For inverse analysis, the  $B_{jk}$  is the similarity between species  $j$  and  $k$ ;  $x_{ij}$  and  $x_{ik}$  are the abundances of species  $j$  and  $k$  in sample  $i$ .

Normal similarity matrices were clustered using the group averaging method of clustering, and inverse similarity matrices were clustered using the flexible sorting method of clustering (Boesch, 1973). Flexible sorting was performed with  $\beta = -0.25$ , a widely accepted value for this analysis (Boesch, 1973). For the additional cluster analyses of individual sand resource areas, normal and inverse similarity matrices were clustered by the group averaging method.

The extent to which sample groups formed by normal cluster analysis of the entire data set could be explained by environmental variables was examined by canonical discriminant analysis (SAS Institute Inc., 1989). Environmental variables used were survey (categorical), water depth, percent gravel, percent sand, and percent fines (percent silt + percent clay). Canonical discriminant analysis identifies the degree of separation among pre-defined groups of variables in multivariate space. This analysis examined the relationships among the environmental variables and the station groups as indicated by the normal cluster analysis.

#### **6.2.4.4 Epifauna and Demersal Ichthyofauna**

Trawl data were summarized by numbers of taxa and number of individuals per tow in each sand resource area. Normal and inverse cluster analyses as described above (Section 6.2.4.3) were used to examine patterns in the epifaunal/demersal ichthyofaunal data set. Both normal and inverse clustering were performed with the group averaging algorithm.

### **6.3 RESULTS**

#### **6.3.1 Water Column**

Temperature, salinity, and dissolved oxygen recorded in surface, middle, and bottom waters of the sand resource areas differed among surveys and sample locations (Appendix D2, Table D2-1). Bottom values for temperature, salinity, and dissolved oxygen for the May and December surveys are shown in Figure 6-7. During the May survey, values for all three parameters indicated some stratification with depth in all sand resource areas. Surface temperatures averaged 25.7°C and ranged from 26.9°C in Area 3 to 24.4°C in Area 1. Middle depth temperatures averaged 22.8°C and ranged from 21.4°C in Area 3 to 23.8°C in Area 5. Bottom temperatures averaged 21.5°C and ranged from 21.2°C in Area 4 to 21.8°C in Area 1. Surface salinities averaged 20.6 ppt and ranged from 17.2 ppt in Area 3 to 27.2 ppt in Area 1. Middle depth salinities averaged 28.9 ppt and ranged from 26.2 ppt in Area 2 to 31.9 ppt in Area 4. Bottom salinities averaged 31.1 ppt and ranged from 28.2 ppt in Area 3 to 33.9 ppt in Area 4. Surface values of dissolved oxygen averaged 5.14 mg/L and ranged from 4.37 mg/L in Area 5 to 7.49 mg/L in Area 1. In middle depths, the values averaged 4.19 mg/L and ranged from 2.07 mg/L in Area 3 to 7.21 mg/L in Area 1. In bottom waters, dissolved oxygen averaged 3.16 mg/L and ranged from 1.22 mg/L in Area 4 to 6.19 mg/L in Area 1.

During the December survey, values for temperature, salinity, and dissolved oxygen revealed much less stratification with depth than was observed during May (Appendix D2, Table D2-2). Surface temperatures averaged 15.6°C and ranged from 14.2°C in Area 5 to 16.9°C in Area 3. Middle depth temperatures averaged 16.1°C and ranged from 14.9°C in Area 2 to 18.1°C in Area 4. Bottom temperatures averaged 16.9°C and ranged from 14.9°C in Area 2 to 18.5°C in Area 4. Salinities in surface waters averaged 30.9 ppt and ranged from 29.2 ppt in Area 5 to 31.7 ppt in Area 3. In middle depths, salinities averaged 31.3 ppt and ranged from 30.2 ppt in Area 5 to 32.0 ppt in Area 4. Bottom salinities averaged 31.7 ppt and ranged from 31.2 in Area 2 to 32.1 ppt in Areas 2 and 5. Surface dissolved oxygen values averaged 7.08 mg/L and ranged from 6.43 mg/L in Area 2 to 7.79 mg/L in Area 1. Middle depth values averaged 6.86 mg/L and ranged from 6.39 mg/L in Area 4 to 7.60 mg/L in Area 1. Bottom values averaged 6.78 mg/L and ranged from 6.37 mg/L in Area 4 to 7.65 mg/L in Area 1.

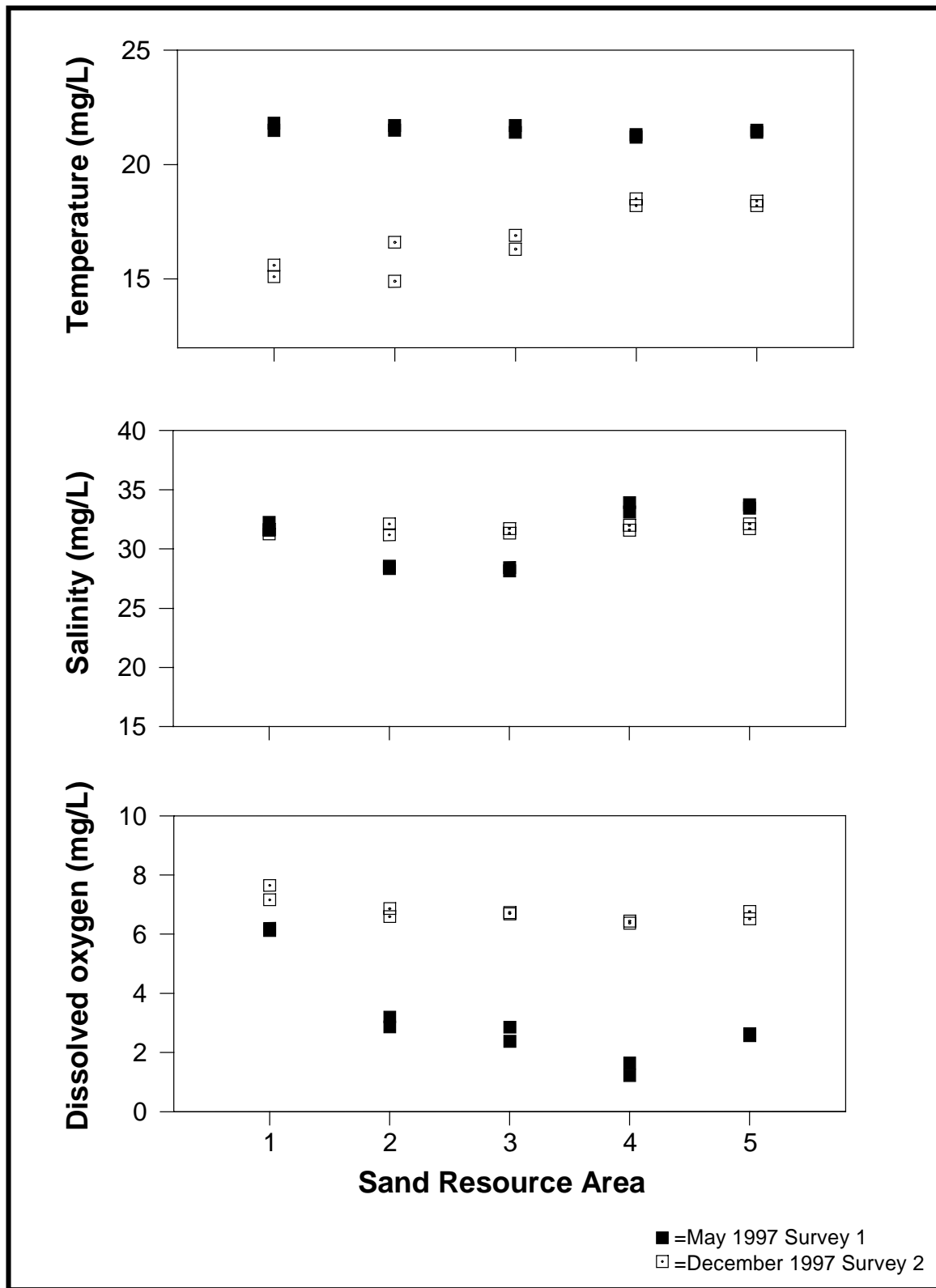


Figure 6-7. Temperature ( $^{\circ}\text{C}$ ), salinity (ppt), and dissolved oxygen (mg/l) measured near-bottom by Hydrolab during May and December 1997 at the five sand resource areas offshore Alabama. Two sets of measurements were made in each sand resource area.

### 6.3.2 Sediment Grain Size

Sediment grain size from the grab samples ranged from sand to mud during Survey 1 (Appendix D3, Table D3-1) and Survey 2 (Appendix D3, Table D3-2). Sand Resource Areas 1, 2, and 3 were primarily sand. In Area 1, all samples contained >95% sand with lesser amounts of gravel and no mud. All but two samples from Area 2 and two samples from Area 3 contained >96% sand with some gravel.

Grain size was much more variable in Area 4, with many stations containing more silt and clay than expected. Ten of the 16 samples within Area 4 during the May survey had sand percentages <90%. Seven of the 16 samples within Area 4 during the December survey had sand percentages <90%. Sediment grain size for Stations 1, 2, and 7, which are located within the primary sand resource site of Area 4, was <90% sand in the May survey, but >90% in the December survey. This may be because the December samples were not taken in exactly the same spot as the May samples, small-scale grain size variability may exist, or physical processes occurred causing winnowing of fine-grained sediment from surface samples. However, grain size at Area 4 Stations 10, 11, 13, and 14 remained <90% sand.

Grain size also was variable in Area 5. Ten of the 16 samples from the May survey in Area 5 had <90% sand. Eight of the 16 samples from the December survey in Area 5 had <90% sand.

Visual observations indicated that the gravity core from Area 4 Station 14 was mud from top to bottom. The same was true for sediment retrieved from Area 4 Station 14 using a Van Veen sampler. Laboratory analyses indicated that all of the Survey 2 grain size samples from Area 4 Station 14 were <60% sand.

### 6.3.3 Infauna

The phylogenetic list of infauna collected in bottom grabs during Surveys 1 (May) and 2 (December) is presented in Appendix D4, Table D4-1, and complete data summaries are provided in Appendix D4, Tables D4-2 through D4-7. For both surveys combined, 91,964 individuals were collected, representing 834 taxa in 13 separate phyla. Infauna were more abundant during the May survey, when 64,613 individuals (70% of the project total) were collected. Three hundred ninety-four taxa (47% of the project total) were common to both surveys. Of those taxa found in just one of the two surveys, 70% (308 taxa) were sampled during the May cruise. Numerical dominants were the gastropods *Caecum pulchellum* and *C. cooperi*, which represented 24% and 9%, respectively, of all infauna censused over both surveys.

Numerically dominant taxa sampled during the May survey (Table 6-2) were *C. pulchellum* (25% of all individuals collected during the May survey), *C. cooperi* (10%), unidentified bivalve mollusks (5%), and the spionid polychaetes *Paraprionospio pinnata* (4.5%) and *Spiophanes bombyx* (4%). Most *C. pulchellum* and *C. cooperi* occurred in the easternmost areas during the May survey, with 99.6% of these individuals sampled from Areas 1, 2, and 3. Densities of these two species were particularly high in Areas 1 and 2. Areas 4 and 5 were numerically dominated by *P. pinnata* (28% and 11% of collected individuals, respectively) and the capitellid polychaete *Mediomastus* (lowest practical identification level [LPIL]) (12% and 4%, respectively) during the May survey.

Numerically dominant taxa collected during the December survey (Table 6-2) were *C. pulchellum* (21% of all individuals collected during the December survey), the archiannelid *Polygordius* (LPIL) (8%), *C. cooperi* (7%), the polychaete *Scoletoma verrilli* (3%), and the amphipod *Eudevenopus hondurans* (3%). As was the case during the May survey, *C. pulchellum* and *C. cooperi* were obtained nearly exclusively from the easternmost areas, with 99.8% of these individuals sampled from Areas 1, 2, and 3, and again were particularly abundant in Areas 1 and 2. Area 4 was numerically dominated by the lancelet *Branchiostoma* (9% of collected individuals) and the polychaetes *Armandia maculata* (7%), *Mediomastus* (LPIL) (7%), and *Nereis micromma*

Table 6-2. Five most abundant infaunal taxa from samples collected during the May 1997 Survey 1 and December 1997 Survey 2 in the five sand resource areas offshore Alabama.					
May 1997			December 1997		
Area	Taxonomic Name	Count	Area	Taxonomic Name	Count
1	<i>Caecum pulchellum</i>	5,866	1	<i>Caecum pulchellum</i>	3,835
	<i>Caecum cooperi</i>	2,296		<i>Caecum cooperi</i>	1,019
	Bivalvia (LPIL)	781		<i>Polygordius</i> (LPIL)	1,001
	<i>Spiophanes bombyx</i>	600		<i>Eudevenopus honduranus</i>	503
	<i>Tellina</i> (LPIL)	379		<i>Scoletoma verrilli</i>	268
2	<i>Caecum pulchellum</i>	9,183	2	<i>Caecum pulchellum</i>	1,737
	<i>Caecum cooperi</i>	3,059		<i>Caecum cooperi</i>	623
	Bivalvia (LPIL)	1,440		<i>Polygordius</i> (LPIL)	615
	<i>Spiophanes bombyx</i>	766		<i>Scoletoma verrilli</i>	357
	<i>Tellina</i> (LPIL)	557		<i>Eudevenopus honduranus</i>	190
3	<i>Caecum pulchellum</i>	960	3	<i>Polygordius</i> (LPIL)	321
	<i>Caecum cooperi</i>	851		<i>Caecum pulchellum</i>	278
	<i>Spiophanes bombyx</i>	772		<i>Caecum cooperi</i>	244
	Bivalvia (LPIL)	717		<i>Oligochaeta</i> (LPIL)	165
	<i>Mediomastus</i> (LPIL)	574		<i>Mediomastus</i> (LPIL)	132
4	<i>Paraprionospio pinnata</i>	1,680	4	<i>Branchiostoma</i> (LPIL)	250
	<i>Mediomastus</i> (LPIL)	729		<i>Armandia maculata</i>	209
	<i>Spiophanes bombyx</i>	243		<i>Nereis micromma</i>	201
	<i>Apoprionospio pygmaea</i>	202		<i>Mediomastus</i> (LPIL)	199
	<i>Magelona sp.H</i>	198		<i>Magelona sp.H</i>	172
5	<i>Paraprionospio pinnata</i>	561	5	<i>Nereis micromma</i>	341
	Bivalvia (LPIL)	225		<i>Mediomastus</i> (LPIL)	211
	<i>Mediomastus</i> (LPIL)	192		<i>Armandia maculata</i>	205
	<i>Aricidea taylori</i>	189		<i>Phascolion strombi</i>	103
	<i>Polygordius</i> (LPIL)	149		<i>Aricidea taylori</i>	75
May Total	<i>Caecum pulchellum</i>	16,042	December Total	<i>Caecum pulchellum</i>	5,855
	<i>Caecum cooperi</i>	6,254		<i>Polygordius</i> (LPIL)	2,065
	Bivalvia (LPIL)	3,238		<i>Caecum cooperi</i>	1,899
	<i>Paraprionospio pinnata</i>	2,901		<i>Scoletoma verrilli</i>	894
	<i>Spiophanes bombyx</i>	2,487		<i>Eudevenopus honduranus</i>	835

LPIL = Lowest practical identification level.

(7%). Area 5 was numerically dominated by *N. micromma* (14%), *Mediomastus* sp. (9%), and *A. maculata* (8%).

Table 6-3 summarizes the number of taxa, number of individuals, density, species diversity, evenness, and richness for each sand resource area during the May and December surveys. During the May survey, the mean number of taxa per station was highest in Area 3 (99 taxa), while Area 1 stations averaged the highest number of taxa (67) in the December survey. The highest number of infaunal taxa collected from a single station was collected at Station 20 in Area 2 (126) during the May survey and at Station 19 in Area 1 (116) in the December survey. During both the May and December surveys, the mean number of taxa per station was lowest in Area 4, with values

Table 6-3. Summary of infaunal statistics by survey and sand resource area offshore Alabama.

May 1997 (Survey 1)												
Area	No. of Taxa		No. of Individuals		Density (individuals/m <sup>2</sup> )		H' Diversity		J' Evenness		D Richness	
	Mean Per Station	Standard Deviation	Mean Per Station	Standard Deviation	Mean Per Station	Standard Deviation	Mean Per Station	Standard Deviation	Mean Per Station	Standard Deviation	Mean Per Station	Standard Deviation
1	84	18	838	503	8,384	5,031	2.96	0.61	0.67	0.14	12.69	2.14
2	95	15	1,182	527	11,823	5,274	2.78	0.61	0.61	0.13	13.54	2.05
3	99	21	643	286	6,433	2,858	3.66	0.41	0.80	0.07	15.21	2.75
4	49	13	305	146	3,046	1,464	2.82	0.74	0.72	0.15	8.52	2.35
5	62	20	262	158	2,622	1,582	3.32	0.55	0.81	0.08	11.01	3.02
December 1997 (Survey 2)												
Area	No. of Taxa		No. of Individuals		Density (individuals/m <sup>2</sup> )		H' Diversity		J' Evenness		D Richness	
	Mean Per Station	Standard Deviation	Mean Per Station	Standard Deviation	Mean Per Station	Standard Deviation	Mean Per Station	Standard Deviation	Mean Per Station	Standard Deviation	Mean Per Station	Standard Deviation
1	67	20	571	389	5,714	3,891	2.97	0.59	0.71	0.13	10.63	2.97
2	57	18	345	187	3,447	1,867	2.93	0.36	0.73	0.08	9.69	2.40
3	47	11	184	83	1,839	831	3.20	0.25	0.84	0.06	8.99	1.53
4	35	12	145	73	1,449	725	2.83	0.41	0.81	0.09	6.85	1.90
5	36	15	123	60	1,229	603	2.85	0.59	0.81	0.12	7.27	2.51

of 49 and 35 taxa, respectively. The lowest number of infaunal taxa collected from a single station was collected in Area 5 during both the May (17) and December (15) cruises at Stations 13 and 3, respectively.

During the May survey, highest infaunal abundances were sampled from Area 2 (station average = 1,182 individuals), while Area 1 yielded the greatest abundances in the December survey (571). The highest number of individuals collected from a single station was sampled from Station 16 in Area 1 in both the May and December surveys, with 2,050 and 1,954 individuals collected, respectively. Areas 4 and 5 yielded the lowest mean abundances in both the May survey (305 and 262, respectively) and December survey (145 and 123, respectively). The fewest number of individuals sampled from a single station during the May survey (117) came from Station 13 in Area 5, while the December survey yielded its lowest count (35) from Station 2 in Area 5.

Mean values of species diversity ( $H'$ ) were similar in all five sand resource areas and between surveys (Table 6-3). Per station averages of species evenness ( $J'$ ) also were similar in the five areas and between surveys. Mean values of species richness ( $D$ ) were significantly higher during the May survey than during the December survey.

During the May survey, mean station values of species diversity and richness were highest in Area 3 (3.66 and 15.21, respectively), while the highest measure of mean species evenness was from Area 5 (0.81) (Table 6-3). Lowest mean values of species diversity and evenness during the May survey were in Area 2 (2.78 and 0.61, respectively). During the December survey, the highest mean values of species diversity and evenness were in Area 3 (3.20 and 0.84, respectively), while the highest measure of mean species richness was from Area 1 (10.63). During the December survey, the lowest mean values of species diversity and evenness were from Area 4 (2.83) and Area 1 (0.71), respectively. Lowest mean values of species richness were from Area 4 in both the May (8.52) and December (6.85) surveys.

## Cluster Analysis

Patterns of infaunal similarity among stations were examined with cluster analysis. When examined over both surveys, normal cluster analysis produced six groups (Groups A through F) of stations that were similar with respect to species composition and relative abundance (Appendix D4, Table D4-8). Cluster analysis revealed a strong seasonal effect. With the exception of station Group E, which consisted of stations sampled during both surveys, station groups were comprised of samples collected exclusively during one of the two surveys (Figure 6-8). Three of the six station groups were each represented by few stations, primarily in Areas 4 and 5, and were characterized by low abundance during the May (Group A) and December (D and F) cruises. Station Groups B and C represent the *Caecum*-associated assemblages sampled from Areas 1, 2, and 3 during the May and December surveys, respectively. Group E stations were represented in Areas 4 and 5 during both surveys, and were dominated with respect to the number of taxa and abundance by polychaetous annelids, especially *Mediomastus* and *P. pinnata*. Sediment grain size characteristics for all infaunal sampling stations indicate that, except for Station Group E, sedimentary regime is homogeneous within station groupings (Figure 6-9).

Inverse cluster analysis resulted in 13 groups of taxa (Groups 1 through 13) that reflected their co-occurrence in station samples (Table 6-4). Many of these species groups were dominated either by molluscan or crustacean taxa, or by a combination of both of these taxa. Species Groups 3, 5, 6, 8, and 12 were made up primarily or exclusively of molluscan taxa, while amphipod and ostracod crustaceans dominated Group 2. Species Groups 1, 10, 11, and 13 were comprised of a mixture of crustaceans, molluscans, and polychaetes, while Groups 4, 7, and 9 were dominated by polychaete taxa. These latter species groups generally were associated with the western areas (Station Group E), while the remainder of the species groups were found primarily in the eastern half of the study area (Station Groups B and C).

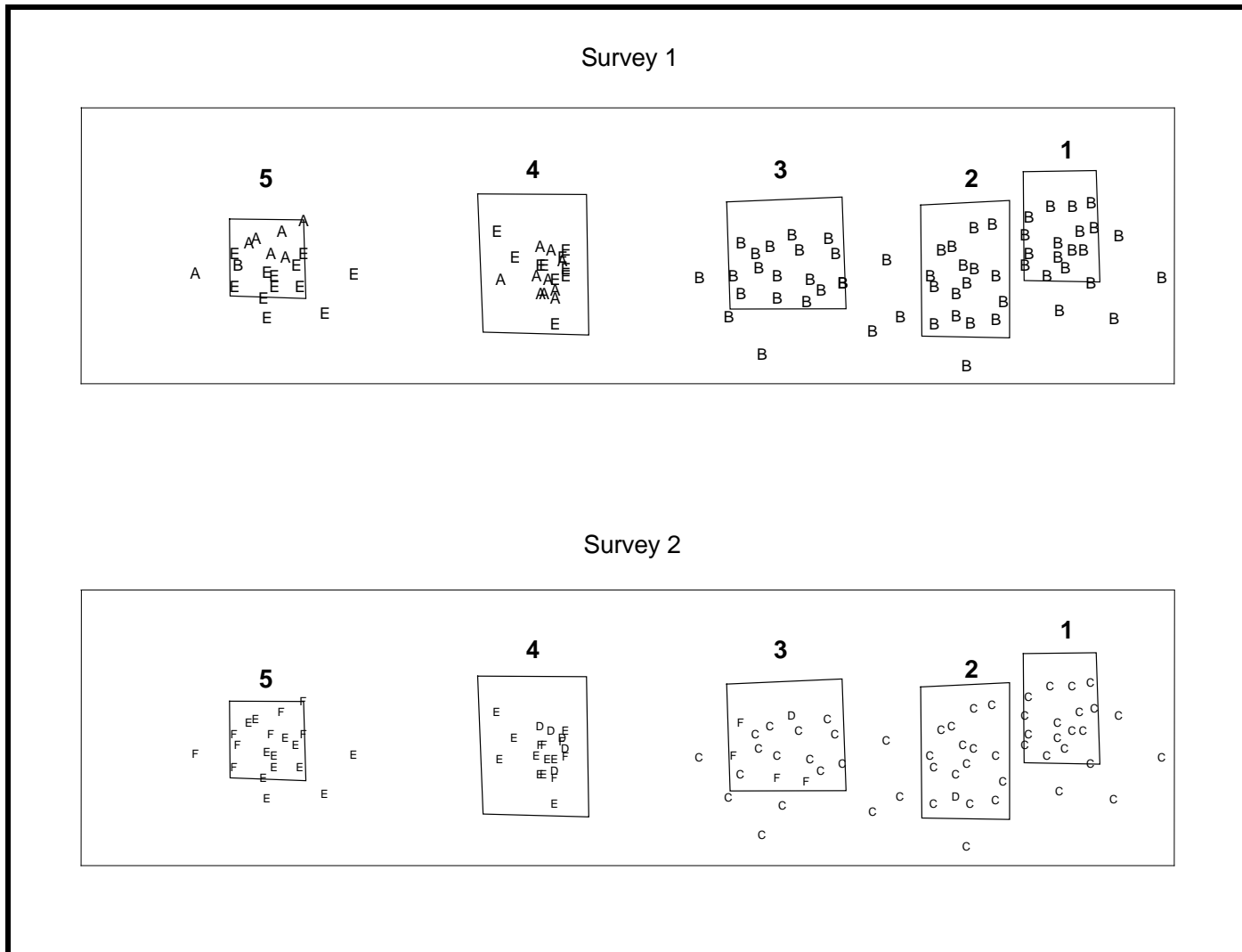


Figure 6-8. Station groupings (A to F) based on normal cluster analysis of infaunal samples collected during the May 1997 Survey 1 and December 1997 Survey 2 in the five sand resources areas (1 to 5) offshore Alabama.

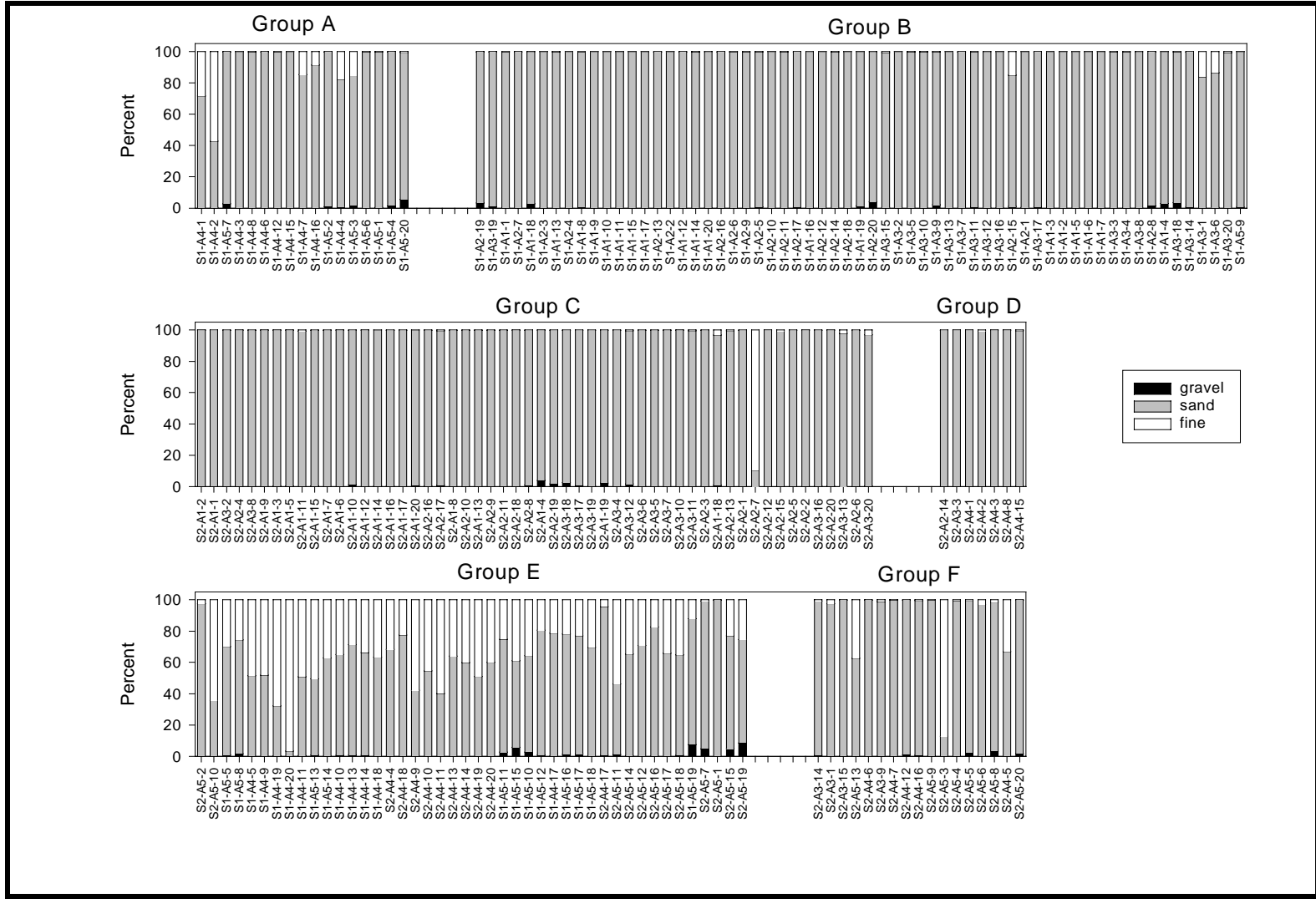


Figure 6-9. Grain size composition of infaunal samples collected during the May 1997 Survey 1 and December 1997 Survey 2 in the five sand resource areas offshore Alabama. Sample order and Groups A-F are based on normal cluster analysis.

Table 6-4. Infaunal species groups resolved from inverse cluster analysis of all samples collected during the May 1997 Survey 1 and December 1997 Survey 2 in the five sand resource areas offshore Alabama.

**GROUP 1**

*Caecum pulchellum*  
*Caecum cooperi*  
*Armanda maculata*  
*Eudevenopus honduranus*  
*Metharpinia floridana*  
*Spiophanes bombyx*  
*Prionospio cristata*  
*Nephtys picta*  
*Tectonatica pusilla*  
*Apoprionospio pygmaea*  
*Ervilia concentrica*  
*Acteocina candei*

**GROUP 2**

*Aricidea wassi*  
*Monticellina dorsobranchialis*  
*Acanthohaustorius uncinus*  
*Eusarsiella childi*  
*Asteropterygion oculitristis*  
*Haplocytheridea setipunctata*  
*Ampelisca agassizi*  
*Listriella barnardi*  
*Olivella dealbata*

**GROUP 3**

*Pythinella cuneata*  
*Golfingia* sp. V  
*Nuculana acuta*  
*Nassaricus albus*  
*Anachis obesa*  
*Argissa hamatipes*

**GROUP 4**

*Nereis micromma*  
*Magelona* sp. H  
*Phascolion strombi*  
*Paraprionospio pinnata*  
*Scoletoma verrilli*  
*Aspidosiphon albus*  
*Ampelisca* sp. A  
*Glycinde solitaria*  
*Aricidea taylori*  
*Cossura soyeri*  
*Diopatra cuprea*  
*Scoletoma ernesti*

**GROUP 5**

*Chione latilirata*

**GROUP 6**

*Lucina multilineata*  
*Photis pugnator*  
*Melinna maculata*  
*Lucina nassula*  
*Strombiformis bilineatus*  
*Anadara transversa*  
*Vitrinella floridana*  
*Haminocea succinea*  
*Abra aequalis*  
*Sthenelais* sp. A

**GROUP 7**

*Lumbrineris latreilli*  
*Scoloplos rubra*  
*Tellina versicolor*  
*Spio pettiboneae*  
*Cyclaspis pustulata*  
*Ampharete* sp. A  
*Sigambra tentaculata*  
*Aglaophamus verrilli*  
*Spiophanes* cf. *Missionensis*  
*Eusarsiella texana*  
*Goniada littorea*  
*Paramphinome* sp. B  
*Glycera americana*

**GROUP 8**

*Anomia simplex*  
*Varicorbula operculata*  
*Lyonsia hyalina floridana*  
*Amphictene* sp. A  
*Crassinella martinicensis*  
*Strombiformis hemphilli*  
*Phyllodoce arenae*  
*Rictaxis punctostriatus*  
*Galathowenia oculata*  
*Oxyurostylis smithi*  
*Ampelisca* sp. C  
*Ampelisca bicarinata*  
*Volvulella persimilis*  
*Acteocina bidentata*  
*Spiochaetopterus oculatus*  
*Travisia hobsonae*  
*Crenella divaricata*  
*Philine saga*  
*Chione grus*  
*Pitar fulminatus*  
*Diplodonta punctata*  
*Verticordia ornata*

**GROUP 9**

*Polycirrus* sp. G  
*Cirrophorus branchiatus*  
*Glycera* sp. A  
*Pandora trilineata*  
*Levinsenia* sp. E  
*Nereis succinea*  
*Aspidosiphon muelleri*  
*Glycera* sp. I  
*Brania wellfleetensis*  
*Bhawania heteroseta*  
*Goniadides caroliniae*

**GROUP 10**

*Armandia agilis*  
*Onuphis eremita oculata*  
*Magelona pettiboneae*  
*Linga amiantus*  
*Albunea paretii*  
*Diplodonta semiaspera*  
*Harbansus paucichelatus*  
*Aricidea philbiniae*  
*Antalis eborum*  
*Lumbrineris* sp. D  
*Ceratocephale oculata*  
*Edotia triloba*

**GROUP 11**

*Bogaea enigmatica*  
*Aonides paucibranchiata*  
*Protohaustorius* sp. C  
*Tellina alternata*  
*Chione intapurpurea*  
*Ophelia denticulata*  
*Crassinella lunulata*  
*Cyclaspis* sp. N  
*Strigilla mirabilis*

**GROUP 12**

*Caecum imbricatum*  
*Caecum bipartitum*  
*Natica pusilla*

**GROUP 13**

*Magelona* sp. B  
*Owenia fusiformis*  
*Protohaustorius bousfieldi*  
*Americhelidium americanum*  
*Cyclaspis varians*  
*Semele nuculoides*  
*Cumingia tellinoides*  
*Caecum johnsoni*  
*Synelmis ewingi*  
*Acanthohaustorius intermedius*  
*Glycera* sp. D  
*Caecum nitidum*  
*Cyclaspis* sp. O  
*Pectinaria gouldii*

## Canonical Discriminant Analysis

Data collected during the two surveys were analyzed using canonical discriminant analysis to determine which environmental factors most affected the distribution of the infaunal assemblages. The first two canonical discriminant variates were used to analyze variability among those station groups identified by normal cluster analysis as being similar with respect to species composition and relative abundance. The first canonical variate strongly correlated with survey (0.9867). Within surveys, the second canonical variate correlated well with percent sand (0.9024), percent fine sediments (-0.8857), and to a lesser degree with station depth (0.6118).

The selection of any sand resource area as a sediment source for nourishment projects will be based largely on its environmental characteristics. Patterns of infaunal similarity among stations (normal cluster analysis) and the co-occurrence of taxa within samples (inverse cluster analysis) were therefore examined for each sand resource area. The following describes the results of this area-by-area analysis for each survey, as well as the affinities of the station groups and species groups identified by cluster analyses.

### Area 1

Normal cluster analysis resulted in two station groups (Groups A and B) in Area 1 that were separated entirely by survey (Figure 6-10). Group A consisted of all 20 stations sampled during May, while Group B was comprised of all Area 1 stations sampled during December. Differences in assemblage composition between the two station groups were evident both in the relative densities of taxa common to both surveys and also in the presence of particular taxa within either station group. Group A stations yielded relatively high numbers of the bivalves *Chione* (LPIL), *Ervilia concentrica*, and *Tellina* (LPIL) and the spionid polychaetes *Paraprionospio pinnata*, *Prionospio cristata*, and *Spiophanes bombyx*. The amphipod *Protohaustorius bousfieldi* and the bivalves *Anomia simplex* and *Nearomya* (LPIL) were exclusive to Group A stations. Group B stations yielded relatively high numbers of the amphipod *Ampelisca agassizi*, the archiannelid *Polygordius* (LPIL), and the ostracod *Haplocytheridea setipunctata*. Certain polychaetes were relatively more abundant in Group B stations as well, including *Armandia maculata*, *Aricidea wassi*, and *Scoletoma verrilli*. Taxa collected exclusively during the December survey (Group B) included the amphipod *Protohaustorius* sp. C, the bivalve *T. alternata*, the echinoid *Encope* (LPIL), and the polychaete *Aonides paucibranchiata* (Table 6-5).

Inverse cluster analysis produced four groups of taxa (Groups 1 through 4) that reflected their co-occurrence in samples collected in Area 1 (Figure 6-11). Species Groups 1 and 2 were characterized by a single taxon and by a pair of co-occurring taxa, respectively, that were rare in samples. Group 1 was represented by the gastropod *Caecum nitidum*. Group 2 included a pair of the molluscan taxa (*C. imbricatum* and *Nearomya*) that were found predominantly at a single station. Group 3 represented the *Caecum cooperi* and *C. pulchellum*-associated assemblage. Along with those two numerically dominant taxa, Group 3 included the amphipods *A. agassizi*, *Eudevenopus honduranus*, and *Metharpinia floridana*, the lancelet *Branchiostoma*, the polychaetes *A. maculata*, *A. wassi*, *Nephtys picta*, and *Scoletoma verrilli*, and the archiannelid *Polygordius*. Species Group 4 taxa included the amphipod *Protohaustorius bousfieldi*, the bivalves *A. simplex*, *Chione* (LPIL), *E. concentrica*, and *Tellina* (LPIL), the gastropods *Caecum johnsoni* and *Acteocina candei*, and the polychaetes *P. pinnata*, *P. cristata*, *Monticellina dorsobranchialis*, and *S. bombyx* (Table 6-5).

Sediment texture was characterized as slightly gravelly sand at all Area 1 stations during both surveys. The spatial homogeneity of sediment composition was reflected in the broad distribution of the *Caecum*-associated assemblage (Species Group 3) in this area, especially during the December survey (Station Group B). Because area sediment composition was spatially homogeneous, some other environmental factor(s) presumably had a greater influence on those

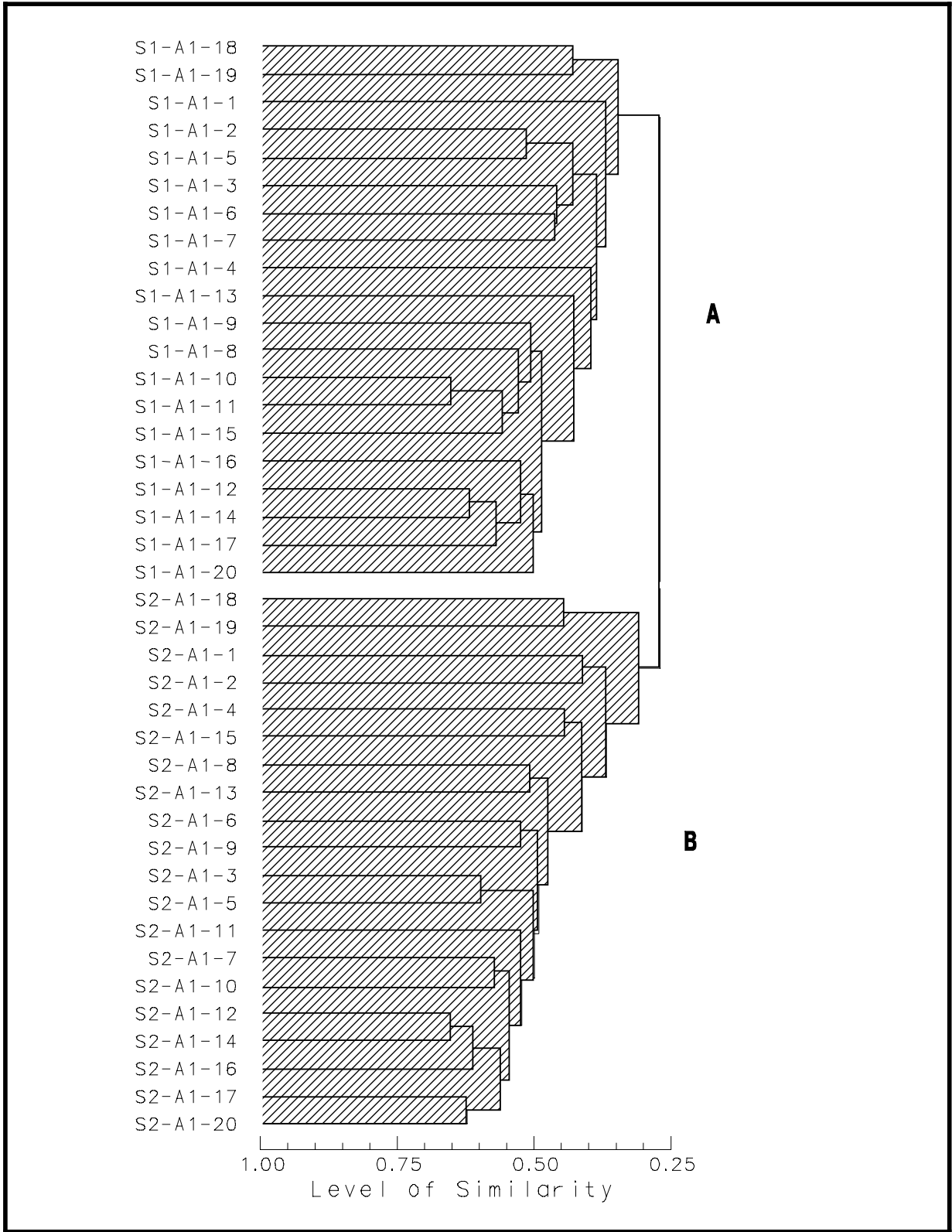


Figure 6-10. Normal cluster analysis of infaunal samples collected during the May 1997 Survey 1 (S1) and December 1997 Survey (S2) in Sand Resource Area 1 offshore Alabama.



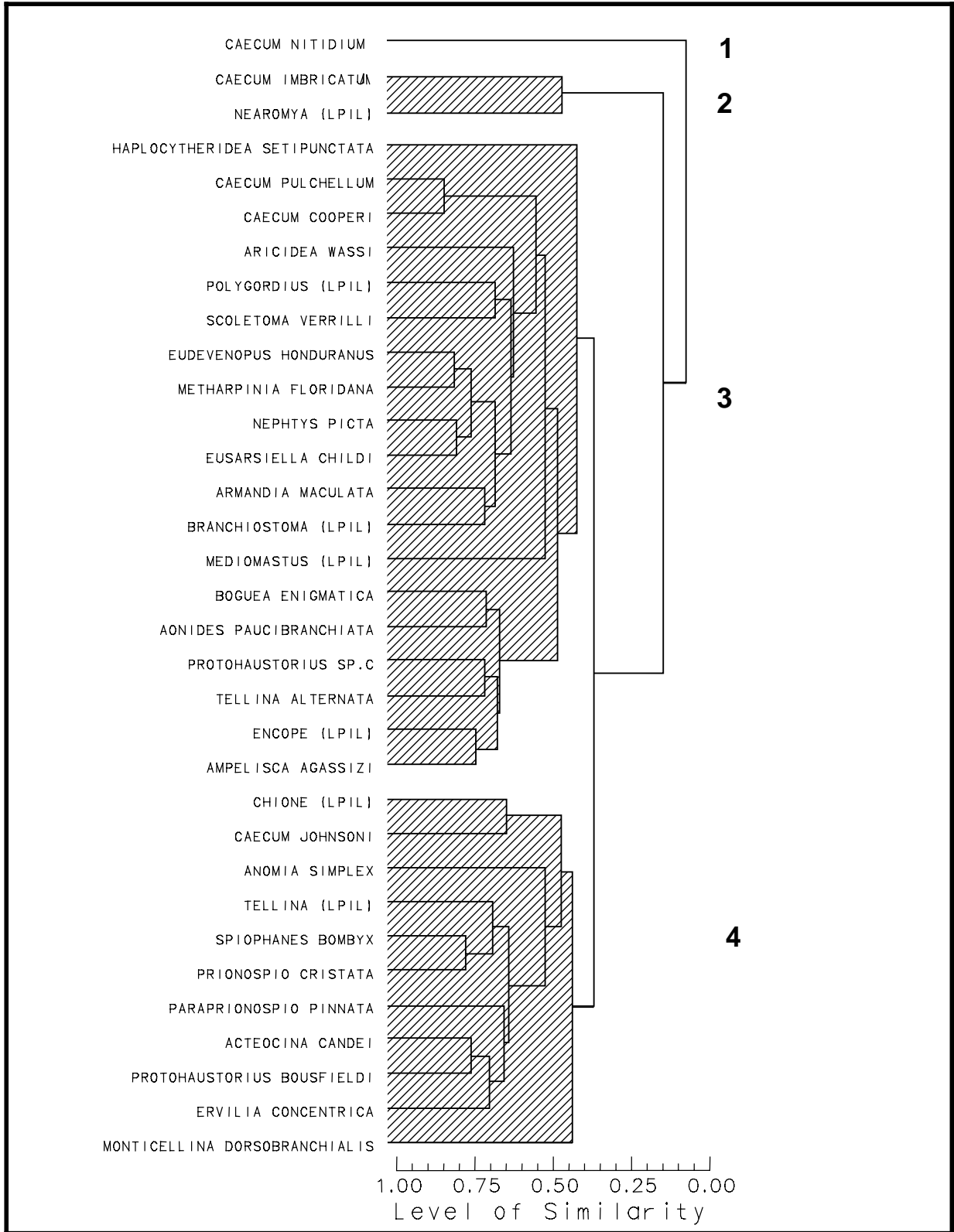


Figure 6-11. Inverse cluster analysis of infaunal taxa from samples collected during the May 1997 Survey 1 and December 1997 Survey 2 in Sand Resource Area 1 offshore Alabama.

differences in assemblage distribution and composition that were indicated by station groupings generated from normal analysis. Canonical discriminant analysis indicated that after season and sediment composition, depth was the environmental factor that most affected the distribution of the infaunal assemblages censused during the present study. Some indication of a depth factor was apparent in Area 1, with the two deepest stations [Stations 18 (21 m) and 19 (23 m)] closely associated with one another within station groupings (Table 6-5). These two stations also were the most dissimilar to other stations. The average depth at Area 1 stations was 14 m.

## Area 2

Station groupings in Area 2 were defined by survey, and normal cluster analysis resulted in three station groups (Groups A through C) (Figure 6-12). Group A consisted of one station during the September survey that was depauperate both in numbers of taxa and individual abundance. Station Group B was comprised of all Area 2 stations sampled during May. This group was distinguished by relatively high abundances of most of the numerically dominant taxa collected from Area 2. In addition to *C. cooperi* and *C. pulchellum*, the bivalves *Chione*, *E. concentrica*, *Lyonsia hyalina floridana*, and *Tellina*, and the polychaetes *Amphictene* sp. A, *N. picta*, *P. cristata*, *P. pinnata*, and *S. bombyx* were relatively abundant in Station Group B. The bivalves *A. simplex* and *Varicorbula operculata* were exclusive to the May survey (Group B). Station Group C was further distinguished from Group B by yielding relatively high abundances of *Polygordius* and the ostracod *Haplocytheridea setipunctata*.

Inverse cluster analysis produced three species groups (1 through 3) from the surveys of Area 2 (Figure 6-13). Group 1 was comprised of three co-occurring taxa: *Branchiostoma*, *C. johnsoni*, and the sipunculid *Aspidosiphon mulleri*. Group 2 was represented only by *V. operculata*, which did not show any pattern of association with other numerically dominant taxa. Species Group 3 was the *Caecum*-associated assemblage, and included 21 of the 25 numerically dominant taxa collected from Area 2. Taxa included in this group were mostly polychaetes, including *A. pygmaea*, *Amphictene* sp. A, *Aricidea wassi*, *A. maculata*, *M. dorsobranchialis*, *Mediomastus*, *N. picta*, *P. cristata*, *P. pinnata*, *S. bombyx*, and *S. verrilli*. Bivalves were well represented in Group 3, including *A. simplex*, *Chione* (LPIL), *E. concentrica*, *L.h. floridana*, *Tellina*, and *V. operculata*. Other taxa included in Group 3 were *A. candei*, *M. floridana*, and *Polygordius* (Table 6-6).

As in Area 1, Area 2 stations were characterized by slightly gravelly sand. The spatial homogeneity of sediment composition was reflected in the broad distribution of the *Caecum*-associated assemblage (Group 3) during both surveys. Two stations (8 and 19) were closely associated within station groups (surveys) and also were most dissimilar to other stations (Table 6-6). These stations had depths of 12 and 13 m, respectively, compared to a station average of 14 m in Area 2.

## Area 3

As in Areas 1 and 2, station groupings in Area 3 were separated by survey (Figure 6-14). Normal cluster analysis resulted in two station groups (Groups A and B). Group A was comprised of 19 of the 20 Area 1 stations sampled during May and yielded generally higher abundances than did stations in Group B. Taxa found at higher densities in Group A relative to Group B included the molluscs *C. johnsoni*, *Pythinella cuneata*, and *Semele nuculoides*, the polychaetes *N. picta*, *P. cristata*, *P. pinnata*, and *S. bombyx*, and the sipunculid *Golfingia* sp. V. Several taxa were found nearly exclusively at Group A stations, including the molluscs *Chione*, *L. h. floridana*, and *V. persimilis* and the polychaetes *Ampharete* sp. A and *Phyllodoce arenae* (Table 6-7). The polychaete *Nereis micromma* was collected almost exclusively in Group B stations. The echinoid *Encope* (LPIL) was collected only from Group B stations (December survey).

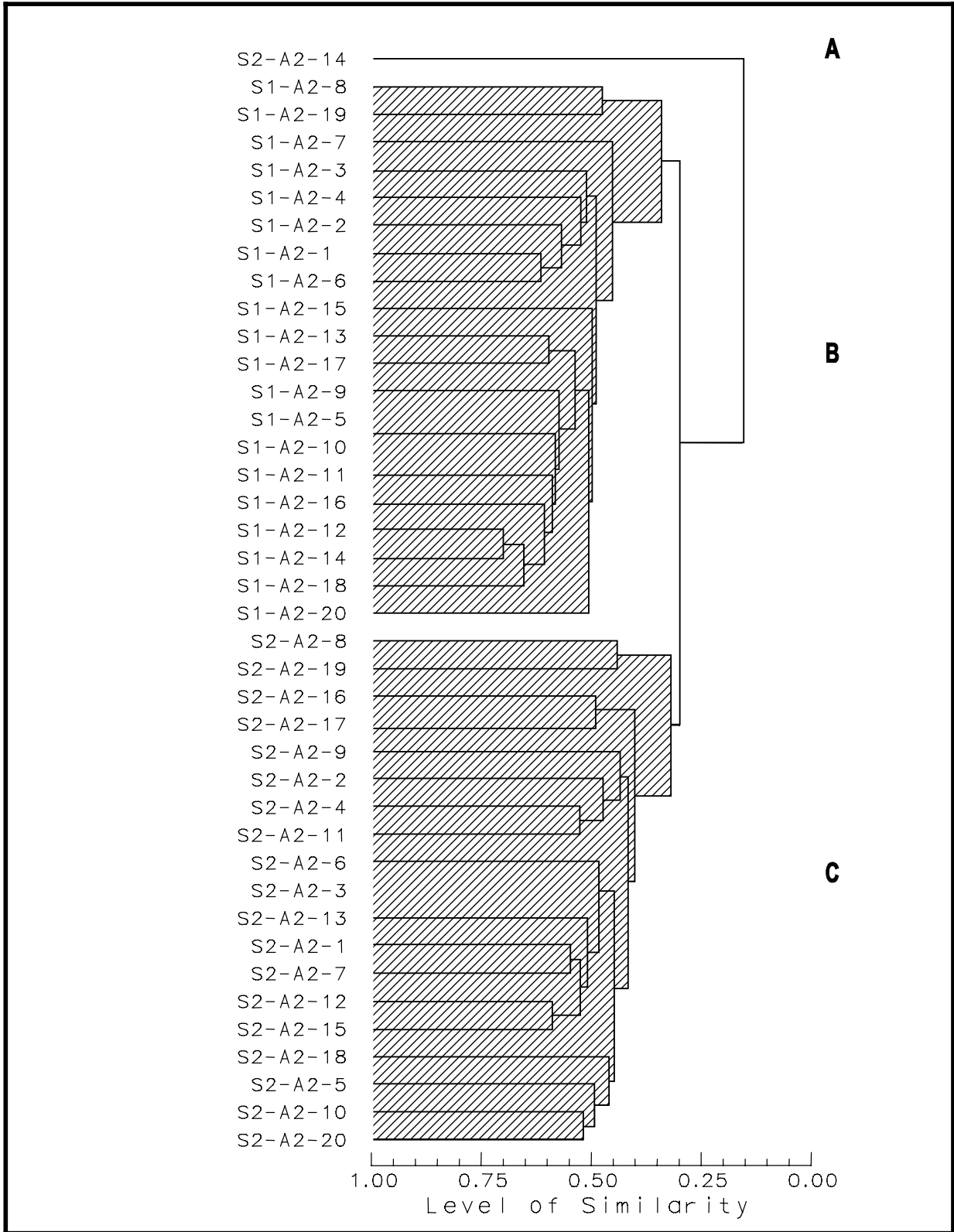


Figure 6-12. Normal cluster analysis of infaunal samples collected during the May 1997 Survey 1(S1) and December 1997 Survey 2 (S2) in Sand Resource Area 2 offshore Alabama.

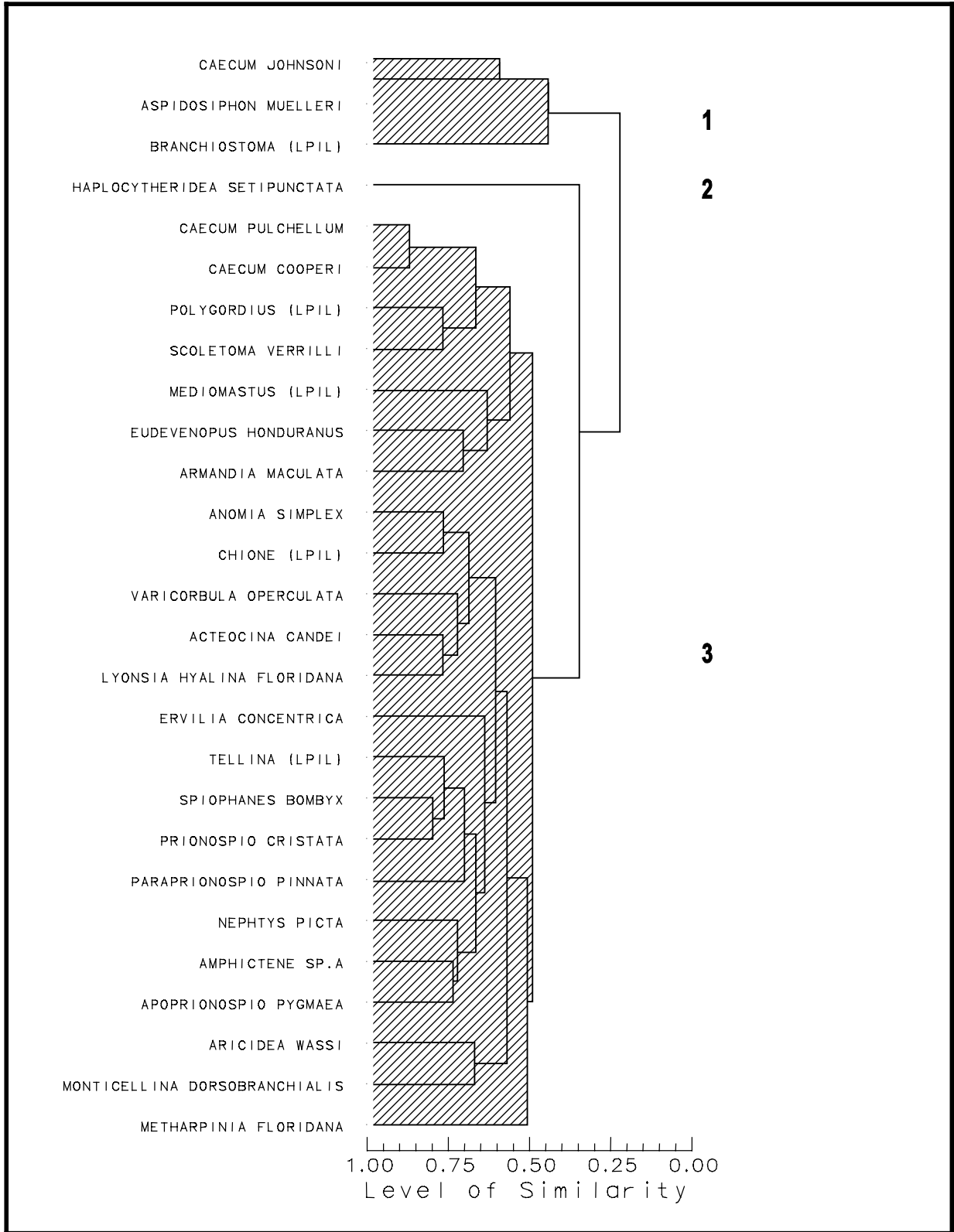


Figure 6-13. Inverse cluster analysis of infaunal taxa from samples collected during the May 1997 Survey 1 and December 1997 Survey 2 in Sand Resource Area 2 offshore Alabama.



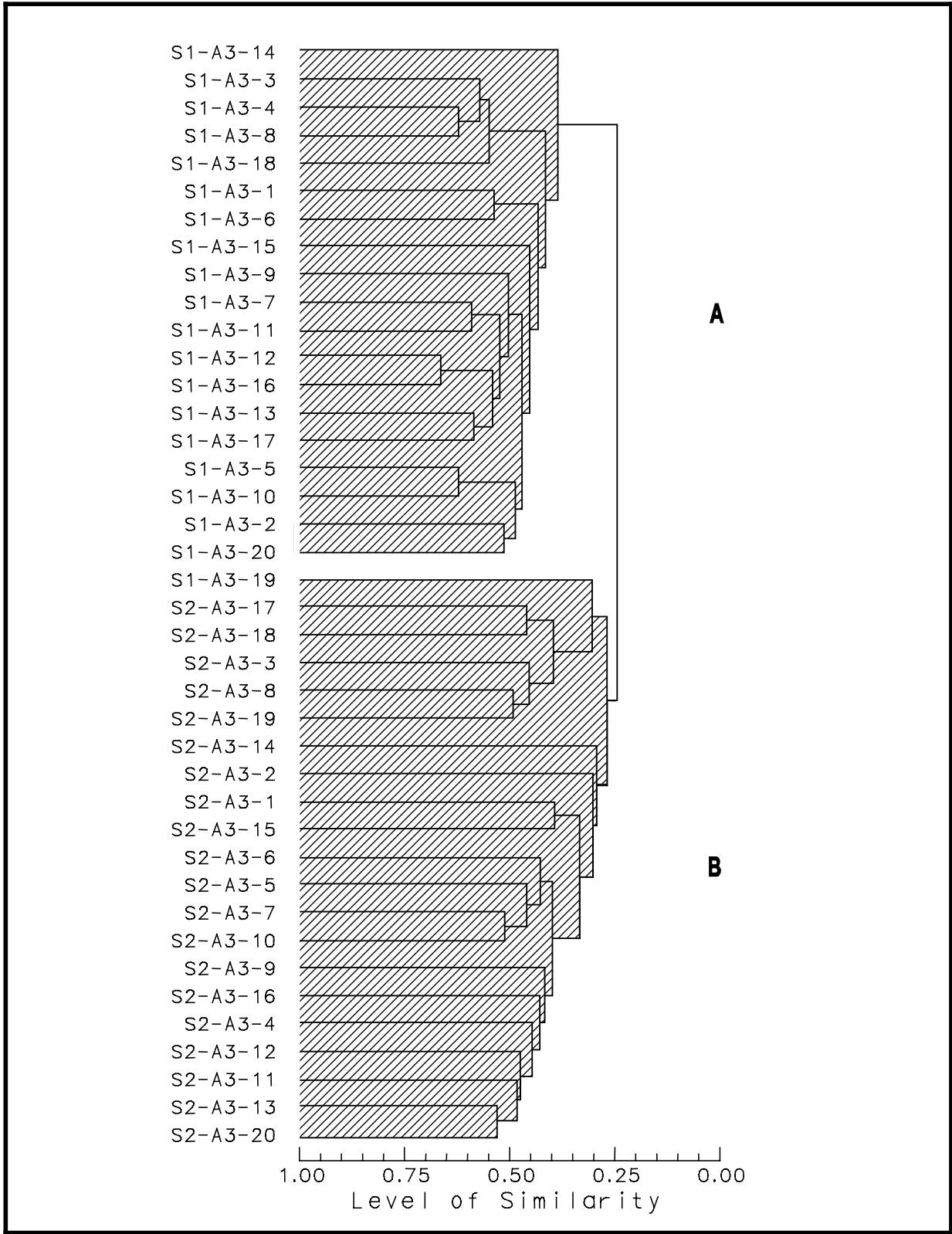


Figure 6-14. Normal cluster analysis of infaunal samples collected during the May 1997 Survey (S1) and December 1997 Survey 2 (S2) in Sand Resource Area 3 offshore Alabama.



Four groups of taxa (Groups 1 through 4) were observed in Area 3 (Figure 6-15). Species Groups 1 and 2 each were characterized by a single taxon that showed no pattern of association with other taxa: *Encope* (Group 1) and *N. micromma* (Group 2). These two groups were collected mostly during the December survey. A co-occurring pair of molluscan taxa (*C. johnsoni* and *S. nukuloides*) collected primarily during the May survey represented Species Group 3. Twenty-nine of the 33 numerically dominant taxa collected from Area 3 were included in Group 4. In addition to the gastropods *C. cooperi* and *C. pulchellum*, this group consisted of annelids (12 taxa), bivalves (5), other gastropods (3), crustaceans (3), *Polygordius*, and miscellaneous taxa, including *Branchiostoma* and the sipunculids *Phascolion strombi* and *Golfingia* sp. V (Table 6-7).

Area 3 stations were fairly consistent with respect to sediment texture. There was some variability in sediment composition in Area 3 during the May survey (Station Group A), with two stations (1 and 6) characterized by slightly gravelly muddy sand, compared to slightly gravelly sand at all other stations. Those two stations yielded relatively high numbers of *Mediomastus* (LPIL), *P. strombi*, and the polychaete *Sigambra tentaculata* relative to other Area 3 stations. Station water depth also may have influenced assemblage composition in Area 3. May survey Stations 3, 4, 8, and 18 were closely associated within Station Group A and had depths averaging 11.5 m. These stations yielded high densities of *C. johnsoni* and *S. nukuloides* (Species Group 3). The remaining Group A stations had an average depth of 14.2 m.

#### Area 4

Three station groups (Groups A through C) were identified by normal cluster analysis (Figure 6-16). Groups A and B were comprised of the same stations sampled during the May and December surveys, respectively. Group C included stations from both surveys. Station Group A (nine stations) was distinguished from other groups by yielding relatively high numbers of the polychaetes *A. pygmaea*, *Magelona* sp. B, and *S. bombyx*. Group B yielded relatively high numbers of *A. maculata* and *Branchiostoma*. Groups A and B both yielded low numbers of several of the numerically dominant taxa found at Group C stations (Table 6-8). Group C taxa were mostly polychaetes, including *Aricidea taylori*, *Cossura soyeri*, *Diopatra cuprea*, *Glycinde solitaria*, *Magelona* sp. H, *Mediomastus*, *N. micromma*, *P. pinnata*, *S. tentaculata*, and *Scoletoma verrilli*. Other Group C taxa included *Ampelisca* sp. A and the rhynchocoel *Tubulanus*.

Inverse cluster analysis delineated three groups of co-occurring taxa (Groups 1 through 3) in Area 4 (Figure 6-17). Group 1 was represented by the acorn worm *Balanoglossus* (LPIL) and showed no pattern of association with other taxa. Species Group 2 included the amphipods *E. honduranus* and *Protohaustorius bousfieldi*, the bivalves *Chione* and *E. concentrica*, *Branchiostoma*, the decapod *Pagurus* (LPIL), the gastropod *Nassarius albus*, the polychaetes *A. pygmaea*, *Magelona* sp. B, and *S. bombyx*, and *Polygordius*. Species Group 3 was comprised predominantly of polychaetes, including *Magelona* sp. H, *Mediomastus* (LPIL), *N. micromma*, *P. pinnata*, *S. tentaculata*, and *S. verrilli* (Table 6-8).

Sediment composition in Area 4 stations was variable during both surveys. Species groups were clearly associated with particular station groupings. Those Area 4 stations with slightly gravelly sand (Station Groups A and B) supported amphipods, lancelet, pagurid decapods, polychaetes such as *A. pygmaea*, *Magelona* sp. B, and *S. bombyx*, and *Polygordius* (Species Group 2). Those stations with slightly gravelly muddy sand, muddy sand, slightly gravelly sandy mud, or clayey sand (Station Group C) yielded a preponderance of polychaetes, including *Magelona* sp. H, *Mediomastus*, and *P. pinnata* (Species Group 3) (Table 6-8). No relationship between the composition of infaunal assemblages and station depth was apparent in Area 4.

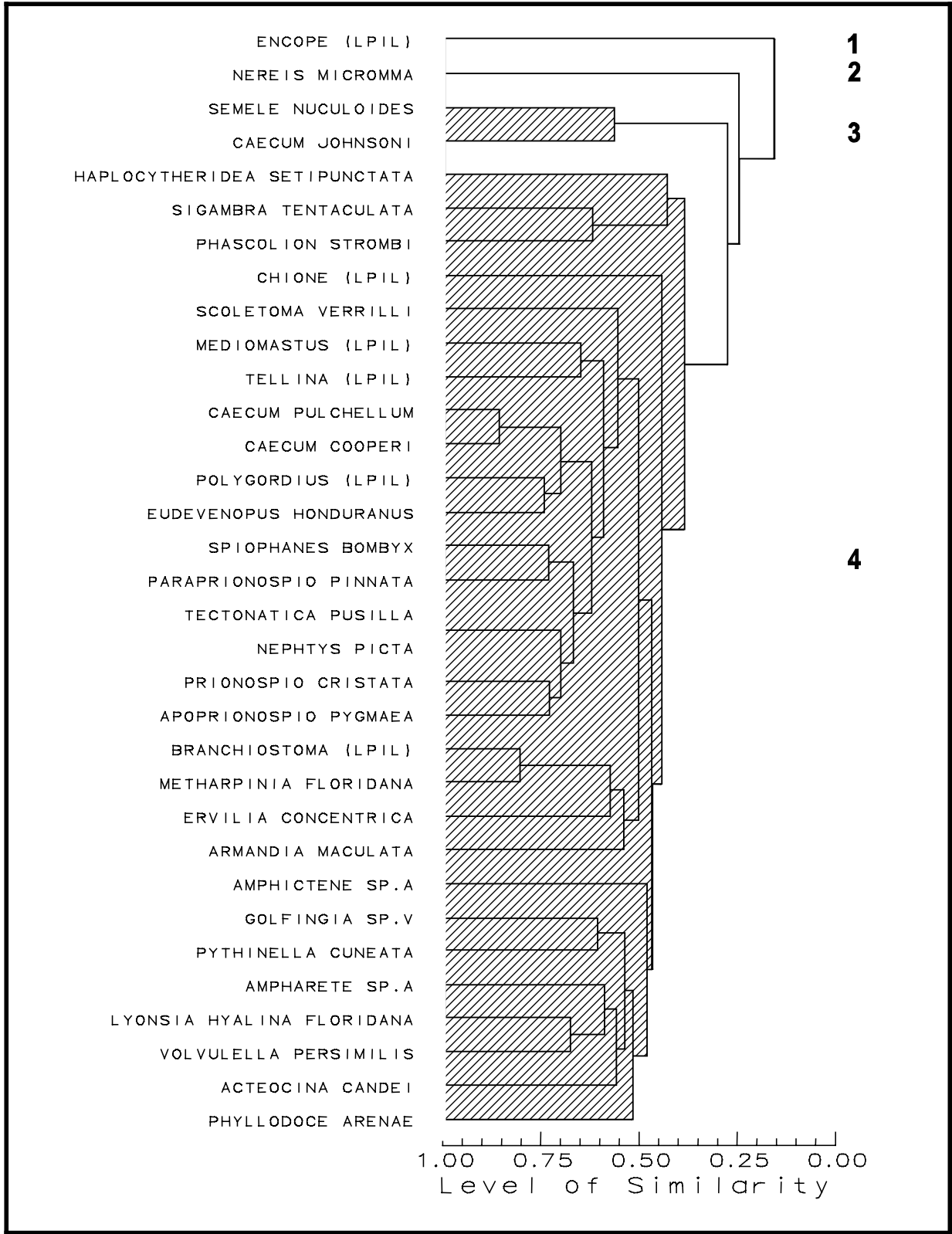


Figure 6-15. Inverse cluster analysis of infaunal taxa from samples collected during the May 1997 Survey 1 and December 1997 Survey 2 in Sand Resource Area 3 offshore Alabama.

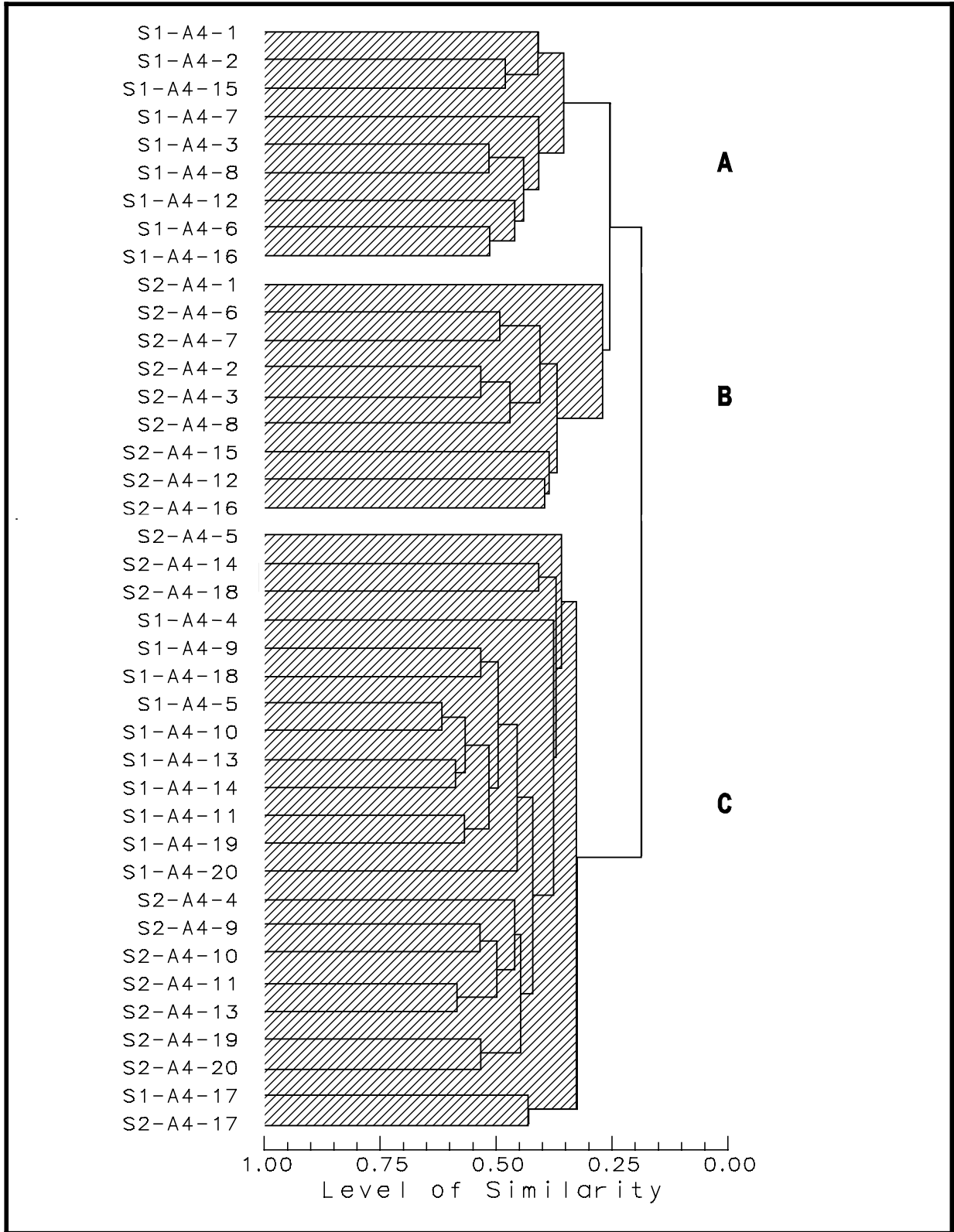


Figure 6-16. Normal cluster analysis of infaunal samples collected during the May 1997 Survey 1 (S1) and December 1997 Survey 2 (S2) in Sand Resource Area 4 offshore Alabama.

Table 6-8. Two-way matrix from cluster analysis of infaunal samples collected during the May 1997 Survey 1 (S1) and December 1997 Survey 2 (S2) in Sand Resource Area 4 offshore Alabama.

TAXA	STATION GROUPS																																												
	A										B										C																								
	S1- A4- 1	S1- A4- 2	S1- A4- 15	S1- A4- 7	S1- A4- 3	S1- A4- 8	S1- A4- 12	S1- A4- 6	S1- A4- 16	S2- A4- 1	S2- A4- 6	S2- A4- 7	S2- A4- 2	S2- A4- 3	S2- A4- 8	S2- A4- 15	S2- A4- 12	S2- A4- 16	S2- A4- 5	S2- A4- 14	S2- A4- 18	S1- A4- 4	S1- A4- 9	S1- A4- 18	S1- A4- 5	S1- A4- 10	S1- A4- 13	S1- A4- 14	S1- A4- 11	S1- A4- 19	S1- A4- 20	S2- A4- 4	S2- A4- 9	S2- A4- 10	S2- A4- 11	S2- A4- 13	S2- A4- 19	S2- A4- 20	S1- A4- 17	S2- A4- 17					
<i>Balanoglossus</i> (LPIL)																					1																								
<i>Armandia maculata</i>	1 1 3 1										1 3 10 2 31 4 7 137 10										1 1 2 1 1																								
<i>Branchiostoma</i> (LPIL)	11	5	15	2	27	5	1	2	1	27	5	14	24	80	19	66	6	4	3	1																									
<i>Polygordius</i> (LPIL)		4	17	1	3	9	10	3	1	1	4	7	20	8	24	17	6	19				1																							
<i>Eudevenopus honduranus</i>	10	1		3	1	1				9		1	6	5	1	5	1	1	4			1																							
<i>Spiophanes bombyx</i>	5	9	7	100	6	18	35	25	20			8	2	3	4		3					7	2	2		1															5				
<i>Apoprionospio pygmaea</i>	7	3	4	78	7	11	25	25	21		1						1	1				20				1																1			
<i>Nassarius albus</i>	2	2		2	10	8	6	1	3													23			2																		2		
<i>Pagurus</i> (LPIL)	5	4	2	1		14	10															4			3																				
<i>Nephtys picta</i>			4	1	2	3	8	9	3	2			1	1	2				1																								3		
<i>Ervilia concentrica</i>	9	6	3			4				17				3		1																												1	
<i>Magelona sp.B</i>	5		13		14	20	2	6					5	2	1	5	7																												
<i>Chione</i> (LPIL)	5		12			20		1			1																																		
<i>Protohaustorius bousfieldi</i>	20				7	9																			2																				
<i>Prionospio cristata</i>				8	1		1	3	5	1	3			1		5							4		1	2	2	1																	
<i>Tellina</i> (LPIL)	1			16		2		2	2				1		2							7			1	1																			
<i>Pinnixa</i> (LPIL)	1	1	5		3	2				2		1	1		3		1					3	4		3		1		1	2															
<i>Ampharete sp.A</i>		1	1	1	1						2			2	1	1	1					7	1	1		1	1		2																
<i>Phascolion strombi</i>			3		16	8	7	10	4		6	17	1	3	2	1	7	4	20	1	2	3	4	4	20	9	5	2	6																
<i>Tectonatica pusilla</i>	4	3	5		7	7	6	2	2	2	7	7	5	4									10	2	2	4	6	5		1	1	1	1	1	1	1	4								
<i>Paraprionospio pinnata</i>				4	3	3	13	9	24		1	1					1	2	1	4	10	172	243	42	255	98	152	98	162	94	294	49	9	1	5	5	4	5	14	13					
<i>Mediomastus</i> (LPIL)	1	4	6	25	4	2	18	8	17	5	3		2	1	3	1	6	8				154	75	5	129	82	42	20	19	61	51	82	15	19	11	14	13	6	6	10					
<i>Magelona sp.H</i>									1			1					2	9	10	8	42	29	14	18	16	18	13	12	16	14	22	10	18	21	18	36	5	5	11						
<i>Nereis micromma</i>	2			2	1			1	9						1	2	4	1	9	12	4	9	2	6	1	18	19	19	5		1	18	21	36	5	29	11	7	3	41		3			
<i>Scoletoma verrilli</i>				1					4			1							3	3	8		5	7	3	6	9	3	1	5	1	10	16	6	8	11	13	1	12	23					
<i>Tubulanus</i> (LPIL)	1		1	1		1	3	2				1							2		11	14			12	2		2		2		10	8	8	9	7	4	6	3	5					
<i>Ampelisca sp.A</i>					2			2											3		9	9	26		10	2	1	1		4	4	12				1		1	2	4					
<i>Sigambra tentaculata</i>		2		1				1			1											4	14	1	3	5	4		2	1	8	9	3	1	4	3	1	1	2	1					
<i>Glycinde solitaria</i>			1																2	4	1	5		1	2		1	1	4	1	1	4	3	2	3	1	7	1							
<i>Cossura soyeri</i>																								1	3	5	1		4	7	49														
<i>Aricidea taylori</i>									2																																				
<i>Aglaophamus verrilli</i>												1							2	3	6		2																						
<i>Diopatra cuprea</i>	3																																												
<i>Scoletoma ernesti</i>	2	2		9																																									

LPIL= Lowest practical identification levels.

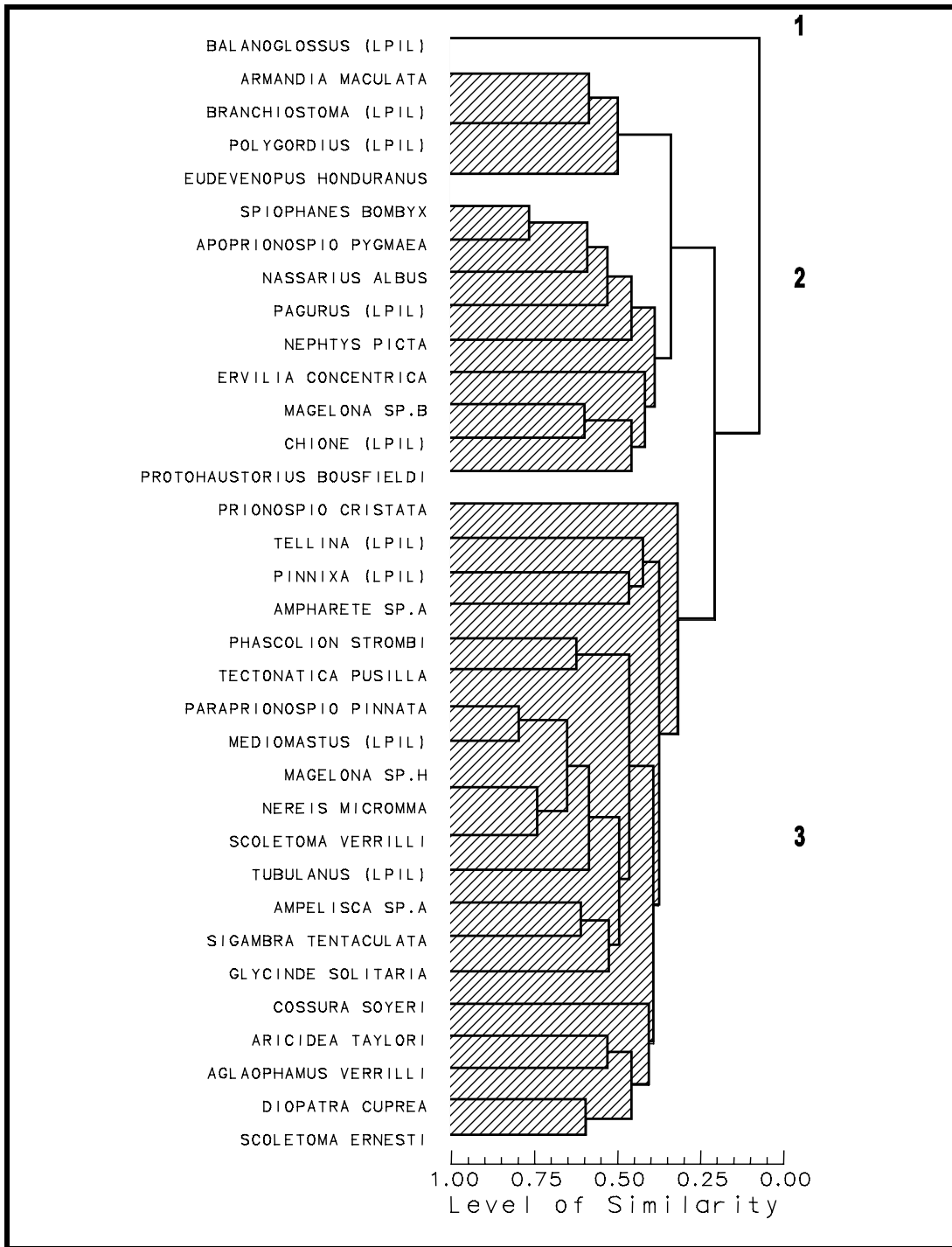


Figure 6-17. Inverse cluster analysis of infaunal taxa from samples collected during the May 1997 Survey 1 and December 1997 Survey 2 in Sand Resource Area 4 offshore Alabama.

## Area 5

Normal cluster analysis resulted in three station groups (Groups A through C) in Area 5 (Figure 6-18). As was the case in Area 4, Groups A and B were restricted by survey, with Group A (six stations) comprised of December samples and Group B (nine stations) comprised of May samples. Four of the six Group A stations also were included in Group B. Group C included stations from both surveys, although May survey stations were closely associated within the grouping. Group A was distinguished from other station groups by yielding relatively low numbers of infauna, and by lacking many of the numerically dominant taxa found at other stations in Area 5. Group B stations contained high numbers of the molluscans *Chione*, *N. albus*, and *Tellina*, *Pagurus*, the polychaetes *A. pygmaea*, *P. cristata*, and *S. bombyx*, and *Polygordius*. Group C stations were distinguished from Group B by relatively high densities of *C. soyeri*, *D. cuprea*, and *S. verrilli*, and low numbers of, or lacking altogether, many of the taxa found at Group B stations (Table 6-9).

Four groups of co-occurring taxa (Groups 1 through 4) were observed in Area 5 (Figure 6-19). Group 1 consisted of a single gastropod species (*C. cooperi*) that showed no pattern of association with other Area 5 taxa. Group 2 included two co-occurring taxa that were distributed across all station groups: *A. maculata* and *Branchiostoma*. Group 3 was comprised mostly of polychaetes, including *A. taylori*, *A. verrilli*, *C. soyeri*, *D. cuprea*, *Magelona* sp. H, *Mediomastus*, *M. dorsobranchialis*, *N. micromma*, *N. picta*, *P. pinnata*, *Sabaco americanus*, and *S. verrilli*. Group 3 also included *Ampelisca* sp. A, the sipunculids *Aspidosiphon albus* and *P. strombi*, and *Tubulanus*. Most taxa in Species Group 3 were distributed across all station groups. Species Group 4 included *A. pygmaea*, *Chione*, *Golfingia* sp. V, *N. albus*, *P. cristata*, *P. cuneata*, *Pagurus*, *Polygordius*, *S. bombyx*, and *Tellina* (Table 6-9).

Sediment composition across Area 5 stations was variable during both surveys. Area 5 stations were characterized by the presence of slightly gravelly sand or gravelly sand (Station Group B) and supported the molluscans *Chione* and *N. albus*, polychaetes such as *P. cristata* and *S. bombyx*, *Polygordius*, and *Pagurus* (Species Group 4). Stations with slightly gravelly sand or sand (Station Groups A and B) supported fewer polychaete taxa, and exhibited lower abundances generally and higher numbers of *P. cuneata* and *P. strombi*. Stations with slightly gravelly muddy sand and muddy sand (Station Group C) tended to yield more polychaetes, including *C. soyeri*, *Magelona* sp. H, *N. micromma*, *Scoletoma ernesti*, and *S. verrilli* (Species Group 3). *Mediomastus* and *P. pinnata* were evenly distributed across station groups. No relationship between the composition of infaunal assemblages and depth was apparent in Area 5.

### 6.3.4 Epifauna and Demersal Ichthyofauna

Fishes and invertebrates collected in trawls during Surveys 1 and 2 are listed in Tables 6-10 and 6-11, respectively. Twenty trawl hauls made over two field surveys produced 3,619 specimens (1,628 fishes and 1,991 invertebrates) in 70 taxa (44 fishes and 26 invertebrates). The numerically dominant fish taxa in the hauls included longspine porgy (*Stenotomus caprinus*), spot (*Leiostomus xanthurus*), silver seatrout (*Cynoscion nothus*), Atlantic croaker (*Micropogonias undulatus*), and rock seabass (*Centropristis philadelphica*). The most abundant invertebrates collected were roughneck shrimp (*Trachypenaeus constrictus*), squid (*Loligo* sp.), striped sea star (*Luidia clathrata*), and rock shrimps (*Sicyonia* spp.). These taxa collectively accounted for 80% of all specimens collected.

Taxonomic composition, abundance, and richness in trawl hauls differed somewhat between surveys. The May survey trawls yielded 2,068 individuals (1,140 fishes and 928 invertebrates) and 47 taxa (27 fishes and 20 invertebrates) from all five sand resource areas. Most abundant were longspine porgy, rock seabass, lizardfish (*Saurida brasiliensis*), striped sea star, squid, and roughneck shrimp. The total number of individuals (fishes and invertebrates combined) per trawl in the May survey ranged from 42 to 433 and averaged 207 individuals. Fishes averaged 114 individuals and invertebrates averaged 93 individuals per haul. The number of taxa (fishes and

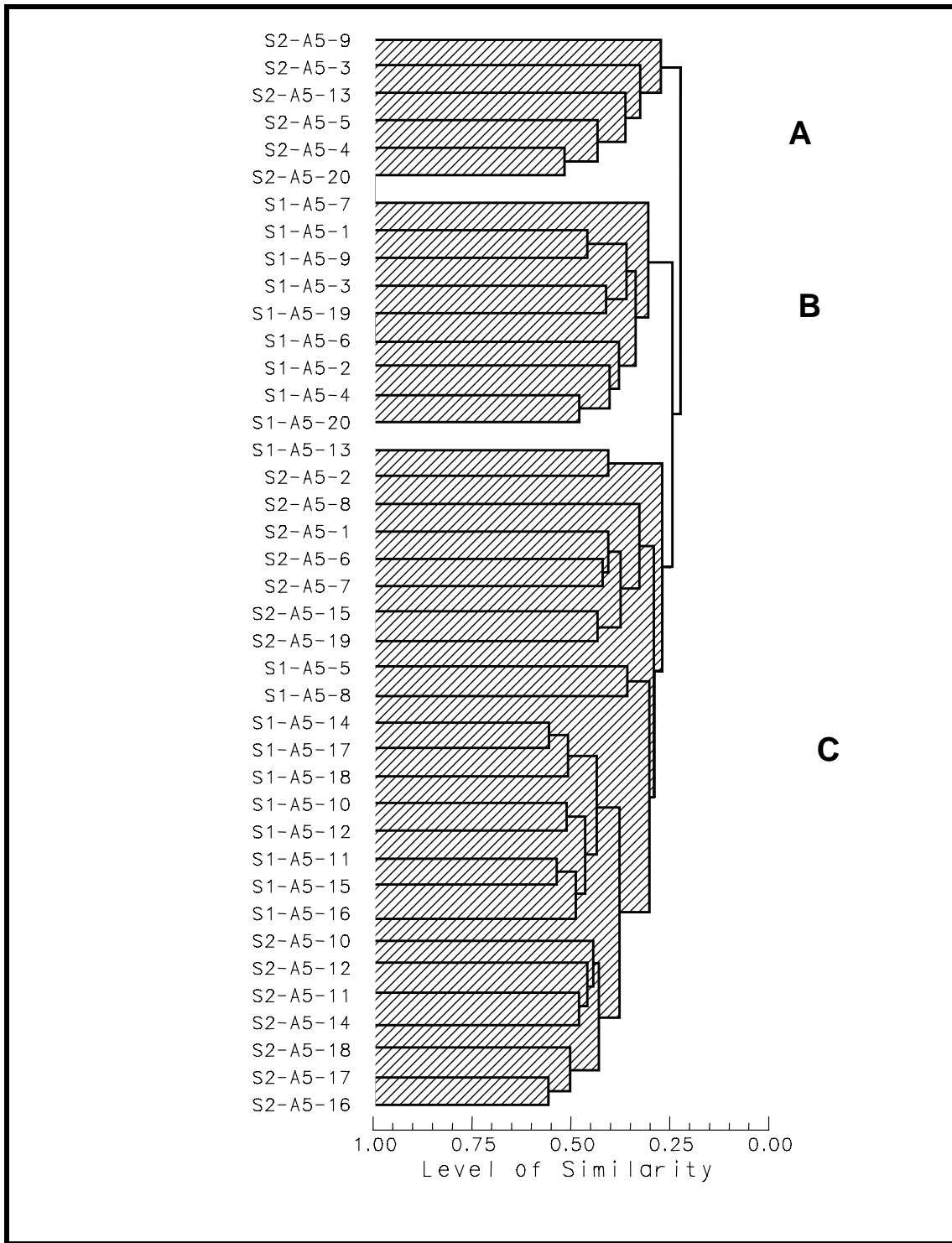


Figure 6-18. Normal cluster analysis of infaunal samples collected during the May 1997 Survey 1 (S1) and December 1997 Survey 2 (S2) in Sand Resource Area 5 offshore Alabama.



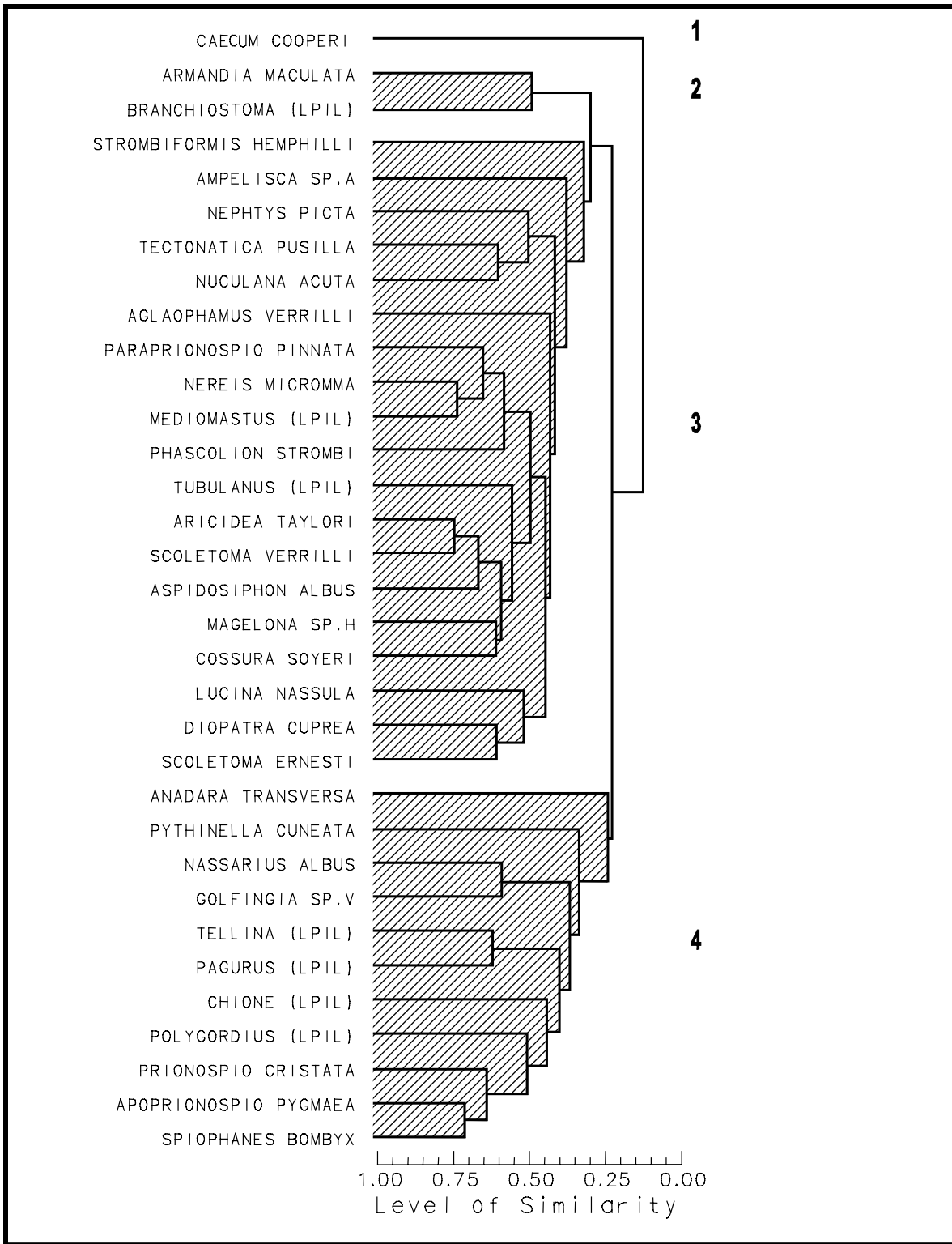


Figure 6-19. Inverse cluster analysis of infaunal samples collected during the May 1997 Survey 1 and December 1997 Survey 2 in Sand Resource Area 5 offshore Alabama.

Table 6-10. Epifauna collected by mongoose trawl and ranked by numerical abundance from the May 1997 Survey (S1) in the five potential sand resource areas (A1 to A5) along north (1) and south (2) transects offshore Alabama.

Species	S1-A1-1	S1-A1-2	S1-A2-1	S1-A2-2	S1-A3-1	S1-A3-2	S1-A4-1	S1-A4-2	S1-A5-1	S1-A5-2	Total
<b>FISHES</b>											
<i>Stenotomus caprinus</i>	32	68	52	7	133	116		47	120	184	759
<i>Centropristis philadelphica</i>					8	2	1	42	4		57
<i>Saurida brasiliensis</i>								14	20	17	51
Bothids juv.								43			43
<i>Anchoa hepsetus</i>									39		39
<i>Diplectrum bivittatum</i>				1		1		15	5	9	31
<i>Peprilus burti</i>		2			4				5	18	29
<i>Prionotus scitulus</i>	2	1	4		4		1	9			21
<i>Ophidion marginatum</i>			2		1	16				1	20
<i>Syacium</i> sp.			12	2		3					17
<i>Prionotus rubio</i>			1		2	7					10
<i>Syacium papillosum</i>	1	1			8						10
<i>Trachurus lathamii</i>										8	8
<i>Prionotus</i> sp.									6		6
<i>Sphoeroides nephelus</i>			2		1	1				2	6
<i>Symphurus plagiusa</i>						2		2		2	6
<i>Upeneus parvus</i>	1	4									5
<i>Etropus crossotus</i>			1					2	1		4
<i>Synodus foetens</i>	2						1		1		4
<i>Ophidion</i> sp.					3						3
<i>Antennarius radiosus</i>			1							1	2
<i>Gobionellus hastatus</i>								2			2
<i>Lutjanus campechanus</i>					1				1		2
<i>Urophycis floridana</i>						1				1	2
<i>Citharichthys spilopterus</i>							1				1
<i>Prionotus tribulus</i>					1						1
<i>Sphoeroides parvus</i>									1		1
<b>INVERTEBRATES</b>											
<i>Luidia clathrata</i>		4	1	42		237					284
<i>Loligo</i> sp.		5	1				53		100	76	235
<i>Trachypenaeus constrictus</i>					71	14		48	1	29	163
<i>Sicyonia burkenroadi</i>								101			101
<i>Sicyonia</i> sp.			2		5	18			7	11	43
<i>Portunus spinimanus</i>								23	1	1	25
<i>Squilla empusa</i>								8		5	13
<i>Portunus gibbesii</i>									11		11
<i>Squilla</i> sp.						11					11
<i>Astropecten</i>	1	6				1					8
<i>Pagurus pollicaris</i>								6			6
<i>Encope michelini</i>	3		2								5
<i>Stenorhynchus seticornis</i>				1		2		1	1		5
<i>Penaeus</i> sp.			3	1							4
<i>Pleurobranchia hedgpethi</i>					4						4
<i>Callinectes sapidus</i>								3			3
<i>Hepatus epheliticus</i>						1				1	2
Nudibranch			1				1				2
<i>Porcellana sayana</i>								1	1		2
<i>Penaeus setiferus</i>								1			1
<b>FISH TOTALS</b>											
Total Individuals	38	76	75	10	166	149	4	176	203	243	1,140
Total taxa	5	5	8	3	11	9	4	9	11	10	27
<b>INVERTEBRATE TOTALS</b>											
Total Individuals	4	15	10	44	80	284	54	192	122	123	928
Total taxa	2	3	6	3	3	7	2	9	7	6	20
<b>FISH AND INVERTEBRATE TOTALS COMBINED</b>											
Total Individuals	42	91	85	54	246	433	58	368	325	366	2,068
Total taxa	7	8	14	6	14	16	6	18	18	16	47

Table 6-11. Epifauna collected by mongoose trawl and ranked by numerical abundance from the December 1997 Survey (S2) in the five potential sand resource areas (A1 to A5) along north (1) and south (2) transects offshore Alabama.

Species	S2-A1-1	S2-A1-2	S2-A2-1	S2-A2-2	S2-A3-1	S2-A3-2	S2-A4-1	S2-A4-2	S2-A5-1	S2-A5-2	Total
<b>FISHES</b>											
<i>Leiostomus xanthurus</i>					10		2	3	4	79	98
<i>Cynoscion nothus</i>							28	3	48	2	81
<i>Micropogonias undulatus</i>					11		2	5	9	53	80
<i>Lagodon rhomboides</i>					6	15	1	2	6	1	31
<i>Prionotus rubio</i>					1	3		2	11	3	20
<i>Larimus fasciatus</i>					4		14	1			19
<i>Ophidion grayi</i>					1		1	12	2		16
<i>Cynoscion arenarius</i>								1	3	10	14
<i>Peprilus burti</i>				4	2				7		13
<i>Engraulis eurystole</i>					2	8					10
<i>Lepophidium brevibarbe</i>									7	3	10
<i>Sphoeroides parvus</i>			1					5	4		10
<i>Symphurus diomedianus</i>						1			4	5	10
<i>Anchoa lyolepis</i>					1	8					9
<i>Etropus crossotus</i>			1				1	2	4	1	9
<i>Diplectrum bivittatum</i>									1	7	8
<i>Lutjanus campechanus</i>							7	1			8
<i>Ophidion selenops</i>								7	1		8
<i>Prionotus martis</i>				5	1						6
<i>Saurida brasiliensis</i>				4							4
<i>Centropristis philadelphica</i>							1		2		3
<i>Ophidion sp.</i>								3			3
<i>Ophidion welshi</i>						1			1	1	3
<i>Citharichthys sp.</i>								2			2
<i>Menticirrhus littoralis</i>					2						2
<i>Syacium papillosum</i>		1						1			2
<i>Symphurus plagiusa</i>								1		1	2
<i>Symphurus sp.</i>							1		1		2
<i>Synodus foetens</i>		1		1							2
<i>Anchoa hepsetus</i>								1			1
<i>Citharichthys spilopterus</i>				1							1
<i>Prionotus tribulus</i>							1				1
<b>INVERTEBRATES</b>											
<i>Trachypenaeus constrictus</i>						126	89	100	84	69	468
<i>Loligo sp.</i>						113	27	31	54	15	240
Penaeidae						26	64	83	33	6	212
<i>Sicyonia dorsalis</i>						50	19	1	18	6	94
<i>Luidia clathrata</i>							5	1	1	2	9
<i>Penaeus aztecus</i>							3	1	1	2	7
<i>Callinectes tricolor</i>									4	2	6
<i>Penaeus setiferus</i>							4		2		6
<i>Sicyonia sp.</i>						2	3				5
<i>Pagurus pollicaris</i>									3	1	4
<i>Squilla neglecta</i>							2		1	1	4
<i>Sicyonia brevirostris</i>						1			1	1	3
<i>Pleurobranchia hedgpethi</i>								2			2
<i>Portunus gibbesii</i>						1	1				2
<i>Portunus spinimanus</i>						1					1
<b>FISH TOTALS</b>											
Total Individuals		2	2	15	41	36	59	52	115	166	488
Total Taxa		2	2	5	11	6	11	17	17	12	33
<b>INVERTEBRATE TOTALS</b>											
Total Individuals						320	217	219	202	105	1,063
Total Taxa						8	10	7	11	10	15
<b>FISH AND INVERTEBRATE TOTALS COMBINED</b>											
Grand Total Individuals		2	2	15	41	356	276	271	317	271	1,551
Grand Total Taxa		2	2	5	11	14	21	24	28	22	47

invertebrates combined) per trawl in the May survey averaged 12. The average number of fish taxa per haul was 8 and the average number of invertebrate taxa per haul was 5.

During the December survey, trawls produced 1,551 individuals (488 fishes and 1,063 invertebrates) in 48 taxa (33 fishes and 15 invertebrates) with roughneck shrimp, squid, penaeid shrimps, rock shrimps, spot, silver seatrout, and Atlantic croaker numerically dominating the catches. Catches during the December survey ranged from 0 to 356 individuals and averaged 155 individuals per haul. Fish catch averaged 49 individuals per tow and ranged from 0 to 166 individuals per tow. Invertebrates were more numerous, averaging 106 individuals per tow and ranging from 0 to 320 individuals. In December, the number of taxa ranged from 0 to 28 and averaged 13 per haul. Fishes averaged 8 taxa and invertebrates averaged 5 taxa per haul, respectively.

During both surveys, trawl catches from Areas 3, 4, and 5 yielded the most individuals and taxa. The highest number of individuals (433) in a single haul was recorded in Area 3 during the May cruise. During the December survey, the highest number of individuals (356) was collected in Area 3. The fewest number of individuals (0) in a single haul came from Area 1 during the December cruise. The highest number of taxa (18) collected during the May survey was from Areas 4 and 5. The highest number of taxa (28) collected during the December survey was from Area 5. Areas 2 and 4 yielded the fewest trawl-caught taxa (6) during the May survey.

Patterns of similarity among trawl samples were examined with cluster analysis. Normal cluster analysis produced four groups of samples that were similar with respect to species composition and relative abundance (Figure 6-20). The first major separation evident in the normal analysis was that, with the exception of Groups 1 and 4, samples from the two surveys formed distinctive groups. Group 1 was comprised of three samples with sparse numbers of taxa and individuals. Group 2 consisted of six samples collected exclusively during the December survey. These samples were characterized by high numbers of roughneck shrimp, squid, penaeid shrimps, silver seatrout, spot, and Atlantic croaker. Samples from Areas 1 to 5 collected exclusively during the May survey formed Group 3. Longspine porgy, striped sea star, and rock shrimp were abundant in these samples.

Inverse cluster analysis generated six groups (A to F) of taxa that reflected the co-occurrence of taxa in the samples (Figure 6-21). Group A consisted of taxa that were commonly collected during the May survey, including longspine porgy, striped sea star, and rock shrimp. Group B was composed of sparsely distributed taxa such as juvenile flounder (*Syacium* sp.) and shrimp (*Penaeus* sp.) collected primarily in Area 2 during the May survey. Group C was a large group of 16 taxa distributed sparsely in samples from both surveys and all sand resource areas. Group D included six taxa that occurred in low numbers at stations from both field surveys. Group E included taxa collected primarily during the December cruise. The most abundant of these were roughneck shrimp, squid, rock shrimp, silver seatrout, spot, and Atlantic croaker. Group F consisted of four infrequently occurring taxa with no particular distribution pattern within the samples.

## 6.4 DISCUSSION

Benthic assemblages surveyed in the five sand resource areas offshore Alabama consisted of members of the major invertebrate and vertebrate groups that are commonly found in the study region. Numerically dominant infaunal groups included numerous crustaceans, echinoderms, molluscs, and polychaetous annelids, while epifaunal invertebrate taxa consisted primarily of sea stars, squid, and various shrimps. These infaunal and epifaunal groups typically dominate abundance in the study area. Similarly, the numerically dominant demersal ichthyofauna collected in trawls within the sand resource areas revealed a consistency with previous surveys. Fishes such as Atlantic croaker (*Micropogonius undulatus*), longspine porgy (*Stenotomus caprinus*), silver seatrout (*Cynoscion nothus*), and spot (*Leiostomus xanthurus*) were numerical dominant during the

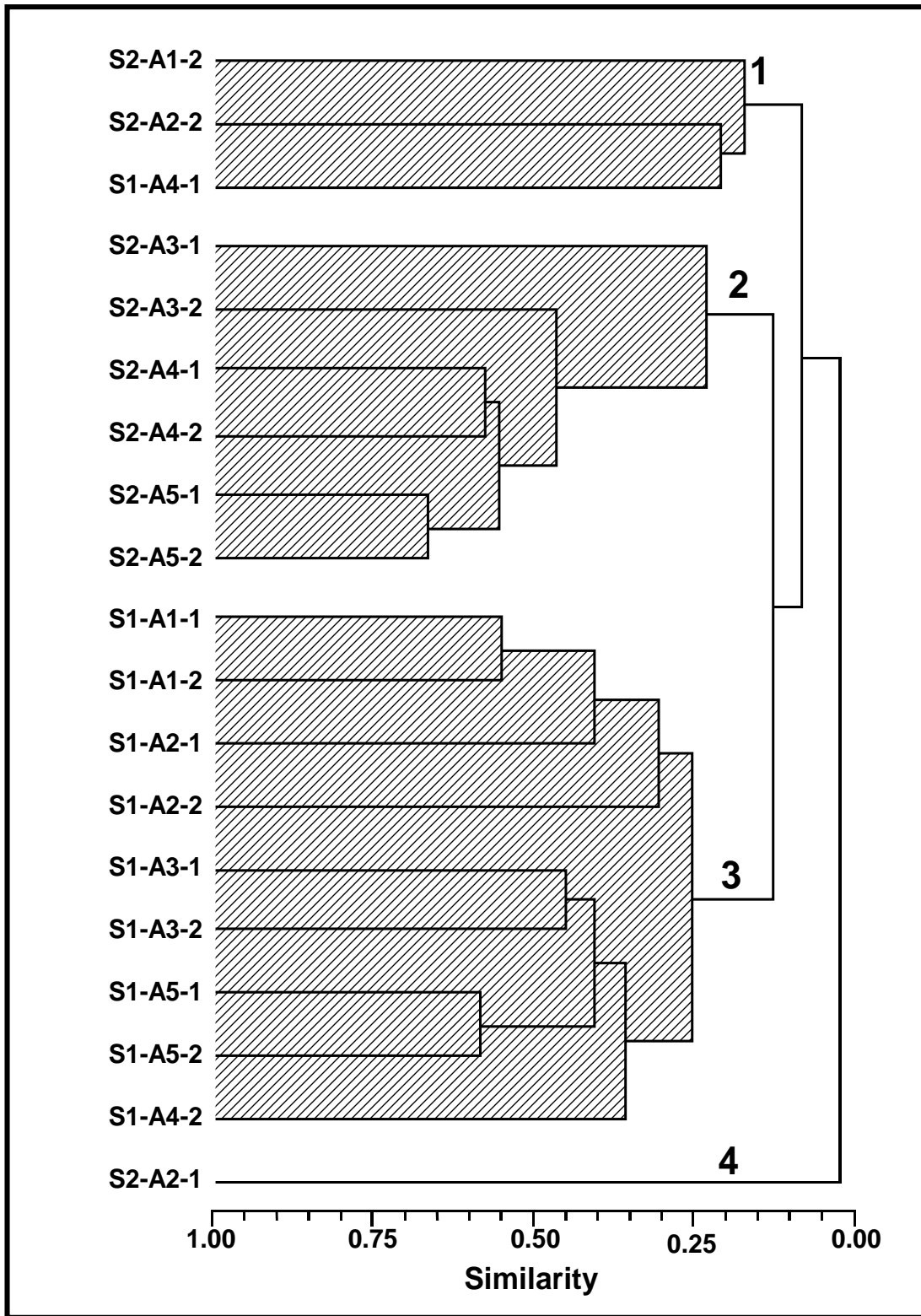


Figure 6-20. Normal cluster analysis of epifaunal trawl samples collected during the May 1997 Survey 1 (S1) and December 1997 Survey 2 (S2) in the five sand resource areas (A1 to A5) along the north (1) and south (2) transects offshore Alabama.

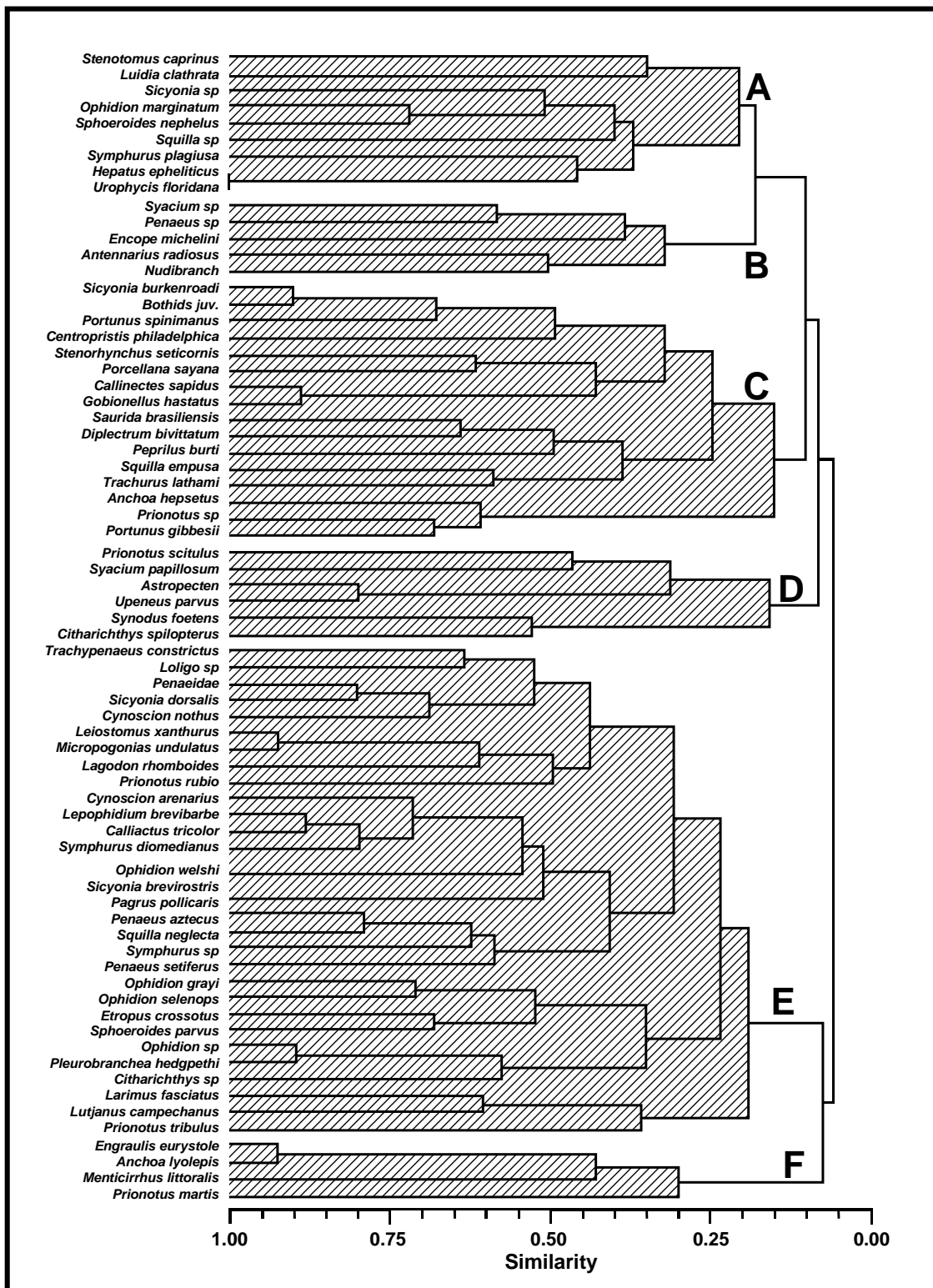


Figure 6-21. Inverse cluster analysis of epifaunal taxa from trawl samples collected during the May 1997 Survey 1 and the December 1997 Survey 2 in the five sand resource areas along north and south transects offshore Alabama.

1997 sand resource area surveys, and these species consistently are among the most ubiquitous and abundant demersal taxa in the region (Chittenden and McEachran, 1976; Barry A. Vittor & Associates, Inc., 1985; Darnell and Kleypas, 1987).

Seasonal variability in the composition of benthic assemblages was apparent in the sand resource area surveys, as the grouping of stations based on similar infaunal composition and abundance was correlated primarily with survey (Figure 6-8). Infaunal abundance was substantially higher during the May survey than was observed in December. This seasonal difference reaffirms the findings of previous area surveys which found substantial temporal variation in the composition of infaunal assemblages, with generally lower densities occurring in winter relative to summer months (Shaw et al., 1982; Continental Shelf Associates, Inc. and Barry A. Vittor & Associates, Inc., 1989; Harper, 1991). Infaunal species richness varied between surveys as well. Nearly half of the infaunal taxa sampled over the entire project were found in both the May and December surveys; however, most (70%) of the remainder of censused taxa were collected only during the May cruise, resulting in higher mean values of species richness compared to the December survey.

Epifaunal and demersal ichthyofaunal taxa collected in trawls differed between surveys as well. Two of the four groups of trawl samples produced by normal cluster analysis were separated by survey. The May survey was characterized by an abundance of longspine porgy, rock shrimps (*Sicyonia* spp.), and striped sea star (*Luidia clathrata*), while December trawls were characterized by high numbers of spot, silver seatrout, croaker, and roughneck shrimp (*Trachypenaeus constrictus*). Although seasonal trends cannot be reliably discerned from relatively limited sampling, the temporal variability in the composition of sand resource area demersal assemblages does agree with previous local sampling efforts that indicated a community of spatially widespread taxa that migrate inshore seasonally (Comiskey et al., 1985).

In addition to seasonal trends, spatial variability was evident in the 1997 sand resource surveys. Infaunal abundance generally increased from west to east in both the May and December surveys (Table 6-3). This result was primarily due to high numbers of the gastropod *Caecum* spp., which accounted for 33% of all infaunal individuals censused over the entire project. *Caecum* (mostly *C. pulchellum*) was found nearly exclusively in Areas 1, 2, and 3 during both surveys. High numbers of *Caecum* collected during the sand resource area surveys resulted in higher infaunal abundance than was found during previous area studies (Barry A. Vittor & Associates, Inc., 1985; Harper, 1991). It may be concluded that a major recruitment episode occurred at some time prior to the 1997 surveys of the sand resource areas. It is unknown whether high *Caecum* densities were indicative of typical benthic assemblages in the area, or whether members of the genus form an opportunistic group of taxa that can occur in offshore sandy areas on an intermittent basis, exploiting available habitat when suitable conditions exist. Previous benthic surveys of the area did not find *Caecum* in such high numbers. *Caecum* does include several epibenthic species that generally inhabit areas of sandy substrata, especially seagrass beds and beach drift (Andrews, 1971).

As with previous surveys, infaunal assemblage type was closely tied to sediment grain size. Overall, canonical discriminant analysis indicated that season was the most important factor that affected the composition and distribution of infaunal assemblages offshore Alabama. Within season, discriminant analysis indicated that sedimentary regime most affected infaunal assemblages. Surface sediment included a mixture of sand and mud at most stations in the western sand resource areas (Areas 4 and 5), as compared to the easternmost areas (Areas 1, 2, and 3) which were predominantly sand (Figure 6-9). Infaunal assemblage types reflected sediment type distributions; station groupings based on cluster analysis of infaunal samples from the May and December surveys indicated spatial homogeneity of assemblage distributions in the eastern sand resource areas and heterogeneity of assemblage distributions in Areas 4 and 5, regardless of season (Figure 6-8). Of the six station groups identified through cluster analysis, Group E was comprised of stations in Areas 4 and 5 common to both the May and December surveys. Apparently, infaunal assemblages in the western sand resource areas are affected as much by

sedimentary regime as by seasonal effects. This contrasts with Areas 1, 2, and 3 where assemblages differed between seasons. The results of the sand resource area surveys therefore reflect a sediment-related longitudinal arrangement of infaunal assemblages.

The eastern areas tended to support assemblages numerically dominated by the gastropod *Caecum* spp. and included many arthropods, bivalves, and gastropods, while the western areas supported assemblages that tended to be dominated by polychaetes in terms of abundance and species richness. Stations in Areas 4 and 5 that had sandier sediments supported taxa commonly associated with Areas 1, 2, and 3, including the archiannelid *Polygordius*, lancelet *Branchiostoma*, and polychaete *Spiophanes bombyx*. Furthermore, stations characterized by sandy substrate in Areas 4 and 5 exhibited different infaunal assemblages between seasons, as did the entirety of the eastern sand resource areas (Figure 6-8). The numerically dominant taxa in Areas 4 and 5, especially the polychaetes *Mediomastus* and *Paraprionospio pinnata*, are more ubiquitous species that typically inhabit areas characterized by fine sediment. These ubiquitous taxa are less abundant in the eastern areas, which provide less suitable habitat due to relatively coarser sediments and higher salinities.

The density of infaunal taxa was high during both field surveys when compared with historical surveys. Other surveys have recorded values of species richness comparable to the present study (Shaw et al., 1982; Continental Shelf Associates, Inc. and Barry A. Vittor & Associates, Inc., 1989); however, those earlier estimates were calculated for stations where multiple samples were taken, thus increasing the potential of sampling more taxa. Stations sampled during the present surveys were censused with just a single bottom grab and, therefore, high values of species richness were generated from relatively limited areas. It may be that a period of higher than usual recruitment levels preceded the surveys of the candidate borrow areas.

Variability between sand resource areas also was evident in the composition of trawl samples. Trawl catches from Areas 3, 4, and 5 yielded the most individuals and taxa during both the May and December surveys, while Areas 1 and 2 yielded the fewest trawl-caught taxa and individuals. A similar geographic trend was identified by pattern analyses performed by Comiskey et al. (1985) on various data sets from previous trawl surveys in the region. Their analyses indicated that the nearshore environment off Alabama was characterized by low numbers of taxa and individuals relative to areas nearer the Mississippi Delta, where the environment is under the influence of considerable riverine discharge. The influence of Mobile Bay outflow on the western sand resource areas relative to the eastern sand resource areas apparently affects demersal assemblages in much the same way, albeit on a smaller scale.

Temperature, salinity, and dissolved oxygen measurements were taken in each of the sand resource areas during the field surveys (Figure 6-7) and compared to the community parameters in Table 6-3 to assess any apparent hydrographic influences upon infauna. Temperatures were lower during the December survey than the May survey. During the December survey, Areas 4 and 5 showed higher bottom water temperatures than Areas 1, 2, and 3. Possible effects of relatively higher temperatures in Areas 4 and 5 during the second survey were not discernable in the infaunal data when comparing surveys or areas. Salinity was similar among sand resource areas during both surveys. Dissolved oxygen values measured during the May survey were low in Areas 2, 3, 4, and 5, and were very low in Area 4, where bottom values were measured as low as 1.22 mg/L. The mean number of infaunal taxa collected per station was substantially lower in Area 4 than in other areas during the May survey (Table 6-3), although it is ultimately unknown whether this was a result of hypoxic conditions. A negative relationship between hypoxia and infaunal density can only be inferred from the data; however, a significant negative effect does occur for many benthic invertebrates at concentrations of 2.0 mg/L or lower (Diaz and Rosenberg, 1995). Trawl catches in Area 4 also may have been influenced by hypoxic conditions during the May survey.

Hummell and Smith (1995, 1996) indicate that the surficial sediment texture of the primary sand source in Area 4 should be sand. However, results from the biological field surveys indicate that grain size in Area 4 is actually quite variable, with more silt and clay than expected. This may have been due to the fact that much of the primary sand source within Area 4 also is within the limits of a dredge disposal area (see Figure 33 in Hummell and Smith, 1995). Approximately 13 MCM of sediment were placed offshore as the Mobile Outer Mound (Hands, 1994). Storm-induced resuspension of sediments on this site may result in transport to parts of Area 4, resulting in a layer of fine-grained material at the sediment surface. Changes in Area 4 surficial sediments also could be attributed to annual disposal of maintenance dredging material from the Mobile Ship Channel and Bar Channel.

In summary, the results of the sand resource area surveys agree well with previous descriptions of benthic assemblages residing in shallow waters off the Alabama coast. Seasonality had the greatest effect on community composition; normal cluster analysis revealed that most groups of biologically similar stations were separated according to survey. Spatial differences in community composition also were obvious, with western areas supporting assemblages dominated by those taxa capable of exploiting the fluctuating, riverine-influenced habitats nearer Mobile Bay. Certain euryhaline opportunists, including infauna such as *Mediomastus* and *P. pinnata*, are widespread over all surveyed areas, while the *Caecum*-associated assemblages of the eastern areas apparently are restricted to the more stable environmental characteristics of those sand sediment areas. The composition of demersal assemblages across the Alabama sand resource areas is influenced by fluctuating hydrographic parameters in the western areas relative to the more stable eastern areas.

## 7.0 POTENTIAL EFFECTS

One of the primary purposes of this project is to provide site-specific information for decisions on requests for non-competitive leases from other local, State, and Federal agencies. The information may be used to determine whether or not stipulations need to be applied to a lease. The information also may be incorporated into an Environmental Assessment (EA) or Environmental Impact Statement (EIS), if so required.

Environmental impact analyses of mining operations should be based on commodity-specific, technology-specific, and site-specific information, whenever possible (Hammer et al., 1993). First, the specific mineral of interest and the technological operations for a specific mining operation need to be defined because these two parameters determine the impact producing factors that need to be considered. Once the impact producing factors are known, this information can be translated into statements concerning the impacts that might occur to the full suite of potentially affected environmental resources that may need to be addressed, including geology, chemical and physical oceanography, air quality, biology, and socioeconomics. Then, decisions can be made regarding the type of mitigation necessary to determine the preferred alternative for a specific marine mining operation to acquire project approval.

This section focuses on providing information on potential impacts related to physical processes and biological considerations of sand mining for beach nourishment from four of the five sand resource areas offshore Alabama. Sand for beach replenishment is the commodity of interest. Two primary dredging technologies are available for offshore sand mining operations, depending on distance from source to project site, the quantity of sand being dredged, and the depth to which sand is extracted at a site (Herbich, 1992). They are: 1) cutterhead suction dredge, where excavated sand is transported through a direct pipeline to shore, and 2) hopper dredge, where sand is pumped to the hopper, transported close to the replenishment site, and pumped to the site through a pipeline from the hopper or from a temporary offshore disposal area close to the beach fill site. As a general rule, cutterhead suction dredging is most effective for projects where the sand resource is close to shore (within 8 km), the dredging volumes are large (>8 MCM), and the excavation depth is on the order of 2.5 to 4 m (Taylor, 1999). Hopper dredging becomes a more efficient procedure when the sand resource areas are greater than 8 km from shore, dredging volumes are relatively small (<2 MCY), and the excavation depth at the sand resource area is less than 2 m (Taylor, 1999). Ultimately, a combination of these factors will be evaluated by dredgers to determine the most cost effective method of sand extraction and beach replenishment for a given project. Availability of dredging equipment also may be a factor for determining the technique to be used; however, the number of cutterhead suction and hopper dredges in operation is about equal in the industry today (Taylor, 1999). As such, both technologies will be evaluated for potential biological effects.

### 7.1 POTENTIAL SAND BORROW SITES

Five potential sand resource areas were identified offshore Alabama in Federal waters by the Alabama Geological Survey and the U.S. Minerals Management Service, INTERMAR (Parker et al., 1993). Each site has specific geologic and geographic characteristics that make it more or less viable as a sand resource for specific segments of coast. Areas 1, 2, 3, and 4 contain borrow sites with the greatest potential for use in the future. Area 5 is unlikely to be used due to its location and geological composition relative to beach replenishment needs.

Areas 1, 2, and 3 are very similar geologically (medium-to-fine sand sheet deposit), whereas the identified borrow site in Area 4 has from zero to 30 cm of silt and clay overburden before encountering a medium-to-fine sand deposit. Currently, Areas 1, 2, and 3 (east of Mobile Bay) are

thought to be of greatest interest to the State, due primarily to their proximity to beaches severely impacted by storms and hurricanes in 1998. Physical processes (waves and currents) and biological habitat illustrate minor variability offshore eastern Alabama. Although these three potential sand resource areas were designated in 1993 (Parker et al., 1997), it is possible that sand could be dredged from intervening areas because consistency of geologic deposits is widespread seaward of the eastern Alabama coast. Proximity to the beach replenishment site will be the significant factor for determining specific borrow area locations.

Area 4, west of the Mobile Bay entrance channel in an EPA-designated dredged material disposal area, has quite different physical characteristics (surface and subsurface sediment, and currents and flow from Mobile Bay) and biological communities than Areas 1, 2, and 3 (Hummell et al., 1996). Spatial and temporal variability in surface sediment characteristics reflect the influence of sediment and flow from Mobile Bay, as well as the impact of dredged material placement at or near the site (Douglas et al., 1995). Although the ecosystem dynamics at Area 4 appear significantly more variable than those offshore eastern Alabama, the sand resource identified by Parker et al. (1993, 1997) and Hummell et al. (1995, 1996) in this area could be a significant source of beach-quality sand for beaches along Dauphin Island.

The amount of dredging that occurs at any given site is a function of Federal, State, and local needs for beach replenishment. There is no way of predicting the exact sand quantities needed in the foreseeable future, so an upper value was estimated based on discussions with State personnel and the MMS, as well as the geological characteristics of specific resource targets. Preliminary analysis of short-term storm impacts at specific sites along eastern Alabama beaches indicates that about 750,000 m<sup>3</sup> of sand could be needed for beach replenishment after each event. Long-term shoreline change data sets suggest that a replenishment interval of about 10 years would be expected to maintain beaches. This does not consider the potential for multiple storm events impacting the coast over a short time interval, nor does it consider longer time intervals absent of destructive storm events. Instead, the estimate represents average change over decades that is a reasonable measure for coastal management applications.

Given the quantity of 750,000 m<sup>3</sup> of sand per beach replenishment event, the surface area covered for evaluating potential environmental impacts is a function of the average dredging depth. Two factors should be considered when establishing dredging practice and depth limits for proposed extraction scenarios. First, regional shelf sediment transport patterns should be evaluated to determine net transport directions and rates. It is more effective to dredge the leading edge of a migrating shoal, and infilling of dredged areas occurs more rapidly at these sites (Byrnes and Groat, 1991; Van Dolah et al., 1998). Second, shoal relief above the ambient shelf surface should be a determining factor controlling depth of dredging. Geologically, shoals form and migrate on top of the ambient shelf surface, indicating a link between fluid dynamics, sedimentology, and environmental evolution (Swift et al., 1976). As such, average shoal relief is a reasonable depth threshold for maintaining environmentally-consistent sand extraction procedures.

In Area 4, southwest of the Mobile Bay entrance channel, a relatively small, low-relief shoal was identified by the GSA as a potential borrow area (Hummell et al., 1996). Average sand thickness, as determined from core samples, for a  $2.8 \times 10^6$  m<sup>2</sup> resource site in this area is 3 m (Figure 7-1), resulting in a potential sand volume of 8.4 MCM. Table 7-1 provides coordinate pairs defining the potential borrow site. Again, this volume of sand likely represents multiple beach replenishment events, meaning the cumulative impact of successive dredging events at the borrow site were estimated.

For Areas 1, 2, and 3, seaward of the eastern Alabama coast, maximum shoal relief is on the order of 4.5 m, and average shoal relief is about 3.0 m. Although specific beach replenishment practice is unknown for the Alabama coast, it is reasonable to expect multiple replenishment events over the next 50 years from the designated sand resource areas. As such, one shoal deposit was

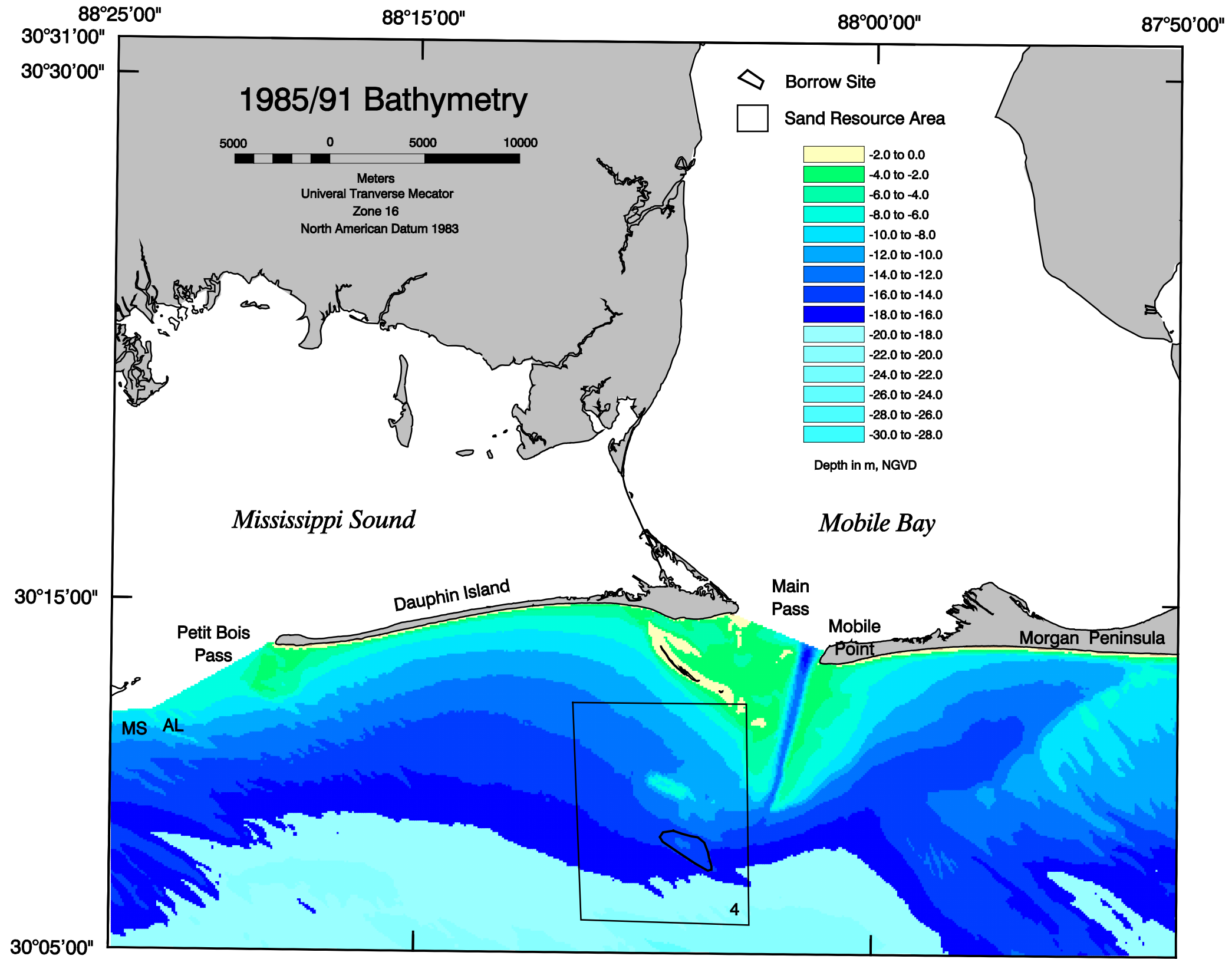


Figure 7-1. Location of potential borrow sites for Resource Area 4.

selected from Areas 1, 2, and 3 based on geological characteristics. A maximum excavation depth was determined for each specific site. In Area 1, a  $1.94 \times 10^6 \text{ m}^2$  borrow site was defined based on shoal morphology (Figure 7-2; see Table 7-1 for coordinate locations). Bathymetry data and geological samples (McBride and Byrnes, 1995) indicate a maximum excavation depth of 3.0 m, resulting in a 5.8 MCM extraction scenario. The same procedure was used for selecting borrow sites in Areas 2 and 3. The selected shoal borrow site in Area 2 encompassed  $0.57 \times 10^6 \text{ m}^2$  of seafloor to a depth of 3.0 m, resulting in 1.7 MCM of sand. Area 3 covers  $1.19 \times 10^6 \text{ m}^2$  of seafloor to a maximum excavation depth of 4.0 m. The resource site contains 4.7 MCM of sand. The sand volume at each of these borrow sites is greater than any single expected replenishment event, so all analyses were used to estimate potential cumulative effects of multiple extraction scenarios.

UTM Coordinates (Zone 16, NAD83)	Borrow Site 1	Borrow Site 2	Borrow Site 3	Borrow Site 4
	433830.4, 3341520.5	426592.1, 3340396.3	412989.2, 3339789.3	393244.8, 3335024.1
435593.5, 3341748.7	427163.0, 3340505.3	413053.5, 3339070.8	392701.1, 3334940.5	
436663.6, 3340943.7	427748.1, 3339248.1	414776.8, 3339000.6	392533.8, 3334689.4	
435291.6, 3340440.6	427621.6, 3339137.4	414724.2, 3339660.8	392680.2, 3334438.5	
	426949.5, 3339872.8		393579.4, 3333832.0	
			394374.1, 3333309.2	
			395064.2, 3332911.9	
			395252.4, 3332974.6	
			395252.4, 3333141.9	
			395210.6, 3333288.3	
			395127.0, 3333602.0	
			395064.2, 3333894.8	
			394876.0, 3334396.8	
			394541.4, 3334668.6	
			394185.9, 3334731.4	
			393704.9, 3334856.8	

A primary question addressed by the modeling efforts relates to sediment transport and infilling estimates at potential borrow sites and the impact of dredging operations on these estimates. Combined wave-current interaction (waves mobilize the seabed and currents transport the sediment) at the borrow areas results in a net direction of transport into and out of potential sand resource sites. Historical sediment transport dynamics suggest that the net direction of sediment movement is from east to west at all potential sand resource sites, and the rate at which sand moves along the shelf is relatively slow. For a 65-yr period of record, very little net erosion or accretion was documented throughout the study area, except on the seafloor in Area 4, where net deposition occurred in response to natural outflow from Mobile Bay and dredged material disposal activities by the U.S. Army Corps of Engineers. Consequently, it is expected that the time required to refill borrow areas will be on the order of decades for Areas 1, 2, and 3 and years in Area 4 where net fine-grained sediment deposition is prevalent. Area 4 is a problem for multiple sand extraction because the material expected to fill the borrow area after excavation is silt and clay. As such, increasing overburden to the sand resource may result in abandoning the site for a more viable alternative.

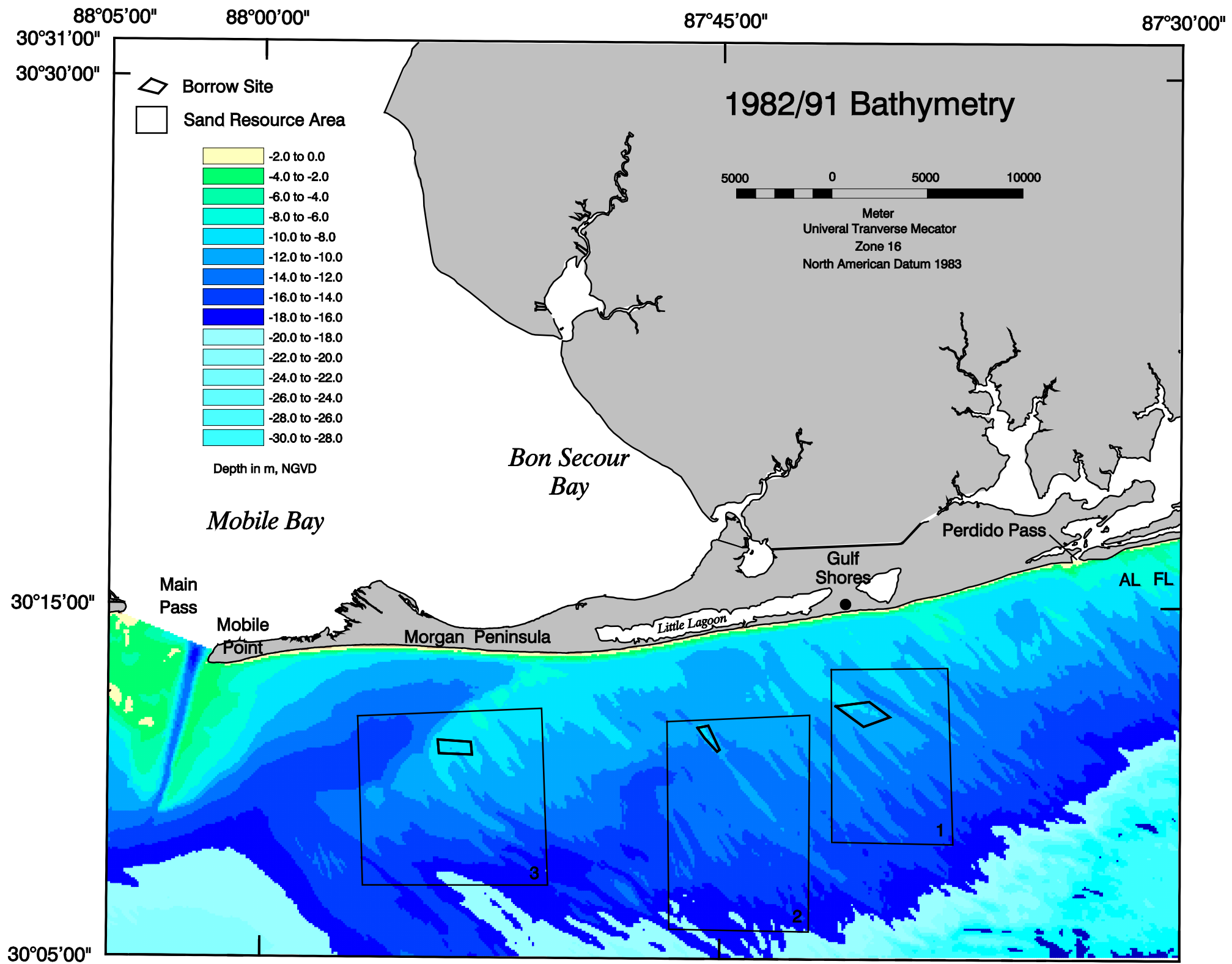


Figure 7-2. Location of potential borrow sites for Resource Areas 1, 2 and 3.

Applied Coastal  
Research and Engineering, Inc

## 7.2 WAVE TRANSFORMATION

Extraction of sediment from potential borrow sites may result in modifications to physical processes at local borrow sites and in the nearshore zone of Alabama. Wave modeling results indicate that minor changes will occur to wave fields under typical significant seasonal conditions and sand extraction scenarios representing multiple replenishment events. Changes in localized regions near borrow sites are apparent (maximum increases of 0.2 to 0.4 m in significant wave height; 12 to 24% of the initial wave height), but will not result in serious impact to the prevailing wave climate at the coast. Modifications to wave heights caused by extraction of sediment offshore Alabama decay as they approach the coastline. Under seasonal conditions, maximum changes in wave height dissipate significantly by the time the shoreline is encountered.

Under extreme conditions (i.e., the simulated 50-yr storm event), the same percentage change occurred to the wave field (12 to 24% of the initial wave height), although the magnitude of change increased (maximum increases of 1.0 to 2.0 m relative to initial waves). The 50-yr storm event and large sand extraction scenarios simulated in the present study represent a worst-case scenario (cumulative extraction impacts and storm waves). Although most events will not be as large as a 50-yr storm, during any storm event, dredged regions can be expected to have significant impact on the wave field in certain areas along the coastline. The magnitude of the impact will depend on the size and duration of the storm, the amount of material removed from the borrow site, and the time passed since dredging.

The most significant cumulative physical environmental impact appears to occur at the borrow site located within Sand Resource Area 2. Proximity of the borrow site to the coastline, orientation of the borrow site, and focusing of offshore wave energy seaward of the borrow site all contribute to the relative increase in wave height (0.4 m) at this location. A similar increase in wave energy is also evident near Sand Resource Area 3 due to the relatively large sand extraction depth (4 m).

Figures 7-3 and 7-4 show the present coastline configurations (thick line) versus differences in wave height, taken at approximately 100 m offshore, between pre- and post-dredging scenarios (thin line). These figures indicate approximate locations along the coastline where increases or decreases in wave height will occur due to potential sand extraction scenarios. Only small changes in wave height occur during typical significant seasonal conditions (<5 cm [ $<3\%$  increase] for all of coastal Alabama), while storm results show a slightly larger modification to wave heights. A notable amount of wave energy decay is illustrated at transect locations, and because wave heights are taken at 100 m offshore, an additional reduction in the magnitude of change is expected as waves enter shallower water and decay.

## 7.3 CURRENTS AND CIRCULATION

Throughout the study area, currents were predominantly parallel to shelf depth contours and driven by wind stress. Winds were shown to produce an approximate five-fold increase in current speed, with order 10 cm/sec currents during mild wind conditions to order 50 cm/sec during strong wind conditions. Frictional effects on the continental shelf modified currents as well; currents were strongest in the surface layer and weaker along the bottom and nearshore boundary areas. Major bathymetric and shoreline features, for example, the ebb-tidal shoals encompassing Pelican Island and vicinity at the western margin of Main Pass, were shown to modify predominant flow directions, and provide turning points that signaled major shifts in large-scale circulation patterns. Less significant bathymetric features, such as the dredged material disposal mound located at Sand Resource Area 4 or shore-oblique shoals prevalent in Areas 1 and 2, were found to have little effect on large-scale circulation. No direct observations of currents were obtained near Sand Resource Area 3 immediately east of Mobile Bay.

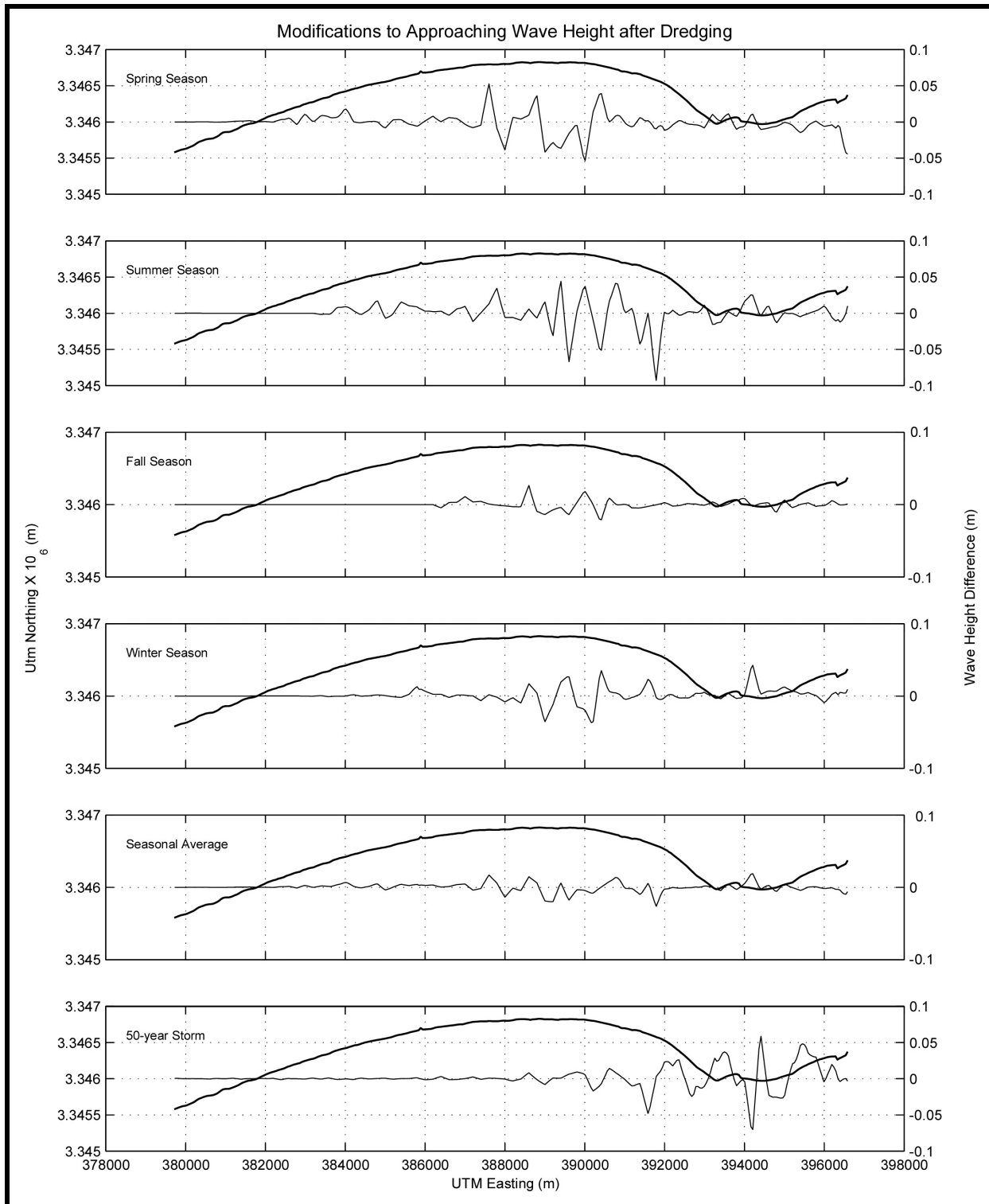


Figure 7-3. Present shoreline configuration (thick line) compared to differences in wave heights (thin line) caused by potential dredging scenarios offshore Dauphin Island. Wave heights (post-dredging minus pre-dredging) were taken from a baseline approximately 100 m seaward of the coastline.

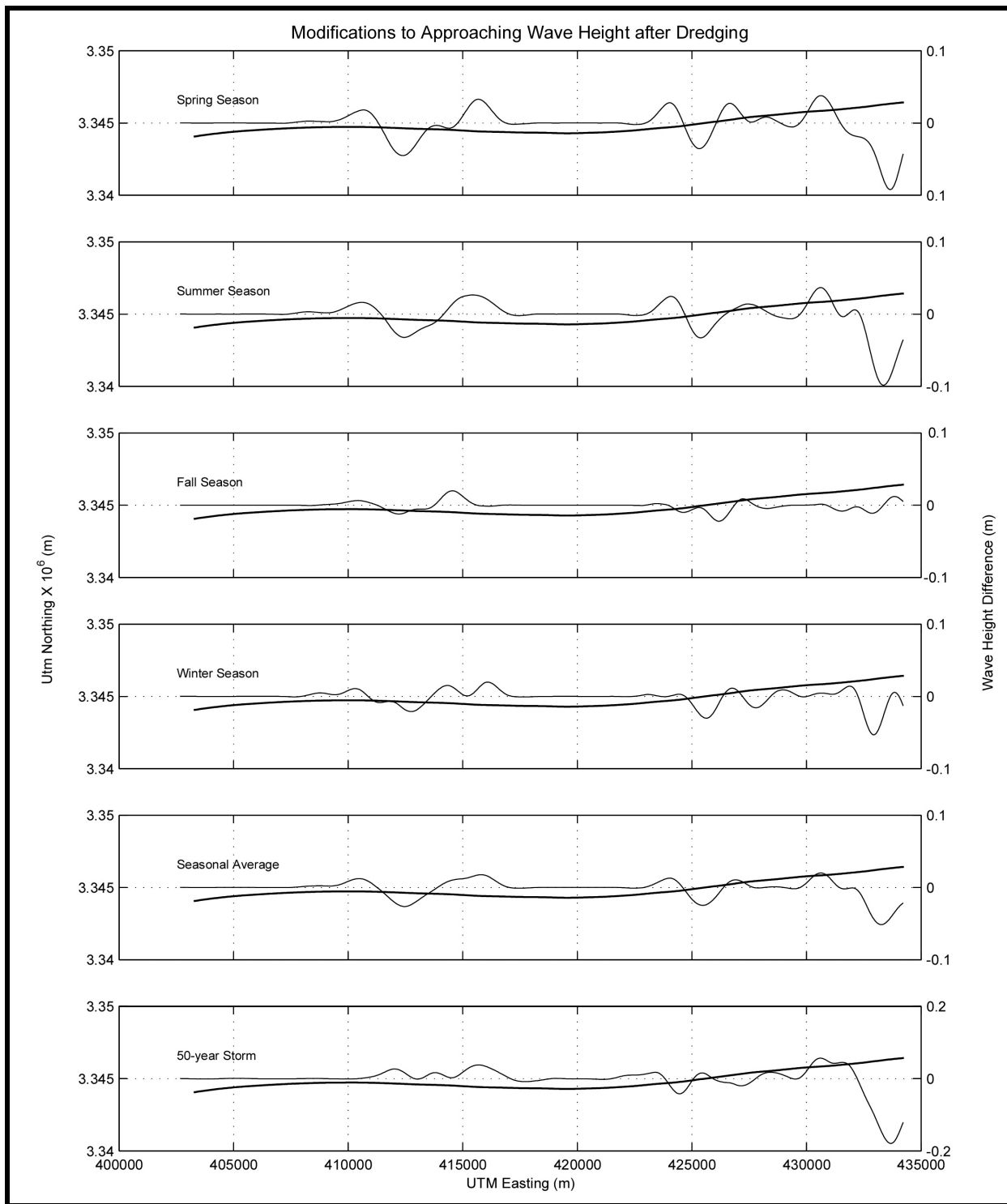


Figure 7-4. Present shoreline configuration (thick line) compared to differences in wave heights (thin line) caused by potential dredging scenarios offshore Morgan Peninsula. Wave heights (post-dredging minus pre-dredging) were taken from a baseline approximately 100 m seaward of the coastline.

While no large-scale predictive circulation models were developed to quantify effects of dredging in sand resource areas, the analysis of current patterns resulting from this study suggests proposed sand mining will have negligible impact on large-scale shelf circulation. The proposed sand mining locations are small relative to the entire shelf area, and it is anticipated that resulting dredging will not remove enough material to significantly alter major bathymetric features in the region. Therefore, the forces and/or geometric features that principally affect circulation patterns will remain relatively unchanged.

Currents within Sand Resource Area 4 were influenced primarily by Pelican Island, which produced a significant steering effect to divert flow along a general northwest/southeast axis, parallel to bathymetry contours. Mobile Outer Mound, with elevations approximately 2 to 6 m above average shelf elevation, also exists within this region. The ADCP field surveys showed highly localized bottom flow vectors influenced weakly by the presence of the dredged material mound, specifically with currents shown flowing around the feature. Adjacent flow vectors (of order 100's of meters removed from the mound) did not appear to be influenced by the mound, but they were directed along the depth contours, consistent with prevailing flow through the region. This suggests that small-scale bathymetric irregularities, such as a sand borrow site, while producing a localized effect on currents, will not impact prevailing or ambient flow characteristics. The proposed borrow site, approximately equal in area to the dredged material mound, is presumed to result in similar effects. Specifically, there is potential for localized impact on currents near the area but no effect on flow in adjacent areas.

For Areas 1 and 2, surface shape is rough with numerous ridges and troughs. Dredging is targeted to remove a portion of these shoal ridges. Circulation in the region did appear to be affected by bottom friction, but the influence was found to be manifest as weaker flow at the bottom and nearshore areas than at the surface. By removing a shoal ridge or a portion of a ridge, one may argue that there may be a resulting change to the bottom roughness, thus changing local current patterns. However, Areas 1 and 2 contain numerous ridges and troughs. Thus, it is unlikely the alteration of a single ridge would significantly impact bottom roughness. Also, these sand ridges migrate across the shelf surface (east to west), suggesting that any localized impacts due to dredging may be approximately equal to localized impacts due to natural transience of these sand ridges and shoals. As such, data suggest it is doubtful that removal or alteration of a small region of shoal ridges will have any measurable impact on regional current flow.

The sand borrow site in Sand Resource Area 3 is located on the seaward tip of a major sand shoal (Figure 7-2). While no analysis of flow was performed for Area 3, extrapolating our understanding of flow behavior from areas west and east suggests this large shoal may influence circulation. The shoal provides significant elevation and extent to modify alongshore flow, likely in terms of deceleration due to increased frictional effects and deflection of flow. The shape of the shoal suggests that westward-directed flow will be deflected slightly offshore, and that eastward flow may be slowed by friction as currents pass over the feature. Removing a small portion of the seaward tip of the shoal may reduce the steering effects of flow and possibly lessen frictional damping. Even so, the proposed borrow site represents a relatively small fraction of the shoal, hence effects on currents in Area 3 due to dredging will likely be negligible.

## **7.4 SEDIMENT TRANSPORT**

Current measurements and analyses, and wave transformation modeling, provide baseline information on incident processes impacting coastal environments under existing conditions and with respect to proposed sand mining activities for beach replenishment. Ultimately, the most important data set for understanding physical processes impacts from offshore sand extraction is changes in sediment transport dynamics resulting from potential sand extraction scenarios relative to existing conditions.

Three independent sediment transport analyses were completed to evaluate physical environmental impacts due to sand mining. First, historical sediment transport trends were quantified to document regional, long-term sediment movement throughout the study area using historical bathymetry data sets. Erosion and accretion patterns were documented, and sediment transport rates in the littoral zone and at offshore borrow sites were evaluated to assess potential changes due to offshore sand dredging activities. Second, sediment transport patterns at proposed offshore borrow sites were evaluated using wave modeling results and current measurements. Post-dredging wave model results were integrated with regional current measurements to estimate sediment transport trends for predicting borrow site infilling rates. Third, nearshore currents and sediment transport were modeled using wave modeling output to document potential impacts to the longshore sand transport system (beach erosion and accretion). All three methods were compared for evaluating consistency of measurements relative to predictions, and potential physical environmental impacts were identified.

#### **7.4.1 Historical Sediment Transport Patterns**

Regional geomorphic changes between 1917/20 and 1982/91 were documented for assessing long-term, net coastal sediment transport dynamics. Although these data do not provide information on the potential impacts of sand dredging from proposed borrow sites, they do provide a means of calibrating predictive sediment transport models relative to infilling rates at borrow sites and longshore sand transport.

A comparison of erosion and deposition volumes at proposed borrow sites provided a method for quantifying net sediment transport rates (or borrow site infilling rates). For borrow sites in Sand Resource Areas 1, 2, and 3, net transport rates ranged from about 9,000 to 34,000 m<sup>3</sup>/yr. This compared well with sediment transport predictions made near borrow sites using wave model output and currents measurements (13,000 to 100,000 m<sup>3</sup>/yr). The net longshore sand transport rate for the Morgan Peninsula was determined by comparing zones of erosion and accretion in the littoral zone (seaward to 6-m depth contour [NGVD]) between Perdido Pass and Main Pass (Mobile Bay entrance) in a sediment budget formulation. The net transport rate for that portion of the study area was approximately 106,000 m<sup>3</sup>/yr. Net transport rates determined via sediment transport modeling ranged from about 50,000 to 150,000 m<sup>3</sup>/yr under seasonal conditions. These rates compare well and provide a measured level of confidence in wave and sediment transport modeling predictions relative to impacts associated with sand dredging from proposed borrow sites.

#### **7.4.2 Sediment Transport Modeling at Potential Borrow Sites**

In addition to predicted modifications to the wave field, potential sand mining at offshore borrow sites results in minor changes in sediment transport pathways in and around the dredged regions. The modifications to bathymetry caused by sand mining only influence local hydrodynamic and sediment transport processes in the offshore area. Although wave heights may change at the dredged borrow sites, areas adjacent to the sites do not experience dramatic changes in wave or sediment transport characteristics.

Initially, sediment transport at borrow sites will experience mild changes after sand dredging is complete. Given the water depths at the proposed borrow sites, it is expected that minimal impacts to waves and sediment transport will occur during infilling. Sediment that replaces the dredged material will fluctuate based on the location, time of dredging, and storm characteristics following dredging episodes. Borrow sites at Sand Resource Areas 1, 2, and 3 are expected to fill with the same material that was excavated (the entire shelf surface south of the Morgan Peninsula is at least 95% medium-to-fine sand). Sediment characteristics in this region are consistent, high-quality, and compatible with beach sand. The potential borrow site at Sand Resource Area 4, however, will likely be filled with fine sediment (i.e., fine sand to clay) exiting Mobile Bay by natural processes or human activities (maintenance channel dredging and disposal). Because the potential

transport rate plus sediment flux from Mobile Bay is substantially greater than shelf transport rates alone, the borrow site in Sand Resource Area 4 will fill faster than other borrow sites, limiting the likelihood for multiple dredging events from the same area.

### **7.4.3 Nearshore Sediment Transport Trends**

Development of the REF/DIF S wave model, the wave-induced current model, and the longshore sediment transport model provided a basis for comparing existing conditions with post-dredging coastal processes conditions. Dredging of major offshore borrow sites can have a significant effect on coastal erosion/accretion, since changes to the offshore bathymetry can focus wave energy by altering the nearshore wave characteristics. For example, waves encountering a hole created by dredging activities can be refracted toward the edges of the dredged area (refraction tends to bend waves parallel to shallower depth contours). Through this process, wave energy will be focused toward either side of a dredged area and a shadow zone of lower wave energy will be created directly landward of the borrow area.

For the coast of Alabama, the physical effects of dredging four different borrow sites were evaluated. Average annual sediment transport patterns for existing conditions, as well as post-dredging scenarios, were documented for the Morgan Peninsula and Dauphin Island sub-grids to determine whether dredging would cause a significant effect above normal conditions. In addition, sediment transport effects were evaluated for a 50-yr storm event. The physical environmental impacts of dredging in Sand Resource Areas 1, 2, and 3 are shown on Figure 7-5 for average annual conditions and on Figure 7-6 for a 50-yr storm event. The impacts of dredging in Resource Area 4 are shown on Figure 7-7 for average annual conditions and on Figure 7-8 for a 50-yr storm event.

#### **7.4.3.1 Eastern Alabama Coast**

Figure 7-5 illustrates that there is a defined, but somewhat minor impact, from dredging in Areas 1, 2, and 3. Due to the naturally higher transport rates at the eastern end of Morgan Peninsula, the magnitude of impacts associated with borrow sites at Resource Areas 1 and 2 appear to be higher than those associated with Resource Area 3. However, the net transport rate associated with pre-dredging conditions at Resource Area 3 is significantly lower than the rate associated with adjacent borrow sites. For all three borrow sites, the maximum variation in annual longshore sand transport rate is approximately 8 to 15% of the existing value. In general, the increase or decrease in longshore sediment transport rates associated with each potential borrow site amounts to approximately 3 to 8% of the net littoral drift, distributed over an approximate 10 km stretch of shoreline.

The predominant wave direction from the southeast shifts the wave-induced impacts of dredging towards the west. As described above, a shadow zone typically is created immediately shoreward of a borrow site, as wave energy is directed away from the shoreline immediately landward of the borrow site. Based on Figure 7-5, the shadow zone landward of Resource Area 3 is approximately 3 km to the west of the Easting coordinates for this area. This shadow zone is indicated by a significant reduction in west-directed wave energy. Due to the close proximity of Resource Areas 1 to 2, it is difficult to discern the individual impacts of each dredging scenario.

According to Figure 7-6, dredging in Resource Areas 1 and 2 will create a slight increase in west-directed transport during a storm. Again, the maximum impact of this dredging activity would be an approximate 8 to 15% increase in potential transport rates over a short stretch of shoreline. The average increase in west-directed transport would be 5 to 8%; however, a similar reduction in west-directed transport is associated with the shadow zone generated by the borrow site at Resource Area 1. Impacts associated with dredging at Resource Areas 2 and 3 are slightly lower than impacts associated with Area 1.

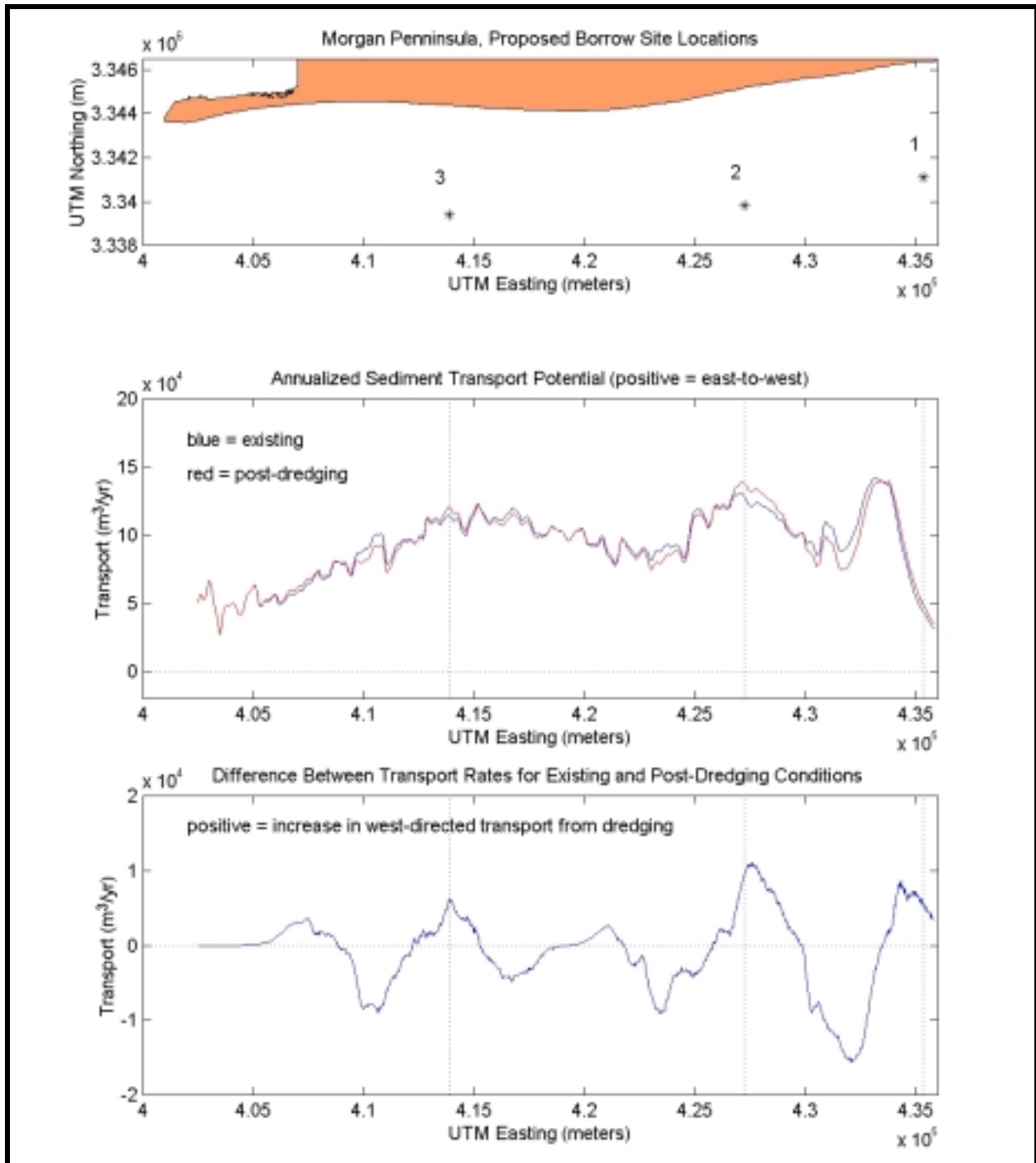


Figure 7-5. Difference in average annual transport rates associated with dredging sand resource sites along Morgan Peninsula.

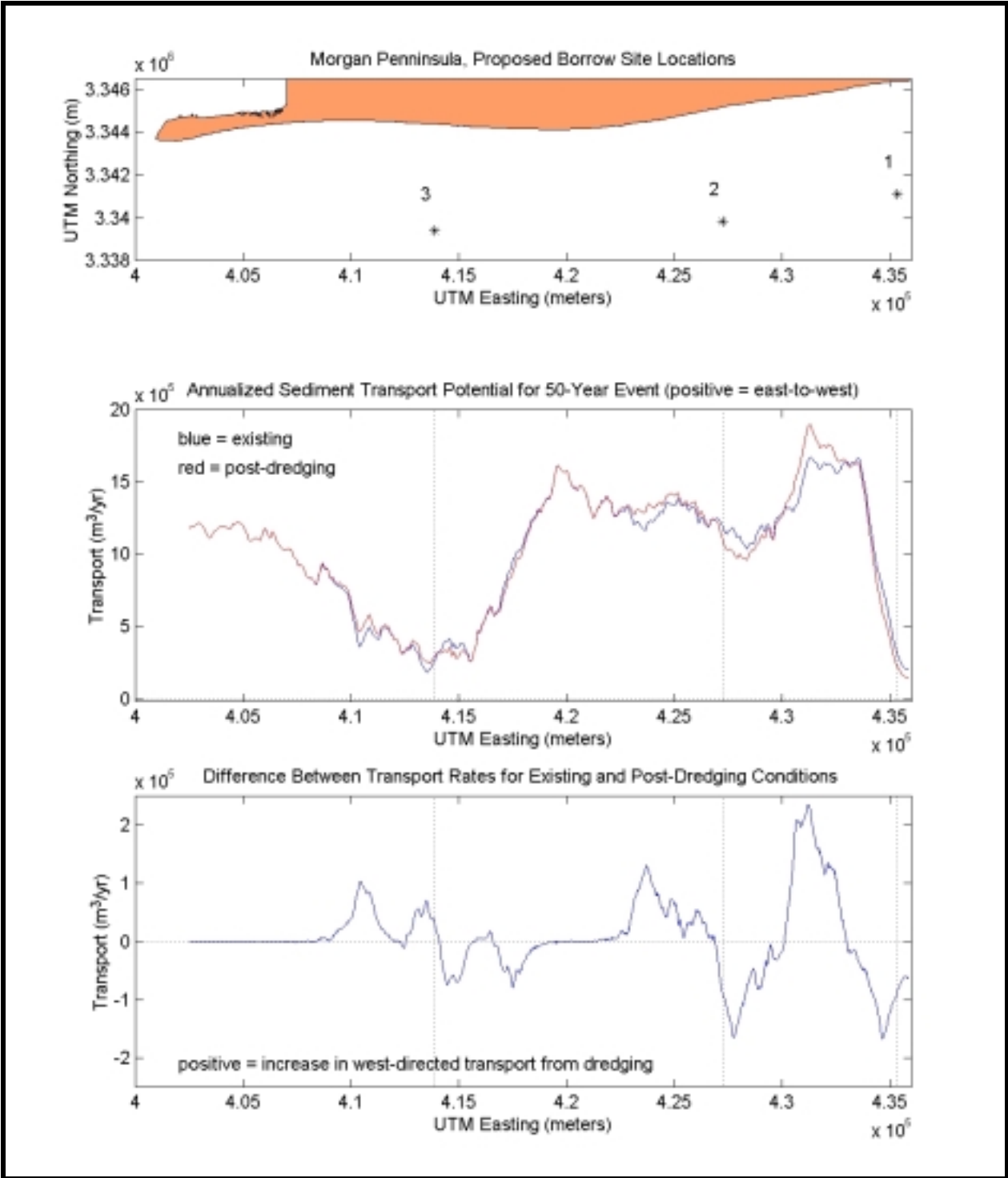


Figure 7-6. Difference in transport rates for 50-yr storm event associated with dredging sand resource sites along Morgan Peninsula.

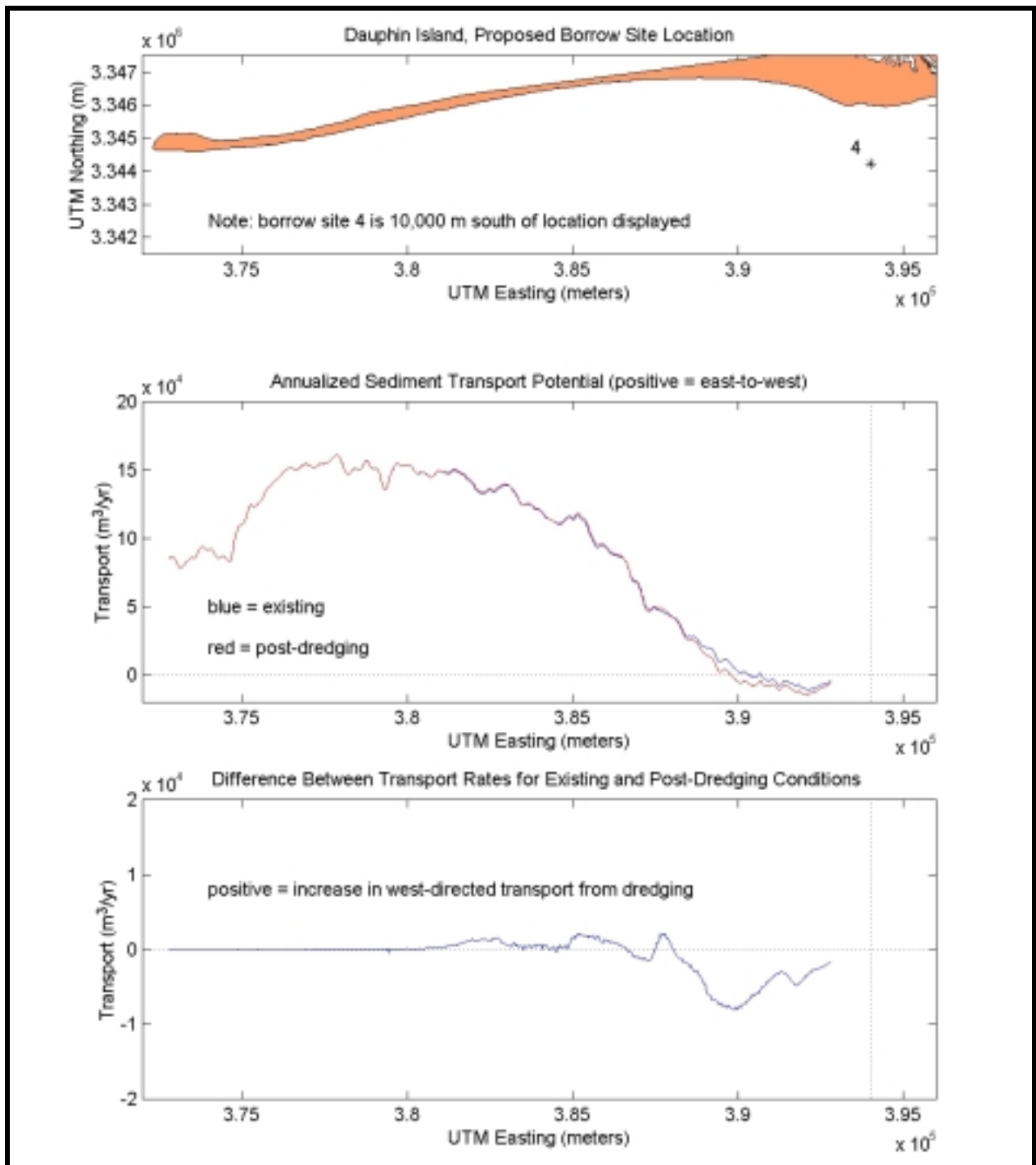


Figure 7-7. Difference in average annual transport rates associated with dredging sand resource area along Dauphin Island.

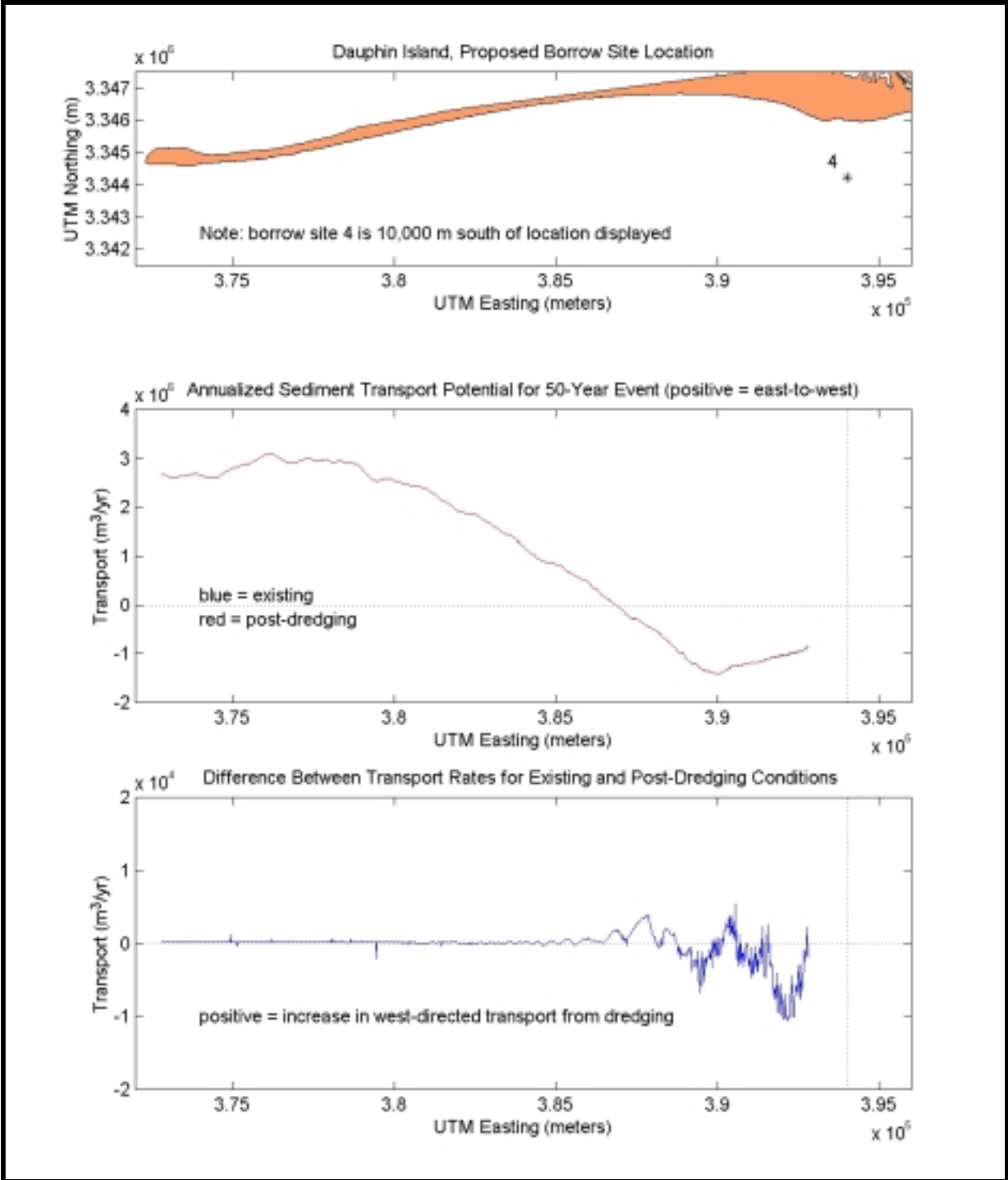


Figure 7-8. Difference in transport rates for 50-yr storm event associated with dredging sand resource area along Dauphin Island.

### 7.4.3.2 Western Alabama Coast

The potential impacts of dredging Resource Area 4 are insignificant in relation to Resource Areas 1 through 3. Average annual conditions illustrated in Figure 7-7 indicate a relatively high percentage change in transport rates along the eastern portion of Dauphin Island; however, the existing net littoral drift is almost non-existent at this location. The net effect of dredging the borrow site at Resource Area 4 would be to direct a greater percentage of sand transport to the east, with a maximum increase of approximately 8,000 m<sup>3</sup>/yr. The limited influence of borrow site dredging is exemplified in the scenario for the 50-yr event, shown in Figure 7-8. The two lines showing existing conditions and the post-dredging scenario are nearly coincident. A slight increase (maximum of approximately 10,000 m<sup>3</sup>/yr if this condition existed for an entire year) in east-directed transport is created as a result of dredging Area 4. As such, there is no significant impact to longshore transport rates on Dauphin Island as a result of potential sand mining activities in Resource Area 4.

### 7.4.3.3 Significance of Transport Trends

Quantitative evaluation of potential effects to nearshore sediment transport rates associated with dredging scenarios was performed using a statistical analysis of predicted rates for both annual average conditions (Table 7-2) and the 50-year event (Table 7-3). The region of influence for each borrow site was characterized using four calculated parameters, in addition to a visual comparison of existing and post-dredging sediment transport rates.

Table 7-2. Statistical parameters for annual average sediment transport conditions associated with Sand Resource Areas 1 through 4.				
	Resource Area			
	1	2	3	4
Mean Transport (m <sup>3</sup> /yr)	97,000	106,000	103,000	33,000
Absolute (Mean Difference in Transport (m <sup>3</sup> /yr))	8,000	5,200	3,200	3,200
Standard Deviation (m <sup>3</sup> /yr)	4,600	3,200	2,400	2,300
Percentage Difference	8.3	4.9	3.1	9.6

Table 7-3. Statistical parameters for 50-year event sediment transport conditions associated with Sand Resource Areas 1 through 4.				
	Resource Area			
	1	2	3	4
Mean Transport (m <sup>3</sup> /yr)	1,220,000	1,240,000	580,000	-620,000
Absolute (Mean Difference in Transport (m <sup>3</sup> /yr))	102,000	69,000	33,000	2,200
Standard Deviation (m <sup>3</sup> /yr)	60,000	51,000	27,000	2,400
Percentage Difference	8.3	5.6	5.8	0.3

For average annual conditions, mean longshore sand transport rates were approximately equal landward of borrow sites in Resource Areas 1, 2, and 3. Mean annual transport rates along the eastern portion of Dauphin Island (landward of Resource Area 4) were estimated to be approximately 35% of the rates associated with the Morgan Peninsula. The absolute value of the mean difference between existing and post-dredging conditions generally decreased from east-to-west, with a maximum difference of approximately 8,000 cubic meters per year (8.3%) along the shoreline stretch influenced by dredging in Resource Area 1. Because the net sediment transport rate predicted for the borrow site in Resource Area 4 was relatively low (approximately 33,000 cubic meters per year), the percentage difference between existing and post-dredging conditions was greatest for this site (9.6%). Results from analyses of the 50-year event indicated a similar trend,

where the absolute value of the mean difference decreased from east-to-west. The maximum difference in transport rates was approximately 102,000 cubic meters per year at Resource Area 1. Due to wave breaking associated with Pelican Island and the shallow shoals seaward of the eastern end of Dauphin Island, the 50-year event created variations in transport similar in magnitude to those predicted for average annual conditions at Resource Area 4 (absolute value of the mean difference was 2,200 and 3,200 cubic meters per year for the 50-year event and average annual wave conditions, respectively).

Upon initial inspection, the differences between existing and post-dredging transport rates appear to be significant. To determine the relative significance of this difference, a simple analysis of uncertainties associated with nearshore sediment transport calculations was performed. An estimate of uncertainties was based on procedures described by Rosati and Kraus (1991). Although the sediment transport calculation technique used in this study was slightly different than the method employed by Rosati and Kraus (1991), both procedures were based on wave height and direction. Using conservative estimates for error associated with wave height and wave direction of 10%, sediment transport rates can be predicted to within  $\pm 35\%$ . These errors can be attributed to the inherent uncertainties in the WIS data set (wave height and directional accuracy) used to develop offshore wave conditions. The  $\pm 35\%$  value is significantly higher than the impacts associated with any of the borrow sites evaluated along the Alabama coast.

Analysis of uncertainties related to longshore sediment transport estimates indicates that variations in transport associated with potential dredging scenarios are an order of magnitude lower than the uncertainty associated with sediment transport calculations. Therefore, the potential effects of offshore sand mining seaward of the Alabama coast on longshore sand transport rates are insignificant for the scenarios tested in this study. Alternative scenarios are not expected to pose any greater effects unless the quantity of sand dredged from a site is substantially larger than potential dredged volumes selected for this study.

## **7.5 BENTHIC ENVIRONMENT**

The purpose of this section is to address potential effects of offshore dredging activity on benthic organisms, including analyses of the potential rate and success of recolonization following cessation of dredging activities. This section is divided into three parts. The first two parts summarize information from the existing literature on effects and recolonization. The first part (Section 7.5.1) describes potential impacts to benthic organisms from the physical disturbance of dredging, which causes removal, suspension/dispersion, and deposition of sediments. The second part (Section 7.5.2) discusses the potential rate and success of recolonization. Finally, the third part (Section 7.5.3) provides predictions of impacts and recolonization relative to the five borrow sites off Alabama.

Ecological effects of marine mining and beach nourishment operations have been reviewed by numerous authors (Thompson, 1973; Naqvi and Pullen, 1982; Nelson, 1985; Cruickshank et al., 1987; Goldberg, 1989; Grober, 1992; Hammer et al., 1993; National Research Council, 1995). Effects vary from detrimental to beneficial, short- to long-term, and direct and indirect (National Research Council, 1995).

Most reviews on the effects of beach nourishment operations have focused on potential impacts at the beach. Comprehensive assessments of the effects on biological resources at open ocean sand borrow sites have been limited (National Research Council, 1995). Alterations to biological resources in offshore sand borrow areas are generally of longer duration, and the consequences of those changes have not been well-defined (National Research Council, 1995). The remainder of this section focuses on potential impacts of dredging operations at offshore borrow sites.

### **7.5.1 Effects of Offshore Dredging on Benthic Fauna**

The primary impact producing factor relative to dredging offshore borrow areas is mechanical disturbance of the seabed. This physical disruption includes removal, suspension/dispersion, and deposition of dredged material. This section focuses on the potential biological effects of these physical processes on benthic fauna.

#### **7.5.1.1 Sediment Removal**

Physical removal of sediments from a borrow area removes benthic habitat along with infaunal and epifaunal organisms which are incapable of avoiding the dredge, resulting in drastic reductions in the number of individuals, number of species, and biomass. Extraction of habitat and biological resources may in turn disrupt the functioning of existing communities. Removal of benthic resources is of concern because they are important in the food web for commercially and recreationally important fishes and invertebrates, and contribute to the biodiversity of the pelagic environment through benthic-pelagic coupling mechanisms. These mechanisms include larval transport and diurnal migrations of organisms which may have substantial impact on food availability, feeding strategies, and behavioral patterns of other members of the assemblage (Hammer and Zimmerman, 1979; Hammer, 1981).

Removal of sand resources can expose underlying sediment and change the sediment structure and composition of a borrow area, consequently altering its suitability for burrowing, feeding, or larval settlement of some benthic organisms. Many studies show decreases in mean grain size, and in some cases, increases in silt and clay in borrow sites following dredging (National Research Council, 1995). Changes in sediment composition could potentially prevent recovery to an assemblage similar to that which occurred in the borrow area prior to dredging and could by implication affect the nature and abundance of food organisms for commercial and recreational fishery stocks (Coastline Surveys Limited, 1998; Newell et al., 1998). In some cases, dredging borrow areas may create new and different habitat from surrounding substrates which could result in increased habitat complexity and biodiversity of an area.

The influence of sediment composition on benthic community composition has been recognized since the pioneer studies of Peterson (1913), Thorson (1957), and Sanders (1958). However, more recent reviews suggest that precise relationships between benthic assemblages and specific sediment characteristics are poorly understood (Gray, 1974; Snelgrove and Butman, 1994; Newell et al., 1998). Sediment grain size, chemistry, and organic content may influence recolonization of benthic organisms (McNulty et al., 1962; Thorson, 1966; Snelgrove and Butman, 1994), although the effects of sediment composition on recolonization patterns of various species are not always significant (Zajac and Whitlatch, 1982). Because the complexity of soft-sediment communities may defy any simple paradigm relating to any single factor, Hall (1994) and Snelgrove and Butman (1994) proposed a shift in focus towards understanding relationships between organism distributions and the dynamic sedimentary and hydrodynamic environments. It is likely that the composition of benthic assemblages is controlled by a wide array of physical, chemical, and biological variables which interact in complex ways which are variable with time.

Removal of sediments from borrow areas can alter seabed topography, creating pits which may refill rapidly or cause detrimental impacts for extended periods of time. Borrow areas have been known to remain well-defined 8 years after dredging (Marsh and Turbeville, 1981; Turbeville and Marsh, 1982). Although nearly 12 years may be required for some offshore borrow sites to refill to pre-dredge profiles, intentionally locating borrow sites in highly depositional areas may dramatically reduce the time for refilling (Van Dolah et al., 1998). In general, shallow dredging over large areas causes less harm than small but deep pits, particularly pits opening into a different substrate surface (Thompson, 1973; Applied Biology, Inc., 1979). Deep pits also can hamper commercial trawling activities and harm level-bottom communities (Thompson, 1973). If borrow pits

are deep, current velocity is reduced at the bottom, which can lead to deposition of fine particulate matter and in turn a biological assemblage much different in composition than the original. Deep holes may decrease dissolved oxygen to hypoxic or anoxic levels and increase hydrogen sulfide levels (Murawski, 1969; Saloman, 1974; National Research Council, 1995).

#### **7.5.1.2 Sediment Suspension/Dispersion**

Dredging causes suspension of sediments which increases turbidity over the bottom. This turbidity undergoes dispersion in a plume that drifts with the water currents. The extent of suspension/dispersion depends on sediment composition, sediment transport processes, the type of dredging equipment, techniques for operating the equipment, amount of dredging, thickness of the dredged layer, etc. Herbich and Brahme (1991) and Herbich (1992) reviewed sediment suspension caused by existing dredging equipment, and discussed potential technologies and techniques to reduce suspension and the associated environmental impacts. In general, cutterhead suction dredges produce less turbidity than hopper dredges.

A cutterhead suction dredge consists of a rotating cutterhead, positioned at the end of a ladder, that excavates the bottom sediment. The cutterhead is swung in a wide arc from side to side as the dredge is stepped forward on pivoting spuds, and the excavated material is picked up through a suction pipe and transferred by pipeline as a slurry (Hrabovsky, 1990; LaSalle et al., 1991). Sediment suspension is caused by the rotating action of the cutterhead and the swinging action of the ladder (Herbich, 1992). A properly operated cutterhead dredge can limit sediment suspension to the lower portion of the water column (Herbich and Brahme, 1991; Herbich, 1992).

A well-designed cutterhead, selection of an appropriate cutterhead for a given sediment, the correct relationship between rotational speed of the cutterhead and the magnitude of hydraulic suction, and suitable swing rate of the cutterhead, along with hooded intakes, may reduce turbidity at the cutterhead, although these conditions are rarely achieved (Herbich, 1992). Measurements around properly operated cutterhead dredges show that elevated levels of suspended sediments can be confined to the immediate vicinity of the cutterhead and dissipate rapidly with little turbidity reaching surface waters (Herbich and Brahme, 1991; LaSalle et al., 1991; Herbich, 1992). Maximum suspended sediment concentrations typically occur within 3 m above the cutterhead and decline exponentially to the sea surface (LaSalle et al., 1991). Suspended sediment concentrations in near-bottom waters may be elevated up to several hundred meters laterally from the cutterhead location (LaSalle et al., 1991).

A hopper dredge consists of one, two, or more dragarms and attached dragheads mounted on a ship-type hull or barge with hoppers to hold the material dredged from the bottom (Herbich and Brahme, 1991). As the hopper dredge moves forward, sediment is hydraulically lifted through the dragarm and stored in hopper bins on the dredge (Taylor, 1990; LaSalle et al., 1991). Hopper dredging operations produce turbidity as the dragheads are pulled through bottom sediment. However, the main source of turbidity during hopper dredging operations is sediment release during hopper overflow (Herbich and Brahme, 1991; LaSalle et al., 1991; Herbich, 1992). A plume may occasionally be visible at distances of 1,200 m or more (LaSalle et al., 1991).

Much attention has been given to turbidity effects from dredging, although most reviews have concerned estuaries, embayments, and enclosed waters (e.g., Sherk and Cronin, 1970; Sherk, 1971; Sherk et al., 1975; Moore, 1977; Peddicord and McFarland, 1978; Stern and Stickle, 1978; Herbich and Brahme, 1991; LaSalle et al., 1991; Kerr, 1995). Turbidity effects should be less important in unprotected offshore areas for several reasons. Offshore sand tends to be coarser with less clay and silt than inshore areas. The open ocean environment also provides more dynamic physical oceanographic conditions which minimize settling effects. In addition, offshore organisms are adapted to sediment transport processes which create scouring, natural turbidity, and sedimentation effects under normal conditions. Impacts should be evaluated in light of average

background conditions as well as occasional high level disturbances associated with storms, floods, hypoxia/anoxia, trawling, etc. (Herbich, 1992). Physical disturbance of the bottom and resulting biological impacts from dredging are similar to those of storms but at a much smaller spatial scale.

Turbidity interferes with the food gathering process of filter feeders and organisms that feed by sight by inundation with nonnutritive particles. Large quantities of bottom material placed in suspension decrease light penetration and change the proportion of wavelengths of light reaching the bottom, leading to decreases in photosynthetic activity. Suspension and dispersion of sediment may cause changes in sediment and water chemistry as nutrients and other substances are released from the substratum and dissolved during the dredging process. Coastline Surveys Limited (1998) proposed that for aggregate mining operations using hopper dredges, the far-field visible plume contains an organic admixture of fats, lipids, and carbohydrates from organisms entrained and fragmented during the dredging process and discharged with the overflow. Dredging may produce localized hypoxia or anoxia in the water column due to oxygen consumption of the suspended sediments (LaSalle et al., 1991). Suspension and dispersion processes also uncover and displace benthic organisms, temporarily providing extra food for bottom feeding species (Centre for Cold Ocean Resources Engineering, 1995).

### **7.5.1.3 Sediment Deposition**

Suspended sediment settles and is deposited nearby or some distance from the dredge site. The extent of deposition and the boundaries of biological impact are dependent on the type and amount of suspended sediment and physical oceanographic characteristics of the area.

Dredging effects are not necessarily limited to the borrow area alone. The types of far-field impacts from suspension and deposition of sediment can be detrimental or beneficial. Deposition of sediment can suffocate and bury benthic fauna, although some organisms are able to migrate vertically to the new surface (Maurer et al., 1986). Johnson and Nelson (1985) found decreases in abundances and numbers of taxa at non-dredged stations, although these decreases were not as extreme as those observed in the borrow area. McCaully et al. (1977) as cited by Johnson and Nelson (1985) also observed that dredging effects can extend to other nearby areas, and noted decreases in abundance ranging from 34% to 70% at undredged stations within 100 m of a dredged area. Conversely, benthos may show an increase in biodiversity downstream from the dredge site (Centre for Cold Ocean Resources Engineering, 1995). In some areas, population density and species composition of benthic invertebrates increased rapidly outside dredging sites, with the level of enhancement decreasing with increasing distance from the dredged area up to a distance of 2 km (Stephenson et al., 1978; Jones and Candy, 1981; Poiner and Kennedy, 1984). The enhancement was ascribed to the release of organic nutrients from the dredge plume, a process known from other studies (Ingle, 1952; Biggs, 1968; Sherk, 1972; Oviatt et al., 1982; Coastline Surveys Limited, 1998; Newell et al., 1998). This suggestion was supported by records of nutrient releases from benthic areas during intermittent, wind-driven bottom resuspension events (Walker and O'Donnell, 1981), significant increases in nutrients in the water column from simulated storm events in the laboratory (Oviatt et al., 1982), and review of the literature indicating a major restructuring force in infaunal communities is the response of species to resources released from the sediments by periodic disturbance (Thistle, 1981). Fishing also may improve temporarily down current of the dredging area and continue for some months (Centre for Cold Ocean Resources Engineering, 1995).

## **7.5.2 Recolonization Rate and Success**

### **7.5.2.1 Adaptations for Recolonization and Succession**

In dynamic areas which undergo frequent perturbations, benthic invertebrates tend to be small bodied, short lived, and adapted for maximum rate of population increase with high fecundity,

efficient dispersal mechanisms, dense settlement, and rapid growth rates (MacArthur, 1960; MacArthur and Wilson, 1967; Odum, 1969; Pianka, 1970; Grassle and Grassle, 1974). In contrast, organisms in stable areas tend to be relatively larger and longer lived with low fecundity, poor dispersal mechanisms, slow growth rates, and adaptations for non-reproductive processes such as competition and predator avoidance. Recolonization of a disturbed area often is initiated by organisms which have the adaptive characteristics for rapid invasion and colonization of habitats where space is available due to some natural or man-induced disturbance. These early colonizers frequently are replaced during the course of succession through competition by other organisms, unless the habitat is unstable or frequently perturbed.

Although the distinction between the adaptive strategies is somewhat arbitrary and is blurred in habitats which are subject to only mild disturbance, the lifestyle differences are fundamentally important because they help explain variations in succession and recolonization rate and success following disturbance (Coastline Surveys Limited, 1998; Newell et al., 1998). Knowledge of faunal component lifestyles allows some predictions of dredging impacts and subsequent recolonization and recovery of community composition (Coastline Surveys Limited, 1998; Newell et al., 1998).

### 7.5.2.2 Successional Stages

Successional theory states that organism-sediment interactions result in a predictable sequence of benthic invertebrates belonging to specific functional types following a major seafloor disturbance (Rhoads and Germano, 1982, 1986). Because functional types are the biological units of interest, the succession definition does not rely on the sequential appearance of particular species or genera (Rhoads and Boyer, 1982). This continuum of change in benthic communities has been divided arbitrarily into three stages (Rhoads et al., 1978; Rhoads and Boyer, 1982; Rhoads and Germano, 1982):

- Stage I is the initial pioneering community of tiny, densely populated organisms which appears within days of a natural or anthropogenic disturbance. Stage I communities are composed of opportunistic species that have high tolerance for and can indicate disturbance by physical disruption, organic enrichment, and chemical contamination of sediments. The organisms have high rates of recruitment and ontogenetic growth. Stage I communities tend to physically bind sediments, making them less susceptible to resuspension and transport. For example, Stage I communities often include tube-dwelling polychaetes or oligochaetes that produce mucous to build their tubes which stabilizes the sediment surface. Stage I communities include suspension or surface deposit-feeding animals that feed at or near the sediment-water interface. The Stage I initial community may reach population densities of  $10^4$  to  $10^6$  individuals/m<sup>2</sup>;
- Stage II is the beginning of the transition to burrowing, head-down deposit feeders that rework the sediment deeper and deeper with time and mix oxygen from the overlying water into the sediment. Stage II animals may include tubicolous amphipods, polychaetes, and mollusks. These animals are larger and have very low population densities compared to Stage I animals; and
- Stage III is the mature and stable community of deep-dwelling, head-down deposit feeders. In contrast to Stage I organisms, these animals rework the sediments to depths of 3 to 20 cm or more, loosening the sedimentary fabric and increasing the water content of the sediment. They also actively recycle nutrients because of the high exchange rate with the overlying water resulting from their burrowing and feeding activities. The presence of Stage III taxa can be a good indication that the sediment surrounding these organisms has not been severely disturbed recently, resulting in high benthic stability and health. Loss of Stage III species results in the loss of

sediment stirring and aeration and may be followed by a build-up of organic matter (eutrophication) of the sediment. Because Stage III species tend to have relatively low rates of recruitment and ontogenetic growth, they may not reappear for several years once they are excluded from an area. These inferences are based on past work, primarily in temperate latitudes, showing that Stage III species are relatively intolerant to physical disturbance, organic enrichment, and chemical contamination of sediments. Population densities are low (10 to 10<sup>2</sup> individuals/m<sup>2</sup>) compared to Stage I.

The general pattern of succession of benthic species in a marine sediment following cessation of dredging or other environmental disturbance begins with initial recolonization. Initial recolonization occurs relatively rapidly by small opportunistic species which reach peak population densities within months of a new habitat becoming available after catastrophic mortality of the previous assemblage. As the disturbed area is invaded by additional larger species, the population density of initial colonizers declines. This transitional period and assemblage with higher species diversity and a wide range of functional types may last for years, depending on numerous environmental factors. Provided environmental conditions remain stable, some members of the transitional assemblage are eliminated by competition, and the species assemblage forms a recovered community comprised of larger, long-lived, and slow growing species with complex biological interactions with one another.

### **7.5.2.3 Recolonization Rates**

The rate of recolonization is dependent upon numerous physical and biological factors. Physical factors include the time of year, depth of the borrow area, water currents, sediment composition, bedload transport, temperature and salinity, natural energy levels in the area, frequency of disturbance, latitude, etc. Recovery times may be shorter in warmer waters at lower latitudes as compared to colder waters at higher latitudes (Coastline Surveys Limited, 1998; Newell et al., 1998).

Recolonization of borrow areas may occur by transport of larvae from neighboring populations by currents and subsequent growth to adults, immigration of motile species from adjacent areas, organisms contained in sediment slumping from the sides of pits, or return of undamaged organisms from the dredge plume. The rate of recolonization depends on the size of the pool of available colonists (Bonsdorff, 1983; Hall, 1994). Other biological factors such as competition and predation also determine the rate of recolonization and the composition of resulting benthic communities. Timing of dredging is important because many benthic species have distinct peak periods of reproduction and recruitment. Because larval recruitment and adult migration are the primary recolonization mechanisms, biological recovery from physical impacts generally should be most rapid if dredging is completed before seasonal increases in larval abundance and adult activity (Herbich, 1992). Recovery of a community disturbed after peak recruitment, therefore, will be slower than one disturbed prior to peak recruitment (LaSalle et al., 1991).

Benthic recolonization and succession have been reviewed to varying extents for a wide variety of habitats throughout the world (e.g., Thistle, 1981; Thayer, 1983; Hall, 1994; Coastline Surveys Limited, 1998; Newell et al., 1998). Recolonization is highly variable and ranges from within months (e.g., Saloman et al., 1982) to more than 12 years (e.g., Wright, 1977), depending on the habitat type and other physical and biological factors. Focusing on dredging, Coastline Surveys Limited (1998) and Newell et al. (1998) suggested that in general recovery times of 6 to 8 months are characteristic for many estuarine mud, 2 to 3 years for sand and gravel, and 5 to 10 years as the deposits become coarser.

The Centre for Cold Ocean Resources Engineering (1995) estimated times for recovery of a reasonable biodiversity (number of species and number of individuals) based on sediment type. In

this study, recovery was defined as attaining a successional community of opportunistic species providing evidence of progression towards a community equivalent to that previously present or at non-impacted sites. Fine-grained sediments may need only 1 year before achieving a recovery level biodiversity, medium-grained deposits 1 to 3 years, and coarse-grained deposits 5 or more years. For a hypothetical borrow site dredging scenario off Ocean City, Maryland, the Centre for Cold Ocean Resources Engineering (1995) stated that virtually all benthic species would be lost, but there may be temporary improvement of fishing due to release of nutrients. Recolonization would start within weeks of closure and moderate biodiversity would occur within 1 year. The borrow area would be colonized initially by a very different species complex than originally present. An estimate of 2 to 3 years was given for the community to begin to show succession to pre-impact sand habitat species.

Studies of recolonization listed and discussed by Grober (1992) and the National Research Council (1995) indicate that recolonization of offshore borrow areas is highly variable. This variability is not surprising considering the differences between studies in geographic locations, oceanographic conditions, sampling methods and times, etc. Part of the problem in determining recolonization patterns is seasonal and year to year fluctuations in benthic community characteristics and composition. Without adequate seasonal and yearly data prior to dredging, it is difficult to determine whether differences in community characteristics and composition are due to temporal changes or dredging disturbance.

Results and conclusions from these offshore borrow area studies indicate that recolonization usually begins soon after dredging ends. Recolonization periods range in duration from a few months to several years. Although abundance and diversity of benthic fauna within the borrow sites often returned to levels comparable to pre-dredging or reference conditions within less than 1 year, several studies documented changes in benthic species composition that lasted much longer, particularly where sediment composition was altered (e.g., Johnson and Nelson, 1985; Bowen and Marsh, 1988; Van Dolah et al., 1992, 1993; Wilber and Stern, 1992).

Most recolonization studies of borrow areas concentrated on three main features of infaunal communities, namely the number of individuals (population density), number of species (diversity), and weight (biomass as an index of growth). Dredging is usually accompanied by an immediate and significant decrease in the number of individuals, species, and biomass of benthic infauna. Using biological community parameters (e.g., total taxa, total number of individuals, species diversity, evenness, richness, etc.), previous studies tend to indicate that recovery of borrow areas occurs in approximately 1 year after dredging. However, these parameters do not necessarily reflect the complex changes in community structure and composition which occur during the recovery process. Major changes in species assemblages and community composition usually occur shortly after dredging such that a different type of community exists. Although the number of individuals, species, and biomass of benthic infauna may approach pre-dredging levels within a relatively short time after dredging, recovery of community composition may take longer.

#### **7.5.2.4 Recolonization Success and Recovery**

Assessing impacts of dredging and recolonization and recovery of borrow areas is difficult because most biological communities are complex associations of species that often undergo major changes in population densities and community composition, even in areas which are far removed and unaffected by dredging and other disturbances. Recolonization success and recovery do not necessarily mean communities should be expected to return to the pre-dredged species composition. To gauge recovery, it is important to compare community composition of dredged areas with control areas during the same seasons because community composition changes with time.

When long-term alterations in sediment structure and composition occur as a result of dredging, long-term differences in the composition of benthic assemblages inhabiting those sites may occur as well. The recovery time of benthic assemblages after dredging can depend in large measure on the degree and duration of sediment alteration from sand borrowing (Van Dolah, 1996). Recolonization success and recovery also are controlled by compaction and stabilization processes involving complex interactions between particle size, water currents, waves, and biological activities of the benthos following sediment deposition (Oakwood Environmental Ltd., 1999). While the abundance and diversity of infaunal assemblages may recover relatively rapidly in dredged areas, it may take years to recover in terms of sediment and species composition.

One conclusion commonly held is that perturbations to infaunal communities in borrow areas are negligible because organisms recolonize rapidly (Wilber and Stern, 1992). This conclusion often is based on measures including densities, species diversity/evenness indices, relative distribution of classes or phyla, and species-level dendrograms. For example, many researchers have recognized that borrow and reference area infaunal communities can differ considerably at the species level, although these differences usually are considered insignificant because species diversity is high. According to Wilber and Stern (1992), reliance upon these studies may lead to a premature conclusion that impacts to borrow area infauna are minimal because these measures are relatively superficial and ambiguous characteristics of infaunal communities. Wilber and Stern (1992) re-examined infaunal data from four borrow area projects by grouping species into functional groups called ecological guilds based on similarities in feeding mode, locomotory ability, and sediment depth occurrence. Their analyses showed that infaunal communities in borrow and control areas can differ in several ways and that these differences can last several years. Polychaetes and amphipods that recolonize borrow areas are small-bodied and confine their movement and feeding to the surface sediment or the interface between the sediment and water column. In contrast, control areas have well-developed infaunal communities commonly consisting of large-bodied organisms that move and feed deep in the sediment (Wilber and Stern, 1992). They concluded that the infaunal communities recolonizing borrow areas may remain in an early successional stage for 2 to 3 years or longer as opposed to being completely recovered in shorter time frames.

The conclusions of Wilber and Stern (1992) coincide with the model of succession discussed previously. The model states pioneering or opportunistic species are the first to colonize an area after a physical disturbance to the bottom (e.g., dredging borrow areas). Pioneering species tend to share several ecological traits, including a tendency to confine activities to the sediment-water interface, possibly because subsurface conditions cannot support a significant number of organisms. The subsurface environment changes with time after the disturbance, possibly by actions of early colonizers, and becomes suitable for deposit feeders and mid-depth burrowers. The relative absence of deposit feeders and mid-depth burrowers is interpreted to mean an area is still in the state of recovery.

Although most of the literature on recolonization rate and success in borrow areas concerns infauna, some information exists for epifauna. The numbers of taxa and individuals collected by trawls in a borrow area off Duval County, Florida greatly exceeded the control area numbers 4 months after dredging and were generally higher 7 and 13 months after dredging (Applied Biology, Inc., 1979). There were no detectable differences between pre-dredging and post-dredging (8 and 16 months) epifaunal communities in a borrow area surveyed by otter trawl and video camera off Egmont Key, Florida (Blake et al., 1995).

### **7.5.3 Predictions Relative to the Borrow Sites**

Based upon the commodity-specific, technology-specific, and site-specific information provided in Section 7.0, the following predictions can be made regarding the potential effects of

offshore dredging on benthic organisms (Section 7.5.3.1) and the recolonization rate and success (Section 7.5.3.2) relative to the borrow sites off Alabama.

### **7.5.3.1 Potential Benthic Effects**

#### **Sediment Removal**

The immediate impact of excavating upper sediments from the sand resource areas would be removal of portions of the benthic invertebrate populations that inhabit the seafloor. Lost individuals would be those with slow-moving or sessile lifestyles, primarily individuals of infaunal populations. Surveys within and adjacent to each of the five candidate borrow sites (see Section 6.0), as well as benthic investigations of nearby waters (see Section 2.3.1), reveal that the sand bottom benthic assemblages of inner shelf waters of the study area are comprised predominantly of invertebrates, including crustaceans, echinoderms, mollusks, and polychaetous annelids.

The expected loss of benthic fauna due to sediment excavation from the sand resource areas could be considered to represent a minimal impact to the ecosystem when evaluating the impact on a spatial scale. Impacts most likely would be short-term and localized. It should be noted that use of any of the sand resource areas does not entail complete excavation of those areas. For example, the potential high-end case of 750,000 m<sup>3</sup> of sand excavation would affect roughly 25 ha of seafloor, with an average excavation depth of 3 m. Specific locations within Areas 1 through 4 that are to be dredged will be selected based on particular sediment characteristics, leaving a significant extent of non-dredged areas surrounding and interspersed throughout the sand resource areas. These undisturbed "islands" would be a primary source of colonizing fauna for the excavated sites (Oliver et al., 1977; Van Dolah et al., 1984) and complement colonization of altered substrata via larval recruitment. The great densities and high fecundity of invertebrate populations, along with the relatively small area of impact proposed, likely would preclude significant long-term negative effects on benthic populations and assemblages.

Of the five sand resource areas offshore Alabama, Areas 1, 2, 3, and 4 have the greatest potential for use as borrow sites for beach replenishment projects. Areas 1, 2, and 3 are very similar with respect to sediment type, with all of these areas containing medium-to-fine sands. In contrast, some parts of Area 4 have up to 0.3 m of silt and clay overburden before encountering a medium-to-fine sand deposit. Infaunal assemblages that inhabit these areas are, at least partly, a reflection of these surficial geologic characteristics; Areas 1 to 3 support similar benthic assemblages, while Area 4 is characterized by assemblages that contain taxa adapted to living in finer sediments.

Correlation between sediment composition and the composition of infaunal assemblages has been demonstrated in numerous environmental surveys, including those of the sand resource areas. Invertebrate populations inhabiting marine soft bottoms offshore Alabama exhibit heterogeneous distributions that are largely the result of sedimentary regime and, to a lesser extent, water depth. Sediment removal could result in an alteration of the areal extent and relative distribution of assemblage types by altering the distribution of sediment types capable of supporting those assemblages.

It is possible that a change in the composition of surficial sediments within excavated areas could become a long-term result of dredging. Several factors could contribute to such an outcome, primarily the type of sediments exposed by dredging and the degree of deposition of fine sediments into dredged areas. These factors would depend primarily on the depth of excavation, which would be determined by the vertical extent of those sediments suitable for coastal nourishment projects, the volume of sand required, and the vertical relief of the sand shoal to be excavated.

Because the inner shelf ecosystem of the NEGOM exhibits some heterogeneity in sediment types and their associated assemblages, those transitional infaunal assemblages that would colonize dredged areas likely would be similar to some naturally occurring assemblages that inhabit

nearby non-dredged areas. When viewed within a context of scale, the removal of sediments from portions of the inner continental shelf would, at most, minimally alter the existing spatial balance of habitat (sediment) types. Moreover, those habitats that have relatively high levels of finer sediments are not uninhabitable, or necessarily less desirable, when compared to sandier substrata. These habitat types merely differ in their level of suitability for certain types of infaunal taxa.

Motile populations, including non-migratory foragers, would be less stressed by sediment removal than infauna or sessile epifauna. Most adult epifaunal and demersal ichthyofaunal populations would have a low probability of being adversely impacted directly by dredging because of their mobility; however, adult entrainment is possible and some species release eggs on the bottom which would be vulnerable to sediment removal and deposition. Minimal impacts are expected, especially if dredging activity coincides with the seasonal absence of key epifaunal (e.g., brown shrimp) and demersal taxa. Slow-moving or sessile epifauna inhabiting the project area include echinoderm and cnidarian taxa. Local populations of these types of benthic organisms would most likely experience a reduction in density due to sediment removal. Highest numbers of motile epifaunal taxa are usually sampled from areas of relatively coarse-grained sand; however, these taxa generally are migratory and not endemic to the areas of proposed impact. Most demersal populations exhibit naturally dynamic distributions, as they move between areas within the Gulf of Mexico on a seasonal basis (Comiskey et al., 1985; Brooks and Giammona, 1991; Harper, 1991).

Impacts of sediment removal on epifaunal and demersal taxa would likely be indirect in nature, through habitat alteration. A reduction of infaunal biomass resulting from sediment removal could have an indirect effect upon the distribution of certain demersal ichthyofauna and other epibenthic predators by interrupting established energy pathways to the higher trophic levels represented by these foraging taxa. Reductions in densities of the preferred prey of bottom-feeding taxa could induce migration of foragers to unimpacted areas.

Darnell (1991) reported gut content analyses of demersal fishes sampled from Gulf shelf waters. In that study, large, motile prey items (shrimps, crabs, fishes, and cephalopods) made up 70% of the diet of demersal fishes. The preferred food of most demersal taxa apparently is the abundant motile epifauna (Rogers, 1977; Darnell, 1991), populations of which are not likely to be adversely impacted by mining of the sand resource areas due to their migration and general ability for flight response. A relatively small percentage of infaunal prey items that typically are consumed by these fishes would be rendered unavailable for consumption as a result of their removal along with surficial sediments. Benthic predators would simply select alternative areas in which to forage. Therefore, the loss of infaunal biomass due to sediment excavation is unlikely to adversely affect normal energy flow through Alabama inner shelf sand bottoms.

In addition to widely documented spatial variation, the location and extent of inner shelf-inhabiting infaunal and demersal populations varies seasonally in the study area. This seasonal variability should be considered when evaluating potential impacts due to sand removal. The timing of sand removal would seem to be less critical for minimizing the impact upon infauna than for other faunal categories of concern (e.g., key pelagic species), due to the great abundance and reproductive potential of these invertebrate populations. Surveys of the borrow sites, as well as previous studies (Barry A. Vittor & Associates, Inc., 1985; Harper, 1991), indicate that local benthic assemblages tend to maintain fairly consistent values of species diversity and richness year-round, whereas densities are lower during winter. Additionally, many numerically dominant infaunal taxa inhabiting the study area are known to exhibit year-round or late winter-early spring periods of recruitment. Because of these patterns of recruitment and lower winter densities, removal of sand between late fall and early spring would result in less stress on benthic populations.

## **Sediment Suspension/Dispersion**

Whether cutterhead suction dredging or hopper dredging is ultimately utilized for sand mining activity, the amount of sediment resuspension that results from these excavation methods is not anticipated to be of a scale that would cause significant negative impacts to the benthic community. Impacts of dredging-induced elevations in turbidity would be short-term and localized. Motile taxa could avoid turbid areas. In general, benthic assemblages of the inner Alabama shelf are adapted to periodic resuspension of surficial sediments caused by tropical and extratropical (winter) storms. Along the nearshore area of Alabama, the winter season is characterized by frequent energetic storms and a well-mixed water column, while summer exhibits a reduction of storm-derived mixing and an increase in solar heating, resulting in water column stratification (Section 5.1.1.4; Kjerfve and Sneed, 1984). Removal of sediment during winter may therefore be advantageous in minimizing any adverse impacts upon benthos resulting from dredging-induced turbidity.

## **Sediment Deposition**

Of the various faunal categories, infaunal and sessile epifaunal populations would be most negatively affected by significant deposition of sediments; however, this scenario is unlikely. The methods of sediment excavation that would be utilized will preclude all but a relatively minimal amount of sediment deposition. As a result, the suspension and transport of suspended sediments away from dredging sites should be minimal and, therefore, any subsequent deposition will be insignificant in degree. Areas 1, 2, and 3 are characterized by a lack of fine sediments. In the unlikely event that significant dredging-related excavation of fine-grained sediment does occur in these eastern sand resource areas, the deposited sediment should not persist on the seafloor. Area 4 does exhibit a higher percentage of fine sediments but, given the relatively small amounts of resuspended sediments anticipated to occur during dredging, the concentration will be substantially less than would be required to impact negatively on the infaunal community. Furthermore, the benthic community inhabiting Area 4 is probably adapted to periods of siltation as a result of outflow from Mobile Bay and nearby disposal of dredged material.

### **7.5.3.2 Potential Recolonization Rate and Success**

The rate of post-dredging recovery of benthic assemblages within a sand resource area will depend primarily on the depth of sand excavation. While surface area of impact could be minimized by excavating a shoal to a greater depth, deep excavation likely would require a greater length of time for complete recovery of infaunal assemblages within the impacted area. Creation of a bathymetrically-abrupt pit has potential to inhibit water current flow through such a feature, resulting in a “dead zone” characterized by persistent hypoxia and deposition of fine particles. This situation would extend the duration of ecological impact beyond that which would occur with a more shallow cut over a much larger area. While the initial impact upon benthic assemblages would increase with increasing surface area of sand removal, the persistence of ecological impact that would occur with a relatively shallow excavation would be less than that of a deep pit. Paradoxically, the long-term impact of a maximum excavation of 3 m (Area 1) or 4 m (Area 3) would decrease with an increased area of sand removal because a more smoothly-graded, trough-like feature would allow greater bottom current flow than would an abrupt pit. The inner Alabama shelf sediment sheet does exhibit natural trough features within the sand resource areas.

The length of time required for reestablishment of pre-dredging infaunal assemblages depends in part on the length of time required for refilling of those areas. Sediment types exposed by dredging and deposited in excavated areas are additional considerations. The relatively shallow water benthic habitats of the Alabama inner shelf also are strongly influenced by factors such as Mobile Bay discharge (salinity and turbidity), currents and circulation, and storms (Barry A. Vittor & Associates, Inc., 1985). These same forces would tend to modify impacted areas in the direction

of pre-dredging conditions. Movement of shelf sediment in offshore Alabama waters occurs primarily as a result of the high winds and waves that characterize intense storms, while transport of Alabama shelf sediment due to shelf currents appears to be minimal (Parker et al., 1997). Borrow area refilling probably will occur mainly by storm-induced sediment movement. Tropical and extra-tropical storms impact the offshore Alabama region more or less on an annual basis and these events would tend to refill seafloor depressions formed by dredging. Storm-induced sediment transport can be substantial at relatively shallow depths such as those in the region of the borrow areas. It is expected that the time required to refill borrow areas will be on the order of decades for Areas 1, 2, and 3 and years in Area 4 for the sand extraction scenarios evaluated in this study.

Assuming that the depth of sand excavation will not be so great as to substantially alter local hydrological characteristics, the removal of benthic organisms along with sediment would be followed quickly by initial recolonization of the dredged areas by opportunistic infaunal taxa. This scenario appears likely if the maximum depth of excavation at borrow sites ranges between 3 and 4 m, as is presently anticipated. Early-stage succession will begin within days of sand removal, through settlement of larval recruits, primarily annelids and bivalves. Initial larval recruitment will be dominated by the opportunistic taxa that were numerical dominants in the western sand resource areas during the biological surveys (e.g., *Magelona* sp. H, *Mediomastus* spp., and *Paraprionospio pinnata*). These species are well adapted to environmental stress and exploit suitable habitat (especially fine-grained sediments) when it becomes available. Later successional stages of benthic recolonization will be more gradual, involving taxa that generally are less opportunistic and longer lived. Immigration of motile crustaceans, annelids, and echinoderms into impacted areas also will begin soon after excavation.

Areas 1, 2, and 3 east of Mobile Bay exhibit limited sediment movement during historical time. The process of sediment refilling of excavated sites would be accomplished mainly by storm-induced transport and, to a lesser degree, normal shelf sediment transport processes. The rapidity of the refilling process will depend on the frequency and intensity of storms. However, the rate of refilling may not be a significant issue with respect to benthic recolonization in the eastern sand resource areas because the areas are fairly uniform with respect to biological habitat. Sediment consists of well-sorted sand and appear to be vertically uniform with respect to sedimentary regime. These areas are characterized by an absence of fine sediment. It may be predicted from this that recolonization of dredged areas offshore eastern Alabama likely will occur in a timely manner and without persistent inhabitation by transitional assemblages, not unlike the process which has been documented in comparable regional habitats (Saloman et al., 1982). Recolonization of surficial sediment by later successional stages likely will proceed even if dredged areas are not completely refilled. Furthermore, the horizontal uniformity of biological habitat across the eastern areas will ensure that a supply of non-transitional, motile taxa will be available for rapid migration into dredged areas. Infaunal assemblages that typically inhabit the eastern portion of the study area will most likely become reestablished within 2 years.

Area 4 infaunal assemblages can be expected to recover more quickly than those in the eastern areas. Because of the physical environmental characteristics of Area 4, especially outflow of fresh water and fine material (silts and organics) from Mobile Bay, existing assemblages are comprised of species that colonize perturbed habitats. The infaunal community in Area 4 is adapted to environmental instability and probably never fully reaches a stable Stage III community (Continental Shelf Associates, Inc. and Barry A. Vittor & Associates, Inc., 1989). As a result, many infaunal taxa that inhabit Area 4 are the transitional taxa that would colonize areas of sand removal. Infaunal assemblages that inhabit the western study areas would therefore become reestablished relatively rapidly, probably within 12 to 18 months.

## **7.6 PELAGIC ENVIRONMENT**

This section discusses the potential effects of hydraulic (cutterhead and hopper) dredging on water column organisms at a borrow site, and seasonal windows that would reduce the effects to particular species or groups. Groups of organisms considered include zooplankton (including eggs and larvae of economically important fish and shellfish species), squids, pelagic fishes, sea turtles, and marine mammals.

### **7.6.1 Zooplankton**

#### **7.6.1.1 Entrainment**

Zooplankters encountering the suction field of hydraulic dredges will be easily drawn into the system (i.e., entrained). Entrained zooplankters are assumed to die from abrasion and physical trauma (LaSalle et al., 1991; Reine and Clarke, 1998). The most detrimental consequence of zooplankton entrainment is the death of fish and invertebrate larvae which ultimately influences the age structure of adult populations.

The rate of zooplankton entrainment by hydraulic dredges depends upon local hydrographic patterns responsible for their transport and the spatial and temporal dynamics of local populations. Hydrographic patterns can be measured, whereas inherently variable zooplankton populations are more difficult to characterize (Sullivan and Hancock, 1977). Because of difficulties in measuring population parameters from field-collected data, direct estimates of zooplankton entrainment (and subsequent population effects) are not available in the dredging literature. An alternative to using field-collected data has been to develop numerical models that predict population effects given specific scenarios (discussed in LaSalle et al., 1991 and Reine and Clarke, 1998). Unfortunately, population effects estimated from models can differ greatly depending upon model assumptions (LaSalle et al., 1991; Reine and Clarke, 1998).

Entrainment rate also depends upon physical aspects of the dredging operation. Because the suction field of hydraulic dredges remains near the seafloor, species most susceptible to entrainment are those occurring in the lower portion of the water column. Taxa or life stages which spend part of their time associated with the benthic environment, such as demersal fish eggs or demersal zooplankton (Hammer, 1979), would be especially vulnerable. Unfortunately, no information exists on the abundance or composition of demersal zooplankton in the sand resource areas. Other zooplankters may occur in the lower water column under certain hydrographic or meteorological conditions (Rogers et al., 1993). Considering the high reproductive capacity of zooplankton along with the relatively small area of the dredge suction field and the volume of water entrained compared to the overall volume of surrounding waters, it is unlikely that entrainment would greatly affect zooplankton populations or assemblages in the Alabama sand resource areas.

#### **7.6.1.2 Turbidity**

Sediment suspended and dispersed by the action of a working dredge can affect zooplankters by 1) interfering with feeding activity; 2) direct mortality and toxicity; and 3) physiological impairment. Most crustacean zooplankters are filter feeders capable of filtering and processing particles between 3 and 10 $\mu$  (Nival and Nival, 1976). Inorganic particles in this size range can easily foul the fine structures (setules) on feeding appendages of crustaceans such as copepods, and crab and shrimp larvae (Sullivan and Hancock, 1977). Laboratory studies have shown that mechanical disruption of feeding can affect growth and reproductive success (Kirk, 1992). Plankters feeding by ciliary action (e.g., echinoderm larvae) also would be susceptible to mechanical effects of suspended particles (Sullivan and Hancock, 1977).

Larval fishes are visual feeders that depend on adequate light levels for their foraging success (Blaxter, 1968). High turbidity reduces light levels in the water column which in turn shortens the

reactive distance between a larval fish and its prey. Laboratory studies have demonstrated the negative influence of elevated turbidity on prey capture rates for larvae of herring, *Clupea harengus harengus* (Johnston and Wildish, 1982), striped bass, *Morone saxatilis* (Morgan et al., 1983; Breitburg, 1988), and dolphin, *Coryphaena hippurus* (Jokiel, 1989). In one laboratory study however, increased turbidity actually enhanced feeding abilities of larval herring (*Clupea harengus pallisi*) (Boehlert and Morgan, 1985). The authors suggested that suspended sediment may have provided better contrast against which small particles were viewed.

Direct mortality and toxicity caused by elevated turbidity varies with species and nature of the sediment and sediment-bound contaminants. Crustacean zooplankters will ingest suspended inorganic particles that may or may not contain contaminants. Contamination is expected to be low in all sand resource areas, although Area 4 may be influenced by Mobile Bay outflow and the dredged material disposal site to the northwest. A laboratory study showed that copepods ingesting high amounts of “red mud” grew slower than control groups feeding only on diatoms (Paffenhofer, 1972). This was attributed to the non-nutritive value of the red mud rather than to any associated toxic compounds. Sediment-bound toxic compounds introduced into the water column may be ingested by zooplankters. These substances can be detrimental to zooplankters. However, studies with copepods exposed to deep sea mine tailings containing trace metals showed minimal effects (Hirota, 1981; Hu, 1981).

High turbidity can cause physiological changes that can kill or retard developing eggs and larvae of fishes and invertebrates (Davis and Hidu, 1969; Rosenthal, 1971). High concentrations of suspended sediment can kill or deform fish eggs (Rosenthal, 1971). Laboratory studies investigating effects of elevated turbidity on eggs and larvae of bivalves show that slight increases in turbidity actually stimulated larval growth, whereas large increases in turbidity caused abnormalities (Loosanoff, 1962; Davis and Hidu, 1969). Hatching success of fish eggs exposed to high suspended concentrations varies, but most studies show minimal effects from acute exposures in the 50 to 500 mg/L range (Auld and Schubel, 1978; Morgan et al., 1983; Jokiel, 1989). In these same studies, artificially high suspended sediment concentrations (1,000 to 8,000 mg/L) were required to induce mortality.

As with entrainment, the effects of suspended sediments on zooplankters is primarily restricted to the lower portion of the water column for a cutterhead dredge because the turbidity plume remains near the cutterhead with little reaching surface waters (LaSalle et al., 1991). Suspended sediment plumes in near-bottom waters may extend for up to several hundred meters laterally from the cutterhead. In contrast, hopper barges may create turbid surface plumes due to overwash (LaSalle et al., 1991). With either dredge type, the turbidity plume is expected to cover a small portion of the water column relative to the surrounding waters. Due to the limited areal extent and transient nature of the sediment plume, it is unlikely that turbidity would greatly affect zooplankton populations or assemblages in the Alabama sand resource areas.

### **7.6.1.3 Project Scheduling**

For open ocean environments, Sullivan and Hancock (1977) generalized that dredging effects on zooplankton would be minimal due to high spatial and temporal variability of the populations, whereas significant effects would be expected in enclosed waters with endemic populations. However, accurate prediction of the local effects of entrainment or dredge-produced turbidity on zooplankton populations of the sand resource areas requires adequate site-specific data. Zooplankton populations in general should not be subject to impacts from dredging, but available regional information (see Section 2.3.1) indicates that planktonic larvae, particularly those of shrimp and blue crab, occur in the project area during summer and fall months. Because adults of these species spawn offshore and larval forms make their way back to inshore nursery areas inside Mobile Bay, Area 4 could be construed as lying in a recruitment corridor. The other sand resource areas

are not within such an important position relative to larval transport and therefore should not require any special project scheduling consideration.

When data are inadequate to accurately predict the magnitude of dredging effects, environmental windows have been required to provide a conservative approach and lessen potential effects on key species. However, LaSalle et al. (1991) and Reine et al. (1998) have stressed the need to base future environmental windows on sound evidence, and have argued against subjectively selected environmental windows. Environmental windows delay projects and greatly increase costs (Dickerson et al., 1998), and their use should not be driven by subjective or overly conservative approaches. If Area 4 is used as a sand source, an environmental window excluding summer and fall months could be considered to avoid dredging when shrimp and blue crab larvae are most prevalent, but only if additional data become available to determine the extent of impacts and justify the restriction. Progress toward understanding the real need for environmental windows can only be achieved by reducing the degree of uncertainty surrounding impacts and the means to avoid them (Dickerson et al., 1998).

## **7.6.2 Squids**

### **7.6.2.1 Entrainment**

No information exists regarding impacts of hydraulic dredging on squids. Nevertheless, squids could be entrained if they encountered the suction field of a hydraulic dredge. Some general aspects of squid behavior increase the chance of encountering the bottom-oriented dredge suction field. Adult squids are generally demersal by day and enter the water column at night to feed on zooplankton (Fischer, 1978). In addition, squids lay their eggs in large clusters on the seafloor (Vecchione, 1981). The early stages (prolarvae) of *Loligunculus brevis* may be susceptible as well.

### **7.6.2.2 Attraction**

Because some squid species are attracted to lights at night (Fischer, 1978), it is likely that squids could be attracted to lights of a working dredge. This could draw them into the suction field and increase the chance of entrainment.

### **7.6.2.3 Project Scheduling**

With no information on local squid populations available, reasonable predictions of demographic effects are difficult to make. As with the other pelagic organisms, dredging is unlikely to significantly impact squid populations in the vicinity of the sand resource areas. Quantitative data are lacking to support the use of an environmental window to protect squid resources.

## **7.6.3 Fishes**

### **7.6.3.1 Entrainment**

Entrainment of adult fishes by hydraulic dredging has been reported for several projects (Larson and Moehl, 1988; McGraw and Armstrong, 1988; Reine and Clarke, 1998). The most comprehensive study of fish entrainment took place in Grays Harbor, WA during a 10-yr period when 27 fish taxa were entrained (McGraw and Armstrong, 1988). Most entrained fishes were demersal species such as flatfishes, sand lance, and sculpin; however, three pelagic species (anchovy, herring, and smelt) were recorded. Entrainment rates for the pelagic species were very low, ranging from 1 to 18 fishes/1,000 cy (McGraw and Armstrong, 1988). Comparisons between relative numbers of entrained fishes with numbers captured by trawling showed that some pelagic species were avoiding the dredge. Another entrainment study conducted near the mouth of the Columbia River, WA reported 14 fish taxa entrained at an average rate of 0.008 to 0.341 fishes/cy (Larson and Moehl, 1988). Few of the coastal pelagic fishes occurring offshore of Alabama should

become entrained because the dredge's suction field exists near the bottom and many pelagic species have sufficient mobility to avoid the suction field.

#### **7.6.3.2 Attraction**

Even though dredges are temporary structures, they can still attract roving pelagic species. Many pelagic fishes of the northern Gulf of Mexico are attracted to large objects or structures such as artificial reefs (Klima and Wickham, 1971) or oil and gas platforms (Stanley and Wilson, 1990). Bluefish, cobia, jacks, and king and Spanish mackerels that migrate through the area could be attracted to the dredge. This may temporarily disrupt a migratory pattern for some members of the stock, but it is unlikely that there would be an appreciable negative effect. There are already several artificial reefs and oil and gas structures in the area, so the presence of a dredge will not be novel.

#### **7.6.3.3 Turbidity**

Turbidity can cause feeding impairment, avoidance and attraction movements, and physiological changes in adult pelagic fishes. As discussed for larval fishes, pelagic species are primarily visual feeders and when turbidity reduces light penetration, the fishes reactive distance decreases (Vinyard and O' Brien, 1976). Light scattering caused by suspended sediment can also affect a visual predator's ability to perceive and capture prey (Benfield and Minello, 1996).

Some species will actively avoid or be attracted to turbid water. Experiments with pelagic kawakawa (*Euthynnus affinis*) and yellowfin tuna (*Thunnus albacares*) demonstrated that these species would actively avoid experimental turbidity clouds, but would also swim directly through them during some trials (Barry, 1978). Turbidity plumes emanating from coastal rivers may retard or affect movements of some pelagic species.

Gill cavities can be clogged by suspended sediment preventing normal respiration and mechanically affecting food gathering in planktivorous species (Bruton, 1985). High suspended sediment levels generated by storms have contributed to the death of nearshore and offshore fishes by clogging gill cavities and eroding gill lamellae (Robins, 1957).

The limited spatial and temporal extents of turbidity plumes from either cutterhead or hopper dredges are expected to be limited. Therefore, there should be no significant impact on adult pelagic fishes.

#### **7.6.3.4 Project Scheduling**

Hydraulic dredging should not present a significant problem for pelagic fishes offshore Alabama. If an environmental window is sought to protect pelagic fishes from dredging impacts, the spring to fall period would encompass the peak seasons for the economically important species. Temporal scheduling as means to avoid impacts is practical if the organism in question is highly concentrated in waters of the area during some specific time period. Quantitative data are lacking to support the use of an environmental window to lessen effects on pelagic fishes.

#### **7.6.3.5 Essential Fish Habitat**

The Magnuson-Stevens Fishery Conservation and Management Act (16 U.S.C. § 1801-1882) established regional Fishery Management Councils and mandated that Fishery Management Plans (FMPs) be developed to responsibly manage exploited fish and invertebrate species in Federal waters of the United States. When Congress reauthorized this act in 1996 as the Sustainable Fisheries Act, several reforms and changes were made. One change was to charge the NMFS with designating and conserving Essential Fish Habitat (EFH) for species managed under existing FMPs. This was intended to minimize, to the extent practicable, any adverse effects on habitat caused by

fishing or non-fishing activities, and to identify other actions to encourage the conservation and enhancement of such habitat.

EFH is defined as “those waters and substrate necessary to fish for spawning, breeding, feeding or growth to maturity”[16 U.S.C. § 1801(10)]. The EFH interim final rule summarizing EFH regulations (62 FR 66531-66559) outlines additional interpretation of the EFH definition. Waters, as defined previously, include “aquatic areas and their associated physical, chemical, and biological properties that are used by fish, and may include aquatic areas historically used by fish where appropriate.” Substrate includes “sediment, hard bottom, structures underlying the waters, and associated biological communities.” Necessary is defined as “the habitat required to support a sustainable fishery and the managed species’ contribution to a healthy ecosystem.” “Fish” includes “finfish, mollusks, crustaceans, and all other forms of marine animal and plant life other than marine mammals and birds,” whereas “spawning, breeding, feeding or growth to maturity” cover the complete life cycle of those species of interest.

The Gulf of Mexico Fishery Management Council (GMFMC) has produced several FMPs including those for coastal migratory pelagic fishes, coral and coral reefs, red drum, reef fishes, shrimp, spiny lobster, and stone crab. To amend these FMPs with respect to EFH of managed species, the GMFMC prepared a generic document that identified and described EFH for 26 species (Gulf of Mexico Fishery Management Council, 1998). This document presented maps depicting EFH for all life stages of the 26 species. Mapped EFH for several of these species (and life stages) overlapped the five sand resource areas offshore Alabama. EFH characteristics for these overlapping species are presented in Table 7-4. Of the species listed, several are hard bottom associates (i.e., gag, scamp, greater amberjack, red snapper, and lane snapper). Hard bottom habitats or inhabitants were not covered in Section 2.0 of this report because no known hard bottom occurs in the immediate vicinity of the sand resource areas.

Table 7-4. Invertebrate and fish species managed by the Gulf of Mexico Fishery Management Council for which Essential Fish Habitat has been identified in the vicinity of the five sand resource areas offshore Alabama (adapted from Gulf of Mexico Fishery Management Council, 1998).	
Species (Phylogenetic Order)	Life Stage (Seasonal Occurrence); Reproductive Activity; Habitat Affinity
<b>Invertebrates</b>	
Brown shrimp ( <i>Penaeus aztecus</i> )	Adults (year-round); spawning year-round in water depth >14 m; soft bottom
Pink shrimp ( <i>Penaeus duorarum</i> )	Adults (year-round); soft bottom
White shrimp ( <i>Penaeus setiferus</i> )	Adults (year-round), spawning from March to October; soft bottom
Stone crab ( <i>Menippe mercineria</i> )	Adults (year-round); soft bottom
<b>Fishes</b>	
Gag ( <i>Mycteroperca microlepis</i> )	Adults (year-round); hard bottom
Scamp ( <i>Mycteroperca phenax</i> )	Adults (year-round); hard bottom
Cobia ( <i>Rachycentron canadum</i> )	Adults (summer); water column
Red drum ( <i>Sciaenops ocellatus</i> )	Adults (year-round); spawning in fall and winter; soft bottom
Greater amberjack ( <i>Seriola dumerili</i> )	Adults (year-round); hard bottom
Red snapper ( <i>Lutjanus campechanus</i> )	Juveniles (year-round); soft bottom
Lane snapper ( <i>Lutjanus synagris</i> )	Adults (year-round); hard bottom
King mackerel ( <i>Scomberomorus cavalla</i> )	Adults (year-round); pelagic
Spanish mackerel ( <i>Scomberomorus maculatus</i> )	Adults (year-round); pelagic

The area encompassed by the five sand resource areas is very small relative to the mapped EFH characteristics. For this reason, the effect of dredging on EFH for the managed species is expected to be minimal.

#### **7.6.4 Sea Turtles**

##### **7.6.4.1 Physical Injury**

The main potential effect of dredging on sea turtles is physical injury or death caused by the suction and/or cutting action of the dredge head. Numerous sea turtle injuries and mortalities have been documented during dredging projects, particularly along Florida's east coast (Studt, 1987; Dickerson et al., 1992; Slay, 1995). Impacts typically can be minimized by some combination of project scheduling and equipment selection, accompanied if necessary by turtle removal and/or monitoring.

Although any of the five sea turtle species may be present in the project area, loggerhead, green, and Kemp's Ridley turtles are considered to be most at risk from dredging activities because of their life cycle and behavioral patterns (Dickerson et al., 1992). Loggerheads are expected to be the most abundant of these three turtles in the project area. Hawksbill turtles are usually associated with coral reef environments and are the least abundant sea turtle in the northern Gulf. Leatherbacks are predominantly found in deep waters over the continental slope (see Section 2.3.2.4).

Physical impact can occur when a turtle resting on (or buried in) the seafloor is contacted by the dredge head. Two types of dredges may be used on the proposed project (see Section 7.0). Cutterhead suction dredges are considered unlikely to kill or injure turtles, perhaps because the cutterhead encounters a smaller area of seafloor per unit time, allowing more opportunity for turtles to escape (Palermo, 1990). Hopper dredges are believed to pose the greatest risk to sea turtles (Dickerson, 1990; NMFS, 1997). There has been considerable research into designing modified hopper dredges with turtle deflectors that reduce the likelihood of entraining sea turtles (Studt, 1987; Berry, 1990; Dickerson et al., 1992; U.S. Army Corps of Engineers, 1999). If a hopper dredge is used on this project, its design is likely to be a significant consideration in minimizing potential impacts to sea turtles.

##### **7.6.4.2 Turbidity and Anoxia**

Sea turtles in and near the project area may encounter turbid water during dredging. For those turtles known to forage visually (e.g., leatherbacks feeding on jellyfishes), this turbidity could temporarily interfere with feeding. However, due to the limited areal extent and transient occurrence of the sediment plume (see Section 7.5.1.2), turbidity is considered unlikely to significantly affect turtle behavior or survival.

In addition to turbidity, dredging may produce localized anoxia in the water column due to oxygen consumption of the suspended sediments (LaSalle et al., 1991). In general, oxygen levels in the plume and near-bottom waters may approach zero, but levels in adjacent waters outside the plume are at or near normal. Due to the limited extent and transient occurrence of anoxia, no significant effects on turtles are expected.

##### **7.6.4.3 Noise**

Dredging is one of many human activities in the marine environment that produce underwater noise. This noise is unlikely to significantly affect sea turtles because of their limited hearing ability (Ridgway et al., 1969; Lenhardt, 1994). These animals do not rely upon sound to any significant degree for communication or food location. Studies in the northern Gulf of Mexico have shown

some evidence for positive association of sea turtles with petroleum platforms (Rosman et al., 1987; Lohoefer et al., 1990) despite the industrial noise associated with these sites.

#### **7.6.4.4 Project Scheduling**

Project scheduling is one way to avoid or minimize turtle impacts during dredging (Studt, 1987; Arnold, 1992). There are currently no turtle-related seasonal restrictions on dredging in the Alabama/Florida Panhandle area (R. Nyc, 1999, personal communication, U.S. Army Corps of Engineers, South Atlantic Region). However, dredging for beach restoration obviously would not occur during the loggerhead nesting season because nesting beaches cannot be disturbed during this time.

Loggerheads are expected to be the most abundant turtle in the project area, and there is a significant nesting subpopulation of loggerhead turtles along the Florida Panhandle, with some loggerhead nesting on Alabama beaches (see Section 2.3.2.4). Increased loggerhead densities may be expected during the nesting season, which in the Panhandle region extends from 1 May through 30 November (Minerals Management Service, 1997). A schedule that avoids the loggerhead nesting season also would avoid potential impacts to occasional nesting green and leatherback turtles.

Although green turtles also may nest on Alabama beaches (Alabama Game and Fish Division, 1997), the Minerals Management Service (1997) indicates that the green turtle nesting in the northern Gulf is “isolated and infrequent” during the season lasting from 1 May through 31 October. Leatherbacks occasionally nest on Florida Panhandle beaches from 1 May through 30 September (Minerals Management Service, 1997) but are not listed as nesting in Alabama by the Alabama Game and Fish Division (1997). Hawksbill and Kemp’s Ridley turtles do not nest anywhere near the project area.

Winter seasonal restrictions have been necessary in some channel dredging projects along Florida’s east coast due to turtles aggregating in bottom sediments (Studt, 1987). From December or January (depending on water temperature) through April, large numbers of loggerhead turtles rest along the bottom in the Canaveral Harbor entrance channel (Carr et al., 1981). These aggregations were a surprising discovery, and little is known of this behavior in other areas (Lutz, 1990). In the northern Gulf, Lohoefer et al. (1990) reported seeing loggerheads with mud trails on their carapaces, suggesting that they had been partially buried during cold spells. However, loggerheads also may move into deeper water during winter (Lohoefer et al., 1990). Similarly, Richardson (1990) reported that turtles do not brumate in the St. Mary’s entrance channel (Georgia) during winter, but instead migrate south to warmer waters (e.g., the Canaveral area).

It is not known whether sea turtles are likely to be brumating in bottom sediments of the project area during winter. Consequently, there is insufficient information to determine whether seasonal restrictions on dredging during winter months would be appropriate. However, this is mainly an issue during channel dredging because narrow channels tend to concentrate turtles moving between estuaries and the open ocean. So far, it has not been an issue for dredging offshore borrow areas (E. Hawk, 1999, personal communication, NMFS Southeastern Regional Office).

#### **7.6.5 Marine Mammals**

##### **7.6.5.1 Physical Injury**

Unlike sea turtles, marine mammals are unlikely to be physically injured during dredging because (1) they generally do not rest on the bottom and (2) they can easily avoid contact with the dredge. The two marine mammals most likely to be found in and near the project area are the Atlantic spotted dolphin and the bottlenose dolphin (Davis and Fargion, 1996; Davis et al., 1998; see

Section 2.3.2.5). Both are fast, agile swimmers and are presumed capable of avoiding direct physical injury by either a cutterhead suction dredge or hopper dredge. Dolphins also may avoid the immediate vicinity of the project due to the associated noise and turbidity.

#### **7.6.5.2 Turbidity**

Marine mammals in and near the project area may encounter turbid water during dredging. This turbidity could temporarily interfere with feeding or other activities, but the animals could easily swim to avoid turbid areas. Due to the limited areal extent and transient occurrence of the sediment plume (see Section 7.5.1.2), turbidity is considered unlikely to significantly affect marine mammal behavior or survival.

#### **7.6.5.3 Noise**

Underwater noise from dredging activities could have minor impacts on marine mammals. Noise can cause marine mammals to temporarily avoid certain areas (Gales, 1982; Richardson et al., 1995). However, sound levels from dredging activities are likely to dissipate to the tolerance of most cetaceans within a few tens of meters from the source. Hearing loss or other auditory discomfort or damage is not likely to result to marine mammals from normal noise produced during dredging operations because the pressure variations produced from most sounds are far less than those which marine mammals must tolerate during dives (Gales, 1982). Furthermore, dolphins could easily move away from noise that would cause them discomfort, danger, or harm, or interfere with normal behaviors. Observations of marine mammals in the vicinity of active platforms (a common source of underwater noise in the northern Gulf of Mexico) suggest that routine operations have little effect on normal behavior (Gales, 1982; Malme et al., 1983).

#### **7.6.5.4 Project Scheduling**

As discussed in Section 2.3.2.5, the two marine mammals most likely to be found in and near the project area are the Atlantic spotted dolphin and the bottlenose dolphin (Davis and Fargion, 1996; Davis et al., 1998). Neither exhibits strong seasonality of occurrence.

Atlantic spotted dolphins can be expected to occur near the project area during all seasons. It has been hypothesized that they are more common during spring, but data supporting this hypothesis are limited (see Section 2.3.2.5). Bottlenose dolphins were sighted on the continental shelf off Mobile Bay during all seasons during GulfCet II aerial and shipboard surveys (Mullin and Hoggard, 1998). For either species, there is no strong seasonal pattern in abundance that would provide an appropriate basis for seasonal restrictions on the project. In addition, the likelihood of significant impact is low even if these animals are present.

### **7.7 POTENTIAL CUMULATIVE EFFECTS**

Cumulative physical environmental impacts from multiple sand extraction scenarios at one or all sand borrow sites within the study area were evaluated to assess long-term effects at potential borrow sites and along the coastline. Results presented above for wave and sediment transport processes reflect the impact of large extraction scenarios that are expected to be within the cumulative sand resource needs of the State for the next 50 years. Therefore, the cumulative impacts of sand mining offshore Alabama on wave propagation and sediment transport processes are expected to be negligible under the conditions imposed. Unless substantially larger borrow sites and extraction volumes are selected for sand mining, no significant impacts to normal and storm physical processes are expected.

Cumulative impacts resulting from multiple sand mining operations within a sand resource area are a concern when evaluating potential long-term effects on benthic and pelagic

assemblages. Given that the expected beach replenishment interval is on the order of a decade, and that the expected recovery time of the affected benthic community after sand removal is anticipated to be much less than that – certainly within 5 years – the potential for significant cumulative benthic impacts is remote. No cumulative impacts to the pelagic environment, including zooplankton, squids, fishes, sea turtles, and marine mammals, are expected from multiple sand mining operations within a sand resource area.

## 8.0 SUMMARY AND CONCLUSIONS

The primary purpose of this study was to address environmental concerns raised by the potential for dredging sand from the OCS offshore the State of Alabama for beach replenishment. Primary concerns focused on physical and biological components of the environment at five proposed sand resource areas. Biological and physical processes data were collected and analyzed to assess the potential impacts of offshore dredging activities within the study area to minimize or preclude long-term adverse environmental impacts at potential borrow sites and along the coastline landward of resource sites. Furthermore, wave transformation and sediment transport numerical modeling were employed to simulate the physical environmental effects of proposed sand dredging operations to ensure that offshore sand resources are developed in an environmentally sound manner. Of the five potential sand resource areas, four were chosen for evaluating sand extraction scenarios based on discussions of beach replenishment needs with Geological Survey of Alabama personnel (Hummell, 1999). Area 5 at the western end of the study area was not evaluated as a sand borrow source because it is substantially removed from beach areas of greatest replenishment need and the sediment was least compatible with native beach sand (see Parker et al., 1997).

The following discussion provides a summary of results and conclusions regarding the potential environmental effects of sand mining on the OCS for replenishing sand to eroding beaches. Because benthic and pelagic biological characteristics are in part determined by spatially varying physical processes throughout the study area, physical processes analyses are summarized first.

### 8.1 WAVE TRANSFORMATION MODELING

A primary component of any physical environmental effects analysis related to sand mining from the OCS must include numerical wave transformation modeling. Potentially rapid and significant changes in bathymetry due to sand extraction from the OCS may have substantial impact on wave propagation patterns on the continental shelf and at the shoreline. In turn, sediment transport patterns may be altered so as to adversely impact erosion problems being mitigated. As such, substantial effort was spent understanding existing wave propagation patterns relative to those resulting from potential sand extraction scenarios.

The spectral wave transformation model REF/DIF S was used to evaluate changes in wave approach resulting from potential sand dredging activities. REF/DIF S is a combined refraction and diffraction spectral wave model, which can simulate the behavior of a random sea and incorporates the effects of shoaling, wave breaking, refraction, diffraction, and energy dissipation. A spectral wave model was selected to simulate wave transformation because of its ability to propagate realistic wave components (a spectrum) simultaneously across the continental shelf surface. By simulating several wave components together, a spectral wave model represents nature more closely.

Accuracy of the wave transformation model is affected by the quality of selected input data and parameters. The spectral wave modeling approach requires the development of precise spectrum in the energy and directional domain. USACE WIS data and NOAA buoy data were used to derive input wave conditions. The Gulf of Mexico experiences minimal variation in wave climate, and with the exception of storm events, typical conditions are directionally narrow and energetically mild.

From the available data, prevalent seasonal conditions were used to generate accurate seasonal wave climates through development of combined directional/energy spectra. Seasonal wave conditions were selected to represent the differences in spectral wave approach and to investigate long-term average trends in wave and sediment transport patterns (nearshore and

offshore). Input spectra (rather than specific directions and/or frequencies) were represented through empirical approximations and verified through comparison to observed wave data. In this manner, actual conditions are simulated rather than using approximations of the frequency and directional spectra based on primary wave periods and directions. In addition, an extreme storm event (50-yr storm) was developed to investigate potential impacts during high energy conditions.

Wave transformation results identify key areas of wave convergence, wave divergence, and shadow zones offshore Alabama. For seasonal simulations, significant wave heights and wave angles experience little variation to the 15-m depth contour where the wave field begins to feel the influence of bathymetry. Seaward of Dauphin Island, wave heights are relatively consistent along the shoreline while the eastern end of the island is protected from significant wave energy by a shadow zone produced from Pelican Island (subaerial portion of the ebb-tidal delta) and subaqueous shoals associated with the ebb delta. Several areas of wave convergence were identified from the Dauphin Island simulations, including those associated with the Mobile Outer Mound disposal site, which focuses wave energy near Pelican Island during most seasons. Wave focusing caused by Mobile Outer Mound most likely results in an unnatural increase in the erosion rate at Pelican Island, and during a storm event may significantly erode the protective island. Areas of wave convergence and divergence along Morgan Peninsula are primarily caused by southwest-oriented shoals on the continental shelf. For the 50-yr storm simulation, wave patterns are similar to normal seasonal results. An increase in wave height is significant in many areas where wave convergence occurs. For example, the Mobile Outer Mound disposal site concentrates 4.0- to 4.5-m storm wave heights on Pelican Island.

Wave height results also were compared with historical shoreline change rates for Dauphin Island and Morgan Peninsula. Approaching wave heights under existing conditions correlate relatively well to historical erosion/accretion rates. Along most stretches of coastline, areas of high waves correspond to historical shoreline retreat, while reduced wave energy corresponds to areas that are historically stable or accreting. The correlation provides an increased level of confidence in the wave modeling results.

Similar results (as those shown for existing conditions) were illustrated for post-dredging simulations to investigate the potential physical environmental impacts to the propagating wave field. Differences in wave propagation are difficult to visualize, so quantitative wave height comparisons were made between pre- and post-dredging simulations. At Dauphin Island, maximum wave height differences (both reduction and augmentation) for seasonal simulations ranged from  $\pm 0.02$  to 0.2 m. These maximum changes dissipate relatively rapidly as waves break and advance towards the coast. At Morgan Peninsula, maximum wave height differences were slightly larger ( $\pm 0.2$  to 0.4 m) due to borrow site sizes and orientations, as well as their proximity to the shoreline. However, wave energy is dissipated as waves propagate toward the shoreline, and increases in wave height of 0.1 m or less are observed at the potential impact areas along the coast. Overall, the physical environmental impact caused by offshore sand extraction during seasonal simulations is minimal.

During extreme wave conditions (i.e., the 50-yr storm), wave heights are modified between  $\pm 1.5$  and 2.0 m, suggesting a rather significant change. For the sand resource site in Sand Resource Area 4, a significant amount of wave energy is dissipated before waves reach the coast. For example, wave height increases are less than 0.5 m along a majority of Pelican Island. Furthermore, under storm conditions, wave heights are substantially larger relative to normal wave conditions, regardless of modifications caused by the sand dredging. Therefore, a maximum change of 0.5 m may not significantly increase nearshore erosion above existing conditions near Dauphin Island.

Sand borrow sites within Sand Resource Areas 1, 2, and 3, which are located closer to the shoreline than Sand Resource Area 4, have a greater impact on the wave field. A smaller amount

of wave energy is dissipated before reaching the shoreline, and changes to wave heights are large enough to result in measured impacts at certain locations along Morgan Peninsula.

## **8.2 CIRCULATION AND SEDIMENT TRANSPORT DYNAMICS**

Current measurements and analyses and wave transformation modeling provided baseline information on incident processes impacting coastal environments under existing conditions and with respect to proposed sand mining activities for beach replenishment. Ultimately, the most important data set for understanding physical processes impacts from offshore sand extraction is changes in sediment transport dynamics resulting from potential sand extraction scenarios relative to existing conditions.

Three independent sediment transport analyses were completed to evaluate impacts due to sand mining. First, historical sediment transport trends were quantified to document regional, long-term sediment movement throughout the study area using historical bathymetry data sets. Erosion and accretion patterns were documented, and sediment transport rates in the littoral zone and at offshore borrow sites were evaluated to assess potential changes due to offshore sand dredging activities. Second, sediment transport patterns at proposed offshore borrow sites were evaluated using wave modeling results and current measurements. Post-dredging wave model results were integrated with regional current measurements to estimate sediment transport trends for predicting borrow site infilling rates. Third, nearshore currents and sediment transport were modeled using wave modeling output to document potential impacts to the longshore sand transport system (beach erosion and accretion). All three methods were compared for evaluating consistency of measurements relative to predictions, and potential impacts were identified.

### **8.2.1 Historical Sediment Transport Patterns**

Regional geomorphic changes between 1917/20 and 1982/91 were documented for assessing long-term, net coastal sediment transport dynamics. Although these data do not provide information on the potential impacts of sand dredging from proposed borrow sites, they do provide a means of calibrating predictive sediment transport models relative to infilling rates at borrow sites and longshore sand transport.

A comparison of erosion and deposition volumes at proposed borrow sites provided a method for quantifying net sediment transport rates (or borrow site infilling rates). For borrow sites in Sand Resource Areas 1, 2, and 3, net transport rates ranged from about 9,000 to 34,000 m<sup>3</sup>/yr. This compared well with sediment transport predictions made near borrow sites using wave model output and currents measurements (13,000 to 43,000 m<sup>3</sup>/yr). For Sand Resource Area 4, net deposition at a rate of about 65,000 m<sup>3</sup>/yr recorded the influence of sediment input from Mobile Bay and local transport processes.

The net longshore sand transport rate for the Morgan Peninsula was determined by comparing cells of erosion and accretion in the littoral zone (seaward to 6-m depth contour [NGVD]) between Perdido Pass and Main Pass (Mobile Bay entrance) in a sediment budget formulation. The net transport rate for that portion of the study area was determined to be approximately 106,000 m<sup>3</sup>/yr to the west. Net transport rates determined via sediment transport modeling ranged from about 50,000 to 150,000 m<sup>3</sup>/yr. These rates compare well and provide a measured level of confidence in wave and sediment transport modeling predictions relative to impacts associated with sand dredging from proposed borrow sites.

### **8.2.2 Sediment Transport at Potential Borrow Sites**

In addition to predicted modifications to the wave field, potential sand mining at offshore borrow sites results in minor changes to sediment transport pathways in and around the sites.

Modification to bathymetry caused by sand mining influences local hydrodynamic and sediment transport processes, but areas adjacent to the borrow site do not experience dramatic changes in wave and transport characteristics.

Initially, sediment transport at borrow sites will experience mild changes after sand dredging activities. For example, sediment entering the dredged area will settle and have difficulty exiting. After several years of seasonal and storm activity, sediment will be deposited at the borrow sites, eventually re-establishing pre-dredging conditions. Given the water depths at the proposed borrow sites, it is expected that minimal impacts will occur during sediment infilling of the borrow site. The pre- and post-dredging differences will be reduced as sediment infills the borrow site, and wave and resulting sediment transport patterns will steadily return to pre-dredging conditions.

Sediment that replaces the dredged material will fluctuate based on location, time of dredging, and storm characteristics following dredging episodes. Borrow sites at Sand Resource Areas 1, 2, and 3 are expected to fill with the same material that was excavated (the entire shelf surface south of the Morgan Peninsula is at least 95% medium-to-fine sand). The sediment type in this region is consistent, high-quality, and compatible for beach replenishment. The potential borrow site at Sand Resource Area 4, however, will likely be filled with fine sediment (i.e., fine sand to clay) exiting Mobile Bay by natural processes or human activities (maintenance channel dredging and disposal). Because the potential transport rate plus sediment flux from Mobile Bay is substantially greater than shelf transport rates alone, the borrow site in Sand Resource Area 4 will fill faster than other borrow sites, limiting the likelihood for multiple dredging events from the same area.

### **8.2.3 Nearshore Sediment Transport Modeling**

For this study, the potential effects of offshore sand mining on nearshore sediment transport patterns are of interest, because dredged holes can intensify wave energy at the shoreline and create erosional hot-spots. Therefore, numerical techniques were developed to utilize the nearshore wave information derived from REF/DIF S to evaluate longshore sediment transport patterns. First, a wave-induced current model was developed to determine the magnitude and distribution of the surf zone current. Bathymetry, wave height, and radiation stress information from the wave modeling provided the site-specific data needed to compute wave-induced current patterns. The nearshore current distribution results then were incorporated into a longshore sediment transport model based on the wave energy dissipation rate in the surf zone (Bodge, 1986). This approach yielded net longshore sediment transport rates for existing conditions, as well as post-dredging scenarios.

Application of the REF/DIF S wave model, a wave-induced current model, and a longshore sediment transport model provided the basis for comparing existing conditions to post-dredging conditions with regards to coastal processes. Average annual sediment transport patterns for existing conditions, as well as post-dredging scenarios, were evaluated for the Morgan Peninsula and Dauphin Island sub-grids to determine whether offshore sand dredging would cause a significant effect on average littoral sand transport conditions. In addition, sediment transport effects were evaluated for the 50-yr storm event. Extremal conditions indicate “worst-case” scenarios, where potential impacts of dredging are amplified in the predicted longshore sediment transport rates.

Sand dredging impacts for Sand Resource Areas 1, 2, and 3 illustrate that there is a defined, but somewhat minor, change in littoral transport. Due to naturally higher transport rates at the eastern end of coastal Alabama, the magnitude of impacts associated with Sand Resource Areas 1 and 2 appear to be higher than those associated with Sand Resource Area 3; however, the net transport rate landward of Sand Resource Area 3 is significantly lower than the rate associated with Sand Resource Areas 1 and 2. For all three sand resource sites, the maximum variation in annual littoral transport rate, along the beach landward of the site, is approximately 8% to 10% of the

existing value. In general, the increase or decrease in longshore sediment transport rates associated with each potential sand resource area amounts to approximately 1% to 2% of the net littoral drift, distributed over an approximate 10 km stretch of shoreline.

The potential impacts of dredging Sand Resource Area 4 on littoral transport rates are insignificant in relation to Sand Resource Areas 1, 2, and 3. Average annual conditions indicate a relatively high percentage change in transport rates along the eastern portion of Dauphin Island; however, the existing net littoral drift is almost non-existent at this location. The net effect of dredging Sand Resource Area 4 would direct a greater percentage of littoral sand transport to the east, with a maximum increase of approximately 8,000 m<sup>3</sup>/yr.

### 8.3 BENTHIC ENVIRONMENT

Results of the biological field surveys in the five sand resource areas agreed well with previous descriptions of benthic assemblages residing in shallow waters off the Alabama coast. Benthic assemblages surveyed in the five sand resource areas consisted of members of the major invertebrate and vertebrate groups that are commonly found in the study region. Numerically dominant infaunal groups included numerous crustaceans, echinoderms, molluscs, and polychaetous annelids, while epifaunal invertebrate taxa consisted primarily of sea stars, squid, and various shrimps. Fishes such as Atlantic croaker (*Micropogonius undulatus*), longspine porgy (*Stenotomus caprinus*), silver seatrout (*Cynoscion nothus*), and spot (*Leiostomus xanthurus*) were numerical dominants during the 1997 surveys and these species consistently are among the most ubiquitous and abundant demersal taxa in the region.

Seasonality was apparent from the biological field surveys. Infaunal abundance was substantially higher during the May survey than was observed in December. Nearly half of the infaunal taxa sampled over the entire project were found in both the May and December surveys; however, most (70%) of the remaining taxa were collected only during the May cruise, resulting in higher mean values of species richness compared to the December survey. Within season, sedimentary regime most affected infaunal assemblages. Sediment in the easternmost areas (Areas 1, 2, and 3) was predominantly sand as compared to the western sand resource areas (Areas 4 and 5) which were a mixture of sand and mud at most stations. Spatial differences in community composition were obvious. The eastern areas tended to support assemblages numerically dominated by the gastropod *Caecum* spp. and included many arthropods, bivalves, and gastropods, while the western areas supported assemblages that tended to be dominated by polychaetes in terms of abundance and species richness. The *Caecum*-associated assemblages of the eastern areas apparently are restricted to the more stable environmental characteristics of those sand sediment areas, whereas the western areas support assemblages numerically dominated by those taxa capable of exploiting the fluctuating, riverine-influenced habitats nearer Mobile Bay.

Trawl catches of epifauna and demersal ichthyofauna from Areas 1 and 2 yielded the fewest taxa and individuals during both the May and December surveys, while Areas 3, 4, and 5 yielded the most individuals and taxa. The composition of demersal assemblages across the Alabama sand resource areas is influenced by fluctuating hydrographic parameters in the western areas relative to the more stable eastern areas.

Potential benthic effects from dredging will result from sediment removal, suspension/dispersion, and deposition. Potential effects are expected to be short-term and localized. Seasonality and recruitment patterns indicate that removal of sand between late fall and early spring would result in less stress on benthic populations. Early-stage succession will begin within days of sand removal, through settlement of larval recruits, primarily annelids and bivalves. Initial larval recruitment will be dominated by the opportunistic taxa that were numerical dominants

in the western sand resource areas during the biological surveys (e.g., *Magelona* sp. H, *Mediomastus* spp., and *Paraprionospio pinnata*). These species are well adapted to environmental stress and exploit suitable habitat (especially fine-grained sediments) when it becomes available. Later successional stages of benthic recolonization will be more gradual, involving taxa that generally are less opportunistic and longer lived. Immigration of motile crustaceans, annelids, and echinoderms into impacted areas also will begin soon after excavation.

Recolonization of Areas 1, 2, and 3 east of Mobile Bay likely will occur in a timely manner and without persistent inhabitation by transitional assemblages. Infaunal assemblages that typically inhabit the eastern portion of the study area will most likely become reestablished within 2 years. Area 4 infaunal assemblages can be expected to recover more quickly than those in the eastern areas. Because of the physical environmental characteristics of Area 4, especially outflow of fresh water and fine sediment (silts and organics) from Mobile Bay, existing assemblages are comprised of species that colonize perturbed habitats. Infaunal assemblages that inhabit the western study areas would therefore become reestablished relatively rapidly, probably within 12 to 18 months. Given that the expected beach replenishment interval is on the order of a decade, and that the expected recovery time of the affected benthic community after sand removal is anticipated to be much less than that, the potential for significant cumulative benthic impacts is remote.

#### **8.4 PELAGIC ENVIRONMENT**

Based on existing information, potential effects from offshore dredging could occur to transitory pelagic species. Dredging effects on most zooplankton from entrainment and turbidity should be minimal due to high spatial and temporal variability of the populations. If Area 4 is used as a sand source, an environmental window excluding summer and fall months could be considered to avoid dredging when shrimp and blue crab larvae are most prevalent, but only if additional data become available to determine the extent of impacts and justify the restriction. Dredging is unlikely to significantly affect squid populations in the vicinity of the sand resource areas. Although entrainment, attraction, and turbidity could occur from dredging, quantitative data are lacking to support the use of an environmental window for pelagic fishes.

The main potential effect of dredging on sea turtles is physical injury or death caused by the suction and/or cutting action of the dredge head. No significant effects on turtles are expected from turbidity, anoxia, or noise. Loggerheads are expected to be the most abundant turtle in the project area. Increased loggerhead densities may be expected during the nesting season, which extends from 1 May through 30 November. A schedule that avoids the loggerhead nesting season also would avoid potential impacts to occasional nesting green and leatherback turtles. Hawksbill and Kemp's Ridley turtles do not nest anywhere near the project area. It is not known whether sea turtles are likely to be brumating in bottom sediments of the project area during winter. Consequently, there is insufficient information to determine whether seasonal restrictions on dredging during winter months would be appropriate.

The two marine mammals most likely to be found in and near the project area are the Atlantic spotted dolphin and the bottlenose dolphin. There is no strong seasonal pattern in abundance for either species that would provide an appropriate basis for seasonal restrictions on the project. In addition, the likelihood of significant impact from physical injury, turbidity, or noise is low even if these animals are present.

Zooplankton, squids, fishes, sea turtles, and marine mammals were groups in the pelagic environment considered to be potentially affected by offshore dredging. No cumulative effects to any of these pelagic groups are expected from multiple sand mining operations.

## 8.5 SYNTHESIS

The data collected, analyses performed, and simulations conducted for this study indicate that proposed sand dredging at sites evaluated on the OCS should have minimal environmental impact on fluid and sediment dynamics and biological communities. Short-term impacts to benthic communities are expected due to the physical removal of borrow material, but the potential for significant cumulative benthic impacts is remote. Additionally, no cumulative effects to any of the pelagic groups are expected from potential sand mining operations.

Minimal physical environmental impacts due to potential sand dredging operations have been identified through wave and sediment transport simulations. However, under normal wave conditions, the maximum change in sand transport dynamics is about 5% of existing conditions. Because wave and sediment transport predictions are only reliable to within about  $\pm 25\%$ , predicted changes are not deemed significant. Although changes during storm conditions illustrate greater variation, the ability of models to predict storm wave transformation and resultant sediment transport is less certain. Because minimal impacts were documented to wave and sediment transport dynamics and biology, particularly along the eastern portion of the study area, additional data may be required for a specific sand extraction scenario to determine the extent of impacts.

## 9.0 LITERATURE CITED

- Ackerman, B.B., 1995. Aerial Surveys of Manatees: A Summary and Progress Report. In: T.J. O'Shea, B.B. Ackerman, and H.F. Percival (eds.), Population Biology of the Florida Manatee. National Biological Service Information and Technical Report No. 1, pp. 13-33.
- Adams, K.T., 1942. Hydrographic Manual. U.S. Department of Commerce, Coast and Geodetic Survey, Special Publication 143, 940 pp.
- Alabama Game and Fish Division, 1997. Federally listed endangered/threatened species. Department of Conservation and Natural Resources, Montgomery, AL.
- Alexander, J.E., T.T. White, K.E. Turgeon, and A.W. Blizzard, 1977. Baseline Monitoring Studies, Mississippi, Alabama, Florida Outer Continental Shelf, 1975-1976, Volume III: Results. Final Report Prepared for U.S. Department of the Interior, Bureau of Land Management, Washington, DC., Report No. BLM-ST-78-32.
- Anders, F.J. and M.R. Byrnes, 1991. Accuracy of shoreline change rates as determined from maps and aerial photographs. *Shore and Beach*, 59(1): 17-26.
- Andrews, J., 1971. Shells and Shores of Texas. University of Texas Press, Austin and London. 365 pp.
- Applied Biology, Inc., 1979. Biological Studies Concerning Dredging and Beach Nourishment at Duval County, Florida with a Review of Pertinent Literature. U.S. Army Corps of Engineers, Jacksonville District, Jacksonville, FL.
- Arnold, D.W., 1992. The Scientific Rationale For Restricting Coastal Construction Activities During The Marine Turtle Nesting Season. In: L.S. Tait (comp.), New Directions in Beach Management. Proceedings of the 5th Annual National Conference on Beach Preservation Technology, St. Petersburg, FL, pp. 374-380.
- Auld, A.H. and J.R. Schubel, 1978. Effects of suspended sediment on fish eggs and larvae: A laboratory assessment. *Estuarine and Coastal Marine Science*, 6: 153-164.
- Bakker, W.T., 1974. Sand concentration in an oscillatory flow. Proceedings of the 14<sup>th</sup> Conference on Coastal Engineering, ASCE, New York, pp. 1,129-1,148.
- Bakker, W.T. and Th. Van Doorn, 1978. Near-bottom velocities in waves with a current. Proceedings of the 16<sup>th</sup> Conference on Coastal Engineering, ASCE, New York, pp. 1,394-1,413.
- Balech, E., 1967. Dinoflagellates and tintinnids in the northeastern Gulf of Mexico. *Bulletin of Marine Science in the Gulf and Caribbean*, 17(2): 280-298.
- Barry A. Vittor & Associates, Inc., 1985. Tuscaloosa Trend Regional Data Search and Synthesis Study, Synthesis Report, Volume I. U.S. Department of the Interior, Minerals Management Service, New Orleans, LA. OCS Study MMS 85-0056.
- Barry A. Vittor & Associates, Inc., 1988. Environmental Report, Jubilee Pipeline Systems. Final Report to Jubilee Pipeline Company, Houston, TX. 105 pp.
- Barry, M., 1978. Behavioral Response of Yellowfin Tuna, *Thunnus albacares*, and Kawakawa, *Euthynnus affinis*, to Turbidity. U.S. Department of Commerce, National Oceanic and Atmospheric Administration, Environmental Research Laboratories, Pacific Marine Environmental Laboratory, Seattle, WA. Deep Ocean Mining Environmental Study (DOMES), Unpublished Manuscript Number 31. National Technical Information Service No. PB-297, 106 pp.

- Bearden, B.L. and R.L. Hummell, 1990. Geomorphology of Coastal Sand Dunes, Morgan Peninsula, Baldwin County, Alabama. Geological Survey of Alabama Circular 150, 71 pp.
- Bedford, K.W., and J. Lee, 1994. Near-bottom sediment response to combined wave-current conditions, Mobile Bay, Gulf of Mexico. *Journal of Geophysical Research*, 16: 161-177.
- Benfield, M.C. and T.J. Minello, 1996. Relative effects of turbidity and light intensity on reactive distance and feeding of an estuarine fish. *Environmental Biology of Fishes*, 46: 211-216.
- Berkhoff, J.C.W., N. Booij and A.C. Radder, 1972. Verification of numerical wave propagation models for simple harmonic linear waves. *Coastal Engineering*, 6: 255-279.
- Berry, S.A., 1990. Canaveral Harbor Entrance Channel Operational Measures to Protect Sea Turtles. In: D.D. Dickerson and D.A. Nelson (comps.), *Proceedings of the National Workshop on Methods to Minimize Dredging Impacts on Sea Turtles*, Jacksonville, FL. U.S. Army Engineer Waterways Experiment Station, Environmental Effects Laboratory, Vicksburg, MS, Miscellaneous Paper EL-90-5, pp. 49-52.
- Biggs, R.B., 1968. Environmental Effects of Overboard Spoil Disposal. *Journal of Sanitary Engineering Division* 94, No. SA3, Proceeding Paper 5979, pp. 477-478.
- Birkemeier, W.A. and R.A. Dalrymple, 1976. Numerical Models for the Prediction of Wave Set-up and Nearshore Circulation. Ocean Engineering Report No. 3, Department of Civil Engineering, University of Delaware, Newark, DE.
- Blake, N.J., L.J. Doyle, and J.J. Culter, 1995. Impacts and Direct Effects of Sand Dredging for Beach Renourishment on the Benthic Organisms and Geology of the West Florida Shelf. U.S. Department of the Interior, Minerals Management Service, Office of International Activities and Marine Minerals, Herndon, VA. Executive Summary, OCS Report MMS 95-0004, 23 pp. Final Report, OCS Report MMS 95-0005, 109 pp. Appendices, OCS Report MMS 95-0005.
- Blanton, J.O., 1994. U.S. Southeast Continental Shelf Inner Shelf Processes Relevant to the Northeast Gulf of Mexico Inner Shelf. *Proceedings of the Northeast Gulf of Mexico Physical Oceanography Workshop*, U.S. Department of the Interior, Minerals Management Service, OCS Study 94-0044.
- Blaxter, J.H.S., 1968. Visual thresholds and spectral sensitivity of herring larvae. *Journal of Experimental Biology*, 48: 39-53.
- Blaylock, R.A., J.W. Hain, L.J. Hansen, D.L. Palka, and G.T. Waring, 1995. U.S. Atlantic and Gulf of Mexico Marine Mammal Stock Assessments. NOAA Tech. Mem. NMFS-SEFSC-363, 211 pp.
- Bodge, K.R., 1986. Short Term Impoundment of Longshore Sediment Transport. Ph.D. Dissertation, Department of Coastal and Ocean Engineering, University of Florida, Gainesville, FL, 346 pp.
- Bodge, K.R. and R.G. Dean, 1987. Short-term Impoundment of Longshore Transport. *Proceedings of Coastal Sediments '87*, ASCE, pp. 468-483.
- Bodge, K.R., 1989. A literature review of the distribution of longshore sediment transport across the surf zone. *Journal of Coastal Research*, 5(2): 307-328.
- Boehlert, G.W. and J. B. Morgan, 1985. Turbidity enhances feeding abilities of larval Pacific herring, *Clupea harengus pallasii*. *Hydrobiologia*, 123: 161-170.
- Boesch, D.F., 1973. Classification and community structure of macrobenthos in the Hampton Roads area, Virginia. *Marine Biology*, 21: 226-244.

- Bonsdorff, E., 1983. Recovery Potential of Macrozoobenthos from Dredging in Shallow Brackish Waters. In: L. Cabioch et al. (eds), *Fluctuations and Succession in Marine Ecosystems, Proceedings of the 17th European Symposium on Marine Biology*, Brest: Oceanologica Acta., pp. 27-32.
- Booij, N., 1983. A note on the accuracy of the mild-slope equation. *Coastal Engineering*, 7: 191-203.
- Boone, P.A., 1973. Depositional systems of the Mississippi, Alabama, and western Florida coastal zone. *Gulf Coastal Association of Geological Societies Transactions*, 23: 266-277.
- Borgman, L.E., 1985. Directional Spectrum Estimation for the  $S_{xy}$  Gauges. Technical Report, U.S. Army Engineer Waterways Experiment Station, Coastal Engineering Research Center, Vicksburg, MS, pp. 1-104.
- Borror, A.C., 1962. Ciliate protozoa of the Gulf of Mexico. *Bulletin of Marine Science in the Gulf and Caribbean*, 12(3): 333-349.
- Bowen, P.R. and G.A. Marsh, 1988. Benthic Faunal Colonization of an Offshore Borrow Pit in Southeastern Florida. U.S. Army Engineer Waterways Experiment Station, Dredged Material Research Station, Vicksburg, MS. Miscellaneous Paper D-88-5.
- Boyd, I.L. and M.P. Stanfield, 1998. Circumstantial evidence for the presence of monk seals in the West Indies. *Oryx*, 32: 310-316.
- Breitburg, D.L., 1988. Effects of turbidity on prey consumption by striped bass larvae. *Transactions of the American Fisheries Society*, 117: 72-77.
- Bretschneider, C.L., 1968. Significant waves and wave spectrum. *Ocean Industry*, 40-46.
- Brooks, J.M. and C.P. Giamonna (eds.), 1991. Mississippi-Alabama Continental Shelf Ecosystem Study Data Summary and Synthesis, Volume II: Technical Narrative. U.S. Department of the Interior, Minerals Management Service, OCS Study MMS 91-0063.
- Brooks, R.M. and W.D. Corson, 1984. Summary of Archived Study Pressure, Wind, Wave, and Water Level Data. U.S. Army Engineer Waterways Experiment Station, Wave Information Study, Vicksburg, MS, WIS Report 13.
- Bruton, M.N., 1985. The effects of suspensoids on fish. *Hydrobiologia*, 125: 221-241.
- Burke, V.J., E.A. Standora, and S.J. Morreale, 1993. Diet of juvenile Kemp's ridley and loggerhead sea turtles from Long Island, New York. *Copeia*, 1993: 1,176-1,180.
- Burke, W.D., 1975. Pelagic Cnidaria of the Mississippi Sound and adjacent waters. *Gulf Research Report*, 5(1): 23-38.
- Burke, W.D., 1976. Biology and distribution of the macrocoelenterates of the Mississippi Sound and adjacent waters. *Gulf Research Report*, 5(2): 17-28.
- Byles, R.A., 1988. Satellite Telemetry of Kemp's Ridley Sea Turtle, *Lepidochelys kempii*, in the Gulf of Mexico. Report to the National Fish and Wildlife Foundation, 40 pp.
- Byles, R.A. and C.K. Dodd, 1989. Satellite Biotelemetry of a Loggerhead Sea Turtle (*Caretta caretta*) from the East Coast of Florida. In: S.A. Eckert, K.L. Eckert, and T.H. Richardson (comps.), *Proceedings of the Ninth Annual Workshop on Sea Turtle Conservation and Biology*. U.S. Department of Commerce, Miami, FL. NOAA Tech. Mem. NMFS-SEFSC-232, pp. 215-218.
- Byles, R.A., C. Caillouet, D. Crouse, L. Crowder, S. Epperly, W. Gabriel, B. Gallaway, M. Harris, T. Henwood, S. Heppell, R. Marquez, S. Murphy, W. Teas, N. Thompson, and

- B. Witherington, 1996. A report of the turtle expert working group: Results of a series of deliberations held in Miami, Florida, June 1995-June 1996.
- Byrnes, M.R. and C.G. Groat, 1991. Characterization of the Development Potential of Ship Shoal Sand for Beach Replenishment of Isles Dernieres. Final Report, U.S. Department of the Interior, Minerals Management Service, Office of International Activities and Marine Minerals, Herndon, VA, 164 pp.
- Byrnes, M.R. and M.W. Hiland, 1994a. Shoreline Position and Nearshore Bathymetric Change (Chapter 3). In: N.C. Kraus, L.T. Gorman, and J. Pope (editors), Kings Bay Coastal and Estuarine Monitoring and Evaluation Program: Coastal Studies. Technical Report CERC-94-09, U.S. Army Engineer Waterways Experiment Station, Coastal Engineering Research Center, Vicksburg, MS, pp. 61-143.
- Byrnes, M.R. and M.W. Hiland, 1994b. Compilation and analysis of shoreline and bathymetry data (Appendix B). In: N.C. Kraus, L.T. Gorman, and J. Pope (editors), Kings Bay Coastal and Estuarine Monitoring and Evaluation Program: Coastal Studies. Technical Report CERC-94-09, U.S. Army Engineer Waterways Experiment Station, Coastal Engineering Research Center, Vicksburg, MS, pp. B1-B89.
- Byrnes, M.R., R.A. McBride, S. Penland, M.W. Hiland, and K.A. Westphal, 1991. Historical Changes in Shoreline Position Along the Mississippi Sound Barrier Islands. In: Coastal Depositional Systems in the Gulf of Mexico: Quaternary Framework and Environmental Issues, GCS-SEPM 12<sup>th</sup> Annual Research Conference, pp. 43-55.
- Carr, A.F. Jr, L. Ogren, and C. McVea, 1981. Apparent hibernation by the Atlantic loggerhead turtle *Caretta caretta* off Cape Canaveral. Biol. Conserv., 19: 7-14.
- Centre for Cold Ocean Resources Engineering (C-CORE), 1995. Proposed Marine Mining Technologies and Mitigation Techniques: A Detailed Analysis with Respect to the Mining of Specific Offshore Mineral Commodities. Contract report for U.S. Department of the Interior, Minerals Management Service, OCS Report MMS 95-0003, C-CORE Publication 96-C15, 280 pp. + apps.
- Chandler, C.R., R.M. Sanders, Jr., and A.M. Landry, Jr., 1985. Effects of three substrate variables on two artificial reef fish communities. Bulletin of Marine Science, 37(1): 129-142.
- Chermock, R.L., P.A. Boone, and R.L. Lipp, 1974. The Environment of Offshore and Estuarine Alabama. Geological Survey of Alabama Information Series 51, 135 pp.
- Chittenden, M.E., Jr. and J.D. McEachran, 1976. Composition, Ecology, and Dynamics of Demersal Fish Communities on the Northwestern Gulf of Mexico Continental Shelf, with a Similar Synopsis for the Entire Gulf. Texas A&M Univ. Sea Grant Pub. No. 76-208, 104 pp.
- Christmas, J.Y., 1973. Cooperative Gulf of Mexico estuarine inventory and study, Mississippi. Gulf Coast Research Laboratory, Oceans Springs, MS. 434 pp.
- Christmas, J.Y., G. Gunter, and P. Musgrave, 1966. Studies of annual abundance of postlarval penaeid shrimp in the estuarine waters of Mississippi, as related to subsequent commercial catches. Gulf Research Report, 2(2): 177-212.
- Clarke, A.J., 1994. Overview of the Physical Oceanography of the Florida Shelf in the Study Region. Proceedings of the Northeast Gulf of Mexico Physical Oceanography Workshop, U.S. Department of the Interior, Minerals Management Service, OCS Study 94-0044.
- Coastal Oceanographics, 1996. Hypack Navigation Software Version 6.4.

- Coastline Surveys Limited, 1998. Marine Aggregate Mining Benthic and Surface Plume Study. Final report to the U.S. Department of the Interior, Minerals Management Service and Plume Research Group. Report 98-555-03, 168 pp.
- Comiskey, C., T. Farmer, C. Brandt, Y. Jager, and E. Burrell, 1985. Quantitative Characterization of Demersal Finfish and Shellfish Populations and Communities in the Tuscaloosa Trend Region, Appendix C. In: Tuscaloosa Trend Regional Data Search and Synthesis Study, Synthesis Report, Volume II. U.S. Department of the Interior, Minerals Management Service, New Orleans, LA, OCS Study MMS 85-0056, 236 pp.
- Continental Shelf Associates, Inc., 1989. Diver Tow and Photographic Survey Around a Proposed Drillsite in Pensacola Area Block 881. Report Prepared for Conoco, Inc., New Orleans, LA. 3 pp. + app.
- Continental Shelf Associates, Inc. and Barry A. Vittor & Associates, Inc., 1989. Environmental Monitoring in Block 132 Alabama State Waters. Report Prepared for Shell Offshore, Inc., New Orleans, LA. 75 pp.
- Crowell, M., S.P. Leatherman, and M.K. Buckley, 1991. Historical shoreline change: error analysis and mapping accuracy. *Journal of Coastal Research*, 7(3): 839-852.
- Cruikshank, M.J., J.P. Flanagan, B. Holt, and J.W. Padan, 1987. Marine Mining on the Outer Continental Shelf: Environmental Effects Overview. U.S. Department of the Interior, Minerals Management Service, OCS Report 87-0035, 66 pp.
- Da Silva, J.A. and R.E. Condrey, 1998. Discerning patterns in patchy data: A categorical approach using Gulf menhaden, *Brevoortia patronus*, bycatch. *Fishery Bulletin*, 96(2): 193-209.
- Dames & Moore, 1979. Mississippi, Alabama, Florida Outer Continental Shelf Baseline Environmental Survey; MAFLA, 1977/78. Final Report Prepared for the U.S. Department of the Interior, Bureau of Land Management, Contract No. AA550-CT7-34.
- Darnell, R.M., 1991. Summary and Synthesis. In: J.M. Brooks and C.P. Giamonna (eds.), Mississippi-Alabama Continental Shelf Ecosystem Study Data Summary and Synthesis, Volume II: Technical Narrative. U.S. Department of the Interior, Minerals Management Service, OCS Study MMS 91-0063, pp. 15: 1-147.
- Darnell, R.M. and J.A. Kleypas, 1987. Eastern Gulf Shelf Bio-atlas: A Study of the Distribution of Demersal Fishes and Penaeid Shrimp of Soft Bottoms of the Continental Shelf from the Mississippi River Delta to the Florida Keys. U.S. Department of the Interior, Minerals Management Service, OCS Study MMS 86-0041, 548 pp.
- Davis, H.C. and H. Hidu, 1969. Effects of turbidity-producing substances in sea water on eggs and larvae of three genera of bivalve mollusks. *Veliger*, 11(4): 316-323.
- Davis, R.W. and G.S. Fargion (eds.), 1996. Distribution and Abundance of Cetaceans in the North-central and Western Gulf of Mexico, Final Report, Volume II: Technical report. Prepared by the Texas Institute of Oceanography and the National Marine Fisheries Service. U.S. Department of the Interior, Minerals Management Service, Gulf of Mexico OCS Region Office, New Orleans, LA, OCS Study MMS 96-0027, 357 pp.
- Davis, R.W., G.S. Fargion, N. May, T.D. Leming, M. Baumgartner, W.E. Evans, L.J. Hansen, and K. Mullin, 1998. Physical habitat of cetaceans along the continental slope in the north-central and western Gulf of Mexico. *Marine Mammal Science*, 14(3): 490-507.
- Defenbaugh, R.E., 1976. A Study of the Benthic Macroinvertebrates of the Continental Shelf of the Northern Gulf of Mexico. Ph.D. dissertation, Texas A&M University, College Station, TX, 476 pp.

- Diaz, R.J. and R. Rosenberg, 1995. Marine benthic hypoxia: A review of its ecological effects and the behavioural responses of benthic macrofauna. *Oceanographic Marine Biology Annual Review*, 33: 245-304.
- Dickerson, D.D., 1990. Workgroup 1 Summary. In: D.D. Dickerson and D.A. Nelson (comps.), *Proceedings of the National Workshop on Methods to Minimize Dredging Impacts on Sea Turtles*, Jacksonville, FL. U.S. Army Engineer Waterways Experiment Station, Environmental Effects Laboratory, Vicksburg, MS, Miscellaneous Paper EL-90-5, pp. 74-75.
- Dickerson, D.D., D.A. Nelson, M. Wolff, and L. Manners, 1992. Summary of Dredging Impacts on Sea Turtles: King's Bay, Georgia and Cape Canaveral, Florida. In: M. Salmon and J. Wyneken (comps.), *Proceedings of the Eleventh Annual Workshop on Sea Turtle Biology and Conservation*, Jekyll Island, GA. NOAA Tech. Mem. NMFS-SEFSC-302, pp. 148-151.
- Dickerson, D.D., K.J. Reine, and D.G. Clarke, 1998. Economic Impacts of Environmental Windows Associated with Dredging Operations. U.S. Army Engineer Waterways Experiment Station, Research and Development Center, Vicksburg, MS. DOER Tech. Note: Collection (TN DOER-E3).
- Dinnell, S., 1997. Personal communication and provision of electronic data.
- Ditty, J.G., 1986. Ichthyoplankton in neretic waters of the northern Gulf of Mexico off Louisiana: Composition, relative abundance, and seasonality. *Fishery Bulletin*, 84(4): 935-946.
- Ditty, J.G., G.G. Zieske, and R.F. Shaw, 1988. Seasonality and depth distribution of larval fishes in the northern Gulf of Mexico above 26°00'N. *Fishery Bulletin*, 86: 811-823.
- Dodd, C.K., Jr., 1988. Synopsis of the Biological Data on the Loggerhead Sea Turtle *Caretta caretta* (Linnaeus 1758). U.S. Fish and Wildlife Service Biological Report 88(4), 110 pp.
- Douglass, S.L., D.T. Resio, and E.B. Hands, 1995. Impact of Near-Bottom Currents on Dredged Material Mounds Near Mobile Bay. Technical Report DRP-95-6, U.S. Army Engineers Waterways Experiment Station, Dredged Material Research Program, Vicksburg, MS.
- Doyle, L.J. and T.N. Sparks, 1980. Sediments of the Mississippi, Alabama, and Florida (MAFLA) Continental Shelf. *Journal of Sedimentary Petrology*, 50(3): 905-915.
- Early, G., 1998. Comment on Boyd and Stanfield (1998) paper, posted on Marine Mammals Research and Conservation Discussion (MARMAM@UVVM.UVIC.CA) listserv, 2 November 1998. Greg Early, Edgerton Research Laboratory, New England Aquarium, Central Wharf, Boston, MA. gearly@neaq.org.
- Ebersole, B.A. and R.A. Dalrymple, 1979. A Numerical Model for Nearshore Circulation Including Convective Acceleration and Lateral Mixing. Ocean Engineering Report No. 21, Department of Civil Engineering, University of Delaware, Newark, DE.
- Ebersole, B.A. and R.A. Dalrymple, 1980. Numerical Modeling of Nearshore Circulation. *Proceedings of the 17<sup>th</sup> Coastal Engineering Conference*, Sydney, pp. 2,710-2,725.
- Eckert, K.L., 1995. Leatherback Sea Turtle, *Dermochelys coriacea*. In: P.T. Plotkin (ed.), *National Marine Fisheries Service and U. S. Fish and Wildlife Service Status Reviews for Sea Turtles Listed under the Endangered Species Act of 1973*, Silver Spring, MD.
- Eckert, S.A., D.W. Nellis, K.L. Eckert, and G.L. Kooyman, 1986. Diving patterns of two leatherback sea turtles (*Dermochelys coriacea*) during interesting intervals at Sandy Point, St. Croix, U.S. Virgin Islands. *Herpetologica*, 42(3): 381-388.
- Edmiston, H.L., 1979. The Zooplankton of the Apalachicola Bay system. M.S. thesis, Florida State University, Tallahassee, FL., 104 pp.

- Ehrhart, L.M., 1977. Cold water stunning of marine turtles in Florida east coast lagoons: Rescue measures, population characteristics and evidence of winter dormancy. Paper presented at the 1977 American Society of Ichthyologists and Herpetologists Meeting, Gainesville, FL. (as cited in Fritts et al., 1983).
- Ellis, M.Y., 1978. Coastal Mapping Handbook. U.S. Department of the Interior, Geological Survey, U.S. Department of Commerce, National Ocean Service, U.S. Government Printing Office, Washington, D.C., 199 pp.
- Exxon Company, U.S.A., 1986. Production of Hydrocarbon Resources From Offshore State Leases in Mobile and Baldwin Counties, Alabama. An Environmental Information Document Submitted in Support of Applications for Permits from the U.S. Army Corps of Engineers, Mobile District, Mobile, AL.
- Fauchald, K. and P. Jumars, 1979. The diet of worms: A study of polychaete feeding guilds. *Oceanography and Marine Biology Annual Review*, 17: 193-284.
- Fischer, W. (ed.), 1978. FAO Species Identification Sheets for Fishery Purposes, Western Central Atlantic (Fishing Area 31), Volume VI.
- Frazier, N.B., 1995. Loggerhead Sea Turtle, *Caretta caretta*. In: P.T. Plotkin (ed.), National Marine Fisheries Service and U. S. Fish and Wildlife Service Status Reviews for Sea Turtles Listed Under the Endangered Species Act of 1973, Silver Spring, MD.
- Fredsoe, J. and R. Deigaard, 1992. Mechanics of Coastal Sediment Transport. World Scientific, New Jersey, 392 pp.
- Fritts, T.H., A.B. Irvine, R.D. Jennings, L.A. Collum, W. Hoffman, and M.A. McGehee, 1983. Turtles, Birds, and Mammals in the Northern Gulf of Mexico and Nearby Atlantic Waters. U.S. Fish and Wildlife Service, Office of Biological Services, Washington, DC, FWS/OBS-82/65, 455 pp.
- Fuller, D.A., A.M. Tappan, and M.C. Hester, 1987. Sea turtles in Louisiana's coastal waters. Louisiana Sea Grant College.
- Gales, R.S., 1982. Effects of Noise of Offshore Oil and Gas Operations on Marine Mammals -- An Introductory Assessment. Technical Report 844, Naval Ocean Systems Center, San Diego, CA.
- Garcia, A. W., 1977. Dauphin Island Littoral Transport Calculations. U.S. Army Engineer Waterways Experiment Station, Hydraulics Laboratory, Vicksburg, MS, Miscellaneous Paper H-77-11, 12 pp.
- Gelfenbaum, G., 1994. U.S.G.S Coastal Studies in the Northeast Gulf of Mexico. Proceedings of the Northeast Gulf of Mexico Physical Oceanography Workshop, April 5-7, 1994. U.S. Department of the Interior, Minerals Management Service OCS Study 94-0044.
- Gelfenbaum, G. and R.P Stumpf, 1993. Observations of currents and density structure across a buoyant plume front. *Estuaries*, 16(1): 40-52.
- Gilbert, R.O., 1987. Statistical Methods for Environmental Pollution Monitoring. Van Nostrand Reinhold, New York, NY. 320 pp.
- Goldberg, W.M., 1989. Biological Effects of Beach Nourishment in South Florida: The Good, the Bad, and the Ugly. Proceedings of Beach Preservation Technology, 1988, Shore and Beach Preservation Association, Tallahassee, FL.
- Govoni, J.J. and C.B. Grimes, 1992. The surface accumulation of larval fishes by hydrodynamic convergence within the Mississippi River plume front. *Continental Shelf Research*, 12(11): 1,265-1,276.

- Govoni, J.J., D.E. Hoss, and D.R. Colby, 1989. The spatial distribution of larval fishes about the Mississippi River plume. *Limnology and Oceanography*, 34: 178-187.
- Grant, U.S., 1943. Waves as a transporting agent. *American Journal of Science*, 241: 117-123.
- Grant, W.D. and O.S. Madsen, 1978. Bottom Friction Under Waves in the Presence of a Weak Current. NOAA Tech Rep. ERL-MESA-29, 150 pp.
- Grant, W.D. and O.S. Madsen, 1979. Combined wave and current interaction with a rough bottom. *Journal of Geophysical Research*, 84 (C4): 1,797-1,808.
- Grassle, J.F. and J.P. Grassle, 1974. Opportunistic life histories and genetic systems in marine benthic polychaetes. *Journal of Marine Research*, 32: 253-284.
- Gray, J.S., 1974. Animal-sediment relationships. *Oceanography and Marine Biology Annual Review*, 12: 223-261.
- Greenberg, M.D., 1988. *Advanced Engineering Mathematics*. Prentice Hall, Inc., Englewood Cliffs, New Jersey.
- Grimes, C.B. and J.H. Finucane, 1991. Spatial distribution and abundance of larval and juvenile fish, chlorophyll and macrozooplankton around the Mississippi River discharge plume, and the role of the plume in fish recruitment. *Marine Ecology Progress Series*, 75: 109-119.
- Grober, L.E., 1992. The Ecological Effects of Beach Replenishment. M.S. thesis, Duke University, School of the Environment, North Carolina, 109 pp.
- Gulf of Mexico Fishery Management Council, 1998. Generic Amendment for Addressing Essential Fish Habitat Requirements in the Following Fishery Management Plans of the Gulf of Mexico: Shrimp Fishery of the Gulf of Mexico, United States Waters, Red Drum Fishery of the Gulf of Mexico, Reef Fishery of the Gulf of Mexico, Coastal Migratory Resources (Mackerels) in the Gulf of Mexico and South Atlantic, Stone Crab Fishery of the Gulf of Mexico, Spiny Lobster Fishery of the Gulf of Mexico and South Atlantic, and Coral and Coral Reefs of the Gulf of Mexico. Gulf of Mexico Fishery Management Council, Tampa, Florida, 238 pp. +app.
- Hall, S.J., 1994. Physical disturbance and marine benthic communities: Life in unconsolidated sediments. *Oceanography and Marine Biology Annual Review*, 32: 179-239.
- Hallermeier, R.J., 1981. A profile zonation for seasonal sand beaches from wave climate. *Coastal Engineering*, 4: 253-277.
- Hammer, R.M., 1981. Day-night differences in the emergence of demersal zooplankton from a sand substrate in a kelp forest. *Marine Biology*, 62: 275-280.
- Hammer, R.M. and R.C. Zimmerman, 1979. Species of demersal zooplankton inhabiting a kelp forest ecosystem off Santa Catalina Island, California. *Bulletin of the Southern California Academy of Sciences*, 78(3): 199-206.
- Hammer, R.M., B.J. Balcom, M.J. Cruickshank, and C.L. Morgan, 1993. Synthesis and Analysis of Existing Information Regarding Environmental Effects of Marine Mining. Final Report by Continental Shelf Associates, Inc. for the U.S. Department of the Interior, Minerals Management Service, Office of International Activities and Marine Minerals, Herndon, VA, OCS Study MMS 93-0006, 392 pp.
- Hands, E.B., 1994. Shoreward Movement and Other 5-yr Changes at the Sand Island Berms, Alabama. In: *Proceeding of the 15<sup>th</sup> Western Dredging Association Conference*, College Station, TX, pp. 223-235.
- Hansen, L.J. and R.A. Blaylock, 1994. South Atlantic Regional Draft Stock Assessment Reports.

- Hansen, L.J., K.D. Mullin, T.A. Jefferson, and G.P. Scott, 1996. Visual Surveys Aboard Ships and Aircraft. In: R.W. Davis and G.S. Fargion (eds.), Distribution and Abundance of Cetaceans in the North-central and Western Gulf of Mexico, Final Report, Volume II: Technical Report. Prepared by the Texas Institute of Oceanography and the National Marine Fisheries Service for the U.S. Department of the Interior, Minerals Management Service, Gulf of Mexico OCS Region Office, New Orleans, LA. OCS Study MMS 96-0027, pp. 55-132.
- Hardin, J.D., C.D. Sapp, J.L. Emplaincourt, and K.E. Richter, 1976. Shoreline and Bathymetric Changes in the Coastal Area of Alabama: A Remote Sensing Approach. Geological Survey of Alabama Information Series 50, 125 pp.
- Harper, D.E., Jr., 1991. Macroinfauna and Macroepifauna. In: J.M. Brooks and C.P. Giamonna (eds.), Mississippi-Alabama Continental Shelf Ecosystem Study Data Summary and Synthesis, Volume II: Technical Narrative. U.S. Department of the Interior, Minerals Management Service, OCS Study MMS 91-0063.
- Harris, T.F.W., J.M. Jordan, W.R. McMurray, C.J. Verwey and F. P. Anderson, 1963. Mixing in the surf zone. International Journal of Air and Water Pollution, 7: 649-667.
- Hart, A.D., R.A. Shaul, B.A. Vittor, 1989. Environmental Monitoring in Block 132, Alabama State Waters. Summary Report for Shell Offshore, Inc., Continental Shelf Associates, Inc., Jupiter, FL. Technical Report.
- Hasselmann, K.T., Barnett, E. Bouws, H. Carlson, D. Cartwright, K. enke, J. Ewing, H. Gienapp, D. Hasselmann, P. Kruseman, A. Meerburgh, P. Muller, D. Olbers, K. Richter, W. Sell, and H. Walden, 1973. Measurement of wind-wave growth and swell decay during the joint north sea wave project (JONSWAP). Deutsches Hydrographisches Zeitschrift Reihe A (8<sup>0</sup>), No. 12.
- Henwood, T.A. and L.H. Ogren, 1987. Distribution and migrations of immature Kemp's ridley turtles (*Lepidochelys kempî*) and green turtles (*Chelonia mydas*) off Florida, Georgia and South Carolina. Northeast Gulf Science, 9: 153-159.
- Herbich, J.B., 1992. Handbook of Dredging Engineering. McGraw-Hill, Inc., New York, 740 pp.
- Herbich, J.B. and S.B. Brahme, 1991. Literature Review and Technical Evaluation of Sediment Resuspension During Dredging. U.S. Army Engineer Waterways Experiment Station, Hydrolics Laboratory, Vicksburg, MS. Contract Report HL-91-1.
- Hildebrand, H., 1982. A Historical Review of the Status of Sea Turtle Populations in the Western Gulf of Mexico. In: K.A. Bjorndal (ed.), Biology and Conservation of Sea Turtles. Smithsonian Institution Press, Washington, DC, pp. 447-453.
- Hirota, J., 1981. Potential effects of deep-sea minerals mining on macrozooplankton in the north equatorial Pacific. Marine Minerals, 3(1/2): 19-57.
- Hopkins, T.L., 1966. The plankton of the St. Andrew Bay system, Florida. Publ. Inst. Mar. Sci. Univ. Tex., 11: 12-64.
- Houston, J.R., 1995. Beach nourishment, coastal forum. Shore and Beach, January, 21-24.
- Hrabovsky, L., 1990. Hydraulic cutterhead pipeline dredging. In: D.D. Dickerson and D.A. Nelson (comps.), Proceedings of the National Workshop on Methods to Minimize Dredging Impacts on Sea Turtles, Jacksonville, FL. U.S. Army Engineer Waterways Experiment Station, Environmental Effects Laboratory, Vicksburg, MS, Miscellaneous Paper EL-90-5, pp. 56-58.
- Hu, V.J.H., 1981. Ingestion of deep-sea mining discharge by five species of tropical copepods. Water, Air, and Soil Pollution, 15: 433-440.

- Hubertz, J.M., R.M. Brooks, W.A. Brandon, and B.A. Tracy, 1993. Hindcast Wave Information for the U.S. Atlantic Coast. WIS Report 30, U.S. Army Engineer Waterways Experiment Station, Coastal Engineering Research Center, Wave Information Study, Vicksburg, MS.
- Hughes, S.A., 1984. The TMA Shallow-water Spectrum Description and Applications. Technical Report, CERC-84-7, U.S. Army Engineer Waterways Experiment Station, Coastal Engineering Research Center, Vicksburg, MS.
- Hummell, R.L., 1990. Main Pass and the Ebb-Tidal Delta of Mobile Bay, Alabama. Geological Survey of Alabama Circular 146, 45 pp.
- Hummell, R.L., 1996. Holocene Geologic History of the West Alabama Inner Continental Shelf, Alabama. Geological Survey of Alabama Circular 189, 131 pp.
- Hummell, R.L., 1999. Telephone conversation regarding potential beach replenishment requirements for erosion hazard areas along the Alabama coast. Table of estimated sand volumes faxed to Mark Byrnes on March 31, 1999.
- Hummell, R.L. and S.J. Parker, 1995. Holocene Geologic History of Mobile Bay, Alabama. Geological Survey of Alabama Circular 186, 96 pp.
- Hummell, R.L. and W.E. Smith, 1995. Geologic and Environmental Characterization and Near-term Lease Potential of an Offshore Sand Resource Site for Use in Beach Nourishment Projects on Dauphin Island, Alabama. Final Report, Prepared by the Geological Survey of Alabama in fulfillment of U.S. Department of the Interior, Minerals Management Service Cooperative Agreement No. 14-35-0001-30725, 165 pp.
- Hummell, R.L. and W.E. Smith, 1996. Geologic Resource Delineation and Hydrographic Characterization of an Offshore Sand Resource Site for Use in Beach Nourishment Projects on Dauphin Island, Alabama. Final Report, Prepared by the Geological Survey of Alabama in cooperation with the Department of Geology, University of Alabama in fulfillment of U.S. Department of the Interior, Minerals Management Service Cooperative Agreement No. 14-35-0001-30781, 169 pp.
- Ingle, R.M., 1952. Studies on the Effect of Dredging Operations Upon Fish and Shellfish. Florida State Board of Conservation, Technical Series 5, 26 pp.
- Jefferson, T.A. and A. J. Schiro, 1997. Distribution of cetaceans in the offshore Gulf of Mexico. Mammal Review, 27(1): 27-50.
- Johnson, A.G., W.E. Fable, Jr., C.B. Grimes, L. Trent, and J.V. Perez, 1994. Evidence for distinct stocks of king mackerel, *Scomberomorus cavalla*, in the Gulf of Mexico. Fishery Bulletin, 92: 91-101.
- Johnson, R.O. and W.G. Nelson, 1985. Biological effects of dredging in an offshore borrow area. Florida Scientist, 48: 166-188.
- Johnston, D.D. and D.J. Wildish, 1982. Effect of suspended sediment on feeding by larval herring (*Clupea harengus harengus* L.). Bulletin of Environmental Contamination and Toxicology, 29: 61-67.
- Jokiel, P.L., 1989. Effects of marine mining dredge spoils on eggs and larvae of a commercially important species of fish, the Mahimahi (*Coryphaena hippurus*). Marine Minerals, 8: 305-315.
- Jones, G. and S. Candy, 1981. Effects of dredging on the macrobenthic infauna of Botany Bay. Australian Journal of Marine and Freshwater Research, 32: 379-399.
- Jonsson, I.G., 1966a. Wave boundary layers and friction factors. Proceedings of the 10<sup>th</sup> Conference on Coastal Engineering, Tokyo, ASCE, New York, NY, pp. 1: 127-148.

- Jonsson, I.G., 1980. A new approach to oscillatory rough turbulent boundary layers. *Ocean Engineering*, 7: 109-152.
- Kajiura, K., 1964. On the bottom friction in an oscillatory current. *Bulletin of Earthquake Research, Inst. Tokyo University*, 42(99): 147-174.
- Kajiura, K., 1968. A model for the bottom boundary layer in water waves. *Bulletin of Earthquake Research, Inst. Tokyo University*, 46: 75-123.
- Kamphuis, J.W., 1975. Friction under oscillatory waves. *Journal of Waterways and Harbors, Coastal Engineering Division, ASCE*, 101: 135-144.
- Kelly, F. J. and A.C. Vastano, 1994. A Census of Loop Current Related Intrusions Onto the Mississippi-Alabama Continental Slope and Shelf. *Proceedings of the Northeast Gulf of Mexico Physical Oceanography Workshop, OCS MMS Study 94-0044*.
- Kerr, S.J., 1995. Silt, Turbidity and Suspended Sediments in the Aquatic Environment: An Annotated Bibliography and Literature Review. Ontario Ministry of Natural Resources, Southern Region Science and Technology Transfer Unit, Technical Report TR-008, 277 pp.
- Kinoshita, K. and M. Noble, 1995. Current Data from the Northern Gulf of Mexico. *Open File Report 95-633, U.S. Department of the Interior, U.S. Geological Survey*.
- Kirby, J.T., 1983. Propagation of weakly-nonlinear surface water waves in regions with varying depth and current. *ONR Tech. Rept. 14, Res. Rept. CE-83-37, Department of Civil Engineering University of Delaware, Newark*.
- Kirby, J.T., 1984. A note on linear surface wave-current interaction. *Journal of Geophysical Research*, 89: 745-747.
- Kirby, J.T. and H.T. Özkan, 1994. Combined refraction/diffraction model for spectral wave conditions, REF/DIF S. v. 1.1, no. CACR-94-04, Center for Applied Coastal Research, Newark, DE.
- Kirby, J.T. and R.A. Dalrymple, 1983a. A parabolic equation for the combined refraction-diffraction of stokes waves by mildly varying topography. *Journal of Fluid Mechanics* 136: 543-566.
- Kirby, J.T. and R.A. Dalrymple, 1983b. The propagation of weakly nonlinear waves in the presence of varying depth and currents. *Proceedings of the 20<sup>th</sup> Congress I.A.H.R., Moscow*.
- Kirby, J.T. and R.A. Dalrymple, 1984. Verification of a parabolic equation for propagation of weakly non-linear waves. *Coastal Engineering*, 8: 219-232.
- Kirk, K. L., 1992. Effects of suspended clay on *Daphnia* body growth and fitness. *Freshwater Biology*, 28: 102-109.
- Kjerfve, B. and J.E. Sneed, 1984. Analysis and Synthesis of Oceanographic Conditions in the Mississippi Sound Offshore Region. Final Report, Volume 1. U.S. Army Corps of Engineers, Mobile District, Mobile, AL, Contract No. DCW01-83-R-0014, 253 pp.
- Klima, E.F. and D.A. Wickham, 1971. Attraction of coastal pelagic fishes with artificial structures. *Transactions of the American Fisheries Society* , 100(1): 86-99.
- Knight, D.W., 1978. Review of oscillatory boundary layer flow. *Journal of the Hydraulics Division, ASCE*, 104(HY6): 839-855.
- Komar, P.D. and D.L. Inman, 1970. Longshore sand transport on beaches. *Journal of Geophysical Research*, 75(30): 5,914-5,927.

- Kraus, N.C. and M. Larson, 1991. NMLONG: Numerical Model for Simulating the Longshore Current; Report 1, Model Development and Tests. Technical Report DRP-91-1, U.S. Army Engineer Waterways Experiment Station, Dredged Material Research Program, Vicksburg, MS, 166 pp.
- Kraus, N.C. and T.O. Sasaki, 1979. Influence of wave angle and lateral mixing on the longshore current. *Marine Science Communications*, 5(2): 91-126.
- Larson, K.W. and C.E. Moehl, 1988. Entrainment of Anadromous Fish by Hopper Dredge at the Mouth of the Columbia River. In: C.A. Simenstad (ed.), *Effects of Dredging on Anadromous Pacific Coast Fishes*, Workshop Proceedings, University of Washington Sea Grant, pp. 102-112.
- Larson, M. and N.C. Kraus, 1995. Prediction of Cross-shore Sediment Transport at Different Spatial and Temporal Scales. In: J.H. List and J.H.J. Terwindt (eds.), *Large-Scale Coastal Behavior*, *Marine Geology Special Issue*, 126(1/4): 111-128.
- LaSalle, M.W., D.G. Clarke, J. Homziak, J.D. Lunz, and T.J. Fredette, 1991. A Framework for Assessing the Need for Seasonal Restrictions on Dredging and Disposal Operations. Technical Report D-91-1, U.S. Army Engineer Waterways Experiment Station, Dredged Material Research Program, Vicksburg, MS, 74 pp.
- Lefebvre, L.W., T.J. O'Shea, G.B. Rathbun, and R.C. Best, 1989. Distribution, Status, and Biogeography of the West Indian Manatee. In: C.A. Woods, (ed.), *Biogeography of the West Indies*, Sandhill Crane Press, Gainesville, FL, pp. 567-610.
- Leis, J.L., 1991. The Pelagic Stage of Reef Fishes: The Larval Biology of Coral Reef Fishes. In: P.F. Sale (ed.), *The Ecology of Fishes on Coral Reefs*, Academic Press, New York, NY, pp. 183-230.
- Lenhardt, M.L., 1994. Seismic and Very Low Frequency Sound Induced Behaviors in Captive Loggerhead Marine Turtles (*Caretta caretta*). In: K.A. Bjorndal, A.B. Bolten, D.A. Johnson, and P.J. Eliazar (comps.), *Proceedings of the Fourteenth Annual Symposium on Sea Turtle Biology and Conservation*, Hilton Head, SC. U.S. Department of Commerce, National Oceanic and Oceanographic Administration, National Marine Fisheries Service, Southeast Fisheries Science Center, Miami, FL.
- Lewis, J.K. and R.O. Reid, 1985. Local wind forcing of a coastal sea at subinertial frequencies. *Journal of Geophysical Research*, 90: 934-944.
- Lipka, D.A., 1975. The Systematics and Zoogeography of Cephalopods from the Gulf of Mexico. Ph.D. dissertation, Texas A&M University, Department of Oceanography, College Station, TX, 351 pp.
- Lohofener, R., W. Hoggard, K. Mullin, C. Roden, and C. Rogers, 1990. Association of Sea Turtles with Petroleum Platforms in the North-central Gulf of Mexico. U.S. Department of the Interior, Minerals Management Service, Gulf of Mexico OCS Region, New Orleans, LA, OCS Study MMS 90-0025, 90 pp.
- Longuet-Higgins, M.S., 1970. Longshore currents generated by obliquely incident sea waves, parts 1 and 2. *Journal of Geophysical Research*, 75(33): 6,778-6,801.
- Loosanoff, V.L., 1962. Effects of turbidity on some larval and adult bivalves. *Proceedings of the 14<sup>th</sup> Annual Session*, Gulf and Caribbean Fisheries Institute, pp. 80-95.
- Lowery, G.H., 1974. *The Mammals of Louisiana and Its Adjacent Waters*. Louisiana State University Press, Baton Rouge, LA, 565 pp.

- Lozano, C.J. and P.L.F. Liu, 1980. Refraction-diffraction model for linear surface water waves. *Journal of Fluid Mechanics*, 101(4): 705-720.
- Ludwick, J.C., 1964. Sediments in Northeastern Gulf of Mexico. In: R.L. Miller (ed.), *Papers in Marine Geology*, Macmillan Co., New York, NY, pp. 204-238.
- Lundgren, H., 1972. Turbulent currents in the presence of waves. *Proceedings of the 13<sup>th</sup> Coastal Engineering Conference*, Vancouver, B.C., (1): 623-634, ASCE, New York, NY.
- Lutcavage, M. and J.A. Musick, 1985. Aspects of the biology of sea turtles in Virginia. *Copeia*, 1985(2): 449-456.
- Lutz, P., 1990. Sea Turtle Hibernation in the Cape Canaveral Ship Channel. In: D.D. Dickerson and D.A. Nelson (comps.), *Proceedings of the National Workshop on Methods to Minimize Dredging Impacts on Sea Turtles*, Jacksonville, FL. U.S. Army Engineer Waterways Experiment Station, Environmental Effects Laboratory, Vicksburg, MS, Miscellaneous Paper EL-90-5, pp. 64-65.
- MacArthur, R.H., 1960. On the relative abundance of species. *American Naturalist*, 94: 25-36.
- MacArthur, R.H. and E.O. Wilson, 1967. *Theory of Island Biogeography*. Princeton University Press, Princeton, New Jersey, 203 pp.
- Madsen, O.S. and W.D. Grant, 1976. *Sediment Transport in the Coastal Environment*. Report No. 209, MIT, Department of Civil Engineering, Cambridge, MA, 105 pp.
- Madsen, O.S. and W.D. Grant, 1977. Quantitative description of sediment transport by waves. *Proceedings 15<sup>th</sup> International Coastal Engineering Conference*, ASCE, New York, NY, pp. 1,093-1,112.
- Malme, C.I., P.R. Miles, C.W. Clark, P. Tyack, and J.E. Bird, 1983. *Investigations of the Potential Effects of Underwater Noise from Petroleum Industry Activities on Migrating Gray Whale Behavior*. Report by Bolt, Beranek and Newman, Inc., Cambridge, MA, for the U.S. Department of the Interior, Minerals Management Service, Anchorage, AK. BBN Rep. 5366.
- Marine Mammal Commission, 1986. *Habitat Protection Needs for the Subpopulation of West Indian Manatees in the Crystal River Area of Northwest Florida*. National Technical Information Service, Silver Spring, MD, PB86-200 250, 46 pp.
- Marley, R.D., 1983. Spatial distribution patterns of planktonic fish eggs in lower Mobile Bay, Alabama. *Transactions of the American Fisheries Society*, 112: 257-266.
- Marquez, R.M., 1990. *Sea Turtles of the World*. FAO Species Catalogue, Volume 11. FAO, Rome. 81 pp.
- Marsh, G.A. and D.B. Turbeville, 1981. The environmental impact of beach nourishment: Two studies in southeastern Florida. *Shore and Beach*, 1981: 40-44.
- Maurer, D., R.T. Keck, J.C. Tinsman, W.A. Leathem, C. Wethe, C. Lord, and T.M. Church, 1986. Vertical migration and mortality of marine benthos in dredged material: A synthesis. *Internationale Revue der gesamten Hydrobiologie*, 71: 49-63.
- McBride, R.A., 1997. *Synthesis of Hard Mineral Resources of the Florida Panhandle Shelf: Spatial Distribution and Subsurface Evaluation*. Final Report, U.S. Department of the Interior, Minerals Management Service, Contract No. 1435-01-96-CT-30812, 5 p. + 727 p. appendix.
- McBride, R.A. and M.R. Byrnes, 1995. Surficial sediments and morphology of the Southwestern Alabama/Western Florida panhandle coast and shelf. *Gulf Coast Association of Geological Societies Transactions*, 45: 393-404.

- McBride, R.A., M.R. Byrnes, S. Penland, D.L. Pope, and J.L. Kindinger, 1991. Geomorphic History, Geologic Framework, and Hard Mineral Resources of the Petit Bois Pass Area, Mississippi-Alabama. In: Coastal Depositional Systems in the Gulf of Mexico: Quaternary Framework and Environmental Issues, GCS-SEPM 12<sup>th</sup> Annual Research Conference, pp. 116-127.
- McCaully, J.E., R.A. Parr, and D.R. Hancock, 1977. Benthic infauna and maintenance dredging: A case study. *Water Research*, 11: 233-242.
- McGehee D., J.P. McKinney, W.E. Grogg, and E.B. Hands, 1994. Monitoring of Waves and Currents at the Dredged Material Mounds Offshore of Mobile Bay, Alabama. Technical Report DRP-94-4, U.S. Army Engineer Waterways Experiment Station, Dredged Material Research Program, Vicksburg, MS.
- McGraw, K.A. and D.A. Armstrong, 1988. Fish Entrainment by Dredges in Grays Harbor, Washington. In: C.A. Simenstad (ed.), Effects of Dredging on Anadromous Pacific coast Fishes, Workshop Proceedings, University of Washington Sea Grant, pp. 113-131.
- McIlwain, T., 1968. Seasonal occurrence of pelagic Copepoda in Mississippi Sound. *Gulf Research Report*, 2(3): 257-270.
- McLelland, J.A., 1984. Observations on chaetognath distributions in the northeastern Gulf of Mexico during the summer of 1974. *Northeast Gulf Science*, 7(1): 49-59.
- McLelland, J.A., 1989. An illustrated key to the Chaetognatha of the northern Gulf of Mexico with notes on their distribution. *Gulf Research Report*, 8(2): 145-172.
- McNulty, J.K., R.C. Work, and H.B. Moore, 1962. Some relationships between the infauna of the level bottom and the sediment in South Florida. *Bulletin of Marine Science in the Gulf and Caribbean*, 12: 322-332.
- Meyer, G.H. and J.S. Franks, 1996. Food of cobia, *Rachycentron canadum*, from the northeastern Gulf of Mexico. *Gulf Research Report*, 9(3): 161-168.
- Meylan, A., 1992. Hawksbill Turtle *Eretmochelys imbricata*. In: P. Moler (ed.), Rare and Endangered Biota of Florida, University Press of Florida, Gainesville, FL, pp. 95-99.
- Miller, M.L., 1993. The rise of coastal marine tourism. *Ocean and Coastal Management*, 20: 181-199.
- Minerals Management Service, 1997. Gulf of Mexico OCS Oil and Gas Lease Sales 169, 172, 175, 178, and 182, Central Planning Area: Final Environmental Impact Statement. OCS EIS/EA MMS 97-0033, U.S. Department of the Interior, Minerals Management Service, Gulf of Mexico OCS Region, New Orleans, LA.
- Modlin, R.F., 1982. Contributions to the ecology of the mysid crustaceans in the shallow waters of Dauphin Island, Alabama. *Northeast Gulf Science*, 5(2): 45-49.
- Moore, P.G., 1977. Inorganic particulate suspensions in the sea and their effects on marine animals. *Oceanography of Marine Biology Annual Review*, 15: 225-363.
- Morgan, R.P., V.J. Rasin, Jr., and L.A. Noe, 1983. Sediment effects on eggs and larvae of striped bass and white perch. *Transactions of the American Fisheries Society*, 112: 220-224.
- Morisawa, M., 1968. Streams, Their Dynamics and Morphology. McGraw-Hill, New York, NY. 175 pp.
- Mortimer, J.A., 1982. Feeding Ecology of Sea Turtles. In: K.A. Bjorndal (ed.), Biology and Conservation of Sea Turtles, Smithsonian Institution Press, Washington, DC, pp. 103-109.

- Mullin, K. and W. Hoggard, 1998. Aerial Surveys of Marine Mammals and Sea Turtles from Ships and Aircraft. In: R. Davis, W. Evans, M. Horning, S. Lynn, and P. Canton (eds.), Distribution and Abundance of Cetaceans in the Northern Gulf of Mexico, Interim Report No. 2. Prepared by the Texas Institute of Oceanography and the National Marine Fisheries Service, U.S. Geological Survey, Biological Resources Division. USGS/BRD/CR-1998-001, 259 pp.
- Murawski, W.S., 1969. A Study of Submerged Dredge Holes in New Jersey Estuaries With Respect to Their Fitness as Finfish Habitat. New Jersey Department of Conservation and Economic Development, Division of Fish and Game, Miscellaneous Report No. 2M, 32 pp.
- Murray, S.P., 1970. Bottom currents near the coast during hurricane Camille. Journal of Geophysical Research, 75(24): 4579-4582.
- Naqvi, S. and E. Pullen, 1982. Effects of Beach Nourishment and Borrowing on Marine Organisms. U.S. Army Corps of Engineers, Coastal Engineering Research Center, Fort Belvoir, VA, Miscellaneous Report No. 82-14.
- National Marine Fisheries Service and U.S. Fish and Wildlife Service, 1991. Recovery Plan for U.S. Population of Atlantic Green Turtle. National Marine Fisheries Service, Washington, DC, 52 pp.
- National Marine Fisheries Service and U.S. Fish and Wildlife Service, 1992. Recovery Plan for the Kemp's Ridley Sea Turtle (*Lepidochelys kempii*). National Marine Fisheries Service, St. Petersburg, FL, 40 pp.
- National Marine Fisheries Service and U.S. Fish and Wildlife Service, 1993. Recovery Plan for Hawksbill Turtles in the U.S. Caribbean Sea, Atlantic Ocean, and Gulf of Mexico. National Marine Fisheries Service, St. Petersburg, FL, 47 pp.
- National Marine Fisheries Service, 1990. Recovery Plan for U.S. Population of Loggerhead Turtle. National Marine Fisheries Service, St. Petersburg, FL.
- National Marine Fisheries Service, 1997. Regional Biological Opinion for Hopper Dredging of Channels and Beach Nourishment Activities in the Southeastern United States from North Carolina Through Florida East Coast. October 1997.
- National Marine Fisheries Service, 1998. Office of Protected Resources website, information on pinnipeds (seals and sea lions), URL: <http://www.nmfs.gov/tmcintyr/pinniped/pinniped.html>
- National Research Council, 1990. Decline of the Sea Turtles: Causes and Prevention. National Academy Press, Washington, DC, 259 pp.
- National Research Council, 1995. Beach Nourishment and Protection. National Academy Press, 334 pp.
- Nelson, W.G., 1985. Physical and Biological Guidelines for Beach Restoration Projects, Part 1, Biological Guidelines. Florida Sea Grant College Program, Report No. 76.
- Newell, R.C., L.J. Seiderer, and D.R. Hitchcock, 1998. The impact of dredging works in coastal waters: A review of the sensitivity to disturbance and subsequent recovery of biological resources on the seabed. Oceanography and Marine Biology Annual Review, 36: 127-178.
- Nival, P. and S. Nival, 1976. Particle retention efficiencies of an herbivorous copepod, *Acartia clausi* (adult and copepodite stages): Effects of grazing. Limnology and Oceanography, 21(1): 24-38.
- Nummedal, D., S. Penland, R. Gerdes, W. Schramm, J. Kahn, and H. Roberts, 1980. Geologic response to hurricane impact on low-profile Gulf coast barriers. Gulf Coast Association of Geological Societies, Transactions, 30: 183-195.

- Oakwood Environmental Ltd., 1999. Strategic Cumulative Effects of Marine Aggregates Dredging (SCEMAD). Prepared for the U.S. Department of the Interior, Minerals Management Service, 175 pp.
- Odum, E.P., 1969. The strategies of ecosystem development. *Science*, 16: 262-270.
- Oliver, J.S., P.N. Slattery, L.W. Hulberg, and J.N. Nybakken, 1977. Patterns of Succession in Benthic Infaunal Communities Following Dredging and Dredged Material Disposal in Monterey Bay. Technical Report D-77-27, U.S. Army Engineer Waterways Experiment Station, Dredged Material Research Program, Vicksburg, MS.
- Otvos, E.G., 1979. Barrier Island Evolution and History of Migration, North-central Gulf Coast. In: S.P. Leathermen (ed.), *Barrier Islands*, Academic Press, New York, NY, pp. 291-319.
- Oviatt, C.A., C.D. Hunt, G.A. Vargo, and K.W. Kopchynski, 1982. Simulation of a storm event in a marine microcosm. *Journal of Marine Research*, 39: 605-618.
- Paffenhofer, G.A., 1972. The effects of "red mud" on mortality, body weight, and growth of marine planktonic copepod, *Calanus helgolandicus*. *Water, Air, and Soil Pollution*, 1: 314-321.
- Palermo, M.R., 1990. Workgroup 2 Summary. In: D.D. Dickerson and D.A. Nelson (comps.), *Proceedings of the National Workshop on Methods to Minimize Dredging Impacts on Sea Turtles*, Jacksonville, FL, U.S. Army Engineer Waterways Experiment Station, Environmental Effects Laboratory, Vicksburg, MS. Miscellaneous Paper EL-90-5, pp. 76-80.
- Parker, R.H., 1960. Ecology and Distributional Patterns of Marine Macroinvertebrates, Northern Gulf of Mexico. In: F.P. Shephard (ed.), *Recent Sediments, Northwest Gulf of Mexico*, American Association Petroleum Geologists, Tulsa, OK, pp. 302-337.
- Parker, S.J., 1990. Assessment of Nonhydrocarbon Mineral Resources in the Exclusive Economic Zone Offshore Alabama. Geological Survey of Alabama Circular 147, 73 pp.
- Parker, S.J., A.W. Shultz, and W.W. Schroeder, 1992. Sediment Characteristics and Seafloor Topography of a Palimset Shelf, Mississippi-Alabama Continental Shelf. In: *Quaternary Coasts of the United States: Lacustrine and Marine Systems*. SEPM Special Publication 48, pp. 243-251.
- Parker, S.J., D.J. Davies, and W.E. Smith, 1997. Geologic, Economic, and Environmental Characterization of Selected Near-term Leasable Offshore Sand Deposits and Competing Onshore Sources for Beach Nourishment. Geological Survey of Alabama, Environmental Geology Division, Tuscaloosa, AL. Circular 190, 173 pp. + app.
- Parker, S.J., D.J. Davies, W.E. Smith, T.G. Crawford, and R. Kelly, 1993. Geological, Economic, and Environmental Characterization of Selected Near-term Leasable Offshore Sand Deposits and Competing Onshore Sources for Beach Nourishment. Final Report. Prepared by the Geological Survey of Alabama in fulfillment of U.S. Department of the Interior, Minerals Management Service Cooperative Agreement No. 14-35-0001-30630, 223 pp.
- Peddicord, R.K. and V.A. McFarland, 1978. Effects of suspended dredged material on aquatic animals. U.S. Army Engineer Waterways Experiment Station, Dredged Material Research Program, Vicksburg, MS, Technical Report D-78-29, 102 pp. + app.
- Perrin W.F., E.D. Mitchell, J.G. Mead, D.K. Caldwell, M.C. Caldwell, P.J.H. van Bree, and W.H. Dawbin, 1987. Revision of the spotted dolphins, *Stenella* spp. *Marine Mammal Science*, 3(2): 99-170.
- Perrin, W.F., D.K. Caldwell, and M.C. Caldwell, 1994. Atlantic Spotted Dolphin, *Stenella frontalis* (G. Cuvier, 1829), pp. 173-190. In: S.H. Ridgway and R. Harrison (eds.), *Handbook of Marine Mammals*, Volume 5, *The First Book of Dolphins*, Academic Press, London, 416 pp.

- Perry, H.M., C.K. Eleuterius, C.B. Trigg, and J.R. Warren, 1995. Settlement patterns of *Callinectes sapidus* megalope in Mississippi Sound: 1991, 1992. *Bulletin of Marine Science*, 57(3): 821-833.
- Peterson, C.G.J., 1913. Valuation of the Sea. II. The Animal Communities of the Sea-Bottom and Their Importance for Marine Zoogeography. Report of the Danish Biological Station to the Board of Agriculture, 21: 1-44.
- Phillips, P.J., W.D. Burke, and E.J. Keener, 1969. Observations on the trophic significance of jellyfishes in Mississippi Sound with quantitative data on the associative behavior of small fishes with medusae. *Transactions of the American Fisheries Society*, 98(4): 703-712.
- Pianka, E.R., 1970. On r- and K-selection. *American Naturalist*, 104: 592-597.
- Pielou, E.C., 1966. Species-diversity and pattern-diversity in the study of ecological succession. *Journal of Theoretical Biology*, 10: 370-383.
- Poiner, I.R. and R. Kennedy, 1984. Complex pattern of change in the macrobenthos of a large sandbank following dredging. I. Community analysis. *Marine Biology*, 78: 335-352.
- Powell, J.A. and G.B. Rathbun, 1984. Distribution and abundance of manatees along the northern coast of the Gulf of Mexico. *Northeast Gulf Science*, 7: 1-28.
- Pritchard, P.C.H., 1989. Evolutionary Relationships, Osteology, Morphology and Zoogeography of Kemp's Ridley Sea Turtle. In: Proceedings of the Second Western Atlantic Turtle Symposium, U.S. Department of Commerce, Panama City, FL, NOAA Tech. Mem. NMFS-SEFC-226, pp. 17-32.
- Rabalais, N.N., F.R. Burditt, Jr., L.D. Coen, B.E. Cole, C. Eleuteris, K.L. Heck, Jr., T.A. McTigue, S.G. Morgan, H.M. Perry, F.M. Truesdale, R.K. Zimmer-Faust, and R.J. Zimmerman, 1995. Settlement of *Callinectes sapidus* megalopae on artificial collectors in four Gulf of Mexico estuaries. *Bulletin of Marine Science*, 57(3): 855-876.
- Radder, A.C., 1979. On the parabolic equation method for water-wave propagation. *Journal of Fluid Mechanics*, 95: 159-176.
- Ramsey, J.S., 1991. A Study of Wave-Induced Currents Behind Shore Parallel Breakwaters. M.C.E. Thesis, Dept. of Civil Engineering, University of Delaware, Newark, DE, 101 pp.
- Raudkivi, A.J., 1990. Loose Boundary Hydraulics. 3<sup>rd</sup> Edition, Pergamon Press, Oxford.
- Reeve, M.R. and M.A. Walter, 1978. Nutritional ecology of ctenophores - a review of recent research. *Advances in Marine Biology*, 15: 249-287.
- Reid, R.O., 1994. Preliminary Results of LATEX Relevant to the Proposed Study. Proceedings of the Northeast Gulf of Mexico Physical Oceanography Workshop, U.S. Department of the Interior, Minerals Management Service OCS Study 94-0044.
- Reine, K.J. and D.G. Clark, 1998. Entrainment by Hydraulic Dredges – A Review of Potential Impacts. U. S. Army Engineer Waterways Experiment Station, Research and Development Center, Vicksburg, MS, DOER Tech. Notes Collection (TN DOER-E1).
- Reine, K.J., D.D. Dickerson, and D.G. Clarke, 1998. Environmental Windows Associated with Dredging Operations. U. S. Army Engineer Waterways Experiment Station, Research and Development Center, Vicksburg, MS, DOER Tech. Notes Collection (TN DOER-E2).
- Renaud, M., 1993. Satellite Tracking of Juvenile Kemp's Ridley Sea Turtles Near Sabine Pass, Texas. In: B.A. Schroeder and B.E. Witherington (comps.), Proceedings of the Thirteenth Annual Symposium on Sea Turtle Biology and Conservation, U.S. Department of Commerce, Miami, FL. NOAA Tech. Mem. NMFS-SEFC-341, p. 147.

- Resio, D.T., and B.A. Tracy, 1983. A Numerical Model for Wind-Wave Prediction in Deepwater. WIS Report 12, U.S. Army Engineer Waterways Experiment Station, Coastal Engineering Research Center, Wave Information Study, Vicksburg, MS.
- Rhoads, D.C., 1974. Organism-sediment relations on the muddy seafloor. *Oceanograph. Marine Biology Annual Review*, 12: 263-300.
- Rhoads, D.C. and J.D. Germano, 1982. Characterization of organism-sediment relations using sediment profile imaging: An efficient method of remote ecological monitoring of the seafloor (REMOTS™ System). *Marine Ecology Progress Series*, 8: 115-128.
- Rhoads, D.C. and J.D. Germano, 1986. Interpreting long-term changes in benthic community structure: a new protocol. *Hydrobiologia*, 142: 291-308.
- Rhoads, D.C. and L.F. Boyer, 1982. The Effects of Marine Benthos on Physical Properties of Sediments: A Successional Perspective. In: P.L. McCall and M.J.S. Tevesz (eds.), *Animal-Sediment Relations, The Biogenic Alteration of Sediments*, Plenum Press, New York, NY, pp. 3-52.
- Rhoads, D.C., P.L. McCall, and J.Y. Yingst, 1978. Disturbance and production on the estuarine seafloor. *American Science*, 66: 577-586.
- Richardson, J.I., 1990. The Sea Turtles of the King's Bay Area and the Endangered Species Observer Program Associated with Construction Dredging of the St. Marys Entrance Ship Channel. In: D.D. Dickerson and D.A. Nelson (comps.), *Proceedings of the National Workshop on Methods to Minimize Dredging Impacts on Sea Turtles*, Jacksonville, FL. U.S. Army Engineer Waterways Experiment Station, Environmental Effects Laboratory, Vicksburg, MS, Miscellaneous Paper EL-90-5, pp. 32-46.
- Richardson, W.J., C.R. Greene, Jr., C.I. Malme, and D.H. Thomson, 1995. *Marine Mammals and Noise*. Academic Press, San Diego. 576 pp.
- Ridgway, S.H., E.G. Wever, J.G. McCormick, J. Palin, and J.H. Anderson, 1969. Hearing in the giant sea turtle, *Chelonia mydas*. *Proceedings of the National Academy of Sciences*, 64(3): 884-890.
- Robins, C.R., 1957. Effects of storms on the shallow-water fish fauna of southern Florida with records of fishes from Florida. *Bulletin of Marine Science in the Gulf and Caribbean*, 7(3): 266-275.
- Rogers, B.D., R.F. Shaw, W.H. Herke, and R.H. Blanchet, 1993. Recruitment of postlarval and juvenile brown shrimp (*Penaeus aztecus* Ives) from offshore to estuarine waters of the northwestern Gulf of Mexico. *Estuarine, Coastal and Shelf Science*, 36: 377-394.
- Rogers, R.M., 1977. Trophic Interrelationships of Selected Fishes on the Continental Shelf of the Northern Gulf of Mexico. Ph.D. dissertation, Texas A&M University, College Station, TX, 244 pp.
- Rosati, J.D. and N.C. Kraus, 1991. Practical Considerations in Longshore Transport Calculations. CETN II-24, U.S. Army Engineer Waterways Experiment Station, Coastal and Hydraulics Laboratory, Vicksburg, MS, 6 pp.
- <http://bigfoot.wes.army.mil/cetn.index.html#part2>.
- Rosenthal, H.S., 1971. Effects of "red mud" on embryos and larvae of the herring *Clupea harengus*. *Helgolander Wiss. Meeresuntersuchungen*, 22: 366-376.

- Rosman, I., G.S. Boland, L. Martin, and C. Chandler, 1987. Underwater Sightings of Sea Turtles in the Northern Gulf of Mexico. U.S. Department of the Interior, Minerals Management Service, Gulf of Mexico OCS Region, New Orleans, LA, OCS Study MMS 87-0107, 37 pp.
- Rudloe, A., J. Rudloe, and L. Ogren, 1991. Occurrence of immature Kemp's ridley turtles, *Lepidochelys kempi*, in coastal waters of northwest Florida. *Northeast Gulf Science*, 12(1): 49-53.
- Saloman, C.H., 1974. Physical, Chemical, and Biological Characteristics of Nearshore Zone of Sand Key, Florida, Prior to Beach Restoration. National Marine Fisheries Service, Gulf Coastal Fisheries Center, Panama City Laboratory, Panama City, FL.
- Saloman, C.H. and S.P. Naughton, 1983a. Food of King Mackerel, *Scomberomorus cavalla*, From the Southeastern United States Including the Gulf of Mexico. NOAA Tech. Mem. NMFS-SEFC-126, 25 pp.
- Saloman, C.H. and S.P. Naughton, 1983b. Food of Spanish Mackerel, *Scomberomorus maculatus*, from the Gulf of Mexico and Southeastern Seaboard of the United States. NOAA Tech. Mem. NMFS-SEFC-128, 22 pp.
- Saloman, C.H. and S.P. Naughton, 1984a. Food of Crevalle Jack (*Caranx hippos*) from Florida, Louisiana, and Texas. NOAA Tech. Mem. NMFS-SEFC-134, 34 pp.
- Saloman, C.H. and S.P. Naughton, 1984b. Food of Bluefish (*Pomatomus saltatrix*) From the U.S. South Atlantic and Gulf of Mexico. NOAA Tech. Mem. NMFS-SEFC-150, 37 pp.
- Saloman, C.H., S.P. Naughton, and J.L. Taylor, 1982. Benthic Community Response to Dredging Borrow Pits, Panama City Beach, Florida. U.S. Army Corps of Engineers, Coastal Engineering Research Center, Fort Belvoir, VA, Miscellaneous Report No. 82-3, 138 pp.
- Sanders, H.L., 1958. Benthic studies of Buzzards Bay. I. Animal-sediment relationships. *Limnology and Oceanography*, 3: 245-258.
- SAS Institute Inc., 1989. SAS/STAT® User's Guide, Version 6, Fourth Edition, Volume 1. SAS Institute Inc., Cary, NC, 943 pp.
- Sawaragi, T. and I. Deguchi, 1978. Distribution of Sand Transport Rate Across a Surf Zone. Proceedings, 16<sup>th</sup> International Conference on Coastal Engineering, ASCE, pp. 1,596-1,613.
- Schmidly, D.J., 1981. Marine Mammals of the Southeastern United States Coast and the Gulf of Mexico. U.S. Department of the Interior, Fish and Wildlife Service, Office of Biological Services, Coastal Ecosystems Project, Washington, DC, FWS/OBS-80/41, 166 pp.
- Schroeder, W.W., S.P. Dinnel, F.J. Kelly, W.J. Wiseman, 1994. Overview of the Physical Oceanography of the Louisiana-Mississippi-Alabama Continental Shelf. Proceedings of the Northeast Gulf of Mexico Physical Oceanography Workshop, U.S. Department of the Interior, Minerals Management Service OCS Study 94-0044.
- Seim, H. E., B. Kjerfve, and J.E. Sneed, 1987. Tides of Mississippi Sound and the adjacent continental shelf. *Estuarine, Coastal and Shelf Science*, 25: 143-156.
- Shalowitz, A.L., 1964. Shoreline and Sea Boundaries, Volume 2. U.S. Department of Commerce Publication 10-1, U.S. Coast and Geodetic Survey, U.S. Government Printing Office, Washington, DC, 420 pp.
- Shaver, D.J., 1991. Feeding ecology of wild and headstarted Kemp's ridley sea turtles in south Texas waters. *Journal of Herpetology*, 25(3): 327-334.

- Shaw, J.K., P.G. Johnson, R.M. Ewing, C.E. Comiskey, C.C. Brandt, and T.A. Farmer, 1982. Benthic Macroinfauna Community Characterization in Mississippi Sound and Adjacent Waters. U.S. Army Corps of Engineers, Mobile District, Mobile, AL, 442 pp.
- Shaw, R.F., B.D. Rogers, J.H. Cowen, Jr., and W.H. Herke, 1988. Ocean-estuary coupling of ichthyoplankton and nekton in the northern Gulf of Mexico. *American Fisheries Society Symposium*, 3: 77-89.
- Sherk, J.A., J.M. O'Connor, and D.A. Newman, 1975. Effects of Suspended and Deposited Sediments on Estuarine Environments. In: L.F. Cronin (ed.), *Estuarine Research Volume 2*, Academic Press, New York, NY, pp. 541-558.
- Sherk, J.A., Jr., 1971. The Effects of Suspended and Deposited Sediment on Estuarine Organisms: Literature Summary and Research Needs. University of Maryland, Natural Resources Institute, Chesapeake Biological Laboratory Contribution No. 43, 73 pp.
- Sherk, J.A., Jr., 1972. Current status of the knowledge of the biological effects of suspended and deposited sediments in Chesapeake Bay. *Chesapeake Science*, 13(Suppl.): S137-S144.
- Sherk, J.A., Jr. and L.E. Cronin, 1970. The Effects of Suspended and Deposited Sediments on Estuarine Organisms, An Annotated Bibliography of Selected References. University of Maryland, Chesapeake Biological Laboratory, Natural Resources Institute. Reference No. 70-19, 62 pp.
- Shields, I.A., 1936. Application of similarity principles and turbulence research to bed-load movement (in German). *Mitteilunden der Preoss. Versuchsanst. Fur Wasserbau and Schiffbau*, Berlin, No. 26.
- Shipp, R.L., 1987. Temporal Distribution of Finfish Eggs and Larvae Around Mobile Bay. In: T.A. Lowery (ed.), *Symposium on the Natural Resources of the Moblie Bay Estuary*. Alabama Sea Grant Extension Service, Alabama Cooperative Extension Service, Auburn University, MASGP-87-007, pp. 44-54.
- Shipp, R.L., 1982. Larval Fish Stocks. Dauphin Island Sea Lab Technical Report 82-003.
- Shipp, R.L., 1984. Fish Stocks of the Alabama Coastal Area. Dauphin Island Sea Lab Technical Report 84-002.
- Slay, C.K., 1995. Sea Turtle Mortality Related to Dredging Activities in the Southeastern U.S.: 1991. In: J.I. Richardson and T.H. Richardson (comps.), *Proceedings of the Twelfth Annual Workshop on Sea Turtle Biology and Conservation*, Jekyll Island, GA, NOAA Tech. Mem. NMFS-SEFSC-361, pp. 132-133.
- Smith, J.D., 1977. Modeling of Sediment Transport on Continental Shelves. In: *The Sea*, Volume 6, Edited by Goldberg, E.D., McCave, I.N., O'Brien, J.J., and Steele, J.H., Wiley-Interscience, New York, NY.
- Snelgrove, P.V.R. and C.A. Butman, 1994. Animal-sediment relationships revisited: Cause versus effect. *Oceanography and Marine Biology Annual Review*, 32: 111-177.
- Stanley, D.S. and C.A. Wilson, 1990. A fishery-based study of fish species composition and associated catch rates around oil and gas structures off Louisiana. *Fisheries Bulletin*, 88(2): 719-730.
- Stephenson, W.W.T., S.D. Cook, and S.J. Newlands, 1978. The macrobenthos of the Middle Banks of Moreton Bay. *Mem. Queensl. Mus.*, 18: 95-118.

- Stern, E.M. and W.B. Stickle, 1978. Effects of Turbidity and Suspended Material in Aquatic Environments: Literature Review. U.S. Army Engineer Waterways Experiment Station, Dredged Material Research Program, Vicksburg, MS, Technical Report D-78-21, 117 pp.
- Stickle, W.B., M.A. Kapper, L. Liu, E. Gnaiger, and S.Y. Wang, 1989. Metabolic adaptation of several species of crustaceans and molluscs to hypoxia: Tolerance and microcalorimetric studies. *Biological Bulletin*, 177: 301-312.
- Stone, G.W., F.W. Stapor, J.P. May, and J.P. Morgan, 1992. Multiple sediment sources and a cellular, non-integrated, longshore drift system: northwest Florida and southeast Alabama coast, USA. *Marine Geology*, 105: 141-154.
- Stuck, K.C. and H.M. Perry, 1981a. Observations on the distribution and seasonality of portunid megalopae in Mississippi coastal waters. *Gulf Research Report*, 7: 93-95.
- Stuck, K.C. and H.M. Perry, 1981b. Ichthyoplankton Community Structure in Mississippi Coastal Waters, p. IV-1 to VI-1-53. In: *Fishery Monitoring and Assessment Completion Report*, 1 January 1977 to 31 December 1981, Gulf Coast Research Laboratory, Project No. 2-296-R.
- Stuck, K.C., H.M. Perry, and R.W. Heard, 1979. Records and range extensions of Mysidacea from coastal and shelf waters of the eastern Gulf of Mexico. *Gulf Research Report*, 6(3): 239-248.
- Studt, J.F., 1987. Amelioration of Maintenance Dredging Impacts on Sea Turtles, Canaveral Harbor, Florida. In: W. Witzell (ed.), *Ecology of East Florida Sea Turtles*. Proceedings of the Cape Canaveral, Florida Sea Turtle Workshop, Miami, FL. NOAA Technical Report NMFS 53, pp. 55-58.
- Stumpf, R.P., and G. Gelfenbaum, 1990. Effects of high river discharge on suspended sediments in Mobile Bay, Alabama. *EOS*, 71: 1,406-1,407.
- Stumpf, R.P., G. Gelfenbaum, J.R. Pennock, 1993. Wind and tidal forcing of a buoyant plume, Mobile Bay, Alabama. *Continental Shelf Research*, 13(11): 1281-1301.
- Sullivan, B.K. and D. Hancock, 1977. Zooplankton and dredging: Research perspectives from a critical review. *Water Research Bulletin*, 13(3): 461-468.
- Sutter, F.C., III, R.O. Williams, and M.F. Godcharles, 1991. Movement patterns of king mackerel in the southeastern United States. *Fisheries Bulletin*, 89: 315-324.
- Svendson, I.A., and I.G. Jonsson, 1976. *Hydrodynamics of Coastal Regions*. Technical University of Denmark, 285 pp.
- Swift D.J.P., 1976. Continental Sedimentation. In: Stanley D.J., and Swift D.J.P. Jr, (eds.), *Marine Sediment Transport and Environmental Management*, New York, N.Y, John Wiley and Sons, pp. 225-310.
- Swift, D.J.P. and A.W. Niedoroda, 1985. Fluid and Sediment Dynamics on Continental Shelves. In: Tillman, R.W., D.J.P. Swift, and R.G. Walker (editors), *Shelf Sands and Sandstone Reservoirs*, SEPM Short Course No. 13, Tulsa, OK, pp. 47-133.
- Tanaka H. and N. Shuto, 1981. Friction coefficient for a wave-current coexisting system. *Coastal Engineering of Japan*, 24: 105-128.
- Taylor, A.S., 1990. The Hopper Dredge. In: D.D. Dickerson and D.A. Nelson (comps.), *Proceedings of the National Workshop on Methods to Minimize Dredging Impacts on Sea Turtles*, Jacksonville, FL. U.S. Army Engineer Waterways Experiment Station, Environmental Effects Laboratory, Vicksburg, MS, Miscellaneous Paper EL-90-5, pp. 59-63.

- Taylor, A.S., 1999. Personal communication regarding offshore dredging operations (conversation with Mark Byrnes, January 26, 1999). Mr. Taylor is Vice President and General Manager of Bean Dredging Corporation.
- TechCon, Inc., 1980. Environmental Monitoring Program for Mobil Oil Exploration & Producing Southeast, Inc. Test Well in Mobile Bay, Alabama. Contract Report to Mobil Oil Exploration & Producing Southeast, Inc., New Orleans, LA.
- Thayer, C.W., 1983. Sediment-mediated Biological Disturbance and the Evolution of Marine Benthos. In: M.J.S. Tevesz and P.L. McCall (eds.), *Biotic Interactions in Recent and Fossil Benthic Communities*, Plenum Press, NY, pp. 479-625.
- Thistle, D., 1981. Natural physical disturbances and communities of marine soft bottoms. *Marine Ecology Progress Series*, 6: 223-228.
- Thompson, J.R., 1973. Ecological Effects of Offshore Dredging and Beach Nourishment: A Review. U.S. Army Engineer Waterways Experiment Station MP 1-73, U.S. Army Corps of Engineers, Coastal Engineering Research Center, Fort Belvoir, VA, Report 1-73.
- Thompson, N.B. and H. Huang, 1993. Leatherback turtles in the southeast U.S. waters. NOAA Tech. Mem. MNFS-SESFC-318, 11 pp.
- Thornton, E.B., 1968. A Field Investigation of Sand Transport in the Surf Zone. *Proceedings, 11<sup>th</sup> International Conference on Coastal Engineering, ASCE*, pp. 335-351.
- Thornton, E.B. and R.T. Guza, 1983. Transformation of wave height distribution. *Journal of Geophysical Research*, 88: 5,925-5,938.
- Thornton, E.B. and R.T. Guza, 1989. Models for Surf Zone Dynamics. In: *Nearshore Sediment Transport*, R.J. Seymour, (ed.), Plenum Press, New York, NY, pp. 337-369.
- Thorson, G., 1957. Bottom communities (sublittoral or shallow shelf). *Geological Society of America Memoir*, 67: 461-534.
- Thorson, G., 1966. Some factors influencing the recruitment and establishment of marine benthic communities. *Netherlands Journal of Sea Research*, 3(2): 267-293.
- Todd, T.W., 1968. Dynamic diversion: influence of longshore current-tidal flow interaction on chenier and barrier island plains. *Journal of Sedimentary Petrology*, 38: 734-746.
- Trowbridge, J. and O. Madsen, 1984. Turbulent wave boundary layers, 1. model formulation and first-order solution. *Journal of Geophysical Research*, 89: 7,989-7,997.
- Trowbridge, J. and V.C. Agrawal, 1995. Glimpses of a wave boundary layer. *Journal of Geophysical Research*, 100: 729-744.
- Truesdale, F.M. and B.L. Andryszak, 1983. Occurrence and distribution of reptant decapod crustacean larvae in neritic Louisiana waters: July 1976. *Contributions in Marine Science*, 26: 37-53.
- Turbeville, D.B. and G.A. Marsh, 1982. Benthic Fauna of an Offshore Borrow Area in Broward County, Florida. U.S. Army Corps of Engineers, Coastal Engineering Research Center. Miscellaneous Report 82-1, 43 pp.
- Turner, J.T., 1984a. Zooplankton feeding ecology: Contents of fecal pellets of the copepods *Acartia tonsa* and *Labidocera aestiva* from continental shelf waters near the mouth of the Mississippi River. *Marine Ecology*, 5(3): 265-282.

- Turner, J.T., 1984b. Zooplankton feeding ecology: Contents of fecal pellets of the copepods *Temora turbinata* and *T. stylifera* from continental shelf and slope waters near the mouth of the Mississippi River. *Marine Biology*, 82: 73-83.
- Turner, J.T., 1984c. Zooplankton feeding ecology: Contents of fecal pellets of the copepods *Eucalanus pileatus* and *Paracalanus quasimodo* from continental shelf waters of the Gulf of Mexico. *Marine Ecology*, 6(4): 285-298.
- Turner, J.T., 1984d. Zooplankton feeding ecology: Contents of fecal pellets of the copepod *Anomalocera ornata* from continental shelf and slope waters of the Gulf of Mexico. *Marine Ecology Progress Series*, 15: 27-46.
- Turner, J.T., 1986. Zooplankton feeding ecology: Contents of fecal pellets of the cyclopoid copepods *Oncaea venusta*, *Corycaeus amazonicus*, *Oithona plumifera*, and *O. simplex* from the northern Gulf of Mexico. *Marine Ecology*, (4): 289-302.
- Turner, R.E. and N.N. Rabalais, 1994. Coastal eutrophication near the Mississippi River Delta. *Nature*, 368: 619-621.
- U.S. Army Corps of Engineers, 1955. Perdido Pass (Alabama Point) Alabama Beach Erosion Control Study. Mobile District, Mobile, AL.
- U.S. Army Corps of Engineers, 1967. Hurricane Survey of the Alabama Coast. U.S. 90<sup>th</sup> Congress, 1<sup>st</sup> Session, House Document 99, 92 pp.
- U.S. Army Corps of Engineers, 1984. Shore Protection Manual. U.S. Army Engineer Waterways Experiment Station, Coastal Engineering Research Center, Vicksburg MS.
- U.S. Army Corps of Engineers, 1984. Exploration and Production of Hydrocarbon Resources in Coastal Alabama and Mississippi. Mobile District, Mobile, AL, 615 pp.
- U.S. Army Corps of Engineers, 1999. Hopper Dredge Sea Turtle Deflector Draghead and Operational Requirements. <http://www.saj.usace.army.mil/pd/turtle.htm>
- U.S. Department of Commerce, National Marine Fisheries Service, 1998. Alabama Landings Data. <http://www.nmfs.gov/st1/commercial/index.html>
- U.S. Department of Commerce, 1991. Our Living Resources. NOAA Tech Mem. NMFS-F/SP0-2, 123 pp.
- U.S. Fish and Wildlife Service, 1996. Florida Manatee Recovery Plan (*Trichechus manatus latirostris*), Second Revision. Prepared by the Florida Manatee Recovery Team for the Southeast Region, U.S. Fish and Wildlife Service, Atlanta, GA.
- Underwood, A.J. and P.G. Fairweather, 1989. Supply side ecology and benthic marine assemblages. *Trends in Ecological Evolution*, 4(1): 16-20.
- Van de Voorde, N.E and S.P. Dinnel, 1998. Observed directional wave spectra during a frontal passage. *Journal of Coastal Research*, 14: 337-346.
- Van Dolah, R.F, 1996. Impacts of Beach Nourishment on the Benthos: What Have We Learned?. Twenty-fourth Annual Benthic Ecology Meeting, Columbia, SC, pp. 82.
- Van Dolah, R.F., B.J. Digre, P.T. Gayes, P. Donovan-Ealy, and M.W. Dowd, 1998. An Evaluation of Physical Recovery Rates in Sand Borrow Sites Used for Beach Nourishment Projects in South Carolina. Final Report to the U.S. Department of the Interior, Minerals Management Service, Office of International Activities and Marine Minerals, by the South Carolina Department of Natural Resources, Marine Resources Research Institute, 76 pp. + app.

- Van Dolah, R.F., D.R. Calder, and D.M. Knott, 1984. Effects of dredging and open-water disposal on benthic macroinvertebrates in a South Carolina estuary. *Estuaries*, 7: 28-37.
- Van Dolah, R.F., P.H. Wendt, R.M. Martore, M.V. Levisen, and W.A. Roumillat, 1992. A Physical and Biological Monitoring Study of the Hilton Head Beach Nourishment Project. Final Report submitted to the Town of Hilton Head Island and South Carolina Coastal Council by the South Carolina Wildlife and Marine Resources Department, Marine Resource Research Institute, 159 pp.
- Van Dolah, R.F., R.M. Martore, and M.V. Levisen, 1993. Supplemental Report for the Physical and Biological Monitoring Study of the Hilton Head Beach Nourishment Project. Prepared by the South Carolina Marine Resources Division, Marine Resources Research Institute for the for the Town of Hilton Head Island, SC.
- Vecchione, M., 1981. Aspects of the early life history of *Loligo pealei* (Cephalopoda; Myopsida). *Journal of Shellfish Research*, 1: 171-180.
- Vincent, C.L. and M.J. Briggs, 1989. Refraction-diffraction of irregular waves over a mound. *Journal of Waterway Port, Coastal And Ocean Engineering*, 115(2): 269-284.
- Vinyard, G.L. and J.W. O'Brien, 1976. Effects of light and turbidity on the reactive distance of bluegill (*Lepomis macrochirus*). *Journal of the Fisheries Research Board of Canada*, 33: 2,845-2,849.
- Walker, T.A. and G. O'Donnell, 1981. Observations on nitrate, phosphate and silicate in Cleveland Bay, Northern Queensland. *Australian Journal of Marine and Freshwater Research*, 32: 877-887.
- Weber, M., 1995. Kemp's ridley sea turtle, *Lepidochelys kempii*. In: P.T. Plotkin (ed.), National Marine Fisheries Service and U. S. Fish and Wildlife Service Status Reviews for Sea Turtles Listed under the Endangered Species Act of 1973. Silver Spring, MD.
- Werner, S.A. and A.M. Landry, Jr., 1994. Feeding Ecology of Wild and Head Started Kemp's Ridley Sea Turtles (*Lepidochelys kempii*). In: K.A. Bjorndal, A.B. Bolten, D.A. Johnson, and P.J. Eliazar (comps.), Proceedings of the Fourteenth Annual Symposium on Sea Turtle Biology and Conservation. U.S. Department of Commerce, Miami, FL, NOAA Tech. Mem. NMFS-SEFSC-351, pp. 163.
- Wilber, P. and M. Stern, 1992. A Re-examination of Infaunal Studies That Accompany Beach Nourishment Projects. In: New Directions in Beach Management: Proceedings of the 5th Annual National Conference on Beach Preservation Technology, Florida Shore and Beach Preservation Association, Tallahassee, FL, pp. 242-257.
- Williams, S.J., 1992. Coasts in Crisis. U.S. Geological Survey Circular 1075, 32 pp.
- Winer, H., 1988. Numerical Modeling of Wave-Induced Currents Using a Parabolic Wave Equation. Technical Report No. 80, Dept. of Coastal and Oceanographic Engineering, University of Florida, Gainesville, FL.
- Wiseman, W.J., W.W. Schroeder, and S.P. Dinnel, 1988. Shelf-estuarine water exchanges between the Gulf of Mexico and Mobile Bay, Alabama. *American Fisheries Society Symposium*, 3: 1-8.
- Wright, D.G., 1977. Artificial Islands in the Beaufort Sea: A Review of Potential Impacts. Department of Fisheries and Environment, Winnipeg, Manitoba. 38 pp.
- Yan, Y., 1987. Numerical Modeling of Current and Wave Interactions on an Inlet-beach System. Technical Report No. 73, Dept. of Coastal and Oceanographic Engineering, University of Florida, Gainesville, FL.

Zajac, R.N. and R.B. Whitlatch, 1982. Responses of estuarine infauna to disturbance. I. Spatial and temporal variation of initial recolonization. *Marine Ecology Progress Series*, 10: 1-14.